

**AN INVESTIGATION INTO THE SUSTAINABLE DESIGN  
OF GREEN ROOFS IN RELATION TO THEIR  
HYDROLOGICAL PERFORMANCE**

**KINGA ELZBIETA OWCZAREK**

**A thesis submitted in partial fulfilment of the requirements of the  
University of East London for the degree of Doctor of Philosophy**

**March 2017**

## ABSTRACT

It became paramount for resilient cities to mitigate negative effects of climate change such as extreme weather, heat waves or flooding. Implementation of green roofs in urban regions could help to improve local microclimate through evapotranspiration from green roof surfaces and vegetation, and mitigate flood risk by providing additional storage for stormwater surface runoff. This research investigates the sustainable design of green roofs using conventional and alternative materials, in relation to their hydrological performance under UK climatic conditions. The assessment of the hydrological performance of green roofs was performed by means of laboratory-based and in-situ experiments. This research has identified and selected the alternative materials, suitable for the use in extensive green roof systems. Subsequently, the properties of these materials were assessed using appropriate British Standards, showing that properties-based, as opposed to type-based, selection of the materials is of high importance to the sustainable green roof design. The in-situ experiment demonstrated high retention performance across eight green roof designs with median retention above 99% and cumulative retention for the entire monitoring period of 4 years ranging from 61.5% to 77.9%. The highest retention was recorded for the green roof design of the deepest substrate (100mm) and drainage layer (40mm). Green roofs investigated in the laboratory under extreme rainfall events demonstrated much lower hydrological performance (6% - 11.5% of median retention) than these assessed in-situ. However, their maximum retention capacity ranged from 61% to 78%, given specific conditions such as long inter-event dry period prior to the extreme rainfalls. The green roofs made of alternative materials performed as well as or better than the conventional green roofs in regards to retention. The preliminary multiple linear regression models confirmed the significance of the rainfall depth and temperature in predicting runoff depth and retention as well as porosity of the substrate material and water absorption of drainage layer material. These models could be the basis for further development of tools for accurate prediction of green roof responses to rainfall events in order to assist green roof designers, standardisation bodies, specifiers, manufacturers, and contractors.

**Keywords:** Sustainability, Green roof, Stormwater management, Retention, Runoff, Alternative materials, Extreme rainfall events

# TABLE OF CONTENTS

Abstract.....	ii
List of Figures .....	viii
List of Tables.....	xxi
List of Abbreviations.....	xxxii
Acknowledgment.....	xxxii
Chapter 1 Introduction .....	1
1.1 Problem statement.....	3
1.2 Aim and objectives of the research.....	5
1.3 Contribution to knowledge .....	5
1.4 Development effort .....	10
1.5 Boundaries of research.....	10
1.6 Structure of the thesis.....	11
Chapter 2 Knowledge fundamentals and literature review.....	14
2.1 Knowledge fundamentals.....	14
2.1.1 Hydrology .....	15
2.1.2 Green roofs .....	21
2.1.3 Statistics.....	24
2.2 Literature review .....	31
2.2.1 Green roof rainfall-runoff monitoring.....	32
2.2.2 Green roof construction materials .....	38
2.2.3 Hydrological performance of green roofs .....	44
2.2.4 Research in the UK.....	54
Chapter 3 Green roof materials and their properties.....	57
3.1 Selection of the materials.....	57
3.1.1 Selection criteria.....	57
3.1.2 Description of selected materials.....	58
3.2 Properties of the materials.....	62

3.2.1	Selection of the test methods .....	63
3.2.2	Sample preparation – adjustment of organic matter content in substrate materials .....	66
3.2.3	Material properties procedures.....	68
3.2.4	Data analysis and results .....	73
3.2.5	Discussion.....	85
3.3	Conclusions .....	106
Chapter 4	Hydrological performance of small scale conventional extensive green roofs: in-situ experiment.....	109
4.1	Methodology .....	110
4.1.1	Description of in-situ green roof experiment at Barking Riverside 111	
4.1.2	Analysis methods .....	123
4.1.3	Data preparation.....	123
4.2	Overview of the data .....	127
4.2.1	Weather condition data .....	127
4.2.2	Green roof design data.....	128
4.2.3	Green roof hydrological performance data .....	128
4.3	Results and discussion .....	129
4.3.1	London climatic conditions .....	129
4.3.2	Rainfall - Barking Riverside .....	132
4.3.3	Hydrological performance of the green roofs: experimental replicates 137	
4.3.4	Hydrological performance of the green roofs of different designs	154
4.3.5	Preliminary multiple linear regression analysis.....	183
4.4	Conclusions .....	189
Chapter 5	Rainfall simulator system .....	192
5.1	Background.....	192
5.2	Rainfall simulator design.....	194

5.2.1	The structural frame .....	195
5.2.2	Water supply system .....	197
5.2.3	Rainfall simulator drop-forming box.....	199
5.3	Modifications .....	202
5.4	Rainfall simulator performance .....	202
5.4.1	Calibration of the flow meter.....	203
5.4.2	Calibration of the rainfall simulator system.....	206
5.4.3	Assessment of the spatial variability of rainfall (coefficient of uniformity).....	207
5.5	Conclusions .....	212
Chapter 6 Hydrological performance of small scale extensive green roofs: laboratory experiment .....		213
6.1	Methodology .....	214
6.1.1	Description of laboratory green roof experiment .....	214
6.1.2	Analysis methods .....	230
6.1.3	Data preparation.....	231
6.2	Overview of data .....	234
6.2.1	Simulated rainfall events characteristics and laboratory microclimate conditions data .....	235
6.2.2	Green roof design data.....	235
6.2.3	Green roof hydrological performance data .....	236
6.3	Results and discussion .....	236
6.3.1	Vegetation cover analysis .....	236
6.3.2	Green roof response to the simulated rainfalls: the effect of vegetation presence .....	245
6.3.3	Green roof response to the simulated rainfalls: experimental replicates.....	250
6.3.4	Green roof response to the simulated rainfalls: green roofs of different design.....	258

6.3.5	Preliminary multiple linear regression analysis.....	288
6.4	Conclusions .....	295
Chapter 7	Green roof hydrological performance – an overview.....	298
7.1	Hydrological behaviour of the conventional green roof (W/40/100 – ‘A’ design) based on laboratory and in-situ experiments .....	298
7.2	Discussion of preliminary multiple linear regression models developed based on results of in-situ and laboratory experiments.....	301
7.3	Sustainable green roof design for hydrological performance in the UK - best practice .....	304
Chapter 8	Conclusions and recommendations .....	308
8.1	Overall conclusions.....	308
8.1.1	Green roof materials and their properties.....	309
8.1.2	Hydrological performance of conventional extensive green roofs.....	310
8.1.3	Hydrological performance of green roofs made with alternative materials subjected to extreme rainfall events.....	313
8.2	Contribution to knowledge .....	315
8.2.1	Green roof materials and their properties.....	315
8.2.2	Experimental setup to assess the hydrological performance of green roofs in laboratory conditions.....	315
8.2.3	Hydrological performance of green roofs subjected to extreme rainfall events .....	316
8.2.4	Prediction models for the hydrological performance of the green roofs	316
8.3	Recommendations for further work.....	316
8.3.1	Green roof materials and their properties.....	316
8.3.2	Improvement of the rainfall simulator system .....	317
8.3.3	Improvement of the prediction models for the hydrological performance of the green roofs .....	317
	References.....	318
	Appendix A .....	333

Appendix B ..... 335  
Appendix C ..... 340  
Appendix D ..... 341  
Appendix E ..... 350  
Appendix F ..... 354  
Appendix G ..... 355

## LIST OF FIGURES

Figure 1.1 Global temperature spiral in 2D and 3D showing the increase in global temperatures between 1850 and 2016 (Hawkins, 2016).....	2
Figure 1.2 Outline of the structure of the thesis. ....	13
Figure 2.1 Natural hydrological cycle.....	17
Figure 2.2 Urban hydrological cycle.....	17
Figure 2.3 Effect of urbanisation on rainfall distribution (not to scale); (a) water movement prior to urbanisation with large proportion of water infiltrated (b) water movement post-urbanisation with reduced quantities of water evapotranspired and infiltrated.....	18
Figure 2.4 Typical IDF relationship curves.....	19
Figure 2.5 Rainfall and runoff hydrograph.....	20
Figure 2.6 Typical green roof configuration (a) extensive green roof with substrate depth between 60 mm to 200 mm (b) intensive green roof with substrate depth between 150mm to 400mm.....	22
Figure 2.7 Normal distribution with distinctive bell-shaped density (Johnson and Bhattacharyya, 2011).....	25
Figure 2.8 Example of a histogram, graphical display of the distribution of data. ....	26
Figure 2.9 Example of a boxplot, graphical display of the distribution of data. It presents summary information in the quartiles. ....	27
Figure 2.10 Example of a normal quantile plot (Q-Q plot), graphical display of the distribution of data. It shows relation between the empirical and theoretical distribution of data.....	28
Figure 2.11 Example of a scatterplot. It is a graphical representation of pair of observations x and y.....	28
Figure 2.12 Graphical verification of an assumption of the independence of residuals (Faraway, 2002). ....	31
Figure 2.13 Green roof stormwater retention – cumulative or average retention values reported in published literature and a median retention determined based on these values.....	46

Figure 2.14 Green roof peak flow reduction values reported in published literature and a median peak flow reduction determined based on these values. ....	47
Figure 3.1 Loss on ignition test: (a) Crushed Red Brick, Lytag, Sewage Sludge Pellets and compost samples in crucibles (b) samples were combusted at $(450 \pm 25)$ °C in muffle furnace. ....	67
Figure 3.2 Loose bulk density test: standard mould filled with Wool-rich Carpet Shred. ....	70
Figure 3.3 Particle density and water absorption test: (a) three pycnometers filled with Crushed Red Brick (b) three pycnometers filled with Granulated Rubber. ....	71
Figure 3.4 Constant head permeability test: (a) apparatus diagram (Whitlow, 1995) (b) Sewage Sludge Pellets test (c) Wool-rich Carpet Shred test ....	72
Figure 3.5 Substrate materials: (a) Crushed Red Brick: conventional substrate, widely used in the UK (b) Lytag: selected alternative material (c) Sewage Sludge Pellets: selected alternative material. ....	76
Figure 3.6 Particle size distribution (PSD) curve for Crushed Red Brick, including PSD envelope for extensive substrates recommended by FLL. .	77
Figure 3.7 Particle size distribution (PSD) curve for Lytag, including PSD envelope for extensive substrates recommended by FLL. ....	78
Figure 3.8 Particle size distribution (PSD) curve for Sewage Sludge Pellets, including PSD envelope for extensive substrates recommended by FLL. .	79
Figure 3.9 Drainage layer materials: (a) Roofdrain40: conventional drainage layer, widely used in the UK (b) Granulated Rubber: selected alternative material (c) Wool-rich Carpet Shred: selected alternative material. ....	82
Figure 3.10 Particle size distribution (PSD) curve for Granulated Rubber, including PSD envelope for drainage layer recommended by FLL (author's interpretation). ....	83
Figure 3.11 The particle distribution: (a) in a well-graded soil, the spaces between larger particles are filled with smaller (b) in a poorly-graded soil the spaces are unfilled. ....	86
Figure 3.12 Particle size distribution (PSD) chart for all substrate materials tested and FLL recommended limits. ....	96
Figure 3.13 Loose bulk density, saturated density, particle density of substrate materials tested (based on Table 3.7). ....	97

Figure 3.14 The porosity, effective size, and maximum capillary rise of Crushed Red Brick, Lytag and Sewage Sludge Pellets (based on Table 3.7).....	99
Figure 3.15 The porosity, coefficient of permeability and water absorption of Crushed Red Brick, Lytag and Sewage Sludge Pellets (based on Table 3.7). .....	101
Figure 3.16 Loose bulk density, saturated density, particle density of all drainage layer materials based on test results (Table 3.9) and manufacturer specification. ....	103
Figure 3.17 The porosity, coefficient of permeability and water absorption of all drainage layer materials based on test results (Table 3.9) and manufacturer specification. ....	105
Figure 4.1 The location of Barking Riverside in-situ experimental setup (Imagery ©2016 Google, Map data ©2016 Google). ....	110
Figure 4.2 Barking Riverside experimental setup: (a) green roof plots on the top of the transport containers; (b) green roof plots; (c) central cover over drainage outlet in each green roof plot; (d) drainage pipe under each green roof plot.....	111
Figure 4.3 Generic Barking Riverside green roof profile. ....	112
Figure 4.4 Randomised position of the green roof test plots. Green roof design: letter represents vegetation type: S-sedum, W-wildflower, first number corresponds to drainage layer depth: 25mm or 40mm, second number represents substrate depth: 50mm or 100mm. ‘Control’ refers to empty test plot, ‘Non-experimental’ refers to plot not included in the experiment.....	113
Figure 4.5 Vantage Pro 2 weather station at Barking Riverside experiment site. ....	114
Figure 4.6 Runoff monitoring instrument at Barking Riverside: (a) tipping bucket rain gauges inside the transport container (b) tipping bucket rain gauge, fitted with the sieve acting as filter, on the top of the water collection box. ....	115
Figure 4.7 Tipping bucket rain gauge: (a) internal components, where A-Magnet, B-Reed Switch (Davis Instruments, 2012) (b) schematics of the mechanism. ....	116
Figure 4.8 Calibration of the tipping bucket rain gauges at Barking Riverside, phase one: flow rate 1 (around 2.3 l/h). ....	118

Figure 4.9 Modelled calibration curve for the green roof S/25/100 based on Table 4.4.....	121
Figure 4.10 Weather station output data as a 'text' file. ....	124
Figure 4.11 Daily rain gauge output data sheet ('csv' file). First column includes time, remaining columns contain records of tip – '1' or no tip – '0' per test plot.....	125
Figure 4.12 The historical rainfall data for Heathrow, London (UK Meteorological Office, 1948-current). Annual rainfall depth is presented for each year of research period and compared to long term average rainfall depth based on data between years 1948 and 2015.....	130
Figure 4.13 The historical temperature data, Heathrow, London (UK Meteorological Office, 1948-current). Chart presents monthly averages (minimum and maximum) for each year of research period, monthly averages (minimum and maximum) for the period between 2010 and 2014, and long term monthly averages (minimum and maximum) for the period between 1948 and 2015. ....	131
Figure 4.14 The historical monthly rainfall data, Heathrow, London (UK Meteorological Office, 1948-current). Chart presents monthly averages for each year of research period, monthly averages for the period between 2010 and 2014, and long term monthly averages for the period between 1948 and 2015.....	132
Figure 4.15 Data exploratory analysis of rainfall at Barking Riverside (a) boxplot showing distribution of the initial rainfall data (b) histogram presenting the frequency of rainfall data - initial data set. Boxplot confirms non-normal distribution of rainfalls. Histogram shows exponential distribution of rainfalls. ....	133
Figure 4.16 Data exploratory analysis of rainfall at Barking Riverside (a) boxplot showing distribution of the final rainfall data (b) histogram presenting the frequency of rainfall data - final data set. Boxplots confirms non-normal distribution of rainfalls. Histogram shows exponential distribution of rainfalls. ....	134
Figure 4.17 The annual rainfall data recorded at Barking Riverside, London-Heathrow, London-Crossness STW, July 2010 – August 2014. ....	135
Figure 4.18 Rainfall characteristics for Barking Riverside rainfall data, July 2010 – August 2014 compared with return period estimated for London.....	136

Figure 4.19 Stormwater retention data distribution for the following roofs: Control-1, Control-2, Control-3.....	138
Figure 4.20 Stormwater retention data distribution for green roofs: S/25/50-1, S/25/50-2, S/25/50-3.....	139
Figure 4.21 Stormwater retention data distribution for green roofs: S/25/100-1, S/25/100-2, S/25/100-3.....	140
Figure 4.22 Stormwater retention data distribution for green roofs: S/40/50-1, S/40/50-2, S/40/50-3.....	141
Figure 4.23 Stormwater retention data distribution for green roofs: S/40/100-1, S/40/100-2, S/40/100-3.....	142
Figure 4.24 Stormwater retention data distribution for green roofs: W/25/50-1, W/25/50-2, W/25/50-3.....	143
Figure 4.25 Stormwater retention data distribution for green roofs: W/25/100-1, W/25/100-2, W/25/100-3.....	144
Figure 4.26 Stormwater retention data distribution for green roofs: W/40/50-1, W/40/50-2, W/40/50-3.....	145
Figure 4.27 Stormwater retention data distribution for green roofs: W/40/100-1, W/40/100-2, W/40/100-3.....	146
Figure 4.28 Control roof at Barking Riverside in-situ experiment setup. The drainage outlet is located on the overlapping waterproof material.....	149
Figure 4.29 Distribution of stormwater runoff depth data for selected green roofs in relation to their overall performance.....	156
Figure 4.30 Distribution of stormwater retention data for selected green roofs in relation to their overall performance. ....	158
Figure 4.31 Distribution of stormwater peak flow reduction data for selected green roofs in relation to their overall performance.....	160
Figure 4.32 The annual retention for each year of the monitoring period and cumulative retention 2010-2014 based on full monitoring period between July 2010 and August 2014. ....	168
Figure 4.33 Cumulative rainfall and runoff depth for green roofs of different designs over full monitoring period between July 2010 and August 2014. .....	169
Figure 4.34 Cumulative runoff depth over period of study July 2010 – August 2014. Runoff depth data were grouped based on vegetation type: (a) sedum; (b) wildflower.....	172

Figure 4.35 Cumulative runoff depth over period of study July 2010 – August 2014. Runoff depth data were grouped based on substrate depth: (a) 100mm; (b) 50mm. ....	172
Figure 4.36 Cumulative runoff depth over period of study July 2010 – August 2014. Runoff depth data were grouped based on drainage layer depth: (a) 40mm; (b) 25mm. ....	173
Figure 4.37 Distribution of stormwater runoff depth data by season. ....	174
Figure 4.38 Distribution of stormwater retention data by season. ....	176
Figure 4.39 Distribution of stormwater peak flow reduction data by season. ...	178
Figure 4.40 Rainfall depth data distribution by season. ....	180
Figure 4.41 Linear regression model assumptions graphical tests (a) residuals vs. fitted values (b) residuals Q-Q plot. ....	185
Figure 4.42 Retention linear regression model assumptions graphical tests (a) residuals vs. fitted values (b) residuals Q-Q plot. ....	186
Figure 5.1 Example of the rainfall intensity distribution produced by spray-nozzle type of rainfall simulator. The rainfall intensity ranges between 40mm/h and 140mm/h for the target intensity of 127mm/h (Grismer, 2011). ....	193
Figure 5.2 Rainfall simulator system - general view. ....	195
Figure 5.3 The structural frame of the rainfall simulator system supporting water supply system, drop-forming box, and green roof trays. ....	195
Figure 5.4 Rainfall simulator system diagram – elevation view. ....	196
Figure 5.5 The water supply system through which the water is supplied to the drop-forming box of the rainfall simulator (a) upper part of the water supply system (b) drop-forming box connected to the water supply system. ....	198
Figure 5.6 Rainfall simulator drop-forming box: (a) drop-forming box elevation (b) rain drops formed at the end of hypodermic needles (c) drop-forming box – plan view. ....	200
Figure 5.7 Rainfall simulator drop-forming box cross section and plan view. ...	201
Figure 5.8 The relationship between the volume of water collected and the collection time for each displayed flow rates. The slope of each best fit line indicates the average actual flow rate corresponding to selected displayed flow rate. ....	204

Figure 5.9 The relationship between the actual and displayed flow rates for the DigiFlow 6710M flow rate meter. The coefficient of discharge is taken as a slope of the best fit line. ....	205
Figure 5.10 The relationship between the actual and displayed flow rate for the rainfall simulator system. The coefficient of discharge is taken as a slope of the best fit line.....	207
Figure 5.11 Uniformity test (a) circular measuring cups covering tested area, (b) determination of the water volume in circular cups, (c) square measuring cups covering tested area (b) determination of the water volume in square cups. ....	209
Figure 5.12 Comparison of the coefficient of uniformity obtained for different flow rates and durations based on Table 5.2. ....	210
Figure 5.13 Maps showing simulated rainfall distribution for the tests of the following characteristics: (a) low flow rate of 0.05l/min and short duration of 5min, (b) high flow rate of 0.28l/min and long duration of 10min.....	211
Figure 6.1 Laboratory experiment setup overview: (a) small scale green roof trays (b) rainfall simulator system with green roof trays.....	215
Figure 6.2 Green roof trays: (a) assembly of green roof tray (b) ready green roof trays (c) micro-pores on the wall surface of tray (d) tray lain with pond liner. ....	218
Figure 6.3 Green roof trays preparation: (a) empty tray (b) first layer of geotextile (c) drainage layer (d) second layer of geotextile (e) substrate layer compaction (f) ready green roof tray. Note: these photos were taken for green roof design A and before trays were lain with pond liner. The same procedure applied to all green roof designs after the pond liner was introduced.....	219
Figure 6.4 The growth of the wildflowers from seeds (a) signs of light depravation (b) seedlings suffering from damping-off.....	222
Figure 6.5 The green roof plots under LED grow lights in the laboratory setup. ....	223
Figure 6.6 Green roof trays plug-planting: (a) wildflower plugs in plug tray (b) green roof trays plug-planted in four by four matrix (c) Common Knapweed in bloom (d) Oxeye Daisy in bloom. ....	224

Figure 6.7 Runoff monitoring equipment: (a) the data-logging bench scales with water collection containers atop (b) the computer to which all scales were connected to for continuous data-logging. ....	228
Figure 6.8 The green roof tray image (a) before colour conversion of the vegetated area (b) after colour conversion of the vegetated area.....	232
Figure 6.9 Data-logging scale output data sheet ('csv' file). The first column includes reading number, the second contains cumulative mass of water in the collection container and finally the third column indicates date and time of the reading taken. ....	233
Figure 6.10 Vegetation cover over the 12-week testing programme for green roof design A. The vegetation cover for replicates A1, A2, and A3 is shown by solid lines, the average of replicates is shown by dashed line. ....	237
Figure 6.11 Vegetation cover over the 12-week testing programme for green roof design B. The vegetation cover for replicates B1, B2, and B3 is shown by solid lines, the average of replicates is shown by dashed line. ....	237
Figure 6.12 Vegetation cover over the 12-week testing programme for green roof design C. The vegetation cover for replicates C1, C2, and C3 is shown by solid lines, the average of replicates is shown by dashed line. ....	238
Figure 6.13 Vegetation cover over the 12-week testing programme for green roof design D. The vegetation cover for replicates D1, D2, and D3 is shown by solid lines, the average of replicates is shown by dashed line. ....	238
Figure 6.14 Vegetation cover over the 12-week testing programme for green roof design E. The vegetation cover for replicates E1, E2, and E3 is shown by solid lines, the average of replicates is shown by dashed line. ....	239
Figure 6.15 The comparison between average vegetation cover of each green roof design over the 12-week testing programme.....	239
Figure 6.16 The average vegetation cover data distribution for all green roof designs: A, B, C, D, and E. ....	240
Figure 6.17 Poorly performing cowslip. Its poor performance was observed across all green roof designs: (a) cowslip growing in Crushed Red Brick (b) cowslip growing in Lytag.....	242
Figure 6.18 Slugs being found in green roof trays: (a) slug feeding on plant (b) slug trap – small container filled with beer sunk into the soil.....	243
Figure 6.19 Stormwater retention data distribution for green roofs with and without vegetation.....	247

Figure 6.20 The usual and preferential flow paths for stormwater through plug-planted green roof substrate.....	250
Figure 6.21 Retention data distribution for green roofs: A-1, A-2, A-3. The retention data included observations for green roof trays with vegetation. ....	252
Figure 6.22 Retention data distribution for green roofs: B-1, B-2, B-3. The retention data included all observations for green roof trays with and without vegetation.....	253
Figure 6.23 Retention data distribution for green roofs: C-1, C-2, C-3. The retention data included observations for green roof trays with vegetation. ....	254
Figure 6.24 Retention data distribution for green roofs: D-1, D-2, D-3. The retention data included observations for green roof trays with vegetation. ....	255
Figure 6.25 Retention data distribution for green roofs: E-1, E-2, E-3. The retention data included observations for green roof trays with vegetation. ....	256
Figure 6.26 Stormwater runoff depth data distribution for green roofs designs A-E. ....	260
Figure 6.27 Stormwater retention data distribution for green roof designs A-E. ....	262
Figure 6.28 Stormwater peak flow reduction data distribution for green roof designs A-E. ....	263
Figure 6.29 Relationship between runoff depth and substrate material porosity (S_porosity) and water absorption (S_water_abs) for green roofs design A-E. ....	270
Figure 6.30 Relationship between runoff depth and coefficient of permeability of substrate material (S_coeff_perm) and drainage layer material (DL_coeff_perm) for green roofs design A-E. ....	270
Figure 6.31 Relationship between runoff depth and water absorption of drainage layer material (DL_water_abs) and capillary rise of substrate material (S_cap_rise) for green roofs design A-E.....	271
Figure 6.32 Relationship between runoff depth and sand to gravel ratio of substrate material for green roofs design A-E.....	271

Figure 6.33 Relation between retention and substrate material porosity (S_porosity) and water absorption (S_water_abs) for green roofs design A-E. ....	272
Figure 6.34 Relation between retention and coefficient of permeability of substrate material (S_coeff_perm) and drainage layer material (DL_coeff_perm) for green roofs design A-E. ....	272
Figure 6.35 Relation between retention and water absorption of drainage layer material (DL_water_abs) and capillary rise of substrate material (S_cap_rise) for green roofs design A-E.....	273
Figure 6.36 Relation between retention and sand to gravel ratio of substrate material for green roofs design A-E. ....	273
Figure 6.37 Time-series of per-event retention for the control green roof design A and treatment green roof designs B and C.....	274
Figure 6.38 Time-series of per-event retention for the control green roof design A and treatment green roofs D and E. ....	274
Figure 6.39 Green roof design B water-logging problem: (a) green roof tray filled with undrained water (b) lump of deposited low permeability layer.....	276
Figure 6.40 Stormwater runoff depth data distribution categorised by the rainfall magnitude. ....	281
Figure 6.41 Stormwater retention data distribution categorised by the magnitude of rainfall event. ....	283
Figure 6.42 Linear regression model assumptions graphical tests (a) residuals vs. fitted values (b) residuals Q-Q plot.....	290
Figure 6.43 Retention linear regression model assumptions graphical tests (a) residuals vs. fitted values (b) residuals Q-Q plot.....	291
Figure 7.1 Distribution of rainfall depth data (a) recorded during the in-situ experiment (b) recorded during the laboratory experiment. ....	299
Figure 7.2 Retention data distribution (a) for green roofs investigated in-situ: W/40/100-1, W/40/100-2, W/40/100-3 (b) for green roofs investigated in laboratory: A-1, A-2, A-3. ....	301
Figure B.1 Modelled calibration curves for the sedum green roof plots with drainage layer depth being 25mm. ....	335
Figure B.2 Modelled calibration curves for the sedum green roof plots with drainage layer depth being 40mm. ....	336

Figure B.3 Modelled calibration curves for the wildflower green roof plots with drainage layer depth being 25mm. ....	337
Figure B.4 Modelled calibration curves for the wildflower green roof plots with drainage layer depth being 40mm. ....	338
Figure B.5 Modelled calibration curves for the control roof plots. ....	339
Figure C.1 Data exploratory analysis of rainfall at Barking Riverside – initial data set: (a) Q-Q plot showing relationship between sample and theoretical quantiles. It confirms non-normal distribution of rainfalls (b) histogram presenting the density of rainfall data. It shows exponential distribution of rainfalls. ....	340
Figure C.2 Data exploratory analysis of rainfall at Barking Riverside – final data set: (a) Q-Q plot showing relationship between sample and theoretical quantiles. It confirms non-normal distribution of rainfalls (b) histogram presenting the density of rainfall data. It shows exponential distribution of rainfalls. ....	340
Figure D.1 Data exploratory analysis of retention data for replicates of control roof. Q-Q plots and density histograms confirm non-normal distribution of retention.....	341
Figure D.2 Data exploratory analysis of retention data for replicates of S/25/50 roof. Q-Q plots and density histograms confirm non-normal distribution of retention.....	342
Figure D.3 Data exploratory analysis of retention data for replicates of S/25/100 roof. Q-Q plots and density histograms confirm non-normal distribution of retention.....	343
Figure D.4 Data exploratory analysis of retention data for replicates of S/40/50 roof. Q-Q plots and density histograms confirm non-normal distribution of retention.....	344
Figure D.5 Data exploratory analysis of retention data for replicates of S/40/100 roof. Q-Q plots and density histograms confirm non-normal distribution of retention.....	345
Figure D.6 Data exploratory analysis of retention data for replicates of W/25/50 roof. Q-Q plots and density histograms confirm non-normal distribution of retention.....	346

Figure D.7 Data exploratory analysis of retention data for replicates of W/25/100 roof. Q-Q plots and density histograms confirm non-normal distribution of retention.....	347
Figure D.8 Data exploratory analysis of retention data for replicates of W/40/50 roof. Q-Q plots and density histograms confirm non-normal distribution of retention.....	348
Figure D.9 Data exploratory analysis of retention data for replicates of W/40/100 roof. Q-Q plots and density histograms confirm non-normal distribution of retention.....	349
Figure E.1 Maps showing simulated rainfall distribution for the displayed flow rate of 0.05 l/min (a) test duration 5min (b) test duration 10min.....	350
Figure E.2 Maps showing simulated rainfall distribution for the displayed flow rate of 0.1 l/min (a) test duration 5min (b) test duration 10min.....	351
Figure E.3 Maps showing simulated rainfall distribution for the displayed flow rate of 0.2 l/min (a) test duration 5min (b) test duration 10min.....	352
Figure E.4 Maps showing simulated rainfall distribution for the displayed flow rate of 0.28 l/min (a) test duration 5min (b) test duration 10min.....	353
Figure F.1 Data exploratory analysis of retention data for vegetated and unvegetated green roofs. Each group includes all green roof designs. Q-Q plots and density histograms confirm non-normal distribution of retention. ....	354
Figure G.1 Data exploratory analysis of retention data for replicates of green roof design A. Q-Q plots and density histograms confirm non-normal distribution of retention. ....	355
Figure G.2 Data exploratory analysis of retention data for replicates of green roof design B. Q-Q plots and density histograms confirm non-normal distribution of retention. ....	356
Figure G.3 Data exploratory analysis of retention data for replicates of green roof design C. Q-Q plots and density histograms confirm non-normal distribution of retention. ....	357
Figure G.4 Data exploratory analysis of retention data for replicates of green roof design D. Q-Q plots and density histograms confirm non-normal distribution of retention. ....	358

Figure G.5 Data exploratory analysis of retention data for replicates of green roof design E. Q-Q plots and density histograms confirm non-normal distribution of retention. ....359

## LIST OF TABLES

Table 1.1 Mapping objectives to specific research questions and contributions.	7
Table 2.1 Collation of conventional materials used as a green roof substrate based on published literature. The materials are categorised in regards to the location of the study.	39
Table 2.2 Collation of alternative materials used as a green roof substrate based on published literature. The materials are categorised in regards to the location of the study.	40
Table 2.3 Collation of green roof substrate additives based on published literature. The materials are categorised in regards to the location of the study.	41
Table 2.4 Collation of drainage layer materials based on published literature. The materials are divided into three groups: conventional, alternative and recommended by FLL (2008).	43
Table 2.5 Summary of the UK based research in relation to hydrological performance and use of alternative materials or additives. Studies belong to one of the two groups of research focus: HP-hydrological performance or B/PGE – Biodiversity/Plant Growth Enhancement.	56
Table 3.1 Summary of the green roof construction material selection.	60
Table 3.2 British Standards describing the test methods for relevant material properties.	63
Table 3.3 Summary of material properties, corresponding British Standards describing test of material properties and materials tested.	65
Table 3.4 Results of the loss on ignition test, initial organic matter content.	67
Table 3.5 Results of the loss on ignition test, final organic matter content.	68
Table 3.6 The results of the visual inspection of the substrate materials: Crushed Red Brick, Lytag and Sewage Sludge Pellets.	76
Table 3.7 Summary of the Crushed Red Brick, Lytag and Sewage Sludge Pellets properties and corresponding values recommended by FLL.	80
Table 3.8 The description of drainage layer materials (Roofdrain40, Granulated Rubber and Wool-rich Carpet Shred) based on the visual inspection.	81

Table 3.9 Summary of the Roofdrain40, Granulated Rubber and Wool-rich Carpet Shred properties and corresponding values recommended by FLL. .....	84
Table 3.10 The FLL recommendation for particle size distribution of drainage layer and its interpretation adopted in this study.....	94
Table 3.11 Percentage difference in densities (loose bulk, saturated, particle) for Lytag and Sewage Sludge Pellets in comparison to Crushed Red Brick. .....	98
Table 3.12 The percentage difference in porosity and maximum capillary rise of Lytag and Sewage Sludge Pellets in comparison to Crushed Red Brick. ...	99
Table 3.13 The percentage difference of porosity, coefficient of permeability and water absorption of Lytag and Sewage Sludge Pellets in comparison to Crushed Red Brick.....	101
Table 3.14 The percentage difference in densities (bulk and saturated) of Granulated Rubber and Wool-rich Carpet Shred in comparison to Roofdrain40. ....	104
Table 4.1 In-situ experimental green roof at Barking Riverside. Green roof design: letter represents vegetation type: S-sedum, W-wildflower, first number corresponds to drainage layer depth: 25mm or 40mm, second number represents substrate depth: 50mm or 100mm. ....	113
Table 4.2 Weather data specifications for the Vantage Pro 2 weather station installed at the Barking Riverside experiment site. ....	114
Table 4.3 Results of the two initial calibrations of tipping bucket rain gauges at Barking Riverside.....	119
Table 4.4 The results of the calibrations showing the runoff low rate (tips/hour) and corresponding volume of individual tip (ml) for the green roof S/25/100. .....	120
Table 4.5 Summary of the calibration equations and corresponding goodness of fit of a model coefficient ( $R^2$ ). ....	122
Table 4.6 The runoff data excluded from the analysis: reason for exclusion and corresponding dates for the monitoring period between July 2010 and August 2014.....	126
Table 4.7 Summary statistics of initial and final rainfall data sets recorded at Barking Riverside. Initial data set contains all identified rainfall events, whilst final data set contains rainfall events greater than 2mm. ....	133

Table 4.8 Summary statistics of stormwater retention data for following roofs: Control-1, Control-2, Control-3.....	138
Table 4.9 Summary statistics of stormwater retention data for following green roofs: S/25/50-1, S/25/50-2, S/25/50-3. ....	139
Table 4.10 Summary statistics of stormwater retention data for following green roofs: S/25/100-1, S/25/100-2, S/25/100-3. ....	140
Table 4.11 Summary statistics of stormwater retention data for following green roofs: S/40/50-1, S/40/50-2, S/40/50-3. ....	141
Table 4.12 Summary statistics of stormwater retention data for following green roofs: S/40/100-1, S/40/100-2, S/40/100-3. ....	142
Table 4.13 Summary statistics of stormwater retention data for following green roofs: W/25/50-1, W/25/50-2, W/25/50-3. ....	143
Table 4.14 Summary statistics of stormwater retention data for following green roofs: W/25/100-1, W/25/100-2, W/25/100-3. ....	144
Table 4.15 Summary statistics of stormwater retention data for following green roofs: W/40/50-1, W/40/50-2, W/40/50-3. ....	145
Table 4.16 Summary statistics of stormwater retention data for following green roofs: S/25/100-1, S/25/100-2, S/25/100-3. ....	146
Table 4.17 Wilcoxon rank test results – significance for each combination of the data sets for control roofs. ....	147
Table 4.18 P-values from Wilcoxon rank tests between replicates of the sedum green roof designs: S/25/50, S/25/100, S/40/50, S/40/100. Highlighted numbers demonstrate no statistically significant difference between plots. .....	148
Table 4.19 P-values from Wilcoxon rank tests between replicates of the wildflower green roof designs: W/25/50, W/25/100, W/40/50, W/40/100. Highlighted numbers demonstrate no statistically significant difference between plots.....	148
Table 4.20 Summary statistics of stormwater runoff depth data for selected green roofs in relation to their overall performance.....	156
Table 4.21 P-values from Dunn’s Kruskal-Wallis multiple comparison test results with Bonferroni correction applied for each combination of the runoff depth data sets. Highlighted numbers demonstrate a statistically significant difference between plots. Italicised numbers show a statistically significant difference between plots based on uncorrected p-value.....	157

Table 4.22 Summary statistics of stormwater retention data for selected green roofs in relation to their overall performance.....	158
Table 4.23 P-values from Dunn’s Kruskal-Wallis multiple comparison test results with Bonferroni correction applied for each combination of the retention data sets. Highlighted numbers demonstrate a statistically significant difference between plots. Italicised numbers show a statistically significant difference between plots based on uncorrected p-value.....	159
Table 4.24 Summary statistics of stormwater peak flow reduction data for selected green roofs in relation to their overall performance. ....	160
Table 4.25 P-values from Dunn’s Kruskal-Wallis multiple comparison test results with Bonferroni correction applied for each combination of the peak flow reduction data sets. Highlighted numbers demonstrate a statistically significant difference between plots. Italicised numbers show a statistically significant difference between plots based on uncorrected p-value.....	161
Table 4.26 Median stormwater retention determined for four rainfall depth quantiles. ....	164
Table 4.27 Median stormwater peak flow reduction determined for four rainfall depth quantiles. ....	164
Table 4.28 Annual and cumulative retention over full monitoring period between July 2010 and August 2014. ....	168
Table 4.29 Summary statistics of stormwater runoff depth data in relation to their overall performance in different seasons over a period of study July 2010 – August 2014. Statistically significant differences are represented by p-values obtained from Dunn’s Kruskal-Wallis multiple comparison test results with Bonferroni correction. Highlighted numbers demonstrate a statistically significant difference in runoff depth between seasons. ....	174
Table 4.30 Median runoff depth for selected green roofs in relation to season and p-values from Dunn’s Kruskal-Wallis multiple comparison test results with Bonferroni correction applied between seasons for selected roofs. Highlighted numbers demonstrate a statistically significant difference in runoff depth between seasons.....	175
Table 4.31 Summary statistics of stormwater retention data in relation to their overall performance in different seasons over a period of study July 2010 – August 2014. Statistically significant differences are represented by p-values obtained from Dunn’s Kruskal-Wallis multiple comparison test	

results with Bonferroni correction. Highlighted numbers demonstrate a statistically significant difference in retention between seasons. ....	176
Table 4.32 Median retention for selected green roofs in relation to season and p-values from Dunn’s Kruskal-Wallis multiple comparison test results with Bonferroni correction applied between seasons for selected roofs. Highlighted numbers demonstrate a statistically significant difference in retention between seasons. ....	177
Table 4.33 Summary statistics of stormwater retention data in relation to their overall performance in different seasons over a period of study July 2010 – August 2014. Statistically significant differences are represented by p-values obtained from Dunn’s Kruskal-Wallis multiple comparison test results with Bonferroni correction. Highlighted numbers demonstrate a statistically significant difference in peak flow reduction between seasons. ....	178
Table 4.34 Median peak flow reduction for selected green roofs in relation to season and p-values from Dunn’s Kruskal-Wallis multiple comparison test results with Bonferroni correction applied between seasons for selected roofs. Highlighted numbers demonstrate a statistically significant difference in peak flow reduction between seasons. ....	179
Table 4.35 Summary of multiple linear regression predicting runoff depth using rainfall depth (RD), rainfall duration (DUR), temperature (TEMP), humidity (HUM), dew point (DEW), wind speed (WIND) and air pressure (BAR) (N=1355). ....	185
Table 4.36 Summary of multiple linear regression predicting retention using rainfall depth (RD), rainfall duration (DUR), temperature (TEMP), humidity (HUM), dew point (DEW), wind speed (WIND) and air pressure (BAR) (N=1355). ....	186
Table 5.1 Displayed flow rates and corresponding actual flow rates based on Figure 5.8. ....	204
Table 5.2 Spatial variability of rainfall (coefficient of uniformity) for various flow rates and durations. ....	209
Table 6.1 Summary of the green roof construction materials selection. ....	216
Table 6.2 Summary of green roof designs tested in laboratory experiment. ....	217

Table 6.3 Mass of the 100mm depth of the substrate material and 40mm depth of drainage layer material (compacted). This technique applies to granular and fibre-like materials, hence the Roofdrain40 is not included.....	220
Table 6.4 Two types of the frequencies recommended by BS EN 752: 2008 for storm sewers design, both related to the location of the building (British Standards Institution, 2013).....	225
Table 6.5 The example of the predicted climate change effect on rainfall characteristics – the most unfavourable prediction of 30% increase in depth and intensity of winter rainfalls. The intensity and depth of the rainfall events were determined using Wallingford Procedure (DoE/NWC, 1981) and are specific to London.....	226
Table 6.6 Summary of the extreme rainfall event characteristics selected for the laboratory testing. The intensity and depth of the rainfall events were determined using Wallingford Procedure (DoE/NWC, 1981) and are specific to London. The flow rate was calculated for the area of the green roof trays.....	227
Table 6.7 The schedule for the programme of testing green roofs with no vegetation. ....	229
Table 6.8 The schedule for the programme of testing green roofs with vegetation. This included the vegetation establishment time and the rainfall simulation tests .....	230
Table 6.9 Daily green roof laboratory test schedule for both testing programmes. This includes number of tests per day and corresponding inter-event dry period.....	230
Table 6.10 Summary statistics of average vegetation cover data for all green roof designs: A, B, C, D, and E.....	240
Table 6.11 P-values from Dunn’s Kruskal-Wallis multiple comparison test results with Bonferroni correction applied for each combination of the green roof vegetation cover data sets. Highlighted numbers demonstrate a statistically significant difference between green roof designs.....	241
Table 6.12 Summary statistics of retention data in relation to vegetation presence.....	247
Table 6.13 P-values from Mann-Whitney U test results with Bonferroni correction applied for each combination of the retention data sets.	

Highlighted numbers demonstrate a statistically significant difference between green roof with and without vegetation.....	248
Table 6.14 Median retention for each green roof design in relation to vegetation presence and p-values from Dunn’s Kruskal-Wallis multiple comparison test results with Bonferroni correction. Highlighted numbers demonstrate a statistically significant difference in retention between green roofs with and without vegetation.....	248
Table 6.15 Summary statistics of stormwater retention data for following green roofs: A-1, A-2, A-3. The retention data included observations for green roof trays with vegetation.....	252
Table 6.16 Summary statistics of stormwater retention data for following green roofs: B-1, B-2, B-3. The retention data included observations for green roof trays with vegetation.....	253
Table 6.17 Summary statistics of stormwater retention data for following green roofs: C-1, C-2, C-3. The retention data included observations for green roof trays with vegetation.....	254
Table 6.18 Summary statistics of stormwater retention data for following green roofs: D-1, D-2, D-3. The retention data included observations for green roof trays with vegetation.....	255
Table 6.19 Summary statistics of stormwater retention data for following green roofs: E-1, E-2, E-3. The retention data included observations for green roof trays with vegetation.....	256
Table 6.20 Median of vegetation cover, air temperature and substrate water content corresponding to each green roof design replicate. Italicised numbers show values that could have been possibly critical to green roof replicates performance such as low vegetation cover or high substrate water content. ....	257
Table 6.21 P-values from Mann-Whitney tests between replicates of the following green roof designs: A, B, C, D, and E. Highlighted numbers demonstrate no statistically significant difference in retention between green roof design replicates. The retention data included all observations for green roof trays with and without vegetation. ....	257
Table 6.22 Summary statistics of stormwater runoff depth data for the following green roofs: A, B, C, D, and E. ....	260

Table 6.23 P-values from Dunn’s Kruskal-Wallis multiple comparison test results with Bonferroni correction applied for each combination of the runoff depth data sets. Highlighted numbers demonstrate a statistically significant difference between green roof designs.....	261
Table 6.24 Summary statistics of stormwater retention data for selected green roofs.....	261
Table 6.25 P-values from Dunn’s Kruskal-Wallis multiple comparison test results with Bonferroni correction applied for each combination of the retention data sets. Highlighted numbers demonstrate a statistically significant difference between green roof designs. Italicised numbers show a statistically significant difference between green roof designs based on uncorrected p-value. ....	262
Table 6.26 Summary statistics of stormwater peak flow reduction data for selected green roofs. ....	263
Table 6.27 P-values from Dunn’s Kruskal-Wallis multiple comparison test results with Bonferroni correction applied for each combination of the peak flow reduction data sets. Highlighted numbers demonstrate a statistically significant difference between green roof designs. Italicised numbers show a statistically significant difference between green roof designs based on uncorrected p-value. ....	264
Table 6.28 Summary statistics of inter-event dry period and substrate water content prior to the tests. This is based on observations green roof trays with vegetation, for all green roof designs.....	266
Table 6.29 Summary statistics of runoff depth data in relation to rainfall event magnitude. Statistically significant differences are represented by p-values obtained from Dunn’s Kruskal-Wallis multiple comparison test results with Bonferroni correction. Highlighted numbers demonstrate a statistically significant difference in runoff depth between rainfall events of different return period. Italicised numbers show a statistically significant difference between green roof designs based on uncorrected p-value. ....	280
Table 6.30 Median runoff depth for selected green roofs in relation to rainfall magnitude and p-values from Dunn’s Kruskal-Wallis multiple comparison test results with Bonferroni correction. Highlighted numbers demonstrate a statistically significant difference in runoff depth between rainfall events of different return period. ....	281

Table 6.31 Summary statistics of retention data in relation to rainfall event magnitude. Statistically significant differences are represented by p-values obtained from Dunn’s Kruskal-Wallis multiple comparison test results with Bonferroni correction. Highlighted numbers demonstrate a statistically significant difference in retention between rainfall events of different return period. Italicised numbers show a statistically significant difference between green roof designs based on uncorrected p-value.....	282
Table 6.32 Median retention for selected green roofs in relation to rainfall magnitude and p-values from Dunn’s Kruskal-Wallis multiple comparison test results with Bonferroni correction. Highlighted numbers demonstrate a statistically significant difference in retention between rainfall events of different return period. ....	283
Table 6.33 Summary of multiple linear regression predicting runoff depth using rainfall depth [RD], inter-event time [IET], temperature [TEMP], substrate water content prior rainfall event [WC], substrate porosity [SPOR], drainage layer water absorption [DLWA] and substrate sand to gravel ratio [SSG] (N=180).....	289
Table 6.34 Summary of multiple linear regression predicting retention using rainfall depth [RD], inter-event time [IET], temperature [TEMP], substrate water content prior rainfall event [WC], substrate porosity [SPOR], drainage layer water absorption [DLWA] and substrate sand to gravel ratio [SSG] (N=180).....	290
Table 7.1 Summary statistics of rainfall data sets recorded during the in-situ and laboratory experiments. ....	299
Table 7.2 Summary statistics of stormwater retention data for green roofs analysed for the in-situ experiment: W/40/100-1, W/40/100-2, W/40/100-3 and for the laboratory experiment: A-1, A-2, A-3. ....	300
Table 7.3 Median stormwater retention determined for different rainfall depth for the in-situ and laboratory experiment, where T is the return period of the rainfall event. ....	301
Table 7.4 Summary of the predictor variables used to develop runoff depth and retention multiple linear regression models based on in-situ and laboratory data sets.....	302
Table 7.5 Multiple linear regression models to predict runoff depth based on in-situ and laboratory data sets.....	302

Table 7.6 Multiple linear regression models to predict retention based on in-situ and laboratory data sets. ....	303
Table 7.7 British Standards describing the test methods for relevant material properties.....	306

## **LIST OF ABBREVIATIONS**

BS	British Standards
CSV	Comma Separated Values (File)
EN	European Standards
FLL	Guidelines for the Planning, Construction and Maintenance of Green Roofing – Green Roofing Guideline
GRO	The Green Roof Organisation
HLS	Heather with Lavender Substrate
IET	Inter-event time/dry period
LECA	Lightweight Expanded Clay Aggregate
SCS	Sedum Carpet Substrate
THW	Temperature-Humidity-Wind (Index)

## **ACKNOWLEDGMENT**

I would like to express my sincere gratitude to my supervisors: Dr Mihaela Anca Ciupala, Dr Stuart Connop and Professor Darryl Newport for their meticulous supervision and continued encouragement.

I would like to thank the Sustainability Research Institute, University of East London, and partners of an EU FP7 research and innovation programme, Transitioning towards Urban Resilience and Sustainability (TURAS), for the PhD studentship and continued support without which this work would not have been possible.

I am grateful to the ABG Ltd., Murfitts Industries Ltd., and Ecosheet Ltd. for donating materials for laboratory experiments.

I wish to thank all of my colleagues at the Architecture, Computing and Engineering School, University of East London, especially Miss Sarah Catmur, Mr Ian Lemon, and Mr Graham Ford for their help, stimulating discussions and for providing motivating atmosphere just when it was needed.

This project would not be possible without the helpful assistance of the following departmental technical staff: Mr Joe Kennedy, Mr Trevor Rhoden, Mr Neil Goodin, Mr Chris Donovan and Mr Tom Juffs.

I would like to thank Leonti Bielski for developing rainfall event separation program and his support with Python programming.

Particular thanks must go to Ertion, William, Laissa, Mara, Mira, and Anisha for their valuable help at various stages of the research.

The thesis would not have been possible without the constant patience, support, and encouragement from my husband Tolu and my daughter Gabi. Special thanks also go to my parents, sisters, and friends for their continuous support.

Lastly, I offer my regards and blessings to all of those who supported me in any respect during the completion of this research.

*"Gutta cavat lapidem non vi sed saepe cadendo - A drop (of water) hollows out  
a stone not by force, but by falling often."*

*- Ovid (Epistulae Ex Ponto 4.10.5)*

*To my beloved family*

# CHAPTER 1

## INTRODUCTION

Cities worldwide are challenged by frequent critical problems related to climate change and its consequences, ecological degradation, economic development and social polarisation, amongst others (Spaans and Waterhout, 2017). The effects of climate changes, such as extreme weather, heat waves, flooding or rising sea levels, are observed both globally and locally. Figure 1.1 presents the global temperature change based on historical temperature data from 1850 to 2016. This clearly shows global temperature increase over the last century. Moreover, such changes are expected to continue to happen in the future. Murphy et al. (2009) projected changes of summer, winter, and annual means of various climate characteristics by the 2080s. Their projection stated that the increase in mean daily temperatures across UK will be on average 5.4°C in summer and between 1.5° to 2.5°C in winter. Precipitation was also projected to increase in winter up to 33% along western side of the UK, and decrease during summer down to 40% south of England.

The global changes in climate have a significant effect on Earth's ecosystem balance (Skinner and Porter, 1995). The projection of increased precipitation is an indicator of the changes occurring in one of the Earth's cycles – the hydrological cycle. The hydrological cycle comprises of the movement of water from Earth's surface (land and oceans) via evaporation and transpiration into atmosphere and return of water via precipitation and surface runoff into the oceans. The equilibrium between all stages of the hydrological cycle is affected by changes in climate but also by the type of landscape.

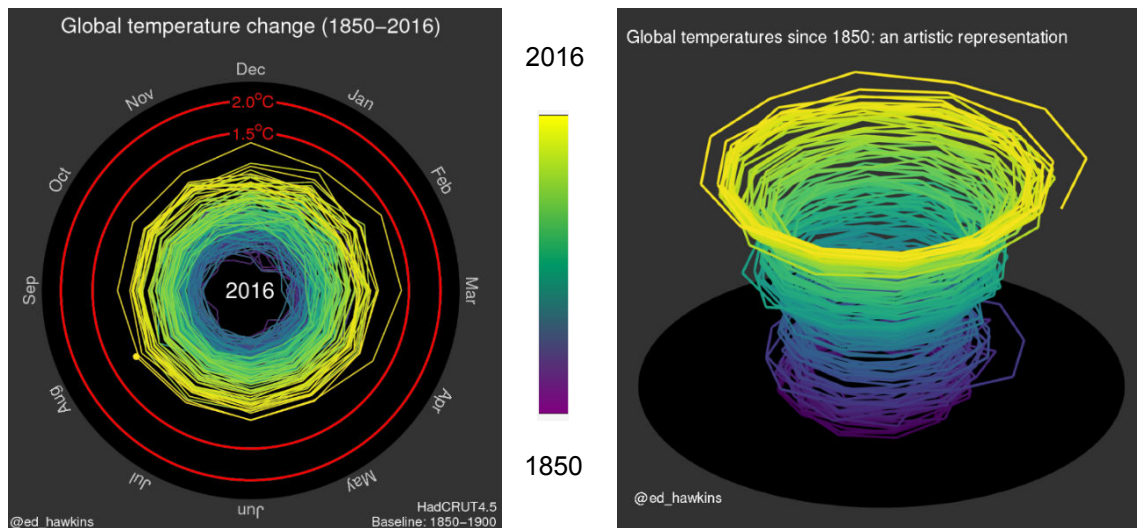


Figure 1.1 Global temperature spiral in 2D and 3D showing the increase in global temperatures between 1850 and 2016 (Hawkins, 2016).

Extensive urbanisation results in increased impervious surfaces and reduction in vegetated areas, which change the water balance: i) the surface runoff rises significantly, ii) evaporation and transpiration decreases in comparison to rural areas (Mansell, 2003). Lower water content in the soil and smaller evaporation surfaces limit the evaporation of moisture, which is a key factor in the local climate response to warming, causing the heat island effect in urban areas. Therefore, it became paramount to mitigate the negative effects of climate change and to search for solutions supporting urban resilience.

Implementation of green roofs in urban regions could help to restore the water cycle through evapotranspiration from green roof surfaces and vegetation, and by providing additional storage for stormwater surface runoff. Higher evapotranspiration would also mitigate the heat island effect. However, green roof contribution to the hydrological cycle strongly depends on its design. The plant type influences evapotranspiration, while the substrate and drainage layer material type and depth control the reduction in surface runoff called also retention capacity (Snodgrass and McIntyre, 2010, Czemieli Berndtsson, 2010). Currently, in the UK, there is a trend towards a one-size-fits-all approach to green roof systems. This results in poor green roof performance and missed opportunities for urban resilience enhancement. Simmons et al. (2008) and Snodgrass and McIntyre (2010), amongst others emphasised that green roofs should be designed according to specific performance objectives, and not on assumed performance attributes.

The enhanced hydrological performance of green roofs could be achieved by varying green roof geometry but most of all, by selecting specific substrate/drainage layer materials. However, certain materials such as pumice or lava (used worldwide for the green roof design) are not available in the UK and would have to be imported, consequently increasing the green roof cost and carbon footprint. Promising results were obtained by Molineux et al. (2009), who showed the potential for recycled materials to be used as green roof substrate. However, their research concentrated mainly on the influence of the substrate materials on vegetation growth, without specifically studying the hydrological performance of green roofs with such substrate materials. The majority of UK-based green roof hydrology research focuses on conventional green roof systems (Kasmin, 2010, Stovin, 2010, Nagase and Dunnett, 2012). Therefore, there is a need to find and investigate new, alternative, locally sourced, ideally recycled, lightweight materials, suitable for green roofs in the UK. Introducing new, alternative materials as green roof components would help to overcome barriers for green roof implementation in the UK, such as high cost or problems with excessive weight of the roof, and could potentially reduce the carbon footprint of green roofs. Green roof design using new, alternative materials would have to be supported by guidelines specific to UK climatic conditions. Lack of common standards and policy for green roof design in the UK also hinders the widespread construction of the green roofs. This study intends to address the above-mentioned issues.

## **1.1 PROBLEM STATEMENT**

One of the significant challenges in green roof hydrological performance studies is the availability of large samples of observations of green roof responses to rainfall events. The collection of such data in natural conditions is a long process, which requires monitoring of green roof systems over a long period. Moreover, these observations usually include large numbers of smaller rainfall events occurring commonly. Hence, the responses of green roofs to small, frequent rainfall events has been widely documented. Only a limited number of observed rainfalls are extreme rainfall events, which are rare but due to climate changes are expected to become frequent in the future. The extreme rainfalls can have a huge impact on the urban environment and human inhabitants. During extreme rainfall events drainage systems can become overloaded resulting in flooding in

urban areas, which poses a huge risk to human life, but also damage to buildings and infrastructure. The performance of the green roofs subjected to extreme rainfall events has not been yet thoroughly investigated.

It should also be noted that characteristics of climatic conditions, including rainfall events pattern, intensity, duration, and frequency, depend strongly on geographical location. Thus, the green roof systems and solutions may not be transferable across the world and each location may require a specific green roof design to effectively respond to these specific climatic conditions, especially to extreme rainfall events. The mitigation of the negative effects of those extreme rainfall events, such as flooding, is crucial for the development of resilient cities.

Resilient cities should also be resourceful, which means recognising alternative ways to use resources. Urban resilience could be, therefore, strengthened through design of the green roofs constructed of recycled, reused or secondary materials (alternative materials). However, the research into alternative green roof construction materials is still very limited. Moreover, the availability of such green roof materials differs amongst locations. Hence, the green roof design should be specific to local climatic conditions and material availability, and should be supported by appropriate guidelines.

Based on the stated problems the following research questions were formulated around the main three themes:

1. Potential for the use of recycled materials in green roof design:
  - What recycled, reused or secondary (alternative) materials could be used to enhance the hydrological performance of the green roofs?
  - Are they suitable for the green roof construction in the UK?
  - Can green roof design in the UK be supported by existing British Standards?
  - What would be the general rules governing green roof design in the UK?
2. Effectiveness of conventional green roofs for storm water management:
  - How effective are the conventional green roofs as a stormwater management tool in the UK?
  - What factors determine their effectiveness?

### 3. Green roof hydrological behaviour in extreme conditions:

- Are green roofs effective in stormwater runoff mitigation and what are the factors influencing green roof hydrological behaviour under extreme rainfall events?
- How does the performance of green roofs constructed from alternative materials compare to conventional green roofs under extreme UK climatic conditions?

## 1.2 AIM AND OBJECTIVES OF THE RESEARCH

The main aim of this research is to investigate the sustainable design of green roofs using alternative materials, in relation to their hydrological performance under UK climatic conditions.

In line with the aforementioned aim of the research and in relation to research questions, following objectives of the present study were identified:

1. **Potential for the use of recycled materials in green roof design:** To identify recycled, reused or waste materials, other than conventional and commercially used materials, suitable for green roof construction in the UK and to assess their physical properties in relation to hydrological performance of the green roofs.
2. **Effectiveness of conventional green roofs for storm water management:** To assess the performance of conventional extensive green roofs under the UK climatic conditions based on long term monitoring data obtained through in-situ experiment.
3. **Green roof hydrological behaviour in extreme conditions:** To assess the hydrological responses of extensive green roofs, constructed using identified alternative materials, to extreme rainfall events specific to the UK climatic conditions through laboratory experiments.

## 1.3 CONTRIBUTION TO KNOWLEDGE

This research contributes to several aspects of civil, environmental, and hydrological engineering using interdisciplinary approaches. It explores the limitations of current green roof monitoring systems, data collection and analysis, showing the complexity of the green roof hydrological behaviour and the challenges of its assessment.

This study highlights the importance of the laboratory experiments such as geotechnical engineering techniques for soil testing and laboratory tests investigating green roof performance as a system subjected to simulated rainfall events. The former allows a better understanding of the properties of individual green roof construction materials, while the latter gives a unique insight into green roof behaviour as a system, with the conclusion that such tests should become standard in order to support the green roof design.

Currently, worldwide and in the UK, the properties of the green roof materials are assessed in accordance with guidelines published by the German Landscape Research, Development and Construction Society - Forschungsgesellschaft Landschaftsentwicklung Landschaftsbau (FLL). There is no British Standard regulating green roof design and installation. There is, however, a guidance developed by Green Roof Organisation (GRO) (The Green Roof Organisation, 2014). *The GRO Green Roof Code* is based mainly on the German FLL guidelines (FLL, 2008) with adjustments to suit the UK market. The GRO code outlines the main considerations for green roof design, installation, and maintenance. However, sections related to green roof materials and their properties are limited. This research recommends specific British Standards as being appropriate for the testing of green roof materials in the UK. The procedures described in these British Standards could successfully replace those recommended by the German FLL guidelines.

This study also contributes to the identification, selection and comprehensive characterisation of the physical properties of alternative materials suitable for green roof systems.

Finally, this research covers a significant gap in the knowledge of the hydrological behaviour of green roofs subjected to extreme rainfall events based on a unique, large set of observations collected through laboratory experiments.

Table 1.1 maps the objectives to the specific research questions, case studies, main contributions, and chapter references.

Table 1.1 Mapping objectives to specific research questions and contributions.

Research questions	Objective	Methods	Contributions	Chapters
<p>Potential for the use of recycled materials in green roof design</p> <ul style="list-style-type: none"> <li>▪ What recycled, reused or secondary (alternative) materials could be used to enhance the hydrological performance of the green roofs? Are these materials suitable for green roof construction in the UK?</li> <li>▪ Can the green roof design in the UK be supported by existing British Standards?</li> <li>▪ What would be the general rules governing the green roof design in the UK?</li> </ul>	<p>To identify alternative materials suitable for green roof construction in the UK and to assess their physical properties in relation to hydrological performance of the green roofs.</p>	<p>Laboratory based experiment – assessment of material properties</p>	<ul style="list-style-type: none"> <li>▪ Identification and selection of alternative materials, suitable for use in extensive green roof systems.</li> <li>▪ Collation of the list of British Standards describing methods for testing of the material properties required for the assessment of green roof performance.</li> </ul>	<p>3, 7</p>

Continued on next page

Table 1.1 Mapping objectives to specific research questions and contributions (continued from previous page).

Research questions	Objective	Methods	Contributions	Chapters
<p><b>Effectiveness of conventional green roofs for storm water management:</b></p> <ul style="list-style-type: none"> <li>▪ How effective the conventional commercially used green roofs are as a stormwater management tool in the UK?</li> <li>▪ What factors determine their effectiveness?</li> </ul>	<p>To assess the hydrological performance of conventional extensive green roof under UK climatic conditions based on long term monitoring data.</p>	<p>In situ experiment - green roof response to natural rainfall events (UK)</p>	<ul style="list-style-type: none"> <li>▪ Evaluation of the strengths and weaknesses of the green roof in-situ monitoring systems.</li> <li>▪ Development of a preliminary regression model to predict runoff depth and retention of conventional green roof system subjected to UK climatic conditions. This includes the evaluation of factors significant to the model.</li> </ul>	<p>4, 7</p>
Continued on next page				

Table 1.1 Mapping objectives to specific research questions and contributions (continued from previous page).

Research questions	Objective	Methods	Contributions	Chapters
<p><b>Green roof hydrological behaviour in extreme conditions:</b></p> <ul style="list-style-type: none"> <li>▪ Are the green roofs effective for the stormwater runoff mitigation and what are the factors influencing the green roof hydrological behaviour when subjected to extreme rainfall events?</li> <li>▪ How does the performance of green roofs constructed with alternative materials compare to conventional green roofs under extreme UK climatic conditions?</li> </ul>	<p>To assess the performance of extensive green roofs, constructed using alternative materials subjected to extreme rainfall events specific to the UK climatic conditions, through laboratory experiment.</p>	<p>Laboratory based experiment – the green roof response to simulated extreme rainfall events (UK)</p>	<ul style="list-style-type: none"> <li>▪ Development of an innovative rainfall simulator to simulate a broad range of rainfall events for the study of the green roof hydrological performance.</li> <li>▪ Development of new experimental method of testing green roof systems in laboratory conditions.</li> <li>▪ Development of the preliminary regression model to predict runoff depth and retention of green roof systems subjected to extreme rainfall events specific to UK climate. This includes evaluation of the factors significant to the model.</li> </ul>	<p>5, 6, 7</p>

## **1.4 DEVELOPMENT EFFORT**

The laboratory work required to develop a rainfall simulator and appropriate procedures for the green roof system testing in laboratory conditions. Different types of rainfall simulators were considered and the drop-former type was chosen as this ensures consistent performance and avoids spatial rainfall variability. Moreover, the rainfall simulator was designed and constructed to allow five green roof plots to be tested consecutively without interrupting the runoff monitoring. Subsequently, an appropriate green roof system testing procedure for laboratory conditions was developed and employed. The rainfall simulator and testing procedures are described in detail in Chapter 5 and 6, respectively.

## **1.5 BOUNDARIES OF RESEARCH**

The research has been carried out within the limits of specific research boundaries. Each study was subjected to the constraint of time, instruments, opportunities, and location.

### **General**

The research was conducted under UK climatic conditions and using alternative materials available in the UK and therefore the research outcome may not be applicable to other climatic or location contexts. The analysis of the green roof responses to extreme rainfall events was based on London climatic conditions. All of the green roofs investigated were extensive.

### **Laboratory-based experiments of material properties**

The following properties of materials have been assessed: bulk density, particle density, saturated density, particle size distribution, organic matter content, permeability, water absorption, porosity, void ratio, and maximum capillary rise. These tests were carried out in accordance to the selected British Standards used in civil engineering field.

### **Green roof in-situ experiment**

The in-situ experiment was set up prior to the commencement of the current research, hence the author of this thesis did not have any influence on the experimental design. The analysis of the green roofs hydrological performance was based on data collected between July 2010 and August 2014. Preliminary

multiple linear regression analysis was limited to investigation of the effect of rainfall characteristics and climate conditions on the runoff and retention of the green roofs.

### **Green roof laboratory experiment**

The space available in the laboratory for conducting the experimental work allowed for only fifteen green roof trays to be tested in this study. The rainfall simulator system could support five green roof trays at any one time, while ten additional green roof trays were kept on the laboratory benches under LED grow lights.

The effect of green roof material type and their properties on hydrological performance was investigated in this part of the study. Factors such as the layer depth or slope were not included in this experimental investigation. Green roof systems were subjected to rainfall events of three relevant magnitude, including return period of 1:30, 1:50 and 1:100 years.

The research results apply only to the green roofs constructed with the materials investigated in this study and they should not be extrapolated to green roofs made of materials of different type and properties.

Preliminary multiple linear regression analysis was limited to the investigation of the effect of rainfall characteristics, laboratory microclimate conditions, material properties and vegetation cover on the green roof hydrological performance.

## **1.6 STRUCTURE OF THE THESIS**

The thesis contains 8 chapters. The schematic structure of the thesis is presented in Figure 1.2.

**Chapter One** includes the background, research questions, aim and objectives, the boundaries of the research and the brief description of the contribution to knowledge of this research.

**Chapter Two** presents the knowledge fundamentals underpinning the study. It also provides the context of the research, presenting the state-of-art in the hydrological performance of green roof studies. It critically reviews the methods and materials, especially non-conventional ones, employed in green roof investigations, expanding to non-hydrological studies when appropriate.

Subsequently, the gaps in the current knowledge related to the hydrological performance of the green roofs and use of alternative materials for green roof construction are identified.

**Chapter Three** describes the selection process of appropriate materials for the laboratory tests of green roof systems. It also presents the experimental programme, testing techniques and apparatus used to determine the properties of materials employed in the in-situ and laboratory experiment.

**Chapter Four** presents the green roof in-situ experiment including the experimental programme, description of the monitoring and materials used for the investigation of the hydrological performance of green roofs subjected to natural rainfall events.

**Chapter Five** describes the laboratory experimental setup including the design, construction, and performance of a custom designed rainfall simulator to simulate a broad range of rainfall events for green roof hydrological performance assessment.

**Chapter Six** describes the laboratory-based experimental programme, the appropriate testing techniques, apparatus, and materials used to study the hydrological performance of the green roof systems constructed using conventional and alternative materials. The green roof response to extreme rainfall events is evaluated and the outcomes of this investigation are presented.

**Chapter Seven** presents the overview of the hydrological performance of the green roofs based on the results of in-situ and laboratory experiments. It summarises the research findings supporting sustainable green roof design in the UK.

**Chapter Eight** presents the overall conclusions of the study, the contribution to knowledge and recommendations for future research.

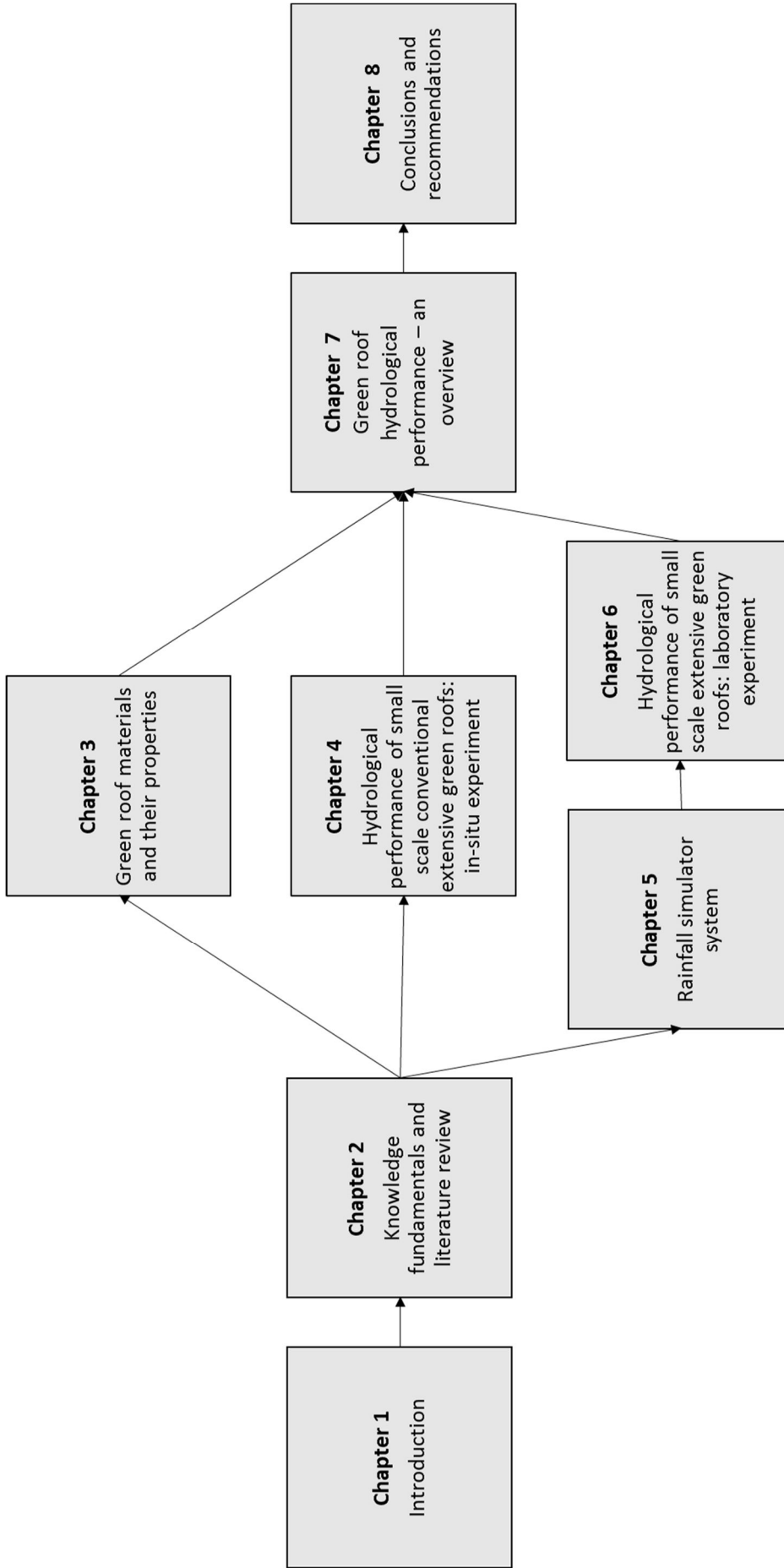


Figure 1.2 Outline of the structure of the thesis.

## **CHAPTER 2**

### **KNOWLEDGE FUNDAMENTALS AND LITERATURE REVIEW**

This chapter provides the context of the research, presenting both the knowledge fundamentals upon which the research was built and the state-of-art related to the research topic. This includes the critical assessment of the hydrological performance of green roofs with emphasis on the role of the green roof construction materials. The following hydrological behaviour aspects in relation to green roofs were discussed: quantification of stormwater runoff, retention, and flow peak reduction. Special attention has been given to factors affecting the green roof performance including extreme weather conditions, green roof geometry and type of materials. A thorough and critical literature review has been conducted, as this is important to identify the current state of art in the field and to identify existing gaps in research.

#### **2.1 KNOWLEDGE FUNDAMENTALS**

This section presents key concepts on hydrology, green roofs, and statistics, which are relevant to analysis and discussion of the experimental results. The hydrology subsection gives insight into the hydrological cycle in rural and urban areas, rainfall characteristics and the rainfall-runoff relation. The green roofs subsection introduces green roofs, their structure, and benefits of their installation. The knowledge of hydrological processes helps to demonstrate the role that green roofs play in urban areas and how hydrological performance could be improved. Finally, the statistics subsection discusses the techniques used to analyse experimental data, based on which the conclusions were drawn. The aim of this section is to give a general understanding of hydrological processes, green

roof fundamentals and statistics background. It does not, however, explain the theories in depth, which can be found in many textbooks.

### **2.1.1 HYDROLOGY**

Hydrology is a scientific and engineering discipline that studies the complex water system of the Earth. It deals with water occurrence, distribution, movement, and properties amongst others. Hydrological knowledge is crucial in many areas of engineering and helps to solve problems related to wastewater treatment, irrigation, design and operation of water resources, flood risk management, ecosystem modelling, etc. This section summarises the fundamental theories of hydrological processes in which green roofs take part, such as the hydrological cycle, precipitation, evaporation and transpiration, infiltration and soil water, their measurements and analysis.

#### **2.1.1.1 THE HYDROLOGICAL CYCLE**

The hydrological cycle, also known as the water cycle, is one of the Earth's cycles, which describes the continuous movement of the water on and within the Earth (Shaw, 2011). Figure 2.1 presents natural water circulation: the water vapour in the atmosphere condenses and precipitates on land and seas, infiltrates into the ground, flows under the surface (ground water flow) to open water (surface runoff and sea) from where it evaporates or is transpired through plants back to the atmosphere (Mansell, 2003).

*Precipitation:* includes rainfall but also snowfall, hail, fog drip or sleet. It occurs when condensed water vapour in the atmosphere falls to the land or open water surface.

*Infiltration:* the passage of water through a surface into the ground.

*Ground Water Flow:* the flow of the underground water (water that has infiltrated into the ground). The flow of groundwater is very slow; it also replenishes slowly.

*Runoff:* ways by which water moves across the land, both on the surface or in channels such as streams or rivers.

*Evaporation:* the movement of the water from the ground or open water surface into the atmosphere. This water transfer involves change of water state from liquid to vapour.

*Transpiration:* evaporation loss through the vegetation.

*Evapotranspiration:* total water loss by both evaporation and transpiration from the ground surface and vegetation.

The interaction between human activity and the natural water cycle resulted in alterations in the latter (Figure 2.2). In addition to natural water cycle components, the urban water cycle includes urban drainage (stormwater and wastewater management) and water supply network.

*Urban drainage:* drainage system, which diverts waste- and stormwater. Wastewater is a product of domestic or industrial water usage, while stormwater is rainwater fallen to the urbanised area. Usually, urban drainage is an artificial system of sewers, i.e. pipes and structures that collect and dispose of water.

*Water supply:* the system, which transports water into urban areas and distributes within it.

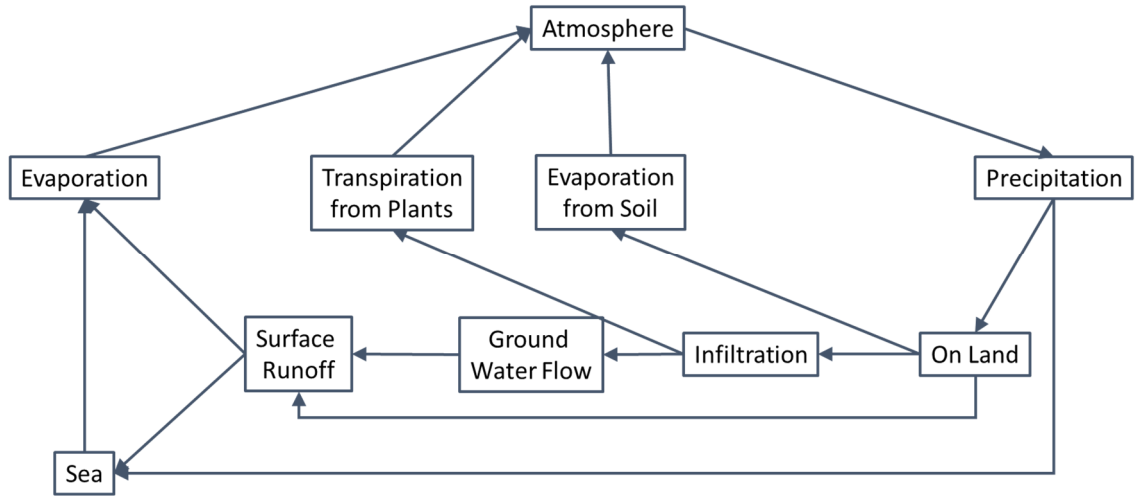


Figure 2.1 Natural hydrological cycle.

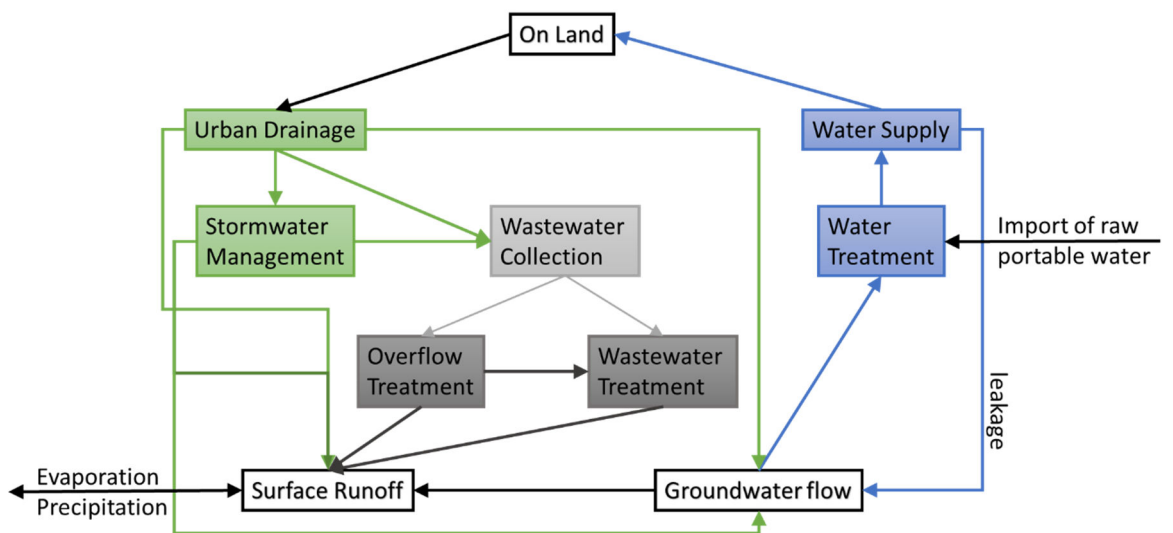
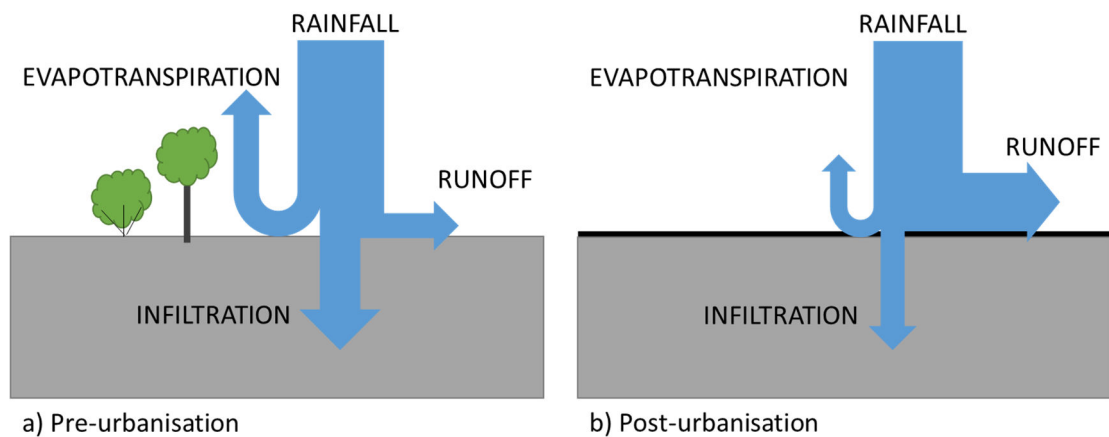


Figure 2.2 Urban hydrological cycle.

Urbanisation has a great impact on the hydrological cycle. The increase of impermeable areas reduces water evapotranspiration and infiltration into the ground and results in increased runoff (Figure 2.3).



*Figure 2.3 Effect of urbanisation on rainfall distribution (not to scale); (a) water movement prior to urbanisation with large proportion of water infiltrated (b) water movement post-urbanisation with reduced quantities of water evapotranspired and infiltrated.*

In the context of green roof study, the main focus is precipitation, water flow through the green roof system including runoff, evaporation from the green roof surface and transpiration from green roof vegetation.

#### **2.1.1.2 RAINFALL**

Rainfall is the main form of precipitation contributing to stormwater runoff. The key properties of rainfall events include depth, duration, intensity, and frequency (Butler and Davies, 2010).

*Depth (in mm):* the common measurement of the rainfall quantity. It is representative of one specific location.

*Intensity (in mm/h):* the rainfall depth collected over the time unit. Also, a common way to quantify the rainfall.

*Duration (in min):* time period over which the rainfall falls. This may not necessarily represent the duration of the whole storm. In some cases, the storm event can be subdivided into the range of durations for analysis purposes.

*Frequency:* the rainfall event frequency is a probability of the rainfall occurring and it is represented by return period. The return period of T years defines the

annual maximum rainfall event which is equalled or exceeded in magnitude once every T years (on average).

Intensity-Duration-Frequency (IDF) analysis is employed to assess the occurrence of the rainfall events. The typical IDF curves are presented in Figure 2.4.

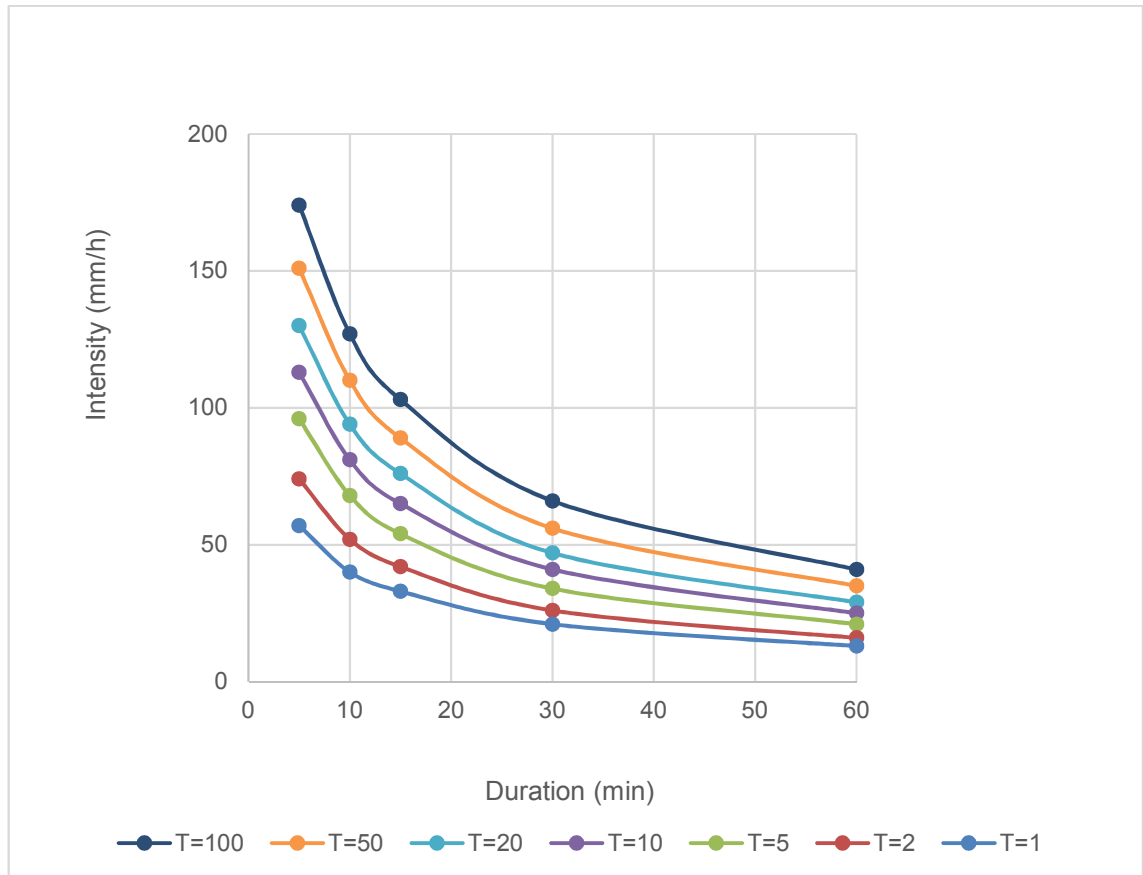


Figure 2.4 Typical IDF relationship curves.

The IDF relationship is specific to a location. The procedures to derive IDF curves are included in Flood Studies Report (Natural Environment Research, 1975) or Wallingford Procedure (DoE/NWC, 1981). The IDF curves are often replaced with Depth-Duration-Frequency (DDF) curves, when depth of the rainfall, rather than intensity, is of interest. This is achieved through conversion of the rain intensities to depths by multiplying the former by precipitation durations.

### 2.1.1.3 RAINFALL – RUNOFF RELATIONSHIP

The rainfall – runoff relationship can be represented by plotting a hydrograph of the particular rainfall falling over a specific area and the runoff resulting from the event. The generic hydrograph is shown in Figure 2.5.

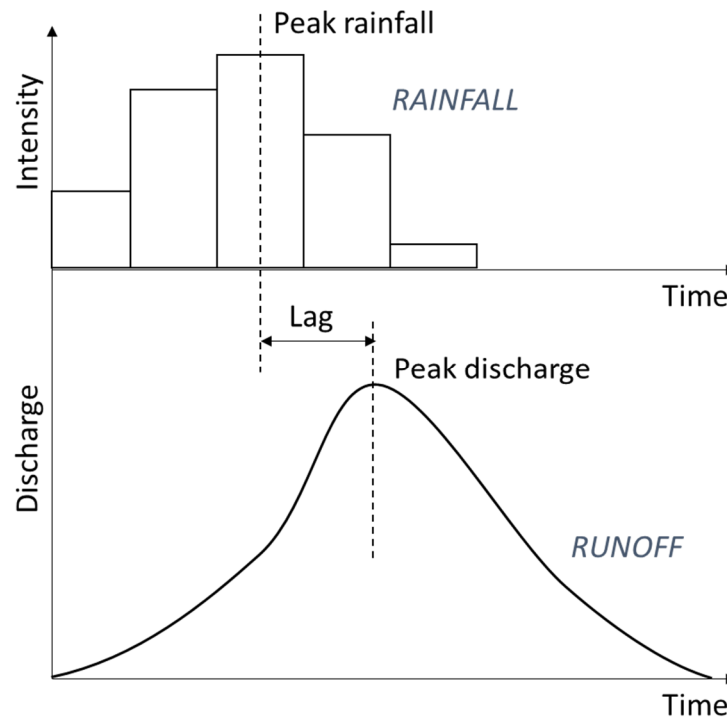


Figure 2.5 Rainfall and runoff hydrograph.

The hydrograph shows the time history of the change in the discharge resulting from the rainfall. The rainfall is represented by intensity change over time, usually in discrete block intervals of time, while runoff is represented by discharge over time as a smooth curve. Both rainfall and runoff have a distinctive peak, i.e. the time of the highest magnitude. The difference in time between peak rainfall and peak discharge is called time lag.

#### 2.1.1.4 EVAPOTRANSPIRATION

Evapotranspiration is the total water that is evaporated from the surface of the ground or open water and transpired from vegetation (Shaw, 2011). The evaporation depends on:

*Solar radiation*: the energy from the Sun in the form of heat that allows the change of water from liquid to vapour.

*Temperature and water vapour capacity of the air*: the temperature of the ground surface and the air. The water vapour capacity of the air increases with the temperature rise. Hence, at higher temperatures, which are common in tropical climate or during summer the evaporation is much higher in comparison to much lower evaporation in low temperature climates or during winter.

*Wind speed:* wind plays a significant role in replacing humid air with dryer air, hence increasing evaporation rate.

*Atmospheric pressure:* low pressure is associated with damp weather; when the air is humid the evaporation rate is lower.

The rate and magnitude of transpiration depends on various factors such as type of vegetation, its ability to transpire and the availability of the water in the soil. The quantification of the effect of these factors on transpiration, however, were outside of the scope of this thesis.

### **2.1.2 GREEN ROOFS**

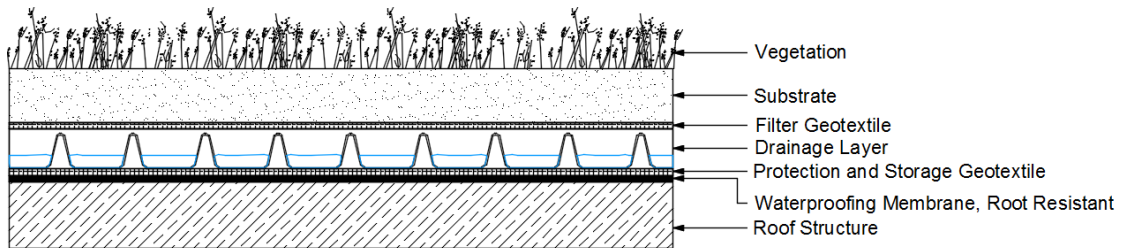
Green roofs are roofs on which vegetation is intentionally grown. There are three categories of green roof: intensive, extensive, and less commonly constructed semi-intensive. The division is made based on the substrate depth and the type of the vegetation supported (FLL, 2008). Intensive green roofs have a deeper soil substrate (growing medium) layer (150mm to 400mm). They are generally used for amenity areas such as gardens and parks, and support lawn, shrubs, and trees. Semi-intensive green roofs generally have grass, herbs and/or shrubs with the soil substrate depth ranging from 120-250 mm. Within the group of semi-intensive green roofs there are bio-diverse green roofs. These types of roofs are intended to mimic the local habitats. They are designed to support biodiversity objectives specific to location. The last category includes extensive green roofs, the most common type of green roof installed. They support moss, herbs, sedums and grasses, creating ecological landscapes. The depth of the soil substrate falls between 60 mm to 200 mm (*Introduction to Types of Green Roof*, 2012).

#### **2.1.2.1 GREEN ROOF CONFIGURATIONS**

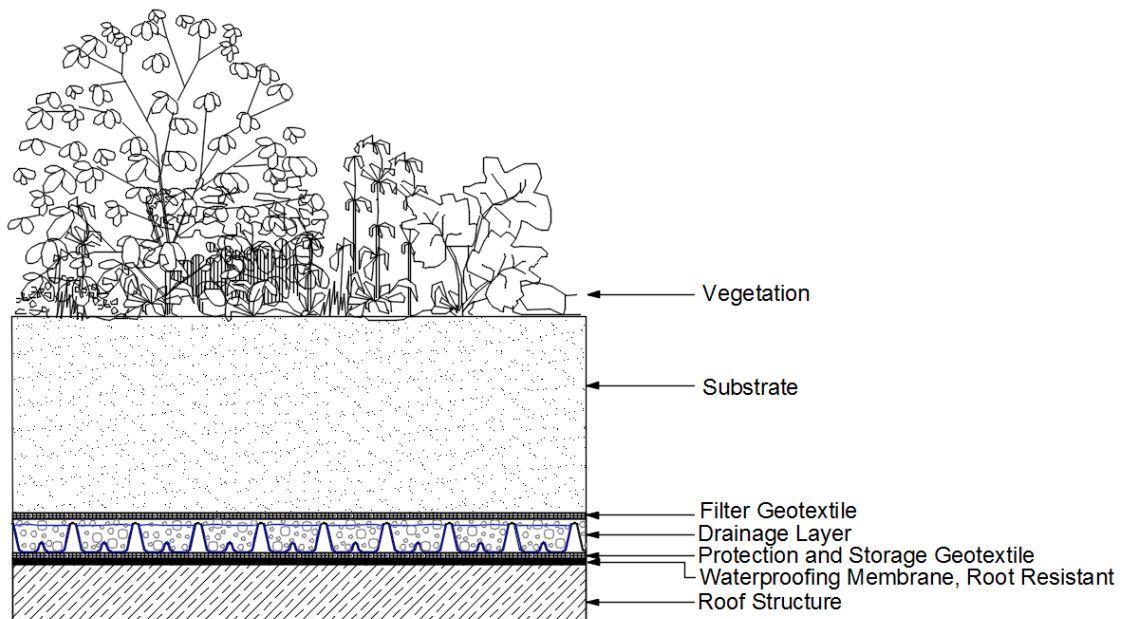
The typical green roof configuration consists of the following layers (Figure 2.6):

- Waterproofing, root resistance membrane – a waterproofing layer which protects the roof structure from plant root penetration and water damage;
- Protection and storage geotextile – protects waterproofing, root resistance membrane, it can contribute to stormwater retention;
- Drainage layer – prevents water logging, usually it's made of polymer sheets or aggregates;

- Filter geotextile – stops the fine soil particles from soil substrate migrating into the drainage layer;
- Substrate – supports the plants, usually a mixture of aggregates and organic matter (compost);
- Vegetation – plant selection varies depending on the type of roof and its purpose and location



(a)



(b)

Figure 2.6 Typical green roof configuration (a) extensive green roof with substrate depth between 60 mm to 200 mm (b) intensive green roof with substrate depth between 150mm to 400mm

### 2.1.2.2 GREEN ROOF INSTALLATION BENEFITS

Green roofs installed in urban areas have the potential to reduce the effects of environmental problems and could become a significant tool towards achieving

sustainable construction in the UK. The installation of a green roof has the potential to bring environmental, economic, and aesthetic benefits:

- Mitigation of stormwater runoff (Hathaway et al., 2008, Getter et al., 2007, Villarreal and Bengtsson, 2005, VanWoert et al., 2005, Fioretti et al., 2010), which is achieved through water retention within the green roof layers and evapotranspiration from the green roof surface and plants. Slow release of the excess water stored within a green roof results in runoff distribution over a time period.
- Improvement of stormwater runoff quality (Vijayaraghavan et al., 2012, Berndtsson et al., 2009). However, it was also noted that whilst some pollutants are absorbed and filtered by green roof layers, other can be released (Gregoire and Clausen, 2011, Carpenter and Kaluvakolanu, 2011).
- Mitigation of the urban heat island effect (Lee et al., 2014, Qin et al., 2012, Takebayashi and Moriyama, 2007, Susca et al., 2011). The cooling effect is achieved through water evapotranspiration from the green roof surface and plants, which reduces the temperature of the surroundings.
- Air quality improvement through removal of airborne particles which includes dust, dirt, soot, smoke, and liquid droplets emitted into the air (Currie and Bass, 2008, Speak et al., 2012, Rowe, 2011), and also through absorption of carbon dioxide and release of oxygen by plants (Li et al., 2010, Rowe, 2011, Getter et al., 2009).
- Energy savings in the building onto which the green roof is installed. The green roof layers insulate roof structure, reducing temperature variations in the building (Alexandri and Jones, 2007, Castleton et al., 2010, Coma et al., 2016).
- Extend roof life through protection of the roof membrane (Liu, 2003, Kosareo and Ries, 2007).
- Sound insulation in buildings and noise absorption (Van Renterghem and Botteldooren, 2011, Van Renterghem and Botteldooren, 2014, EcoSchemes Ltd, 2003).
- Enhancement of biodiversity through mimicking various habitats, reduction of habitat loss (Benvenuti, 2014, Dunnett and Kingsbury, 2008, Nagase

and Dunnett, 2010, Ksiazek et al., 2012, Brenneisen, 2006, Maclvor and Lundholm, 2011).

- Provision of recreational and agricultural spaces (Bianchini and Hewage, 2012, Snodgrass and McIntyre, 2010, Whittinghill et al., 2013).

### **2.1.2.3 GREEN ROOF HYDROLOGICAL PERFORMANCE**

The following aspects of the green roof hydrological performance were of interest of this study:

- Runoff depth (mm) – quantity of the stormwater, which has been discharged from the green roof subjected to rainfall. It can be obtained as a direct measurement of the runoff depth or as a measured volume of the water discharged per area of the green roof.
- Retention (%) – a percentage of the rainwater, which has been retained within the green roof system subjected to rainfall.
- Peak flow reduction (%) – a percentage difference between the peak flow of the runoff from green roof subjected to rainfall (peak discharge, Figure 2.5) and peak flow of the rainfall (peak rainfall, Figure 2.5)

### **2.1.3 STATISTICS**

Statistics is a discipline that concerns itself with process of data collection, summarising and interpreting leading to conclusions and generalisations (Johnson and Bhattacharyya, 2011). Statistics provides principles, methodologies, and techniques for obtaining knowledge from given data. There are two main groups of techniques used in statistics:

- Descriptive statistics concentrating on presenting information in comprehensive and usable format, describing the features of data.
- Inferential statistics focusing on generalisation of the information, drawing conclusions, deciding on further courses of action based on data.

### 2.1.3.1 DESCRIPTIVE STATISTICS

The descriptive statistics techniques allow the organisation of the data into a readable and usable format. During this process the patterns in the data are explored and the distribution is defined as one of the following:

- Normal distribution (Gaussian distribution) – the data distribution that follows a bell shape curve as presented in Figure 2.7. The mean is at the peak of the bell and creates an axis of symmetry for the curve.

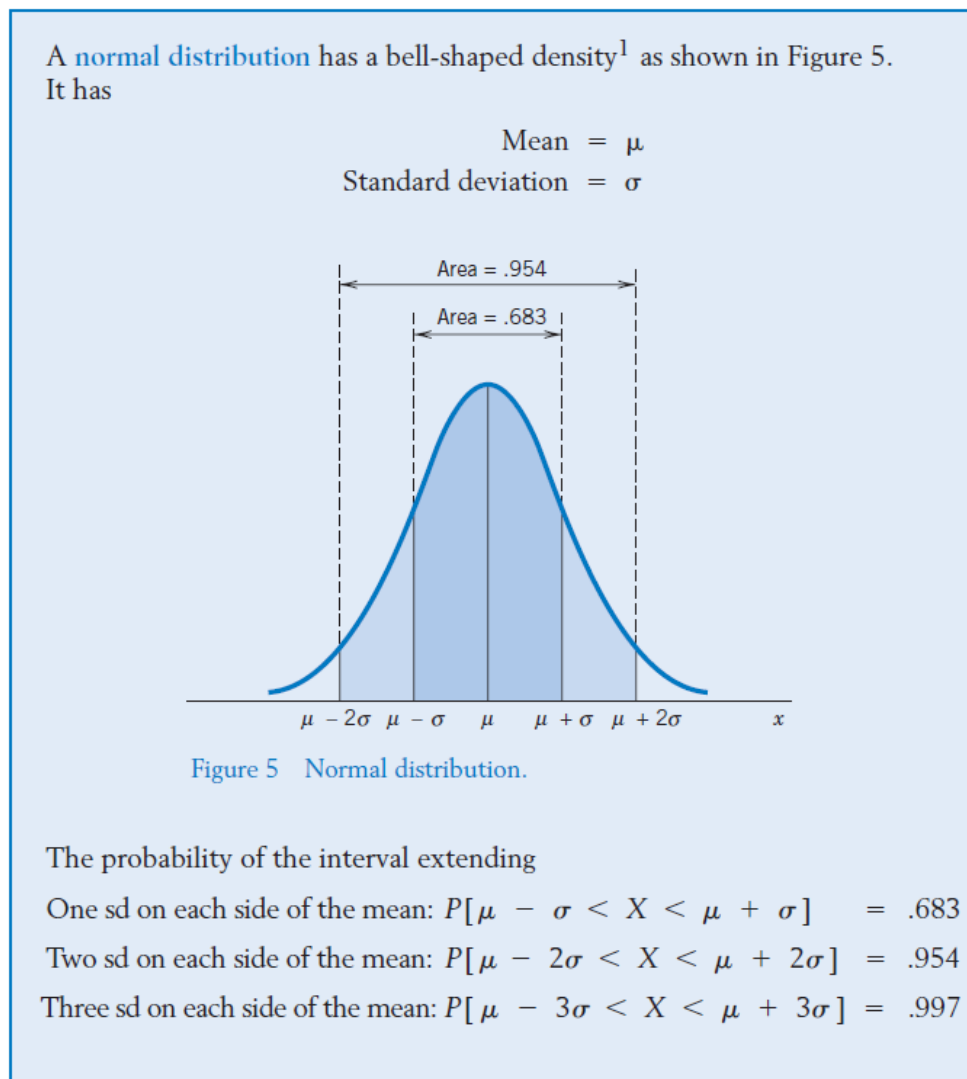


Figure 2.7 Normal distribution with distinctive bell-shaped density (Johnson and Bhattacharyya, 2011).

- Non-normal distribution – other than normal distribution, e.g. binomial distribution, the Poisson distribution, the gamma distribution, etc.

The application of descriptive statistics techniques results in set of parameters, such as:

- Mean, median – forms of average, first is the arithmetic mean, second is the centre of a set of observations placed in order
- Extremes - maximum and minimum values, as well as outliers
- Standard deviation - a measure of dispersion, the data concentration around the mean.
- Correlation coefficient – measure of the strength of the linear relation between two random variables. The values of correlation coefficient are in the range between '-1' and '1'. The perfect linear relation between variables is represented by the correlation coefficient of value '-1' (negative linear relation) or '1' (positive linear relation). Coefficient of correlation of value 0 shows absence of a linear relation.

Other techniques result in graphical representations of the data, such as:

- Histogram– graphical representations of the distribution of data. The histogram presents the distribution of data by dividing observations into groups and showing the frequency or density for each group of data (Figure 2.8).

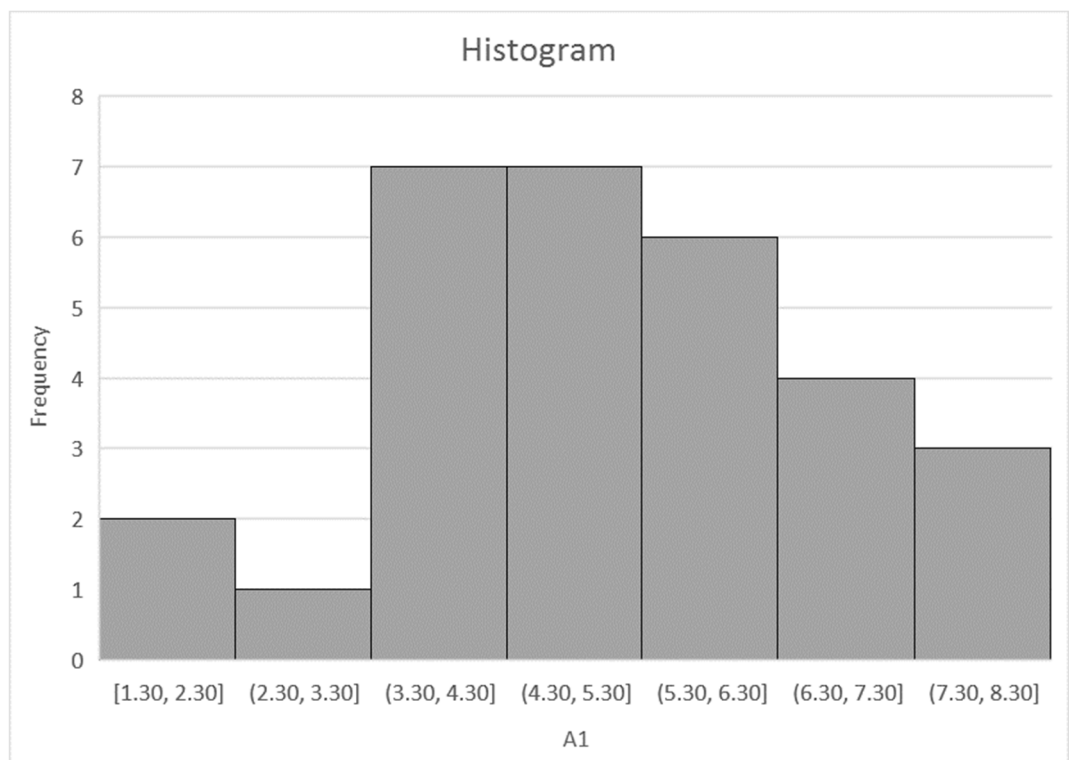
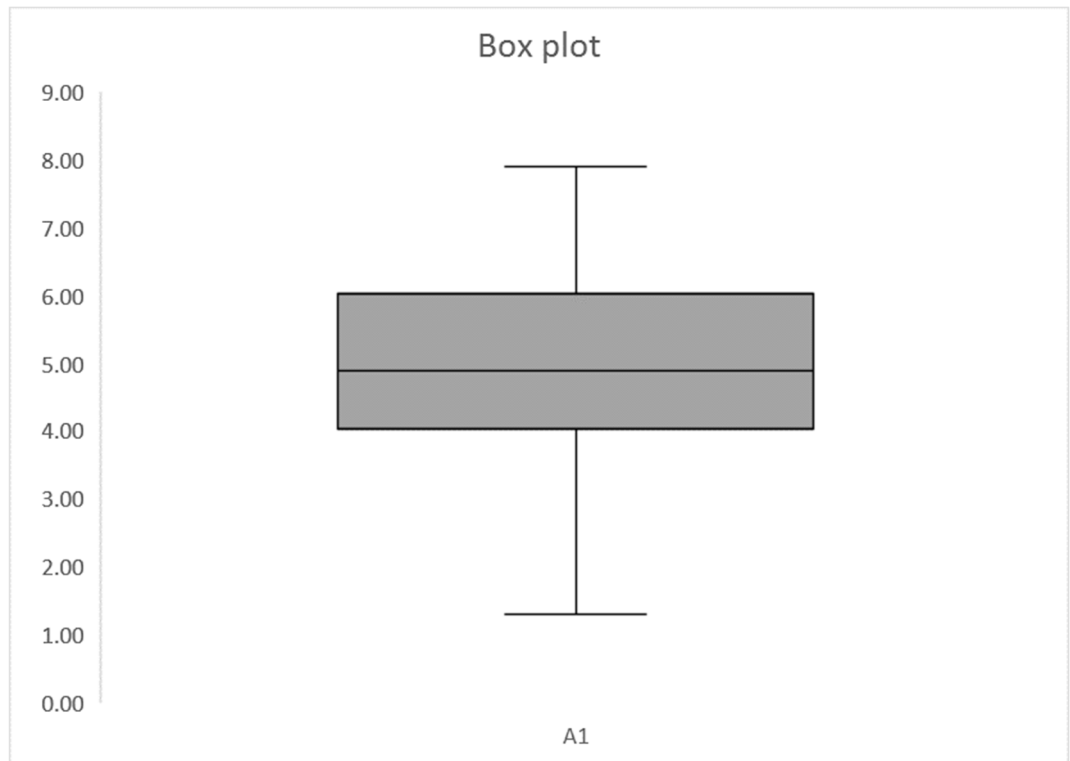


Figure 2.8 Example of a histogram, graphical display of the distribution of data.

- Boxplot – it is also graphical representations of the distribution of data. The box plot shows the following quantities of the data set: minimum value, first quartile (first 25<sup>th</sup> percent of observations), median (50<sup>th</sup> percent of observations), third quartile (75<sup>th</sup> percent of observations) and maximum value (Figure 2.9). Boxplots are usually used to investigate distribution, show the variability or to compare two data sets.



*Figure 2.9 Example of a boxplot, graphical display of the distribution of data. It presents summary information in the quartiles.*

- Quantile – quantile (Q-Q) plot – graphical representations of the distribution of data. The Q-Q plot is a graph showing relation between the empirical and theoretical distribution (Figure 2.10). The Q-Q plot is used to test the normality of the data distribution, when the points are close to reference line, deviating in the random fashion. It is frequently used to check the behaviour (normality) of the residuals during multiple linear regression analysis

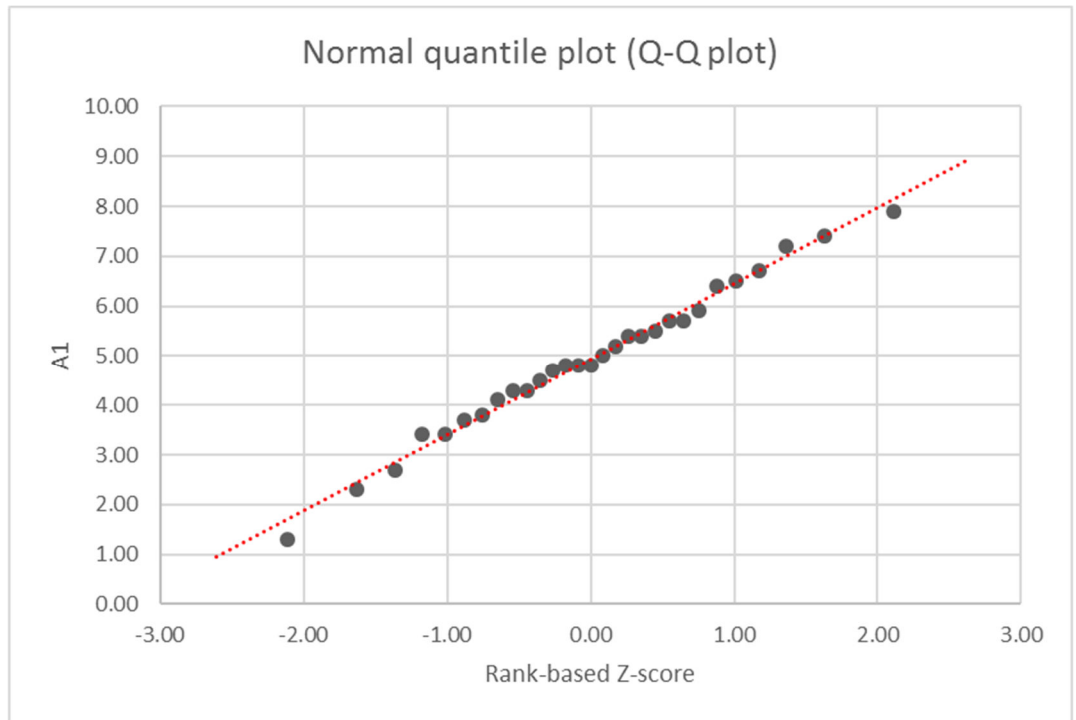


Figure 2.10 Example of a normal quantile plot (Q-Q plot), graphical display of the distribution of data. It shows relation between the empirical and theoretical distribution of data.

- Scatterplot – graphical representation of pair of observations  $(x_i; y_i)$ ,  $i=1,2,3,\dots, n$  (Figure 2.11).

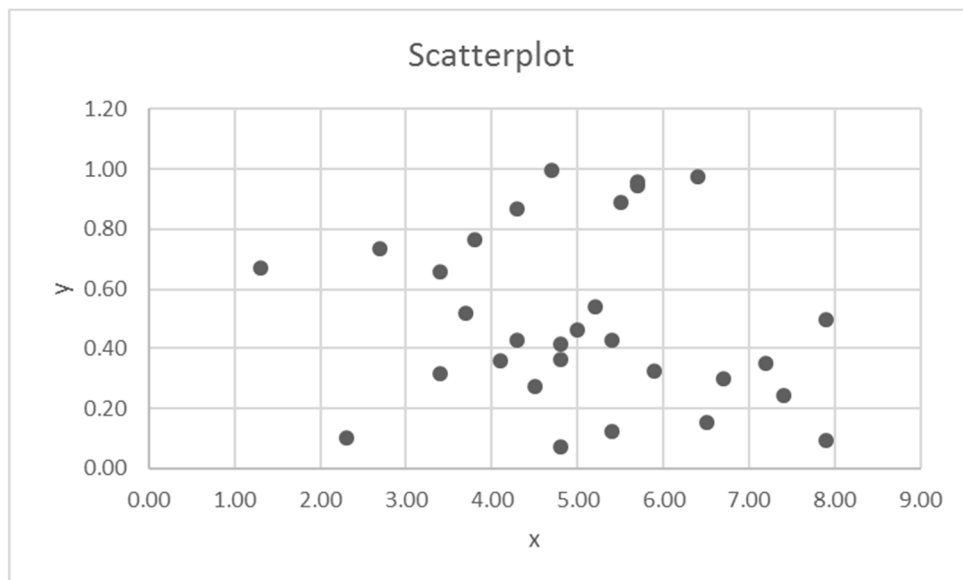


Figure 2.11 Example of a scatterplot. It is a graphical representation of pair of observations  $x$  and  $y$ .

### 2.1.3.2 INFERENCE STATISTICS

Inferential statistics allow to gain the knowledge from the analysis of the sample that applies to the population. There is a wide range of methods of statistical inference. This section will concentrate on the following:

- Hypothesis testing – this technique allows to confirm or reject the hypothesis, a statement about a parameter or probability distribution of a population. There are two complementary hypotheses tested: alternative hypothesis ( $H_1$ ), which is a claim we wish to establish and null hypothesis ( $H_0$ ), which is a negation of the claim. The starting hypothesis for hypothesis testing procedure is the null hypothesis, it can be confirmed or rejected in the favour of alternative hypothesis

The following are involved in hypothesis testing:

- Formulation of hypothesis, e.g.  $H_0$  – there is no statistically significant difference between two things, such as hydrological performance of green roofs of different design
- Determination of the significance level of the test  $\alpha$  – it is a probability of rejecting the null hypothesis  $H_0$  when it is true. For the purpose of this research the  $\alpha=5\%$  ( $\alpha=0.05$ ).
- Determination of the appropriate hypothesis test and calculation of the corresponding test statistic:
  - ♦ Parametric tests when the observations follow normal distribution, e.g. student test.
  - ♦ Non-parametric tests, when there is no need to specify the distribution of the observations, e.g. Wilcoxon test, the Mann–Whitney test, the Kruskal–Wallis test, or the Kolmogorov–Smirnov test.
- Comparison of p-value to the selected significance level  $\alpha$ . The p-value is the probability (calculated under null hypothesis) of the test statistic to be equal or more extreme than the value observed. P-value shows the strength of evidence against the null hypothesis:
  - ♦  $p \leq \alpha$  : the null hypothesis  $H_0$  should be rejected in the favour of the alternative hypothesis  $H_1$ , the result is highly statistically significant.
  - ♦  $p > \alpha$  : the null hypothesis  $H_0$  should be accepted

- Regression analysis – the technique, which allows the determination of the type of relation between two or more variables and presentation of the relation as a function (Lewis-Beck, 1993). The variable that is being explained, the response, is called dependant variable (Y). The variables that explain, predict the variations of dependent variable (Y) are called independent variables (X). Simple regression analysis is conducted when there is only one independent variable, while multiple regression analysis is carried out when there are more than one independent variables. If the relation between independent and dependent variable is linear then the linear regression analysis is performed.

In this section the multiple linear regression will be discussed. The multiple linear regression analysis is performed to model the linear relation between the dependant variable (Y) and many independent variables ( $X_1, X_2, \dots, X_k$ ).

When performing multiple linear regression analysis, the following should be checked:

- The strength of the linear relation – the strength of the linear relation is represented by coefficient of determination  $R^2$ , which takes values between 0 (dependent variable cannot be predicted from the independent variables) to 1 (dependent variable can be predicted without error from the independent variable). The value of coefficient of determination being between 0 and 1 suggests that only certain percentage of the variability of y is explained by the model.
- The independence of residuals. It is confirmed by interpreting residuals vs. fitted values plot. Random distribution of the residuals vs. fitted values confirms independence of errors (Figure 2.12).

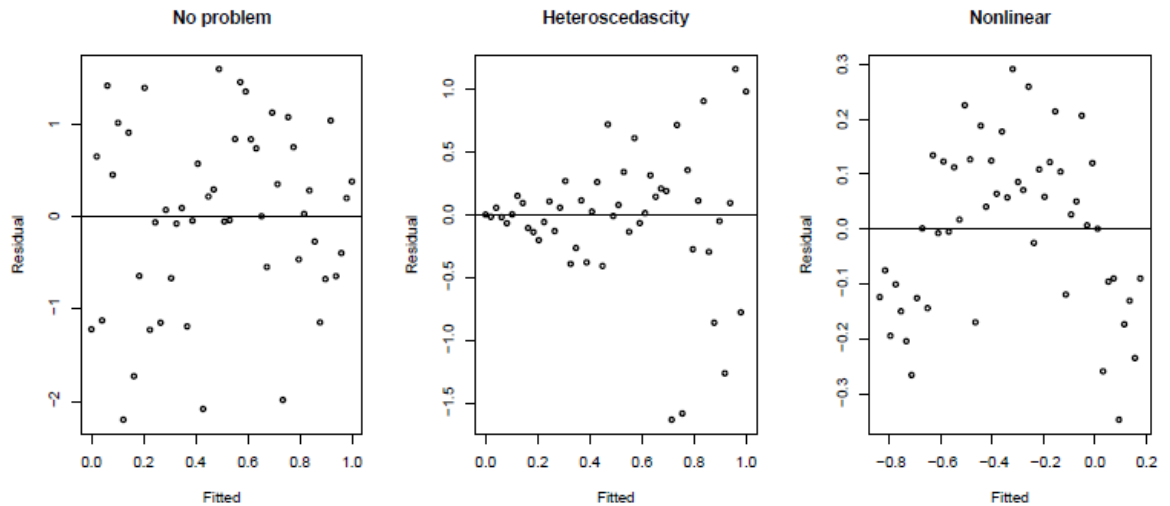


Figure 7.5: Residuals vs Fitted plots - the first suggests no change to the current model while the second shows non-constant variance and the third indicates some nonlinearity which should prompt some change in the structural form of the model

Figure 2.12 Graphical verification of an assumption of the independence of residuals (Faraway, 2002).

- Normality of the residuals with mean zero and common variance. This is confirmed by investigating residuals Q-Q plot. Close alignment to reference line ensures normal distribution of residuals.

## 2.2 LITERATURE REVIEW

Green roofs contribute to water balance restoration in urban areas:

- Larger vegetated areas enhance evapotranspiration
- Green roof substrate and drainage layer provide additional storage for stormwater resulting in surface runoff reduction

Better understanding of hydrological processes, in which green roofs take part, would lead to efficient green roof designs satisfying the project objectives. In regards to hydrological performance this includes green roof design optimisation to enhance stormwater retention capacity as well as attenuation ability.

The retention capability of green roofs was investigated during various studies around the world (VanWoert et al., 2005, Voyde et al., 2010, Stovin et al., 2012, Mentens et al., 2006, Vijayaraghavan, 2016, Czemieli Berndtsson, 2010). The early research concentrated mostly on quantifying water volumes retained by

green roofs. The majority of authors also documented the attenuation properties of green roofs, emphasising green roof value in stormwater management. Having proved the effectiveness of green roofs to reduce surface runoff, several studies focused on investigating different factors controlling hydrological performance of vegetated roofs. It was noticed that the effectiveness of green roof hydrological performance depends on local climatic conditions (Snodgrass and McIntyre, 2010, Czemieli Berndtsson, 2010) and green roof design, including the number and type of layers, materials, roof geometry and vegetation type (Czemieli Berndtsson, 2010). Hence, this review will critically assess studies of hydrological performance of green roofs concentrating on retention and attenuation efficiency of green roofs. It will also evaluate factors influencing the hydrological performance of green roofs with the emphasis on green roof construction materials and their properties. However, before that, green roof monitoring systems will be assessed as a critical but overlooked aspect of green roof hydrological behaviour studies.

### **2.2.1 GREEN ROOF RAINFALL-RUNOFF MONITORING**

Green roof experiments can be divided with regards to scale of the roof (small or full scale) or the nature of the rainfall (natural or artificial/simulated). Most of the reviewed green roof experiments described full scale green roofs subjected to the natural rainfall events and small scale green roofs subjected to the simulated rainfalls. Few experiments, however, included small scale green roofs exposed to natural rainfall events. For the purpose of this review, green roof experiments were categorised as in-situ or laboratory. The in-situ studies include full scale and small scale green roofs subjected to natural rainfall events, while the laboratory investigations concentrate on small scale green roof plots subjected to simulated rainfalls. In both types of study the evaluation of the hydrological performance of the green roofs involves the measurement of the amount of rain falling onto a green roof and the determination of runoff from it. The majority of green roof studies fell into in-situ group, only a few were laboratory based.

#### **2.2.1.1 IN-SITU GREEN ROOF STUDIES**

In-situ green roof studies refer to green roofs established outdoors, usually full scale and exposed to natural rainfall events. However, in this group there are also small scale plots subjected to natural precipitation as well as irrigated green roofs.

The rainfalls were monitored using widely available individual or weather station built-in rain gauges installed on site (Hathaway et al., 2008, Fassman-Beck et al., 2013, Schroll et al., 2011, VanWoert et al., 2005). Some researchers quantified rainfalls based on data from national rain gauge networks (Fassman-Beck et al., 2013, Graceson et al., 2013, Getter et al., 2007). In that case a correction should be applied when estimating rainfall volumes, which would take under consideration the distance between the rain gauge and the location of the experimental green roof.

Documented runoff monitoring systems are based on methods employed to measure flow in open channels or closed conduits (Owczarek et al., 2016). Common methods which will be briefly described in this section including cubature method, critical depth method, tipping bucket rain gauge, weighing method and method utilizing custom designed devices. The most common method used in monitoring in-situ green roof experiments was the cubature method (Villarreal and Bengtsson, 2005, Teemusk and Mander, 2006, Schroll et al., 2011, Harper et al., 2015, Beecham and Razzaghmanesh, 2015, Stovin et al., 2012, Locatelli et al., 2014). The principle of this method is the measurement of the volume of water stored or released, directly or as a product of surface area and change in water level, at a known time interval. Direct measurement of water volume is cost effective since no specialist equipment is required. However, it is not suitable for continuous monitoring. The procedure is more applicable for the laboratory setups, with low amounts of runoff collected within a short period, when only the retention capacity of the green roof is of interest. The determination of water volumes through water level monitoring allows long term, continuous monitoring and eliminates the need for manual labour. However, the accuracy of the results and the cost involved depend on the choice of the water level sensor. It is worth noting that installing costly water level sensors for high accuracy readings will not be effective or justified if the area of the water collection container is large. The larger the area of the container, the higher the volume per unit depth, hence the resolution and the accuracy of the water volume readings will decrease. Unfortunately, none of the reviewed papers reported the cross-section area of the container used for water collection. Hence, the accuracy or reliability of the results can't be confirmed.

A number of researchers used a critical depth method to quantify stormwater runoff from green roofs (Hathaway et al., 2008, Gregoire and Clausen, 2011, Speak et al., 2013a, Bliss et al., 2009, Carpenter and Kaluvakolanu, 2011). Critical depth method is a technique which involves installation of a flow measuring structure, a flume or a regular barrier such as a weir or notch across an open channel. The runoff flow rate is calculated as a function of the level of water upstream or at the throat (flume) or head over the crest of the structure (weir, notch). It is an effective method of flow rate determination, although there are certain restrictions of the use such as minimum effective head, below which the measurement of flow rate would not be accurate or even not possible. Hence, usage of this type of monitoring system may lead to overestimating green roof retention properties resulting from missing values of the low rates of the discharge. Reviewed papers do not disclose any information of how the researchers dealt with this problem or what proportion of the runoff could have been not accounted for.

The next popular but also questionable method of green roof runoff determination is use of tipping bucket rain gauges. The flow rate is measured by recording the number of bucket tips over a known time. The water is collected in a funnel and subsequently directed to one of two buckets on a pivot. When the bucket is filled, the lever of the pivot system tips releasing water. The volume of the bucket is known and the time of the tip is recorded, thus allowing the calculation of the flow rate. The tipping bucket rain gauge is a popular device used to sample rainfall quantity and rate (Butler and Davies, 2010). It was employed by several researchers to measure the runoff from the green roofs (VanWoert et al., 2005, Volder and Dvorak, 2014, Razzaghmanesh and Beecham, 2014, Hakimdavar et al., 2014). One of the advantages of the gauge is its small size and easy installation. It works very well measuring low flow rates such as rate of the rainfall. However, the accuracy of the gauge is not constant and it varies with the flow rate - the higher the rain/runoff rate, the higher the error. Therefore, it is not suitable to measure the discharge from large green roofs, where high flow rate is expected. In this case the stormwater retention of the green roof could be over- or underestimated.

The accurate measurement of a wide range of flow rates was achieved by Fassman-Beck et al. (2013), who installed a custom designed device (orifice

restricted device) at a green roof experimental site. The orifice restricted device (ORD) consists of a 1200mm long tube with a series of orifices located along the device (Voyde et al., 2010). As the tube is filled, the water is discharged through one, two or more orifices depending on the water flow rate. The flow rate is calculated as a function of the water level in the tube. The depth of the water is recorded using a pressure transducer. One of the advantages of the ORD is simplicity of installation – it is fitted in a downpipe, which is very practical as it doesn't require additional space. Despite the functionality and efficiency of the device, it is not widely used since it is not available commercially.

One of the methods that provides accurate and reliable readings is the weighing method. Moreover, weighing equipment is widely available and many have automatic data logging functions. This method allows the assessment of both retention and attenuation properties of green roofs. Many researchers successfully used this method in their studies (Graceson et al., 2013, Morgan et al., 2013, Wong and Jim, 2014). It is suitable for small laboratory setups, but less feasible to monitor full scale in-situ green roofs, where installation of apparatus would be difficult due to the site constraints.

The variety of the methods and equipment utilised in green roof studies is very wide and all present different levels of accuracy and functionality, as presented above. Beside the validity issues associated with the monitoring equipment of in-situ green roofs, the reliability of such experiments could be argued as well. Many of the researchers such as Carter and Rasmussen (2006), Stovin et al. (2012) or Palla et al. (2011) investigated hydrological behaviour of only one green roof. Others such as Fioretti et al. (2010), Fassman-Beck et al. (2013) or Razzaghmanesh and Beecham (2014) studied the performance of two or more green roofs. However, there was only one replicate of each roof investigated, which is not sufficient to draw definite conclusions. There is a chance that another factor contributed to the results and findings. The high retention could be a result of roof structure imperfections, such as depressions, storing stormwater and not necessarily the effect of green roof retention abilities (Voyde et al., 2010). In such a situation, the error would be propagated to an entire data set of observations collected during the green roof monitoring period. Ideally, the results should be confirmed through the studies of replicates of the green roofs of the

same design. However, replicating large scale green roofs is challenging due to financial and space constraints.

A certain degree of repeatability is achieved through green roofs being subjected to multiple rainfall events. Still, the number of rainfall events depends on climatic conditions as well as on the duration of the experiment. Usually a lower number of rainfall events was recorded for the green roofs observed for a short time. For example, Hakimdavar et al. (2014) investigated the behaviour of three different green roofs and recorded a different number of rainfall events at each roof. Two of the green roofs were studied for 12 months during which 63 and 79 rainfall events were recorded. The last roof was investigated for 3 months with only 6 rainfall events observed. In the case of long term green roof monitoring, a higher numbers of rainfall events were noted. Fassman-Beck et al. (2013) recorded green roof response to 198 rainfall events over 28 months research and Razzaghmanesh and Beecham (2014) documented 226 rainfall events over 23 months. It needs to be stressed that monitoring system failures could significantly reduce the number of valid observations. Stovin et al. (2015) documented 324 rainfall events during a 48-month study, however runoff data for only 49 events was valid for all 9 green roofs. The noticeable issue with in-situ green roof experiments is lack of control over the factors related to weather conditions such as temperature, wind speed, rainfall intensity and duration amongst others. Consequently, even large data sets could possibly not include observations reflecting the same conditions. Hence, the reliability of the findings can be put into question.

#### **2.2.1.2 LABORATORY GREEN ROOF STUDIES**

The reliability and validity of green roof investigations could be improved through a choice of suitable monitoring equipment and greater control over the factors such as intensity and duration of rainfall events and temperature amongst others. This could be achieved in laboratory conditions. There are only a few papers published on green roof studies in indoor laboratory conditions. In this type of setup, the green roofs are of small scale and subjected to simulated rainfall events.

Simulated rainfall events are generated using various types of rainfall simulator or in some cases watering cans or sprinklers. A sprinkler was used by

Vijayaraghavan and Joshi (2015) and Alfredo et al. (2010), the latter also used a watering can. However, using sprinklers and watering cans can't produce reliable rainfalls. Total volume of the rain could be determined, however there is little control over intensity or distribution of the simulated rainfall. Use of rainfall simulators ensures greater control over tests. The most common type of rainfall simulator is the nozzle type (Beck et al., 2011, Lee et al., 2015, Carbone et al., 2014). However, the distributions of the rain generated by this type of simulator depend on a water pressure. Higher pressures result in good rainfall distributions but potentially excessive intensities, while low pressures produce lower, desired intensities but very poor rainfall distributions. The most efficient and suitable for green roof investigation are drop former type of rainfall simulators. This type of simulator was employed by Nagase and Dunnett (2012) and Mickovski et al. (2013). However, both investigations concentrated mainly on assessing plant growth rather than hydrological response to rainfall events.

Although, use of a rainfall simulator presents an opportunity to conduct several rainfall simulations independent in time and with control over intensity and duration of the event, only a few researchers have collected a large numbers of observations. Vesuviano and Stovin (2013) generated rainfall events of 5 different intensities, which were applied to 20 physical configurations of drainage layer. All tests were repeated 3 times giving a data set of 300 observations. Data sets of that size ensure more robust analysis as opposed to analysis based on a small number of observations, such as taken by Beck et al. (2011) or Lee et al. (2015). The former performed two rainfall events over six roofs resulting in a data set of 12 observations only; the latter recorded the response of four roofs subjected to seven rainfall events giving data set of 28 observations. The results of the analysis conducted on such small data sets are more likely to be biased.

The runoff monitoring methods employed in green roof laboratory studies included cubature method (Alfredo et al., 2010, Nagase and Dunnett, 2012, Mickovski et al., 2013, Lee et al., 2015, Vesuviano and Stovin, 2013), use of tipping bucket rain gauge (Carbone et al., 2014) or the combination of the above (Palla et al., 2010). All the methods were described in section 2.2.1.1.

Clearly, the study of green roofs in laboratory conditions ensures reliability and validity of the data collected. Robust results achieved through laboratory

experiments can lead to better understanding of the behaviour of green roofs. Consequently, better green roof designs can be produced to fulfil the required objectives.

## **2.2.2 GREEN ROOF CONSTRUCTION MATERIALS**

The major components of the extensive green roof system are the substrate and drainage layer. The main role of the substrate is to support plants. However, it could also enhance retention capacity of the green roofs or improve the quality of stormwater passing through the substrate. The drainage layer ensures proper stormwater draining, preventing water logging, which could lead to roof structure damage and an unhealthy environment for most of the plants. Certain types of drainage layer can also retain stormwater, increasing the retention capacity of the green roof. Both layers can be altered either through the use of alternative materials or introducing additives to conventional ones.

### **2.2.2.1 SUBSTRATE LAYER**

Extensive green roof the substrates are composed of a mixture of aggregates and organic matter. Conventional substrates are made of locally available materials, usually natural aggregates. Their choice varies depending on location and availability (Fassman and Simcock, 2012) (Table 2.1).

Table 2.1 lists various materials implemented by researchers as a substrate across the world. The majority of them are also listed in the FLL guidelines. However, some researchers did not specify the type of substrate used for green roof construction. Some vaguely describe substrate as soil (Locatelli et al., 2014, Qin et al., 2012), others stated the content of the specific grain size fraction such as sand, silt or clay only (Getter et al., 2007, Beck et al., 2011), but did not specify material composition.

*Table 2.1 Collation of conventional materials used as a green roof substrate based on published literature. The materials are categorised in regards to the location of the study.*

<b>Region</b>	<b>Country</b>	<b>Materials</b>	<b>Reference</b>
<b>Australia</b>	Australia New Zealand	pumice, zeolite, scoria, crushed brick, expanded clay	Beecham and Razzaghmanesh (2015), Fassman-Beck et al. (2013), Voyde et al. (2010)
<b>North America</b>	USA Canada	expanded slate, expanded clay, pumice, decomposed granite	Carter and Rasmussen (2006), Hathaway et al. (2008), Carpenter and Kaluvakolanu (2011), Gregoire and Clausen (2011), Hilten et al. (2008), Simmons et al. (2008), Van Seters et al. (2009)
<b>Europe</b>	Mainland	lapillus, pumice, zeolite, crushed clay, crushed limestone, crushed brick	Fioretti et al. (2010), Locatelli et al. (2014), Palla et al. (2011), Villarreal and Bengtsson (2005) Ondono et al. (2016), Nektarios et al. (2015)
	UK	crushed red brick, crushed tile	Graceson et al. (2013), Stovin (2010), Stovin et al. (2012)
<b>FLL Guidelines</b>		lava, pumice, brick, expanded clay, expanded slate, dolomite, tuff, slate slug, mining slug	FLL (2008)

Although, widely used, the conventional substrate materials are criticised for contributing to the negative environmental impact of green roofs (Eksi and Rowe, 2016). Expanded clay, shale or slate are a popular choices as a main component of green roof substrate in North American countries. However, production of lightweight expanded aggregate requires the natural material such as slate, shale or clay to be heated to temperatures at or near 1100°C (Solano et al., 2012). Although, in the process the bulk density is reduced, which is desirable in extensive green roofs, the carbon footprint and embodied energy is significantly increased. In Australia and New Zealand common materials implemented as substrate are pumice, scoria, lapillus, and zeolite, similarly to mainland Europe. These are raw materials that need to be mined. Any natural material extraction is environmentally disruptive. Subsequently, the materials need to be transported to green roof construction site, which further increase the carbon footprint and

embodied energy. The most sustainable conventional materials are crushed brick or crushed tile, which are predominant in the United Kingdom but also used in the USA or in mainland Europe. Crushed brick or tile are recycled materials, the product of breaking defective red or yellow bricks or tiles. Clearly, the selection of the environmentally friendly materials is rather narrow. In order to make green roofs truly sustainable, several researchers studied alternative materials and their influence on green roof performance (Table 2.2). The majority of the listed materials (e.g. porcelain) are recycled or made of components that are recycled (e.g. Lytag or sewage sludge clay pellets). Although, the study of alternative green roof materials has been more dynamic in recent years, especially in the UK, the list of the materials available and suitable for green roof construction is still narrow. Moreover, many of the materials have been investigated in a limited way; mostly for plant growth enhancement (Eksi and Rowe, 2016, Matlock and Rowe, 2016, Molineux et al., 2009, Molineux et al., 2015, Bates et al., 2015, Mickovski et al., 2013), thermal properties (Sailor and Hagos, 2011) or carbon sequestration (Luo et al., 2015).

*Table 2.2 Collation of alternative materials used as a green roof substrate based on published literature. The materials are categorised in regards to the location of the study.*

<b>Region</b>	<b>Country</b>	<b>Materials</b>	<b>Reference</b>
<b>North America</b>	USA	foamed glass, porcelain, porous silica	Eksi and Rowe (2016), Matlock and Rowe (2016), Sailor and Hagos (2011)
<b>Asia</b>	China	sewage sludge	Luo et al. (2015)
<b>Europe</b>	UK	crushed demolition aggregate, solid municipal waste incinerator bottom ash aggregate, Lytag, construction and demolition waste aggregate, sewage sludge clay pellets, paper ash pellets, Carbon8 pellets, Superlite (crushed aircrete),	Bates et al. (2015), Graceson et al. (2014a), Mickovski et al. (2013), Molineux et al. (2009)

Only a few researchers explored multiple properties of the alternative materials in relation to green roof performance. Small scale green roof plots at Harper Adams University were tested for hydrological performance (Graceson et al.,

2013) as well as for plant growth response (Graceson et al., 2014b). Also Mickovski et al. (2013) looked at plant growth and stormwater runoff volumes, however only in relation to vegetation type, not to material type. Similarly, Eksi and Rowe (2016) concentrated on plant response and water retention analysis was based on physical properties of the substrate rather than direct measurements of rainfall and runoff volumes.

Substrate properties can be also altered using additives (Table 2.3). Several researchers studied the influence of hydrogels on green roof hydrological performance (Beck et al., 2011), plant growth (Olszewski et al., 2010, Young et al., 2014, Farrell et al., 2013). Many investigated the effect of perlite on water quality and/or quantity (Gregoire and Clausen, 2011, Lee et al., 2015, Simmons et al., 2008). Natural materials like coir fibre (Beecham and Razzaghmanesh, 2015) or seaweed (Vijayaraghavan and Raja, 2015) were also tested as substrate additives to improve stormwater runoff quality. All of the mentioned additives proved to enhance green roof performance. However, similarly to alternative material tests, the additives studies were also limited concentrating on one type the green roof performance such as plant growth or runoff water quality and/or quality.

*Table 2.3 Collation of green roof substrate additives based on published literature. The materials are categorised in regards to the location of the study.*

<b>Region</b>	<b>Country</b>	<b>Additives</b>	<b>Reference</b>
<b>North America</b>	USA Canada	Paper fibre biochar, hydrogel, perlite	Beck et al. (2011), Gregoire and Clausen (2011), Simmons et al. (2008), Olszewski et al. (2010)
<b>Asia</b>	Korea India	Perlite, Sargassum wightii (seaweed)	Lee et al. (2015), Vijayaraghavan and Raja (2014), Vijayaraghavan and Raja (2015)
<b>Australia</b>	Australia New Zealand	polyacrylamide hydrophilic polymer (hydrogel), silicon-based additive, perlite, coir fibre, hydro-cell flake	Fassman and Simcock (2012), Beecham and Razzaghmanesh (2015), Farrell et al. (2013)
<b>Europe</b>	UK	polyacrylamide gel (hydrogel)	Young et al. (2014)

Finally, the properties of substrates can be modified by amending the organic matter content. Nagase and Dunnett (2011) and Olszewski et al. (2010) demonstrated that increased organic matter resulted in increased plant growth. It need to be noted that, although healthy plants are essential elements of green roofs, the increased plant growth is not always desired. Certain plant species can become excessively dominant, compromising green roof plant diversity, and also damage green roof profile layers.

Many of the alternative materials and additives discussed have a great potential of enhancing green roof functions in various ways including hydrological or thermal performance and plant growth enhancement amongst others. However, there is a need for comprehensive studies exploring the effect of these materials on multiple aspects of green roof performance.

#### **2.2.2.2 DRAINAGE LAYER**

There is little research published on the drainage layer effect on green roof performance. Many researchers use conventional drainage layers (Table 2.4). There is only one type of alternative drainage layer identified in the literature: rubber crumb (also called shredded tires or granulated rubber). However, the focus of rubber crumb studies was mainly in terms of energy or zinc sequestration (Solano et al., 2012, Pérez et al., 2012). Only Vesuviano and Stovin (2013) investigated the effect of various drainage layers on the hydrological performance of green roofs. However, their study included only conventional drainage layers. Clearly, there is a gap in this knowledge area, which should be thoroughly explored and filled. The drainage layer is a major component of the green roof, which could significantly improve green roof performance. It should not be, in any way, omitted or underestimated.

Table 2.4 Collation of drainage layer materials based on published literature. The materials are divided into three groups: conventional, alternative and recommended by FLL (2008).

Type	Material	Reference
<b>Conventional</b>	Floradrain - thermoformed recycled polyolefin board  Hydrodrain - high density polyethylene board  Xero Flor – mat made of looped polyamide filaments  Lapillus Pebbles Mineral wool Polystyrene  Plastic chips	Carter and Rasmussen (2006), Hathaway et al. (2008), Stovin et al. (2012), Carpenter and Kaluvakolanu (2011)  Hathaway et al. (2008)  Getter et al. (2007)  Fioretti et al. (2010), Palla et al. (2011)  Qin et al. (2012)  Locatelli et al. (2014), Wong and Jim (2014), Teemusk and Mander (2006)  Versini et al. (2015), Wong and Jim (2014), Vesuviano and Stovin (2013)  Mickovski et al. (2013)
<b>FLL</b>	lava, pumice, brick, expanded clay, expanded slate, crushed brick, crushed tiles, basalt gravel, dolomite gravel, granite gravel, tuff gravel, structure fleece matting, studded plastic matting, fibre-type woven matting, shaped hard plastic boards, shaped foam drainage boards, insulation material drainage boards	FLL (2008)
<b>Alternative</b>	Rubber crumbs	Perez et al. (2012), Rincón et al. (2014), Solano et al. (2012)

### **2.2.3 HYDROLOGICAL PERFORMANCE OF GREEN ROOFS**

The hydrological performance of the green roofs is of special interest in this research. Hence, this section will focus on the current state-of-art of the hydrological performance of the green roofs. The results of the retention and attenuation investigations as well as factors affecting these results were reviewed and presented in this section.

#### **2.2.3.1 QUANTIFYING RETENTION AND ATTENUATION**

High retention capacity, peak runoff reduction and delay are crucial when a green roof is installed as a stormwater management tool (Stovin, 2010, Mentens et al., 2006, Vijayaraghavan, 2016). Water storage capability is also vital for vegetation and its survival during drought periods (Wolf and Lundholm, 2008) and during frost (VanWoert et al., 2005). The ability of the green roof to retain stormwater has been demonstrated through several studies around the world (Figure 2.13). Mentens et al. (2006) reviewed and summarised the results of some early green roof research available in German and published the review in English. According to their analysis, median retention for extensive green roofs was 55% of annual precipitation. In this review studies published in the English language were considered. The outcome of various research was collated and median, minimum, and maximum green roof hydrological characteristics were established. The median retention was 62%, maximum was 87% and minimum 11% (Figure 2.13). The median peak flow reduction was 81% with maximum of 91% and minimum of 31% (Figure 2.14). The differences between the retention and attenuation values in published research could occur as a result of the influence of various factors such as climate conditions including rainfall characteristics, temperature and humidity of the air, the green roof geometry including type and depth of green roof layers, green roof construction materials characteristics (Czemiel Berndtsson, 2010, Krishnan and Ahmad, 2012). The effect of these factors will be discussed in detail in sections 2.2.3.2 to 2.2.3.4.

It needs to be stressed that most of the published retention analysis are based on short term (a few months) in-situ green roof experiments. The distribution of the rainfall events is of an exponential nature, resulting in a high number of small rainfalls for which the retention is very high, and a low number of high rainfalls for which the retention is usually low (subject to other factors). Consequently, the average or cumulative retention values based on such data sets are usually high.

However, a high overall rainfall retention will not necessarily lead to a high retention of extreme rainfalls, which would be of greater interest to engineers and policy makers due to the flood risk posed by such rainfall events. Average or cumulative retention values could be used, however, as an indicator of overall performance of green roofs. The randomness of natural rainfall events is a major weakness of the in-situ green roof experiments. Conducting tests in laboratory conditions would allow control over simulated rainfall events, leading to more reliable results.

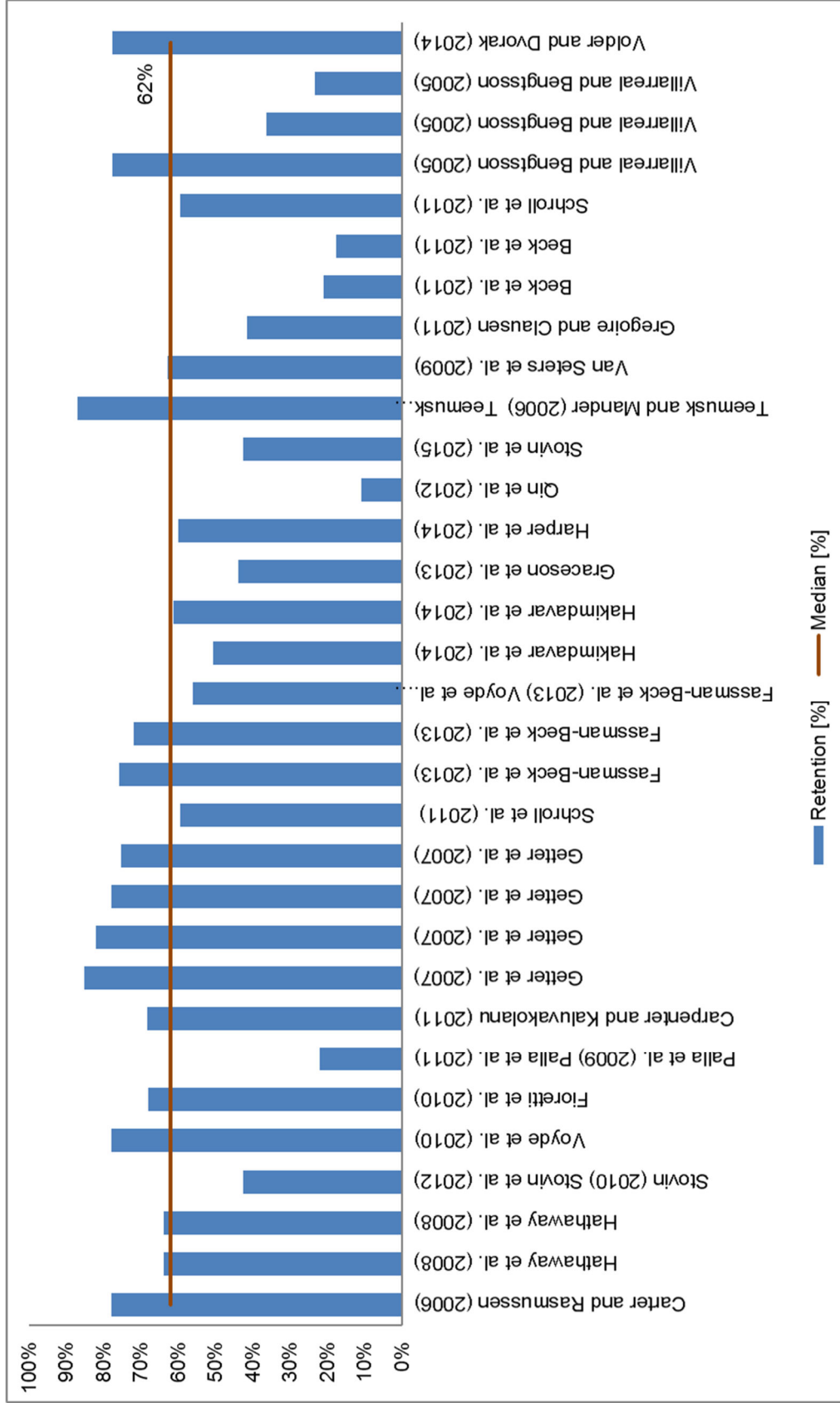


Figure 2.13 Green roof stormwater retention – cumulative or average retention values reported in published literature and a median retention determined based on these values

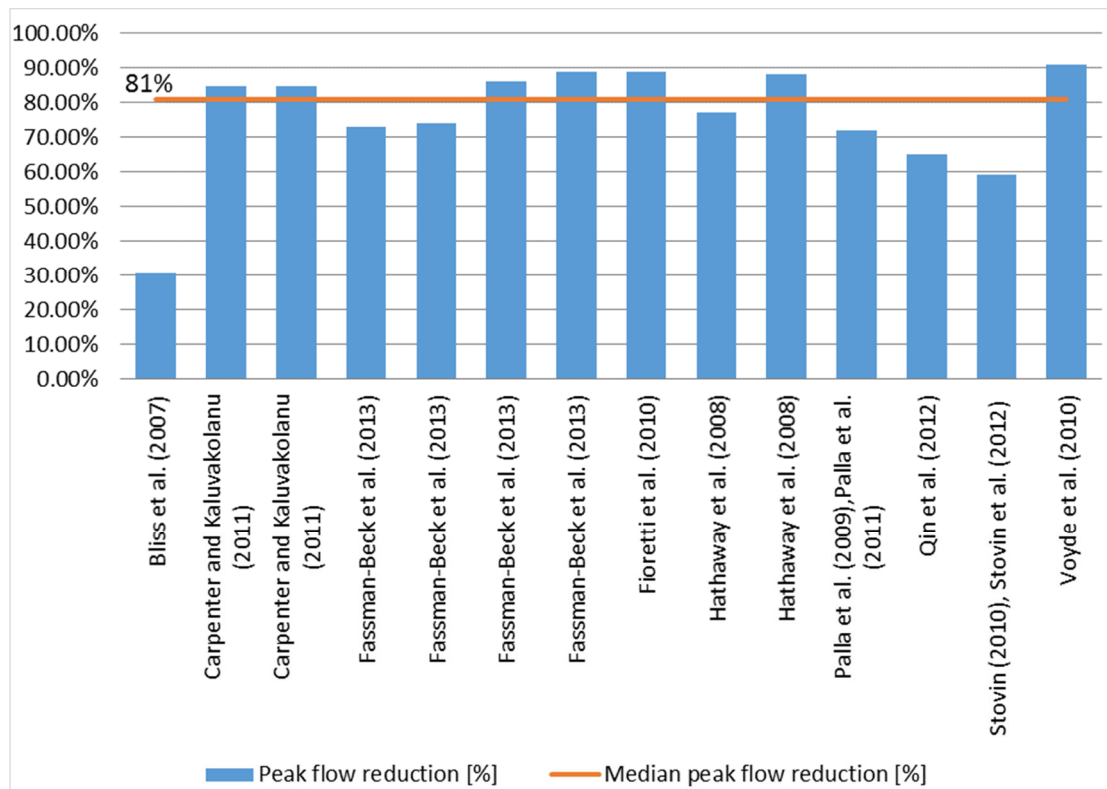


Figure 2.14 Green roof peak flow reduction values reported in published literature and a median peak flow reduction determined based on these values.

### 2.2.3.2 INFLUENCE OF CLIMATE CONDITIONS

Green roof performance differs under varied climatic conditions (Carpenter and Kaluvakolanu, 2011, Stovin et al., 2012, Voyde et al., 2010, Getter et al., 2007). Snodgrass and McIntyre (2010) emphasised the impact of the geographical location on green roof performance based on a study of different green roofs in North America, where the climate is very heterogeneous and the rainfall regime varies drastically. The variation in green roof hydrological response was also noticed through seasonal analysis (Fassman-Beck et al., 2013, Mentens et al., 2006, Bengtsson et al., 2005). Higher retention capacity was noted during warm seasons 70% (Mentens et al., 2006), 88% (Bengtsson et al., 2005), 83-92% (Fassman-Beck et al., 2013) as opposed to cold seasons 33%, 19% and 66% respectively. The seasonal differences occur due to higher evapotranspiration during warm periods, when green roof retention capacity regenerates faster than during cold seasons (Mentens et al., 2006, Czemieli Berndtsson, 2010, Stovin et al., 2012, Fassman-Beck et al., 2013). Also, during colder months the occurrence of intense storms is more frequent as opposed to warmer months. Although

seasonal differences are noticeable and justified the influence of the climate is not that obvious due to additional factors influencing green roof response such as variations in green roof design across studies. These factors could be of high significance, yet through existing green roof experimental design they could not be investigated, e.g. studying a single roof does not reveal the influence of the design on green roof performance.

Climate characteristics such as rainfall patterns, depth and intensity, solar radiation, temperature are listed as factors affecting green roof retention (Carpenter and Kaluvakolanu, 2011, Stovin et al., 2012, Voyde et al., 2010, Getter et al., 2007). However, those climate elements should be treated as an action to which the green roof is being designed rather than the reaction controlling parameters. Each location has a unique combination of the above mentioned climate characteristics hence, the comparison of the results of in-situ studies is very challenging. A common conclusion amongst all studies was that there is an inverse relationship between water retention and the size of rainfall event. However, the rate of change was not established. Moreover, the retention cannot be explained by rainfall depth only and through simple linear regression analysis (Kasmin, 2010, Nawaz et al., 2015). Stovin et al. (2012) attempted to correlate retention capacity with antecedent dry weather periods concluding that it is not the factor which controls green roof response. To effectively predict green roof hydrological behaviour, design parameters such as material properties and geometry of the roof (area, slope, depth of the layers of the roof) should be investigated in addition to their response to a specific action i.e. size of rainfall events.

The review of the published literature revealed a lack of consistency in green roof experiment methodologies in regards to rainfall characteristics. Firstly, there is no common procedure to determine individual rainfall events. Several researchers based rainfall event separation on a 6h inter-event dry period (Hathaway et al., 2008, Stovin et al., 2012, Voyde et al., 2010, Razzaghmanesh and Beecham, 2014), others used 1h (Locatelli et al., 2014), 12h (Schroll et al., 2011) or 24h (Volder and Dvorak, 2014). Although inter-event dry period of 6h is used by a number of researchers, it was established based on North American rainfall data (Driscoll et al., 1989), hence it is specific to that climate. It is unknown, how the choice of inter-event dry period would affect the final result of green roof

hydrological performance analysis. It may influence retention of stormwater from individual events as well as the average retention based on those events.

Secondly, there is no universal classification of rainfall events. Depending on the environment and local climate, the sizes and classification of rainfall events vary considerably. Sanderson (2010) defines all rainfall events of the return period greater than 1 in 5 years as extreme. VanWoert et al. (2005) categorised rainfall events in relation to the rainfall depth: light: <2mm, medium: 2-6mm, heavy: >6mm. Hakimdavar et al. (2014) also defined rainfall events in relation to the rainfall depth. However, their classification differed significantly from VanWoert et al. (2005): small events: <20mm, medium: 20-40mm, large events: >40mm. Rainfall events defined by VanWoert et al. (2005) as small and medium and in part heavy are considered by Hakimdavar et al. (2014) as small. These differences could lead to results misinterpretation. Carpenter et al. (2016) reported mean retention of 96.8% for rainfall events of depth below 17.6mm. They compared their results to Czemieli Berndtsson (2010), who reported 88% of retention for rainfall events of the depth less than 25.4mm, classified as small storms. As one could notice the comparison is hardly meaningful and very misleading. Clearly there is a need for a common framework for green roof experiments methodology, which would ensure robust results and grounds for comparisons.

Some of the researchers complemented rainfall characteristics by defining the return period of recorded rainfall events (Berretta et al., 2014, Fassman-Beck et al., 2013, Nawaz et al., 2015, Stovin et al., 2015). Berretta et al. (2014) analysed rainfall events of return period greater than 1 year. However, there is no information on the rainfall event of the maximum return period. Fassman-Beck et al. (2013) reported the largest storm is less than a 2 years return period event. The largest rainfall event recorded by Nawaz et al. (2015) was 1 in 61 years event, however all other rainfall events were of return period less than 2 years. Similarly, rainfall events observed by Stovin et al. (2015) were all below 5 years return period with only 2 greater than 2 years return period. Clearly the in-situ green roof experiments do not provide enough data, if any, to determine green roof response to rainfall events of high return period such as 30, 50 or 100 years. Multiple rainfall events of such magnitude could be simulated in the laboratory conditions. However, limited research in this area was carried out to date (section 2.2.1.2). This research will fill the noticeable gap in that field.

### 2.2.3.3 INFLUENCE OF GREEN ROOF GEOMETRY

Wide diversity within green roof design across published studies prevents drawing clear relation between green roof geometry and its hydrological performance. Due to a high degree of complexity, there are many probable parameters regulating green roof response to rainfall events such as depth and composition of substrate, slope of the roof, vegetation type and cover amongst other (Czemiel Berndtsson, 2010, Vijayaraghavan, 2016). To assess the importance of an individual determinant either statistical analysis of a large sample of green roofs or detailed experimental work on each individual factor is required. As for now, there is insufficient data available from existing published studies to conduct reliable analysis and investigations into specific parameters are limited. Efforts towards identification of major geometry factors that influence green roof response were undertaken by a few researchers (VanWoert et al., 2005, Getter et al., 2007, Fassman-Beck et al., 2013, Beecham and Razzaghmanesh, 2015).

Getter et al. (2007) demonstrated the influence of the slope on runoff retention capacity. Their research showed that the higher the slope the lower green roof retention, recording average retention of 75.3% at the 25% slope and 85.2% at the slope 2%. A similar outcome was attained by VanWoert et al. (2005), 65.9% of rainfall was retained by the green roof at the 6.5% slope and 87% at the 2% slope. Villarreal and Bengtsson (2005) and Palla et al. (2010) also support the above conclusion. On the contrary, Mentens et al. (2006) documented no significant correlation between slope angle and water retention capacity of analysed green roofs. Stronger influence of other factors could be one of the possible explanation since the design of investigated roofs varied as opposed to Getter et al. (2007) and VanWoert et al. (2005) studies, where tested roofs differed by slope angle only. Beecham and Razzaghmanesh (2015) also did not find large differences between mean retention of extensive green roofs with the slope 1° and 25°: 79.62% and 78.13% respectively.

It has been suggested that the rainfall-runoff processes depend on vertical water movement (Villarreal and Bengtsson, 2005, cited in Czemiel Berndtsson, 2010, p. 355) and is a function of substrate depth and moisture holding capacity (Stovin et al., 2012). However, there is no available publication investigating scale effect on green roof performance to exclude green roof area as one of the influential

factors. The main geometrical parameter of green roofs studied was thickness of substrate. VanWoert et al. (2005) attempted to quantify the substrate depth influence on water retention. It has been established that by increasing the depth of the substrate green roof stormwater retention capacity also increases. Similarly, green roofs of deeper substrate, tested in New Zealand, stored a greater volume of rain water than shallower substrates (Fassman-Beck et al., 2013). Morgan et al. (2013) argued that although mean retention increases with substrate thickness it is only valid for substrates up to 15cm. There was no significant difference between water storage capacity of 15cm and 20cm deep substrate; moreover, a slight reduction in retention was noticed. According to Mentens et al. (2006) the correlation between substrate depth and yearly runoff is significant. However, the nature of it is not specified. Based on analysed literature thicker substrates would enhance green roof retention to a certain extent. However, simultaneously it would introduce additional load to the supporting structure and increase the cost of green roof construction.

#### **2.2.3.4 INFLUENCE OF TYPE OF MATERIALS**

Further improvement of hydrological performance could be achieved through the selection of the substrate and drainage layer materials as well as vegetation. The green roof conventional materials, alternative materials, and additives are discussed in section 2.2.2. Many of the reviewed studies investigated the effect of the composition of the materials on plant growth, thermal and energy performance, only a few investigated the effect on hydrological performance. Amongst the latter, the majority of researchers employed conventional materials for green roof construction. A limited number of studies involved alternative materials or additives.

##### *2.2.3.4.1 CONVENTIONAL MATERIALS*

Green roofs made of conventional materials are far more common than green roofs made of alternative materials or green roofs incorporating additives. Hence, several researchers investigated hydrological performance of green roofs made with conventional materials (Carter and Rasmussen, 2006, Hathaway et al., 2008, Fioretti et al., 2010, Carpenter and Kaluvakolanu, 2011). However, only a few studied the differences in performance between green roofs made with alternative materials (Stovin et al., 2015, Fassman-Beck et al., 2013).

Stovin et al. (2015) investigated the behaviour of green roofs made with three different substrates: Heather with Lavender Substrate (HLS), Sedum Carpet Substrate (SCS) and Lightweight Expanded Clay Aggregate (LECA) substrate. The inorganic component of the HSL medium was crushed brick and pumice, of SCS medium was crushed brick and the main component of the last substrate was expanded clay. The retention analysis demonstrated higher performance of HLS and SCS (crushed brick based) media in comparison to expanded clay based medium. However, these differences were not statistically significant.

Fassman-Beck et al. (2013) found minor differences in retention between pumice (50% v/v) and zeolite (30% v/v) based green roof and pumice (60% v/v) and expanded clay (20% v/v) based green roof with retention being 72% and 76% respectively. Lower retention (56% and 66%) was observed for green roofs with substrate composed mainly of pumice (70% v/v) and expanded clay (10% v/v). However, it needs to be stressed that factors other than substrate composition could have more significant effect on such an outcome. The green roofs discussed had different area, slope, and substrate depth. It is not clear which, if any, of the factors was a dominant one.

#### *2.2.3.4.2 ALTERNATIVE MATERIALS AND ADDITIVES*

Green roof alternative materials and additives have become of great interest to researchers in recent years. However, the list of these materials is still limited. Moreover, many of the materials have been studied in relation to selected properties: mostly for plant growth enhancement (Eksi and Rowe, 2016, Matlock and Rowe, 2016, Molineux et al., 2009, Molineux et al., 2015, Bates et al., 2015, Mickovski et al., 2013), thermal properties (Sailor and Hagos, 2011) or carbon sequestration (Luo et al., 2015). Only a few studies have been published on the influence of the use of alternative materials or additives on the hydrological performance of green roofs.

Simmons et al. (2008) tested six different green roof designs. The results proved diversity in green roof response to rainfall events retaining from 88% to 26% of 12mm rain and 43% to 8% of 28mm rain. Green roof retention was influenced by drainage layer storage capacity and substrate composition i.e. substrates with a higher percentage of perlite retained larger volumes of runoff. In direct opposition to those findings were results reported by Voyde et al. (2010). No significant

difference in hydrological performance between different green roof designs was found with the exception of a roof where a pre-grown sedum mat was used. The mat consisted of coconut coir fibres which enhanced water retention.

A comprehensive study on the effect of substrate composition on green roof performance was carried out at Harper Adams University, Shropshire, UK (Graceson et al., 2013, Graceson et al., 2014a, Graceson et al., 2014b). Several substrate mixes made with either coarse crushed brick, coarse crushed tile or Lytag were tested. Each inorganic aggregate was amended with 10% v/v or 20% v/v composted green waste. The results showed lower hydrological performance of the green roofs made with crushed tile (retention between 27% and 31%) as opposed to crushed brick and Lytag based green roofs (retention between 42% and 49%). However, crushed tile substrate supported sedum growth significantly better than crushed brick based media. Lytag also outperformed crushed brick in supporting sedum growth.

Mickovski et al. (2013) proved that construction waste as a component of substrate supports plants growth. However, the retention values were not disclosed in the publication. Moreover, the experiment did not include any control roofs made with conventional materials for comparison, making it difficult to assess the benefits of these types of alternative materials.

A few studies were carried out testing impact of different additives on the physical and chemical properties of substrates and their significance to vegetation (Olszewski et al., 2010, Farrell et al., 2013, Beck et al., 2011). Olszewski et al. (2010) concluded that compost and/or hydrogel alterations could improve vegetation growth and survival because of greater water availability in the substrate. A similar outcome was presented by Farrell et al. (2013) where the addition of silicates in the substrate increased plant growth. However, neither of the studies included water retention capacity testing. Beck et al. (2011) investigated the effect of substrate composition and vegetation type on the hydrological performance of the green roof. They observed that by adding biochar to the substrate mix the retention capacity was increased from 17.8% to 21.1% on average.

#### *2.2.3.4.3 VEGETATION TYPE*

VanWoert et al. (2005) demonstrated a higher rainfall retention of roofs covered with vegetation (52.4%) in comparison to roofs covered with substrate only (38.9%). Volder and Dvorak (2014) obtained similar results of 7.5% higher water retention of vegetated roofs compared to substrate only modules. Stovin et al. (2015) concurs with these findings, however the differences were not of statistical significance. A difference in retention between sedum and meadow green roofs was observed by Graceson et al. (2013). Sedum decks retained 40% while meadow roofs retained 48% of rain. The type of the vegetation also influenced Beck et al. (2011) results. Green roofs planted with ryegrass demonstrated increased retention capacity compared with green roofs covered with sedum with an average difference of 3.2%.

#### *2.2.3.4.4 SUMMARY*

The above mentioned studies prove that the selection of material and vegetation type has a significant impact on green roof performance. However, as Voyde et al. (2010) reasonably argued, materials used to construct green roofs should be locally available. Hence, further research is needed to extend the list of currently used materials but also to complement the description and properties of alternative materials already tested. Although there has been rapid growth in green roof studies, the choice of materials is still limited due to insufficient information, lack of appropriate research and coherent guidelines.

### **2.2.4 RESEARCH IN THE UK**

Recently, green roof performance was of increased interest of researchers in the UK. However, the number and diversity of studies is still limited. A summary of reviewed UK based research is presented in Table 2.5. It needs to be stressed that the presented list contains studies related to hydrological performance or/and use of alternative materials or additives. There are several green roof UK based studies, which are related to topics like urban cooling (Speak et al., 2013b) or air pollution reduction (Speak et al., 2012) amongst others. Hence, the list is not in any way concluded. However, it already shows the need for further research, e.g. Bates et al. (2015) and Molineux et al. (2015) demonstrated the potential of alternative materials in regards to biodiversity and plant growth enhancement. Yet, the effect of those materials on hydrological performance is unknown. More comprehensive studies are required to fully characterise and assess the use of

alternative materials for green roof construction in the UK. Moreover, different types of possible green roof construction materials should be considered to expand the existing lists giving greater choice and design diversity. This research will address the highlighted issues. It will complement the list of green roof construction materials by further characterisation of already studied materials and by assessing novel materials. The results of this research will fill the existing knowledge gaps and through this it will support green roof installation in the UK, inform designers and policy makers, enhancing development of more sustainable, resilient cities.

*Table 2.5 Summary of the UK based research in relation to hydrological performance and use of alternative materials or additives. Studies belong to one of the two groups of research focus: HP-hydrological performance or B/PGE – Biodiversity/Plant Growth Enhancement.*

Reference	Conventional material	Alternative material / Additive	Research focus		Comments
			HP	B/PGE	
Bates et al. (2015), Bates et al. (2013)	crushed brick	crushed demolition aggregate, incinerator bottom ash aggregate		+	all treatments supported a similar plant biomass
Graceson et al. (2013), Graceson et al. (2014a), Graceson et al. (2014b)	crushed brick, crushed tile	Lytag	+	+	retention for crushed tile media lower than for crushed brick or Lytag media, sedum growth greater for Lytag and crushed tile media than crushed brick medium
Mickovski et al. (2013)	-	construction waste	±	+	construction waste based substrate can support plants growth
Molineux et al. (2009), Molineux et al. (2015)	crushed brick	crushed aircrete, pellets: sewage sludge clay, paper ash, Carbon8		+	alternative substrates perform as well if not better than crushed red brick in terms of plants growth
Berretta et al. (2014), Stovin et al. (2015)	crushed brick, pumice, expanded clay	-	+		higher retention for HLS and SCS (crushed brick base(d) media than expanded clay medium, but not significant
Stovin (2010), Stovin et al. (2012)	crushed brick	-	+		retention: 34% for short period of observations, 42.74% for long period of observations
Nagase and Dunnett (2011)	crushed brick	-		+	enhanced plants growth for substrate with higher organic content
Nagase and Dunnett (2012)	crushed brick and tile	-	+		plants type influence quantity of runoff: the least runoff for grasses followed by forbs and sedum
Young et al. (2014)	crushed brick	polyacrylamide gel (hydrogel)		+	hydrogel addition increased substrate WHC (+24%) and shoot growth (+8%)
Nawaz et al. (2015)	unknown	unknown	+		retention differs seasonally, no accurate retention model was found

## **CHAPTER 3**

### **GREEN ROOF MATERIALS AND THEIR PROPERTIES**

This chapter focuses on the selection and characterisation of green roof construction materials as a crucial step in the planning and design process of green roof installation. As in every engineering design process, it is essential to firstly understand the objectives of the design, secondly recognise the properties of the materials that are critical to the design and lastly choose the materials that allow the desired results to be achieved. It is essential to understand the nature of the materials and the possibilities that they offer and how they could enhance green roof performance. The aim of this research was to investigate alternatives to conventional green roof construction materials and assess their properties in the context of the hydrological performance of green roofs. This chapter presents the process of selecting materials, followed by a description of methods used to test and assess the selected materials' physical properties such as densities, porosity and void ratio, permeability, water absorption and maximum capillary rise. This chapter summarises the results of those tests and their influence on green roof sustainable design and construction, and potential effects on the hydrological performance of green roofs, which is described in greater detail in Chapter 6.

#### **3.1 SELECTION OF THE MATERIALS**

The process of selecting materials was divided into three steps: determination of the selection criteria, initial selection and final selection of the materials.

##### **3.1.1 SELECTION CRITERIA**

As discussed in Chapter 2, green roofs are built of several layers. Two of these layers are of particular interest to this research, as they account for most of the green roof mass and volume, namely the substrate and the drainage layer. Each

layer performs specific functions in green roof systems (section 2.1.2.1). Hence, the identification of appropriate green roof construction materials focused on materials that were:

- suitable as a substrate – aggregates that support plant growth
- suitable as a drainage layer – materials that are permeable (compulsory) and have significant water retaining ability (optional)

In order to identify and select alternative materials, a critical literature review has been carried out (Chapter 2). The existing materials used for green roof design in the UK and worldwide were recognised and assessed. However, many of the conventional materials such as expanded shale or clay were criticised for contributing to the negative environmental impact of green roofs (Eksi and Rowe, 2016). Hence, the following, additional criteria as been set:

- materials come from sustainable sources such as recycled or secondary aggregates
- materials are locally available as final product or derived from resources widely available in the UK

The process of green roof construction materials selection included the choice of two control materials, one for substrate and one for drainage layer construction (conventional materials commonly used to construct green roofs in the UK) and eight alternative materials, four for substrate and four for drainage layer construction (novel, not commonly used in green roof construction). Such selection ensured diversity of material properties for the experiment. Subsequently, the selection of alternative materials was narrowed down to four (due to laboratory space limitations, cost and time constraints), two substrate materials and two drainage layer materials. The selected materials are described in section 3.1.2 and a summary is presented in Table 3.1.

### **3.1.2 DESCRIPTION OF SELECTED MATERIALS**

The literature review identified a variety of materials commonly used as substrate and drainage layers for green roof construction (section 2.1.2.1). In the UK, crushed red brick (substrate) and polymer sheets (drainage layer) are widely used in the green roof market and are recognised as conventional green roof

materials. Hence, for this study the following materials were selected as control materials:

- substrate: ABG Geosynthetics Meadow Mix, comprised of graded clay aggregate, recycled from red brick, mixed with matured and graded green compost (called Crushed Red Brick hereinafter) (Appendix A)
- drainage layer: ABG Geosynthetics Finesse Roofdrain40, an egg-box shape polymer sheet (called Roofdrain40 hereinafter) (Appendix A)

These two specific materials were selected to replicate one of the green roof designs established in the Barking Riverside experiment as part of an EU FP7 research and innovation programme Transitioning towards Urban Resilience and Sustainability (TURAS) (University of East London, 2010). Details of this are provided in Chapter 4. The Barking Riverside experiment provides long term stormwater runoff data from green roofs of various designs. One of these designs was replicated in the laboratory experiments aiming to compare hydrological performance in the field to that recorded in the laboratory (Chapters 6 and 7).

The initial list of the alternative materials was created based on careful, critical review of the materials currently used within green roof industry as well as within the construction, agricultural and horticultural sectors (Table 3.1). Initially selected materials were assessed against selection criteria (section 3.1.1) and the materials that fit the criteria most closely were chosen, namely: Lytag, Clay and Sewage Sludge Ash Pellets (called Sewage Sludge Pellets hereinafter), Granulated Rubber and Wool-rich Carpet Shred. Other materials were subsequently disregarded as they did not meet the criteria such as not being of waste/recycling origins: rigid polyurethane foam, mineral wool, or low availability: strawboard chippings, glass aggregate. Details of the materials selected in the final stage are described in sections 3.1.2.1 to 3.1.2.4

Table 3.1 Summary of the green roof construction material selection.

Green roof layer		Initial selection	Final selection
<b>Substrate</b>	Control	Crushed Red Brick	Crushed Red Brick
	Treatment	<ul style="list-style-type: none"> <li>➤ Lytag</li> <li>➤ Sewage Sledge Pellets</li> <li>➤ Strawboard Chippings</li> <li>➤ Glass Aggregate</li> </ul>	<ul style="list-style-type: none"> <li>➤ Lytag</li> <li>➤ Sewage Sledge Pellets</li> </ul>
<b>Drainage layer</b>	Control	Roofdrain40	Roofdrain40
	Treatment	<ul style="list-style-type: none"> <li>➤ Granulated Rubber</li> <li>➤ Wool-rich Carpet Shred</li> <li>➤ Rigid Polyurethane Foam</li> <li>➤ Mineral Wool</li> </ul>	<ul style="list-style-type: none"> <li>➤ Granulated Rubber</li> <li>➤ Wool-rich Carpet Shred</li> </ul>

### 3.1.2.1 LYTAG

Lytag is a secondary aggregate manufactured from waste material from coal fired power stations, widely available in UK and Europe (Lytag, 2014). The raw material used in the production of lightweight aggregate is called pulverised fuel ash (PFA) also known as fly ash. Lytag is produced by pelletizing the ash and heating the pellets to the temperature of about 1100°C. The UK Lytag manufacturing plant near Drax Power Station, North Yorkshire diverts around 200,000 tonnes of PFA away from landfill every year (Waterman, 2012). Lytag is mainly used as a lightweight aggregate in lightweight concrete mixes and civil engineering bulk fill for backfills or road construction. Due to its free draining properties, it is also used as drainage medium. There are a very limited number of studies where Lytag was also used as substrate material in green roof designs. Graceson et al. (2013) investigated the correlation between substrate composition and water retention capabilities of green roof system with the conclusion that more detailed study of such a relation is needed.

### 3.1.2.2 SEWAGE SLUDGE PELLETS

Clay and sewage sludge ash pellets are secondary aggregates derived from clay and sewage sludge. Sewage sludge is the by-product of the sewage treatment process, available from waste water treatment works, and clay is a naturally occurring material. It has various applications in the construction industry, mainly earthworks but also clay-based construction materials such as bricks or ceramics

(Smith, 2013). Although, the processed aggregate is not currently produced in the UK, the availability of the raw materials of which Sewage Sludge Pellets are made of is very high. These raw materials are:

- **Sewage sludge**

Around 1.4 million tonnes (dry weight) of sewage sludge is produced annually in the UK (Biomass Energy Centre, 2014), of which less than 20 percent is incinerated and the remaining is used on land to improve soil nutrients levels. The by-product of sewage sludge incineration process is a sewage sludge ash (SSA), which can then be recycled for applications such as the production of lightweight aggregates.

- **Clay**

In the UK, the clay bricks industry produced about 1.5 billion bricks in 2012, consuming more than 4.5 million tonnes of materials (clays, shales, fireclays, etc.). Of this 1-2.5 million tonnes of material were excavated but not used (Smith, 2013). This material could be successfully utilised in the production of secondary aggregates.

Molineux et al. (2009) achieved promising results investigating the growth performance of green roof plants on Sewage Sludge Pellet-based substrate. The hydrological performance of substrate comprised of Sewage Sludge Pellets have, thus far, not been investigated.

### **3.1.2.3 GRANULATED RUBBER**

The main source of Granulated Rubber is waste tyres. In Europe, around 3.3 million tonnes of used tyres are generated annually (European Tyre & Rubber Manufacturers' Association, 2013). Although recycling of the waste tyres is increasing, the majority of them are still sent to landfill. There have been attempts to assess the Granulated Rubber performance as green roof construction material. Perez et al. (2012) and Vila et al. (2012) tested Granulated Rubber as a green roof drainage layer. However, only material properties and energy performance were tested with promising results. The hydrological performance of green roofs incorporating Granulated Rubber has not been studied.

### **3.1.2.4 WOOL-RICH CARPET SHRED**

Between 350,000 and 420,000 tonnes of carpet waste is buried in UK landfill sites every year (Thomas, 2010). Of this, around 100,000 tonnes is wool-rich carpet

waste (Macaulay, 2011). One of the ways that wool-rich carpet is recycled is shredded for use as fertiliser in soil. McNeil et al. (2007) investigated the effect of the wool carpet shred and soil mix on crop yield. The results were positive, showing an increase in the dry matter yield of grass grown by between 24 and 82%. In a similar study, Putwain et al. (2011) provided evidence that Wool-rich Carpet Shred releases considerable amounts of nitrogen, which support strong plant growth. There is no published research investigating the effects of using Wool-rich Carpet Shreds as a green roof construction material. However, high water absorption properties and its positive effect on plants growth makes the Wool-rich Carpet Shred a very favourable alternative to conventional material for green roof construction.

### **3.2 PROPERTIES OF THE MATERIALS**

It is anticipated that the performance of the green roof depends on selection of the green roof materials (Czemiel Berndtsson, 2010, Eksi and Rowe, 2016, Molineux et al., 2009). Each material carries a specific combination of mechanical, physical, and chemical properties. Worldwide, the properties of green roof materials are assessed in accordance with guidelines published by the German Landscape Research, Development and Construction Society - Forschungsgesellschaft Landschaftsentwicklung Landschaftsbau (FLL). The guidelines include information on testing of a green roof material properties as well as recommendations that are used to approve and certify substrate and drainage layer for green roof construction. FLL lists the following characteristics to be tested, as compulsory (FLL, 2008):

- Densities: bulk and dry
- Granulometric distribution
- Organic content
- Water permeability
- Water storage capacity/maximum water capacity
- Air content
- pH value
- Salt content
- Nutrient content

This study concentrated on the following physical properties, as they are those most likely to influence the hydrological performance of green roofs:

- Densities: bulk, particle, saturated
- Particle size distribution
- Organic matter content
- Permeability
- Water absorption, as substitution to water storage capacity/maximum water capacity tests
- Porosity and void ratio
- Maximum capillary rise

### 3.2.1 SELECTION OF THE TEST METHODS

Several researchers worldwide, such as Voyde et al. (2010), conducted material characteristics tests based on procedures recommended by FLL. Others followed national standards such as British Standards, BS EN 13041: Soil improvers and substrate (Graceson et al., 2013), Australian Standards, AS 3743-2003: Australian Standards for potting mixes (Vijayaraghavan and Joshi, 2015), European Standards EN 1097-3: Test for mechanical and physical properties of aggregates. Part 3: Determination of loose bulk density and voids (Ondoño et al., 2014).

The methods selected for the purpose of this research were chosen from techniques described in British Standards. Material properties and the corresponding standards used for their testing, are summarised in the Table 3.2 and described in section 3.2.3.

*Table 3.2 British Standards describing the test methods for relevant material properties.*

<b>Material Property</b>	<b>Standard</b>
<b>Particle Size Distribution</b>	BS 1377-2:1990
<b>Loose Bulk Density</b>	BS 1377-2:1990
<b>Particle Density</b>	BS 1377-2:1990
<b>Water Permeability</b>	BS 1377-5:1990
<b>Water Absorption</b>	BS EN 1097-6:2013
<b>Organic Matter Content</b>	BS EN 13039:2011

The procedures for the tests of the material properties mentioned in Table 3.2 are also listed in the FLL guidelines (FLL, 2008). However, the FLL guidelines are based on German Standards and codes, involving, in many cases, specific equipment that is not widely available in the UK. For that reason, suitable British Standard test procedures were identified and used for this investigation. As such, these selections could be used as recommendations for UK testing procedures that could support the standardisation and mainstreaming of green roof installation in the UK.

There are various means of testing green roof materials, depending on the context or the application they are used in, such as horticulture or engineering. There are also several British Standards describing similar tests depending on the use of the material. When evaluating hydrological performance of green roofs, the properties of the materials should be considered from an engineering viewpoint. The effects of the water in soil masses are known and widely investigated by engineers, whose main interest is in how the behaviour, of different soils, varies with water content and/or water flow within the soil. For that reason, the choice of the material properties testing methods was mostly based on soil mechanics techniques for civil engineering. There are further benefits in using such techniques. The required tests can be carried out in accredited soil mechanics laboratories in the UK with the equipment and robust expertise allowing the material tests to be conducted in an efficient and timely manner. Using existing techniques and standards to assess green roof material properties eliminates the need for additional equipment, staff training and accreditation certificates. This would be an incentive in supporting green roof installation in the UK and allow the UK environment to benefit from the many advantages that green roofs offer. However, the assessment of properties such as water absorption or organic matter content are not covered in soil mechanics codes.

The water absorption test selected was based on techniques used to assess mechanical and physical properties of construction aggregates for structural purposes. Green roof substrate materials, selected in this study, are made of porous aggregates, capable of sealing water within. Soil mechanics deals with soil water content in general, without differentiating between water absorbed and water situated between the soil grains, hence the need for separating the two for this study.

Organic content was determined using methods applicable to soil improvers and growing media. These methods were selected as organic matter is added to substrate to improve plant performance rather than influence the hydrological properties of the green roofs.

The tests were divided into two stages, first stage - sample preparation including organic matter content testing and second stage - material physical properties assessment, which included the remaining material properties tests and evaluation of derived properties. Table 3.3 presents a summary of the stages, material properties, corresponding British Standards and the materials excluded from tests. The materials were excluded from test if there were health and safety issues such as oven drying of Granulated Rubber or the test was only applicable to a certain type of material. For example, sieve analysis is applicable only to granular material.

*Table 3.3 Summary of material properties, corresponding British Standards describing test of material properties and materials tested.*

<b>Stage</b>	<b>Material Property</b>	<b>Standard</b>	<b>Materials Excluded from Tests/Assessment</b>
Stage I: Sample Preparation	Organic Matter Content	BS EN 13039:2011	Granulated Rubber, Wool-rich Carpet Shred
Stage II: Material Testing	Particle Size Distribution	BS 1377-2:1990	Wool-rich Carpet Shred
	Loose Bulk Density	BS 1377-2:1990	None
	Particle Density	BS EN 1097-6:2013	None
	Water Permeability	BS 1377-5:1990	None
	Water Absorption	BS EN 1097-6:2013	Granulated Rubber
	Void Ratio and Porosity	Derived property	None
	Saturated Density	Derived property	None
	Maximum Capillary Rise	Derived property	Wool-rich Carpet Shred

### **3.2.2 SAMPLE PREPARATION – ADJUSTMENT OF ORGANIC MATTER CONTENT IN SUBSTRATE MATERIALS**

Substrate materials (Crushed Red Brick, Lytag and Sewage Sludge Pellets) were amended by adding organic matter (compost) prior to the assessment of their properties. This process was carried out in three steps: initial organic matter content assessment, determination of the amount of supplementary organic matter and final organic matter content assessment.

#### **3.2.2.1 DETERMINATION OF THE INITIAL ORGANIC MATTER CONTENT**

The determination of the organic matter of selected substrate materials was carried out according to BS EN 13039:2011. This standard describes the procedure for determining the proportion of organic matter, by mass, that is lost from a soil by ignition at a specified temperature.

The organic matter of the following materials was determined: Crushed Red Brick, Lytag, Sewage Sludge Pellets, Humost (an organic soil conditioner), and peat free compost (material commercially available). Humost and compost were assessed as materials that could balance organic matter in the remaining substrate materials.

Firstly, each of the materials was oven-dried at a temperature of  $(105 \pm 5)^\circ\text{C}$  for at least 24 hours. Then three random samples of each material were taken, ground, sieved through a 2mm sieve and placed in crucibles (Figure 3.1 (a)). All samples were weighed before being combusted at  $(450 \pm 25)^\circ\text{C}$  for total of 7 hours in a muffle furnace (Figure 3.1 (b)).

The organic matter content was calculated as the loss of mass on ignition, as a percentage of the mass of the dried sample:

$$W_{om} = \frac{m_1 - m_2}{m_1 - m_0} \times 100 \quad (3.1)$$

Where  $W_{om}$  is the organic matter content (%) m/m,  $m_0$  is the mass of the crucible (g),  $m_1$  is the mass of the crucible and the sample after drying (g),  $m_2$  is the mass of the crucible and the sample after combustion (g).

The results of the initial organic matter content tests are presented in Table 3.4.



(a) Material samples

(b) Material samples during the test

Figure 3.1 Loss on ignition test: (a) Crushed Red Brick, Lytag, Sewage Sludge Pellets and compost samples in crucibles (b) samples were combusted at  $(450 \pm 25) ^\circ\text{C}$  in muffle furnace.

Table 3.4 Results of the loss on ignition test, initial organic matter content.

	Initial organic matter - Mean (%)	Standard deviation (%)
<b>Humost</b>	24.91	0.81
<b>Compost</b>	58.16	1.75
<b>Crushed Red brick</b>	3.23	0.32
<b>Sewage Sludge Pellets</b>	3.39	0.04
<b>Lytag</b>	2.56	0.09

### 3.2.2.2 DETERMINATION OF THE AMOUNT OF SUPPLEMENTARY ORGANIC MATTER

The amount of supplementary organic matter was determined based on following objectives:

- to achieve an equal amount of organic matter in substrate mixes
- to achieve the quantity of the organic matter content determined for control substrate material, Crushed Red Brick:  $(3.23 \pm 0.32) \%$  (Table 3.4)

Eliminating differences in organic matter content between substrate materials resulted in reduction of the factors affecting hydrological performance of the green roofs in laboratory experiment (Chapter 6).

Based on the results of initial organic matter content determination only Lytag required organic matter content adjustment. It was amended by adding compost to the aggregate (as opposed to Humost, since compost had a higher organic

content than Humost). The Sludge Pellet organic matter content was acceptable and did not need correction. Subsequently, Lytag was sampled and tested again following previously described procedure.

### 3.2.2.3 DETERMINATION OF THE FINAL ORGANIC MATTER CONTENT

The results of determination of final organic matter content are presented in the Table 3.5.

*Table 3.5 Results of the loss on ignition test, final organic matter content.*

	Final organic matter - Mean (%)	Standard deviation (%)
<b>Crushed Red brick</b>	3.23	0.32
<b>Sewage Sludge Pellets</b>	3.39	0.04
<b>Lytag</b>	3.46	0.14

Substrate materials with balanced organic matter content as well as drainage layer materials were subsequently tested to assess other properties including densities, porosity and void ratio, permeability, water absorption and maximum capillary rise.

The Red Crush Brick, Lytag and Sewage Sludge Pellets will be referring to substrate mix (aggregate and organic matter) hereinafter.

### 3.2.3 MATERIAL PROPERTIES PROCEDURES

The list of the tests carried out, corresponding British Standards and the materials tested is presented in Table 3.3.

#### 3.2.3.1 PARTICLE SIZE DISTRIBUTION

Particle size distribution is one of the most important physical characteristics of soil. The soil classification is based mainly on the particle size distribution. Many geotechnical and geohydrological properties such as permeability, compressibility or frost susceptibility of soils are also related to the particle size distribution.

In the case of coarse soils, the particle size distribution is determined through sieve analysis and that method was selected to investigate the chosen aggregates.

The tests were carried out according to the British Standard BS 1377-2:1990 for all aggregate samples. Firstly, each representative sample was oven dried, then passed through a nest of standard test sieves (mm): <0.063, 0.150, 0.212, 0.300, 0.425, 0.600, 1.18, 4.75 and 9.5, which were arranged in descending order of the mesh size, leading to soil subdivision into discrete classes of the particle sizes. The mass of the soil retained on each of the sieves was determined and the cumulative percentage of the sample mass passing each sieve was calculated. Based on the calculation a grading curve (semi-logarithmic curve) was plotted, analysed, and interpreted.

### 3.2.3.2 LOOSE BULK DENSITY

Density represents the relationship between the quantity of the material and the amount of space it occupies. The density evaluated in the study was loose bulk density, specifically the case of dry loose bulk density (also called dry density). The test was carried out according to the British Standard BS 1377-2:1990. The bulk density is the ratio of the total mass (mass of solids and mass of water) to the total volume. Thus, bulk density was determined by filling a mould of known volume and mass with loose material sample and then weighing (Figure 3.2). The loose bulk density was calculated using following formula:

$$\rho_b = \frac{M}{V} \quad (3.2)$$

Where  $\rho_b$  is bulk density ( $\text{Mg/m}^3$ ),  $M$  is total mass of sample ( $\text{Mg}$ ),  $V$  is total volume of sample ( $\text{m}^3$ ).

The specific case of dry bulk density occurs when the water content (mass of water in the sample) is equal to zero, thus:  $\rho_d = \rho_b$ , where  $\rho_d$  is dry loose bulk density ( $\text{Mg/m}^3$ ) and  $\rho_b$  is bulk density ( $\text{Mg/m}^3$ ). In this study, all tested green roof materials were oven dried prior to the tests, hence the density evaluated was dry loose bulk density.



Figure 3.2 Loose bulk density test: standard mould filled with Wool-rich Carpet Shred.

### 3.2.3.3 PARTICLE DENSITY AND WATER ABSORPTION

The particle density of a soil is the ratio of the mass of the known volume of the material to the mass of the same volume of water. The water absorption is defined as the mass of absorbed water expressed as a percentage of the oven-dried mass of the aggregate/material sample. The tests were carried out according to the British Standard BS EN 1097-6:2000.

Particle density and water absorption are determined using a pycnometer. The sample of the material was placed in a pycnometer and weighed. The pycnometer with sample was filled with de-aired water and left for 24 hours to ensure the entire material was fully saturated (Figure 3.3). After 24h, the remaining air bubbles were removed using a vacuum pump. The pycnometer was topped-up with water and weighed again. Subsequently the pycnometers were emptied, refilled with de-aired water, and weighed again. Finally, the samples of each material were surface dried and weighed, next oven dried and re-weighed. The particle density was calculated using following formula:

$$\rho_s = \frac{M_2 - M_1}{(M_4 - M_1) - (M_3 - M_2)} \rho_w \quad (3.3)$$

Where  $\rho_s$  is particle density ( $\text{Mg/m}^3$ ),  $M_1$  is mass of empty dry pycnometer (g),  $M_2$  is mass of pycnometer with dry sample (g),  $M_3$  is mass of pycnometer, material and water (g),  $M_4$  is mass of pycnometer filled with water only (g),  $\rho_w$  is water density ( $\text{Mg/m}^3$ ).

The water absorption was calculated using following formula:

$$w_s = \frac{M_1 - M_2}{M_2} \times 100 \quad (3.4)$$

Where  $w_s$  is water absorption (%),  $M_1$  is mass of surface dried material (g),  $M_2$  is mass of the oven dried material (g).

The collected data was analysed and the particle density and water absorption was determined.

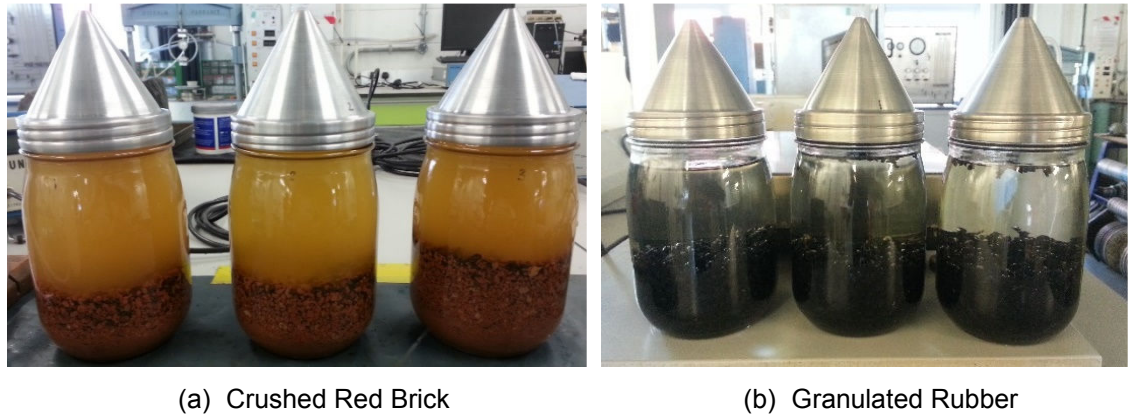


*Figure 3.3 Particle density and water absorption test: (a) three pycnometers filled with Crushed Red Brick (b) three pycnometers filled with Granulated Rubber.*

#### **3.2.3.4 COEFFICIENT OF PERMEABILITY**

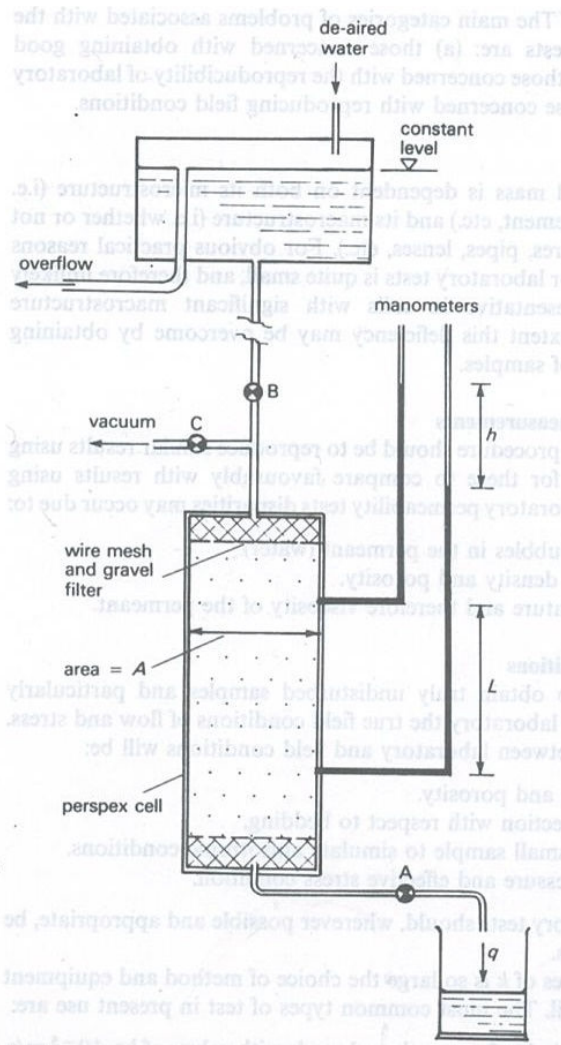
Permeability is the ability of a material to allow the passage of a fluid and is one of the crucial properties of the green roof substrate and drainage layer. The material permeability is affected by several factors such as porosity of the soil, particle-size distribution or the shape and orientation of soil particles and it is represented by the coefficient of permeability.

The coefficient of permeability of the studied materials was determined using the constant head permeability test according to BS 1377-5:1990. The sample was placed in the permeameter cell, and de-aired water was run through the soil (Figure 3.4). Once a steady state had been reached, the flow rate was determined and the two manometers levels noted. The procedure was repeated for different flow rates. The coefficient of permeability was calculated using following formula:

$$k = \frac{QL}{thA} \quad (3.5)$$

Where  $k$  is coefficient of permeability (m/s),  $Q$  is volume of water ( $m^3$ ) collected in time  $t$  (s),  $L$  is distance between manometer tapping points (m),  $h$  is difference in manometer levels (m),  $A$  is cross-sectional area of sample ( $m^2$ ).

Subsequently, the data was analysed and the coefficient of permeability determined.



(a) Constant head permeability apparatus



(b) Sewage Sludge Pellets



(c) Wool-rich Carpet Shred

Figure 3.4 Constant head permeability test: (a) apparatus diagram (Whitlow, 1995) (b) Sewage Sludge Pellets test (c) Wool-rich Carpet Shred test

### 3.2.3.5 VOID RATIO AND POROSITY

Knowledge of the particle density and the bulk density of materials allows other important properties, such as void ratio and porosity, to be calculated. Void ratio was calculated using following formula (Whitlow, 1995):

$$e = \frac{\rho_s}{\rho_d} - 1 \quad (3.6)$$

Where  $e$  is void ratio (-),  $\rho_s$  is particle density ( $\text{Mg/m}^3$ ),  $\rho_d$  is dry bulk density ( $\text{Mg/m}^3$ ).

Porosity was calculated using following formula (Whitlow, 1995):

$$n = \frac{e}{1 + e} \quad (3.7)$$

Where n is porosity (-), e is void ratio (-).

#### **3.2.3.6 SATURATED DENSITY**

Saturated density is the bulk density of the soil when saturated. The saturated density was calculated using following formula (Whitlow, 1995):

$$\rho_{sat.} = \frac{G_s + e}{1 + e} \rho_w \quad (3.8)$$

Where  $\rho_{sat.}$  is saturated density ( $Mg/m^3$ ),  $G_s$  is grain specific gravity (-), e is void ratio (-),  $\rho_w$  is water density ( $Mg/m^3$ ).

#### **3.2.3.7 MAXIMUM CAPILLARY RISE**

The estimation of the maximum capillary rise was done based on the material characteristics, such as void ratio and effective size (grading characteristic). The following formula was used to calculate maximum capillary rise (Whitlow, 1995):

$$h_c = \frac{C}{ed_{10}} \quad (3.9)$$

Where  $h_c$  is maximum capillary rise (mm), e is void ratio (-),  $d_{10}$  is effective size (mm),  $C=30mm^2$ .

#### **3.2.3.8 ANALYSIS METHODS**

Primary data obtained through the laboratory experiments were analysed to assess the suitability and performance of the chosen materials and their correlation to the hydrological performance of green roofs, which will be elaborated in greater details in Chapter 6.

Data analysis was carried out in accordance with the appropriate British Standards (Table 3.3). When required, the average of the results of multiple tests were taken. Finally, the results of the tests for different materials were compared and discussed.

#### **3.2.4 DATA ANALYSIS AND RESULTS**

This section presents the results from laboratory tests of material properties and the calculations of properties derived from the ones tested. Examples of the

detailed calculations of these properties are provided for the Crushed Red Brick. For all the materials, the final results are presented.

### 3.2.4.1 DETAILED CALCULATIONS OF MATERIAL PROPERTIES - CRUSHED RED BRICK

The Crushed Red Brick sample was visually inspected prior to further laboratory tests (Table 3.6). The results of sieve analysis test are presented in Table 3.7 and Figure 3.6.

#### 3.2.4.1.1 LOOSE BULK DENSITY

The loose bulk density of the Red Crushed Brick was calculated using formula 3.2:

$$\rho_b = \frac{860.67 \text{ g}}{1002.32 \text{ cm}^3} = 0.86 \frac{\text{g}}{\text{cm}^3} = 0.86 \frac{\text{Mg}}{\text{m}^3}$$

The test was repeated on three samples. The average of the three readings was taken as a final value of the loose bulk density for all tested materials.

#### 3.2.4.1.2 PARTICLE DENSITY

The particle density of the Red Crushed Brick was calculated using formula 3.3:

$$\rho_s = \frac{877.7 - 493.1}{(1791.0 - 493.1) - (2021.4 - 877.7)} \frac{\text{Mg}}{\text{m}^3} = 2.49 \frac{\text{Mg}}{\text{m}^3}$$

The test was repeated on three samples. The average of the three readings was taken as a final value of the particle density for all tested materials.

#### 3.2.4.1.3 WATER ABSORPTION

The water absorption of the Crushed Red Brick was calculated using formula 3.4:

$$w_s = \frac{169.3 - 131.1}{131.1} \times 100\% = 28.94\%$$

The test was repeated on three samples. The average of the three results was taken as a final value of water absorption for all tested materials.

#### 3.2.4.1.4 COEFFICIENT OF PERMEABILITY

Coefficient of permeability of Crushed Red Brick was calculated using formula 3.5:

$$k = \frac{460 * 10}{30 * 4.3 * 45.36} \frac{\text{cm}}{\text{s}} = 0.79 \frac{\text{cm}}{\text{s}}$$

The test was repeated minimum 10 times. The average of the readings was taken as a final value of the coefficient of permeability for all tested materials.

#### 3.2.4.1.5 VOID RATIO AND POROSITY

Void ratio of the Crushed Red Brick was calculated using equation 3.6:

$$e = \frac{2.47}{0.86} - 1 = 1.87$$

Porosity of the Red Crushed Brick was calculated using equation 3.7:

$$n = \frac{1.87}{1 + 1.87} = 0.65$$

Average values of the particle density and loose bulk density were considered in the calculation of the void ratio and porosity of all materials.

#### 3.2.4.1.6 SATURATED DENSITY

Saturated density of the Crushed Red Brick was calculated using equation 3.8:

$$\rho_{sat.} = \frac{2.47 + 1.87}{1 + 1.87} * 1.00 \frac{Mg}{m^3} = 1.51 \frac{Mg}{m^3}$$

Average values of particle density were considered in the calculation of the void ratio and porosity of all materials.

#### 3.2.4.1.7 MAXIMUM CAPILLARY RISE

Maximum capillary rise of the Crushed Red Brick was calculated using equation 3.9:

$$h_c = \frac{30}{1.87 * 0.2} mm = 80.10 mm$$

The summary of physical characteristics of the Crushed Red Brick are presented in Table 3.7.

### 3.2.4.2 PROPERTIES OF SUBSTRATE MATERIALS: CRUSHED RED BRICK, LYTAG AND SEWAGE SLUDGE PELLETS

All substrate materials were inspected visually before laboratory tests were conducted (Figure 3.5 and Table 3.6). The results from sieve analysis tests for substrate materials are presented in Table 3.7 (grading and classification) and Figure 3.6 to 3.8 (particle size distribution charts).

The summary of the characteristics of substrate materials: Crushed Red Brick, Lytag and Sewage Sludge Pellets, as well as FLL recommended limits are presented in Table 3.7.

*Table 3.6 The results of the visual inspection of the substrate materials: Crushed Red Brick, Lytag and Sewage Sludge Pellets.*

Substrate material	Description
<b>Crushed Red Brick</b>	red sand, some fine gravel, trace fines, well graded, angular, dry (Figure 3.5 (a))
<b>Lytag</b>	grey gravel, some medium sand, trace fines, well graded, sub-angular, dry (Figure 3.5 (b))
<b>Sewage Sludge Pellets</b>	brownish grey gravel, some coarse sand, trace fines, poorly graded, rounded, dry (Figure 3.5 (c))



(a) Crushed Red Brick



(b) Lytag



(c) Sewage Sludge Pellets

*Figure 3.5 Substrate materials: (a) Crushed Red Brick: conventional substrate, widely used in the UK (b) Lytag: selected alternative material (c) Sewage Sludge Pellets: selected alternative material.*

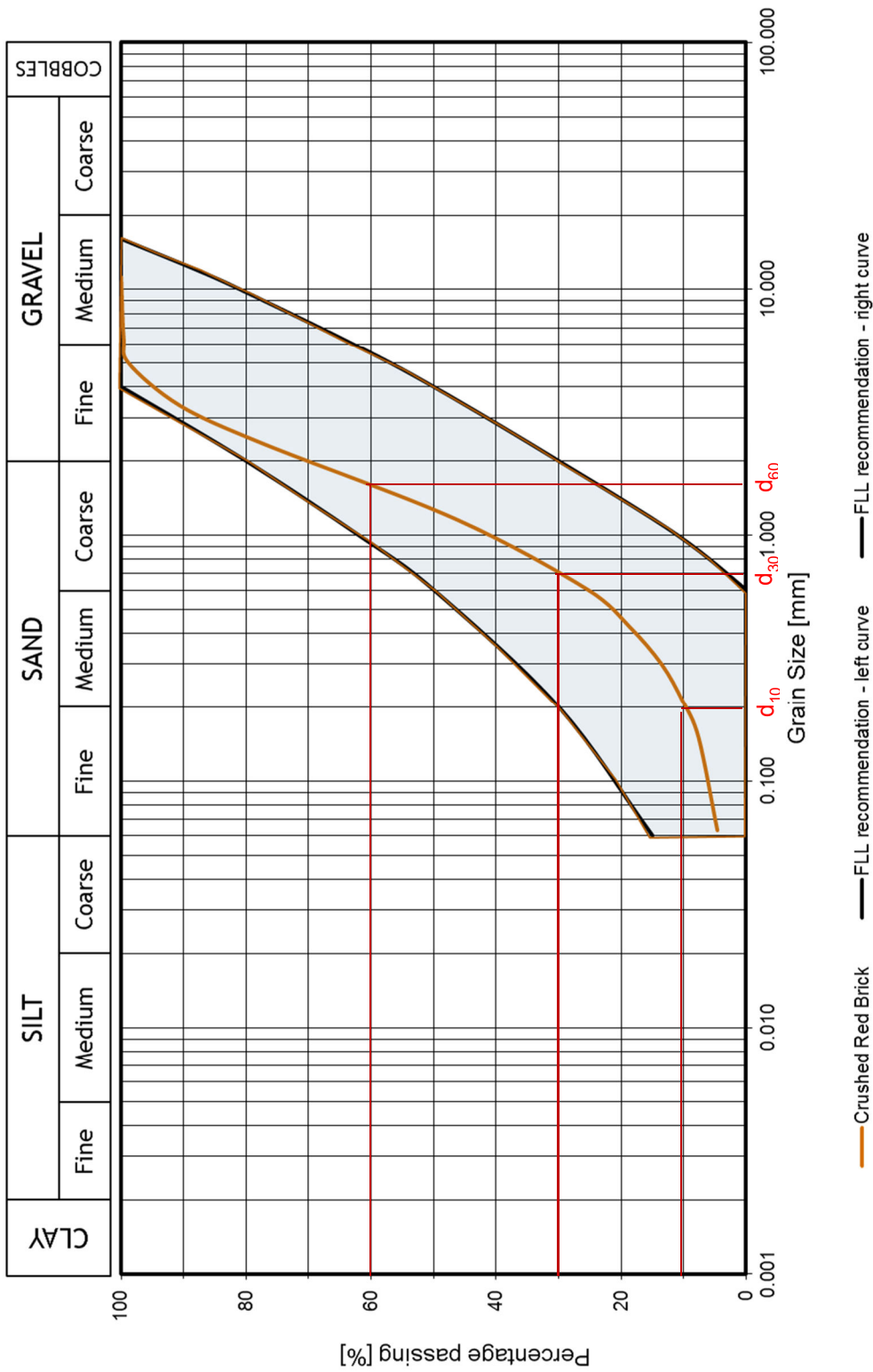


Figure 3.6 Particle size distribution (PSD) curve for Crushed Red Brick, including PSD envelope for extensive substrates recommended by FLL.

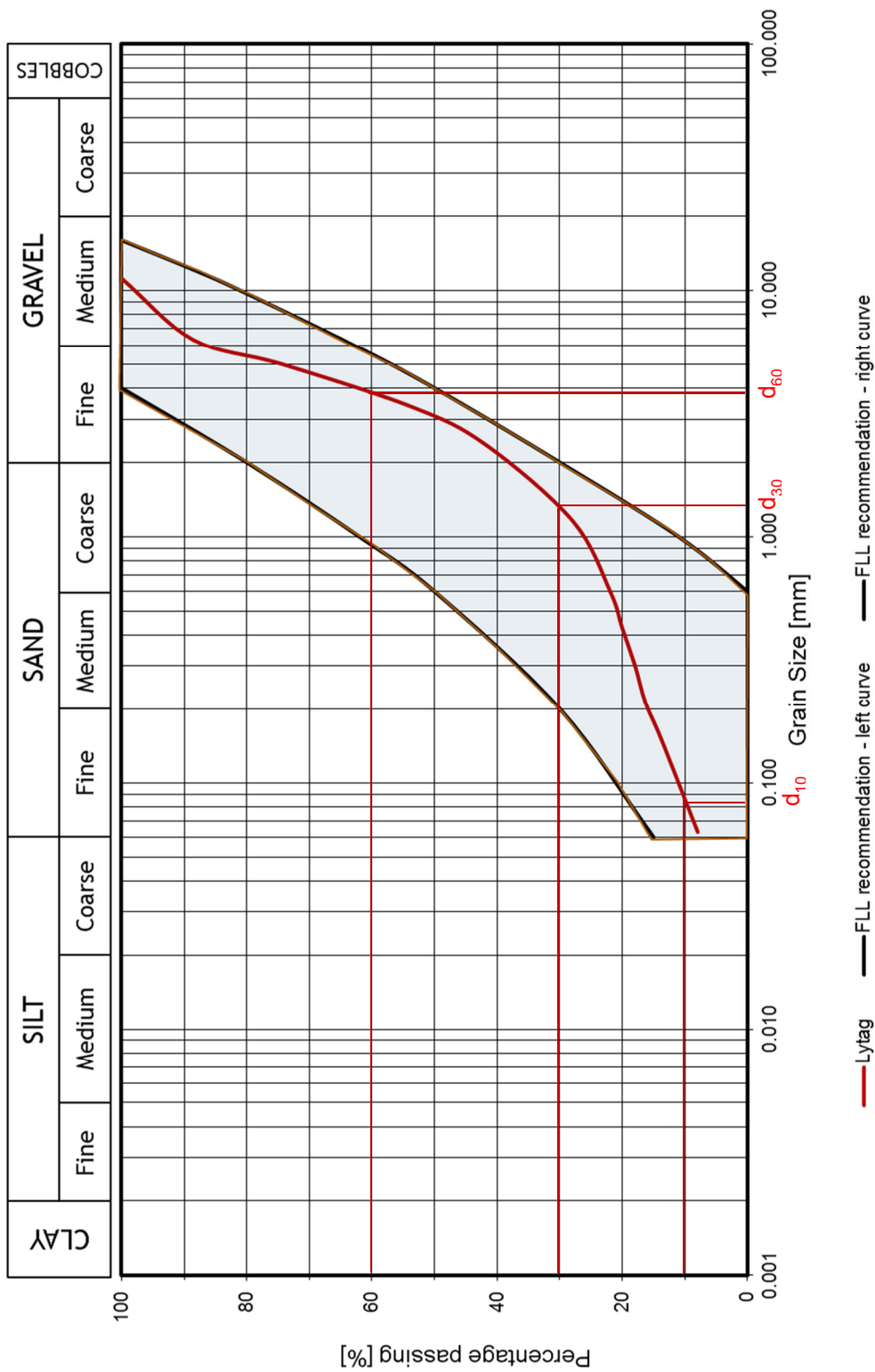


Figure 3.7 Particle size distribution (PSD) curve for Lytag, including PSD envelope for extensive substrates recommended by FLL.

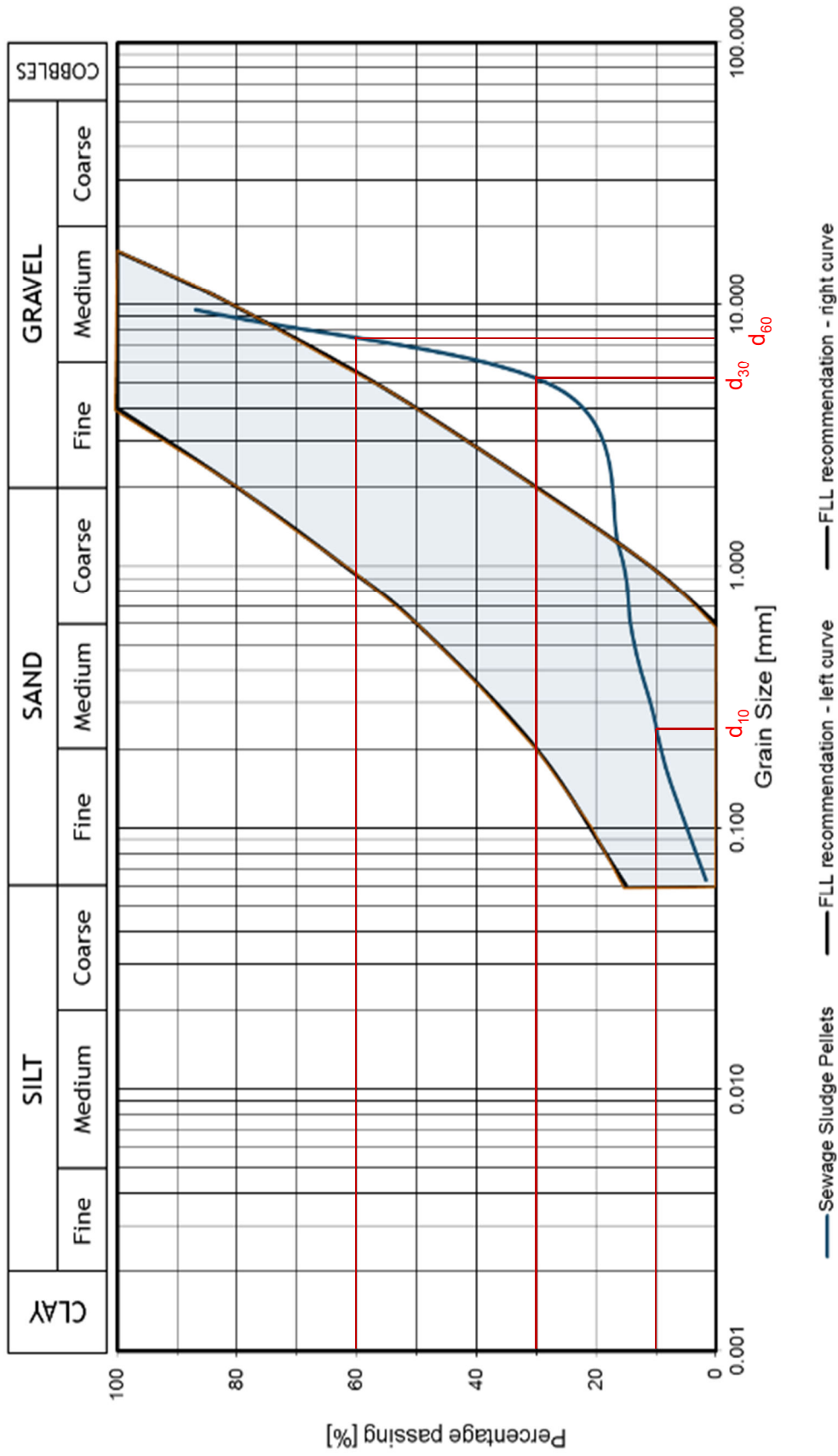


Figure 3.8 Particle size distribution (PSD) curve for Sewage Sludge Pellets, including PSD envelope for extensive substrates recommended by FLL.

Table 3.7 Summary of the Crushed Red Brick, Lytag and Sewage Sludge Pellets properties and corresponding values recommended by FLL.

Material Property	Crushed Red Brick	Lytag	Sewage Sludge Pellets	FLL recommended values
<b>Particle Size Distribution</b>	Silt and Clay: 5% Sand: 65% Gravel: 30%	Silt and Clay: 8% Sand: 30% Gravel: 62%	Silt and Clay: 2% Sand: 16% Gravel: 82%	Silt and Clay: 0-15% Sand: 40-85% Gravel: 60-0% (d>4mm: ≤50%)
<b>Grading Characteristics (mm)</b>	d <sub>10</sub> =0.20 d <sub>30</sub> =0.70 d <sub>60</sub> =1.5	d <sub>10</sub> =0.08 d <sub>30</sub> =1.3 d <sub>60</sub> =3.7	d <sub>10</sub> =0.23 d <sub>30</sub> =5.2 d <sub>60</sub> =7.3	Not specified
<b>Material Classification</b>	well-graded gravelly SAND	well-graded silty sandy GRAVEL	gap-graded sandy GRAVEL	Not specified
<b>Loose Bulk Density - Dry, ρ<sub>b</sub> (Mg/m<sup>3</sup>)</b>	0.86	0.78	0.91	Not specified
<b>Particle Density, ρ<sub>s</sub> (Mg/m<sup>3</sup>)</b>	2.47	1.96	2.05	Not specified
<b>Void Ratio, e (-)</b>	1.87	1.51	1.25	Not specified
<b>Porosity, n (-)</b>	0.65	0.60	0.56	Not specified
<b>Maximum Capillary Rise, h<sub>c</sub> (mm)</b>	80.21	239.37	104.35	Not specified
<b>Saturated Density, ρ<sub>sat</sub>. (Mg/m<sup>3</sup>)</b>	1.51	1.38	1.47	Not specified
<b>Water Absorption, w<sub>s</sub> (%)</b>	30.41	26.21	20.35	Maximum Water Capacity: 35 - 65
<b>Coefficient of Permeability, k (m/s)</b>	8.13 x 10 <sup>-3</sup>	4.84 x 10 <sup>-2</sup>	9.35 x 10 <sup>-2</sup>	1.00 x 10 <sup>-5</sup> < k < 4.2 x 10 <sup>-2</sup>

### 3.2.4.3 PROPERTIES OF SELECTED DRAINAGE LAYER MATERIALS: ROOFDRAIN40, GRANULATED RUBBER AND WOOL-RICH CARPET SHRED

All substrate materials were inspected visually before laboratory tests were carried out (Figure 3.9 and Table 3.8). The results from sieve analysis tests for Granulated Rubber are presented in Table 3.9 (grading and classification) and Figure 3.10 (particle size distribution chart). Due to the fibre-like structure of the Wool-rich Carpet Shred (Table 3.8 and Figure 3.9), the sieve analysis was not conducted. Also, the determination of maximum capillary rise was not carried out since it requires  $d_{10}$  value, the result of sieve analysis.

The summary of the characteristics of drainage layer materials: Roofdrain40 (based on manufacturer's specification, Appendix A), Granulated Rubber, Wool-rich Carpet Shred, as well as FLL recommended limits are presented in Table 3.9.

*Table 3.8 The description of drainage layer materials (Roofdrain40, Granulated Rubber and Wool-rich Carpet Shred) based on the visual inspection.*

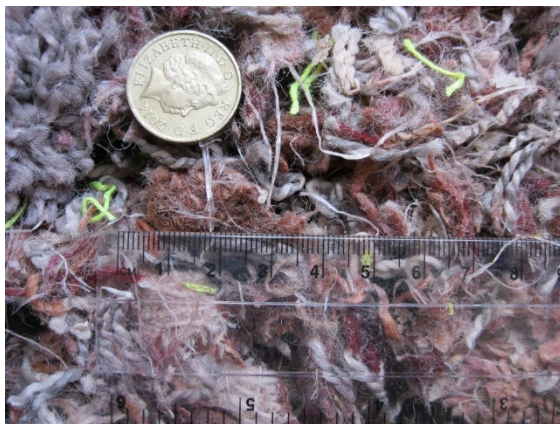
<b>Substrate material</b>	<b>Description</b>
<b>Roofdrain40</b>	black, "egg-box" shaped, polymer sheet (Figure 3.5 (a))
<b>Granulated Rubber</b>	black gravel, trace sand, no fines, poorly graded, angular, dry (Figure 3.5 (b))
<b>Wool-rich Carpet Shred</b>	reddish brown, fibre-like structure lumps (Figure 3.5 (c))



(a) Roofdrain40



(b) Granulated Rubber



(c) Wool-rich Carpet Shred

*Figure 3.9 Drainage layer materials: (a) Roofdrain40: conventional drainage layer, widely used in the UK (b) Granulated Rubber: selected alternative material (c) Wool-rich Carpet Shred: selected alternative material.*

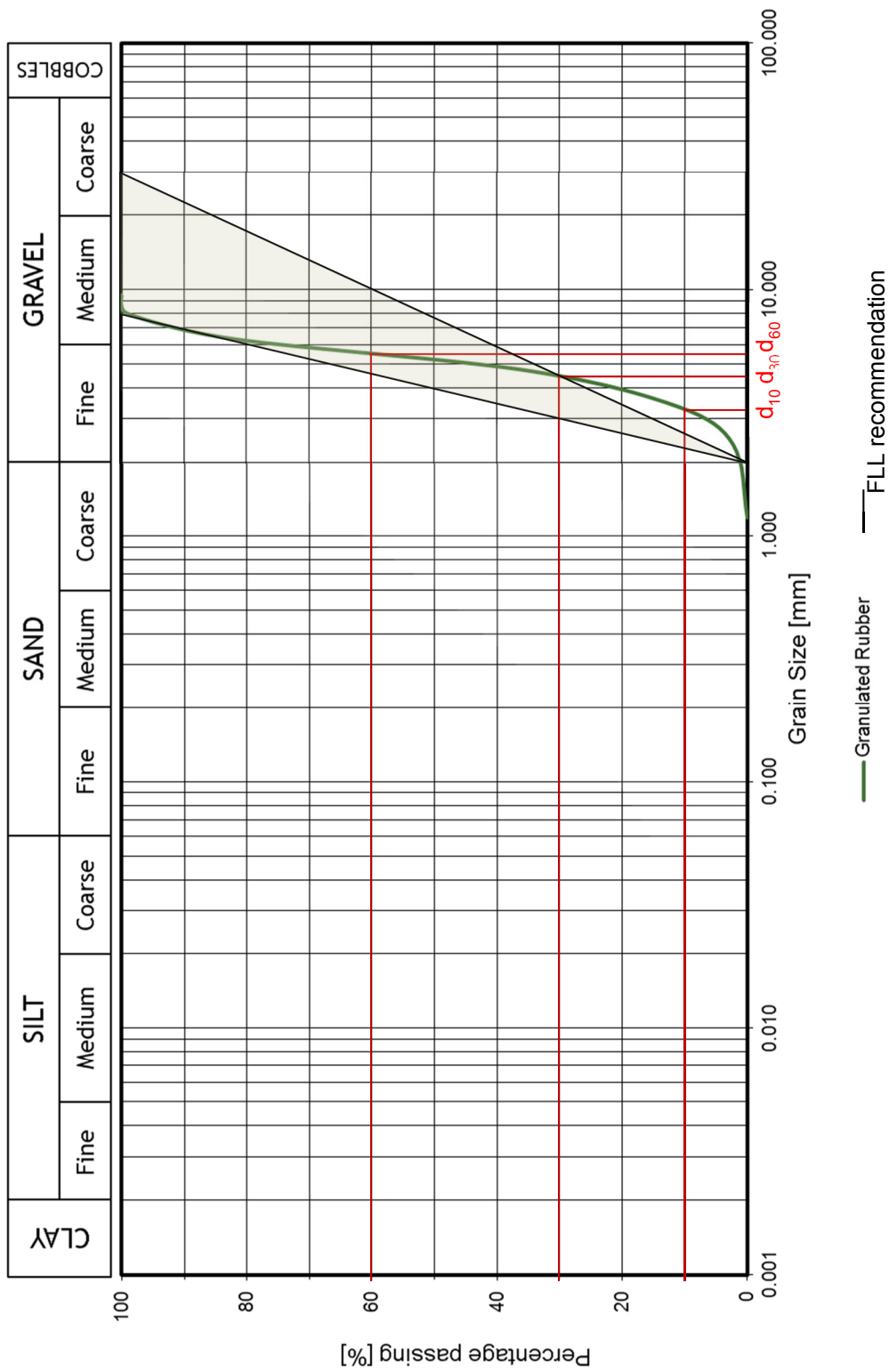


Figure 3.10 Particle size distribution (PSD) curve for Granulated Rubber, including PSD envelope for drainage layer recommended by FLL

Table 3.9 Summary of the Roofdrain40, Granulated Rubber and Wool-rich Carpet Shred properties and corresponding values recommended by FLL.

Material Property	Roofdrain40	Granulated Rubber	Wool-rich Carpet Shred	FLL recommended values
<b>Particle Size Distribution</b>	NA	Silt and Clay: 0% Sand: 1% Gravel: 99%	NA	between 2/8 mm and 2/12 mm for the course depth 4-10 cm, Silt and Clay: ≤10%
<b>Grading Characteristics (mm)</b>	NA	d <sub>10</sub> =3.2 d <sub>30</sub> =4.3 d <sub>60</sub> =5.4	NA	Not specified
<b>Material Classification</b>	NA	poorly (uniformly) - graded GRAVEL	NA	NA
<b>Loose Bulk Density - Dry, pb (Mg/m<sup>3</sup>)</b>	0.064	0.48	0.07	Not specified
<b>Particle Density, ps (Mg/m<sup>3</sup>)</b>	Not given	1.12	0.76	Not specified
<b>Void Ratio, e (-)</b>	NA	1.33	9.86	Not specified
<b>Porosity, n (-)</b>	NA	0.57	0.91	Not specified
<b>Maximum Capillary Rise, hc (mm)</b>	NA	7.05	NA	Not specified
<b>Saturated Density, psat. (Mg/m<sup>3</sup>)</b>	0.415	1.05	0.98	Not specified
<b>Roofdrain40: when fully filled with water</b>				
<b>Water Absorption, ws (%)</b>	NA	negligible	295.82	Not specified
<b>Coefficient of Permeability, k (m/s) or Water Flow Normal to the Plane (m<sup>3</sup>/m<sup>2</sup>s)</b>	1.40 x 10 <sup>-3</sup>	1.01 x 10 <sup>-1</sup>	1.16 x 10 <sup>-2</sup>	k > 3.0 x 10 <sup>-3</sup>
<b>Water Reservoir Volume (l/m<sup>2</sup>)</b>	14	NA	NA	NA

### **3.2.5 DISCUSSION**

Determination of the soil properties is paramount for civil engineers. Engineering analysis and design require assessment of those properties and the relationships between them (Whitlow, 1995). The properties are analysed collectively, as they are interconnected to each other (section 3.2.3). A similar approach should be employed for the assessment of the hydrological performance of the green roofs. However, many researchers such as Stovin et al. (2012) or Razzaghmanesh and Beecham (2014) did not include characteristics of green roof materials. Others, like Harper et al. (2015), determined material properties but did not attempt to assess the relationships between them or their effect on green roof hydrological performance. In this study, an integrated approach to material properties analysis was employed. The properties of each tested material were discussed individually and collectively in sections 3.2.5.1 to 3.2.5.7.

#### **3.2.5.1 CRUSHED RED BRICK**

Based on the sieve analysis results, the Crushed Red Brick was described as well-graded gravelly sand. According to Whitlow (1995), gravel sand mixtures have good drainage, with permeability coefficient values between  $10^{-2}$  and  $10^{-4}$  m/s. This was confirmed by the permeability test, with the result of  $k=8.13 \times 10^{-3}$  m/s (Table 3.7).

The bulk density of the Crushed Red Brick (loose, dry material) was  $0.86 \text{ Mg/m}^3$ , the particle density was  $2.47 \text{ Mg/m}^3$ , and the saturated density was  $1.51 \text{ Mg/m}^3$  (Table 3.7). The densities are necessary to assess the load imposed by the green roof to the building structure, especially the saturated density which results in the maximum load. The dry density impacts the material transportation and the installation process. A depth of 100 mm of Crushed Red Brick would apply a load of  $0.84 \text{ kN/m}^2$  when dry and  $1.48 \text{ kN/m}^2$  when saturated to the supporting structure. For comparison, the standard imposed load to roofs not accessible for normal maintenance and repair is  $0.6 \text{ kN/m}^2$  (roof slope  $<30^\circ$ ) (British Standards Institution, 2002).

The porosity of the Crushed Red Brick (loose material) is  $n=0.65$ , which is at the upper limit of the typical values for soil porosities (0.3 – 0.7) (Nimmo, 2004). The volume of voids represents 65% of the total volume. The voids could be filled with air and/or water available to plants and necessary for healthy plant growth. The

soil compaction decreases soil porosity and negatively impacts on the ability of soil to provide oxygen and water to plants. The character of the pores is also important as it affects the soil water content and movement as well as root growth (Gardner et al., 1999). The larger the voids the higher the soil permeability, hence the water is not retained within the soil but rather drained. The size of the pores is related to the grading of the material. Well-graded materials have much smaller voids as opposed to poorly-graded (Figure 3.11).

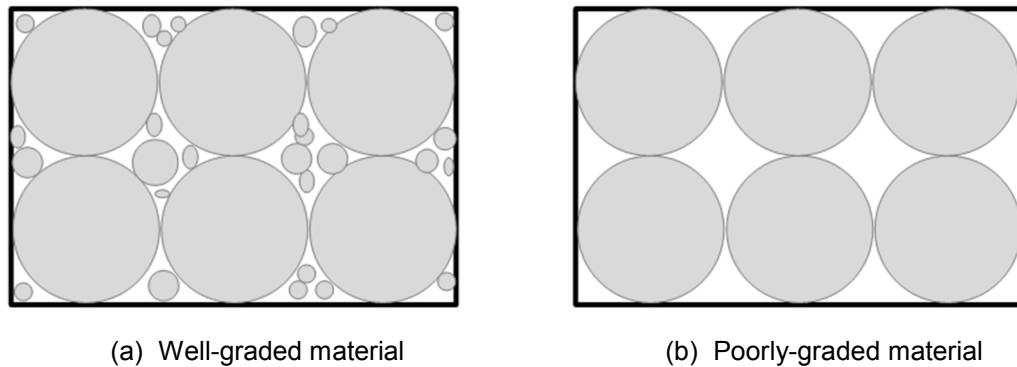


*Figure 3.11 The particle distribution: (a) in a well-graded soil, the spaces between larger particles are filled with smaller (b) in a poorly-graded soil the spaces are unfilled.*

The grading of the soil also has an impact on the capillary rise. The higher the maximum size of the smallest 10 per cent of the sample the lower the maximum capillary rise. The maximum capillary rise is also affected by soil compaction. The compacted soil has lower porosity, hence higher maximum capillary rise. It is due to greater tensions (negative water pressure, with respect to atmospheric pressure) created by smaller pore openings, which holds water against the force of gravity. For the tested Crushed Red Brick (loose material), the maximum capillary rise is  $h_c = 80.21\text{mm}$  (Table 3.7) and is between the approximate capillary rise for a sand and gravel, according to Whitlow (1995). The capillary fringe (subsurface zone where water is present due to the capillary action) can provide water for plants and, if close to the surface, enable evaporation of ground water. Increased evaporation results in regeneration of the green roof retention capacity and decrease of the air temperature leading to urban heat island effect reduction.

The next property investigated was the water absorption. This defines water which is absorbed into the pore structure of the aggregate, but does not include

water adhering to the outside surface of the particles. The result of the water absorption test for the Crushed Red Brick is  $w_s=30.41\%$  (Table 3.7). This indicates that Crushed Red Brick could absorb water of nearly one third of its own weight.

The results of the material properties investigation were compared to those recommended by FLL (Table 3.7). The particle size distribution curve of Crushed Red Brick fits well within FLL recommended particle size limits (Figure 3.6). FLL also suggests that the proportion of silting components ( $d \leq 0.063$  mm) should be less than or equal to 15% by mass and the proportion of gravel ( $d > 4$  mm) should be less than or equal to 50% by mass (FLL, 2008). Crushed Red Brick meets these conditions with the value 5% for the fines and 5% for gravelly particles. However, the same type of green roof material could have more coarser or finer particles depending on the manufacturing process and specification. Different material grading would result in different material properties. In comparison, Molineux et al. (2009) studied red brick substrate, which was described as sandy gravel whilst Graceson et al. (2014a) investigated six different crushed brick substrate mixes ranging from gravelly sand to medium gravel showing the diversity of particle size characteristics within the same substrate type. Both studies were conducted in the UK.

The coefficient of permeability of the Crushed Red Brick lies between the minimum and maximum values suggested by FLL,  $1.00 \times 10^{-5} < k = 8.13 \times 10^{-3} < 4.2 \times 10^{-2}$  m/s (FLL, 2008). The FLL minimum coefficient of permeability, however, corresponds to poor drainage, according to Whitlow (1995). Using materials of such low permeability could lead to water logging, which can result in damage of the supporting structure.

FLL does not specify requirements for densities and pore volume (voids volume). However, it does suggest limits for maximum water capacity (between 35% and 65%), which was substituted in this study with water absorption test ( $w_s=30.4\%$ ) and maximum capillary rise ( $h_c=80.1$ mm). Graceson et al. (2014a) documented the dry bulk density of crushed brick between  $0.824 \text{ Mg/m}^3$  and  $1.4 \text{ Mg/m}^3$  and water holding capacity between 10.5% and 34.6%. Molineux et al. (2009) recorded loose bulk density of red brick to be  $0.83 \text{ Mg/m}^3$  and water holding capacity 20.7%. Those examples reflect the variety within different blends of the

same type of material. All of the materials labelled red brick/crushed brick mix have different properties although they comprise the same aggregate. This leads to the conclusion that the properties and their interconnections should be a primary consideration when selecting material as substrate for green roofs rather than the type of the aggregate alone (Graceson et al., 2014a).

It should be also noted that comparison between the materials and their properties could be difficult to make due to inconsistencies in terminology used. Molineux et al. (2009) refers to water holding capacity of the material although the test described, suggests water absorption determination. There are also discrepancies in density definitions and differentiation between density types is not very clear. This clearly emphasises the need for universal technical green roof guidelines, which could prevent confusion and underpin green roof installation in the UK.

#### **3.2.5.2 LYTAG**

Based on the sieve analysis results the Lytag was described as a well-graded silty sandy gravel. Gravel sand mixtures have a good drainage, with permeability coefficient values between  $10^{-2}$  and  $10^{-4}$  m/s (Whitlow, 1995). This was also confirmed by the permeability test with the result of  $k=4.84 \times 10^{-2}$  m/s (Table 3.7).

The bulk density of the Lytag (loose, dry material) was  $0.78 \text{ Mg/m}^3$ , the particle density was  $1.96 \text{ Mg/m}^3$ , and saturated density was  $1.38 \text{ Mg/m}^3$  (Table 3.7). The densities are essential to assess the load imposed by green roof to the building structure. The depth of the 100mm Lytag would apply load of  $0.76 \text{ kN/m}^2$  when dry, and  $1.35 \text{ kN/m}^2$  when saturated, to the supporting structure. It is more than twice higher than imposed load to roofs not accessible for normal maintenance and repair, which is  $0.6 \text{ kN/m}^2$  (roof slope  $<30^\circ$ ) (British Standards Institution, 2002).

The porosity of the Lytag (loose material) is  $n=0.6$ , which means that the volume of voids comprises 60% of the total volume. As discussed in section 3.2.5.1 those voids could be filled with air and/or water available to plants and necessary for healthy plant growth. The Lytag was determined to be a well-graded material, which would most likely have small size pores as oppose to poorly-graded materials (Figure 3.11). This would result in lower permeability, and potentially higher water retention in comparison to poorly-graded substrates. The 60%

porosity is within the range of typical values for the soils, which is between 30% to 70% (Nimmo, 2004). It needs to be stressed that porosity reduces with material compaction. Hence, it may be lower for matured green roofs.

The grading of the soil impacts the capillary rise. The lower the maximum size of the smallest 10 per cent of the sample the higher the maximum capillary rise. The effective size of Lytag was  $d_{10} = 0.08$  mm. This resulted in high maximum capillary rise  $h_c = 237.24$  mm (Table 3.7). For the substrate depth of 100 mm the capillary fringe would reach the surface increasing evaporation. Consequently, the green roof retention capacity would be restored. Also, increased evaporation leads to air temperature decrease mitigating urban heat island effect.

The next property investigated was the water absorption into the pore structure of the aggregate. The result of the water absorption test for the Lytag is  $w_s = 26.21\%$  (Table 3.7). This indicates that Lytag could absorb water of about a quarter of its own weight. In comparison certain aggregates, such as pumice, can absorb water of about 50% - 80% of its own weight (Evans et al., 1999).

The results of the material properties investigation were also compared to the ones recommended by FLL. The particle size distribution curve of Lytag lays within FLL recommended limits (Table 3.7). The proportion of silting components ( $d \leq 0.063$  mm) is 8%, which is less than 15% (FLL recommendation) and the proportion of gravel ( $d > 4$  mm) is 38%, which is less than 50% (FLL recommendation). Graceson et al. (2013) investigated water retention capabilities of the green roof systems built of substrate comprised of Lytag. The content of gravel particles ( $d > 4$  mm) for all treatments was higher than 70%, exceeding FLL recommended value of 50%. However, that did not affect the hydrological performance of tested green roofs achieving retention between 41% and 49% (Graceson et al., 2013).

The coefficient of permeability of the Lytag slightly exceeds the maximum value suggested by FLL,  $k = 4.84 \times 10^{-2}$  m/s  $>$   $4.2 \times 10^{-2}$  m/s (Table 3.7). Higher permeability can decrease the time lag and increase the peak discharge of the stormwater from the green roof. However, there has been no study quantifying this effect.

FLL does not specify requirements for densities and pore volume (voids volume), it does however suggest limits for maximum water holding capacity (between 35% and 65%), which was substituted in this study with water absorption test ( $w_s=26.21\%$ ) and maximum capillary rise ( $h_c=237.24\text{mm}$ ) (Table 3.7). The water absorption of tested Lytag is lower than FLL maximum water holding capacity. However, it represents only the water that was absorbed into the pore structure of the aggregate. Hence, the maximum water holding capacity would be higher. The water holding capacity of the Lytag substrates studied by Graceson et al. (2013) was recorded between 23.4% and 30.0%. However, the proportion of water absorbed into the pore structure of aggregate was not determined. Comparably to the Crushed Red Brick, there were also variations between the properties of substrates comprised of Lytag, again providing evidence that the properties of the particular material, and not the type, should be taken into consideration when designing green roofs. It also showed that the substrate material could be tailored depending on the objective of the green roof design. Changing the grading of the material would influence its properties to meet design requirements.

#### **3.2.5.3 SEWAGE SLUDGE PELLETS**

The Sewage Sludge Pellets were described as a gap-graded sandy gravel based on the sieve analysis results. The permeability coefficient of the gravel is between  $10^2$  and  $10^{-2}$  m/s and is described as very good drainage (Whitlow, 1995). The soil permeability test result for Sewage Sludge Pellets was  $k=9.35 \times 10^{-2}$  m/s (Table 3.7), which corresponds to the permeability values of gravel. The gap-graded nature of the material, however, can lead to aggregate segregation changing its properties such as permeability.

The bulk density of the Sewage Sludge Pellets (loose, dry material) was  $0.91 \text{ Mg/m}^3$ , the particle density was  $2.05 \text{ Mg/m}^3$ , and saturated density was  $1.47 \text{ Mg/m}^3$  (Table 3.7). The load imposed by the green roof to the building structure of the depth of the 100mm Sewage Sludge Pellets would be  $0.9 \text{ kN/m}^2$  when dry and  $1.44 \text{ kN/m}^2$  when saturated. The density of the material is crucial when the weight of the green roof need to be low.

The porosity of the Sewage Sludge Pellets (loose material) was  $n=0.55$ . This means that the volume of voids comprises 55% of the total volume, hence this is

the volume that could be filled with air and/or water available to plants and necessary for healthy plant growth. It is close to the mid-range of the typical values of soil porosities, which are between 0.3 and 0.7 (Nimmo, 2004). Poorly-graded materials, such as gap-graded, have much greater voids in comparison to well-graded (Figure 3.11), which results in higher permeability and reduced retention capacity of the substrate. However, it also leads to reduction of the degree of substrate compaction, which could be more beneficial for plant growth.

The grading of the soil also impacts the capillary rise. For the Sewage Sludge Pellets (loose material) the maximum capillary rise  $h_c=114.86\text{mm}$  (Table 3.7). The capillary rise estimation, in the case of poorly-graded material, should be taken with caution. The possible segregation of the material leading to concentration of small particles at the lower level would result in multilayer material appearance. The properties of such a system would be very different from the ones estimated for homogenous material.

The water absorption of the Sewage Sludge Pellets was  $w_s=20.35\%$  (Table 3.7). It is lower than FLL maximum water holding capacity (35% to 65%), however it only accounts for water within the pore structure of the aggregate.

Results of the material properties investigation were compared to FLL recommendations (Table 3.7). The particle size distribution curve of Sewage Sludge Pellets did not fit within FLL recommended limits, containing too high proportion of gravel. The Sewage Sludge Pellets gravel particles ( $d>4\text{mm}$ ) comprise 78% of the total mass being higher than FLL maximum of 50%. It was, however, within the limits for the fine particles with the value 2%. Molineux et al. (2009) investigated the effect of sewage sludge pellets (called in their research clay pellets), on the growth of the green roof plants. The study showed that sewage sludge pellets based substrate can successfully support plant development. Interestingly, the clay pellets tested contained over 90% of particles of size greater than 4mm also exceeding the FLL 50% threshold and as proved this did not affect plant growth. However, the hydrological performance of such substrate was not studied.

The coefficient of permeability of the Sewage Sludge Pellets exceeded the maximum value recommended by FLL,  $k=9.35 \times 10^{-2} \text{ m/s} > 4.2 \times 10^{-2} \text{ m/s}$  (Table 3.7), which may result in lower retention capacity of such substrate. FLL does not

specify requirements for densities and pore volume (voids volume), it does however suggest limits for maximum water holding capacity (between 35% and 65%), which was replaced in this study with the water absorption test ( $w_s=20.35\%$ ) and maximum capillary rise ( $h_c=114.86\text{mm}$ ) (Table 3.7). The water absorption is lower than FLL maximum water holding capacity. However, it quantifies only the water absorbed into pore structure of particles. The maximum water holding capacity of the clay pellets investigated by Molineux et al. (2009) was 17.70% and the loose bulk density  $0.83\text{Mg/m}^3$ , which were lower than for the material tested in the current study.

#### **3.2.5.4 ROOFDRAIN40**

The bulk density of the Roofdrain40 (dry material) was  $0.064\text{ Mg/m}^3$  and saturated density was  $0.415\text{ Mg/m}^3$  (Table 3.9). The depth of the Roofdrain40 was 40mm. The load applied to the green roof supporting structure by the Roofdrain40 would be  $0.025\text{ kN/m}^2$  when dry and  $0.163\text{ kN/m}^2$  when saturated.

Water flow, normal to the plane, for Roofdrain40 was  $k=1.4 \times 10^{-3}\text{ m/s}$  (Table 3.9), which places it in the range of good drainage (values between  $10^{-2}$  and  $10^{-4}\text{ m/s}$ ). The water reservoir volume is  $14\text{ l/m}^2$ . To be able to compare Roofdrain40 to other drainage layer materials in terms of water absorption/holding capacity, the percentage of the mass of the water held-in to the mass of the dry Roofdrain40 was determined. The water which the Roofdrain40 can hold accounts for 549.02% of its dry mass.

The rate of the water flow through Roofdrain40 was compared to FLL recommended value for the coefficient of permeability. It was less than the FLL minimum,  $k=1.4 \times 10^{-3}\text{ m/s} < 3.0 \times 10^{-3}\text{ m/s}$  (Table 3.9). Too low permeability of the drainage layer can result in water logging and consequently damage the roof structure. FLL does not specify requirements for densities or water reservoir volumes.

#### **3.2.5.5 GRANULATED RUBBER**

The Granulated Rubber was described as a uniformly-graded gravel. According to Whitlow (1995) gravel has very good drainage, with permeability coefficient values between  $10^2$  and  $10^{-2}\text{ m/s}$ . The permeability coefficient of Granulated Rubber was  $k=1.01 \times 10^{-1}\text{ m/s}$  (Table 3.9), which was within the range stated for materials of similar grading.

The bulk density of the Granulated Rubber (loose, dry material) was  $0.48 \text{ Mg/m}^3$ , the particle density was  $1.12 \text{ Mg/m}^3$ , and saturated density was  $1.05 \text{ Mg /m}^3$  (Table 3.9). The depth of the 40mm Granulated Rubber would impose a load of  $0.19 \text{ kN/m}^2$  when dry and  $0.41 \text{ kN/m}^2$  when saturated, to the green roof supporting structure.

The porosity of the Granulated Rubber (loose material) was  $n=0.57$ , which means that the volume of voids comprises 57% of the total volume.

The Granulated Rubber (loose material) had a maximum capillary rise of only  $h_c=6.96\text{mm}$  (Table 3.9). The estimation of maximum capillary rise for the rubber crumbs should be taken with caution. The obtained value should be corrected taking under consideration irregular shape of the rubber grains. This involves further analysis, which was not undertaken in this study.

The results of the material properties investigation were compared to the ones recommended by FLL. FLL recommendation for granular distribution for drainage layer depths between 40-100mm, is between 2/8mm and 2/12mm. One could notice that the form of representing granular distribution limits is not consistent across FLL guidelines. The FLL recommendation for particle size distribution of substrates is given as coordinates of curve limits and supported by corresponding charts. The FLL recommendation for drainage layer, however, is given as a set of numbers e.g. 2/8mm and 2/12mm, which is confusing and its meaning is unclear. It can lead to misinterpretation and using unsuitable materials for green roof construction. In this study the following interpretation of FLL granular distribution for drainage layers is adopted: the first set of numbers is taken as a left curve limit, while the second as a right curve limit. Subsequently, the first number of a set is interpreted as the lowest grain size, while the second as the highest grain size (Table 3.10 and Figure 3.10).

*Table 3.10 The FLL recommendation for particle size distribution of drainage layer and its interpretation adopted in this study.*

<b>Depth of course - FLL recommendation</b>	<b>Granular distribution - FLL recommendation</b>	<b>Left curve limit – author’s interpretation</b>	<b>Right curve limit – author’s interpretation</b>
<b>4 – 10 cm</b>	between 2/8 mm and 2/12 mm	between 2mm and 8mm	between 2mm and 12mm
<b>&gt; 10 – 20 cm</b>	between 4/8 mm and 8/16 mm	between 4mm and 8mm	between 8mm and 16mm
<b>&gt; 20 cm</b>	between 4/8 mm and 16/32 mm	between 4mm and 8mm	between 16mm and 32mm

Following the adopted interpretation, Granulated Rubber investigated in this study do not met the FLL recommendation (Figure 3.10). The tested material did not have silting components ( $d \leq 0.063\text{mm}$ ) and met the FLL recommendation for fine particles to be less than or equal to 10% by mass. Perez et al. (2012) studied recycled rubber crumbs as a green roof drainage layer material. Three different sizes of the rubber crumbs were investigated, between 2 and 7mm, between 2 and 3.5mm, and between 0.8 and 2.5mm, showing possible variation in particle distribution for the same type of material. Their study demonstrated the potential of use of granulated rubber in green roof systems to improve energy savings in the buildings. However, the hydrological performance of such systems has not been yet investigated.

The coefficient of permeability of Granulated Rubber was greater than the FLL recommended minimum,  $k = 1.01 \times 10^{-1} \text{ m/s} > 3.0 \times 10^{-3} \text{ m/s}$  (Table 3.9). FLL does not specify requirements for densities or water absorption. The permeability coefficient of rubber crumbs investigated by Perez et al. (2012) was around  $2.8 \times 10^{-3} \text{ m/s}$  for particle size between 2 and 7mm, about  $2.1 \times 10^{-3} \text{ m/s}$  for particle size between 2 and 3.5mm and  $1.39 \times 10^{-3} \text{ m/s}$  for particle size between 0.8 and 2.5mm. The permeability coefficient of the Granulated Rubber was much higher than the coefficient of the similarly graded rubber crumbs tested by Perez et al. (2012). This could have been due to the different degree of compaction of the materials. It confirmed the variability in the physical properties of the rubber crumbs and the complexity of the characteristics assessment of green roof materials.

### **3.2.5.6 WOOL-RICH CARPET SHRED**

The permeability coefficient for Wool-rich Carpet Shred was  $k=1.16 \times 10^{-2}$  m/s (Table 3.9). The bulk density of the Wool-rich Carpet Shred (loose, dry material) was  $0.03 \text{ Mg/m}^3$ , the particle density was  $0.38 \text{ Mg/m}^3$ , and saturated density was  $0.98 \text{ Mg/m}^3$  (Table 3.9). Based on the densities the depth of the 40mm Wool-rich Carpet Shred would impose a load, of  $0.07 \text{ kN/m}^2$  when dry and  $0.96 \text{ kN/m}^2$  when saturated, to the green roof supporting structure.

The porosity of the Wool-rich Carpet Shred (loose material) was  $n=0.90$ , which means that the volume of voids comprises 90% of the total volume. It is an extremely high value. The typical porosity for soils is between 30% to 70%. The water absorption was 295.82% (Table 3.9), which is also considered as extremely high. This indicates that Wool-rich Carpet Shred can absorb water of nearly three times of its own weight. Both properties, porosity and water absorption are extremely high due to the fibre-like structure of the Wool-rich Carpet Shred.

The results of the material properties investigation were compared to FLL recommendations. The sieve analysis test was not performed on Wool-rich Carpet Shred so it could not be compared to FLL recommendations. The coefficient of permeability of the Wool-rich Carpet Shred was greater than that suggested as FLL minimum,  $k=1.16 \times 10^{-2} \text{ m/s} > 3.0 \times 10^{-3} \text{ m/s}$  (Table 3.9). FLL does not specify requirements for densities and pore volume (voids volume). There had not been any research published characterising Wool-rich Carpet Shred as a green roof construction material at the time of writing this thesis.

### **3.2.5.7 MATERIALS COMPARISON**

One of the objectives of this research was to assess the suitability of alternative materials as green roof construction materials in comparison to conventionally used materials. In the following section, properties of all tested materials are compared in two groups: substrate materials and drainage layer materials.

#### *3.2.5.7.1 SUBSTRATE MATERIALS*

The Lytag and Sewage Sludge Pellets are alternative substrate materials to conventional Crushed Red Brick materials. Firstly, the particle size distribution of those materials was compared (Figure 3.12). The Crushed Red Brick and Lytag particle size distributions were both within the FLL recommended limits.

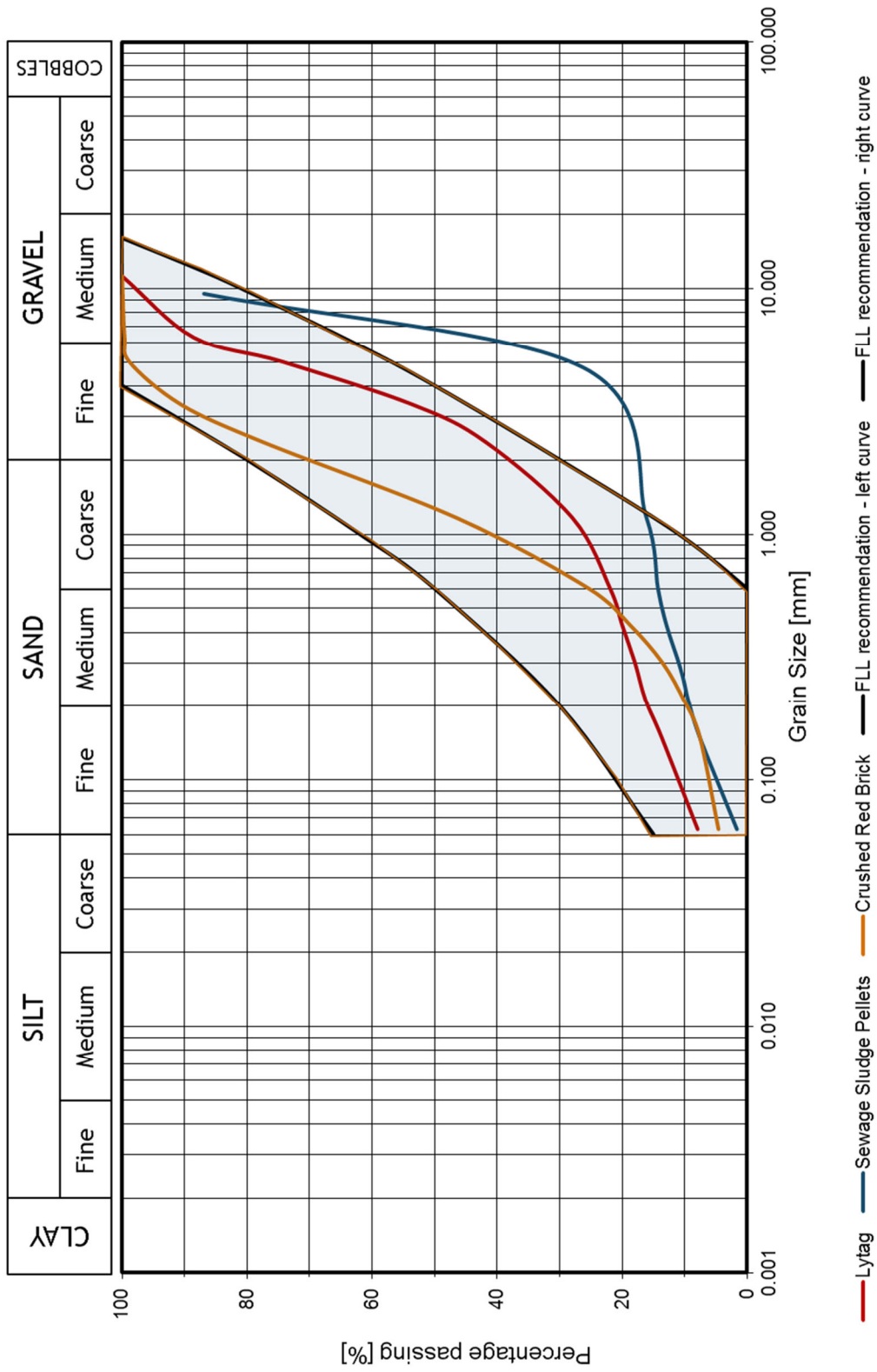


Figure 3.12 Particle size distribution (PSD) chart for all substrate materials tested and FLL recommended limits.

However, Lytag had a higher quantity of gravel-sized particles as opposed to the Crushed Red Brick, which contained a majority of sand-sized particles. Both were well-graded. Although Crushed Red Brick and Lytag met FLL particle size distribution requirements, they exhibited different properties such as permeability or maximum capillary rise (Figure 3.13 to 3.15). Hence, fulfilling particle size distribution requirements does not necessarily mean naturally satisfying the objectives of green roof design. The Sewage Sludge Pellets aggregate did not meet FLL recommendations, as it did not fall within recommended limits, containing a much higher proportion of gravel particles than recommended. This material was poorly-graded, which could lead to material segregation and consequently to alterations in properties such as permeability or capillary rise over time. To be able to assess the changes and their possible impact on green roof system performance, additional tests such as long term rain (simulated or natural) exposure would be required.

Figure 3.13 demonstrates densities of all substrate materials. Table 3.11 presents the percentage difference in densities for Lytag and Sewage Sludge Pellets in comparison with that of Crushed Red Brick.

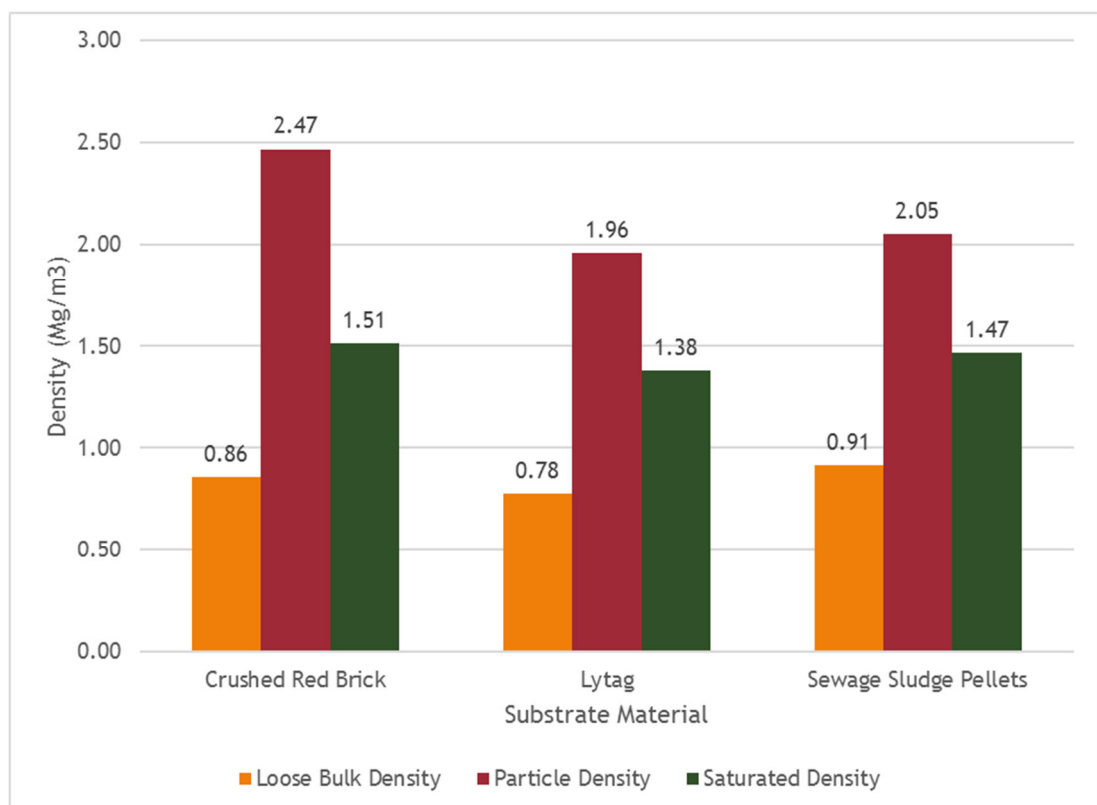


Figure 3.13 Loose bulk density, saturated density, particle density of substrate materials tested (based on Table 3.7).

*Table 3.11 Percentage difference in densities (loose bulk, saturated, particle) for Lytag and Sewage Sludge Pellets in comparison to Crushed Red Brick.*

	<b>Lytag</b>	<b>Sewage Sludge Pellets</b>
<b>Loose Bulk Density, <math>\rho_b</math> (Mg/m<sup>3</sup>)</b>	-9.3%	5.8%
<b>Particle Density, <math>\rho_s</math> (Mg/m<sup>3</sup>)</b>	-20.6%	-17.0%
<b>Saturated Density, <math>\rho_{sat.}</math> (Mg/m<sup>3</sup>)</b>	-8.6%	-2.6%

The densities of the green roof materials affect the load imposed to the structure supporting the roof. The higher the density, the higher the load applied by the material. The green roof construction materials were considered to be in two extreme states: dry and saturated. Lower dry density of the material would likely make the substrate installation easier and material transportation cheaper (Graceson et al., 2014a). The highest bulk density in dry state was Sewage Sludge Pellets  $\rho_b=0.91$  Mg/m<sup>3</sup>, being greater by 6.5% than the density of the conventional material Crushed Red Brick,  $\rho_b=0.86$  Mg/m<sup>3</sup>. However, the relation between the densities of these two materials changed when saturated; the saturated density of the Sewage Sludge Pellets was 2.6% lower than saturated density of the Crushed Red Brick, resulting in a lower maximum load applied to the supporting structure. In the case of Lytag both of the densities were lower than the densities of Crushed Red Brick, bulk density lower by 9.3% and saturated density by 8.6%, making Lytag a more suitable material for construction of light extensive green roofs when the load limit is a main requirement of green roof design. The particle density of Sewage Sludge Pellets and Lytag are both lower than that of Crushed Red Brick, by 17.0% and 20.6% respectively. Particle density represents the mineral composition of the aggregate but also the structure of the soil minerals and particles themselves. Lower particle density indicates that the material is composed of less dense minerals and/or the material particles contain pores, which could be either sealed or too small to become saturated.

Figure 3.14 shows the values of the porosity, effective size, and maximum capillary rise of all the substrate materials examined. Table 3.12 presents the porosity and maximum capillary rise for Lytag and Sewage Sludge Pellets expressed as percentage difference when compared to Crushed Red Brick.

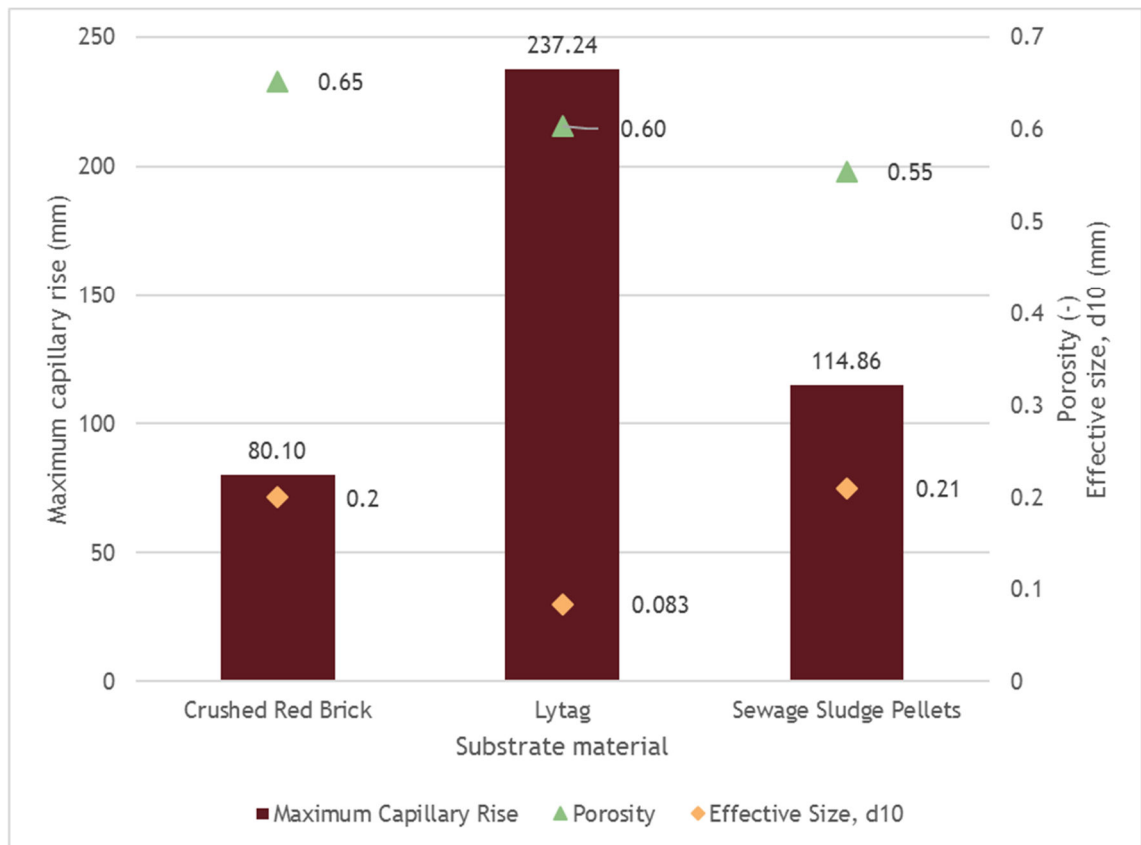


Figure 3.14 The porosity, effective size, and maximum capillary rise of Crushed Red Brick, Lytag and Sewage Sludge Pellets (based on Table 3.7).

Table 3.12 The percentage difference in porosity and maximum capillary rise of Lytag and Sewage Sludge Pellets in comparison to Crushed Red Brick.

Material:	Lytag	Sewage Sludge Pellets
Porosity, n (-)	-7.7%	-13.8%
Maximum Capillary Rise, $h_c$ (mm)	198.4%	30.1%

Crushed Red Brick had the highest porosity value of  $n=0.65$ , followed by Lytag,  $n=0.6$  (7.7% lower than Crushed Red Brick porosity) and Sewage Sludge Pellets  $n=0.55$  (13.8% lower than Crushed Red Brick porosity). This indicates that the highest air/water volume could be stored by Crushed Red Brick. Consequently, Crushed Red Brick based substrate would have the highest quantity of water available to plants necessary for healthy plant growth. The Crushed Red Brick effective size ( $d_{10}$ ) was 0.20mm, the Lytag effective size was 0.08mm and Sewage Sludge Pellets effective size was 0.23mm. The grading characteristics and porosity affect other properties of the green roof materials, such as the

maximum capillary rise. The maximum capillary rise depends on effective size ( $d_{10}$ ) of the aggregate. The lowest effective size of the Lytag resulted in the highest maximum capillary rise  $h_c=237.24\text{mm}$ . It was 198.4% higher in comparison to maximum capillary rise of Crushed Red Brick. Although the effective size of the Crushed Red Brick and Sewage Sludge Pellets were similar, the maximum capillary rise of Sludge Pellet was over 30mm, or 30.1% higher than that of Crushed Red Brick. It was due to the porosity of the materials, which was greater in the case of the Crushed Red Brick. The capillary fringe can provide water for plants and, if close to the surface, enable evaporation of ground water. Increased evaporation results in regeneration of the green roof retention capacity. Therefore, Lytag has the greatest potential of enhancing hydrological performance of the green roofs due to the highest maximum capillary rise. However, in the case of shallow depths of substrates such as 50 – 80 mm, the capillary fringe would be at the surface for all materials increasing water evaporation. It needs to be noted that the values of the maximum capillary rise, presented in Table 3.7 are theoretical and not experimental. The actual maximum capillary rise could be affected by the voids size and distribution within the material. In the case of substrates, the voids are subjected to changes over time due to the growth of the roots of the plants or, in case of a poorly-graded material, due to the particle segregation. To avoid segregation of the material, it is advisable that the substrate aggregate is well-graded.

Figure 3.15 shows the values of the porosity, coefficient of permeability and water absorption of all the substrate materials. Table 3.13 presents the porosity, coefficient of permeability and water absorption of Lytag and Sewage Sludge Pellets expressed as percentage difference when compared to Crushed Red Brick.

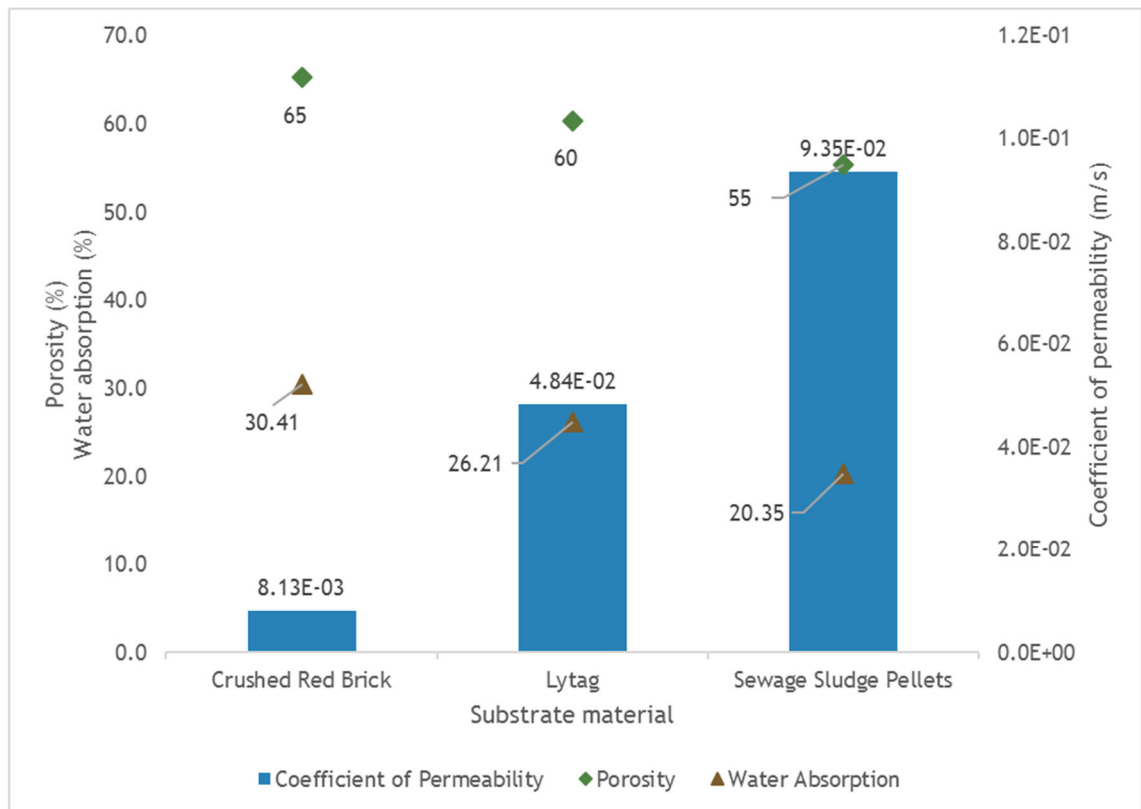


Figure 3.15 The porosity, coefficient of permeability and water absorption of Crushed Red Brick, Lytag and Sewage Sludge Pellets (based on Table 3.7).

Table 3.13 The percentage difference of porosity, coefficient of permeability and water absorption of Lytag and Sewage Sludge Pellets in comparison to Crushed Red Brick.

Material:	Lytag	Sewage Sludge Pellets
Porosity, n (-)	-7.7%	-13.8%
Water Absorption, $w_s$ (%)	-13.8%	-33.1%
Coefficient of Permeability, k (m/s)	495.3%	1050.9%

Both Lytag and Sewage Sludge Pellets had higher coefficient of permeability than the Crushed Red Brick, which means more rapid water release from the substrate material. The coefficient of permeability of Lytag ( $4.84 \times 10^{-2}$  m/s) was 495.3% higher than the coefficient of permeability of Crushed Red Brick. The coefficient of permeability of the Sewage Sludge Pellets ( $9.35 \times 10^{-2}$  m/s) was 1050.9% higher than that of Crushed Red Brick. It would take about 12 seconds for the water to flow through 100mm of saturated Crushed Brick, about 2 seconds through the same depth of Lytag and about 1 second through Sewage Sludge Pellets. The water permeability coefficient should be taken under consideration when the

objective of the green roof installation is stormwater attenuation and retention. Lower permeability increases the duration of water travelling through the green roof structures, delaying the water flow into the drainage system. Lower permeability could also allow sufficient time for the material to absorb water and thus increase stormwater retention of the green roof. Too low water permeability, however, could result in water logging, increasing the load imposed to the supporting structure and, in extreme cases, exceeding the maximum allowable load and possibly causing structural damage.

The Crushed Red Brick had the highest water absorption  $w_s=30.41\%$ , followed by Lytag  $w_s=26.21\%$  (13.8% lower than Crushed Red Brick), and Sewage Sludge Pellets  $w_s=20.35\%$  (33.1% lower than Crushed Red Brick). The water absorption corresponds to the material porosity. Crushed Red Brick had the highest porosity  $n=0.65$ , followed by Lytag  $n=0.60$  and Sewage Sludge Pellets  $n=0.55$ . This provided confirmation of space available within substrate to store air or water, although water absorption refers only to water absorbed by aggregate particles and does not account for the water that could be stored between the material grains.

One could also notice that with increased porosity the permeability of the tested materials decreased. In this case, the size of the voids, rather than the total volume of the voids, influenced the permeability. The Sewage Sludge Pellets material was poorly-graded with a high content of gravel size particles and therefore would be expected to have larger voids, although the total volume of voids was lower compared to Crushed Red Brick. This affected the permeability coefficient of the examined materials.

Based on the coefficient of permeability and water absorption only it could be concluded that Crushed Red Brick was the most suitable material to achieve good retention and attenuation performance when used as the green roof substrate. Sewage Sludge Pellets performance would be expected to be much poorer than that of Crushed Red Brick or Lytag. However, when taking into consideration the maximum capillary rise also Lytag becomes the most favourable material to support hydrological performance of the green roof. The characteristics of the material from properties testing alone cannot give definite answers as to how green roofs constructed using each material type would perform under given rain

conditions. There is therefore a need to assess the green roof as a whole system, under various rain conditions to confirm whether or not material properties could assist in predicting green roof system hydrological performance and if this is the case, what the relationship between the green roof material properties and green roof hydrological performance is. This is further discussed in Chapter 6.

### 3.2.5.7.2 DRAINAGE LAYER MATERIALS

The Granulated Rubber and Wool-rich Carpet Shred are alternative materials to conventional green roof drainage layer such as Roofdrain40. Therefore, the properties of those alternative materials were analysed and compared with properties of Roofdrain40. It should be noted that the full comparison of the materials was not possible due to their different structure. Roofdrain40 is a polymer sheet, whilst Granulated Rubber has an aggregate nature and Wool-rich Carpet Shred has a fibre-like structure.

Figure 3.16 shows the values of the densities of all the drainage layer materials and Table 3.14 presents the densities of Granulated Rubber and Wool-rich Carpet Shred as percentage difference when compared Roofdrain40.

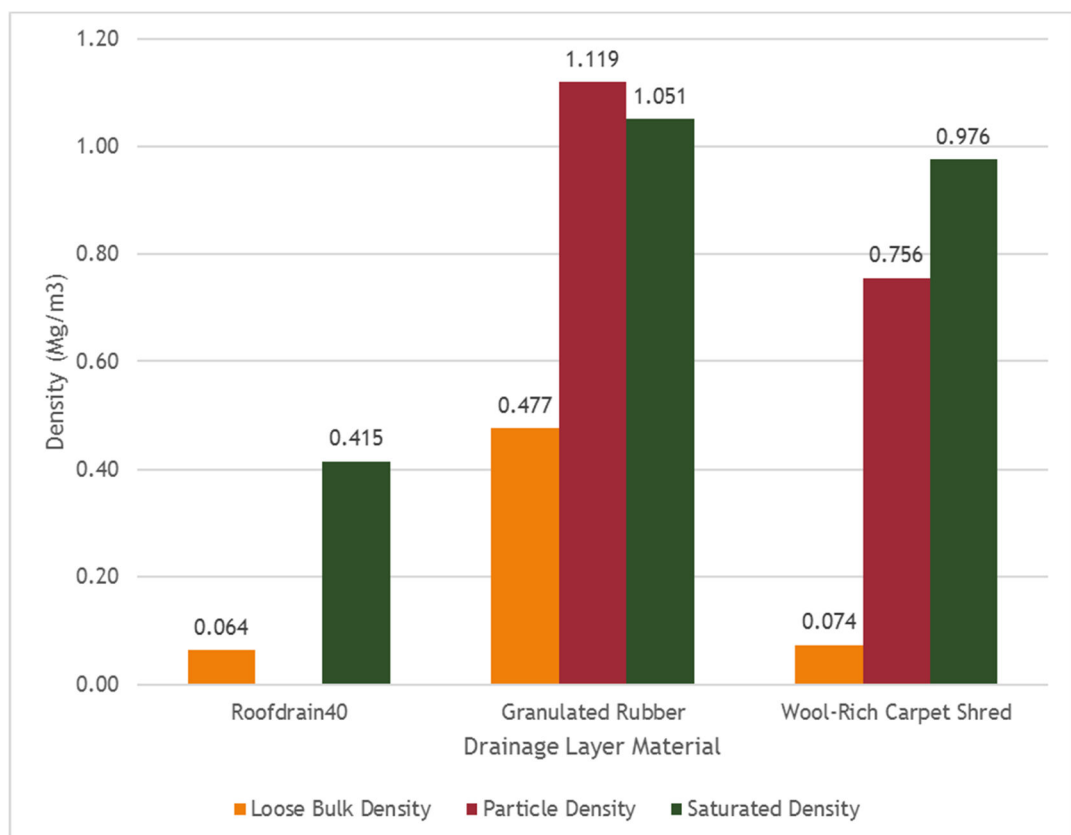


Figure 3.16 Loose bulk density, saturated density, particle density of all drainage layer materials based on test results (Table 3.9) and manufacturer specification.

*Table 3.14 The percentage difference in densities (bulk and saturated) of Granulated Rubber and Wool-rich Carpet Shred in comparison to Roofdrain40.*

<b>Material:</b>	<b>Granulated Rubber</b>	<b>Wool-rich Carpet Shred</b>
<b>Loose Bulk Density, <math>\rho_b</math> (Mg/m<sup>3</sup>)</b>	650.0%	9.4%
<b>Particle Density, <math>\rho_s</math> (Mg/m<sup>3</sup>)</b>	-	-
<b>Saturated Density, <math>\rho_{sat}</math>. (Mg/m<sup>3</sup>)</b>	153.0%	136.1%

The bulk density (dry, loose material) of the Wool-rich Carpet Shred was 9.4% higher than that of Roofdrain40 and the saturated density of the Wool-rich Carpet Shred was 136.1% higher than the density of the Roofdrain40. The Granulated Rubber bulk density was 650.0% higher and saturated density was 153.2% higher than density of the Roofdrain40. Hence, substituting Roofdrain40 with any of the tested alternative materials would result in a significantly higher load applied to the green roof supporting structure. This should be taken into consideration when designing green roofs for retrofitting and particularly when designing for a lightweight green roof system. Higher loose bulk density (especially in the case of Granulated Rubber) would also have an impact on transportation of the material and installation of the green roof. The particle density of the Roofdrain40 is not known. Particle density of Wool-rich Carpet Shred was much lower than the particle density of Granulated Rubber due to a higher organic matter content in the former material.

Figure 3.17 shows the values of the porosity, coefficient of permeability and water absorption of the Granulated Rubber and Wool-rich Carpet Shred in comparison to Roofdrain40.

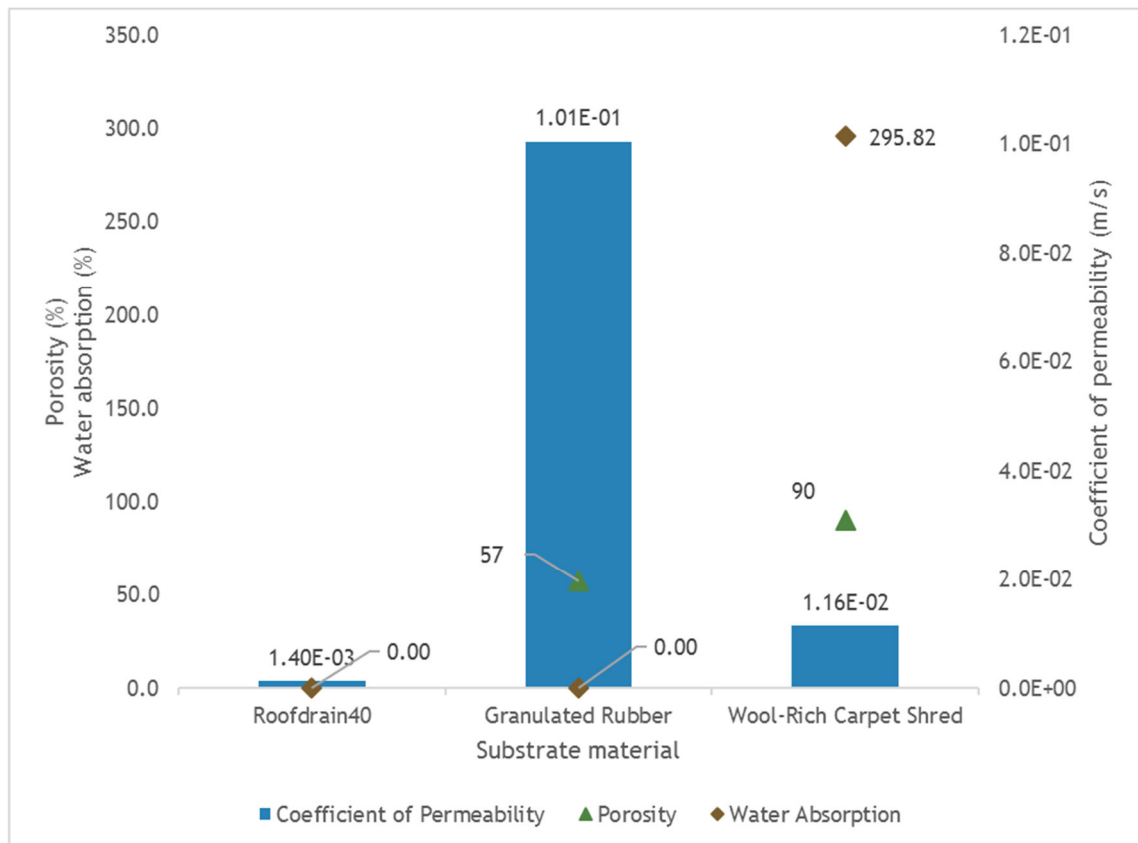


Figure 3.17 The porosity, coefficient of permeability and water absorption of all drainage layer materials based on test results (Table 3.9) and manufacturer specification.

Both the Granulated Rubber and Wool-rich Carpet Shred had higher coefficient of permeability than the Roofdrain40, and would thus result in more rapid stormwater drainage from the green roof. The water absorption of the Granulated Rubber was assumed to be negligible. The water absorption of the Roofdrain40 was not specified by the manufacturer. However, due to the material characteristics one could assume that the water absorption of the Roofdrain40 was also negligible. The water absorption of the Wool-rich Carpet Shred was very high  $w_s=295.82\%$ . It was the highest from all the materials tested, both for the substrate and drainage layer materials. That indicates it would have a positive impact on green roof water retention capacity. High water absorption corresponds to high porosity of the Wool-rich Carpet Shred (dry, loose material)  $n=0.91$ . This means that 91% of the total volume of the material was the voids volume. The porosity of the Granulated Rubber was  $n=0.57$ , the voids volume accounted for 57% of total volume of the material. Due to non-aggregate nature of the Roofdrain40 and Wool-rich Carpet Shred, certain characteristics such as the

maximum capillary rise and the particle size distribution were not determined, preventing direct material comparison for those attributes.

The material properties tests allowed a preliminary assessment of the performance of the materials as green roof layers. The particle size distribution gave an indication of how well the material would drain stormwater as well as the likely maximum capillary rise. Water absorption could be helpful for the estimation of stormwater retention. Based on coefficient of permeability likely green roof retention capacity could be determined. Densities are essential to determine the range of loads applied to the green roof supporting structure, the mineral composition of the material and impact on transportation and installation of the green roof. However, green roofs work as a compound structure, therefore it is crucial to assess their performance in the holistic manner, as a system rather than individual layers of materials. The evaluation of green roof material properties should therefore always be followed by investigation of the performance of the green roof as a composite structure.

### **3.3 CONCLUSIONS**

This chapter concentrated on selection of alternative green roof materials and their properties, as critical aspect for green roof sustainable design and performance assessment. The materials chosen in this study were as follows:

- substrate:
  - Crushed Red Brick – the conventional green roof substrate material taken as control material in this study
  - Lytag and Sewage Sludge Pellets - alternative green roof construction material,
- drainage layer:
  - Roofdrain40 – the conventional green roof drainage layer taken as control material in this study
  - Granulated Rubber and Wool-rich Carpet Shred – alternative green roof construction material.

The properties tested were: loose bulk density, particle density, saturated density, particle size distribution, porosity and void ratio, maximum capillary rise,

coefficient of permeability and water absorption. The material properties analysis led to the following conclusions:

1. The results showed that the type of the material has a significant impact on the physical properties of the substrate and drainage layer materials. It determines material densities and consequently porosity. The saturated density impacts the loads imposed by the green roof to the supporting structure, whilst dry density affects the material transportation and installation process.
2. Particle size distribution also has a great impact on the physical properties of the green roof construction materials. Changes in grading of the same material result in differences in properties such as permeability or maximum capillary rise. The same type of material could present major differences in physical characteristics and performance when particle size distribution has been altered. This highlights the importance of assessing properties of green roof construction materials collectively as they are interconnected to each other. It is paramount to use materials with appropriate characteristics, rather than to rely on the type of the material alone, to meet green roof design objectives specific for the individual project.
3. Crushed Red Brick is the most suitable material to achieve good retention and attenuation performance of the green roof, based on the analysis of coefficient of permeability and water absorption, followed by Lytag, based on maximum capillary rise. In this aspect, the Sewage Sludge Pellets performance is expected to be the least favourable. Amongst drainage layers Wool-rich Carpet Shred offered the highest water absorption and is expected to enhance hydrological performance of green roof.
4. The best choice for lightweight green roof system would be Lytag and Roofdrain40, due to their low densities.

All above indicate but do not prove best performance of the green roof system. Certain tests, such as compaction, were not performed but could provide better understanding of material behaviour. The next phase of this research was to test the materials as green roof system, in order to assess how material testing results compare to real-world performance. The results of this are presented in Chapter 6.

Presently, there is no comprehensive code in the UK addressing test methods for green roof material characterisation. This leads to difficulties in comparison of various materials that have been assessed differently. It also results in confusion in terminology and misconceptions, when material properties are evaluated. Moreover, the inconsistencies in the FLL recommendations for particle size distribution as well as lack of clarity were realised. Clearly, there is a need for collective code presenting best green roof material testing methods and best green roof design practice, underpinning green roof dissemination and installation in the UK and allow UK environment to benefit from many advantages green roofs offer.

## **CHAPTER 4**

### **HYDROLOGICAL PERFORMANCE OF SMALL SCALE**

#### **CONVENTIONAL EXTENSIVE GREEN ROOFS: IN-SITU**

##### **EXPERIMENT**

This chapter addresses the research objective of assessing the hydrological performance of the conventional extensive green roofs by analysing hydrological performance data from the small scale green roof in-situ experiment.

As discussed in Chapter 2, the hydrological performance of green roofs is significantly influenced not only by green roof construction material characteristics (Chapter 3) but also by climate conditions, green roof geometry, and vegetation type and coverage. In order to understand this performance, it is critical to carry out controlled investigations. For example, carrying out controlled hydrological performance tests on green roof systems can increase understanding of how green roofs respond to rainfall events and how green roof design affects this response.

This chapter presents in-situ monitoring results from twenty-seven small scale green roofs at Barking Riverside, London, UK to quantify their hydrological performance. Comparison is made between green roofs of various designs subjected to UK field climatic conditions. Overall hydrological performance (stormwater runoff, retention, and peak flow reduction) is presented, as well as analysis based on per-event and seasonal response. Multiple linear regression analysis is used to investigate the influence of rainfall characteristics and climate conditions on the green roof hydrological performance. Moreover, one of the in-situ experiment green roof designs was replicated and subjected to laboratory

based tests to obtain an in-depth insight to its hydrological performance (Chapter 6).

#### 4.1 METHODOLOGY

The objective of the green roof in-situ monitoring was to provide field experimental data on hydrological performance in order to understand the response of green roofs to UK climatic conditions. The primary data was obtained from the experimental green roof setup at Barking Riverside (location: London Borough of Barking and Dagenham, East London, UK, Figure 4.1).



*Figure 4.1 The location of Barking Riverside in-situ experimental setup (Imagery ©2016 Google, Map data ©2016 Google).*

A series of green roof test plots were installed at Barking Riverside as a part of Barking Riverside Green Roof Research Project (University of East London, 2010). The project commenced in December 2009, prior to the current research, with continuous data logging from the green roof test plots beginning in July 2010. The main aim of the Barking Riverside Green Roof Experiment was to

“investigate the performance of a series of green roof test platforms in terms of their thermal dynamics, water attenuation, water quality of runoff, and flora and associated fauna (...)” (University of East London, 2010). For this study data related to hydrological performance from this green roof experiment, collected between July 2010 and August 2014, was analysed.

#### 4.1.1 DESCRIPTION OF IN-SITU GREEN ROOF EXPERIMENT AT BARKING RIVERSIDE

The Barking Riverside in-situ experiment comprised of thirty-two test plots (27 experimental and 5 non-experimental plots), placed on the top of four transport containers. Each plot measured approximately 2m x 1.37m with a depth of 0.2m, and it was fitted with a centrally located drainage outlet for stormwater runoff (Figure 4.2).

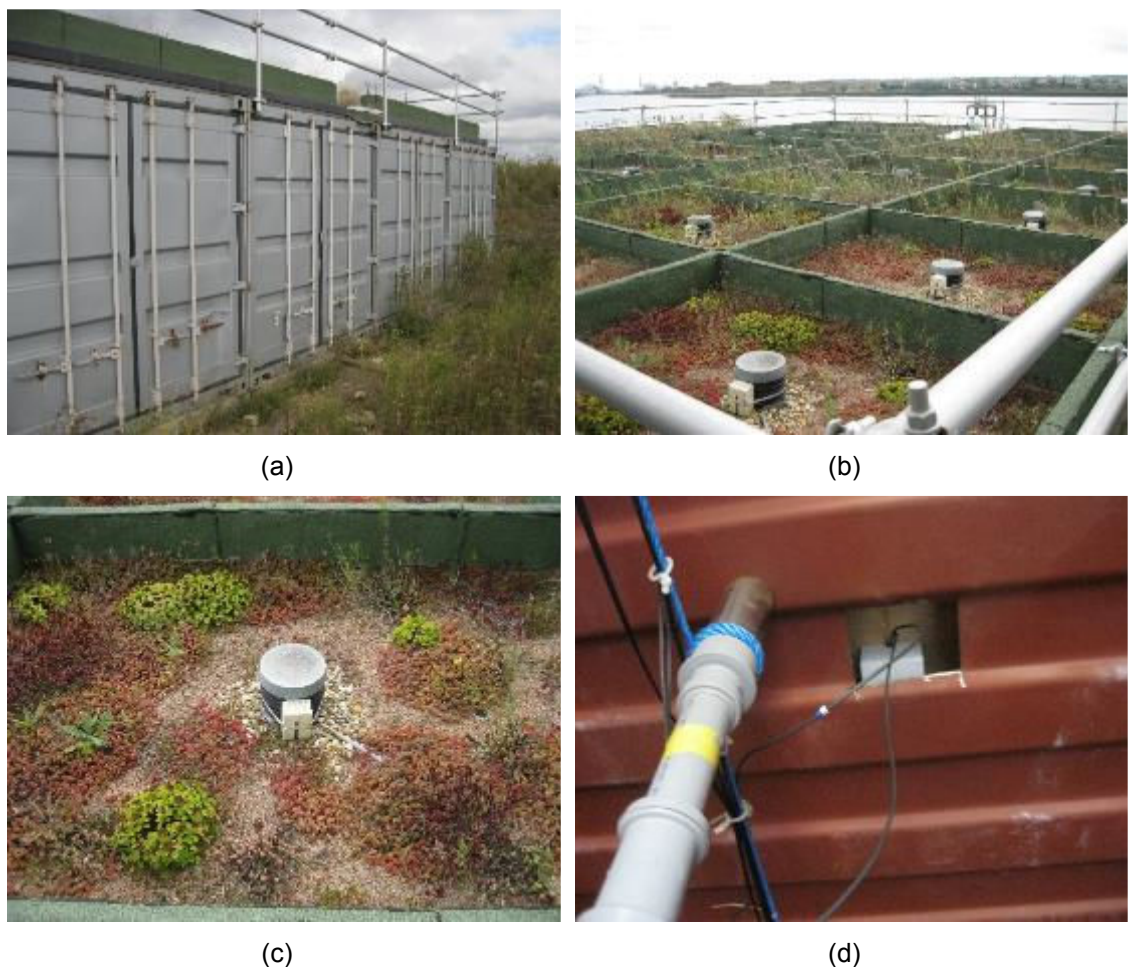


*Figure 4.2 Barking Riverside experimental setup: (a) green roof plots on the top of the transport containers; (b) green roof plots; (c) central cover over drainage outlet in each green roof plot; (d) drainage pipe under each green roof plot.*

All green roofs were designed as standard extensive green roof systems according to German FLL green roof guidelines (University of East London, 2010). Each green roof test plot consisted of a wooden frame lined with an industry standard felt waterproof membrane, followed by a geotextile acting as protective and filter layer. The ABG Geosynthetic Finesse Roofdrain40 drainage layer, an egg-box shape polymer sheet (called Roofdrain40 hereinafter), was placed on top of this. This drainage layer included a geotextile filter layer on top to prevent the drainage volume being filled with aggregates and to prevent root penetration from damaging the drainage layer. ABG Geosynthetic Meadow Mix substrate was placed on top of this. The substrate comprised of graded recycled red brick aggregate, mixed with matured and graded green compost (called Crushed Red Brick hereinafter). Finally, vegetation was planted onto the substrate layer. There were two types of vegetation cover selected: i) sedum, which was considered as being an industry standard/conventional vegetation cover, and ii) wildflowers, which was considered to be more biodiversity-friendly and mimicked the typical ground-level vegetation of the Barking Riverside brownfield site. The generic design profile for green roof experiment is presented in Figure 4.3.

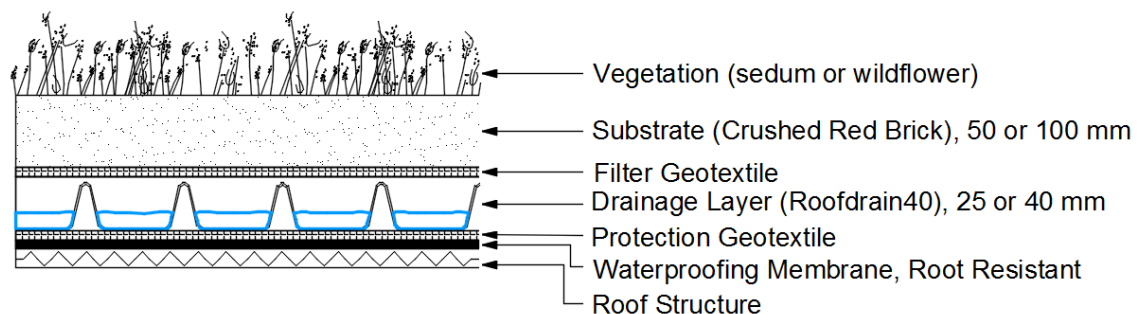


Figure 4.3 Generic Barking Riverside green roof profile.

The Barking Riverside green roof phase 1 experiment test plots varied in design by vegetation type, substrate depth and drainage layer depth. As mentioned previously there were two types of green roof vegetation selected for the purpose of the study: sedum and wildflower. Two depths of substrate were used: 50mm and 100mm. Similarly, there were two depths of drainage layer selected: 25mm and 40mm, corresponding to two different storage volumes: 4.3 l/m<sup>2</sup> and 12 l/m<sup>2</sup> respectively. The combination of those variables resulted in different green roof designs. The in-situ experimental green roof designs are presented in Table 4.1.

Table 4.1 In-situ experimental green roof at Barking Riverside. Green roof design: letter represents vegetation type: S-sedum, W-wildflower, first number corresponds to drainage layer depth: 25mm or 40mm, second number represents substrate depth: 50mm or 100mm.

Green Roof Design	Vegetation Type	Drainage Layer Depth (mm)	Substrate Depth (mm)
<b>S/25/50</b>	Sedum	25	50
<b>S/25/100</b>	Sedum	25	100
<b>S/40/50</b>	Sedum	40	50
<b>S/40/100</b>	Sedum	40	100
<b>W/25/50</b>	Wildflower	25	50
<b>W/25/100</b>	Wildflower	25	100
<b>W/40/50</b>	Wildflower	40	50
<b>W/40/100</b>	Wildflower	40	100
<b>Control</b>	None	None	None

Eight different combinations of green roof design were created and each was replicated three times. The experimental setup also included three empty plots acting as control roofs. The position of each green roof test plot was randomised as shown in Figure 4.4.

<b>S/25/50-1</b>	<b>S/25/50-3</b>	<b>S/40/100-2</b>	<b>W/25/100-1</b>
<b>S/25/50-2</b>	<b>S/25/100-2</b>	<b>W/40/100-3</b>	<b>S/40/100-3</b>
<b>W/25/50-1</b>	<b>W/40/100-1</b>	<b>W/25/50-3</b>	<b>W/25/100-2</b>
<b>W/40/50-1</b>	<b>W/25/50-2</b>	<b>S/25/100-3</b>	<b>W/25/100-3</b>
<b>S/25/100-1</b>	<b>W/40/100-2</b>	<b>Control-2</b>	<b>S/40/50-3</b>
<b>S/40/50-1</b>	<b>S/40/100-1</b>	<b>S/40/50-2</b>	<b>Control-3</b>
<b>Control-1</b>	<b>Non-experimental</b>	<b>Non-experimental</b>	<b>W/40/50-2</b>
<b>Non-experimental</b>	<b>Non-experimental</b>	<b>Non-experimental</b>	<b>W/40/50-3</b>

Figure 4.4 Randomised position of the green roof test plots. Green roof design: letter represents vegetation type: S-sedum, W-wildflower, first number corresponds to drainage layer depth: 25mm or 40mm, second number represents substrate depth: 50mm or 100mm. 'Control' refers to empty test plot, 'Non-experimental' refers to plot not included in the experiment.

#### 4.1.1.1 RAINFALL MONITORING

A Vantage Pro 2 weather station, installed in-situ (Figure 4.5), provided continuous monitoring of environmental conditions. Data collected from the weather station included rainfall depth, temperature, and wind speed amongst others. Table 4.2 presents variables and their corresponding resolution recorded via the weather station, which is relevant to green roof hydrological performance analysis (Davis Instruments, 2015). All data were logged at half an hour intervals.

*Table 4.2 Weather data specifications for the Vantage Pro 2 weather station installed at the Barking Riverside experiment site.*

Variable	Resolution
Rainfall Depth	0.2 mm
Temperature	0.1°C
Humidity	1%
Dew Point	1°C
Wind Speed	0.4 m/ s
Temperature-Humidity-Wind (THW) Index	1°C



*Figure 4.5 Vantage Pro 2 weather station at Barking Riverside experiment site.*

#### 4.1.1.2 RUNOFF MONITORING INSTRUMENT, CALIBRATION, AND VERIFICATION

The runoff volumes were measured using Davis' Rain Collector II tipping bucket rain gauges. The stormwater runoff from each green roof plot was directed from a centrally located drainage outlet, through piping to individual tipping bucket rain gauges, which were placed inside the containers (Figure 4.6). Each tipping bucket was connected to a computer and every individual tip and the corresponding time were logged and saved into 'comma-separated value' file.

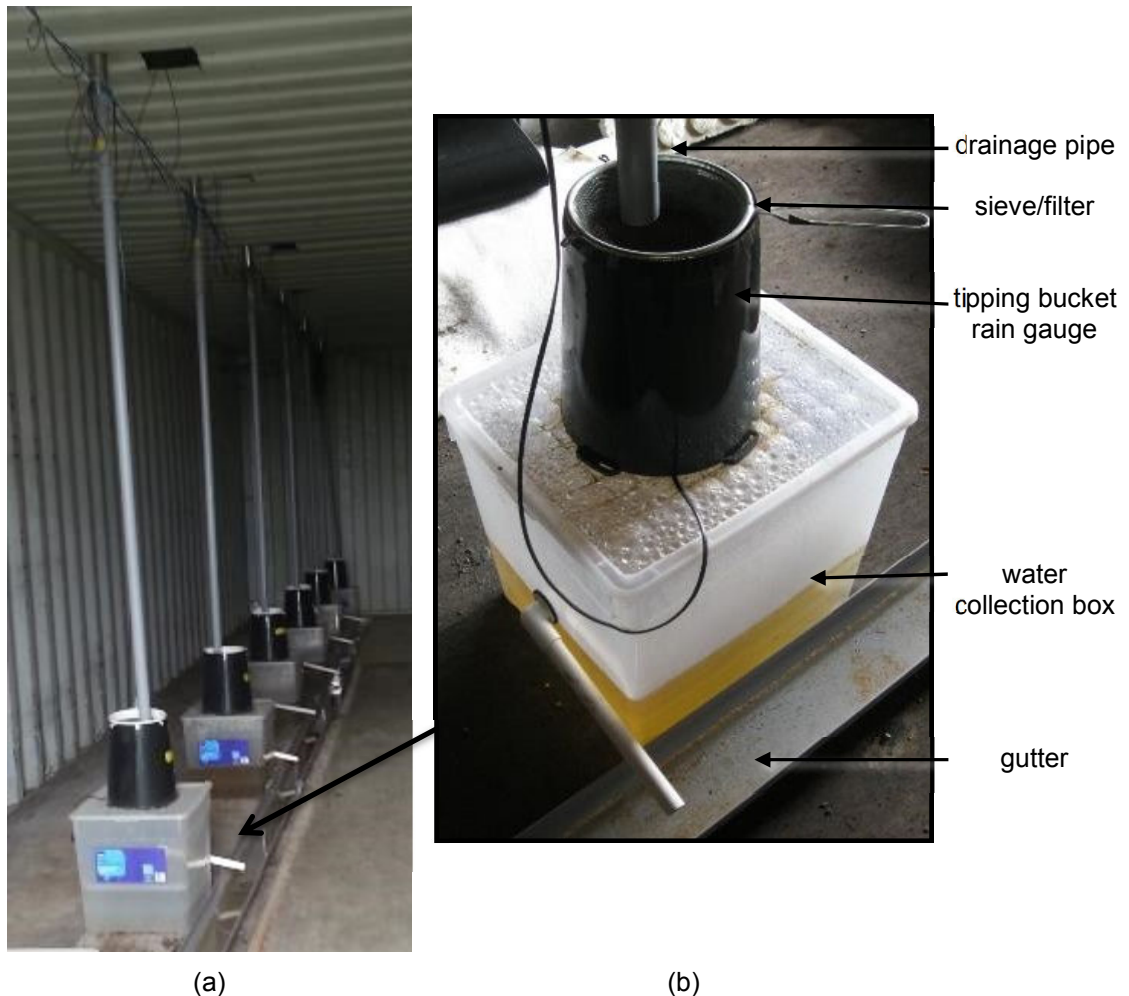


*Figure 4.6 Runoff monitoring instrument at Barking Riverside: (a) tipping bucket rain gauges inside the transport container (b) tipping bucket rain gauge, fitted with the sieve acting as filter, on the top of the water collection box.*

The tipping bucket rain gauge consisted of a funnel also called collector, which directed water into one of the two buckets fitted on pivot (Figure 4.7). Once the bucket was filled with water, it tipped, disposing the collected water to the drain. Each tip emptied one bucket and positioned the other bucket under the funnel. During this process, the magnet fitted below the buckets moved past a sensor

called a reed switch and a signal was sent to the data logger, recording tipping movement (Figure 4.7).

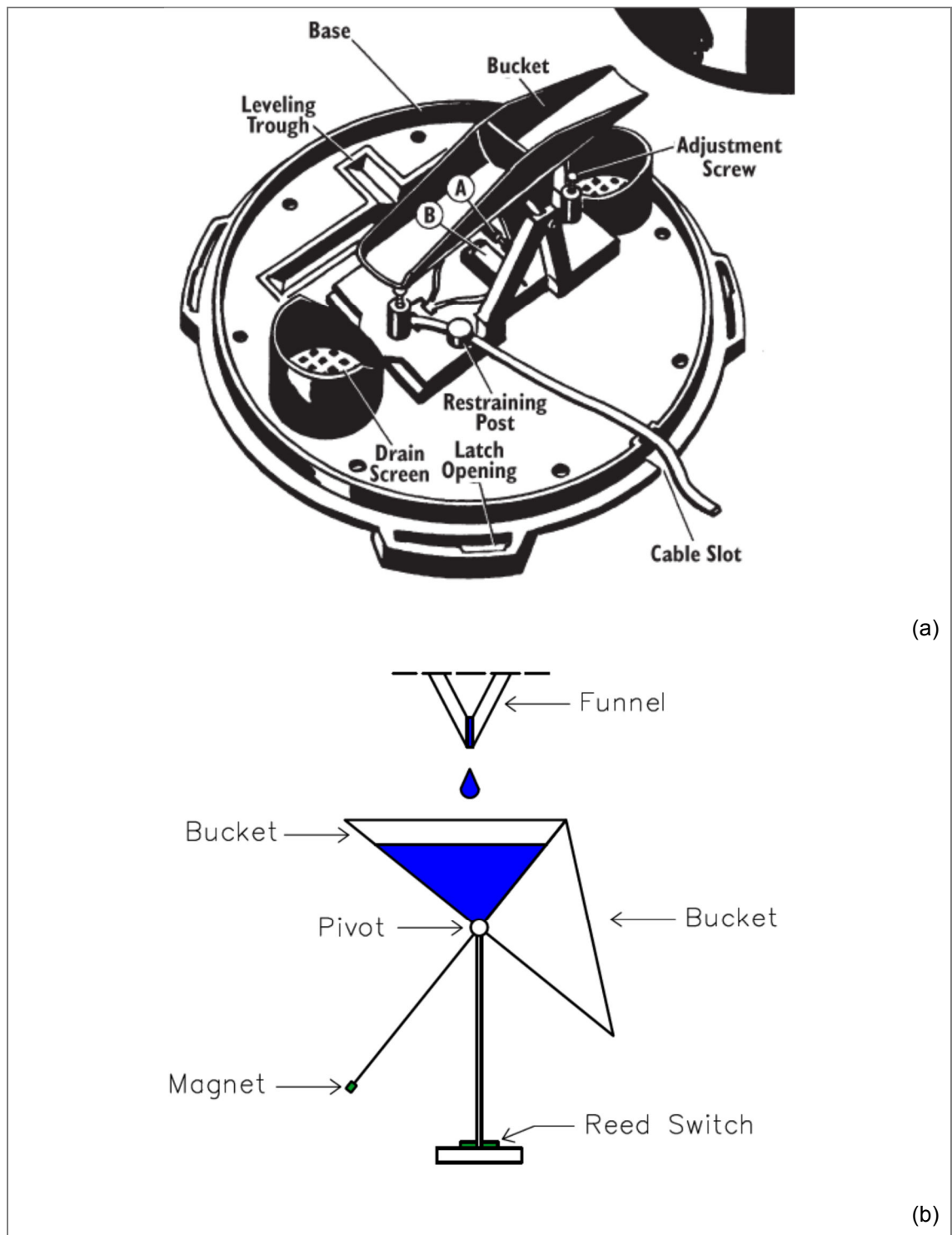


Figure 4.7 Tipping bucket rain gauge: (a) internal components, where A-Magnet, B-Reed Switch (Davis Instruments, 2012) (b) schematics of the mechanism.

The manufacturer stated that 1 tip is equal to a rain depth of 0.01 inch, which is equivalent to 5.43ml of rainfall water (based on 16.5cm bucket diameter). The accuracy stated by manufacturer is  $\pm 4\%$  of total rain for rain rates up to 50 mm/hr

and  $\pm 5\%$  of total rain for rain rates from 50mm/hr to 100mm/hr (Davis Instruments, 2012).

#### *4.1.1.2.1 CALIBRATION OF TIPPING BUCKET RAIN GAUGES*

In order to monitor the stormwater runoff from the green roofs at Barking Riverside in-situ experiment, two initial calibrations of the tipping bucket rain gauges were carried out in July 2010 and July 2011, prior to the current research commencement. Both calibrations were carried out by pouring 1 litre of water through each rain gauge and dividing the total volume by the number of tips measured. During the second calibration the process was repeated three times and an average of the three readings was taken (Connop, 2012). However, the preliminary results of runoff data analysis revealed certain erroneous outcomes, such as unrealistic high runoff volumes. Therefore, there was a need for an additional calibration of the rain gauges to ensure quality of data.

Tipping bucket rain gauges are designed to collect and measure rainfall depths. The intensity of the rainfalls, however, are relatively small compared to the flow rates of stormwater runoff from the roof plots, due to the differences in catchment area. The manufacturer indicates that the accuracy of readings is lower for higher rainfall intensities. Moreover, the observations of tipping bucket performance in laboratory indicated different number of tips corresponding to various flow rates. Taking these into consideration it was assumed that the volume of one tip changes with respect to runoff flow rate. Thus, a new approach to tipping bucket rain gauges calibration was necessary. The new approach involved taking the change in the flow rate and its effect on tip volume into consideration.

#### **Tipping bucket rain gauge calibration method**

The calibration of the tipping bucket rain gauges was conducted on 19<sup>th</sup> August 2013. The calibration apparatus of the rain gauges at the Barking Riverside experiment was partly adopted from the Novalynx Corporation method (NovaLynx Corporation, 2007). The new approach was based on the determination of the volume per tip in relation to runoff rate expressed as number of tips per unit time. The calibration of the rain gauges was conducted in three phases at different flow rates:

- Phase one: flow rate 1 (around 2.3 l/h)

A two-litre plastic bottle was filled with 1 litre of water. It was closed with the cap with  $\text{Ø}1.5\text{mm}$  orifice drilled in. The bottle was carefully placed (cup pointing downwards) on a cardboard support resting on the rain gauge bucket. The water was released allowing free flow (Figure 4.8). The number of tips was recorded.

- Phase two: flow rate 2 (around 8.2 l/h)

A two-litre plastic bottle was filled with 1 litre of water. It was closed with the cap with  $\text{Ø}2.0\text{mm}$  orifice drilled in. The bottle was carefully placed (cap pointing downwards) on a cardboard support resting on the rain gauge bucket. The water was released allowing free flow. The number of tips was recorded.

- Phase three: maximum flow (around 24.5 l/h)

The rain gauge bucket outlet was blocked using silicon plug. The bucket was carefully filled with 1 litre of water. The silicon plug was then removed allowing free flow of water. The number of tips was recorded.

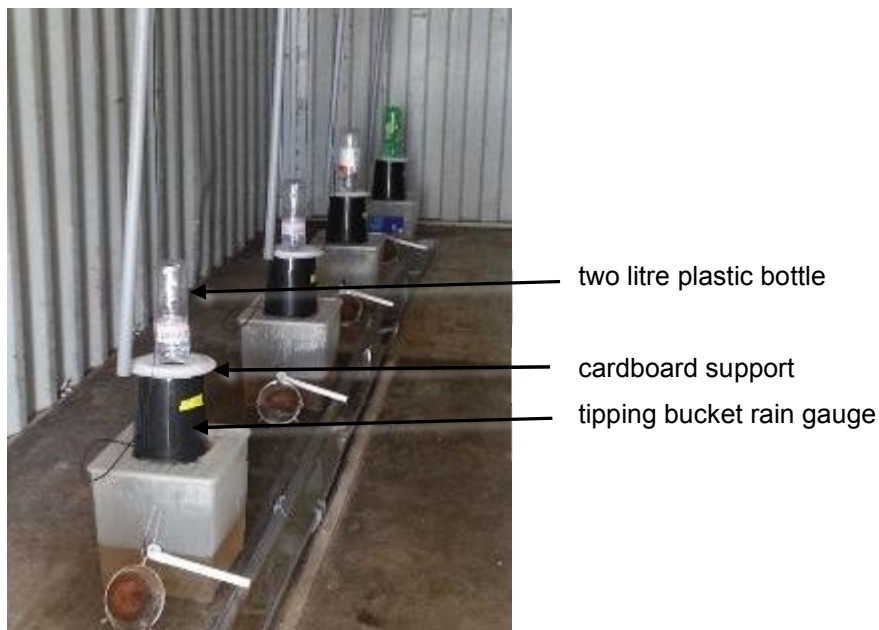


*Figure 4.8 Calibration of the tipping bucket rain gauges at Barking Riverside, phase one: flow rate 1 (around 2.3 l/h).*

### **Tipping bucket rain gauge calibration results and analysis**

Analysis of the tipping bucket rain gauge calibration were based on the results of the initial calibration (July 2010 and July 2011) and three-phase calibration (August 2013). Table 4.3 presents the outcome of the two initial calibrations of the tipping bucket rain gauges.

Table 4.3 Results of the two initial calibrations of tipping bucket rain gauges at Barking Riverside.

Roof Type	2011-1 (tips no)	2011-2 (tips no)	2011-3 (tips no)	2011- average (tips no)	2010 (tips no)	2011- volume per tip (ml)	2010 volume per tip (ml)	2010- 2011 difference (%)
Control-1	157	147	161	155.00	130	6.45	7.69	-16%
Control-2	171	140	158	156.33	143	6.40	6.99	-8%
Control-3	x	x	x	x	x	x	x	x
S/25/50-1	152	119	163	144.67	131	6.91	7.63	-9%
S/25/50-2	149	118	159	142.00	140	7.04	7.14	-1%
S/25/50-3	153	139	156	149.33	134	6.70	7.46	-10%
S/25/100-1	130	113	120	121.00	119	8.26	8.40	-2%
S/25/100-2	153	129	177	153.00	137	6.54	7.30	-10%
S/25/100-3	132	117	132	127.00	123	7.87	8.13	-3%
S/40/50-1	153	124	148	141.67	132	7.06	7.58	-7%
S/40/50-2	177	145	153	158.33	136	6.32	7.35	-14%
S/40/50-3	180	155	147	160.67	147	6.22	6.80	-9%
S/40/100-1	162	134	158	151.33	136	6.61	7.35	-10%
S/40/100-2	x	x	x	x	149	x	6.71	x
S/40/100-3	172	138	159	156.33	144	6.40	6.94	-8%
W/25/50-1	165	124	163	150.67	131	6.64	7.63	-13%
W/25/50-2	160	128	142	143.33	130	6.98	7.69	-9%
W/25/50-3	185	134	187	168.67	137	5.93	7.30	-19%
W/25/100-1	149	165	168	160.67	150	6.22	6.67	-7%
W/25/100-2	171	149	168	162.67	146	6.15	6.85	-10%
W/25/100-3	154	145	142	147.00	140	6.80	7.14	-5%
W/40/50-1	140	118	134	130.67	140	7.65	7.14	7%
W/40/50-2	120	157	176	151.00	152	6.62	6.58	1%
W/40/50-3	163	156	161	160.00	159	6.25	6.29	-1%
W/40/100-1	163	150	162	158.33	140	6.32	7.14	-11%
W/40/100-2	154	126	143	141.00	113	7.09	8.85	-20%
W/40/100-3	127	114	120	120.33	126	8.31	7.94	5%

Of particular interest was that all of the volume per tip values, determined through calibration, exceeded the value stated by the manufacturer (5.43ml). The

difference in volume per tip between the results of calibration carried out in 2010 and 2011 ranged from +7% to -20%. These differences would lead to over- or under-estimating stormwater runoffs and green roof retention capacities. Finally, it would also result in misleading conclusions in regards to green roof hydrological performance. To eliminate the effect of the inaccurate tipping bucket rain gauge calibration on stormwater runoff measurements, a new approach was adopted. This approach took into consideration the variability of the tip number in relation to runoff flow rate. The new approach was based on the determination of the volume per tip in relation to the runoff rate expressed as the number of tips per unit time. The choice of such a unit was influenced by the way the data is logged i.e. tip and corresponding time.

For each calibration phase the number of tips was summed and the total time of runoff determined. Based on these values, the runoff flow rate in tips/hour and the corresponding volume per tip (1litre divided by number of tips) were determined. To represent the calibration for small runoff rates (up to 100 tips/hour), the manufacturers value (corrected to the actual diameter of the rain collector bucket  $\varnothing=17\text{cm}$ ) of 5.77ml was included. Also, it was assumed that the value of the volume per tip determined during phase 3 of the calibration is the maximum value and cannot be exceeded. The values of the calibration conducted in 2011 were also included for a better calibration model fitting. Table 4.4 presents the results of all phases of calibration for the tipping bucket rain gauge monitoring runoff for the S/25/100 green roof. Figure 4.9 shows graph plotted based on Table 4.4. The calibration results and curves for all other green roofs and control roof are included in the Appendix B.

*Table 4.4 The results of the calibrations showing the runoff low rate (tips/hour) and corresponding volume of individual tip (ml) for the green roof S/25/100.*

<b>Date</b>	<b>Runoff flow rate (tips/hour)</b>	<b>Volume per tip (ml)</b>
<b>Jul-11</b>	8041.56	5.81
<b>Jul-11</b>	5018.18	7.25
<b>Jul-11</b>	6980.49	6.29
<b>Manufacturer value</b>	100.00	5.77
<b>Aug-13</b>	434.01	5.78
<b>Aug-13</b>	1186.81	6.67
<b>Aug-13</b>	8928.00	5.38

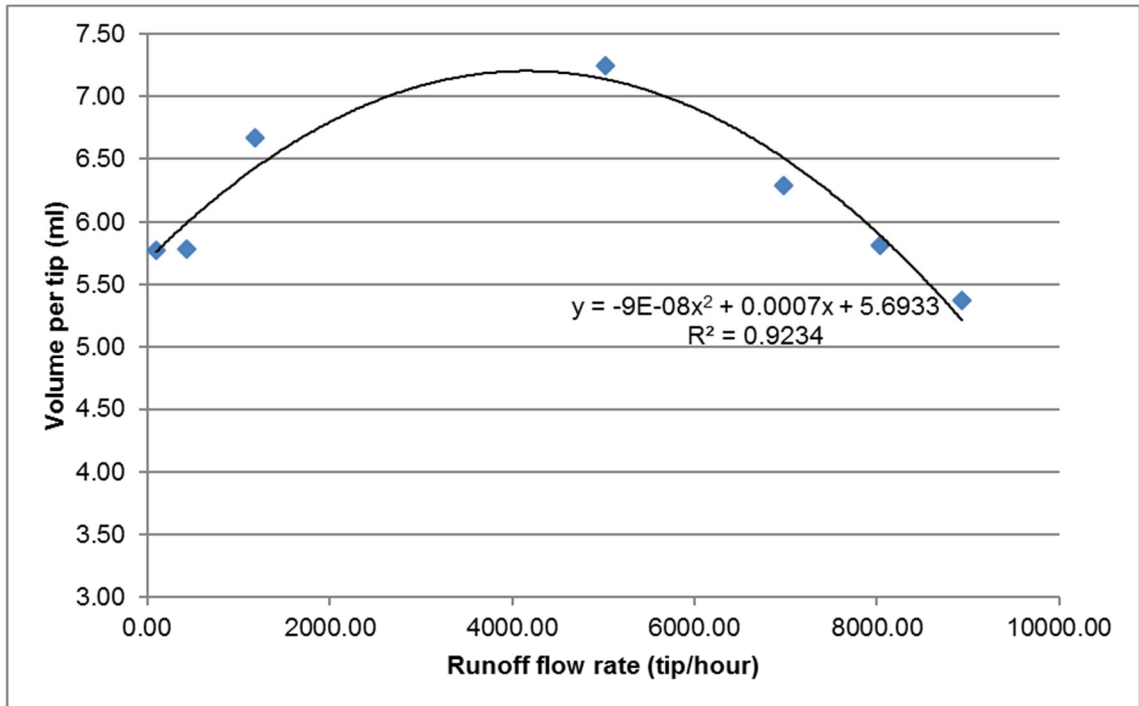


Figure 4.9 Modelled calibration curve for the green roof S/25/100 based on Table 4.4.

Figure 4.9 shows a parabolic relationship between volume per tip and runoff flow rate. The increase of the water volume per tip with the increase of the runoff flow rate could be a result of loss of the water due to water splashing inside the tipping bucket rain gauge and/or missing the bucket between tips. Hence, one tip accounts for water collected plus the water lost. As runoff flow rate increases greater pressure is created as the water flows through funnel. This could force the bucket to tip before being filled resulting in one tip accounting for the water volume of a partially filled bucket. It is believed that when the runoff flow rate is at maximum, these two actions could counterbalance resulting in volume per tip at the value of low runoff flow rates.

Table 4.5 presents the calibration equations for each tipping bucket rain gauge and corresponding the goodness of fit of a model coefficient ( $R^2$ ). The calibration equations (Table 4.5) were incorporated into the analysis of the Barking Riverside green roof in-situ experiment data (section 4.1.3.2).

Table 4.5 Summary of the calibration equations and corresponding goodness of fit of a model coefficient ( $R^2$ ).

Roof Type	Calibration equation Y – volume per tip X – runoff flow rate	$R^2$
Control-1	$y = -1E-07x^2 + 0.0011x + 5.4331$	0.707
Control-2	$y = -7E-08x^2 + 0.0005x + 6.2353$	0.774
Control-3	$y = -1E-07x^2 + 0.0007x + 5.6$	0.791
S/25/50-1	$y = -6E-08x^2 + 0.0005x + 5.9229$	0.810
S/25/50-2	$y = -1E-07x^2 + 0.0009x + 5.6837$	0.804
S/25/50-3	$y = -9E-08x^2 + 0.0007x + 5.8209$	0.796
S/25/100-1	$y = -7E-08x^2 + 0.0006x + 5.9121$	0.707
S/25/100-2	$y = -9E-08x^2 + 0.0007x + 5.6933$	0.923
S/25/100-3	$y = -8E-08x^2 + 0.0007x + 5.6001$	0.919
S/40/50-1	$y = -2E-07x^2 + 0.0016x + 5.5262$	0.951
S/40/50-2	$y = -1E-07x^2 + 0.001x + 5.6373$	0.997
S/40/50-3	$y = -2E-07x^2 + 0.0015x + 5.462$	0.855
S/40/100-1	$y = -2E-07x^2 + 0.0013x + 5.498$	0.905
S/40/100-2	$y = -3E-07x^2 + 0.002x + 5.9164$	0.836
S/40/100-3	$y = -1E-07x^2 + 0.0008x + 5.7014$	0.976
W/25/50-1	$y = -5E-08x^2 + 0.0004x + 5.9172$	0.603
W/25/50-2	$y = -9E-08x^2 + 0.0007x + 5.87$	0.881
W/25/50-3	$y = -6E-08x^2 + 0.0005x + 5.7235$	0.968
W/25/100-1	$y = -2E-07x^2 + 0.001x + 5.6933$	0.997
W/25/100-2	$y = -6E-08x^2 + 0.0004x + 5.9412$	0.512
W/25/100-3	$y = -2E-07x^2 + 0.0015x + 5.4511$	0.775
W/40/50-1	$y = -1E-07x^2 + 0.0007x + 5.6478$	0.683
W/40/50-2	$y = -1E-07x^2 + 0.0009x + 5.8375$	0.768
W/40/50-3	$y = -1E-07x^2 + 0.0008x + 5.5364$	0.702
W/40/100-1	$y = -6E-08x^2 + 0.0005x + 5.9993$	0.934
W/40/100-2	$y = -5E-08x^2 + 0.0004x + 6.0209$	0.535
W/40/100-3	$y = -1E-07x^2 + 0.0008x + 5.7014$	0.976

#### **4.1.2 ANALYSIS METHODS**

During data preparation and analysis, several different techniques and software were employed. Data preparation was mostly conducted using Microsoft Office Excel 2013, except for 'csv' files merging and separating, and individual rainfall event identification, which were carried out using custom designed applications.

Statistical analyses were conducted using R software. Exploratory data analysis of variables was carried out to assess the distribution and to determine subsequent statistical analysis test types. Data normality was assessed using the Shapiro – Wilk normality test. As presented in the Section 4.3 the variables analysed were not normally distributed, therefore non-parametric tests were employed. The Wilcoxon Rank Test was used to investigate statistically significant differences ( $p < 0.05$ ) between per-event runoff depth, retention, and peak flow reduction records from green roof plots of the same design (Fassman and Simcock, 2012, Speak et al., 2013a). Dunn's Kruskal-Wallis Multiple comparison test with a Bonferroni correction was employed to determine statistically significant differences ( $p < 0.05$ ) between individual (per-event) runoff depth, retention, and peak flow reduction observations from green roof plots of different design (Voyde et al., 2010, Nawaz et al., 2015, Stovin et al., 2015). Regression analysis was performed using R software.

#### **4.1.3 DATA PREPARATION**

Prior to the main analysis of the studied green roof hydrological performance, data preparation, including data cleansing, was carried out. In the study, two individual sets of data related to hydrological performance of green roofs were collected: weather conditions data and stormwater runoff from green roofs data. Both of the data sets had to be prepared to ensure quality of the results.

##### **4.1.3.1 WEATHER CONDITIONS DATA**

The weather conditions data was measured by Vantage Pro 2 weather station and logged into 'text' file type at 30min intervals (Figure 4.10).

In Date	In Time	Temp In	Hi In	Low wind In	Out wind In	Dew ISS Pt.	wind Arc. Speed	wind Dir	wind Run	Hi Speed	Hi Dir	wind chill	Heat Index	THW Index	Bar	Rain	Rain Rate
03/06/10	24.8	11:00	18.3	18.3	18.2	49	7.4	6.0	NE	3.00	11.0	NE	18.3	17.3	17.3	30.218	0.00
03/06/10	24.8	11:30	18.7	18.8	18.2	47	7.1	8.0	ENE	4.00	16.0	NNE	18.3	17.6	17.3	30.214	0.00
03/06/10	24.8	12:00	18.7	18.8	18.5	43	5.9	9.0	NE	4.50	14.0	NE	18.0	17.4	16.7	30.206	0.00
03/06/10	23.8	12:30	19.3	19.3	18.7	42	6.0	8.0	NE	4.00	15.0	NE	18.9	18.0	17.7	30.201	0.00
03/06/10	23.7	13:00	19.1	19.3	18.9	57	10.3	10.0	ENE	5.00	18.0	ENE	17.9	18.6	17.4	30.198	0.00
03/06/10	24.6	13:30	19.2	19.2	18.8	45	6.9	13.0	ENE	6.50	20.0	ENE	17.1	18.1	15.9	30.196	0.00
03/06/10	25.3	14:00	18.8	19.6	18.8	50	8.1	12.0	ENE	6.00	21.0	ENE	16.9	17.9	16.0	30.202	0.00
03/06/10	24.5	14:30	18.5	19.1	18.5	46	6.7	14.0	ENE	7.00	21.0	NE	16.1	17.3	14.9	30.195	0.00
03/06/10	24.8	15:00	18.7	18.7	18.3	46	6.8	15.0	ENE	7.50	22.0	NE	16.1	17.6	14.9	30.193	0.00
03/06/10	25.0	15:30	18.4	18.8	18.3	44	5.9	13.0	NE	6.50	20.0	ENE	16.2	17.1	14.9	30.186	0.00
03/06/10	25.4	16:00	18.7	18.7	18.3	49	7.8	11.0	ENE	5.50	20.0	ENE	17.2	17.8	16.2	30.177	0.00
03/06/10	25.6	16:30	18.9	18.9	18.6	45	6.7	10.0	ENE	5.00	19.0	ENE	17.8	17.7	16.6	30.169	0.00
03/06/10	26.0	17:00	18.5	25.2	680	1	99.4	30									

Figure 4.10 Weather station output data as a 'text' file.

The following variables were used in further analysis: rainfall, temperature, humidity, dew point, wind speed and temperature-humidity-wind index (Table 4.2).

The first step of data preparation was the identification and extraction of the relevant data and corresponding date and time. Secondly, the periods with missing rainfall records were identified:

- from 18/08/2011 to 02/09/2011
- from 05/12/2011 to 31/12/2011
- from 08/08/2012 to 10/08/2012
- from 16/05/2013 to 22/05/2013
- from 16/12/2013 to 08/01/2014

Finally, the individual rainfall events (section 4.1.3.1.1) were identified and concatenated to allow a general statistical analysis to be carried out.

#### 4.1.3.1.1 INDIVIDUAL RAINFALL EVENT IDENTIFICATION

There has yet to be a clear definition as to what constitutes a single rainfall event in green roof field research (Chapter 2). Several researchers across the world used 6 hours inter-event dry periods, to separate rainfall events (Stovin et al., 2012, Voyde et al., 2010, VanWoert et al., 2005). However, the inter-event dry period of 6 hours was originally evaluated based on United States rainfall events data (Driscoll et al., 1989). Driscoll et al. (1989) analysis was based on the assumption that for the rainfall event to be independent the arrival time of each storm event must be independent. This is true only for specific inter-event time. They noted that there were differences between the inter-event times for different

parts of the United States, which were characterised by different patterns of rainfall events. It was clear that the rainfall pattern, hence the arrangement of the rainfall data into individual rainfall events, depends on the geographical location. Therefore, based on these observations, similar analysis of the historical rainfall data for London, UK, was performed and this revealed that the inter-event time for rainfall separation in London is 12 hours. This London specific inter-event dry period was subsequently used in this study.

#### 4.1.3.2 RUNOFF DATA

The runoff data was collected by logging each single tip and corresponding time from tipping bucket rain gauges in ‘comma separated values (csv)’ type file (Figure 4.11). There was a ‘csv’ file created for each day of monitoring between July 2010 and August 2014.

	A	B	C	D	E	F	G	H	I	J
31	00:01:38	0	0	0	0	0	0	0	0	0
32	00:01:44	0	0	0	0	0	0	1	0	0
33	00:01:48	0	0	0	0	0	0	0	0	0
34	00:01:49	0	0	0	0	0	0	0	0	0
35	00:01:54	0	1	0	0	0	0	0	0	0
36	00:01:54	1	0	0	0	0	0	0	0	0
37	00:01:55	0	0	0	0	0	0	0	0	0
38	00:02:01	0	0	1	0	0	0	0	0	0
39	00:02:02	0	0	0	0	0	0	0	0	0
40	00:02:05	0	0	0	0	0	0	0	0	0
41	00:02:06	0	0	0	0	0	0	0	0	1
42	00:02:08	0	0	0	0	0	0	0	0	0
43	00:02:09	0	0	0	0	0	1	0	0	0
44	00:02:10	0	0	0	1	0	0	0	0	0

Time (hh:mm:ss)    Individual tips recorded per test plot

Figure 4.11 Daily rain gauge output data sheet (‘csv’ file). First column includes time, remaining columns contain records of tip – ‘1’ or no tip – ‘0’ per test plot.

The runoff data preparation started with the identification of periods of missing recordings due to data logging equipment failures (Table 4.6). There were 28 periods identified, when the runoff was not recorded, accounting for 301 days out of 1523 days of studied period. However, the missing data due to the individual rain gauge failures (e.g. as a result of funnel blockage) were difficult to identify. For example, in the case of individual rain gauge failures, the data record would show ‘0’, which meant that the tip did not occur. However, it was not possible to differentiate between ‘0’ record due to lack of runoff and ‘0’ record due to the rain

gauge failure. Next, the calibration periods were identified (Table 4.6) and the corresponding runoff data were removed from data set. The runoff data corresponding to missing rainfall periods were also excluded from further analysis.

*Table 4.6 The runoff data excluded from the analysis: reason for exclusion and corresponding dates for the monitoring period between July 2010 and August 2014.*

Reason for exclusion	Dates of exclusion					
	2010	2011	2012	2013	2014	
<b>Failure of the runoff logging equipment</b>		01/01 - 05/01				
		20/01 - 27/01				
	14/07 - 15/07	11/02 - 13/02				
	05/08 - 25/08	18/03 - 30/03		01/01 - 24/01	31/03 - 09/06	
	16/10 - 21/10	17/04 - 27/04	26/05 - 30/05	29/04 - 07/05	16/06 - 25/06	
	01/12 - 03/12	06/07 - 12/07	27/09 - 01/10	13/05 - 03/06	22/07 - 24/07	
	07/12 - 07/12	16/07 - 18/07	23/12 - 31/12	24/08 - 17/09		
	22/12 - 31/12	22/07 - 27/07				
		16/08 - 16/08				
		11/09 - 14/09				
		23/11 - 04/12				
		10/12 - 11/12				
	<b>Calibration</b>	05/07 - 05/07			19/08 - 19/08	
					27/11 - 29/11*	

\* calibration not included in analysis due to low reliability of the data

Subsequently, all daily runoff data sets were combined and then separated to data sets corresponding to each green roof plot. The 'zero' fields were removed. Next, the runoff data were arranged at a five-minute interval resolution and the calibration was applied. The runoff data were combined with corresponding rainfall events. However, when the runoff from green roof from the previous rainfall event was still occurring at the start of the subsequent rainfall event, events were merged (Voyde et al., 2010, Stovin et al., 2012).

Data preparation resulted in 358 individual observations over 4-years monitoring period, of which 43 were generated by merging. Rainfall events less than 2mm were excluded from 385-observations data set, as they are unlikely to cause any runoff from a conventional roof (Voyde et al., 2010). The final data set consisted of 181 individual observations.

## **4.2 OVERVIEW OF THE DATA**

This section outlines the variables associated with weather conditions, green roof design and green roof hydrological performance included in the analyses. The final data set consisted of 181 individual observations, recorded between July 2010 and August 2014. Each observation corresponded to independent rainfall event  $\geq 2\text{mm}$  and weather conditions, that twenty-four green roof test plots and three control roofs were subjected to.

### **4.2.1 WEATHER CONDITION DATA**

The following rainfall characteristics were included in further analysis as variables:

- Rainfall event depth (mm)
- Rainfall event duration (h)
- Inter-event time prior to rainfall event (h) (IET)

The following weather data, obtained from the records from weather station at Barking Riverside (section 4.1.1.1), were included in the analyses as variables:

- Temperature ( $^{\circ}\text{C}$ )
- Humidity (%)
- Dew point ( $^{\circ}\text{C}$ )
- Wind speed (km/h)
- Temperature-Humidity-Wind (THW) index ( $^{\circ}\text{C}$ )

For data analysis purposes, seasons were defined as follows: spring was March-May, summer was June – August, autumn was September – November and winter was December – February.

The variables associated with rainfall characteristics, climate conditions are called predictor (independent) variables hereinafter.

#### **4.2.2 GREEN ROOF DESIGN DATA**

As discussed in section 4.1.1, the following variables describing the green roof design were identified and included in further analysis:

- Vegetation type (sedum, wildflower)
- Drainage layer depth (mm)
- Substrate depth (mm)

The individual green roof design was also included as variable (e.g. S/25/50, Table 4.1). The properties of the green roof construction materials were not included since all green roofs were built using the same materials.

Green roof design variables were included into a group of predictor (independent) variables.

#### **4.2.3 GREEN ROOF HYDROLOGICAL PERFORMANCE DATA**

The green roof hydrological performance data were based on the relation between rainfall and corresponding runoff from green roof test plots. The rainfall – runoff relation was described as green roof retention capacity and green roof attenuation ability (Chapter 2). This study concentrates on: runoff depth (mm), retention (%) and peak flow reduction (%) as characteristics of green roof hydrological performance.

It should be noted that in the case when the retention outcome had a negative value (i.e. the runoff was greater than the corresponding rainfall), the listwise deletion was implemented. The negative retention could occur due to the various reasons such as the malfunction of runoff monitoring tipping bucket rain gauges (section 4.1.3.2), the additional runoff from melting of the snow cover (which could take 1 day), melting of the frozen water in the substrate layer (which could take 12 days) (Teemusk and Mander, 2007) or underestimation of rainfall quantity (section 4.3.2).

The hydrological performance characteristics: runoff depth, retention and peak flow reduction are termed as response (dependent) variables hereinafter.

### **4.3 RESULTS AND DISCUSSION**

The following section presents the results and discussion of the climate conditions analysis and hydrological performance of the green roofs analysis. The former includes analysis of climate specific to London, UK and to Barking Riverside experimental site. The latter includes exploratory data analysis, per-event analysis, seasonal analysis, and annual analysis in regards to hydrological performance of green roofs (stormwater runoff, retention, and peak flow reduction). Preliminary multiple linear regression analysis was used to investigate the influence of rainfall characteristics and climate conditions on the green roof hydrological performance.

#### **4.3.1 LONDON CLIMATIC CONDITIONS**

The research concentrated on the hydrological performance of the green roofs under UK climatic conditions. According to the Köppen-Geiger climate classification, the UK climate is defined as a climate with warm temperatures, fully humid with warm summers (Cfb) (Kottek et al., 2006). Due to the Barking Riverside experimental site location (section 4.1.1), the London climate was the focus of this study. London is located in Southern England. Due to the close proximity to the continental Europe, Southern England can be subjected to continental weather such as cold winters and hot, humid summers (UK Meteorological Office, 2016).

The London climate analysis was based on open data provided by the Meteorological Office (Met Office) (UK Meteorological Office, 1948-current). This data came from Heathrow Airport weather station. The average rainfall per year between 1948 and 2015 in London area (Heathrow) was approximately 606 mm. During the green roof monitoring research period, total rainfall in 2012 and 2014 significantly exceeded long term averages for the location, resulting in approximately 707 mm and 864 mm respectively (Figure 4.12).

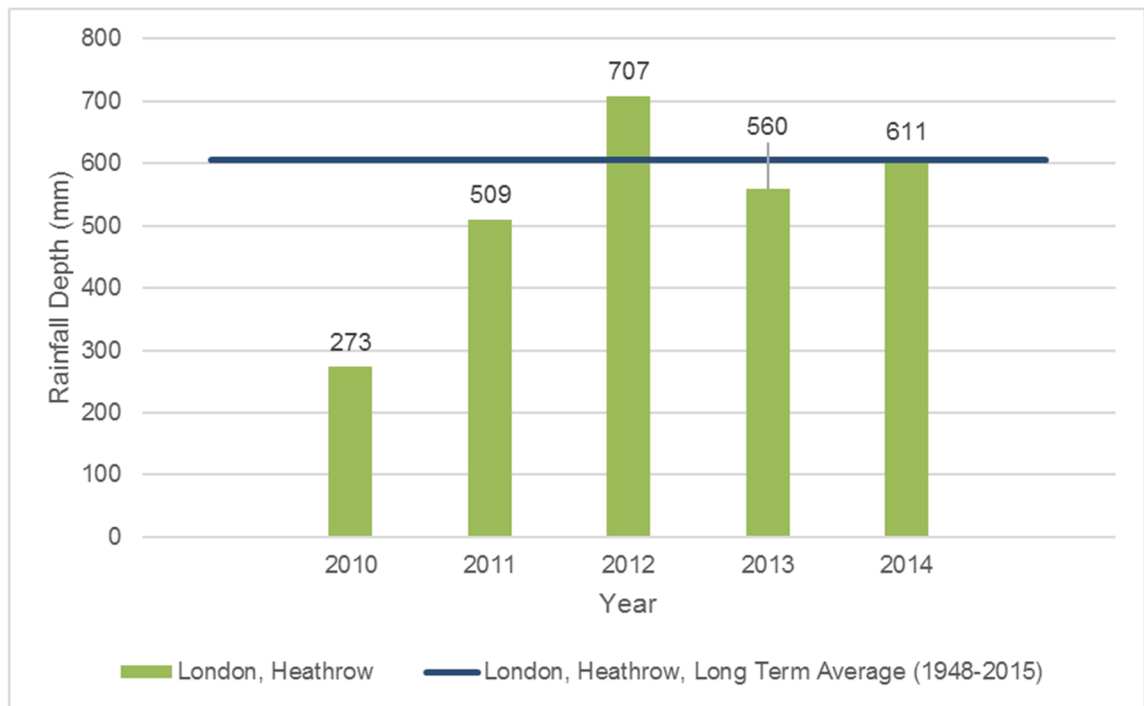


Figure 4.12 The historical rainfall data for Heathrow, London (UK Meteorological Office, 1948-current). Annual rainfall depth is presented for each year of research period and compared to long term average rainfall depth based on data between years 1948 and 2015.

The rainfall and temperatures in London change seasonally. During the period of study, July 2010 – August 2014, the highest mean daily maximum temperature occurred in July 2013 at 27°C, the lowest mean daily minimum temperature was in December 2010 at -1.5°C. The mean daily maximum temperature for the period 2010-2014 was higher than Long Term Average (1948-2015). Similarly, the mean daily minimum temperature for the period 2010-2014 was higher compared to the period 1948-2015 (Figure 4.13).

The highest monthly rainfall was observed in January 2014, 162.4mm and the lowest in April 2011, 2.4mm. The mean monthly rainfall data recorded between 2010 and 2014 exceeded the long-term average rainfall for the period 1948-2015 in all months, with exception to March, May, July, and September (Figure 4.14).

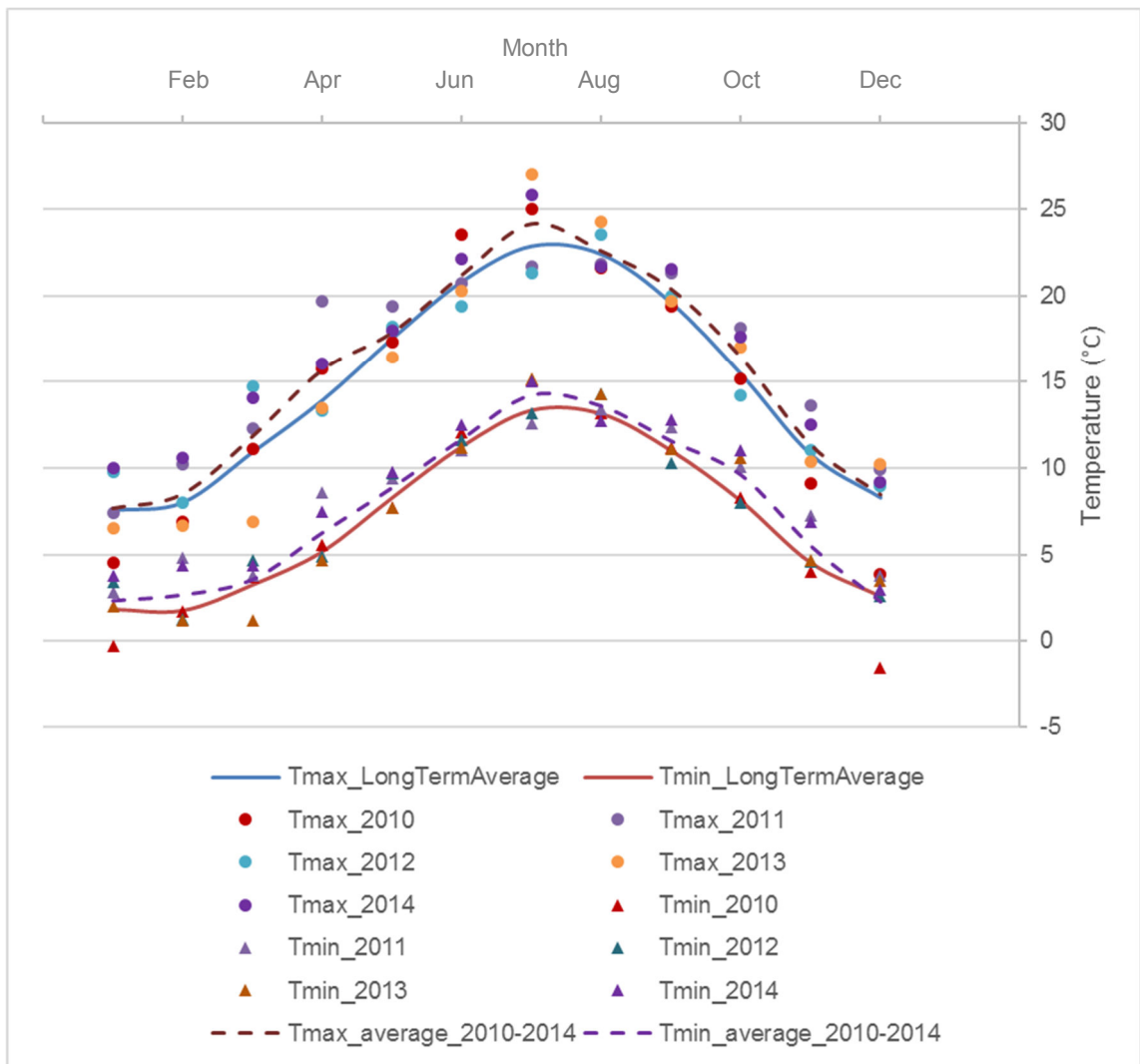


Figure 4.13 The historical temperature data, Heathrow, London (UK Meteorological Office, 1948-current). Chart presents monthly averages (minimum and maximum) for each year of research period, monthly averages (minimum and maximum) for the period between 2010 and 2014, and long term monthly averages (minimum and maximum) for the period between 1948 and 2015.

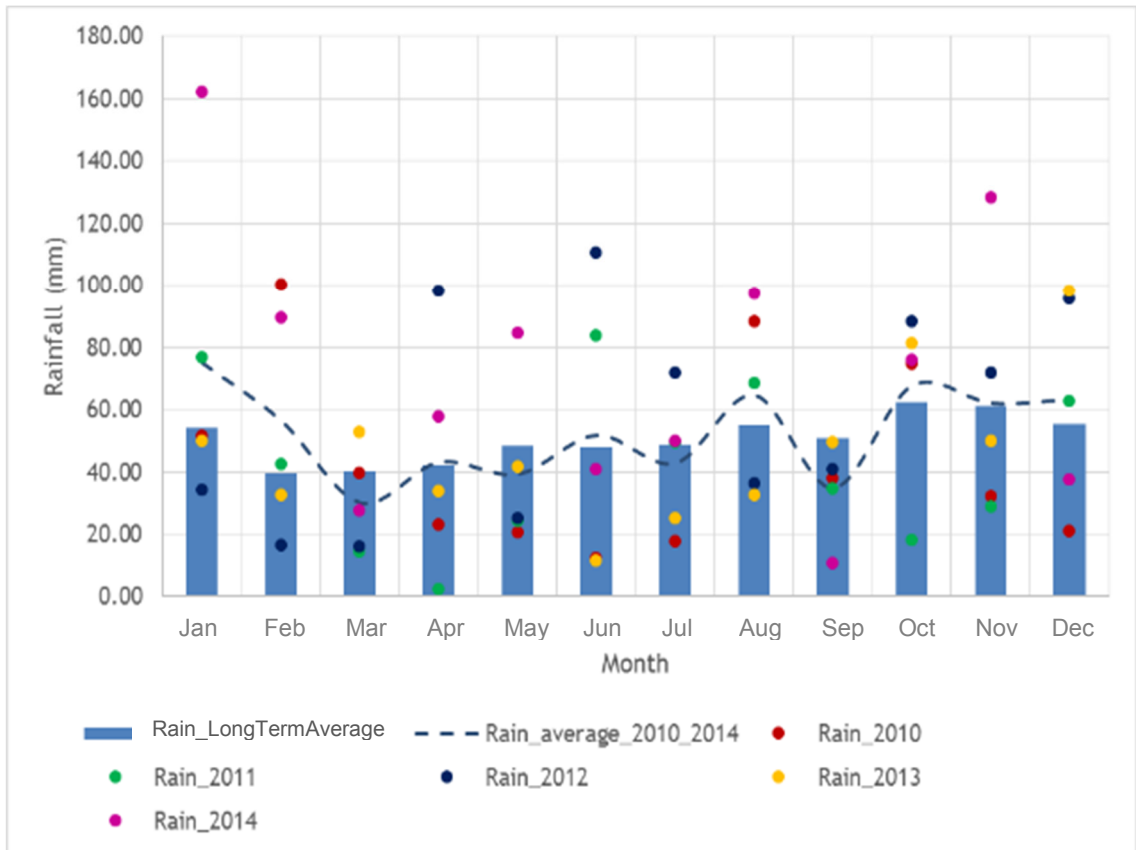


Figure 4.14 The historical monthly rainfall data, Heathrow, London (UK Meteorological Office, 1948-current). Chart presents monthly averages for each year of research period, monthly averages for the period between 2010 and 2014, and long term monthly averages for the period between 1948 and 2015.

#### 4.3.2 RAINFALL - BARKING RIVERSIDE

The rainfall data was prepared as described in the section 4.1.3. Initial number of individual rainfall events was 358. The final number of individual rainfall events ( $\geq 2\text{mm}$ ) was 181. Both data sets were explored, however, only the final was used in green roof hydrological performance analysis.

The summary statistics of initial and final rainfall events data sets are presented in the Table 4.7. Figure 4.15 and 4.16 show boxplots and frequency histograms for both rainfall data sets: initial and final. Q-Q plots and density histograms for these data sets are in Appendix C.

Table 4.7 Summary statistics of initial and final rainfall data sets recorded at Barking Riverside. Initial data set contains all identified rainfall events, whilst final data set contains rainfall events greater than 2mm.

Summary Statistics, Rainfall Depth (mm)			
Rainfall events		initial	final
<b>No</b>		358	181
<b>Mean</b>		4.70	8.69
<b>Median</b>		2.01	6.08
<b>Std. Deviation</b>		6.82	7.70
<b>Percentiles</b>	<b>Min.</b>	0.20	2.00
	<b>25</b>	0.50	3.40
	<b>50</b>	2.01	6.08
	<b>75</b>	6.08	10.89
	<b>Max.</b>	43.55	43.55
<b>Shapiro - Wilk normality test</b>	<b>p-value</b>	< 2.2 x 10 <sup>-16</sup>	1.745 x 10 <sup>-15</sup>
		- non-normal distribution (p<0.05)	

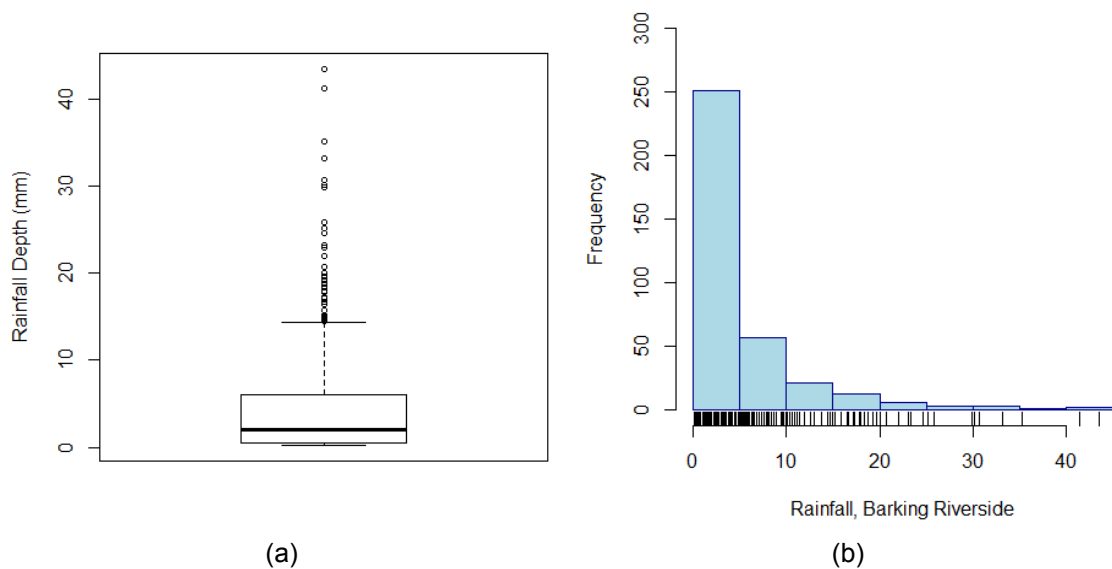
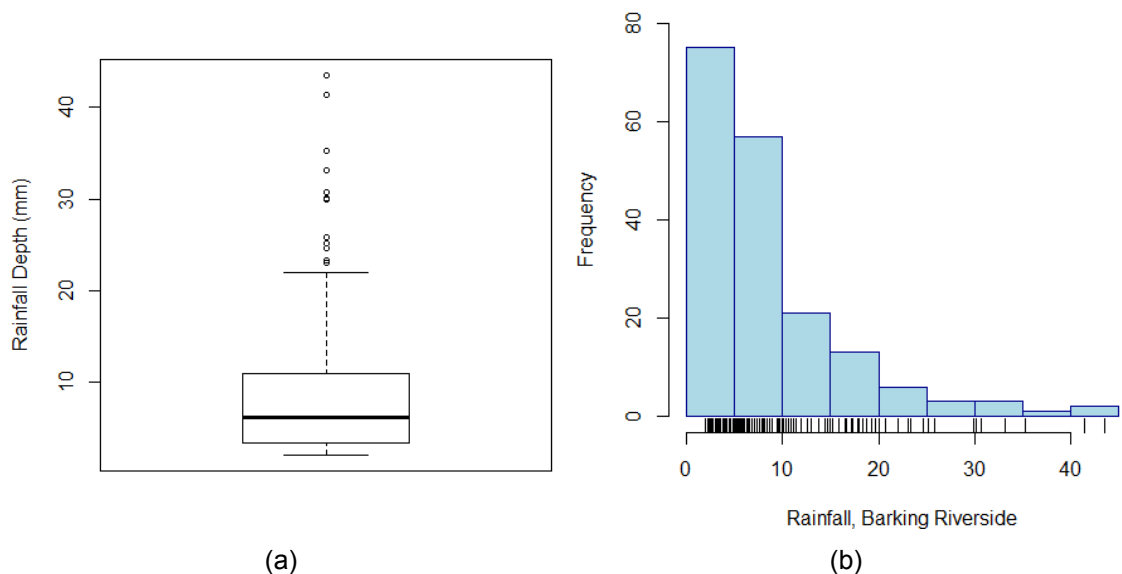


Figure 4.15 Data exploratory analysis of rainfall at Barking Riverside (a) boxplot showing distribution of the initial rainfall data (b) histogram presenting the frequency of rainfall data - initial data set. Boxplot confirms non-normal distribution of rainfalls. Histogram shows exponential distribution of rainfalls.



*Figure 4.16 Data exploratory analysis of rainfall at Barking Riverside (a) boxplot showing distribution of the final rainfall data (b) histogram presenting the frequency of rainfall data - final data set. Boxplots confirms non-normal distribution of rainfalls. Histogram shows exponential distribution of rainfalls.*

Analysing summary statistics results and graphs (Figure 4.15 and 4.16), it was clear that there was a non-normal rainfall data distribution for both data sets: initial with all rainfall events included and final with rainfall events greater than 2mm. The boxplots indicate a positive skewness of the data. The non-normal distribution was also confirmed using Shapiro-Wilk normality test with p-value  $p < 2.2 \times 10^{-16}$  for initial rainfall event data and  $p = 1.745 \times 10^{-15}$  for final rainfall events data. The frequency histogram shows that the depth of the majority of the rainfall events was between 0 and 5 mm in both cases. The two most distant outliers correspond to the following rainfall events (Figure 4.15 (a) and Figure 4.16 (a)):

- 20<sup>th</sup> November 2012, rain depth: 43.5mm, rain duration: 170h
- 23<sup>rd</sup> September 2012, rain depth: 41.34mm, rain duration: 77.5h

Exclusion of small rainfall events improved the overall rainfall distribution. Moreover, it also reduced data that had low explanatory power prior to further green roof hydrological performance analysis.

In order to confirm the reliability of the rainfall data collected at Barking Riverside, it was compared to London, Heathrow rainfall data for the period of study from July 2010 to August 2014 (Figure 4.17). Additionally, Barking Riverside data was also compared to Crossness Sewage Treatment Works (STW) (Met Office,

2012), which is located only 2km away from experiment site as opposed to Heathrow, which is about 40km away (Figure 4.17).

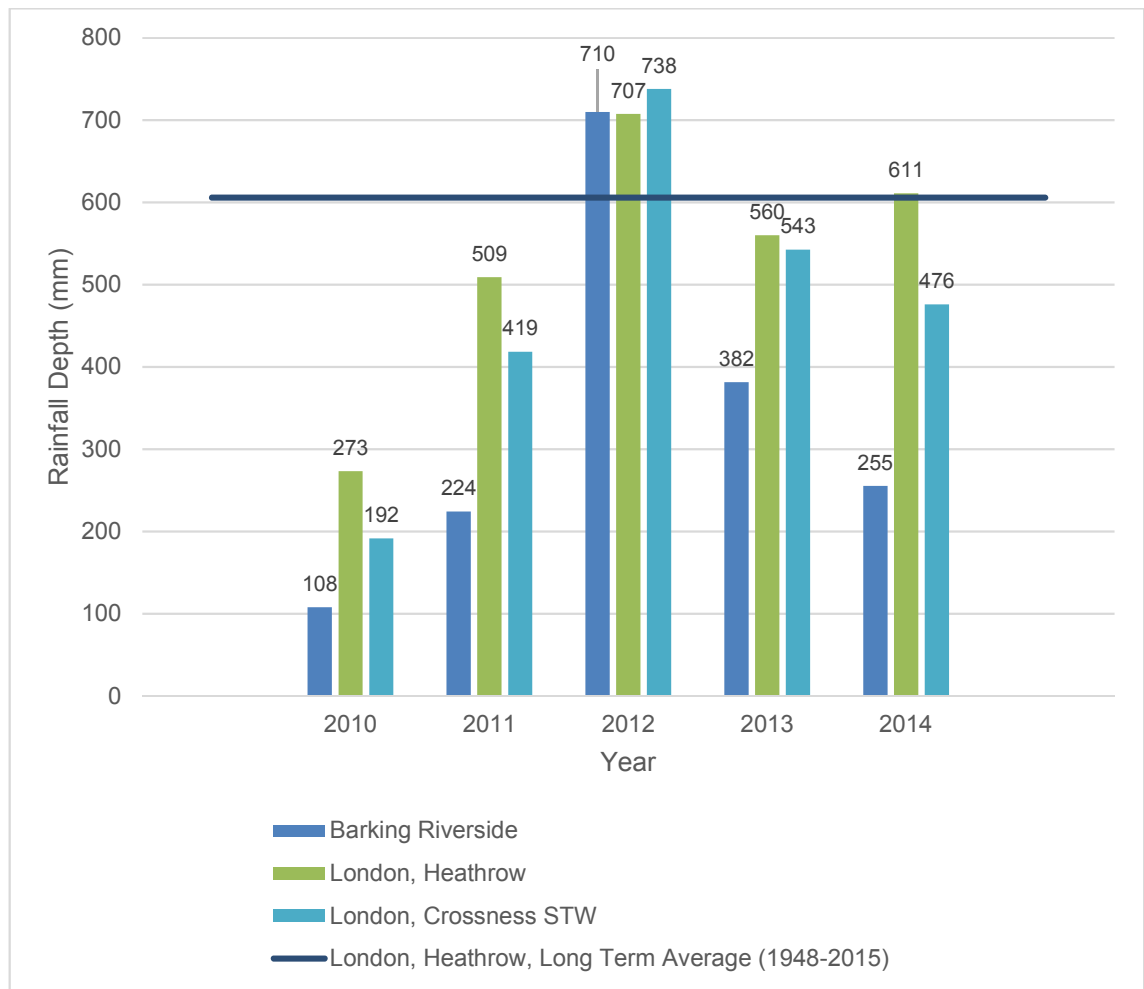


Figure 4.17 The annual rainfall data recorded at Barking Riverside, London-Heathrow, London-Crossness STW, July 2010 – August 2014.

The Barking Riverside rainfall data were significantly lower than London, Heathrow data for the corresponding period. It was also lower than London, Crossness STW. The only exception was the year 2012, when the Barking Riverside data was similar to the Heathrow and Crossness STW records.

The differences in rainfall data between Barking Riverside and Heathrow were likely to be due to the distance of 40km between these weather stations. However, the distance does not explain the significant differences that occurred between Barking Riverside and Crossness STW rainfall data. These stations are located only 2km apart. Hence, the underperformance of the Barking Riverside weather station could be due to equipment failures (section 4.1.3).

The Barking Riverside rainfall events (depths and duration) were compared to London rainfall return period (T) data generated according to Wallingford procedure (Department of the Environment et al., 1981) (Figure 4.18). Figure 4.18 shows initial rainfall events data set indicating rainfalls lower than 2mm and greater or equal to 2mm and merged rainfall events (section 4.1.2). As expected, most of the events fell below the 1 year return period. However, taking into consideration that during the period of study there were months much wetter than the historical average (Figure 4.14), it would be expected than more rainfall events would have had a return period exceeding 1 year. It should be noted that there are rainfall data missing due to the failure of the monitoring equipment (section 4.1.2). It is possible that amongst these missing rainfall records are rainfall events of return period greater than 1 year.

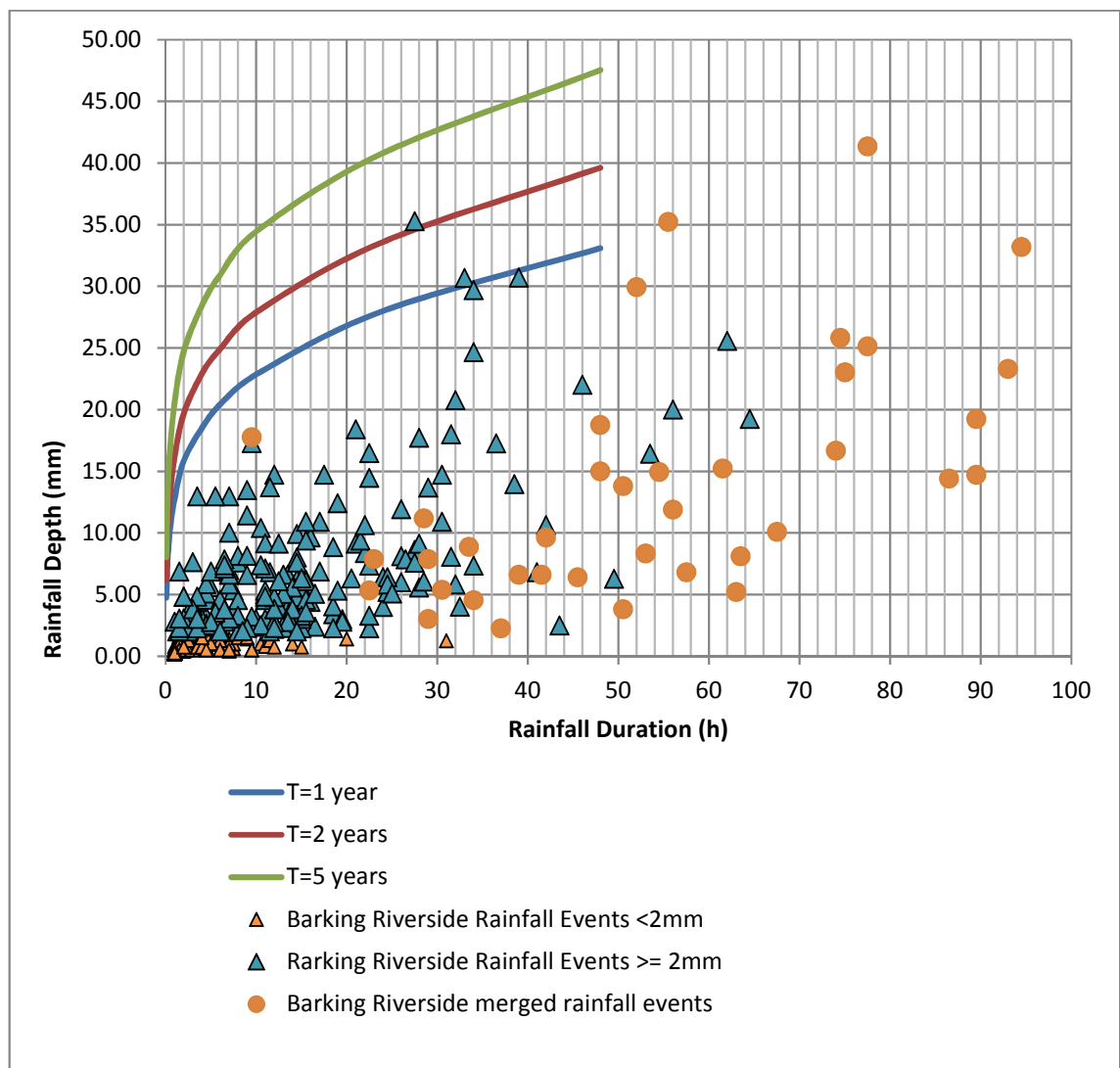


Figure 4.18 Rainfall characteristics for Barking Riverside rainfall data, July 2010 – August 2014 compared with return period estimated for London.

For clarity of presentation, five merged rainfall events were not included in Figure 4.18 due to their extremely long duration (greater than 100h):

- 1<sup>st</sup> October 2010, rainfall depth: 15.8mm, rainfall duration: 101h
- 10<sup>th</sup> January 2011, rainfall depth: 15.0mm, rainfall duration: 105.5h
- 17<sup>th</sup> October 2012, rainfall depth: 30.12mm, rainfall duration: 142h
- 20<sup>th</sup> November 2012, rainfall depth: 43.55mm, rainfall duration: 170h
- 8<sup>th</sup> November 2013, rainfall depth: 17.19mm, rainfall duration: 142.5h

None of these long duration rainfall events had a return period greater than or equal to 1 year.

The following rainfall events had return period  $\geq 1$  year:

- 10<sup>th</sup> June 2012, rainfall depth: 30.69mm, duration: 39h, return period: 1 year
- 23<sup>rd</sup> September 2012, rainfall depth: 35.28mm, duration: 27.5h, return period: 2 years (before merging)
- 27<sup>th</sup> April 2012, rainfall depth: 35.22mm, duration: 55.5h, return period: 1 year (merged rainfall event)
- 23<sup>rd</sup> September 2012, rainfall depth: 41.34mm, duration: 77.5h, return period: 1.5 year (merged rainfall event)

### **4.3.3 HYDROLOGICAL PERFORMANCE OF THE GREEN ROOFS: EXPERIMENTAL REPLICATES**

The hydrological performance of the experimental replicates of each of eight green roof design and control roofs was assessed based on retention as a main characteristic of the hydrological performance. The exploratory data analysis was carried out to determine the nature of data distribution. The summary statistics and boxplots for all roofs are presented in Table 4.7 to 4.16 and Figure 4.19 to 4.27. The Q-Q plots and density histograms for all roofs can be found in Appendix D.

Hydrological performance analyses presented in this section are based on final data set (section 4.2).

## Control roofs

Table 4.8 Summary statistics of stormwater retention data for following roofs: Control-1, Control-2, Control-3.

Summary Statistics, Retention (%)				
Roof type		Control-1	Control-2	Control-3
<b>Mean</b>		81.17	70.18	76.43
<b>Median</b>		94.80	85.05	86.35
<b>Std. Deviation</b>		25.86	31.35	26.31
<b>Percentiles</b>	Min.	0.00	0.00	0.00
	25	68.88	39.92	56.27
	50	94.80	85.05	86.35
	75	98.60	97.20	99.05
	Max.	100.00	100.00	100.00
<b>Shapiro-Wilk normality test</b>	p-value	4.446 x 10 <sup>-16</sup>	2.507 x 10 <sup>-12</sup>	1.247 x 10 <sup>-12</sup>
<div style="display: flex; align-items: center;"> <div style="width: 20px; height: 10px; background-color: #cccccc; margin-right: 5px;"></div> <span>- non-normal distribution (p&lt;0.05)</span> </div>				

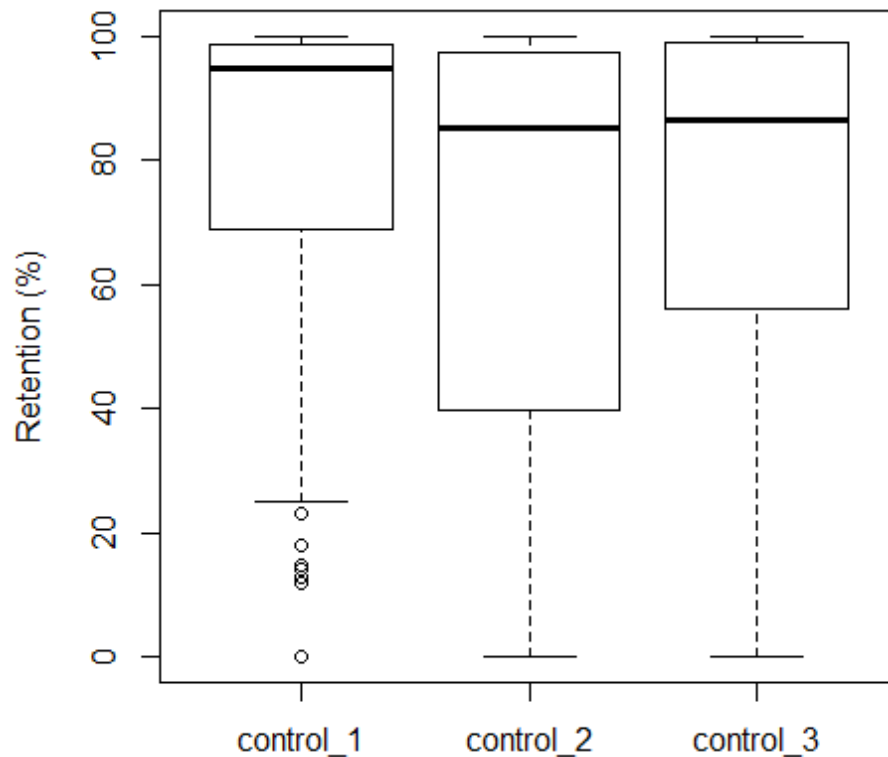


Figure 4.19 Stormwater retention data distribution for the following roofs: Control-1, Control-2, Control-3.

**Vegetation: Sedum, drainage layer: 25mm, substrate: 50mm (S/25/50)**

Table 4.9 Summary statistics of stormwater retention data for following green roofs: S/25/50-1, S/25/50-2, S/25/50-3.

Summary Statistics, Retention (%)				
Roof type		S/25/50-1	S/25/50-2	S/25/50-3
<b>Mean</b>		81.26	77.20	77.12
<b>Median</b>		99.85	99.80	98.85
<b>Std. Deviation</b>		26.35	30.09	29.47
<b>Percentiles</b>	Min.	9.40	0.00	0.00
	25	57.80	48.30	51.65
	50	99.85	99.80	98.85
	75	100.00	100.00	100.00
	Max.	100.00	100.00	100.00
<b>Shapiro-Wilk normality test</b>	p-value	< 2.2 x 10 <sup>-16</sup>	1.849 x 10 <sup>-15</sup>	2.763 x 10 <sup>-15</sup>
<div style="display: flex; align-items: center;"> <div style="width: 20px; height: 10px; background-color: #cccccc; margin-right: 5px;"></div> <span>- non-normal distribution (p&lt;0.05)</span> </div>				

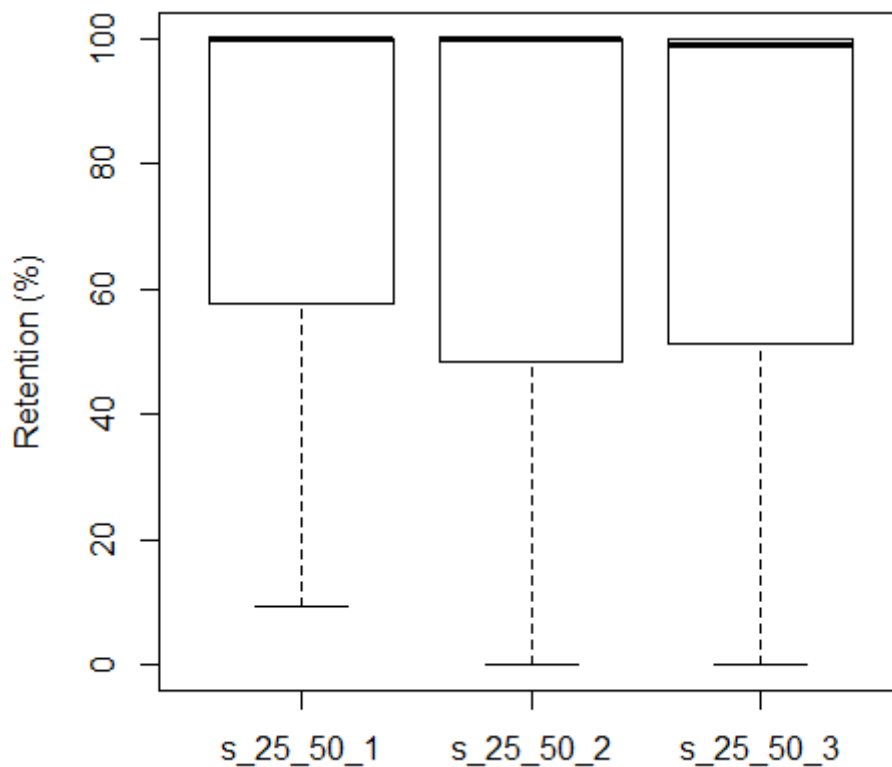


Figure 4.20 Stormwater retention data distribution for green roofs: S/25/50-1, S/25/50-2, S/25/50-3.

**Vegetation: Sedum, drainage layer: 25mm, substrate: 100mm (S/25/100)**

Table 4.10 Summary statistics of stormwater retention data for following green roofs: S/25/100-1, S/25/100-2, S/25/100-3.

Summary Statistics, Retention (%)					
Roof type		S/25/100-1	S/25/100-2	S/25/100-3	
<b>Mean</b>		78.88	77.20	78.83	
<b>Median</b>		100.00	99.80	99.85	
<b>Std. Deviation</b>		28.78	29.18	29.18	
<b>Percentiles</b>	Min.	3.70	0.00	0.00	
	25	55.77	48.30	54.60	
	50	100.00	99.80	99.85	
	75	100.00	100.00	100.00	
	Max.	100.00	100.00	100.00	
<b>Shapiro-Wilk normality test</b>		p-value	5.752 x 10 <sup>-16</sup>	1.849 x 10 <sup>-15</sup>	4.865 x 10 <sup>-16</sup>
		- non-normal distribution (p<0.05)			

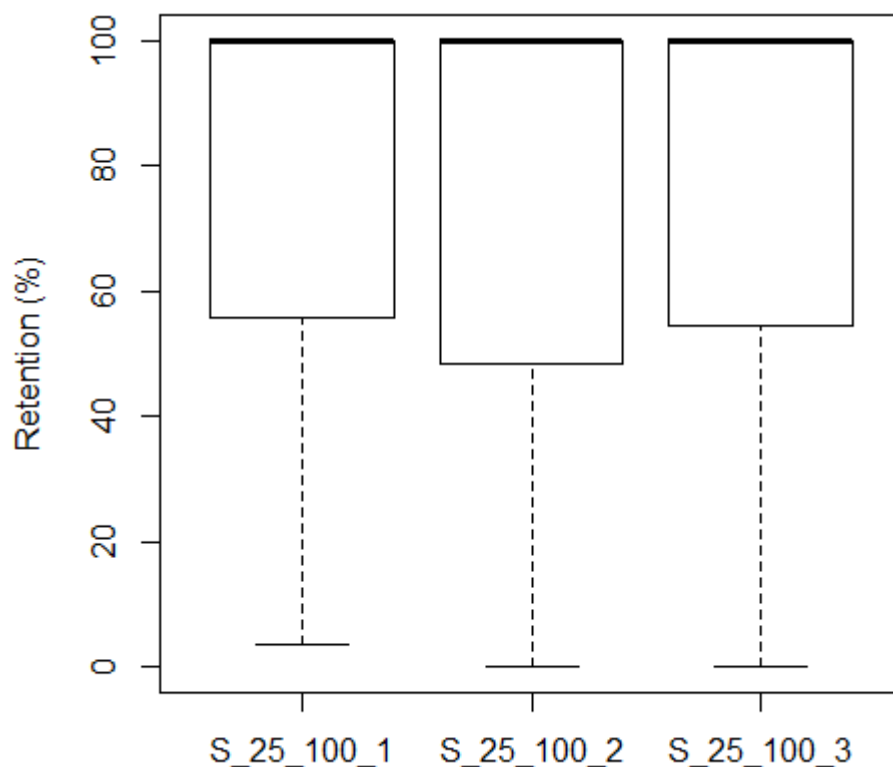


Figure 4.21 Stormwater retention data distribution for green roofs: S/25/100-1, S/25/100-2, S/25/100-3.

**Vegetation: Sedum, drainage layer: 40mm, substrate: 50mm (S/40/50)**

Table 4.11 Summary statistics of stormwater retention data for following green roofs: S/40/50-1, S/40/50-2, S/40/50-3.

Summary Statistics, Retention (%)				
Roof type		S/40/50-1	S/40/50-2	S/40/50-3
<b>Mean</b>		79.24	79.53	77.47
<b>Median</b>		100.00	99.90	98.80
<b>Std. Deviation</b>		28.57	28.46	28.90
<b>Percentiles</b>	Min.	2.50	1.70	1.10
	25	55.90	55.60	49.50
	50	100.00	99.90	98.80
	75	100.00	100.00	100.00
	Max.	100.00	100.00	100.00
<b>Shapiro-Wilk normality test</b>	p-value	6.156 x 10 <sup>-16</sup>	6.123 x 10 <sup>-16</sup>	1.999 x 10 <sup>-15</sup>
<div style="display: flex; align-items: center;"> <div style="width: 20px; height: 10px; background-color: #cccccc; margin-right: 5px;"></div> <span>- non-normal distribution (p&lt;0.05)</span> </div>				

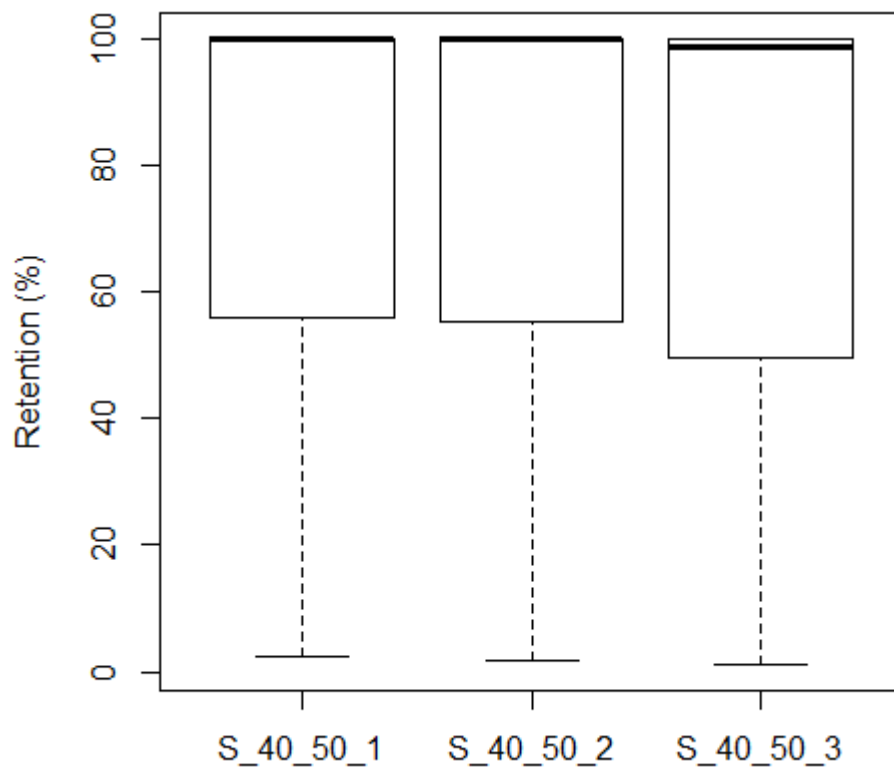


Figure 4.22 Stormwater retention data distribution for green roofs: S/40/50-1, S/40/50-2, S/40/50-3.

**Vegetation: Sedum, drainage layer: 40mm, substrate: 100mm (S/40/100)**

Table 4.12 Summary statistics of stormwater retention data for following green roofs: S/40/100-1, S/40/100-2, S/40/100-3.

Summary Statistics, Retention (%)				
Roof type		S/40/100-1	S/40/100-2	S/40/100-3
<b>Mean</b>		78.12	86.11	86.29
<b>Median</b>		100.00	100.00	100.00
<b>Std. Deviation</b>		29.32	24.79	25.09
<b>Percentiles</b>	Min.	0.00	0.00	0.00
	25	49.20	84.00	87.30
	50	100.00	100.00	100.00
	75	100.00	100.00	100.00
	Max.	100.00	100.00	100.00
<b>Shapiro-Wilk normality test</b>		p-value	7.248 x 10 <sup>-16</sup>	< 2.2 x 10 <sup>-16</sup>
		- non-normal distribution (p<0.05)		

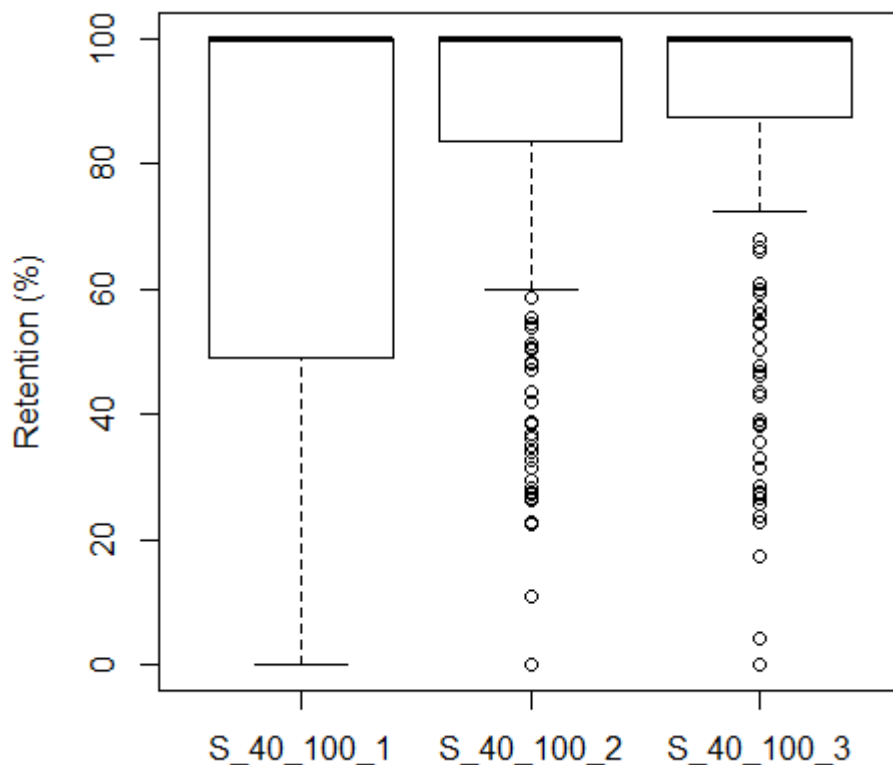


Figure 4.23 Stormwater retention data distribution for green roofs: S/40/100-1, S/40/100-2, S/40/100-3.

**Vegetation: Wildflower, drainage layer: 25mm, substrate: 50mm (W/25/50)**

Table 4.13 Summary statistics of stormwater retention data for following green roofs: W/25/50-1, W/25/50-2, W/25/50-3.

Summary Statistics, Retention (%)				
Roof type		W/25/50-1	W/25/50-2	W/25/50-3
<b>Mean</b>		76.26	83.89	80.14
<b>Median</b>		99.90	100.00	100.00
<b>Std. Deviation</b>		31.1	27.61	28.97
<b>Percentiles</b>	Min.	0.00	0.10	0.00
	25	48.02	71.75	58.02
	50	99.90	100.00	100.00
	75	100.00	100.00	100.00
	Max.	100.00	100.00	100.00
<b>Shapiro-Wilk normality test</b>		p-value	1.885 x 10 <sup>-15</sup>	< 2.2 x 10 <sup>-16</sup>
		- non-normal distribution (p<0.05)		

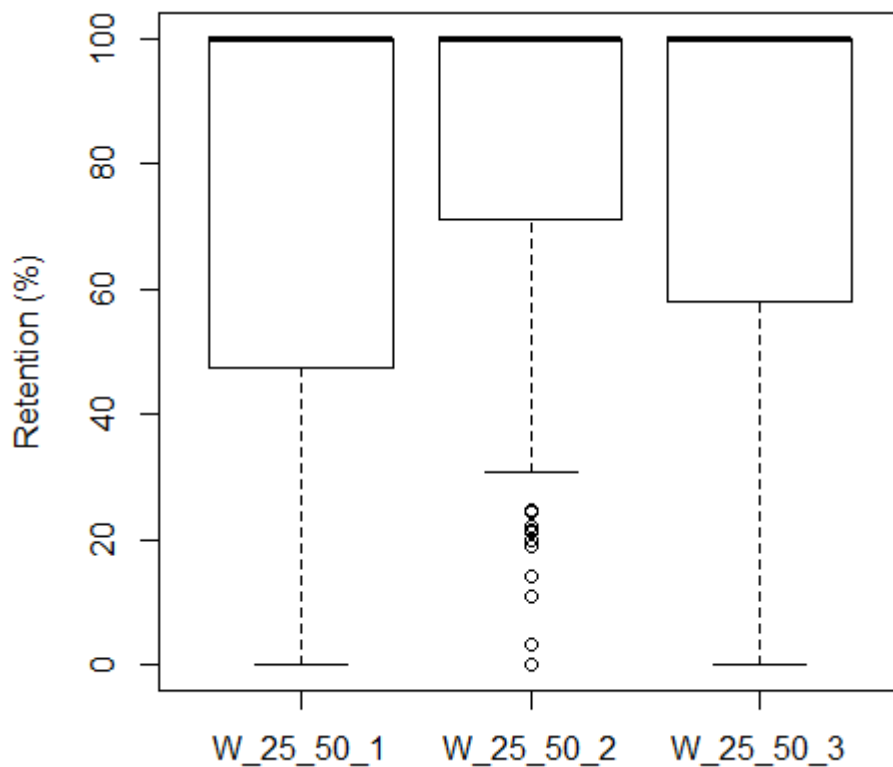


Figure 4.24 Stormwater retention data distribution for green roofs: W/25/50-1, W/25/50-2, W/25/50-3.

**Vegetation: Wildflower, drainage layer: 25mm, substrate: 100mm (W/25/100)**

Table 4.14 Summary statistics of stormwater retention data for following green roofs: W/25/100-1, W/25/100-2, W/25/100-3.

Summary Statistics, Retention (%)				
Roof type		W/25/100-1	W/25/100-2	W/25/100-3
<b>Mean</b>		79.14	77.47	79.33
<b>Median</b>		99.90	99.35	100.00
<b>Std. Deviation</b>		28.15	30.14	28.19
<b>Percentiles</b>	Min.	0.60	0.00	1.30
	25	55.52	52.33	55.67
	50	99.60	99.35	98.95
	75	100.00	100.00	100.00
	Max.	100.00	100.00	100.00
<b>Shapiro-Wilk normality test</b>	p-value	5.299 x 10 <sup>-16</sup>	7.782 x 10 <sup>-16</sup>	6.226 x 10 <sup>-16</sup>
<div style="display: flex; align-items: center;"> <div style="width: 20px; height: 10px; background-color: #cccccc; margin-right: 5px;"></div> <span>- non-normal distribution (p&lt;0.05)</span> </div>				

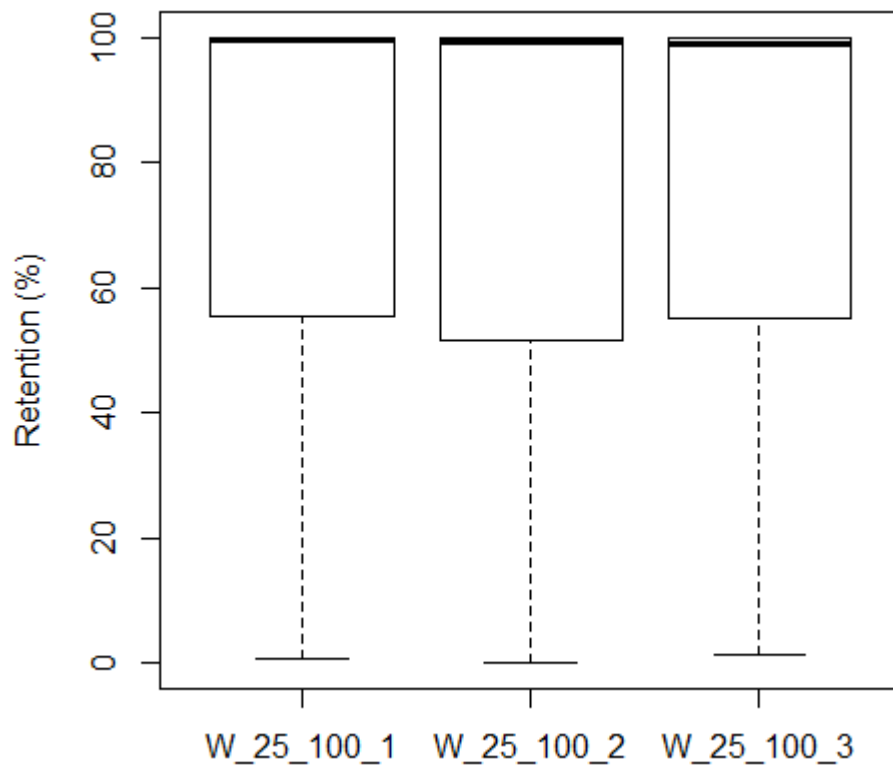


Figure 4.25 Stormwater retention data distribution for green roofs: W/25/100-1, W/25/100-2, W/25/100-3.

**Vegetation: Wildflower, drainage layer: 40mm, substrate: 50mm (W/40/50)**

Table 4.15 Summary statistics of stormwater retention data for following green roofs: W/40/50-1, W/40/50-2, W/40/50-3.

Summary Statistics, Retention (%)				
Roof type		W/40/50-1	W/40/50-2	W/40/50-3
<b>Mean</b>		77.08	78.44	82.81
<b>Median</b>		99.60	99.80	100.00
<b>Std. Deviation</b>		30.40	29.16	24.46
<b>Percentiles</b>	Min.	0.00	0.10	17.00
	25	48.90	52.60	63.00
	50	99.60	99.80	100.00
	75	100.00	100.00	100.00
	Max.	100.00	100.00	100.00
<b>Shapiro-Wilk normality test</b>	p-value	1.033 x 10 <sup>-15</sup>	6.395 x 10 <sup>-16</sup>	< 2.2 x 10 <sup>-16</sup>
<div style="display: flex; align-items: center;"> <div style="width: 20px; height: 10px; background-color: #cccccc; margin-right: 5px;"></div> <span>- non-normal distribution (p&lt;0.05)</span> </div>				

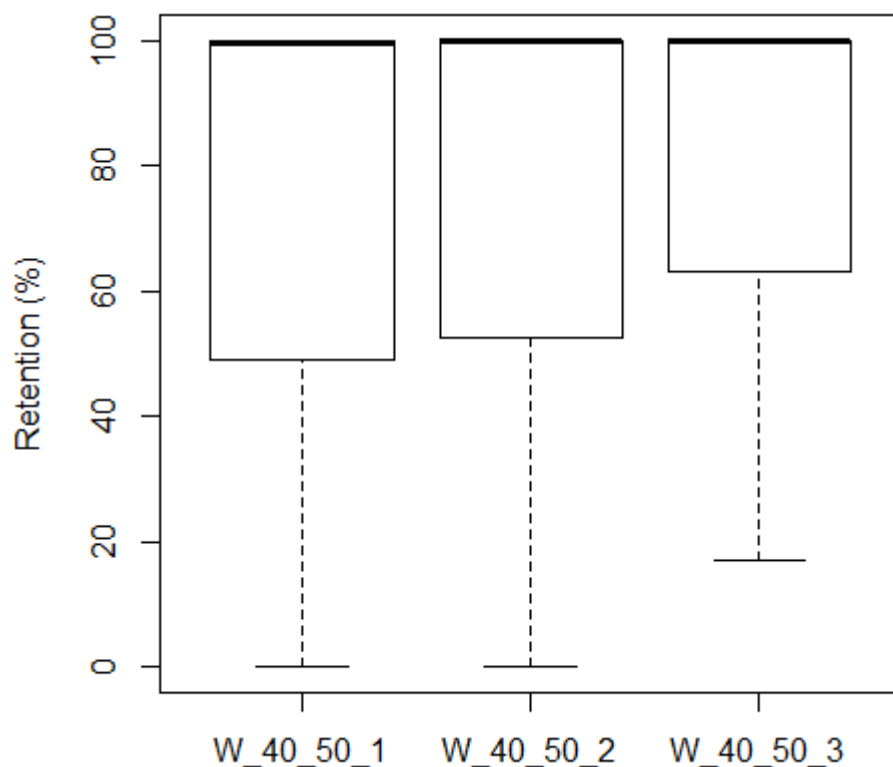


Figure 4.26 Stormwater retention data distribution for green roofs: W/40/50-1, W/40/50-2, W/40/50-3.

**Vegetation: Wildflower, drainage layer: 40mm, substrate: 100mm (W/40/100)**

Table 4.16 Summary statistics of stormwater retention data for following green roofs: W/40/100-1, W/40/100-2, W/40/100-3.

Summary Statistics, Retention (%)				
Roof type		W/40/100-1	W/40/100-2	W/40/100-3
<b>Mean</b>		75.60	76.15	82.65
<b>Median</b>		99.30	99.85	100.00
<b>Std. Deviation</b>		31.71	31.20	27.27
<b>Percentiles</b>	Min.	0.10	6.40	13.30
	25	44.80	47.42	66.22
	50	99.30	99.85	100.00
	75	100.00	100.00	100.00
	Max.	100.00	100.00	100.00
<b>Shapiro-Wilk normality test</b>	p-value	1.267 x 10 <sup>-15</sup>	7.423 x 10 <sup>-16</sup>	< 2.2 x 10 <sup>-16</sup>
		- non-normal distribution (p<0.05)		

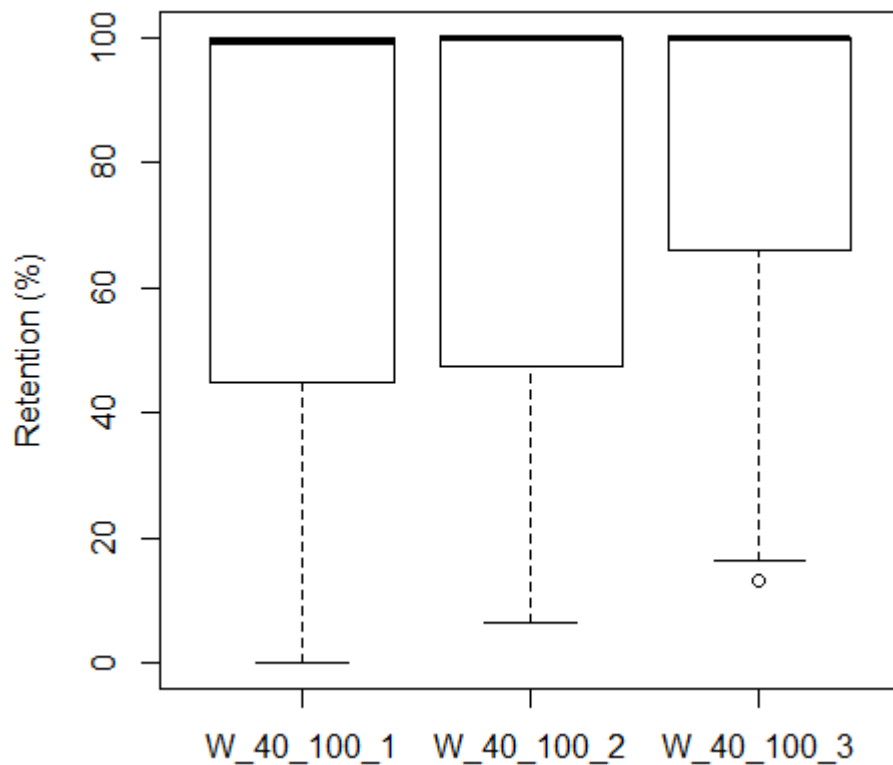


Figure 4.27 Stormwater retention data distribution for green roofs: W/40/100-1, W/40/100-2, W/40/100-3.

It was expected that the replicates of control roofs and green roofs of the same design would perform in a similar manner. Hence, the following null hypothesis was generated and tested: there is no significant difference in retention between green roofs of the same design. The hypothesis was tested using non-parametric test: Wilcoxon Rank Test. The results of the Wilcoxon rank test for three control roofs are presented in Table 4.17, for all sedum green roofs in Table 4.18 and for all wildflower green roofs in Table 4.19.

*Table 4.17 Wilcoxon rank test results – significance for each combination of the data sets for control roofs.*

<b>Roof type</b>	<b>Control-1</b>	<b>Control-2</b>	<b>Control-3</b>
<b>Control-1</b>	-	< 2.200 x 10 <sup>-16</sup>	0.057
<b>Control-2</b>		-	0.066
<b>Control-3</b>			-
<div style="display: flex; align-items: center;"> <div style="width: 20px; height: 10px; background-color: #cccccc; margin-right: 5px;"></div>           - the null hypothesis of no difference should be accepted (p&gt;0.05)         </div>			

Table 4.19 P-values from Wilcoxon rank tests between replicates of the wildflower green roof designs: W/25/50, W/25/100, W/40/50, W/40/100. Highlighted numbers demonstrate no statistically significant difference between plots.

Roof type	W/25/50			W/25/100			W/40/50			W/40/100		
	1	2	3	1	2	3	1	2	3	1	2	3
Replicate												
1	-	0.011	0.210	-	0.451	0.010	-	0.271	2.547 $\times 10^7$	-	0.929	5.674 $\times 10^{-6}$
2		-	0.037		-	0.370		-	1.235 $\times 10^{-11}$		-	9.918 $\times 10^{-9}$
3			-			-			-			-
	- the null hypothesis of no difference should be accepted ( $p > 0.05$ )											

Table 4.18 P-values from Wilcoxon rank tests between replicates of the sedum green roof designs: S/25/50, S/25/100, S/40/50, S/40/100. Highlighted numbers demonstrate no statistically significant difference between plots.

Roof type	S/25/50			S/25/100			S/40/50			S/40/100		
	1	2	3	1	2	3	1	2	3	1	2	3
Replicate												
1	-	0.208	4.094 $\times 10^{-13}$	-	0.503	0.004	-	0.813	0.0002	-	0.008	2.205 $\times 10^{-5}$
2		-	0.872		-	0.661		-	0.071		-	0.878
3			-			-			-			-
	- the null hypothesis of no difference should be accepted ( $p > 0.05$ )											

Boxplots and summary statistics indicate a non-normal, negatively skewed distribution for all control roofs. The non-normal distribution was confirmed through Shapiro-Wilk normality tests ( $p < 0.05$ ) (Table 4.8). The median retention for all control roofs was high, being above 85%. This is an unexpected result for control roofs, as they should mimic conventional roofs, which do not retain stormwater from the rainfalls  $\geq 2\text{mm}$ . The construction of the roof plots could be a reason for such an outcome. The drain outlet is located in the centre of the plot, with no slope towards it. Moreover, the outlet was placed on the waterproof layer overlap, which created an elevation (Figure 4.28). Hence, water logged in roof local depressions, resulting in high retention values.

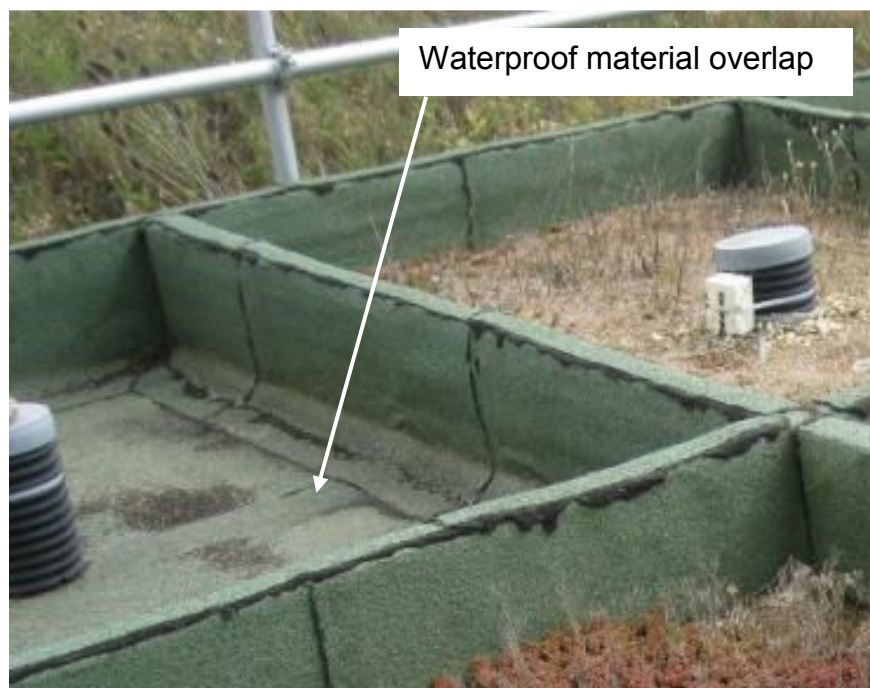


*Figure 4.28 Control roof at Barking Riverside in-situ experiment setup. The drainage outlet is located on the overlapping waterproof material.*

The Wilcoxon rank test showed statistically significant difference ( $p < 0.05$ ) in the stormwater retention between replicate 1 and 2. This result contradicted the assumption that all control roofs would have a similar performance. The difference could be due to the roof plots construction imperfections such as local depressions resulting in retention variations. It can be concluded that the construction of the roof itself could have a significant influence in green roof hydrological performance.

The performance of the control roofs was also questionable. Firstly, the stormwater retention median for all replicates  $\geq 85\%$ , retention mean  $\geq 70\%$ , which is greater than the retention of conventional gravel ballast roof (62% of rainfall volume (VanWoert et al., 2005)). Secondly, they showed statistically significant differences in stormwater retention in two out of three comparisons. As previously mentioned, this could be due to the roof construction imperfections such as surface depressions or drainage outlet construction, resulting in water logging.

The stormwater retention data for the three replicates of green roof S/25/50 failed the Shapiro-Wilk normality test ( $p < 0.05$ ). The boxplot and summary statistics clearly indicate a non-normal, negatively skewed distribution similarly to control roof retention data distribution. Stormwater of the quarter of the rainfall events was fully retained (75<sup>th</sup> percentile = 100%) for all roofs (Table 4.9). The stormwater retention for the half of the rainfall observations was higher than 98% (Table 4.9). This could account for small rainfalls, events preceded by long inter-event dry period as well as events which occurred during high temperature weather when evapotranspiration is high. It could also be an effect of water logging beneath the green roof layers. The inspection of the minimum retentions revealed that the 0% retention occurred for the rainfall event on 10<sup>th</sup> January 2011, rainfall depth: 15mm, rainfall duration: 105.5h, with the inter-event dry period: 62h. This was very likely to happen due to low temperatures and long duration of rain, which would not allow for the sufficient evapotranspiration, hence delaying the drying of the substrate.

The retention data for all replicates of S/25/100 green roofs did not fit the normal distribution and were negatively skewed (Figure 4.21). The non-normal distribution was also confirmed through Shapiro-Wilk normality test ( $p < 0.05$ ) (Table 4.10). The median retention for all roofs was higher than 99%, suggesting that at least half of the rainfall water was retained nearly in full. However, there was also one rainfall event with a retention of 0%. The rainfall event occurred on 6<sup>th</sup> October 2010 with rainfall depth: 4mm, rainfall duration: 9.5h and inter-event dry period: 12h. As one could notice the inter-event dry period prior to the event was only 12h, which could have meant that there was not sufficient time for the green roof to regain its water storage capacity.

All green roofs S/40/50 present a non-normal, negatively skewed distribution for retention (Figure 4.22). The median retention for all green roof replicates was very high, exceeding 98%. However, in contrast to the previously analysed green roof designs, there were no 0% retention events observed. The lowest observed retention was for the green roof S/40/50-3 (1.1%) on 15<sup>th</sup> December 2010 with the rainfall depth: 3.4mm, rainfall duration: 31.5h and inter-event dry period 24h. The rainfall event occurred in winter when evapotranspiration would be significantly lower and it would take longer for the green roof to dry out.

Shapiro-Wilk normality test, summary statistics and boxplot confirmed non-normal, negatively skewed distribution of the retention data for all S/40/100 green roofs. The stormwater was fully retained for at least half of the rainfall events observed for all S/40/100 green roofs (retention median = 100%). Interestingly, the minimum retention for all green roof replicates was 0%, which meant that no stormwater was retained. This happened on two occasions: on 10<sup>th</sup> January 2011 with rainfall depth: 15mm, rainfall duration:105.5h and inter-event dry period 62h (all replicates), and on 31<sup>st</sup> January 2014 with rainfall depth: 7.31mm, rainfall duration: 24h and inter-event dry period 25.5h (replicate 2). Both events occurred in winter, when evapotranspiration would be significantly lower and it would take longer for a green roof to restore retention capacity.

The W/25/50 green roofs retention data distribution was non-normal, negatively skewed based on boxplot analysis and summary statistics. It was also confirmed by a Shapiro-Wilk normality test ( $p < 0.05$  for all replicates). The median retention for replicate W/25/50-2 and W/25/50-3 was 100% and for the replicate W/25/50-1 was 99.90%. This indicates that W/25/50 green roofs retained almost all stormwater from half of the rainfall events. No retention was observed only for the W/25/50-3 green roof on 31<sup>st</sup> January 2014 with rainfall depth: 7.31mm, rainfall duration: 24h and inter-event dry period 25.5h, similarly to green roof S/40/100-2. The observed rainfall event occurred in winter, when the evapotranspiration would have been lower resulting in reduced ability of the green roofs to dry out between rainfall events.

The summary statistics, boxplot and Shapiro-Wilk normality test indicated non-normal, negatively skewed retention data distribution for all replicates of W/25/100 green roofs. The median retention for all W/25/100 was greater than

99%, which meant that stormwater from at least half of the rainfall events observed was retained nearly in full. The only 0% retention was observed for the rainfall event that occurred in winter, on 10<sup>th</sup> February 2013 with rainfall depth: 12.58mm, rainfall duration: 43h and the inter-event dry period: 30h. The evapotranspiration rate in winter would be significantly lower than during other seasons, which would result in longer green roof drying period, reducing the ability of the green roof to restore retention capacity.

Comparably to all green roofs discussed, W/40/50 green roofs retention data distribution was also non-normal, negatively skewed, based on boxplot analysis, summary statistics and the result of Shapiro-Wilk normality test. The W/40/50 green roofs retained over 99% of stormwater of at least half of the rainfall events observed. No retention was observed for the W/40/50-1 green roof on 10<sup>th</sup> January 2011 rainfall event with rainfall depth: 15mm, rainfall duration: 105.5h, with the inter-event dry period: 62h. The event occurred in winter when the evapotranspiration would be low and it would take longer for green roof to regain its retention capacity.

The boxplot and summary statistics show that retention data for W/40/100 had non-normal, negatively skewed distribution, which was also confirmed by the Shapiro-Wilk normality test ( $p < 0.05$ ). Median retention for all W/40/100 replicates was greater than 99%. Hence, W/40/100 green roofs retained stormwater of at least half of the observed rainfall events nearly in full. There was no rainfall event for which corresponding retention was 0%. This could be due to depth of the substrate and drainage layer, 100mm and 40mm respectively, hence having greater water storage ability.

The Wilcoxon rank test demonstrated statistically significant difference ( $p < 0.05$ ) in retention between at least two replicates of green roofs of the same design (Table 4.19 and 4.19). This result does not support the assumption that all control roofs would present similar performance. Similarly to the control roof, the differences could occur due to the construction of the green roof plots. It is very likely that there might have been local depressions in the green roof plots causing water logging. Voyde et al. (2010) argued that all surfaces have certain degree of depression storage. Tested green roofs might have had different degree of depression storage, resulting in retention variations.

Differences in the construction of the green roofs themselves could also be possible. In this study, the depth of the substrate used in the analysis as a variable was nominal, not measured. The degree of compaction and the effect of substrate erosion was unknown. As discussed in Chapter 3, the degree of compaction of the substrate could alter its properties. During the compaction, the volume of voids within the substrate material is reduced, hence the space in which the water could be stored is limited, decreasing stormwater retention. Berretta et al. (2014) also indicated that compaction of the substrate can affect its behaviour during wetting and drying cycles. Hence, it is very likely that different degree of compaction would result in variations in the water retention.

The vegetation coverage was not assessed in this study, therefore its influence on green roof retention capacity could not be quantified. However, some researchers pointed out, that the vegetation coverage and type have significant effect on the green roof retention abilities (VanWoert et al., 2005, Nagase and Dunnett, 2012). In this study, the seed mix sown into green roofs was homogenised. However, the dynamics of the plant development would vary between the roofs over four years of study. The differences in vegetation cover and number of particular plant species between roofs are, therefore, very likely. This could impact green roofs stormwater retention ability.

The organic matter content influences green roof performance (Getter et al., 2007, Graceson et al., 2013, Yio et al., 2013). Over a period of time the organic matter content could change due to the natural plant life cycle. Some of the plants would die increasing the organic matter content, resulting in greater stormwater retention. These factors could affect the green roof response to rainfall and could result in a different green roof performance even between green roofs of the same design.

#### **4.3.3.1 SUMMARY**

The analysis of the hydrological behaviour (retention) of the three replicates of the same green roof design contradicted the assumption of no statistically significant difference between the green roof plots of the same design. There was no green roof design fulfilling that assumption. Hence, there is possibility that there might be non-controlled experimental factors other than the green roof

design (substrate and drainage layer depth) that strongly influenced green roof retention capacity. Those factors could include:

- Vegetation coverage
- Vegetation type
- Organic matter content
- Compaction of substrate material
- Green roof construction imperfections

Great attention should be paid to the construction of the roof itself, especially to unimpeded water transit into drainage outlet or lack of surface depressions. Water logging on the roof could increase the stormwater retention but, most importantly, could cause roof structure and building damage if not designed for. The execution of the green roof is also crucial. Ensuring the correct depth and compaction of the green roof construction materials enables the achievement of green roof design objectives. The effect of factors discussed above should be taken into consideration at the green roof design stage. However, there are no requirements or any guidelines suggesting the use of safety factors in the context of the hydrological performance of green roofs and in many cases this could lead to its overestimation. This is important in the case of utilising green roofs as flood management tool. However, introducing such measures such as safety factors requires further consideration and perhaps carefully designed laboratory trials.

#### **4.3.4 HYDROLOGICAL PERFORMANCE OF THE GREEN ROOFS OF DIFFERENT DESIGNS**

This section presents the analysis of the hydrological performance of the green roofs with different designs. Runoff depth, retention and peak flow reduction data from the control roof and green roofs of various design were analysed and compared. The green roofs chosen for this analysis were selected based on the performance analysis of the green roof replicates (section 4.3.3). In the case of one combination of no statistically significant difference between green roof replicates, the random green roof of that combination was chosen (e.g. W/25/50-1, Table 4.19). In the case of two combinations of no statistically significant difference, green roof replicate common for both combinations was selected (e.g. W/25/100-2, Table 4.19).

The following green roofs were selected for further analysis: Control-3, S/25/50-2, S/25/100-2, S/40/50-2, S/40/100-2, W/25/50-1, W/25/100-2, W/40/50-1, W/40/100-1.

Hydrological performance analyses presented in this section are based on the final rainfall event data set (section 4.2).

#### **4.3.4.1 OVERALL HYDROLOGICAL PERFORMANCE**

This section focuses on overall hydrological performance of the selected green roofs. It is based on the data set for the full monitoring period, from July 2010 to August 2014. It aims to explore general patterns as well as the influence of the design on hydrological performance of the green roofs. The exploratory data analysis was carried out to determine the nature of the data distribution. Summary statistics of the green roof hydrological performance data are presented in Table 4.20 (runoff depth), Table 4.22 (retention) and Table 4.24 (peak flow reduction). Green roof hydrological performance data distribution is presented in Figure 4.29 (runoff depth), Figure 4.30 (retention) and Figure 4.31 (peak flow reduction).

It is assumed that the variations in the green roof design alter the green roof stormwater mitigation capabilities. Hence, a difference in the responses of the green roofs at Barking Riverside to rainfall events would be observed. Based on this assumption, the following null hypothesis was generated: there is no significant difference in hydrological performance (runoff depth, retention, and peak flow reduction) between green roofs of different design.

The hypothesis was tested using non-parametric Dunn's Kruskal-Wallis multiple comparison test with the Bonferroni correction. The results of the test are presented in Table 4.21, Table 4.23 and Table 4.25.

## Runoff depth

Table 4.20 Summary statistics of stormwater runoff depth data for selected green roofs in relation to their overall performance.

Summary Statistics, Runoff depth (mm)									
Roof Type	Control-3	S/25/50-2	S/25/100-2	S/40/50-2	S/40/100-2	W/25/50-1	W/25/100-2	W/40/50-1	W/40/100-1
<b>N</b>	172	165	168	166	176	166	174	171	169
<b>Mean</b>	3.08	3.10	2.80	2.87	1.87	3.14	2.93	3.13	3.20
<b>Median</b>	0.50	0.01	0.03	0.00	0.00	0.01	0.04	0.02	0.04
<b>Std. Deviation</b>	5.60	5.63	5.44	5.55	4.14	5.56	5.06	5.65	5.81
<b>Percentiles</b>	Min.	0.00	0.00	0.00	0.00	0.00	0.00	0.00	0.00
	25	0.04	0.00	0.00	0.00	0.00	0.00	0.00	0.00
	50	0.5	0.01	0.03	0.00	0.00	0.01	0.04	0.02
	75	3.34	3.97	3.33	3.57	1.48	4.13	3.98	3.77
	Max.	30.22	28.28	27.98	28.64	22.37	29.04	26.85	28.03

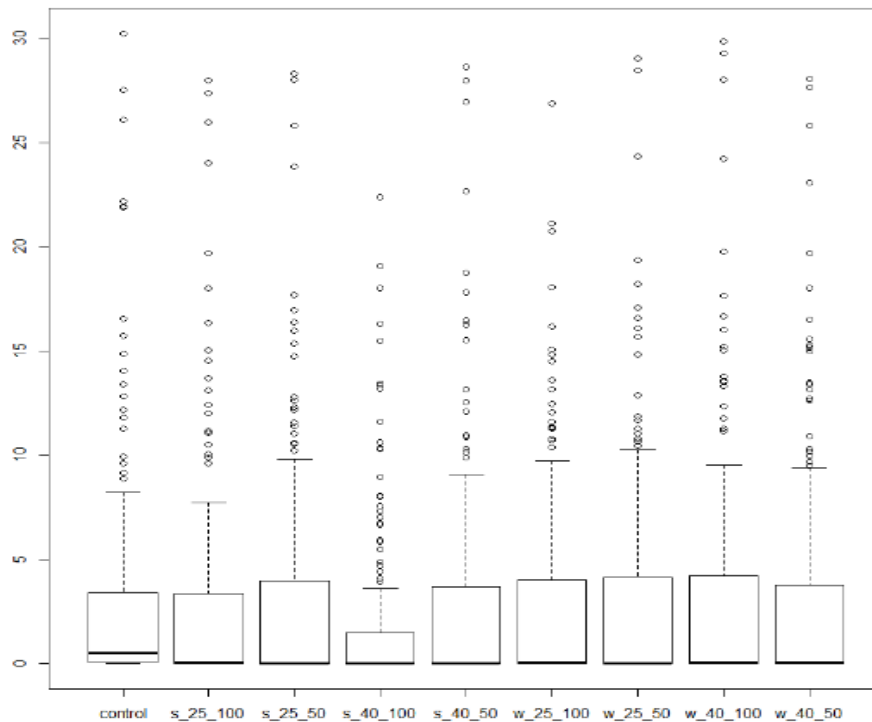


Figure 4.29 Distribution of stormwater runoff depth data for selected green roofs in relation to their overall performance.

Table 4.21 P-values from Dunn's Kruskal-Wallis multiple comparison test results with Bonferroni correction applied for each combination of the runoff depth data sets. Highlighted numbers demonstrate a statistically significant difference between plots. Italicised numbers show a statistically significant difference between plots based on uncorrected p-value.

Dunn's Kruskal-Wallis multiple comparison test – Runoff Depth (mm)									
Roof Type	Control-3	S/25/50-2	S/25/100-2	S/40/50-2	S/40/100-2	W/25/50-1	W/25/100-2	W/40/50-1	W/40/100-1
Control-3	-	0.006	0.010	0.004	<0.001	0.009	0.043	0.008	<i>0.168/0.005*</i>
S/25/50-2		-	1.000	1.000	<i>0.074/0.002*</i>	1.000	1.000	1.000	1.000
S/25/100-2			-	1.000	0.041	1.000	1.000	1.000	1.000
S/40/50-2				-	<i>0.102/0.003*</i>	1.000	1.000	1.000	1.000
S/40/100-2					-	<i>0.050/0.001*</i>	0.007	0.047	0.002
W/25/50-1						-		1.000	1.000
W/25/100-2							-	1.000	1.000
W/40/50-1								-	1.000
W/40/100-1									-
* Uncorrected p-value <span style="background-color: #cccccc; border: 1px solid black; display: inline-block; width: 15px; height: 10px; vertical-align: middle;"></span> Null hypothesis of no statistically significant difference rejected									

## Retention

Table 4.22 Summary statistics of stormwater retention data for selected green roofs in relation to their overall performance.

Summary Statistics, Retention (%)									
Roof Type	Control-3	S/25/50-2	S/25/100-2	S/40/50-2	S/40/100-2	W/25/50-1	W/25/100-2	W/40/50-1	W/40/100-1
<b>N</b>	172	165	168	166	176	166	174	171	169
<b>Mean</b>	76.43	77.20	79.08	79.53	86.11	76.26	77.47	77.08	75.60
<b>Median</b>	86.35	99.80	99.55	99.90	100.0	99.90	99.35	99.60	99.30
<b>Std. Deviation</b>	26.31	30.09	29.18	28.46	24.79	31.10	30.14	30.40	31.71
<b>Percentiles</b>	<b>Min.</b>	0.00	0.00	0.00	1.70	0.00	0.00	0.00	0.10
	<b>25</b>	56.28	48.30	54.98	55.60	84.00	48.03	52.33	44.80
	<b>50</b>	86.35	99.80	99.55	99.90	100.0	99.9	99.35	99.30
	<b>75</b>	99.05	100.0	100.0	100.0	100.0	100.0	100.0	100.0
	<b>Max.</b>	100.0	100.0	100.0	100.0	100.0	100.0	100.0	100.0

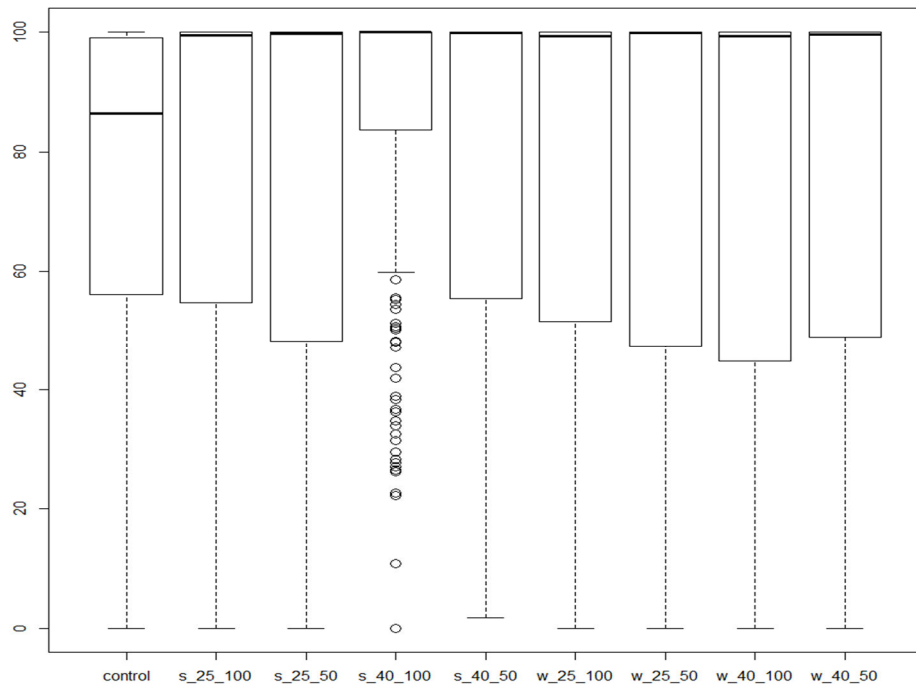


Figure 4.30 Distribution of stormwater retention data for selected green roofs in relation to their overall performance.

Table 4.23 P-values from Dunn's Kruskal-Wallis multiple comparison test results with Bonferroni correction applied for each combination of the retention data sets. Highlighted numbers demonstrate a statistically significant difference between plots. Italicised numbers show a statistically significant difference between plots based on uncorrected p-value.

Dunn's Kruskal-Wallis multiple comparison test – Retention (%)									
Roof Type	Control-3	S/25/50-2	S/25/100-2	S/40/50-2	S/40/100-2	W/25/50-1	W/25/100-2	W/40/50-1	W/40/100-1
Control-3	-	0.010	0.007	0.002	<0.001	0.015	0.023	0.010	<i>0.146</i> <i>/0.004*</i>
S/25/50-2		-	1.000	1.000	0.028	1.000	1.000	1.000	1.000
S/25/100-2			-	1.000	0.034	1.000	1.000	1.000	1.000
S/40/50-2				-	<i>0.089</i> <i>/0.002*</i>	1.000	1.000	1.000	1.000
S/40/100-2					-	0.017	0.008	0.021	0.001
W/25/50-1						-		1.000	1.000
W/25/100-2							-	1.000	1.000
W/40/50-1								-	1.000
W/40/100-1									-

\* Uncorrected p-value  
 Null hypothesis of no statistically significant difference rejected

## Peak flow reduction

Table 4.24 Summary statistics of stormwater peak flow reduction data for selected green roofs in relation to their overall performance.

Summary Statistics, Peak Flow Reduction (%)										
Roof Type	Control-3	S/25/50-2	S/25/100-2	S/40/50-2	S/40/100-2	W/25/50-1	W/25/100-2	W/40/50-1	W/40/100-1	
<b>N</b>	172	165	168	166	176	166	174	171	169	
<b>Mean</b>	84.08	83.28	88.74	86.20	94.79	80.64	86.99	90.76	92.47	
<b>Median</b>	97.00	99.00	99.00	99.00	100	99.00	99.00	99.00	99.00	
<b>Std. Deviation</b>	24.92	28.08	21.29	24.77	13.39	29.87	21.38	16.86	13.25	
<b>Percentiles</b>	<b>Min.</b>	0.00	0.00	0.00	2.00	5.00	0.00	4.00	14.00	22.00
	<b>25</b>	82.50	76.00	88.75	85.00	96.00	63.00	80.00	89.50	91.00
	<b>50</b>	97.00	99.00	99.00	99.00	100	99.00	99.00	99.00	99.00
	<b>75</b>	99.00	100	100	100	100	100	100	100	100
	<b>Max.</b>	100	100	100	100	100	100	100	100	100

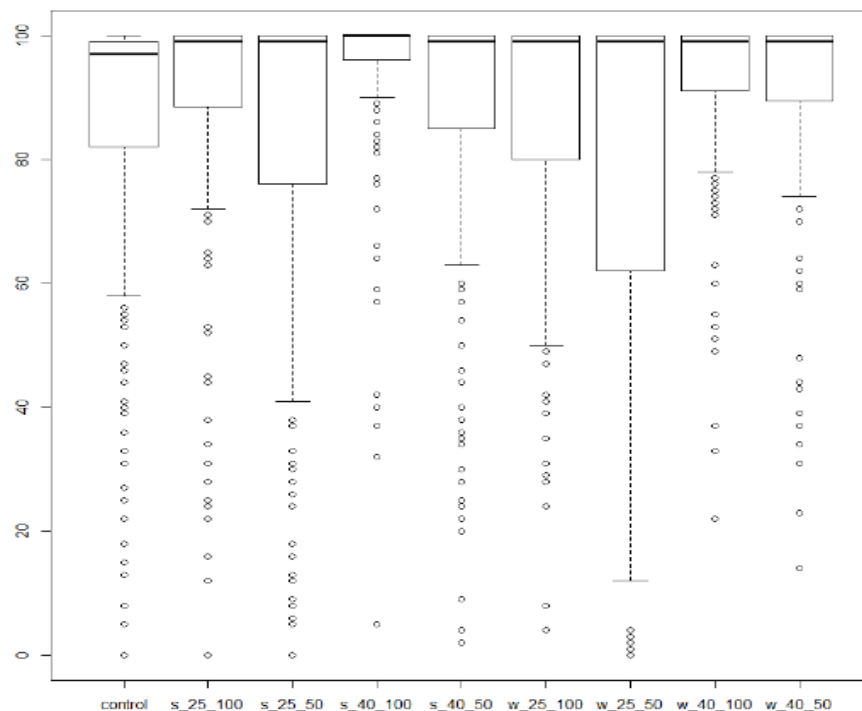


Figure 4.31 Distribution of stormwater peak flow reduction data for selected green roofs in relation to their overall performance.

Table 4.25 P-values from Dunn's Kruskal-Wallis multiple comparison test results with Bonferroni correction applied for each combination of the peak flow reduction data sets. Highlighted numbers demonstrate a statistically significant difference between plots. Italicised numbers show a statistically significant difference between plots based on uncorrected p-value.

Dunn's Kruskal-Wallis Multiple comparison test – Peak Flow Reduction (%)									
Roof Type	Control-3	S/25/50-2	S/25/100-2	S/40/50-2	S/40/100-2	W/25/50-1	W/25/100-2	W/40/50-1	W/40/100-1
Control-3	-	0.008	<0.001	0.001	<0.001	0.021	0.007	<0.001	0.002
S/25/50-2		-	1.000	1.000	0.003	1.000	1.000	1.000	1.000
S/25/100-2			-	1.000	<i>0.058/ 0.002*</i>	1.000	1.000	1.000	1.000
S/40/50-2				-	0.024	1.000	1.000	1.000	1.000
S/40/100-2					-	0.001	0.002	<i>0.057/ 0.002*</i>	0.009
W/25/50-1						-		1.000	1.000
W/25/100-2							-	1.000	1.000
W/40/50-1								-	1.000
W/40/100-1									-
* Uncorrected p-value <span style="background-color: #cccccc; border: 1px solid black; display: inline-block; width: 15px; height: 10px; vertical-align: middle;"></span> Null hypothesis of no statistically significant difference rejected									

Runoff depth, retention and peak flow reduction data from each of the eight green roofs and control roof did not fit the normal distribution. Runoff depth data was positively skewed, while retention and peak flow reduction were negatively skewed (Figure 4.29 to 4.31).

For events with greater than 2mm of rainfall depth, median runoff depth ranged from 0mm (S/40/50 and S/40/100) to 0.04mm (W/25/100 and W/40/100), while mean ranged from 1.87mm (S/40/100) to 3.2mm (W/40/100) (Table 4.20). For comparison, the median runoff depth for control roof was 0.5mm, while mean value was 3.08mm, which is an unexpected result. Due to no retention capacity of the control roof, it was anticipated that the runoff depths from control roof would be higher than that from green roofs. However, these mean and median values of runoff depth were similar. The maximum runoff depth for investigated green roofs ranged from 22.37mm (S/40/100) to 29.83mm (W/40/100) and 30.22mm for control roof. The maximum runoff depth indicates the quantity of water being directed to the drainage system in the most unfavourable conditions. The maximum runoff depth, between 22.37 and 29.83mm, was significantly lower than the maximum runoff depth observed by other researchers. For example, Fassman-Beck et al. (2013) obtained 40.1mm of runoff depth, whilst Razzaghmanesh and Beecham (2014) 34.33mm of runoff depth. The maximum runoff depths from green roofs investigated in the UK studies were: 86.48mm (Stovin et al., 2012) and 75mm (Nawaz et al., 2015). Lower runoff quantities obtained in this study are desirable in the case of stormwater management. However, it needs to be noted that this response was achieved for rainfall events of a return period lower than 2 years.

Although the retention values do not specify the amount of water that sewage system would have to route during the rainfall event, they give an indication of the efficiency of the green roof as a stormwater mitigation tool. The median retention ranged from 99.30% (W/40/100) to 100% (S/40/100) and mean retention ranged from 75.60% (W/40/100) to 86.11% (S/40/100). Control roof median retention was 86.35% and mean 76.43%. The maximum retention for all roofs including the control roof was 100% (Table 4.22). High median retention close to 100% indicated good performance of all green roof designs in relation to stormwater mitigation. However, comparing these results with that obtained by other researchers, it can be noted that they were unexpectedly high. Fassman-

Beck et al. (2013) reported a median retention between 56-76% from six different green roof plots. Stovin et al. (2012) noted a median retention of 30.2% for a single green roof plot. The median retention based on green roof performance described in published literature was 62% (Chapter 2).

Similarly to results of green roof retention analysis, the peak flow reduction values were also high. The median peak flow reduction ranged from 99.00% to 100% (S/40/100) and mean peak flow reduction ranged from 80.64% (W/25/50) to 94.79% (S/40/100). Control roof median peak flow reduction was 97.00% and the mean value was 84.08%. The maximum peak flow reduction for all roof designs including the control roof was 100%. For comparison, Stovin et al. (2012) noted 58.67% of peak flow reduction, while Fassman-Beck et al. (2013) obtained 62-90% of peak flow reduction based on results from six tested roofs.

The high retention and peak flow reduction values could occur due to various reasons such as low rainfall depths or roof construction imperfections. The hydrological performance analysis was based on the data set of the rainfalls of low return periods. The majority of the rainfalls were below 1 year return period (section 4.3.2). Half of the rainfall events were below 6.08mm of the depth. Many researchers have suggested that there is an inverse relationship between rainfall depth and the percentage of rain retained by green roof (Simmons et al., 2008, Carter and Rasmussen, 2006, VanWoert et al., 2005). Table 4.26 and Table 4.27 present median retention and peak flow reduction in relation to rainfall depth divided into rainfall event quantiles.

Table 4.26 shows that the median retention for the 1<sup>st</sup>, 2<sup>nd</sup> and 3<sup>rd</sup> quantile of rainfall events (rain depth  $\leq$  9.65mm) was above 99% for all selected green roofs and 78% for control roof. The median retention for the 4<sup>th</sup> quantile of rainfall events (rain depth  $>$ 9.65) ranged from 42.6% to 72.2% for selected green roofs and it was 46.7% for control roof.

Table 4.27 shows similar results for the median peak flow reduction. For the 1<sup>st</sup>, 2<sup>nd</sup> and 3<sup>rd</sup> quantile of rainfall events the peak flow reduction was above 99% for green roofs and 92.5% for control roof. The 4<sup>th</sup> quantile median peak flow reduction analysis showed the range of variation between 50% and 96% for selected green roofs and 61% for the control roof.

Table 4.26 Median stormwater retention determined for four rainfall depth quantiles.

Median of Retention (%)									
Quantile /Rainfall Depth (mm)	Control-3	S/25/50-2	S/25/100-2	S/40/50-2	S/40/100-2	W/25/50-1	W/25/100-2	W/40/50-1	W/40/100-1
1/ 2 – 3.28	97.1	100.0	100.0	100.0	100.0	100.0	100.0	100.0	100.0
2/ 3.29 – 5.81	94.8	100.0	100.0	100.0	100.0	100.0	100.0	100.0	100.0
3/ 5.82 – 9.64	78.7	99.9	99.7	100.0	100.0	100.0	99.8	100.0	100.0
4/ >9.65	46.7	46.2	53.9	51.9	72.2	42.6	51.6	47.1	44.1

Table 4.27 Median stormwater peak flow reduction determined for four rainfall depth quantiles.

Median of Peak Flow Reduction (%)									
Quantile /Rainfall Depth (mm)	Control-3	S/25/50-2	S/25/100-2	S/40/50-2	S/40/100-2	W/25/50-1	W/25/100-2	W/40/50-1	W/40/100-1
1/ 2 – 3.28	98.0	100.0	100.0	100.0	100.0	100.0	100.0	100.0	100.0
2/ 3.29 – 5.81	98.0	100.0	100.0	100.0	100.0	100.0	100.0	100.0	100.0
3/ 5.82 – 9.64	92.5	99.0	99.0	100.0	100.0	100.0	100.0	100.0	99.0
4/ >9.65	61.0	62.0	79.0	64.0	96.0	50.0	66.0	83.0	88.0

The retention and peak flow reduction in relation to the rainfall depth analysis confirm the assumption that green roofs are very effective in retaining stormwater and mitigating peak flow from small and medium rainfall events. However, for engineering consideration and from regulator perspective the green roof response to the large or/and extreme rainfall events is much more important and relevant. It is crucial to note that 75% of rainfall events (greater or equal to 2mm)

were less than 9.65mm deep (Table 4.26). From the remaining 25% of rainfall events, only 4 rainfall events exceeded 1 year return period (section 4.3.2). To fully understand the potential contribution of green roofs to retaining and attenuating stormwater, a knowledge of their response to extreme rainfall events, such as of 30 or 50 years return period, is needed. In order to achieve that a comprehensive series of laboratory experiments need to be conducted.

Although, in general, there is an inverse relationship between rainfall depth and the green roof retention capacity, some green roof responses did not follow the pattern. For example, the largest event fully retained was a 20.01mm rainfall event in June 2012 that had 411.5 hours (17.15days) inter-event dry period prior to the event (green roof S/40/100). The green roof had a large retention capacity mostly due to the long inter-event dry period before the rainfall occurrence but also due to the depth of the substrate and drainage layer, 100mm and 40mm respectively. For comparison S/25/50 green roof design retained 47.1% of the same rainfall (50 mm substrate depth and 25mm drainage layer depth).

In contrast, the stormwater from a small event of 4.0mm was fully discharged by S/25/100 green roof in October 2010. The inter-event dry period prior to the rainfall event was 12 hours and the preceding rainfall event was of 15.8mm. The large preceding rainfall event of 15.8mm and very short dry period of 12 hours prior to the event did not allow the green roof S/25/100 to fully restore its stormwater retention capacity.

The maximum absolute retention was observed for the rainfall event in September 2012. The S/40/100 green roof retained 38.6mm of 41.3mm rainfall event. The inter-event dry period prior the event was 38.5 hours. However, the preceding rainfall event was only 2.0mm, which did not affect the retention capacity of the S/40/100 green roof.

The analysis of the green roof performance based on the rainfall quantiles showed that the smaller rainfall events are likely to be fully retained. As opposed to the small rainfall events, stormwater from larger events would be only partially retained. Although there is a strong indication that there is an inverse relation between the rainfall depth and retention, there are cases of stormwater from small rainfall events not being retained as well as observations of stormwater from large rainfall events fully retained as presented earlier. This suggests that there are

factors, other than the rainfall depth, influencing the hydrological performance of the green roofs, which should be investigated further.

The rainfall characteristics such as low rainfall depth or low return period could explain high performance of the green roofs, it does not, however, explain the high retention and high peak flow reduction of the control roof. The median runoff depth of 0.5mm was particularly low, while median retention of 86.35% and median peak flow reduction of 97% are extremely high for the control roof performance. As mentioned previously, the roof construction imperfections could partly account for such a result, however there is also a possibility of data bias. As pointed out in section 4.3.2, the rainfall measurement at Barking Riverside are significantly lower than the one at Heathrow and at Crossness STW. Although, it is not expected for the rainfall to be exactly the same in these locations, the difference in rainfall depth between Barking Riverside and Heathrow was greater than 55% and between Barking Riverside and Crossness STW was greater than 44%, in three out of five years of study (Figure 4.17). The runoff data could be also biased. The tipping bucket rain gauges, used to quantify runoff, are not designed to measure high rate flows. The area of the green roof plot is over 120 times greater than the area of the tipping bucket rain gauge, hence the rain gauge is exposed to measurements of water volume 120 times greater than it is designed for. All of the mentioned factors could have a significant impact on the results, hence the outcome of the hydrological performance analysis should be treated with care based on specific circumstances.

The statistical analysis results indicated statistically significant difference ( $p < 0.05$ ) between the runoff depth, retention and peak flow reduction from the control roof and each of the selected green roof designs (Table 4.21, Table 4.23 and Table 4.25). However, in the case of the green roof W/40/100, the null hypothesis of statistically significant difference in runoff depth and retention data was rejected only for uncorrected p-value. Amongst the selected green roof designs, continuously monitored for over 4 years, no statistically significant difference was detected in terms of runoff depth, retention, and peak flow reduction except for the S/40/100 green roof. The runoff depth, retention, and peak flow reduction data from the S/40/100 green roof showed statistically significant difference in comparison to all roofs. The S/40/100 performed better than other roofs for the rainfall events with depths greater than 9.65mm (Table

4.26 and Table 4.27). However, the hypothesis of statistically significance difference in retention between S/40/100 and S/40/50 was accepted only for uncorrected p-value. Similarly, based on the uncorrected p-value, there was no statistically significant difference in runoff depth between S/40/100 and S/25/50, as well as between S/40/100 and S/40/50, and in peak flow reduction between S/40/100 and S/25/100, W/40/50.

These results clearly demonstrated, that except for S/40/100, there was no statistically significant difference in the hydrological performance between different green roof designs. The increase in the drainage layer depth alone or substrate depth alone do not seem have significant effect on green roof hydrologic response. However, the combination of increased drainage layer and substrate depth could potentially provide improvement in the hydrological performance of the green roofs, as demonstrated by S/40/100 green roof design. Nevertheless, the W/40/100 green roof performance did not support that. This could be due to the different type of the vegetation planted onto that green roof, but also due to the other factors such as roof construction imperfections, different level of a substrate compaction or different content of organic matter. Clearly, in the case of analysed green roofs, the change of the substrate depth from 50mm to 100mm or the change in drainage layer depth from 25mm to 40mm did not result in a significant increase in hydrological performance. Although the increase of the substrate depth may not be significantly beneficial in terms of hydrological performance, it can improve plant growth and viability (Voyde et al., 2010, Thuring et al., 2010).

#### **4.3.4.2 CUMULATIVE AND ANNUAL ANALYSIS OF HYDROLOGICAL PERFORMANCE**

This section presents the further investigation into overall hydrological performance of the selected green roofs. It aims to determine the hydrological performance of the green roofs based on cumulative and annual data analysis.

Table 4.28 and Figure 4.32 show annual and cumulative retention of selected green roofs for the full monitoring period between July 2010 and August 2014.

Figure 4.33 presents cumulative rainfall depth and runoff depth from selected roofs for the full monitoring period between July 2010 and August 2014.

Table 4.28 Annual and cumulative retention over full monitoring period between July 2010 and August 2014.

Annual and Cumulative Retention (%)									
Year	Control-3	S/25/50-2	S/25/100-2	S/40/50-2	S/40/100-2	W/25/50-1	W/25/100-2	W/40/50-1	W/40/100-1
<b>Jul-Dec 2010</b>	94.2	67.2	66.3	70.8	92.5	65.7	74.5	79.3	70.0
<b>2011</b>	79.6	72.2	77.6	86.4	93.1	65.1	67.4	68.0	78.6
<b>2012</b>	52.5	57.3	56.6	58.9	76.7	58.9	64.0	58.4	56.0
<b>2013</b>	50.3	61.4	79.1	63.7	71.7	59.2	62.3	61.2	60.1
<b>Jan-Aug 2014</b>	85.6	69.9	70.8	73.6	70.5	69.3	67.3	71.8	69.5
<b>2010-2014</b>	63.0	62.1	66.4	65.1	77.9	61.5	65.0	62.9	61.9

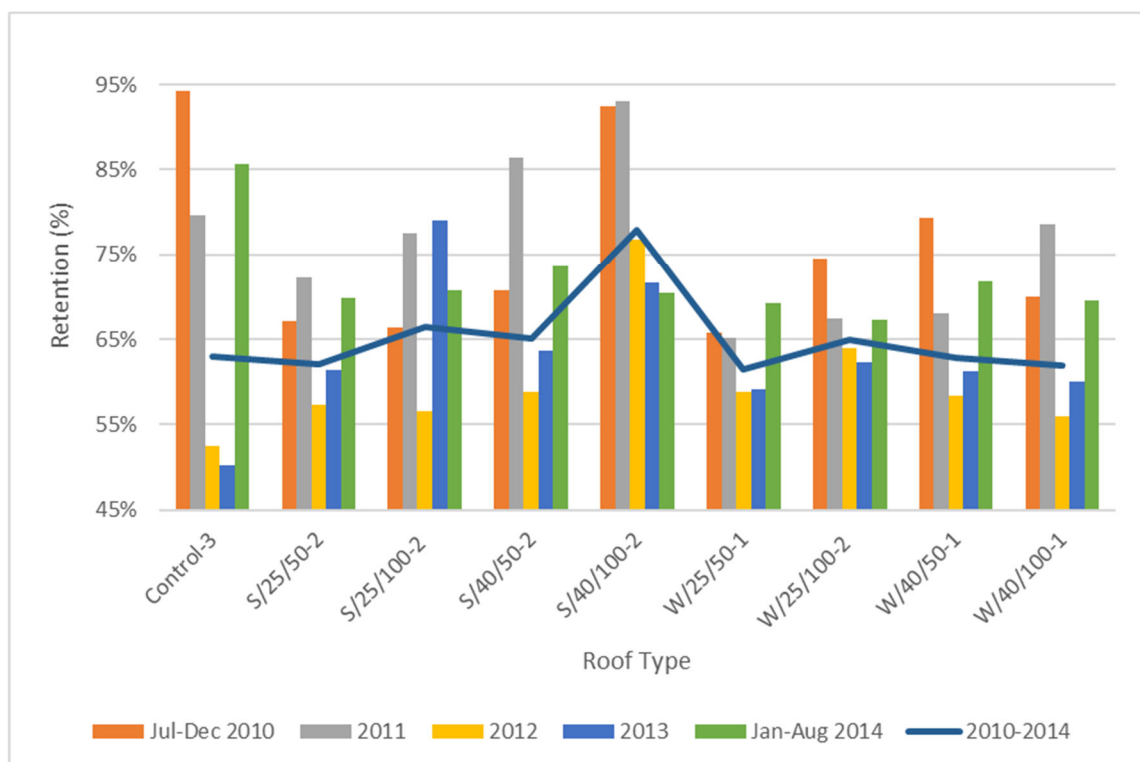


Figure 4.32 The annual retention for each year of the monitoring period and cumulative retention 2010-2014 based on full monitoring period between July 2010 and August 2014.

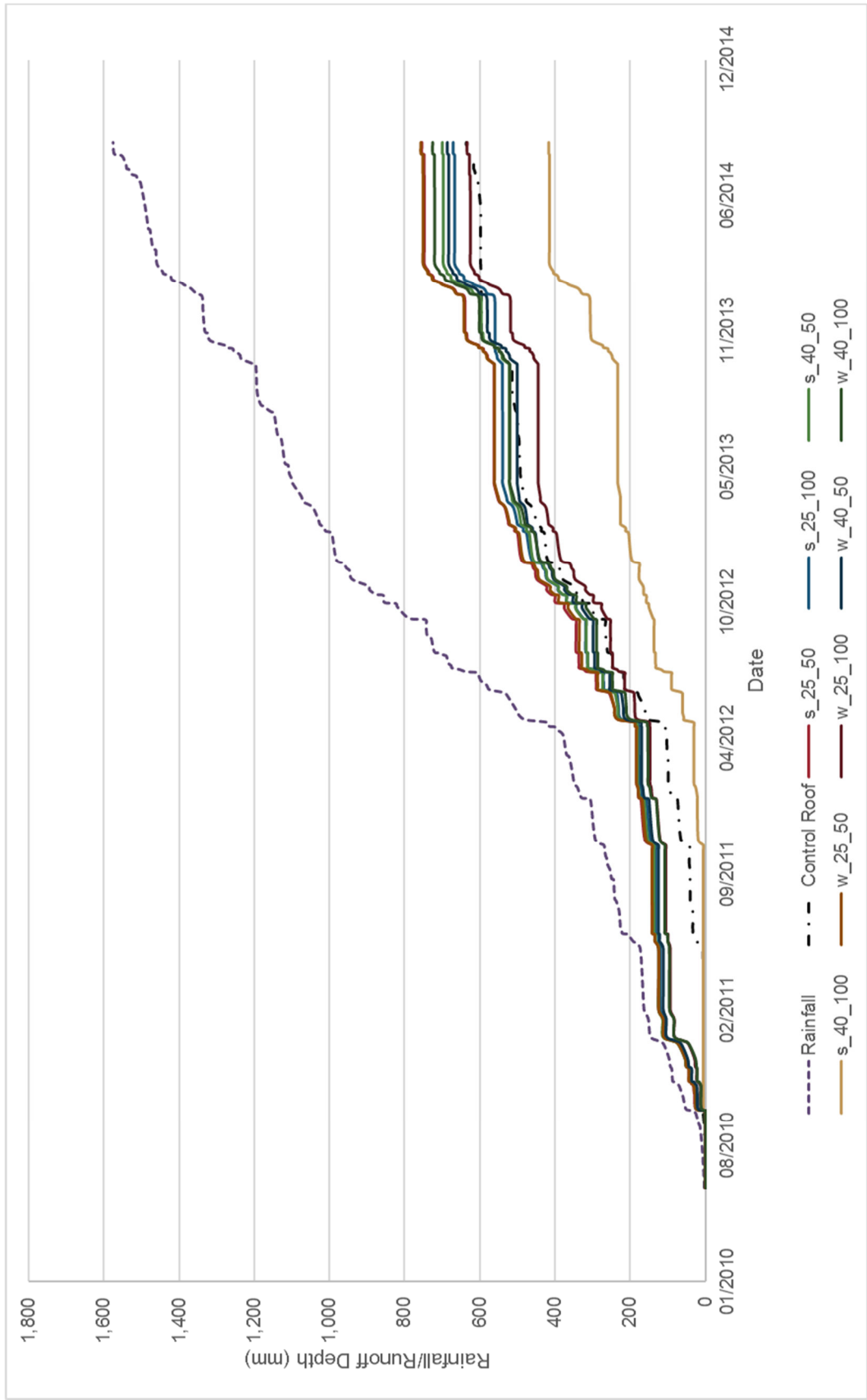


Figure 4.33 Cumulative rainfall and runoff depth for green roofs of different designs over full monitoring period between July 2010 and August 2014.

The annual retention ranged from 56.0% to 93.1% depending on the green roof design and year of monitoring (Table 4.28). The lowest annual retention was recorded for W/25/100 green roof in 2012, the highest retention occurred for S/40/100 green roof in 2011. The lowest annual retention for the control roof was recorded in 2013 (50.3%), the highest in Jul-Dec 2010 (94.2%). The green roof cumulative retention over the entire monitoring period ranged from 61.5% to 77.9% (Table 4.28). Figure 4.32 shows that green roofs performed better in 2010, 2011 and 2014 in comparison to the entire period 2010-2014. The green roof monitoring data in 2010 and 2014 did not include colder months. During colder months the retention is usually lower due to lower evapotranspiration, resulting in elevated cumulative stormwater retention. In 2011 total rainfall recorded was over 3 times less than the rainfall observed in 2012. The difference could occur due to less frequent or smaller rainfall events in 2011, which could result in higher overall retention of the green roofs.

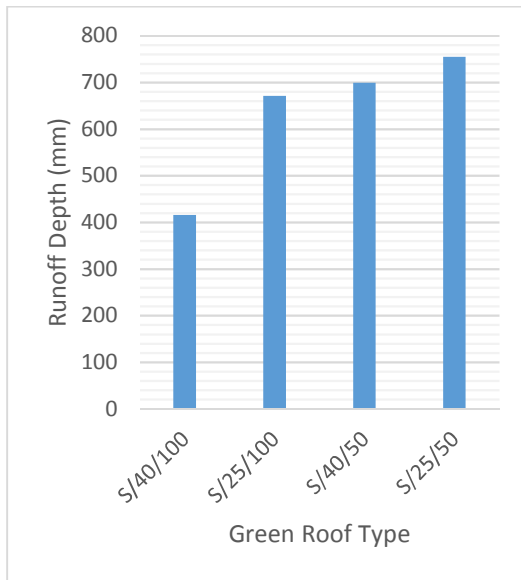
The result of 61.5% to 77.9% of cumulative retention is close to the outcome reported by Carpenter and Kaluvakolanu (2011) – 68.25%, Getter et al. (2007) – ranging from 75.30% to 85.20% or Hathaway et al. (2008) - 64%. However, this is much higher than the retention noted by Palla et al. (2011) – 22% or Stovin et al. (2012) – 42.74%. The wide range of cumulative retention of green roofs highlights the complexity of quantifying the hydrological performance of green roofs. There is no single factor such as rainfall depth that is dominant. Instead it is a combination of different factors that influence hydrologic response of green roofs. Figure 4.33 confirms the efficiency of the green roofs to mitigate stormwater. All green roofs produced runoff significantly lower than the rainfall for the overall period of the study. One roof, in particular, performed significantly better than others: S/40/100 with a total runoff depth 416.0mm. The high retention capacity of the S/40/100 could occur due to the combination of 40mm drainage layer and 100mm of substrate.

Although the differences in runoff depth between the rest of the selected green roofs were not significant (section 4.3.4.1), the possible patterns in hydrological performance of these green roofs were investigated (Figure 4.34 to 3.46). Analysing runoff from green roofs planted with sedum, one could notice that the depth of the substrate is the dominant factor followed by depth of the drainage layer (Figure 4.34 (a)). However, this pattern was not confirmed by the analysis

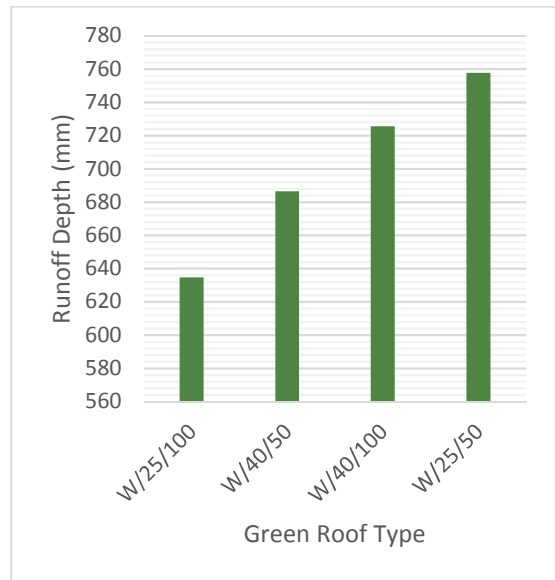
of green roofs planted with wildflowers. In this case, the vegetation coverage might have had more significant influence on green roof retention capacity, than the depth of any of the layers (Figure 4.34 (b)). For the green roofs with shallow substrate, the depth of the drainage layer seemed to influence the cumulative stormwater runoff (Figure 4.35 (b)). For this category of roofs, green roofs with drainage layer of 40mm stored more water than the green roofs with drainage layer of 25mm. However, in the case of green roofs with substrate depth of 100mm, no similar pattern was observed (Figure 4.35 (a)). This pattern could suggest that there is a certain critical depth of a substrate beyond which the layer depth does not influence green roof hydrological performance. It should be noted that such a critical depth could vary for different types of materials. Knowing such critical depths could support sustainable design of the green roofs.

A similar pattern was also observed for the drainage layer. For green roofs with a shallow drainage layer (25mm), the dominant factor enhancing stormwater storage was substrate depth. The runoff from green roofs with substrate depth of 100mm was lower than from green roofs with substrate depth of 50mm. However, in the case of green roofs with drainage layer 40mm, the runoff from all these roofs was about 700mm with exception of the S/40/100 green roof (about 400mm). These results partly supported the findings of VanWoert et al. (2005), who demonstrated that deeper substrate reduced significantly the stormwater runoff, but had little effect on retention values. Similar observations were presented by Graceson et al. (2013). Their study showed that 100% increase in substrate depth resulted in mean retention higher by 20%. However, it should be noted that shallower substrates were planted with sedum, while deeper substrates were covered with wildflowers, which could influence the retention performance. In contrast, Fassman-Beck et al. (2013) demonstrated no significant difference in runoff depth or peak flow reduction between two roofs of differing substrate depths (100mm vs. 150mm).

This analysis demonstrated the complexity of assessment of the hydrological performance of green roofs. Certain patterns in cumulative runoff depth of selected green roofs were identified, even though the differences between green roof designs were not statistically significant. More detailed analysis to determine the dominant factors and their significance to hydrological performance of the green roofs is needed.

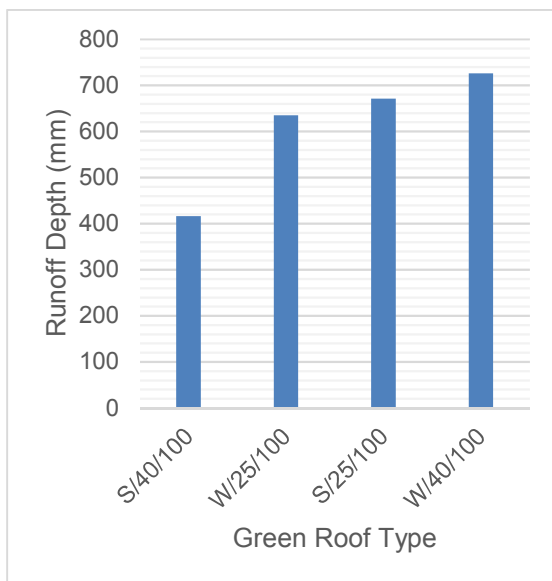


(a)

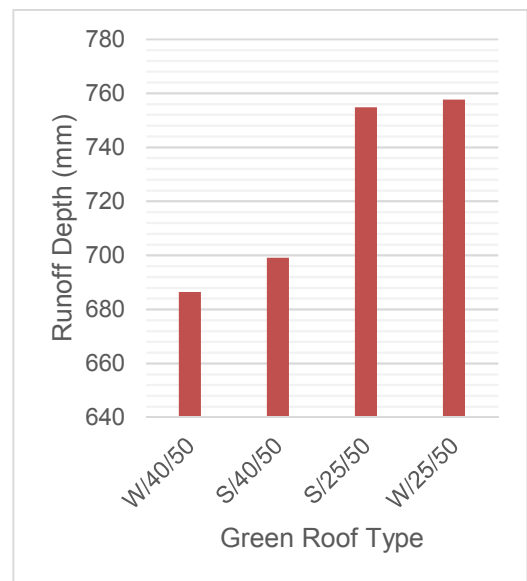


(b)

Figure 4.34 Cumulative runoff depth over period of study July 2010 – August 2014. Runoff depth data were grouped based on vegetation type: (a) sedum; (b) wildflower.



(a)



(b)

Figure 4.35 Cumulative runoff depth over period of study July 2010 – August 2014. Runoff depth data were grouped based on substrate depth: (a) 100mm; (b) 50mm.

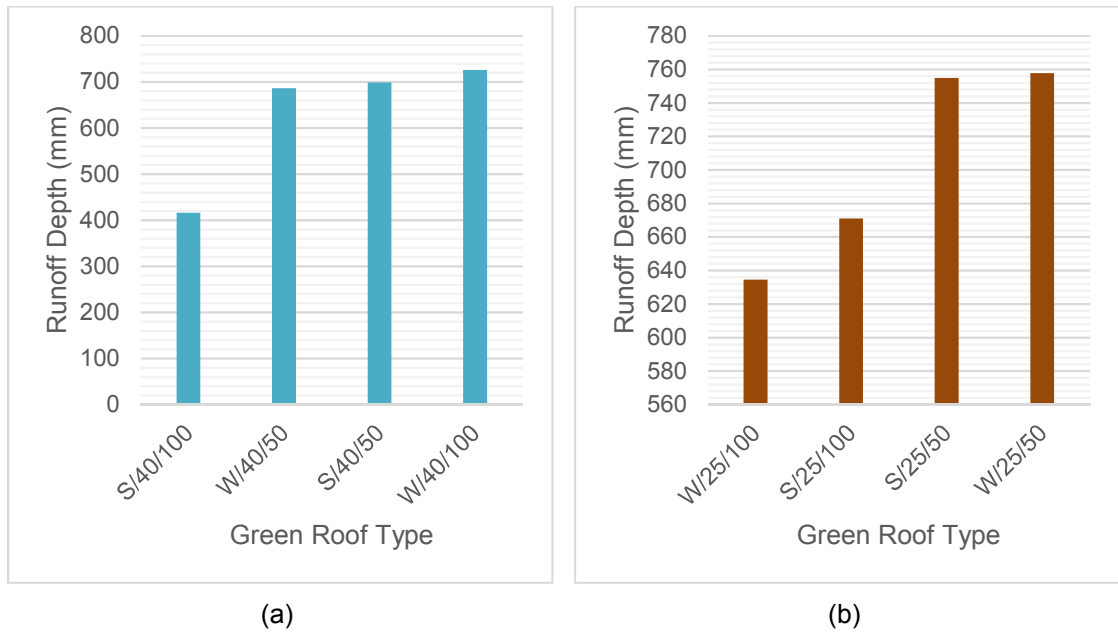


Figure 4.36 Cumulative runoff depth over period of study July 2010 – August 2014. Runoff depth data were grouped based on drainage layer depth: (a) 40mm; (b) 25mm.

#### 4.3.4.3 SEASONAL ANALYSIS OF HYDROLOGICAL PERFORMANCE

This section presents seasonal variations in the hydrological performance of green roofs. It aims to explore general seasonal patterns in hydrological performance of green roofs, as well as the hydrological response of green roof designs to seasonal climate differences. The exploratory data analysis was carried out to determine the nature of data distribution. Summary statistics of the green roof hydrological performance data in relation to season are presented in Table 4.29 (runoff depth), Table 4.31 (retention), and Table 4.33 (peak flow reduction). Green roof hydrological performance data distributions categorised by season are presented in Figure 4.37 (runoff depth), Figure 4.38 (retention) and Figure 4.39 (peak flow reduction).

It was assumed that the seasonal variations in climate conditions would influence the green roof hydrological performance. Based on this assumption, the following null hypothesis was generated: there is no significant difference in green roof hydrological performance (runoff depth, retention, and peak flow reduction) between the seasons.

The hypothesis was tested using a non-parametric test: Dunn's Kruskal-Wallis multiple comparison test with Bonferroni correction. The test was run using all green roof data set (Table 4.29, Table 4.31, and Table 4.33) as well as each selected roof data set (Table 4.30, Table 4.32, and Table 4.34).

## Runoff depth

Table 4.29 Summary statistics of stormwater runoff depth data in relation to their overall performance in different seasons over a period of study July 2010 – August 2014. Statistically significant differences are represented by p-values obtained from Dunn's Kruskal-Wallis multiple comparison test results with Bonferroni correction. Highlighted numbers demonstrate a statistically significant difference in runoff depth between seasons.

Summary Statistics, Runoff Depth (mm)					
Season	Autumn	Summer	Spring	Winter	
<b>N</b>	443	538	285	261	
<b>Mean</b>	3.96	1.59	2.61	4.1	
<b>Median</b>	0.45	0.00	0.00	3.33	
<b>Std. Deviation</b>	6.49	4.31	5.72	4.27	
<b>Percentiles</b>	<b>Min.</b>	0.00	0.00	0.00	0.00
	<b>25</b>	0.00	0.00	0.00	0.00
	<b>50</b>	0.45	0.00	0.00	3.33
	<b>75</b>	4.79	0.48	1.38	6.08
	<b>Max.</b>	30.22	28.02	29.27	19.76
<b>Statistically Significant Differences</b>	<b>Autumn</b>	-	<0.001	<0.001	<0.001
	<b>Summer</b>		-	1.00	<0.001
	<b>Spring</b>			-	<0.001
	<b>Winter</b>				-

Null hypothesis of no statistically significant difference rejected ( $p < 0.05$ )

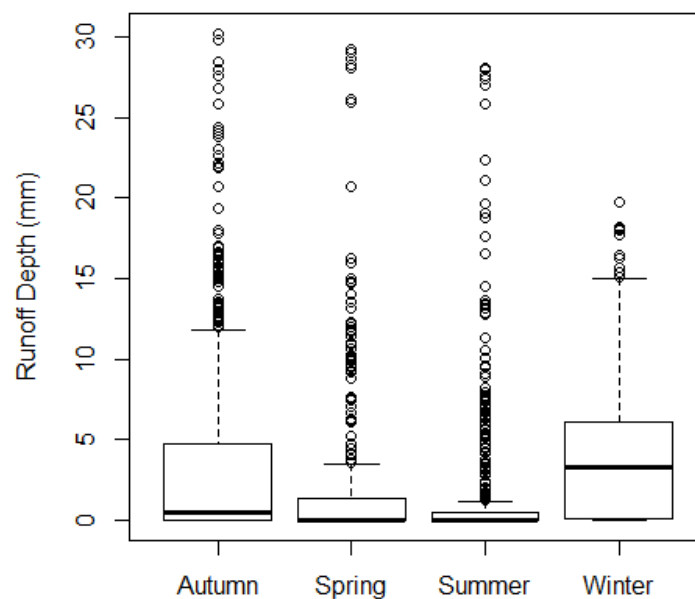


Figure 4.37 Distribution of stormwater runoff depth data by season.

Table 4.30 Median runoff depth for selected green roofs in relation to season and p-values from Dunn's Kruskal-Wallis multiple comparison test results with Bonferroni correction applied between seasons for selected roofs. Highlighted numbers demonstrate a statistically significant difference in runoff depth between seasons.

Median Runoff Depth (mm)										
Season	Control-3	S/25/50-2	S/25/100-2	S/40/50-2	S/40/100-2	W/25/50-1	W/25/100-2	W/40/50-1	W/40/100-1	
Spring	0.89	0.00	0.00	0.00	0.00	0.00	0.00	0.00	0.00	
Summer	1.03	0.00	0.00	0.00	0.00	0.00	0.00	0.00	0.00	
Autumn	0.45	0.84	0.09	0.39	0.00	1.16	0.18	0.66	1.3	
Winter	0.06	3.6	4.22	3.47	0.15	3.75	3.99	3.98	4.26	
Statistically Significant Differences	Autumn - Spring	None	None	None	None	None	None	None	None	
	Autumn - Summer	None	0.017	None	0.009	0.008	0.006	None	0.004	
	Spring - Summer	None	None	None	None	None	None	None	None	
	Autumn - Winter	None	None	0.015	None	None	None	0.018	None	
	Spring - Winter	None	<0.001	<0.001	0.013	0.032	0.002	<0.001	<0.001	
	Summer - Winter	None	<0.001	<0.001	<0.001	0.007	<0.001	<0.001	<0.001	
 Null hypothesis of no statistically significant difference rejected (p<0.05)										

## Retention

Table 4.31 Summary statistics of stormwater retention data in relation to their overall performance in different seasons over a period of study July 2010 – August 2014. Statistically significant differences are represented by p-values obtained from Dunn's Kruskal-Wallis multiple comparison test results with Bonferroni correction. Highlighted numbers demonstrate a statistically significant difference in retention between seasons.

Summary Statistics, all events $\geq$ 2mm, Retention (%)					
Season	Autumn	Summer	Spring	Winter	
<b>N</b>	443	538	285	261	
<b>Mean</b>	72.62	90.11	86.25	55.15	
<b>Median</b>	87.90	100	100	48.60	
<b>Std. Deviation</b>	30.73	19.54	24.20	32.31	
<b>Percentiles</b>	<b>Min.</b>	0.00	8.7	0.00	0.00
	<b>25</b>	41.80	91.88	83.50	29.30
	<b>50</b>	87.90	100	100	48.60
	<b>75</b>	100	100	100	97.00
	<b>Max.</b>	100	100	100	100
<b>p-value</b>	<b>Autumn</b>	-	<0.001	<0.001	<0.001
	<b>Summer</b>		-	1.00	<0.001
	<b>Spring</b>			-	<0.001
	<b>Winter</b>				-

Null hypothesis of no statistically significant difference rejected ( $p < 0.05$ )

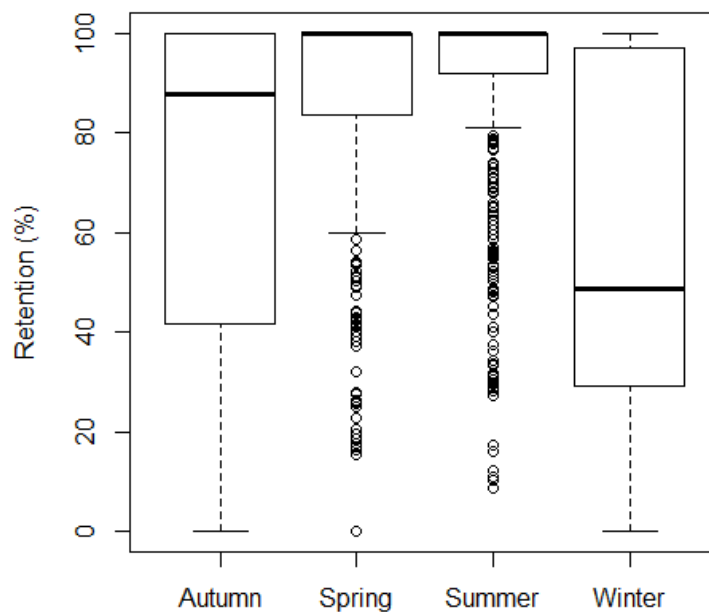


Figure 4.38 Distribution of stormwater retention data by season

Table 4.32 Median retention for selected green roofs in relation to season and p-values from Dunn's Kruskal-Wallis multiple comparison test results with Bonferroni correction applied between seasons for selected roofs. Highlighted numbers demonstrate a statistically significant difference in retention between seasons.

Median Retention (%)										
Season	Control-3	S/25/50-2	S/25/100-2	S/40/50-2	S/40/100-2	W/25/50-1	W/25/100-2	W/40/50-1	W/40/100-1	
Spring	84.0	100.0	100.0	99.95	100.0	100.0	100.0	100.0	100.0	100.0
Summer	84.6	100.0	100.0	100.0	100.0	100.0	99.9	100.0	100.0	100.0
Autumn	86.6	80.35	98.4	87.35	99.9	75.2	95.1	82.85	74.55	
Winter	99.0	49.1	43.15	52.85	93.9	41.5	42.3	44.05	42.1	
p-value	Autumn - Spring	None	0.021	None	None	0.015	None	None	0.050	0.052
	Autumn - Summer	None	0.005	None	0.002	0.005	0.001	None	0.001	0.005
	Spring - Summer	None	None	None	None	None	None	None	None	None
	Autumn - Winter	None	None	0.001	None	None	0.036	<0.001	0.010	0.056
	Spring - Winter	None	<0.001	<0.001	<0.001	0.005	<0.001	<0.001	<0.001	<0.001
	Summer - Winter	None	<0.001	<0.001	<0.001	0.002	<0.001	<0.001	<0.001	<0.001
 Null hypothesis of no statistically significant difference rejected (p<0.05)										

## Peak flow reduction

Table 4.33 Summary statistics of stormwater retention data in relation to their overall performance in different seasons over a period of study July 2010 – August 2014. Statistically significant differences are represented by p-values obtained from Dunn's Kruskal-Wallis multiple comparison test results with Bonferroni correction. Highlighted numbers demonstrate a statistically significant difference in peak flow reduction between seasons.

Summary Statistics, Peak Flow Reduction (%)				
Season	Autumn	Summer	Spring	Winter
<b>N</b>	443	538	285	261
<b>Mean</b>	85.65	92.34	90.75	77.72
<b>Median</b>	98	100	100	86
<b>Std. Deviation</b>	24.67	18.93	20.16	24.62
<b>Percentiles</b>	<b>Min.</b>	1	0	2
	<b>25</b>	87.00	97.00	95.00
	<b>50</b>	85.65	100	100
	<b>75</b>	100	100	100
	<b>Max.</b>	100	100	100
<b>p-value</b>	<b>Autumn</b>	-	<0.001	<0.001
	<b>Summer</b>		-	1.00
	<b>Spring</b>			-
	<b>Winter</b>			

Null hypothesis of no statistically significant difference rejected ( $p < 0.05$ )

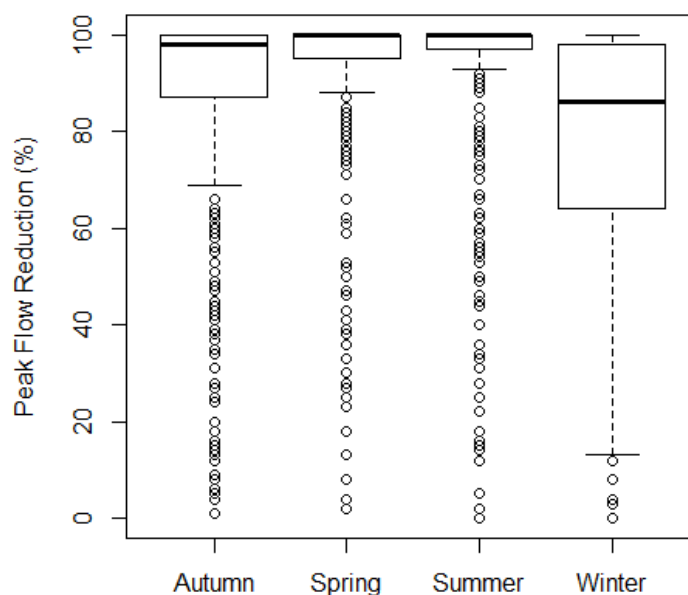


Figure 4.39 Distribution of stormwater peak flow reduction data by season.

Table 4.34 Median peak flow reduction for selected green roofs in relation to season and p-values from Dunn's Kruskal-Wallis multiple comparison test results with Bonferroni correction applied between seasons for selected roofs. Highlighted numbers demonstrate a statistically significant difference in peak flow reduction between seasons.

Median Peak Flow Reduction (%)										
Season	Control-3	S/25/50-2	S/25/100-2	S/40/50-2	S/40/100-2	W/25/50-1	W/25/100-2	W/40/50-1	W/40/100-1	
Spring	96	100	100	99.5	100	100	100	100	100	
Summer	95	100	100	100	100	100	100	100	99	
Autumn	98	98	99	98	100	98	98	97	97	
Winter	99	73	82.5	81.5	98.5	61.5	73	82.5	91.5	
p-value	Autumn - Spring	None	None	None	None	None	None	None	None	None
	Autumn - Summer	None	0.027	None	0.010	0.012	0.008	None	0.013	0.050
	Spring - Summer	None	None	None	None	None	None	None	None	None
	Autumn - Winter	None	None	0.002	None	None	0.046	0.003	0.011	0.017
	Spring - Winter	None	<0.001	<0.001	0.003	0.012	<0.001	<0.001	<0.001	<0.001
	Summer - Winter	None	<0.001	<0.001	<0.001	0.002	<0.001	<0.001	<0.001	<0.001
 Null hypothesis of no statistically significant difference rejected (p<0.05)										

The UK climate is characterised by seasonal variations, which result in cold winters and warm, humid summers as described in section 4.3.1. Therefore, the seasonal variations in green roof hydrological performance was expected. The seasonal performance of all green roofs supported the observations of other researchers, who showed better response to rainfalls in warm season and lower performance during cold seasons (Villarreal and Bengtsson, 2005, Bengtsson et al., 2005, Voyde et al., 2010). The median runoff depth was 0.00mm in spring and summer, 0.45mm in autumn and 3.33mm in winter. These results confirmed better hydrologic response in warm seasons such as spring and summer than colder seasons such as autumn and winter. The higher temperatures during warm seasons would result in higher evapotranspiration rates decreasing runoff quantities from green roofs. In contrast, maximum runoff depth of 30.22mm occurred in autumn, while the lowest maximum runoff depth was observed in winter, 19.76mm. These results followed the distribution of rainfall depth data with the largest rainfalls observed in autumn and with a low number of large events recorded in winter (Figure 4.40). Similar association between green roof hydrological performance and seasonal distribution of rainfall events was observed by Nawaz et al. (2015).

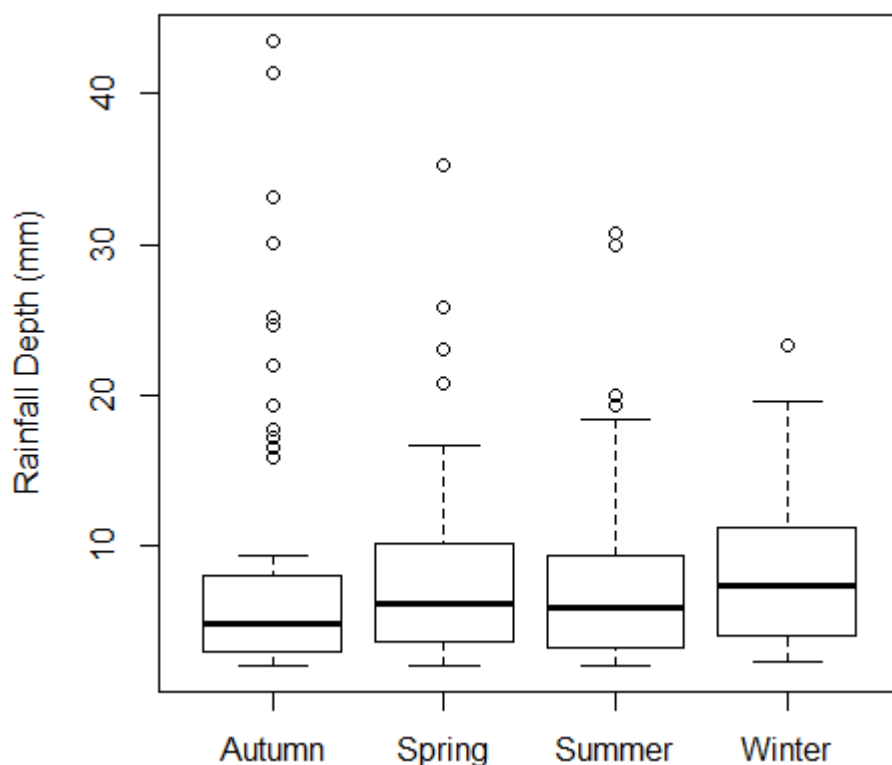


Figure 4.40 Rainfall depth data distribution by season.

The median stormwater retention was 100% in spring, 100% in summer, 87.9% in autumn and 48.6% in winter (Table 4.31). Hence, the retention performance of the green roofs in summer is more effective than in winter. Many researchers suggested that such seasonal variation in a green roofs hydrological performance is a result of changes in evapotranspiration rates between seasons (Fassman-Beck et al., 2013, Graceson et al., 2013). It was observed that higher evapotranspiration during the warm season enhanced green roof stormwater storage regeneration (Mentens et al., 2006) and increased stormwater retention capacity of green roofs. The analysis of the peak flow reduction also followed observed pattern, although with less variations. The median peak reduction was 100% in spring, 100% in summer, 98% in autumn and 86% in winter. Spring performance compared to that of summer showed no statistically significant differences in runoff depth, retention, and peak flow reduction. Kruskal-Wallis tests indicated significant differences in runoff depth, retention, and peak flow reduction between all other seasons. The results clearly showed that there are seasonal variations in green roof hydrological performance. Moreover, green roof response to rainfall is expected to be different in varied climatic conditions. Fassman-Beck et al. (2013) observed seasonal variations in green roof performance in New Zealand. However, the statistically significant difference was noted only between winter and summer and winter and spring for retention and peak flow reduction data. Nawaz et al. (2015) demonstrated difference in green roof retention performance between summer and winter in the UK, although the significance of the difference was not reported. Wong and Jim (2014) found no significant effect of season on retention of green roofs in Hong Kong. These results differed from Barking Riverside data analysis, demonstrating that hydrological performance of green roofs is specific to local climatic conditions.

The analysis of seasonal performance of the specific green roofs showed more variations. The median runoff depth in spring and summer was 0.00mm for all green roofs. It increased slightly in autumn (0.00mm-1.16mm) and more in winter ranging from 0.15mm to 4.26mm (Table 4.30). Median retention per event was 99.95% - 100% in spring, 99.9% - 100% in summer, which decreased to 74.55% - 99.90% in autumn and 41.5% - 93.9% (Table 4.32). Fassman-Beck et al. (2013) also recorded higher retention in spring and summer (81%-92%) and lower retention in autumn (45%-75%) and winter (66%). Median peak flow reduction

per event was 99.5% - 100% in spring, 99.0% - 100% in summer, which decreased to 97.00% - 100% in autumn and 61.5% - 98.5% in winter (Table 4.34).

Similarly, to the overall seasonal performance of the green roofs, there was no statistically significant difference between spring and summer runoff depth, retention and peak flow reduction observations specific to green roof design (Table 4.30, Table 4.32, and Table 4.34). In contrast to the overall seasonal hydrologic response, there was also no statistically significant difference between autumn and spring in specific to green roof design runoff depth and peak flow reduction. In both cases, overall and specific to green roof design hydrological performance in spring and winter as well as in summer and winter differed significantly ( $p < 0.05$ ). In all other combination of seasons, the significance of difference varied depending on green roof design. The analysis, however, confirmed consistent high hydrological performance of S/40/100 green roof design across all seasons. Although, the difference in retention between warm and cold seasons for this green roof design was statistically significant, it was not high. The S/40/100 green roof retained 100% (median) of stormwater in summer and 93.9% (median) of stormwater in winter. This could be a result of greater substrate and drainage layer depth, allowing for high amounts of water to be stored within the green roof. There is no, however, clear pattern or reasons explaining the existence or absence of the differences between other green roof designs. Clearly, climatic conditions play a significant role in green roof hydrological performance. However, the variations in seasonal response between green roofs of different design suggested that there are, other than seasonality, factors influencing green roof behaviour. It could be substrate or drainage layer depth or vegetation type and vegetation coverage.

#### **4.3.4.4 SUMMARY**

The analysis of the hydrological behaviour (runoff depth, retention, and peak flow reduction) between the green roofs of various design were carried out in the context of overall hydrological performance, annual and cumulative response, and seasonal performance.

The overall hydrological performance analysis contradicted the assumption that there would be statistically significant differences between green roofs of different designs. The roofs which demonstrated significantly different response to the

rainfall were S/40/100 and the control roof. All other tested green roof designs did not show statistically significant differences in their hydrological performance.

The green roofs demonstrated very high median retention in general (between 99.3% and 100%). The control roof, unexpectedly, also showed very high retention. The possible causes of such a high retention are:

- Underestimated rainfall depth recorded at Barking Riverside, which is significantly lower than MET Office data at Crossness STW and Heathrow, London
- Roof construction imperfections with local depressions, where stormwater is unintentionally stored
- Possible runoff data bias due to the tipping bucket rain gauges not being designed for runoff measurement

The analysis of green roof hydrological performance concurred with the concept of green roofs being very effective in retaining stormwater and mitigating peak flow from small and medium rainfall events.

The annual and cumulative analysis demonstrated retention abilities in the range from 61.5% to 77.9% across the green roof designs. The wide range of cumulative retention of green roofs and its disparity from overall median retention, indicated complexity of the hydrological performance of green roofs. Although, there was no significant difference in hydrological behaviour of green roofs of various design, cumulative retention suggested that substrate and drainage layer depth have impact on green roof response to rainfall.

The seasonal analysis also supported previous observations of more effective hydrologic response of green roofs during warm seasons as opposed to cold. Clearly, climatic conditions play a significant role in green roof hydrological performance. However, the variations in seasonal response between green roofs of different designs suggest that there are other factors influencing green roof behaviour.

#### **4.3.5 PRELIMINARY MULTIPLE LINEAR REGRESSION ANALYSIS**

This section aims to determine the relationships between green roof hydrological performance characteristics, particularly runoff depth and retention, and various factors such as weather conditions (temperature, humidity, dew point, wind

speed, THW index and air pressure) and rainfall characteristics (rainfall depth, rainfall duration, inter-event time and average rainfall intensity). These relationships were assessed using multiple linear regression analysis.

The preliminary multiple linear regression models were developed based on a unique, large set of 1355 observations. The selection of predictive variables significant to the model was carried out using an automatic stepwise process.

Table 4.35 summarises the results of multiple linear regression analysis for runoff depth, while Table 4.36 presents the results for retention. Figure 4.41 and Figure 4.42 show graphical verification of regression analysis assumptions for runoff depth and retention analysis, respectively.

## Runoff depth

Table 4.35 Summary of multiple linear regression predicting runoff depth using rainfall depth (RD), rainfall duration (DUR), temperature (TEMP), humidity (HUM), dew point (DEW), wind speed (WIND) and air pressure (BAR) (N=1355).

Predictor	$\beta$	p-value
RD	0.514	2.00 x10 <sup>-16</sup> ***
DUR	0.025	6.01 x10 <sup>-10</sup> ***
TEMP	0.849	0.02*
HUM	0.202	0.007**
DEW	-0.958	0.01**
WIND	0.047	0.0001***
BAR	-1.275	9.27 x10 <sup>-5</sup> ***
<b>Linear Regression Model</b>	$\text{RUNOFF} = 0.514 \cdot \text{RD} + 0.025 \cdot \text{DUR} + 0.849 \cdot \text{TEMP} + 0.202 \cdot \text{HUM} - 0.958 \cdot \text{DEW} + 0.047 \cdot \text{WIND} - 1.275 \cdot \text{BAR} + 17.315$ <p>R<sup>2</sup>=0.750, Adjusted R<sup>2</sup> = 0.749, p&lt; 2.2 x10<sup>-16</sup></p>	
Significance codes: 0 '***' 0.001 '**' 0.01 '*' 0.05 '.' 0.1 ' ' 1.0		

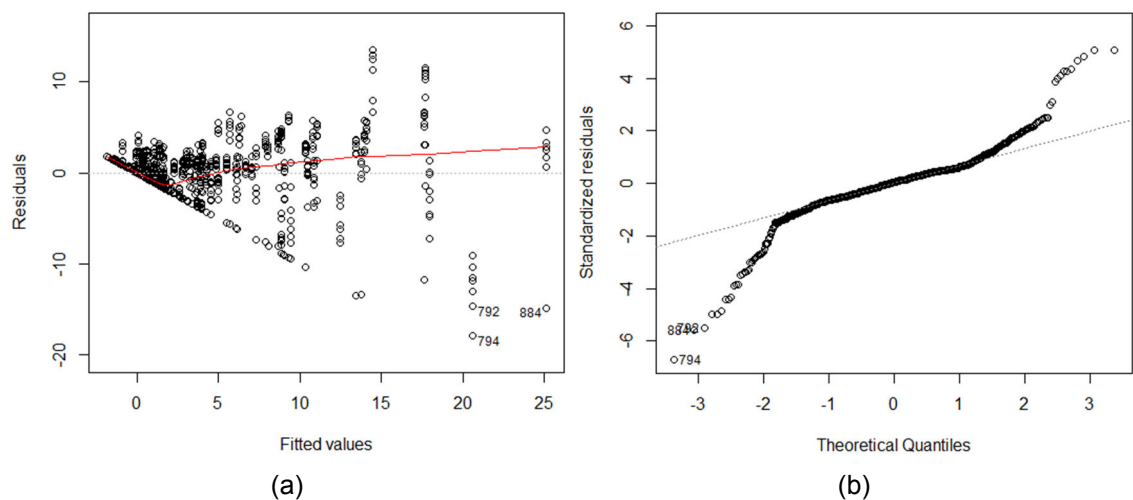


Figure 4.41 Linear regression model assumptions graphical tests (a) residuals vs. fitted values (b) residuals Q-Q plot.

## Retention

Table 4.36 Summary of multiple linear regression predicting retention using rainfall depth (RD), rainfall duration (DUR), temperature (TEMP), humidity (HUM), dew point (DEW), wind speed (WIND) and air pressure (BAR) (N=1355).

Predictor	$\beta$	p-value
RD	-1.173	$<2.00 \times 10^{-16}$ ***
DUR	-0.172	$4.27 \times 10^{-7}$ ***
TEMP	-7.025	0.021*
HUM	-2.084	0.0008***
DEW	8.740	0.005**
WIND	-0.630	0.0001***
BAR	11.500	$1.17 \times 10^{-9}$ ***
<b>Linear Regression Model</b>	$\text{RET} = -1.173 \cdot \text{RD} - 0.172 \cdot \text{DUR} - 7.025 \cdot \text{TEMP} - 2.084 \cdot \text{HUM} + 8.740 \cdot \text{DEW} - 0.630 \cdot \text{WIND} + 11.500 \cdot \text{BAR} - 67.189$ $R^2=0.419, \text{ Adjusted } R^2 = 0.416, p < 2.2 \times 10^{-16}$	
Significance codes: 0 '***' 0.001 '**' 0.01 '*' 0.05 '.' 0.1 ' ' ' '		

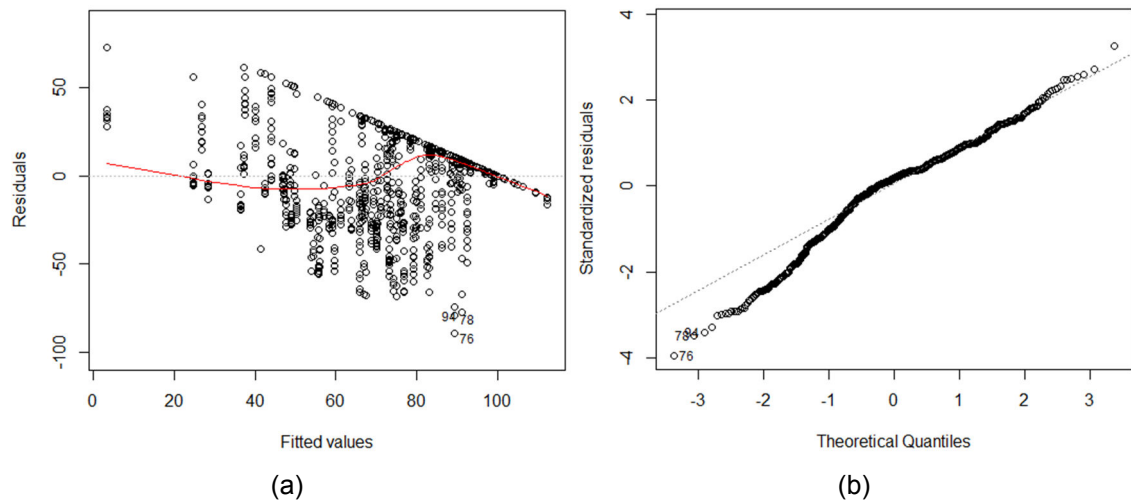


Figure 4.42 Retention linear regression model assumptions graphical tests (a) residuals vs. fitted values (b) residuals Q-Q plot.

The linear regression model to predict runoff depth (RUNOFF) was developed using rainfall depth (RD), rainfall duration (DUR), temperature (TEMP), humidity (HUM), dew point (DEW), wind speed (WIND) and air pressure (BAR) (Table 4.35).

The adjusted coefficient of determination (goodness of fit) for the model  $R^2$  was 0.749. This means that the regression model explains 74.9% of the total variation in runoff depth, which is high. All predictor variables were significant to the model ( $p < 0.05$ ). The most significant predictor was rainfall depth followed by rainfall duration (Table 4.35). The least significant variable was temperature ( $p = 0.020$ ). The significance of the model was also determined ( $p < 2.2 \times 10^{-16}$ ). Very low p-value suggested statistical significance of the model, which means that there was a very low probability for the model to be wrong. However, for the model to be valid it needed to meet further linear regression assumptions such as the independence of the errors and their normal distribution with mean zero and common variance. These assumptions are checked by investigating two plots: residuals (errors) vs. fitted values and Q-Q plot of residuals (Figure 4.41). The residuals vs. fitted values graph should show the residuals centered on zero throughout the range of fitted values. It should not contain any predictive information i.e. random pattern should be observed. However, in the case of runoff depth predictive model, the residuals for low values of runoff depth (0-5mm) formed a distinctive line (Figure 4.41 (a)). Moreover, the residuals Q-Q plot confirmed non-normal distribution of the error (the residuals were expected to follow straight line). Thus, the runoff depth model failed regression assumption tests, which means that it needs improvement.

The linear regression model to predict retention (RET) was also developed using rainfall depth (RD), rainfall duration (DUR), temperature (TEMP), humidity (HUM), dew point (DEW), wind speed (WIND) and air pressure (BAR) (Table 4.36).

The adjusted coefficient of determination for retention model,  $R^2$  was 0.416, which was significantly lower than coefficient of determination for runoff depth model. Only 41.9% of the retention variations can be explained by regression model. All predictor variables were significant for the model ( $p < 0.05$ ). The rainfall depth, duration and air pressure were the most significant variables and

temperature was the least significant predictor (Table 4.36). The analysis demonstrated high statistical significance of the model,  $p < 2.2 \times 10^{-16}$  (Table 4.36). The linear regression assumptions were graphically verified (Figure 4.42). The residuals vs. fitted values of high retention showed similar linear pattern to those observed for runoff depth. The pattern occurred, most likely, for the same rainfall events, since no or low runoff would also mean full or high retention, in most cases. The Q-Q plot confirmed non-normal distribution of residuals, leading to the same conclusion that the retention model did not predict, accurately, green roof retention.

Several researchers have attempted to explain runoff depth and retention through linear regression analysis (Schroll et al., 2011, Carpenter and Kaluvakolanu, 2011, Kasmin, 2010, Wong and Jim, 2015). However, many focused on simple linear regression analysis based on small samples of about 20 observations (Schroll et al., 2011, Carpenter and Kaluvakolanu, 2011). Some, like Kasmin (2010) performed multiple linear regression analysis on a larger data set of 200 observations but also with few predictor variables such as total rainfall, ADWP (inter-event time), rainfall duration, rainfall intensity. Regression analysis in this study was based not only on a large data set of 1355 observations but also incorporated a greater number of variables such as rainfall depth, rainfall duration, inter-event time, average rainfall intensity, temperature, humidity, dew point, wind speed, THW index, air pressure. There were certain similarities in the outcome of the regression analysis of runoff depth between all researches such as significant influence of rainfall depth. However, there was no agreement on linear regression model.

Volder and Dvorak (2014) developed a retention model, however, it was based on one predictor variable being volumetric water content. Kasmin (2010) also developed retention regression models. The results agreed with the outcome of this study showing a strong influence of rainfall depth on retention. The common result for all retention models was low coefficient of determination proving that linear regression models do not explain green roof retention capacity effectively. Moreover, none of the researchers reported on the verification of the regression assumptions. It is crucial for the regression modelling to meet these assumptions, as the evaluation of the coefficient of determination itself is not sufficient.

Both models developed in this study were preliminary and need to be improved. This could be done by introducing new predictor variables, variables transformation or by introducing higher-order terms of predictor variables. The currently developed models did not take under consideration variables such as material properties since the same materials were used to construct all green roofs. The regression model could be improved by transforming variables e.g. log transformation. Other models such as non-linear models should be also explored, especially models supported by machine learning techniques, which do not presume the nature of the response and predictor variables relationship. More in depth analysis is required, to fully and thoroughly investigate the models to predict runoff depth and retention from green roofs.

#### **4.4 CONCLUSIONS**

The aim of this chapter was to assess the hydrological performance of the extensive green roofs under UK climatic conditions. The data collected over a long-term monitoring period (between July 2010 and August 2014) formed a unique data set. The data represented a wide range of green roof hydrological performance under UK, specifically London, climatic conditions. This included comparison of the performance of green roofs of the same design (section 4.3.3), analysis of the overall performance of green roofs of different design performance (section 4.3.4.1), cumulative and annual performance (section 4.3.4.2) as well as green roof response to seasons (section 4.3.4.3). The preliminary multiple linear regression analysis was carried out to assess the effect of UK (London) weather conditions and rainfall characteristics data on hydrological performance of green roofs (section 4.3.5). The in-situ green roof experiment analysis led to the following conclusions:

1. Green roofs are effective in retaining stormwater and mitigating peak flow from rainfall events of return period less than 1 year (cumulative retention abilities in the range from 61.5% to 77.9% across the green roofs).

2. Green roof hydrological performance assessment is a complex problem, which involves large number of factors affecting green roof response to rainfall.
3. Green roofs of the same design (substrate and drainage layer depth and the vegetation type) can behave differently. Factors like vegetation coverage, organic matter content, substrate compaction, design of the underlying roof may influence green roof performance.
4. Green roofs of different design (substrate and drainage layer depth and the vegetation type) can behave similarly. This can also suggest stronger influence of factors such as vegetation coverage, organic matter content, substrate compaction, design of underlying roof or their combination on green roof hydrological performance.
5. Due to the variations in the green roof performance certain safety factors in the context of hydrological performance of green roofs (runoff depth or retention) should be introduced at the design stage, which could account for overestimated response to the rainfall events. This is significant in case of utilising green roofs as flood management tool.
6. For shallow depth of substrate or drainage layer, the depth of the other layer influences the green roof performance. It is anticipated that green roof layers may have a specific critical depth, beyond which the layer depth do not influence green roof hydrological performance. Such a critical depth may vary for different types of materials. However, further investigation to establish such a critical depth is needed.
7. Climatic conditions play a significant role in green roof hydrological performance. Green roofs perform better in warm seasons like summer than in cold such as winter.
8. Green roof design plays a significant role in future green roof response to rainfalls. Special care should be taken to ensure no surface depressions are present, which could lead to stormwater logging and affect supporting structure. Ensuring the correct depth and compaction of the green roof construction materials allow to achieve green roof design objectives.
9. The green roof experiment design is vital for ensuring data quality. The green roofs should be executed as precisely as possible. The green roof monitoring equipment should be adequate for the monitoring objectives.

10. The preliminary multiple linear regression models based on rainfall and weather characteristics did not explain completely runoff depth and retention. Further comprehensive regression analysis is needed. Other models should be explored, especially models supported by machine learning techniques, which do not presume the nature of the response and predictor variables relationship.

The long term in-situ experiment provided great insight into green roof hydrological performance. However, it could not explain the impact of extreme rainfall events such as rainfall events of return period  $T=30$  years or more, as observations for such rainfall events were not present in the analysed data set. Also, green roofs constructed as a part of the Barking Riverside experiment were made of the same green roof construction materials. Therefore, the assessment of the impact of material properties on green roof response to a rainfall event was not possible. To fully understand the green roof response to a greater range of magnitude of rainfall events, one of the on-site experiment green roof designs was replicated and tested in laboratory conditions (Chapter 6). Moreover, the influence of material properties was also investigated in further experimentation in laboratory conditions. It is anticipated that additional laboratory data combined with data collected in-situ could explain the hydrological performance of the green roof in greater detail.

## **CHAPTER 5**

### **RAINFALL SIMULATOR SYSTEM**

This chapter describes, in detail, the development of the experimental setup to assess hydrological performance of green roofs in laboratory conditions.

The determination of green roof hydrologic responses to simulated rainfall in laboratory conditions is still limited. The majority of the reviewed studies were based on monitoring of full scale in-situ green roofs (Chapter 2, section 2.2.1). However, due to the lack of control over the factors related to weather, the in-situ green roof experiments proved to have low reproducibility, especially in the case of extreme rainfall events. The reliability and validity of the green roof investigations could be significantly improved by conducting controlled experiments in laboratory conditions using an efficient and accurate rainfall simulator system.

This chapter presents the description of the laboratory experimental setup, including the design, construction, and performance of a custom designed rainfall simulator to simulate a broad range of rainfall events for green roof hydrological performance assessment. The experimental setup was designed and built based on critical evaluation of the strengths and weaknesses of in-situ and laboratory green roof monitoring systems (Chapter 2, section 2.2.1).

#### **5.1 BACKGROUND**

Rainfall simulators are commonly used in the soil erosion research field. Rainfall simulators allow the precise application of artificial rain with control over rainfall intensity, duration and rain drop size. There are two types of rainfall simulators: the drop-former type and spray-nozzle type (Grismer, 2011). The main advantage of the drop-former type of rainfall simulator is greater density and uniform

distribution of the rain. However, it is difficult to construct and to manoeuvre, which is important in soil erosion field tests. The spray-nozzle type of the rainfall simulator is straightforward in its construction but the rain produced is much less uniform (Figure 5.1) and the coverage changes with intensity of the rainfall (Grismer, 2011).

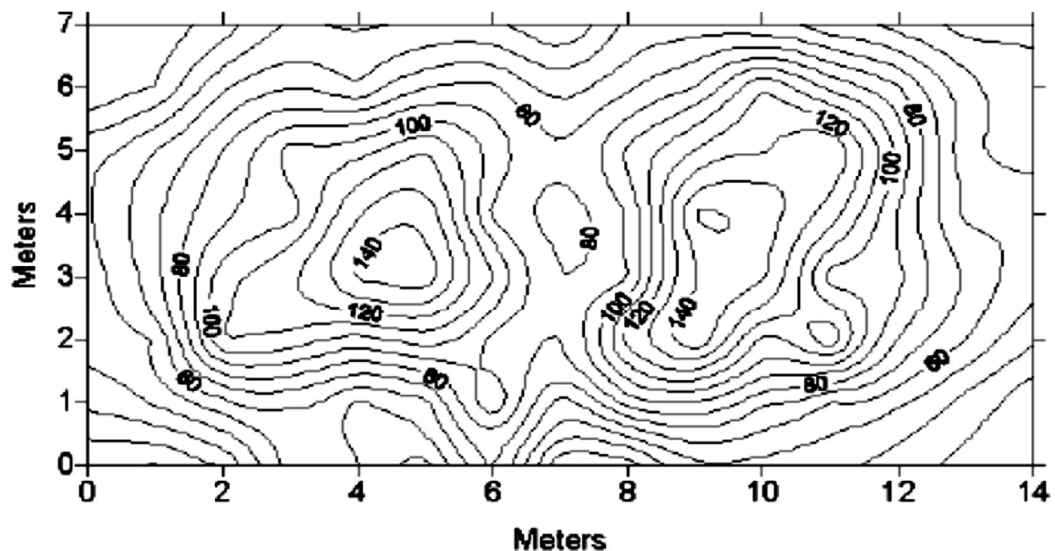


**Figure 17.** Contour map of simulated rainfall intensity (target intensity of 127 mm/h) taken from the mean of three replicated simulations (Munster et al., 2006).

*Figure 5.1 Example of the rainfall intensity distribution produced by spray-nozzle type of rainfall simulator. The rainfall intensity ranges between 40mm/h and 140mm/h for the target intensity of 127mm/h (Grismer, 2011).*

In green roof research, the use of rainfall simulators is increasing in popularity. However, their use is still very limited. Initially, the simulated rainfalls were achieved by irrigation (Schroll et al., 2011). This type of practice was highly inaccurate and did not truly recreate rainfall events. As green roof research has expanded, simulations of the rainfall have become more controlled and accurate through employment of rainfall simulators. However, to date only a few researchers have utilised rainfall simulators in green roof studies, of which the most common simulator is the spray-nozzle type (Beck et al., 2011, Buccola and Spolek, 2011, Lee et al., 2015). Only two studies were identified where a drop-former rainfall simulator was used (Mickovski et al., 2013, Nagase and Dunnett, 2012). Nagase and Dunnett (2012) drop-former rainfall simulator was supplied with water from a tank of limited volume, placed directly above drop-former elements. Rainfall intensity was regulated by monitoring the drop in the level of the water in the tank. The Mickovski et al. (2013) rainfall simulator comprised a

closed line of syringe needles. This posed the risk of reduction of the water pressure at the end of the line, creating uneven rainfall. All of the rainfall simulators were stationary and testing of each green roof tray required removal of the previous. In many cases these operations were not possible to be performed before runoff was ceased, thus limiting the number of tests, which could be done in given time.

Considering the importance of data quality and repeatability, the following objectives for rainfall simulator design were established:

1. The ability to simulate a variety of rainfall events including extreme rainfalls needed for experimental tests; rainfall intensities should be ranging from 0 to 200mm/h and they need to be easily controllable.
2. The rain distribution over the area should be uniform and constant, thus ensuring low spatial variability; the rainfall should be easily repeatable for comparative experiments.
3. The rain distribution should be independent of rain intensity and duration.
4. The rainfall simulator design should ensure the efficiency of the tests in terms of time and workload.

The first three objectives were achieved by implementing a drop-former type of rainfall simulator design which would ensure a consistent performance and avoids spatial rainfall variability. Objective four was achieved by creating a mobile rainfall simulator, thus allowing five green roof trays to be tested consecutively without interrupting the runoff monitoring.

## **5.2 RAINFALL SIMULATOR DESIGN**

The rainfall simulator system was made with the following components: (a) the structural frame, (b) the water supply system, (c) the rainfall simulator drop-forming box (Figure 5.2). All these components are described in detail in sections 5.2.1 and 5.2.2.

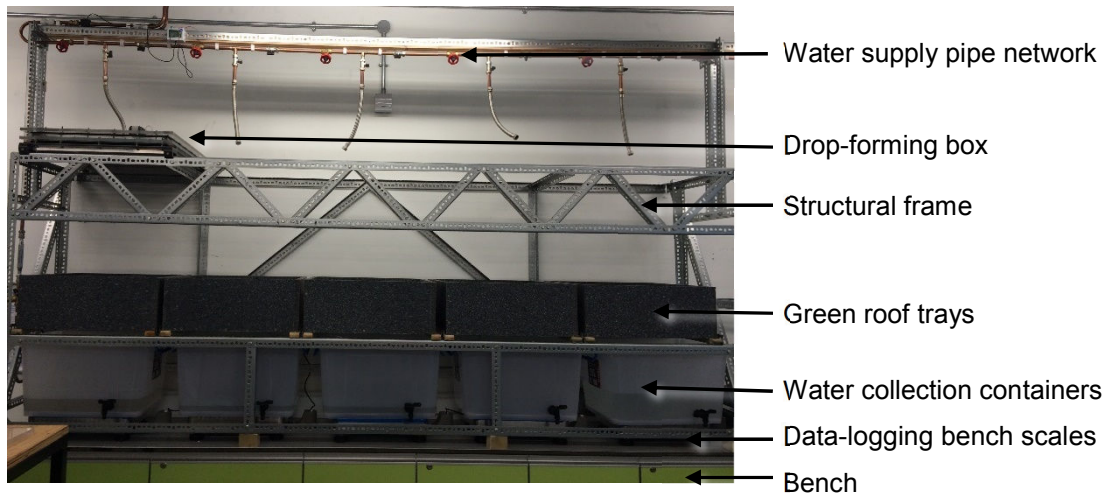


*Figure 5.2 Rainfall simulator system - general view.*

### **5.2.1 THE STRUCTURAL FRAME**

The structural frame was made of steel slotted angles. The frame was designed to support the rainfall simulator, the water supply network and five green roof roof trays (Figure 5.3). It was placed on a heavy-duty bench in the laboratory. The total length of the frame was 3 metres. The green roof trays and rainfall simulator drop-forming box were placed at 400mm and 1150mm above the bench respectively. The water supply network was placed at 1750mm above the bench (Figure 5.4).

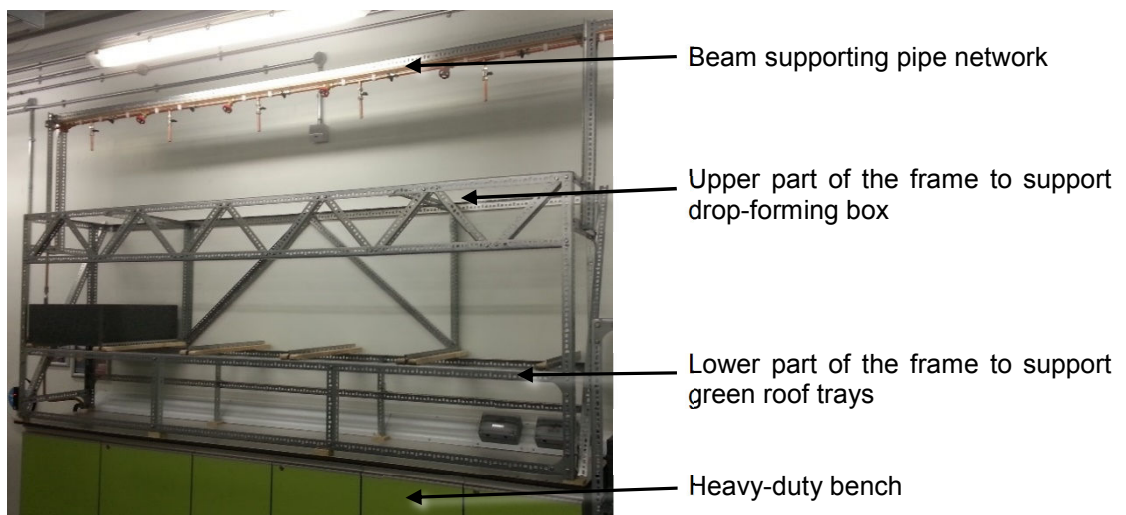


*Figure 5.3 The structural frame of the rainfall simulator system supporting water supply system, drop-forming box, and green roof trays.*

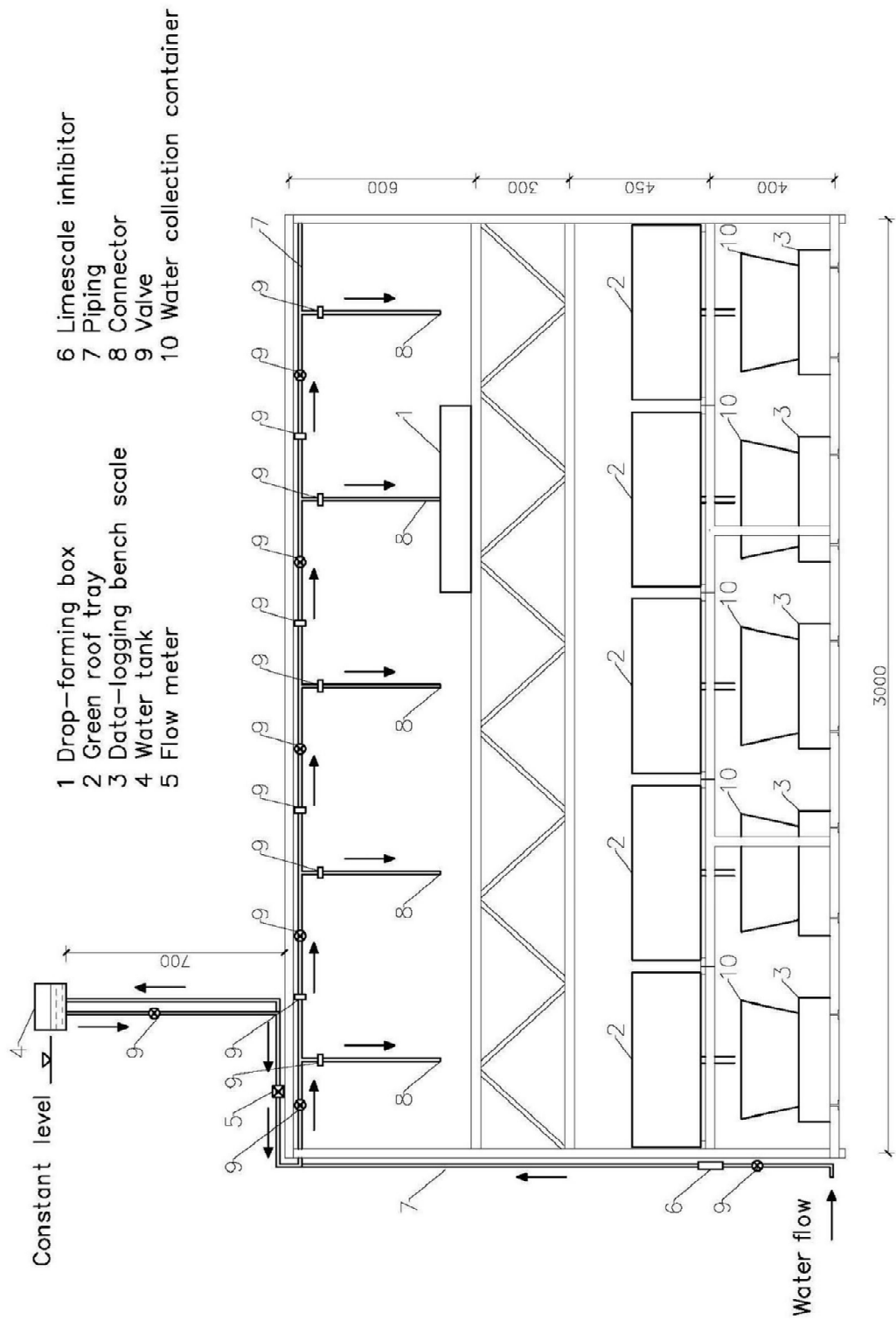
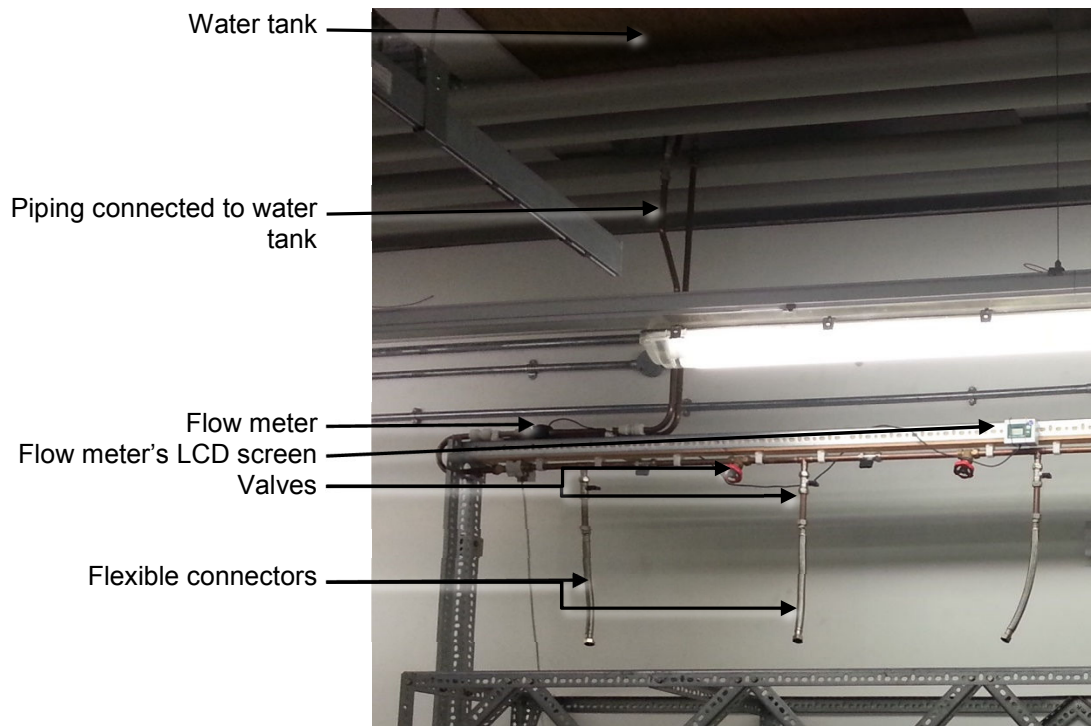


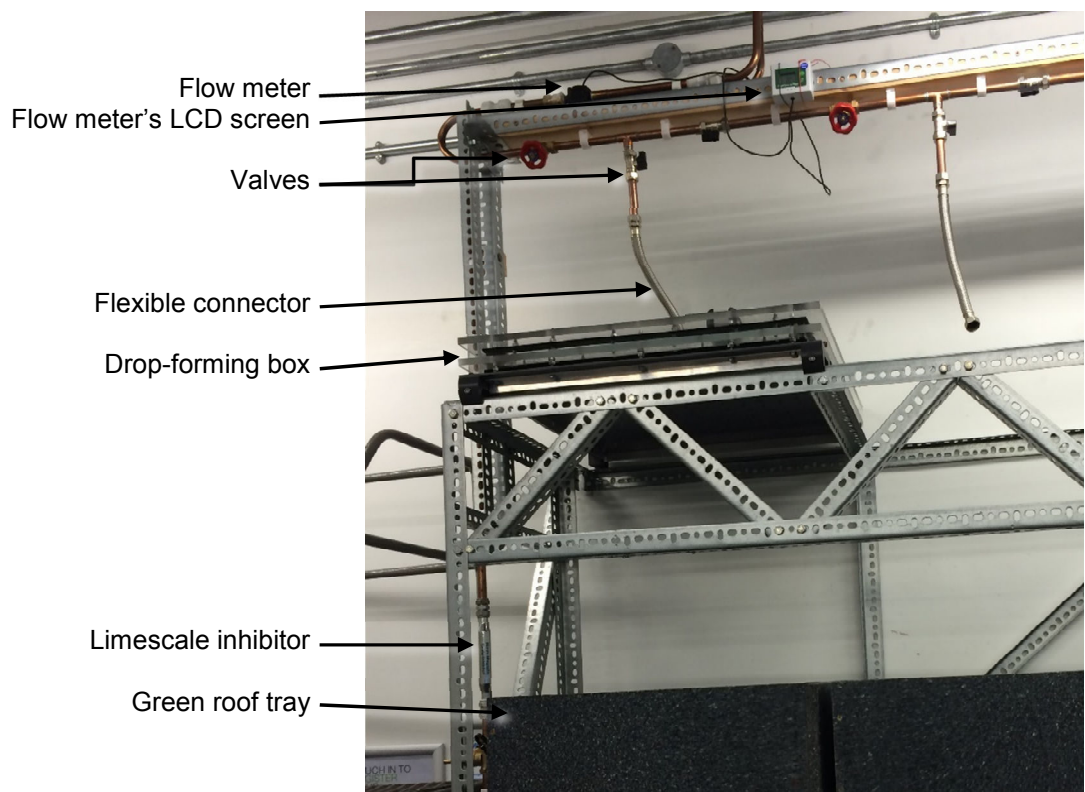
Figure 5.4 Rainfall simulator system diagram – elevation view.

### **5.2.2 WATER SUPPLY SYSTEM**

The header tank of approximately 18 litres capacity was used to supply water to the rainfall simulator drop-forming box. The tank was placed 1.3m above the drop-forming box and it was filled with water from the mains. The header tank was fitted with a ball valve to ensure an approximately constant level (pressure) of water during the tests. To reduce the risk of limescale deposition a limescale inhibitor was fitted inline, before the header tank. Water from the tank was directed through the system of the pipes to the rainfall simulator (Figure 5.5). To ensure full control over the water flow, multiple valves were fitted along pipes. The rainfall intensity was adjusted by manipulating these valves. The in-flow was monitored in two ways: i) a low rate flow meter, DigiFlow 6710M, installed inline between the header tank and the rainfall simulator drop-forming box ii) a digital manometer measuring the pressure changes in a water compartment of drop-forming box. Both measurements are related to the intensity and the volume of rainfall, although measurement of pressure in the water compartment was used to detect needle blockage (indicated by increased pressure) rather than the measurement of the intensity itself. The DigiFlow 6710M flow rate meter was designed to measure flow rates ranging between 0.8 to 8.0 litre/min with an accuracy of  $\pm 5\%$ . The flow rate meter turned on automatically when the water was flowing through.



(a)



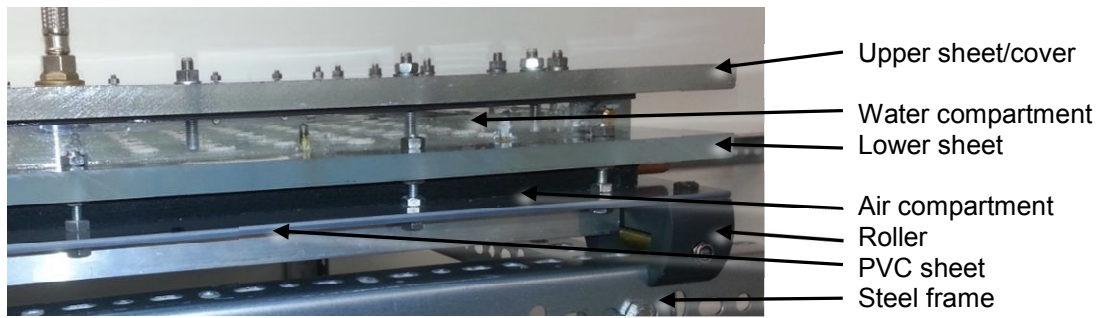
(b)

*Figure 5.5 The water supply system through which the water is supplied to the drop-forming box of the rainfall simulator (a) upper part of the water supply system (b) drop-forming box connected to the water supply system.*

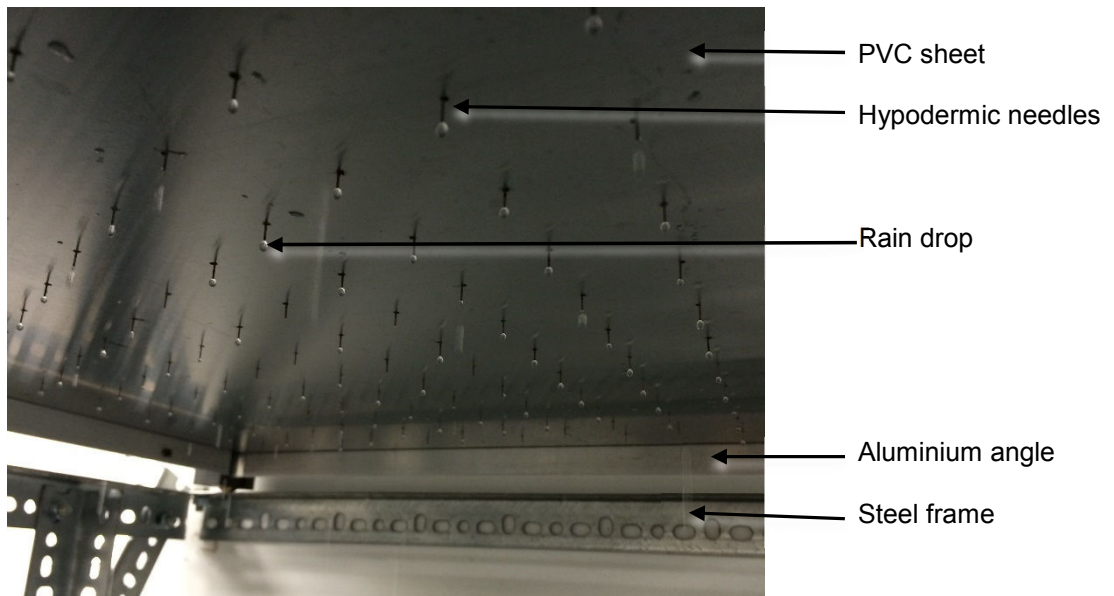
### **5.2.3 RAINFALL SIMULATOR DROP-FORMING BOX**

The rainfall simulator drop-forming box was designed to deliver rainfall over the area 500mm x 500mm (0.25m<sup>2</sup>) of the green roof trays. The external dimensions of the drop-forming box were 600mm x 600mm to allow for fittings. The drop-forming box comprised of two separate compartments: water compartment and air compartment (Figure 5.6 and Figure 5.7).

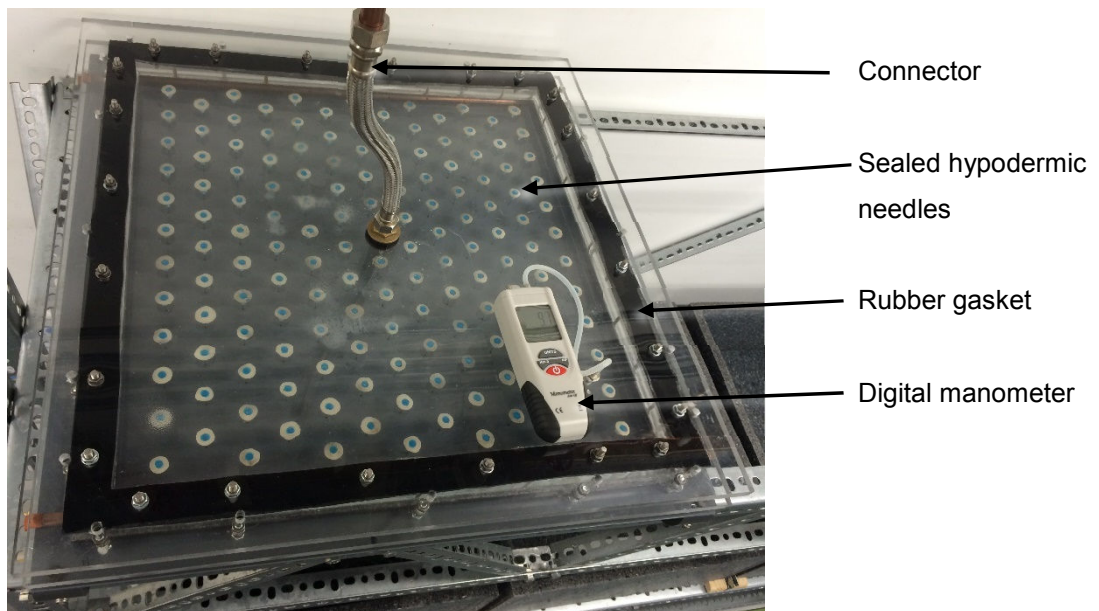
The water compartment was made of acrylic sheets. The top and the bottom sheets were 12mm thick and the side sheets were 25mm thick. The inner dimensions of the compartment were 486mm x 486mm. The bottom and side walls were glued and screwed together and the water compartment corners were sealed with a non-toxic sealant. The removable upper sheet (cover) was attached via bolts to allow access to the interior for maintenance purposes. Between the side sheets and the cover, a rubber gasket was placed to prevent leakage. The drop formers were made from hypodermic needles (23 gauge, Ø 0.6mm and 25mm long), trimmed for safety reasons and inserted into an array of 150 holes drilled into the bottom sheet of the water compartment (the density of drop formers was 600 drop formers/m<sup>2</sup>). The spacing of the holes is shown in Figure 5.7. Each needle was sealed using plumbers' putty. The needles were not permanently sealed in case any of them had to be replaced.



(a)



(b)



(c)

Figure 5.6 Rainfall simulator drop-forming box: (a) drop-forming box elevation (b) rain drops formed at the end of hypodermic needles (c) drop-forming box – plan view.

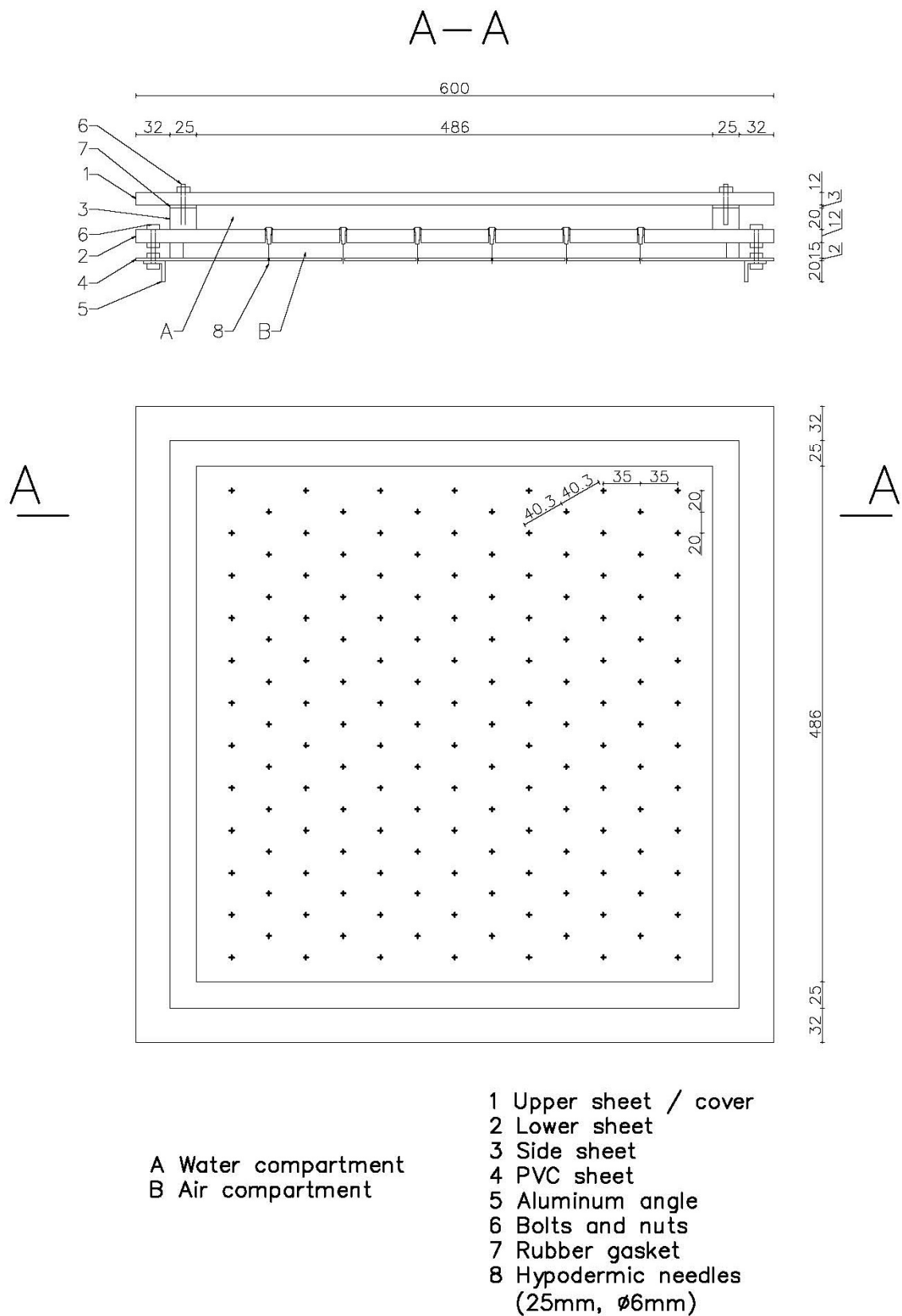


Figure 5.7 Rainfall simulator drop-forming box cross section and plan view.

The air compartment was created by attaching PVC sheet below the water compartment (Figure 5.6 and Figure 5.7) with the 150 holes drilled to allow drop formers. The air compartment was designed to introduce pressurised air, which would manipulate drop size. Although it is not essential for green roof hydrological performance assessment, the ability to manipulate drop size could allow investigation of the green roof erosion processes, which are currently overlooked. However, due to financial and time limitations such analysis was not used in this study.

The drop-forming box was mounted on rollers (Figure 5.6 (a)). This allowed for the drop-forming box to be easily moved along the structural frame to the next green roof trays for consecutive testing.

### **5.3 MODIFICATIONS**

Section 5.2 presented the final design of the rainfall simulator system. It was achieved through several modifications improving its performance. The following modifications were introduced:

- The thickness of the bottom and top sheets of the water compartment was doubled from 6mm to 12mm to prevent leakage due to inner pressure build up. The thickness of the side sheets was also increased from 10mm to 25mm.
- The bottom sheet of the air compartment was initially made of 2mm acrylic sheet. However, it was too brittle for drilling. Hence, it was replaced with a 2mm PVC sheet.
- The water supply was changed from the mains to the header tank, to avoid water pressure fluctuations.
- The flow meter was adjusted to accommodate lower water pressure from the header tank.

### **5.4 RAINFALL SIMULATOR PERFORMANCE**

In order to assess the performance of the rainfall simulator and its readiness for the green roof testing the following tests were initially carried out:

- Calibration of the flow meter (section 5.4.1)
- Calibration of the rainfall simulator (section 5.4.2)

- Assessment of the spatial variability of rainfall (coefficient of uniformity) (section 5.4.3)

The calibration of the flow meter and rainfall simulator was essential for accurate rainfall depth determination. The assessment of the spatial variability was performed to ensure a satisfactory uniform distribution of the rainfall over the testing area.

#### **5.4.1 CALIBRATION OF THE FLOW METER**

The calibration of the flow meter required determination of the coefficient of discharge. This coefficient is obtained as the ratio of the actual flow rate and the flow rate displayed by the flow meter through a graphical method. The flow meter was calibrated without the attachment of the rainfall simulator drop-forming box. The flow meter calibration procedure was as follows:

1. The water flow rate was set at of the following displayed value: 0.05 l/min, 0.10 l/min, 0.2 l/min and 0.30 l/min (the maximum displayed flow rate). The value of the flow rate was recorded.
2. Discharged water was collected in a measuring cylinder over a selected period of time, which included 0.5min, 1min, 1.5min, 3min and 5min. The volume of water collected and selected time were recorded.
3. Steps 1-2 were repeated three times for each combination of the flow rate and the time. The average of the three readings of water volume was taken as a final value.
4. An actual flow rate was determined by plotting average volume of water collected against the time. The average of the actual flow rate was taken as a slope of a best fit line.
5. Subsequently, the average actual flow rate was plotted against the displayed flow rate. The slope of the best fit line was taken as coefficient of discharge.

The results of the flow meter calibration are presented in Figure 5.8, Table 5.1 and Figure 5.9. Figure 5.8 shows the relationship between the average volume of water collected and the time of collection for each displayed flow rate. The slope of each best fit line indicates the average actual flow rate. The displayed and corresponding average actual flow rates are presented in Table 5.1. The coefficient of discharge was determined graphically drawing the average actual

flow rate against displayed flow rate (Figure 5.9). The slope of the best fit line indicates coefficient of discharge.

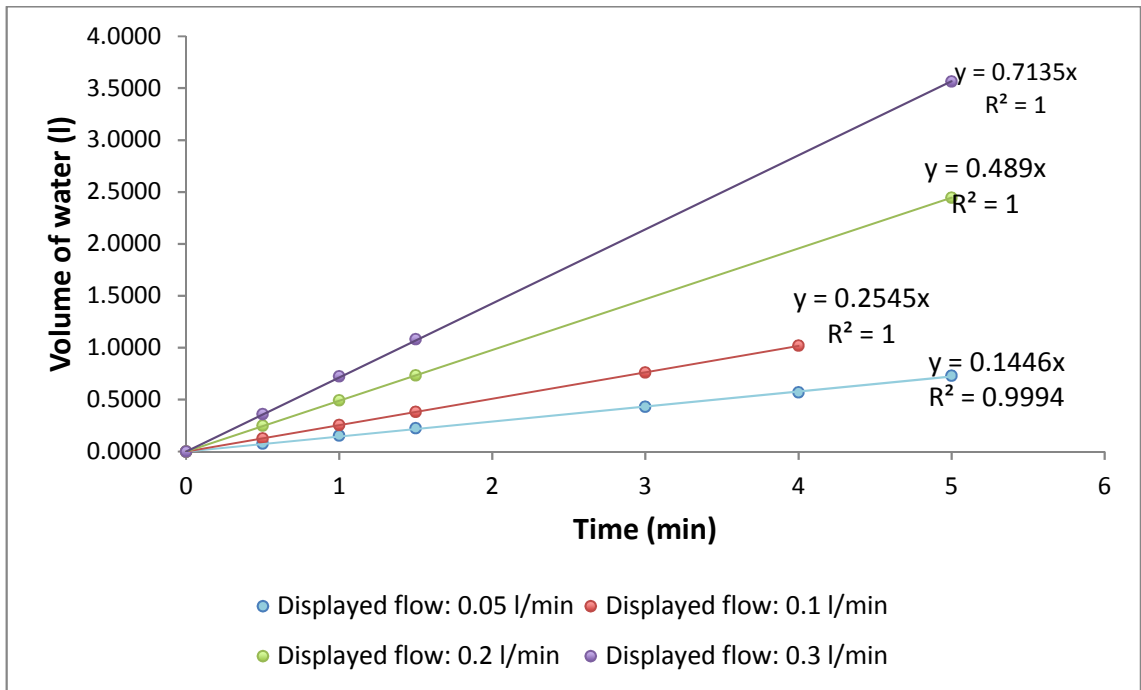
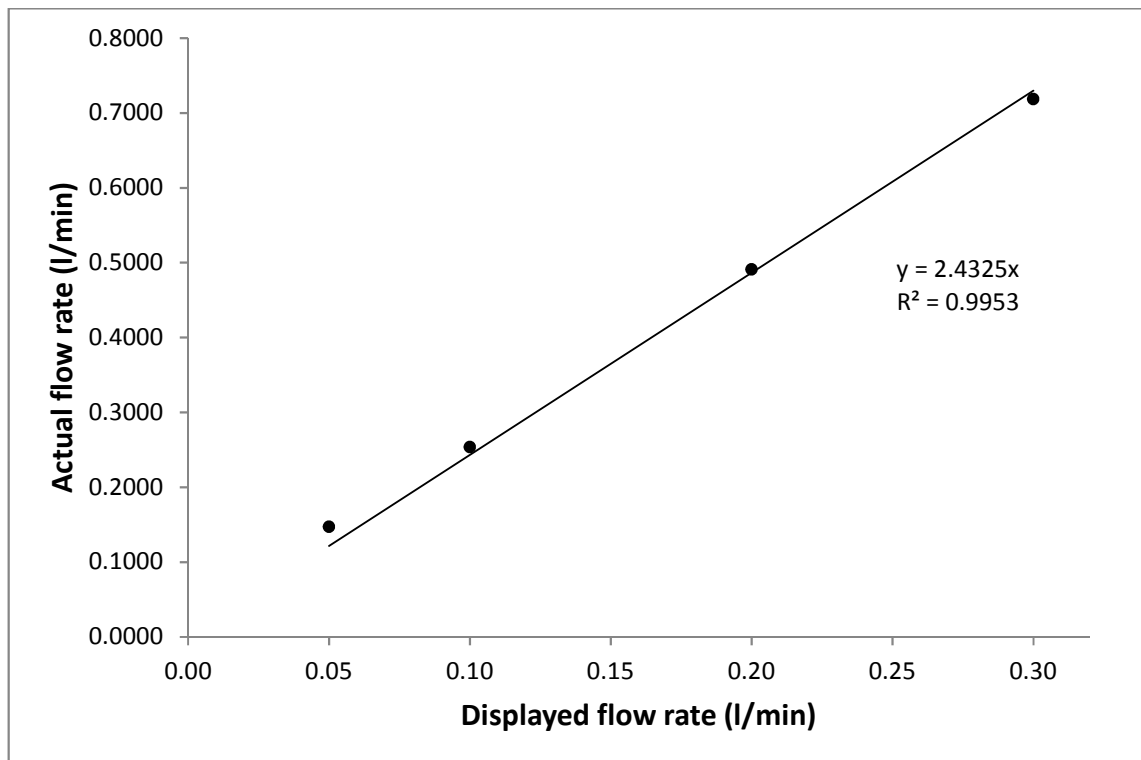


Figure 5.8 The relationship between the volume of water collected and the collection time for each displayed flow rates. The slope of each best fit line indicates the average actual flow rate corresponding to selected displayed flow rate.

Table 5.1 Displayed flow rates and corresponding actual flow rates based on Figure 5.8.

Displayed flow rate (l/min)	Actual flow rate (l/min)
0.00	0.0000
0.05	0.1446
0.10	0.2545
0.20	0.4890
0.30	0.7135



*Figure 5.9 The relationship between the actual and displayed flow rates for the DigiFlow 6710M flow rate meter. The coefficient of discharge is taken as a slope of the best fit line.*

The coefficient of discharge for DigiFlow 6710M flow rate meter was  $C=2.4325$ .

The results of the calibration of the DigiFlow 6710M flow rate meter were considered to be very accurate. Taking into consideration the number of tests and test scenarios (from minimum to maximum flow rate and various collection times) the calculation of actual flow rate was accurate. This was confirmed by the high values of coefficients of determination ( $R^2$ ) ranging from 0.999 to 1.000 (Figure 5.8). The goodness of fit for the coefficient of discharge was also very high ( $R^2 = 0.9953$ , Figure 5.9), ensuring the accuracy of the result and a good model for the actual flow rate prediction.

#### **5.4.2 CALIBRATION OF THE RAINFALL SIMULATOR SYSTEM**

The calibration of the rainfall simulator system was performed to account for any losses in flow through the entire system. As a result, the coefficient of discharge was determined. The following procedure was carried out:

1. The water flow rate was set at of the following displayed value: 0.05 l/min, 0.10l/min, 0.15 l/min 0.2 l/min, 0.25 l/min and 0.28 l/min (the maximum displayed flow rate). The value of the flow rate was recorded.
2. The duration of the generated rainfall was 10 min for each displayed flow rate.
3. The rainwater was directed into the empty tray and, through the centrally located outlet, into a collection container resting on data-logging bench scale.
4. The mass of the collected water and the corresponding time were recorded every 30 seconds using a computer software.
5. Based on total volume of runoff and time of rainfall, the actual flow rate was calculated.
6. Steps 1-5 were repeated three times for each and the average reading was taken as final value of the actual flow rate.
6. Steps 1-6 were repeated three times for each displayed flow rate. The average of the three readings of the actual flow rate was taken as a final value.
7. Subsequently, the average actual flow rate was plotted against the displayed flow rate. The slope of the best fit line was taken as coefficient of discharge.

The coefficient of discharge for the rainfall simulator system was determined graphically by plotting the actual flow rate against the displayed flow rate (Figure 5.10). The slope of the best fit line indicated the coefficient of discharge.

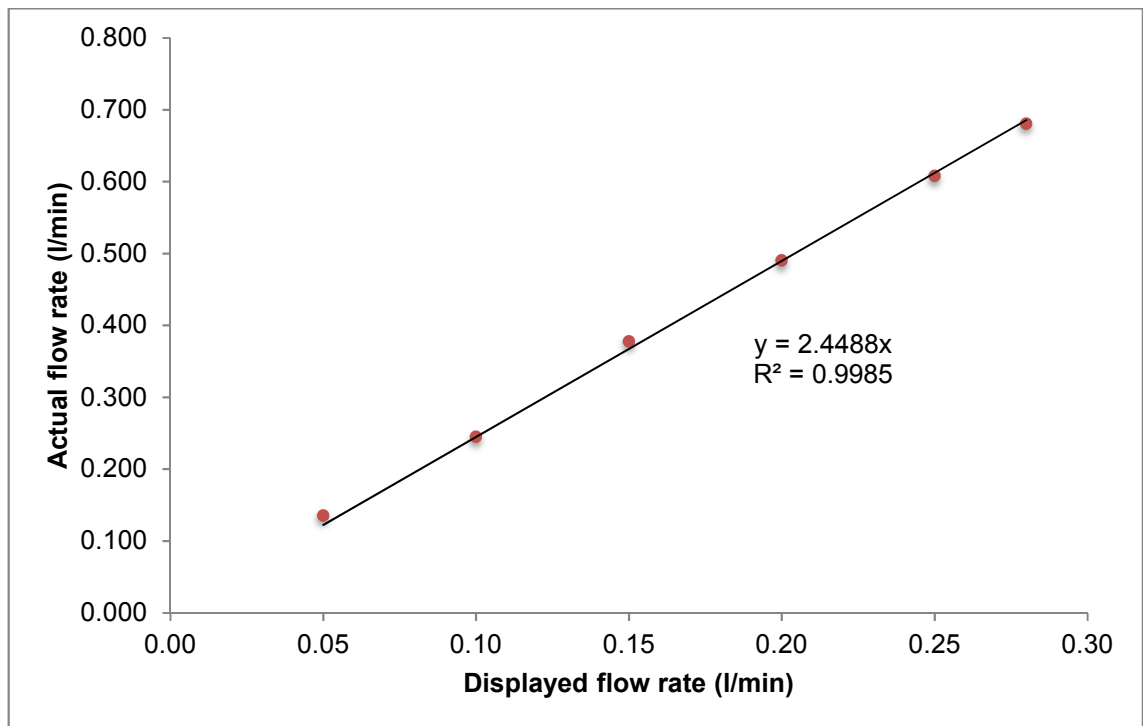


Figure 5.10 The relationship between the actual and displayed flow rate for the rainfall simulator system. The coefficient of discharge is taken as a slope of the best fit line.

The coefficient of discharge for the rainfall simulator system was  $C=2.4488$ .

The trend line fitted well within the data, with a high coefficient of determination  $R^2=0.9985$ , which provided good model for the actual flow rate prediction. The coefficient of discharge for the rainfall simulator was  $C=2.4488$ . This value was used in subsequent determination of the characteristics of simulated rainfall events.

#### 5.4.3 ASSESSMENT OF THE SPATIAL VARIABILITY OF RAINFALL (COEFFICIENT OF UNIFORMITY)

One of the objectives of the rainfall simulator design was to develop a simulator capable of producing uniformly distributed rainfall. The spatial variability was assessed by performing a uniformity test and by determining the Christiansen coefficient of uniformity. Rainfall is considered uniform when the Christiansen coefficient of uniformity is higher than 80% (Aksoy et al., 2012). The following procedure was carried out:

1. Twenty-five circular measurement cups ( $\varnothing = 7.5$  cm and volume of 400ml) were placed in the empty tray over the tested rainfall coverage area (0.5 x 0.5m) to collect the rainfall (Figure 5.11).

2. The rainfall simulator was turned on, setting the actual water flow rate at one of the following values: 0.122l/min, 0.243l/min, 0.487l/min and 0.681l/min and one of the following durations: 5min and 10min.
3. The volume of water in the measuring cups was determined (Figure 5.11 (b)).
4. Subsequently the Christiansen uniformity coefficient was determined by using the following formula:

$$C_u = 100 \times \frac{\sum|x|}{\mu \times n} \quad (5.1)$$

Where  $C_u$  is Christiansen uniformity coefficient,  $x$  is individual deviations from the mean,  $\eta$  is mean of the volume measurements,  $n$  is the number of the volume measurements.

5. Steps 1-4 were repeated for each combination of the actual flow rate and duration.

Due to incomplete area coverage, the circular cups were replaced with 16 squared cups (12.5cm x 12.5cm) and the experiment was repeated for the 0.487l/min and 0.681l/min flow rates and 10min duration (Figure 5.11 (c) and (d)). The results of the tests are presented in Table 5.2 and Figure 5.12.



(a) circular cups in the tray during test



(b) circular cups filled with water after test



(c) square cups in the tray during test



(d) square cups filled with water after test

Figure 5.11 Uniformity test (a) circular measuring cups covering tested area, (b) determination of the water volume in circular cups, (c) square measuring cups covering tested area (b) determination of the water volume in square cups.

Table 5.2 Spatial variability of rainfall (coefficient of uniformity) for various flow rates and durations.

Flow Rate (l/min)	Coefficient of Uniformity Circular Cups Duration - 5 min (%)	Coefficient of Uniformity Circular Cups Duration - 10 min (%)	Coefficient of Uniformity Square Boxes Duration - 10 min (%)
0.122	88.24	84.07	x
0.243	84.92	83.90	x
0.487	84.87	87.58	89.54
0.681	86.98	86.92	88.73
<b>Average</b>	85.93	87.25	89.14
<b>Standard deviation</b>	1.65	1.91	0.58

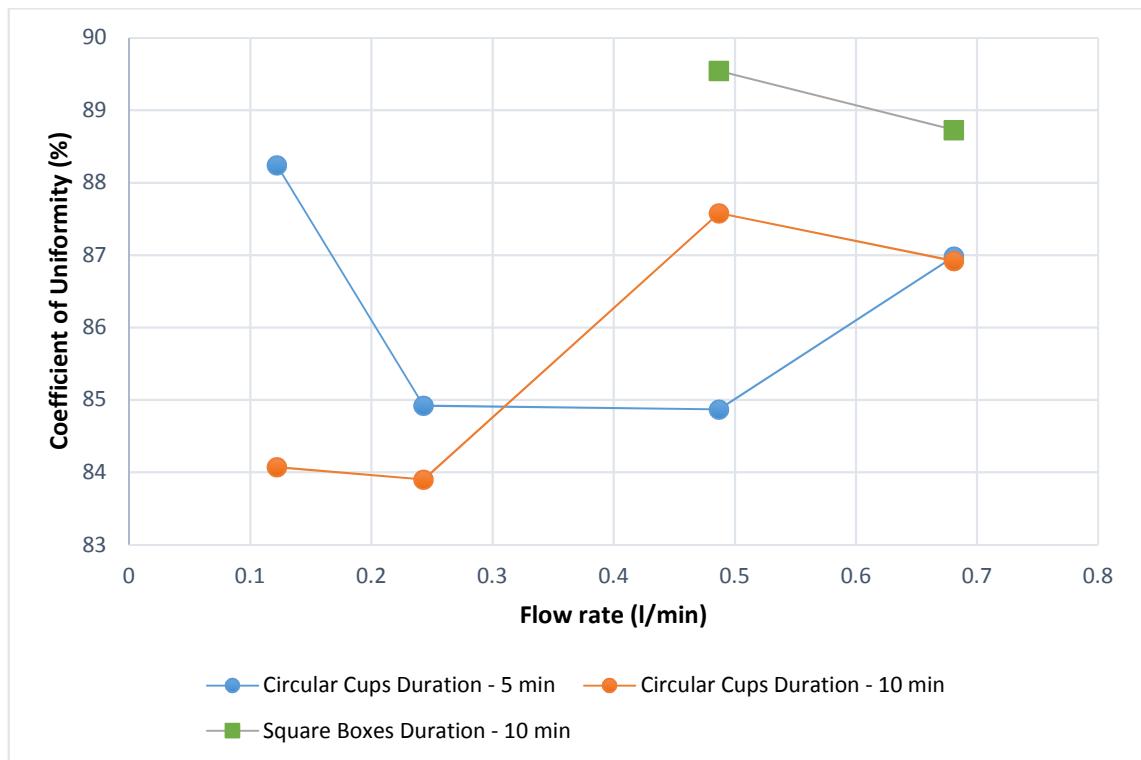


Figure 5.12 Comparison of the coefficient of uniformity obtained for different flow rates and durations based on Table 5.2.

The coefficients of uniformity for all flow rates and durations ranged between 83.90% and 89.54% and were greater than the required threshold of 80%. These results confirmed that the rainfall produced by the rainfall simulator system was uniform at all ranges of the flow rates (rainfall intensities). It also confirms that the change of the flow rate had limited effect on the uniformity of the rain. The standard deviations were very small ( $\sigma=1.65\%$ ,  $\sigma=1.91\%$  and  $\sigma=0.58\%$  for the circular cups - 5min, circular cups - 10min, square boxes - 10min, respectively) suggesting low variations in the coefficient of uniformity. The greatest value of the coefficient of uniformity was achieved during the test with square boxes,  $C_u=89.54\%$ . This could be due to the fact that the entire tested area was covered with squared measuring containers preventing water losses. Nearly total amount of water was captured increasing the accuracy of the results.

The determination of the coefficient of uniformity was based on the uniformity of the set of data (rainfall volumes) (formula (5.1)). However, it did not reflect spatial distribution of the rain across tested area. In order to investigate spatial distribution of the rain, coloured maps were produced (Figure 5.13). The maps

demonstrate differences in volumes collected by each measuring container, showing the areas exposed to different amounts of rain.

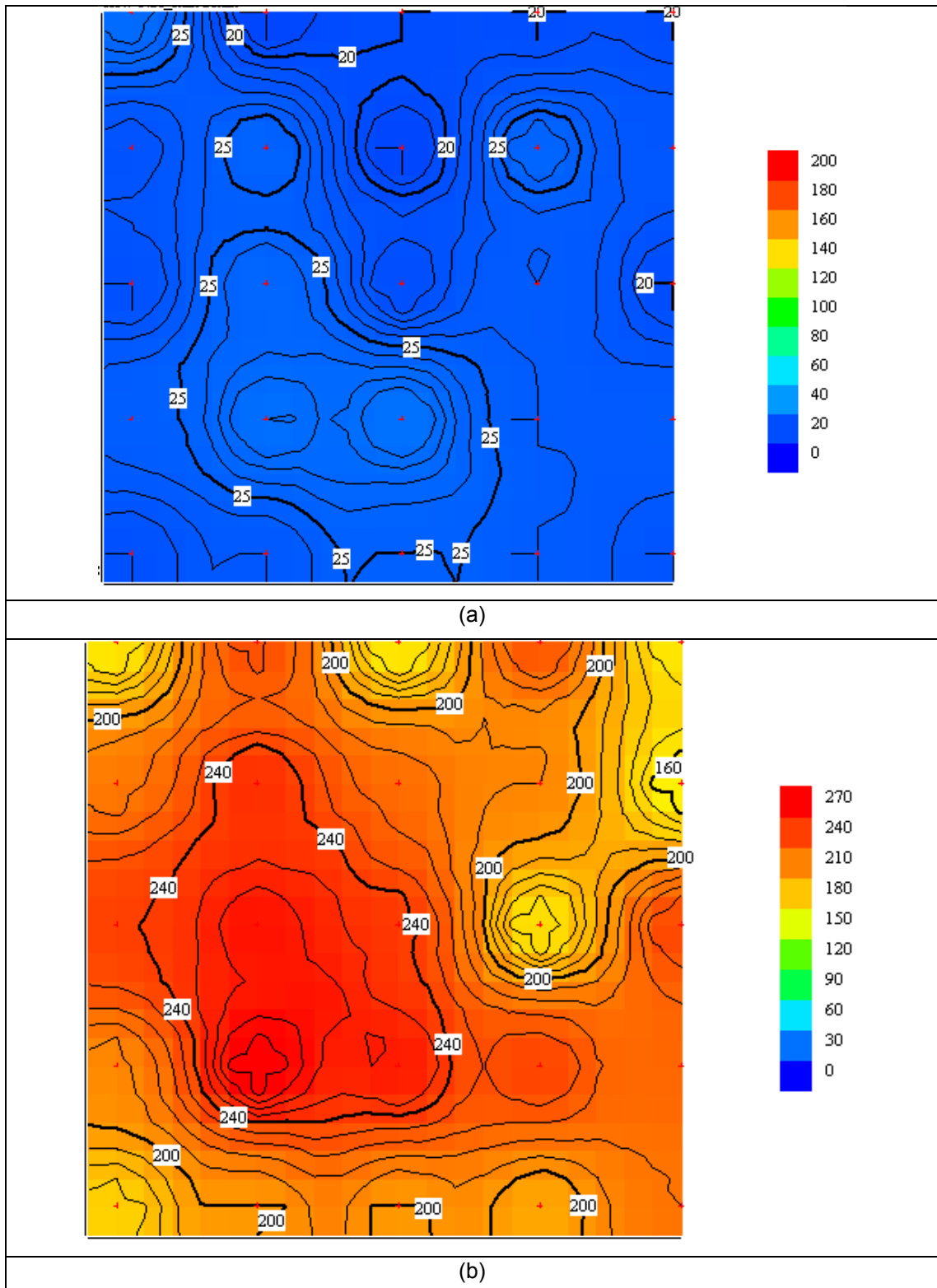


Figure 5.13 Maps showing simulated rainfall distribution for the tests of the following characteristics: (a) low flow rate of 0.05l/min and short duration of 5min, (b) high flow rate of 0.28l/min and long duration of 10min.

The spatial distribution of rainfall (Figure 5.13) shows higher concentration of rainfall in the centre of the tested area and lesser at the edges. However, as indicated by high coefficient of uniformity these differences were not significant. A similar pattern was observed across all ranges of the flow rate and duration Appendix E. These variations should not have a significant effect on quality of the tests performed using the custom designed rainfall simulator system. The use of the rainfall simulator system could, therefore, be considered as an accurate method in reproducing a spatially uniform rainfall over the tested area.

## **5.5 CONCLUSIONS**

A laboratory rainfall simulator system was designed and constructed to deliver a broad range of simulated rain to small scale green roof trays. The performance tests demonstrated that listed objectives for a laboratory rainfall simulator system were satisfactorily complied. The custom designed rainfall simulator system has proved to be both efficient and accurate for use in laboratory conditions.

## **CHAPTER 6**

### **HYDROLOGICAL PERFORMANCE OF SMALL SCALE EXTENSIVE GREEN ROOFS: LABORATORY EXPERIMENT**

This chapter addresses the research objective of assessing the hydrological performance of extensive green roofs constructed using alternative materials subjected to extreme rainfall events by analysing hydrological performance data from the small scale green roof laboratory experiment.

The in-situ green roof experiments provide understanding of green roof hydrologic responses to frequent rainfall events. However, they do not explain the hydrological behaviour of the green roofs subjected to extreme rainfall events, due to their random nature and infrequency (Chapter 2). Extreme rainfall events are rare, but due to the climate changes, they are predicted to occur more often (Butler and Davies, 2010, Murphy et al., 2009). Such rainfall events, independent of time and randomness of nature, could be simulated during comprehensive laboratory experiments. However, such experiments, with large data sets of observations of green roof responses to extreme rainfall events, are not at all documented (Chapter 2). Hence, this part of study aims to fill in this knowledge gap by developing and conducting comprehensive laboratory tests.

This chapter presents the description and results of the laboratory experiment investigating the performance of extensive green roofs under UK (London) extreme climatic conditions. The experiment was carried out using a custom designed rainfall simulator system (described in detail in Chapter 5). Investigated green roofs included conventional extensive green roofs and green roofs constructed using alternative materials as described in Chapter 3. Overall hydrological performance (stormwater runoff, retention, and peak flow reduction)

is presented, as well as hydrologic responses in relation to rainfall magnitude and vegetation presence. Multiple linear regression analysis was used to investigate the influence of rainfall characteristics, laboratory microclimate conditions, and material properties on the green roof hydrological performance.

## **6.1 METHODOLOGY**

The objective of the laboratory monitoring of extensive green roofs was to provide experimental data on their hydrological performance in order to understand the response of the green roofs to extreme rainfall events specific to UK (London) climate. The primary data were obtained from the series of laboratory well-controlled tests including material properties testing (described in detail in Chapter 3), 12-week programme of testing green roof trays without vegetation and 12-week programme of testing green roof trays with vegetation.

### **6.1.1 DESCRIPTION OF LABORATORY GREEN ROOF EXPERIMENT**

The experimental setup was located in the civil engineering laboratory at the University of East London (Figure 6.1). It comprised of five green roof designs replicated three times, resulting in fifteen small scale green roof trays (section 6.1.1.1). The green roofs were subjected to rainfall events generated by a rainfall simulator system (Chapter 5). Stormwater runoff was collected into containers resting on data-logging bench scales (section 6.1.1.3). The scales were connected to a computer, allowing the continuous measurement and logging of the mass of discharged water.



(a) Green roof trays between test periods



(b) Green roof trays during simulated rainfall test

*Figure 6.1 Laboratory experiment setup overview: (a) small scale green roof trays (b) rainfall simulator system with green roof trays.*

#### **6.1.1.1 SMALL SCALE GREEN ROOF DESIGN AND CONSTRUCTION**

All materials used to construct green roof trays and their properties are described in detail in Chapter 3. These materials were divided into two distinctive groups: substrate Table 3.7 and drainage layer Table 3.9. Each group contained one material, which was considered as a control material (conventional material commonly used to construct green roofs in the UK) and two alternative materials (novel, not commonly used in green roof construction) to ensure diversity of material properties (Table 6.1).

Table 6.1 Summary of the green roof construction materials selection.

Green roof layer	Control / Treatment	Final selection
<b>Substrate</b>	Control	Crushed Red Brick
	Treatment	Lyttag
		Sewage Sledge Pellets
<b>Drainage layer</b>	Control	Roofdrain40
	Treatment	Granulated Rubber
		Wool-rich Carpet Shred

Five green roof designs tested in the laboratory experiment included one control and four treatment designs. The control green roof was designed using conventional materials i.e. Crushed Red Brick as a substrate and Roofdrain40, “egg-box” polymer mat as drainage layer, materials most common in the UK market. This design was based on the designs and preliminary results of the analysis of Barking Riverside experimental data (Chapter 4). Preliminary analysis indicated that greater depth of drainage layer and substrate enhance the hydrological performance of green roofs. Hence, the 40mm drainage layer and 100mm substrate was selected. In the case of vegetation, the selection was made based on the benefits of green roofs planted with wildflowers, such as the enhancement of biodiversity and biomimicry. Thus, in order to maximise the potential of green roofs as a stormwater mitigation tool and to support biodiversity, the green roof W/40/100 (wildflower, 40mm drainage layer, 100mm substrate) was selected as the control green roof design for the laboratory experiment.

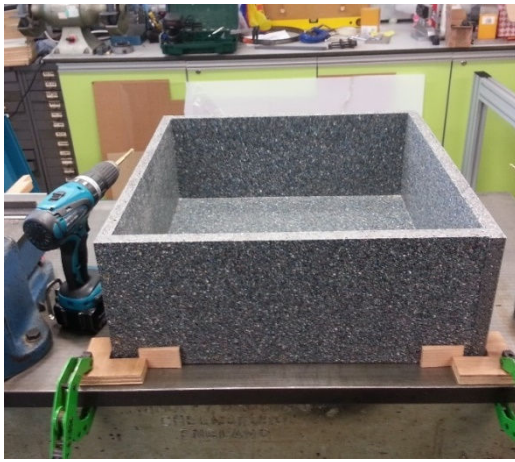
The treatment green roofs were designed to allow meaningful comparison with control green roof. This was achieved by maintaining the same depths of the layers: 100mm substrate and 40mm drainage layer, and the same vegetation type: wildflowers. The materials were changed one layer at a time within each comparative treatment e.g. Crushed Red Brick substrate was replaced by Sewage Sludge Pellets but the conventional Roofdrain40 drainage layer remained unaltered. The summary of green roof designs is presented in Table 6.2. Each green roof design was replicated three times.

Table 6.2 Summary of green roof designs tested in laboratory experiment.

Green Roof Design	Control / Treatment Design	Vegetation	Substrate (100mm)	Drainage Layer (40mm)
A	Control	Wildflower	Crushed Red Brick	Roofdrain40
B	Treatment	Wildflower	Sewage Sludge Pellets	Roofdrain40
C	Treatment	Wildflower	Lytag	Roofdrain40
D	Treatment	Wildflower	Crushed Red Brick	Granulated Rubber
E	Treatment	Wildflower	Crushed Red Brick	Wool-rich Carpet Shred

Each green roof experimental design was placed in one of fifteen custom-made trays (0.5 x 0.5 x 0.2 m internally). The trays were made of Ecosheet, 100% recycled plastic boards (Ecosheet, 2016) (Figure 6.2). The inner edges of the trays were sealed with non-toxic, water resistant sealant. However, after initial tests, some of the trays were leaking water. It was assumed that the weight of the green roof materials in the tray introduced tension into the sealant, thus making the seal ineffective. However, a close inspection of the trays revealed the existence of micro-pores on the surface of the walls, through which the water was leaking. The problem was resolved by lining each tray with waterproof pond liner, before being filled in with green roof construction materials (Figure 6.2).

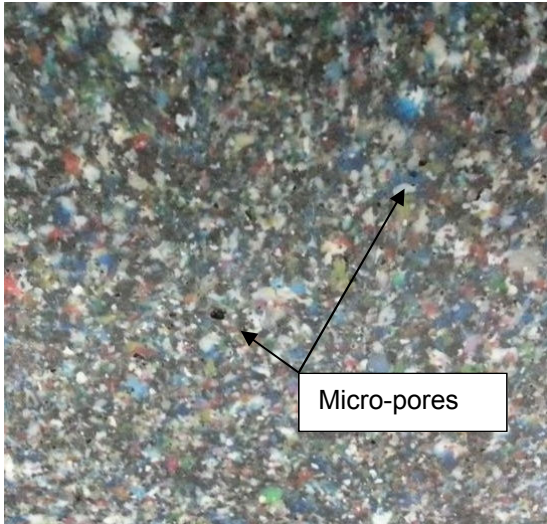
After trays were lined with pond liner, the first layer of geotextile was placed in, followed by 40mm-thick drainage layer. For green roof designs A, B, and C this was Roofdrain40, and for green roof designs D and E, this was Granulated Rubber and Wool-rich Carpet Shred respectively. The drainage layer was covered with a second layer of geotextile and subsequently overlaid with 100mm of substrate. For green roof designs A, D, and E this was Crushed Red Brick, and for green roof designs B and C, this was Sewage Sludge Pellets and Lytag. The green roof tray preparation steps (before pond liner was introduced) for the green roof design A are presented in Figure 6.3.



(a)



(b)



(c)

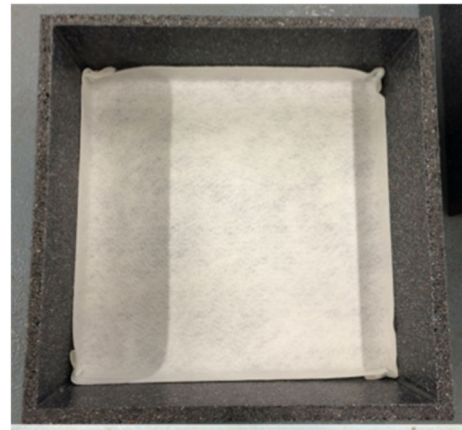


(d)

Figure 6.2 Green roof trays: (a) assembly of green roof tray (b) ready green roof trays (c) micro-pores on the wall surface of tray (d) tray lain with pond liner.



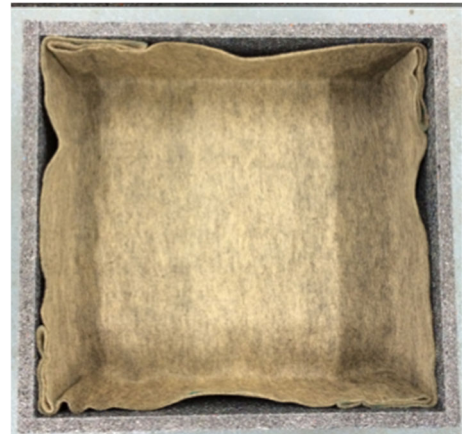
(a)



(b)



(c)



(d)



(e)



(f)

*Figure 6.3 Green roof trays preparation: (a) empty tray (b) first layer of geotextile (c) drainage layer (d) second layer of geotextile (e) substrate layer compaction (f) ready green roof tray. Note: these photos were taken for green roof design A and before trays were lain with pond liner. The same procedure applied to all green roof designs after the pond liner was introduced.*

To ensure as little variations as possible between green roofs of the same design, each tray was filled with the same amount of the material and was compacted

using the same method. Initially, the direct measurement of the depth of material was used. However, this method proved to be unreliable due to the uneven surface beneath the substrate material, which prevented accurate measurement. It was observed that the weight of the substrate material was stretching the geotextile making the depth greater in drainage layer voids and smaller on the notches. Hence, a constant mass of the materials was used for green roof trays construction. Firstly, an empty tray was filled with selected material of known weight to the desired depth (measured in four different places of the tray). The same mass of the material was then used to fill all of the trays for each design. The measured mass of the granular and fibre-like materials is presented in Table 6.3.

*Table 6.3 Mass of the 100mm depth of the substrate material and 40mm depth of drainage layer material (compacted). This technique applies to granular and fibre-like materials, hence the Roofdrain40 is not included.*

<b>Material</b>	<b>Crushed Red Brick</b>	<b>Lytag</b>	<b>Sludge Pellets</b>	<b>Granulated Rubber</b>	<b>Wool-rich Carpet Shred</b>
<b>Mass (kg)</b>	27	22.5	24	5.5	1.25

A compaction procedure for green roof substrates has not been discussed by any researchers in detail. The FLL (2008) states that the material depth should be achieved by compaction but gives no specific compaction procedure. Soils for plant growth should not be over or under-compacted (DeJong-Hughes et al., 2016). For the purpose of this laboratory experiment a moderate compaction was achieved by tamping each substrate layer 20 times with a square-ended tamper. A similar technique is used for the shear box test for dry sands (British Standards Institution, 1990c).

The selection of the wildflower species was made considering the technique for establishing vegetation and to match species planted onto Barking Riverside green roofs. These included: birdsfoot trefoil (*Lotus corniculatus*), small scabious (*Scabiosa columbaria*), wild thyme (*Thymus polytrichus*), wild basil (*Clinopodium vulgare*), common toadflax (*Linaria vulgaris*), autumn hawkbit (*Scorzoneroides autumnalis*), kidney vetch (*Anthyllis vulneraria*), bluebell (*Hyacinthoides non-scripta*), wild daffodil (*Narcissus pseudonarcissus*), wild tulip (*Tulipa sylvestris*),

crocus (*Crocus tommasinianus*), agrimony (*Agrimonia eupatoria*), common knapweed (*Centaurea nigra*), viper's bugloss (*Echium vulgare*), lady's bedstraw (*Galium verum*), perforate St John's wort (*Hypericum perforatum*), field scabious (*Knautia arvensis*), rough hawkbit (*Leontodon hispidus*), oxeye daisy (*Leucanthemum vulgare*), musk mallow (*Malva moschata*), wild marjoram (*Origanum vulgare*), hoary plantain (*Plantago media*), cowslip (*Primula veris*), selfheal (*Prunella vulgaris*), meadow buttercup (*Ranunculus acris*), bulbous buttercup (*Ranunculus bulbosus*), wild mignonette (*Reseda lutea*), salad burnet (*Sanguisorba minor*), bladder campion (*Silene vulgaris*). These species are typical on the Barking Riverside brownfield site (University of East London, 2010).

Techniques for establishing vegetation onto green roofs include seed-sowing, plug-planting, or bulb-planting. Initially, the sowing technique was selected due to the wide range of species in the wildflower mixtures. The selected Wildflower Mixture for green roofs (Emorsgate Seeds, 2016) comprised twenty-two different wildflower species, including many of the species planted onto Barking Riverside green roofs. However, germination under laboratory conditions failed. It is likely that this was due to insufficient light in the laboratory to support healthy growth of the plants (Figure 6.4 (a)). Additionally, the seedlings suffered from damping-off, a common problem with indoor growth as a result of limited air circulation (Planet Natural, 2016) (Figure 6.4 (b)). Moreover, the growth of the plants was very slow. Hence, it was decided that seed-sowing was an unsuitable technique for green roof vegetation establishment under laboratory conditions.

Following the failure of the seed-sowing technique, the plug-planting method was implemented. In order to promote healthy plant growth, energy efficient LED grow lights were installed in the laboratory (Figure 6.5). The LED lights comprised of selected wavelengths (red, far-red and blue light spectra), which is proven to be effective in supporting plant growth (Johkan et al., 2010).



plants were leaning toward a natural light

plants are very light coloured



thin and tough stem of seedlings

stem lesioned at ground level

rotten roots

*Figure 6.4 The growth of the wildflowers from seeds (a) signs of light deprivation (b) seedlings suffering from damping-off.*

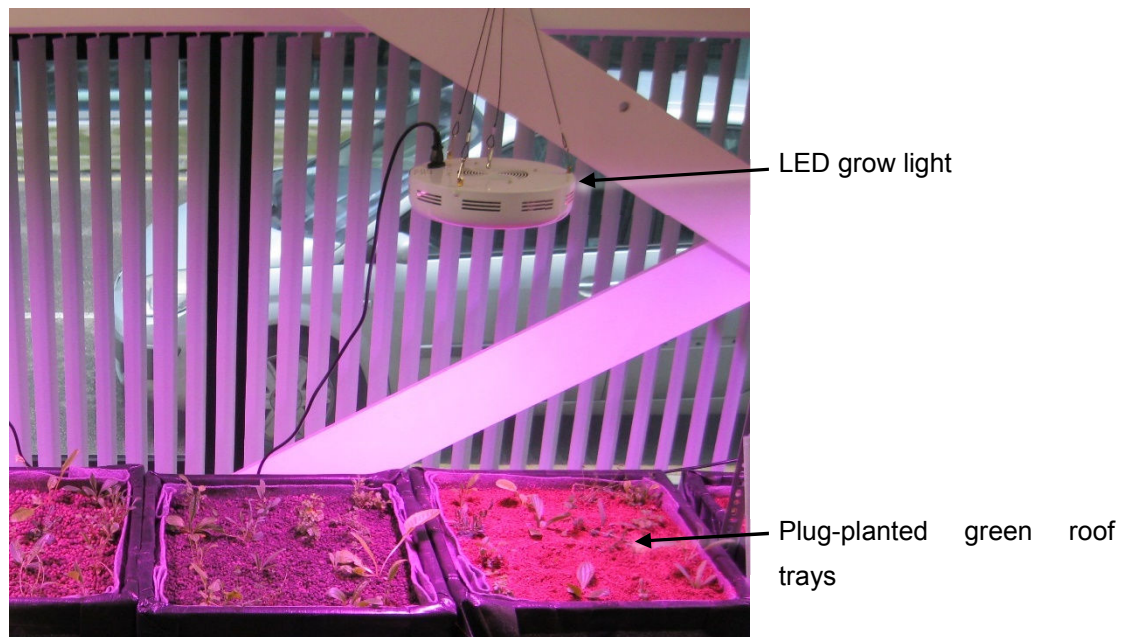


Figure 6.5 The green roof plots under LED grow lights in the laboratory setup.

The choice of the plug-planting technique raised the question of the number of plants per tray. FLL guidelines (2008) recommend 16 plants/m<sup>2</sup>, however this aims at long-term cover and avoidance of competition. Application of this rule would result in 4 plants per tray and would lead to poor short-term vegetation cover. Graceson et al. (2013) planted sedum species approximately 100mm apart in 10 x 10 grid in 1m x 1m plots, resulting in a density of 100 plants/m<sup>2</sup>. Nagase and Dunnett (2012) planted 12 plants in four rows (75 mm interval) and three lines (55 mm interval), resulting in a density of 150 plants/m<sup>2</sup>. Hence, for the purpose of this research, plants were planted approximately 80mm apart in a 4 x 4 grid, resulting in a plant density of 64 plants/m<sup>2</sup>. This equated to 16 plants per tray (Figure 6.6). Each green roof was planted randomly with two plug plants of each of the following species:

- *Anthyllis vulneraria* – KIDNEY VETCH
- *Centaurea nigra* – COMMON KNAPWEED
- *Echium vulgare* – VIPER'S BUGLOSS
- *Leucanthemum vulgare* – OXEYE DAISY
- *Lotus corniculatus* – BIRDSFOOT TREFOIL
- *Malva moschata* – MUSK MALLOW
- *Plantago media* – HOARY PLANTAIN
- *Primula veris* – COWSLIP

The chosen plug plants were grown specifically for green roofing in peat free engineered soil (Boningale Greensky, 2016).



(a)



(b)



(c)



(d)

*Figure 6.6 Green roof trays plug-planting: (a) wildflower plugs in plug tray (b) green roof trays plug-planted in four by four matrix (c) Common Knapweed in bloom (d) Oxeye Daisy in bloom.*

#### **6.1.1.2 RAINFALL EVENTS DESIGN AND SIMULATION**

The selection of the rainfall events magnitude was based on current drain and sewer system design recommendations and climate change predictions. *Sewers for Adoption* guide (Water UK, 2006) recommends the sewers to be design to run full in a 1:30 year storm event. BS EN 752:2008 *Drain and sewer systems outside buildings* suggests two methods for storm sewers design, both related to location of the building. The first is based on storm return period and the second is based on flooding return period (Table 6.4) (British Standards Institution, 2013). BS EN

752:2008 also provides recommendations for the drain and sewer systems design based on the building risk category (British Standards Institution, 2013). Buildings in the risk category 1 should be designed to the design storms of return period of 1 to 2 year, buildings in the risk category 2 should be designed to the design storms of 5 year return period. The return period of the design storms for buildings in the risk category 3 should be 4.5 times higher than period for which building need to be protected. For example, if the building need to be protected from rainwater for 20 years, the return period of the design storm would be 90 years.

*Table 6.4 Two types of the frequencies recommended by BS EN 752: 2008 for storm sewers design, both related to the location of the building (British Standards Institution, 2013)*

<b>Location</b>	<b>Return period for design storm (1 in “n” years)</b>	<b>Return period for design flooding (1 in “n” years)</b>
<b>Rural areas</b>	1	10
<b>Residential areas</b>	2	20
<b>City centres / industrial / commercial areas</b>	5	30
<b>Underground railways / underpasses</b>	10	50

Increased urbanisation and climate change may significantly affect the storm sewers performance in the future (Butler and Davies, 2010, Shaw, 2011). The winter rainfalls are predicted to become 10% to 30% heavier over the majority area of the UK and summer rainfalls become more intense and frequent by the 2080s (Butler and Davies, 2010, Murphy et al., 2009). The example of how the climate change may affect the rainfall characteristics is presented in Table 6.5.

Table 6.5 shows that the predicted increase in rainfall intensity (or depth) of 30% for the rainfall of 1:30 year return period (recommended for sewers design) would exceed the current intensity (depth) of a 1:100 year rainfall event. Similarly, future rainfall event of return period T=10 years would become heavier than a 1:30 year rainfall event is currently. Hence, storm sewers designed to cope with current rainfall intensities may fail to respond to future extreme rainfall events causing flooding.

*Table 6.5 The example of the predicted climate change effect on rainfall characteristics – the most unfavourable prediction of 30% increase in depth and intensity of winter rainfalls. The intensity and depth of the rainfall events were determined using Wallingford Procedure (DoE/NWC, 1981) and are specific to London.*

Rainfall Characteristics Duration 15 min	Return Period (1 in “n” years)			
	1 in 10	1 in 30	1 in 50	1 in 100
Intensity (mm/h)	65	83	89	103
Intensity + 30% (mm/h)	84.5	107.9	115.7	133.9
Depth (mm)	16.25	20.75	22.25	25.75
Depth + 30% (mm)	21.13	26.98	28.93	33.48

Based on the current drain and sewer systems design recommendations and predictions of the impacts of climate change on rainfall event characteristics (Table 6.5) the following frequency of rainfall events were selected to be simulated in the laboratory experiment: 1:30, 1:50 and 1:100 year.

The recommended duration of the design storm should be equal to the concentration time, i.e. the time required for surface runoff to flow from the most remote point in a catchment to the catchment outlet (Butler and Davies, 2010). However, such time of concentration has not been yet defined for the green roofs and it is likely that it would vary with different green roof designs. Therefore, for the purpose of this research, a duration of 15 min of design rainfall event was adopted based on FLL (2008) recommendation for the duration of the test to determine the coefficient of discharge. A summary of the extreme rainfall event characteristics implemented in laboratory experiments is presented in Table 6.6.

All extreme rainfall events were generated using the custom-made rainfall simulator system in the laboratory conditions. The design, construction and performance of the rainfall simulator system are described in detail in Chapter 5.

*Table 6.6 Summary of the extreme rainfall event characteristics selected for the laboratory testing. The intensity and depth of the rainfall events were determined using Wallingford Procedure (DoE/NWC, 1981) and are specific to London. The flow rate was calculated for the area of the green roof trays.*

Rainfall Characteristics Duration 15 min	Return Period (1 in “n” years)		
	Rainfall event 1 1 in 30	Rainfall event 2 1 in 50	Rainfall event 3 1 in 100
Intensity (mm/h)	83	89	103
Depth (mm)	20.75	22.25	25.75
Flow Rate (l/min)	0.346	0.371	0.429

### **6.1.1.3 RUNOFF MONITORING**

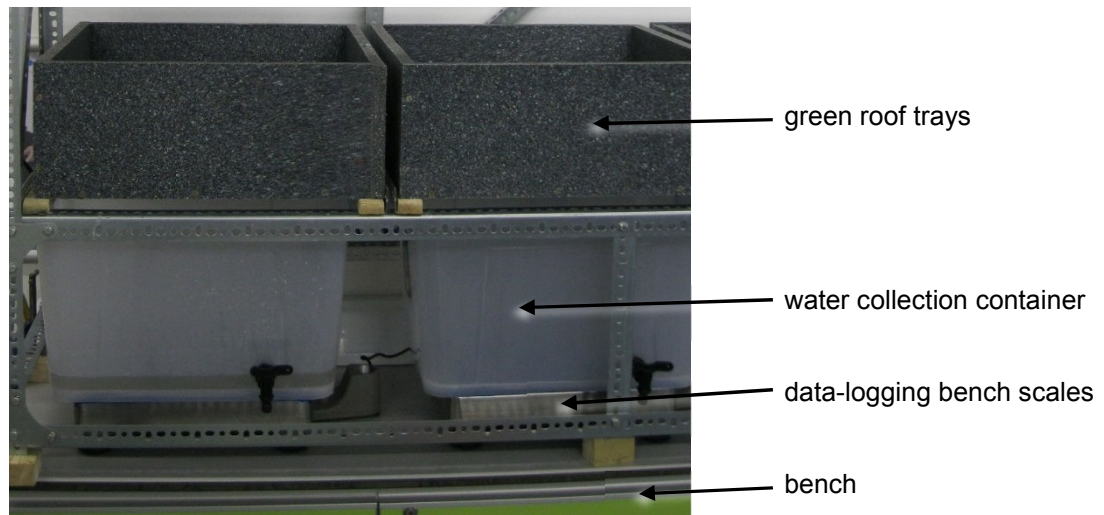
The selection of the appropriate runoff monitoring methods and equipment is crucial for obtaining accurate outcome of the research (Chapter 2). The main objectives for the selection of the runoff monitoring system for laboratory experiment were as follows:

1. To obtain reliable, replicable, and accurate data
2. To ensure time efficient experiments
3. To be easily accommodated in laboratory space

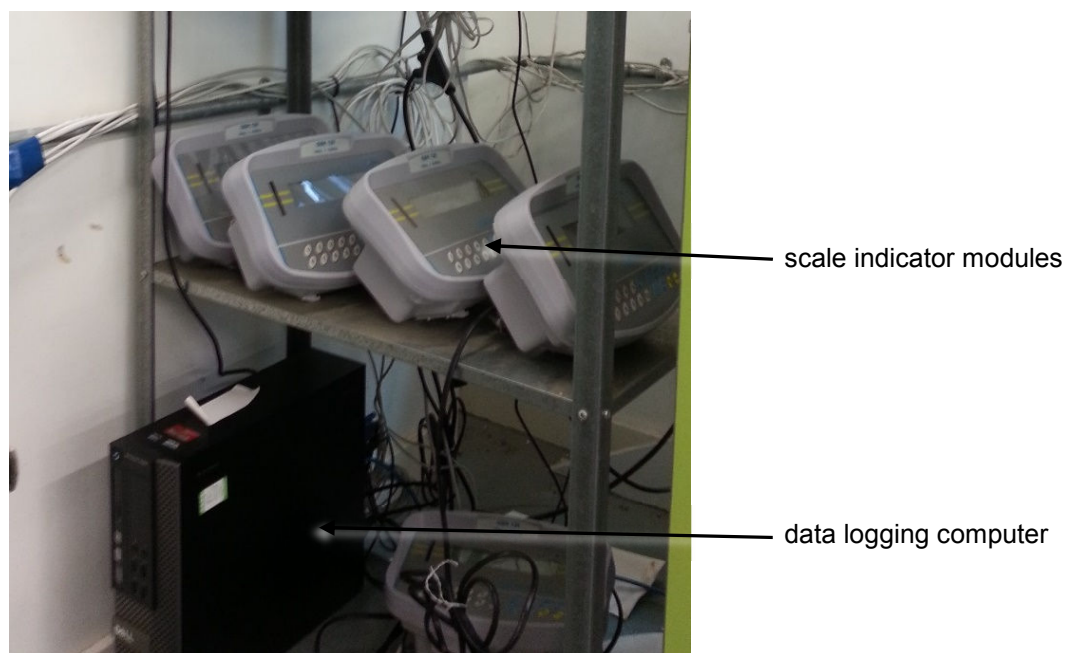
After critical review of the in-situ and laboratory techniques for green roof runoff monitoring (Chapter 2), the weighing method was selected. This technique, although not employed in laboratory conditions in any of the reviewed papers, fulfils all objectives set for the selection of the runoff monitoring for a laboratory experiment. The use of high-resolution scales provides reliable, replicable, and accurate data. The scales fit in the limited laboratory space and can provide an automatic, continuous data-logging, which limits the time and labour requirement.

The scales selected for this experiment were Adam GBK Weighing Scale, GBK 120 Model, with a maximum capacity of 120kg, readability of 5g (equivalent to 5ml of water) and standard deviation 10g (equivalent to 10ml of water). The bench scales were placed under each green roof tray with the collection container placed on top for rainwater runoff collection (Figure 6.7). Each collection container was fitted with a valve to comfortably discharge the collected water.

The scales were connected to a computer for continuous data-logging. The time and mass data was logged into a 'csv' file every 30 seconds. The changes in the mass of rainwater collected over time allowed the calculation of runoff rates.



(a)



(b)

*Figure 6.7 Runoff monitoring equipment: (a) the data-logging bench scales with water collection containers atop (b) the computer to which all scales were connected to for continuous data-logging.*

#### **6.1.1.4 GREEN ROOF TESTING PROGRAMMES**

The laboratory experiment included two 12-week programmes of testing green roofs under simulated extreme rainfall events. The first programme concentrated on testing green roof trays without vegetation to create a comparative quantitative performance for the analysis of the influence of the vegetation on green roof

hydrologic responses to extreme rainfall events. The programme schedule for the green roof trays with no vegetation is presented in Table 6.7. Due to the unexpected green roof tray leakages (section 6.1.1.1), certain weeks of tests were repeated.

After completing tests on the green roof trays with no vegetation cover, the second programme testing green roof trays with plants was initiated. This included the vegetation establishment time and the rainfall simulation tests. The green roof trays were plug-planted so that the age of the plants at the beginning of the tests was the same (three weeks) across all green roofs trays (Table 6.8). The programme schedule for the green roof trays with no vegetation is presented in Table 6.8.

The daily test schedule for green roofs, both with and without vegetation, is presented in Table 6.9. The daily tests were arranged to include various inter-event dry periods prior simulated rainfalls, ranging from about 6 hours to about 408 hours (Table 6.9), but also to ensure efficient use of testing time.

*Table 6.7 The schedule for the programme of testing green roofs with no vegetation.*

<b>Week</b>	<b>Series 1 Green roofs: A1, B1, C1, D1, E1</b>	<b>Series 2 Green roofs: A2, B2, C2, D2, E2</b>	<b>Series 3 Green roofs: A3, B3, C3, D3, E3</b>
1	Rainfall event 1		
2	Rainfall event 2		
3	Rainfall event 2 - repeated		
4	Rainfall event 3		
5	Rainfall event 3 - repeated		
6		Rainfall event 1	
7		Rainfall event 1 - repeated	
8		Rainfall event 2	
9		Rainfall event 3	
10			Rainfall event 1
11			Rainfall event 2
12			Rainfall event 3

*Table 6.8 The schedule for the programme of testing green roofs with vegetation. This included the vegetation establishment time and the rainfall simulation tests*

<b>Week</b>	<b>Series 2 Green roofs: A2, B2, C2, D2, E2</b>	<b>Series 3 Green roofs: A3, B3, C3, D3, E3</b>	<b>Series 1 Green roofs: A1, B1, C1, D1, E1</b>
1	Plug-planting	x	x
2	Plant establishment	Plug-planting	x
3	Plant establishment	Plant establishment	Plug-planting
4	Rainfall event 1	Plant establishment	Plant establishment
5	x	Rainfall event 1	Plant establishment
6	x	x	Rainfall event 1
7	Rainfall event 2	x	x
8	x	Rainfall event 2	x
9	x	x	Rainfall event 2
10	Rainfall event 3	x	x
11	x	Rainfall event 3	x
12	x	x	Rainfall event 3

*Table 6.9 Daily green roof laboratory test schedule for both testing programmes. This includes number of tests per day and corresponding inter-event dry period.*

<b>Day of the week</b>	<b>Number of tests</b>	<b>Inter-event dry period, approximate time (hours)</b>	
		<b>Without vegetation</b>	<b>With vegetation</b>
<b>Monday</b>	1	72	408
<b>Tuesday</b>	1	24	24
<b>Wednesday</b>	none	-	-
<b>Thursday</b>	2	1 <sup>st</sup> test: 48 2 <sup>nd</sup> test: 6	1 <sup>st</sup> test: 48 2 <sup>nd</sup> test: 6
<b>Friday</b>	1	18	18
<b>Saturday</b>	none	-	-
<b>Sunday</b>	none	-	-

### **6.1.2 ANALYSIS METHODS**

Data preparation and analysis required to employ several different techniques and software. At the preparation stage Microsoft Office Excel 2013 was employed

for both rainfall and runoff data. The vegetation cover digital image analysis was conducted using Ulead PhotoImpact 12 and GIMP 2 software.

Statistical analysis was carried out using R software. Exploratory data analysis of variables was conducted to assess the distribution and to determine further statistical analysis test types. The normality of the data distribution was tested through graphical analysis but also using Shapiro – Wilk normality test. All data were not normally distributed, therefore the non-parametric tests were employed. Mann-Whitney U test was used to investigate statistically significant differences ( $p < 0.05$ ) between runoff depth, retention, records from green roof plots of the same design (Carpenter et al., 2016, Fassman-Beck et al., 2013). Dunn's Kruskal-Wallis Multiple comparison test with Bonferroni correction was used to determine statistically significant differences ( $p < 0.05$ ) between runoff depth, retention, and peak flow reduction observations from green roof plots of different design (Voyde et al., 2010, Nawaz et al., 2015, Stovin et al., 2015). Regression analysis was performed using R software.

### **6.1.3 DATA PREPARATION**

Prior to the main analysis of the studied green roof hydrological performance, data preparation, including data transformation and cleansing, was carried out. In this study, the following data sets were collected: laboratory microclimate conditions, rainfall characteristics, stormwater runoff from green roofs data and vegetation cover data. The material properties data (Chapter 3) were also included in this study analysis. All of the data sets were prepared prior the hydrological performance analysis to ensure quality of the results.

#### **6.1.3.1 RAINFALL CHARACTERISTICS DATA**

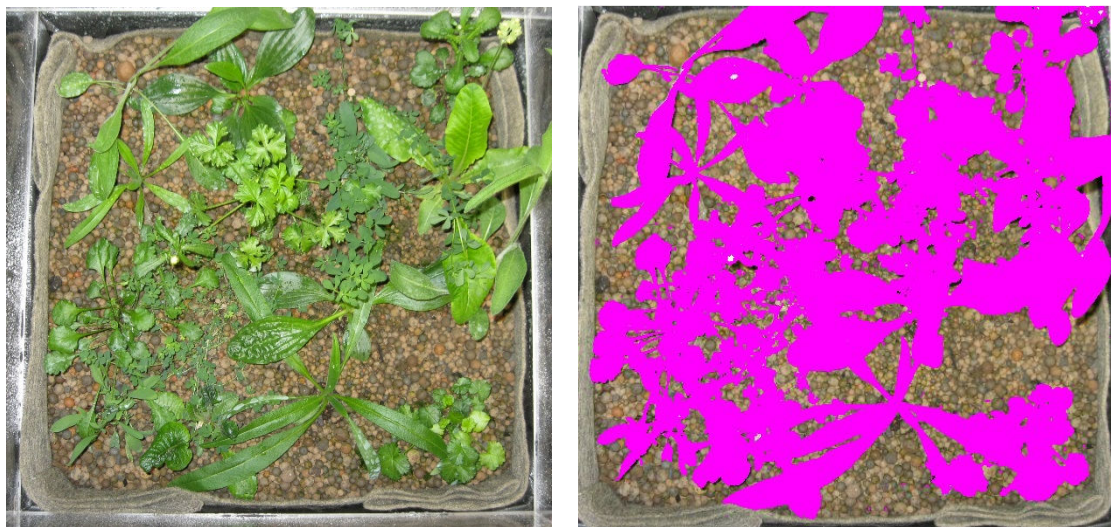
The quality of the rainfall characteristics data was ensured through a high-quality performance of the rainfall simulator. This was ensured by the calibration of the flow meter, calibration of the rainfall simulator and assessment of the spatial variability of rainfall produced through the rainfall simulator (Chapter 5).

#### **6.1.3.2 MATERIAL PROPERTIES DATA**

Material properties data quality was ensured through a series of tests performed according to appropriate British Standards (Chapter 3).

### 6.1.3.3 VEGETATION COVER

Vegetation cover is calculated as the percentage of the ground surface covered by vegetation. The known methods of vegetation cover assessment include point line, grid quadrats or line intercept method amongst other (Bonham, 2013). However, these methods are based on the subjective judgement of the surveyor and apply to large terrain areas. Therefore, these methods are not suitable for the assessment of the vegetation cover of the small green roof trays tested in the laboratory conditions. The vegetation cover assessment was carried out based on the green roof trays digital images analysis (Mickovski et al., 2013). The vegetation cover was determined as the percentage of the green roof tray area (in pixels) covered with vegetation (also counted in pixels). Step one of the digital image analysis was to crop and reduce all images to about 500 x 500 pixels. Secondly, all areas covered with plants were converted to one colour area (Figure 6.8). Colour conversion allows for proper pixel count, reducing errors due to different shades of green and unwanted pixel count.



(a)

(b)

*Figure 6.8 The green roof tray image (a) before colour conversion of the vegetated area (b) after colour conversion of the vegetated area.*

Subsequently, the count of the pixels corresponding to vegetated areas and the count of pixels for the total area of the green roof trays was recorded and the vegetation cover was calculated. Digital photographs of each green roof were taken on a weekly basis. The vegetation cover for days between two consecutive images was interpolated and used in further analysis. The employment of the digital images analysis ensures quality and accurate vegetation cover data.

#### 6.1.3.4 STORMWATER RUNOFF DATA

Runoff data was collected by logging the mass of stormwater accumulated in the collection container and the corresponding date and time. Data was saved in 'csv' file for each green roof and simulated rainfall event (Figure 6.9).

	A	B	C	D	E	F	G	H
1	1	0 g	08/05/2015 09:45					
2	2	0 g	08/05/2015 09:46					
3	3	0 g	08/05/2015 09:46					
4	4	0 g	08/05/2015 09:47					
5	5	0 g	08/05/2015 09:47					
6	6	0 g	08/05/2015 09:48					
7	7	0 g	08/05/2015 09:48					
8	8	0 g	08/05/2015 09:49					
9	9	0 g	08/05/2015 09:49					
10	10	0 g	08/05/2015 09:50					
11	11	0 g	08/05/2015 09:50					
12	12	5 g	08/05/2015 09:51					
13	13	5 g	08/05/2015 09:51					
14	14	5 g	08/05/2015 09:52					
15	15	15 g	08/05/2015 09:52					
16	16	20 g	08/05/2015 09:53					
17	17	40 g	08/05/2015 09:53					
18	18	75 g	08/05/2015 09:54					
19	19	125 g	08/05/2015 09:54					
20	20	210 g	08/05/2015 09:55					
21	21	355 g	08/05/2015 09:55					
22	22	515 g	08/05/2015 09:56					
23	23	725 g	08/05/2015 09:56					
24	24	910 g	08/05/2015 09:57					
25	25	1105 g	08/05/2015 09:57					

Reading number      Mass of water      Date and time (hh:mm:ss)

Figure 6.9 Data-logging scale output data sheet ('csv' file). The first column includes reading number, the second contains cumulative mass of water in the collection container and finally the third column indicates date and time of the reading taken.

Based on the obtained mass of stormwater runoff, the stormwater runoff volumes were calculated using following formula:

$$V = \frac{M}{\rho_w} \quad (6.1)$$

Where  $\rho$  is density of water ( $\text{g}/\text{dm}^3$ ),  $M$  is total mass of water (g),  $V$  is volume of water ( $\text{dm}^3$ ).

However, the density of water depends on the air temperature. Hence, the air temperature was recorded daily and the density of water was adjusted accordingly.

The runoff data had to be cleansed prior to the analysis. The listwise deletion was performed in the following cases:

- When leakage from the trays was observed.
- When there was missing runoff recording due to a power cut.
- The initial tests of green roof with no vegetation, when the substrate material was oven-dried. The soil of 0% water content does not exist in nature.

Where possible, the series of tests were repeated to substitute missing data (Table 6.7).

The events were merged, when the runoff from green roof from the previous rainfall event was still occurring at the start of the subsequent rainfall event (Voyde et al., 2010, Stovin et al., 2012). The final number of observations of the green roofs with no vegetation was 211, of which 52 were generated by merging rainfall events. The final number of observations of the green roofs with vegetation was 180, of which 45 were generated by merging rainfall events. Data preparation resulted in total number of 391 individual observations collected during two 12-week programmes.

## **6.2 OVERVIEW OF DATA**

This section outlines the variables related to simulated rainfall events, laboratory microclimate, green roof design and green roof hydrological performance included in the analyses. The final data set consisted of 391 individual observations, recorded during two 12-week programmes. Each observation corresponded to one green roof tray of specific design subjected to simulated rainfall event and laboratory microclimatic conditions.

This is an exceptional data set of observations of green roofs subjected to extreme rainfall events specific for the UK (London) climate. The analysis of this large data set gives a unique opportunity to generate novel understanding of the hydrological performance of the green roofs, which would not be possible through in-situ experiments.

### **6.2.1 SIMULATED RAINFALL EVENTS CHARACTERISTICS AND LABORATORY MICROCLIMATE CONDITIONS DATA**

The following simulated rainfall characteristics were included in further analysis as variables:

- Rainfall event depth (mm)
- Inter-event time prior to rainfall event (h) (IET)
- Return period of the rainfall (1 in “n” years)

The following laboratory microclimate variables were included in analysis:

- Air temperature (°C)
- Air pressure (mmHg)

The variables associated with simulated rainfall characteristics and laboratory microclimate conditions are called predictor (independent) variables hereinafter.

### **6.2.2 GREEN ROOF DESIGN DATA**

The green roof design data included material properties and vegetation cover records. The following variables related to the material properties were included in the analysis:

- Loose Bulk Density – Dry ( $\text{Mg/m}^3$ )
- Particle Density ( $\text{Mg/m}^3$ )
- Void Ratio (-)
- Porosity (-)
- Maximum Capillary Rise (mm)
- Saturated Density ( $\text{Mg/m}^3$ )
- Water Absorption (%)
- Coefficient of Permeability (m/s)

The following variables reflected the design of the green roof (Table 6.2):

- Green Roof Design (A, B, C, D, or E)

The variables representing the potential influence of vegetation on the green roof hydrological performance included:

- Vegetation Presence (yes or no)
- Vegetation cover (%)

Green roof design variables were included into a group of predictor (independent) variables. In addition to green roof design characteristics the water content of the substrate prior to the test was determined and was also included as predictor variable.

### **6.2.3 GREEN ROOF HYDROLOGICAL PERFORMANCE DATA**

The laboratory green roof hydrological performance data included: runoff depth (mm), retention (%) and peak flow reduction (%) as defined in Chapter 2.

These variables are termed as response (dependent) variables hereinafter.

## **6.3 RESULTS AND DISCUSSION**

This section presents the results and discussion of the vegetation cover analysis and hydrological performance of the small scale extensive green roofs subjected to extreme rainfall events including exploratory data analysis. Preliminary multiple linear regression analysis was used to investigate the influence of rainfall characteristics, laboratory microclimate conditions, and green roof design characteristics on the green roof hydrological performance.

### **6.3.1 VEGETATION COVER ANALYSIS**

Vegetation is considered as one of the variables that affect the green roof hydrological performance (Czemiel Berndtsson, 2010, Lundholm et al., 2010, Nagase and Dunnett, 2012). In this study the effect of the vegetation cover on hydrological performance was also investigated. The vegetation cover was assessed based on digital photographs of plants, prepared for analysis as described in detail in section 6.1.3.3. Figure 6.10 to 6.14 present the vegetation cover recorded over 12 weeks testing programme for each green roof design. The average vegetation cover for all green roof designs is presented in Figure 6.15. The exploratory data analysis was carried out to determine the nature of data distribution. The summary statistics and boxplots for all green roof designs are presented in Table 6.10 and Figure 6.16.

The null hypothesis of no significant difference in vegetation cover between green roofs of the same design using non-parametric test: Mann-Whitney U test. The results of the test for all green roof designs are presented in Table 6.11.

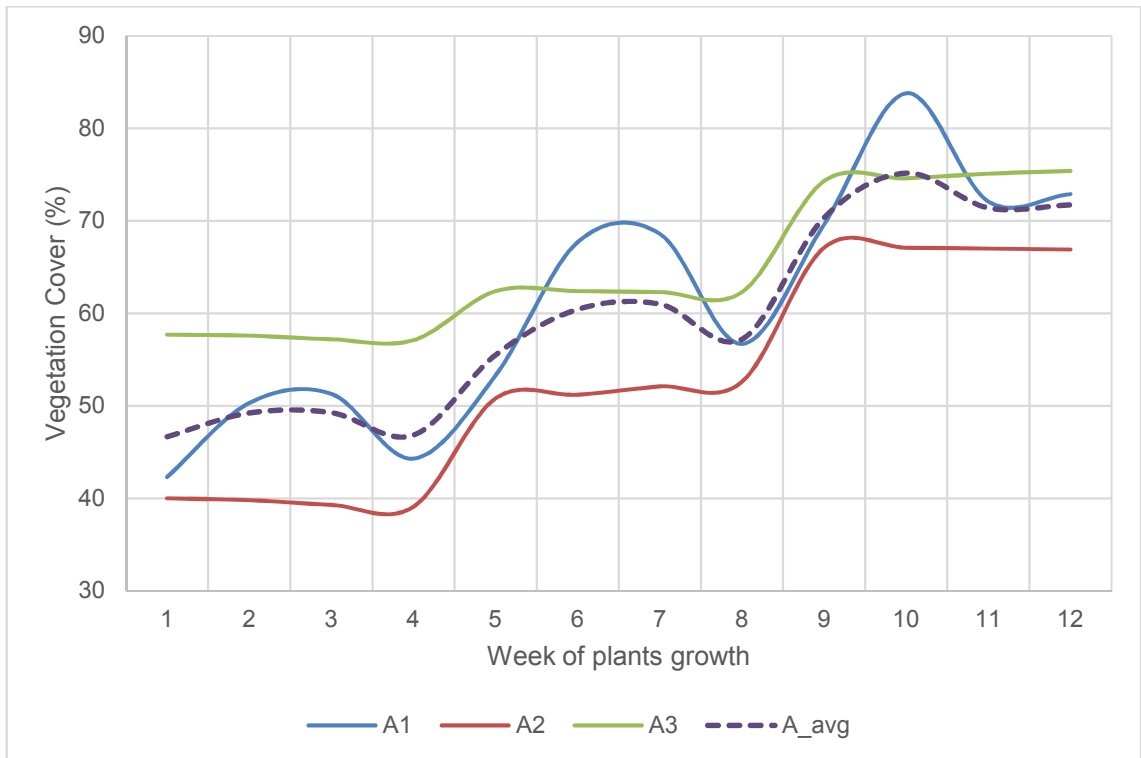


Figure 6.10 Vegetation cover over the 12-week testing programme for green roof design A. The vegetation cover for replicates A1, A2, and A3 is shown by solid lines, the average of replicates is shown by dashed line.

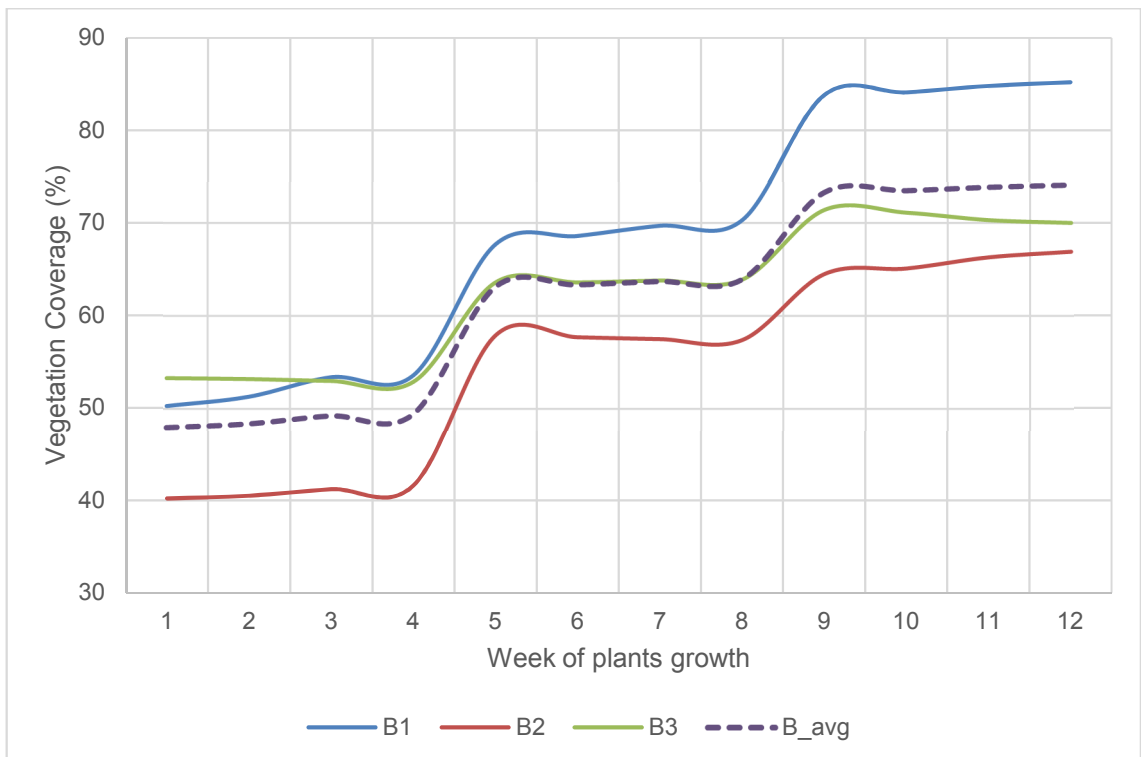


Figure 6.11 Vegetation cover over the 12-week testing programme for green roof design B. The vegetation cover for replicates B1, B2, and B3 is shown by solid lines, the average of replicates is shown by dashed line.

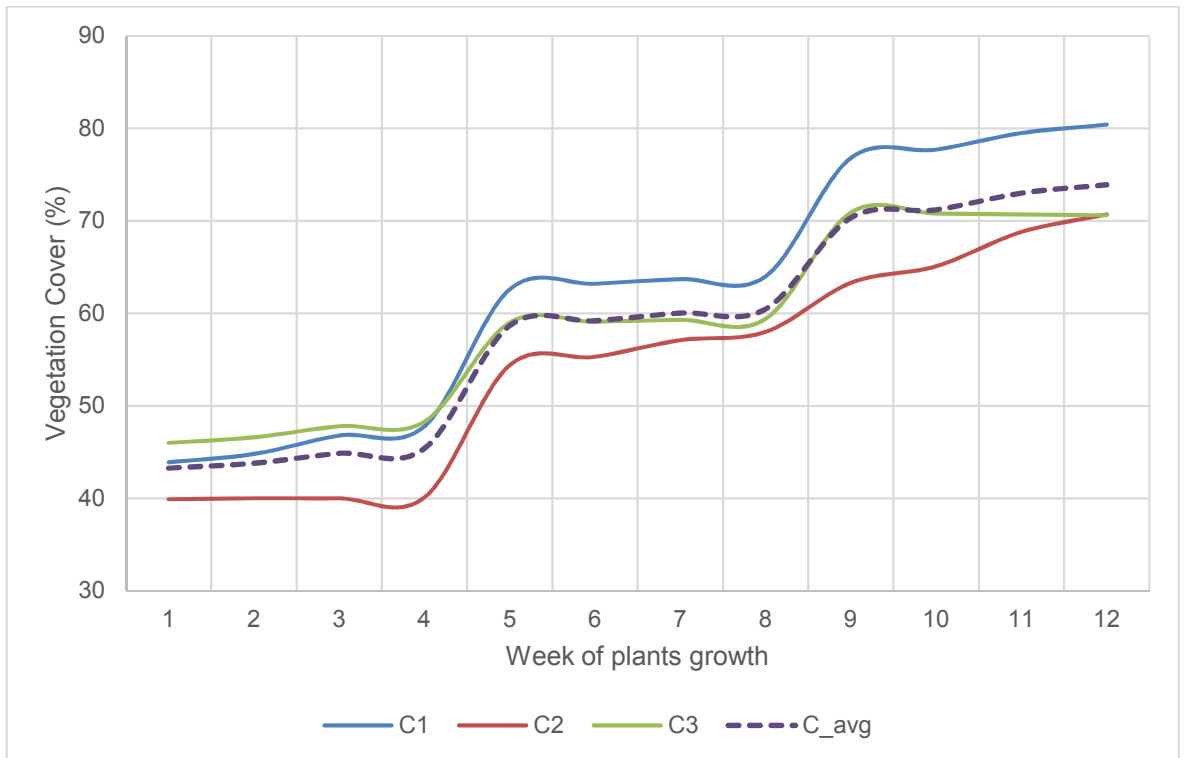


Figure 6.12 Vegetation cover over the 12-week testing programme for green roof design C. The vegetation cover for replicates C1, C2, and C3 is shown by solid lines, the average of replicates is shown by dashed line.

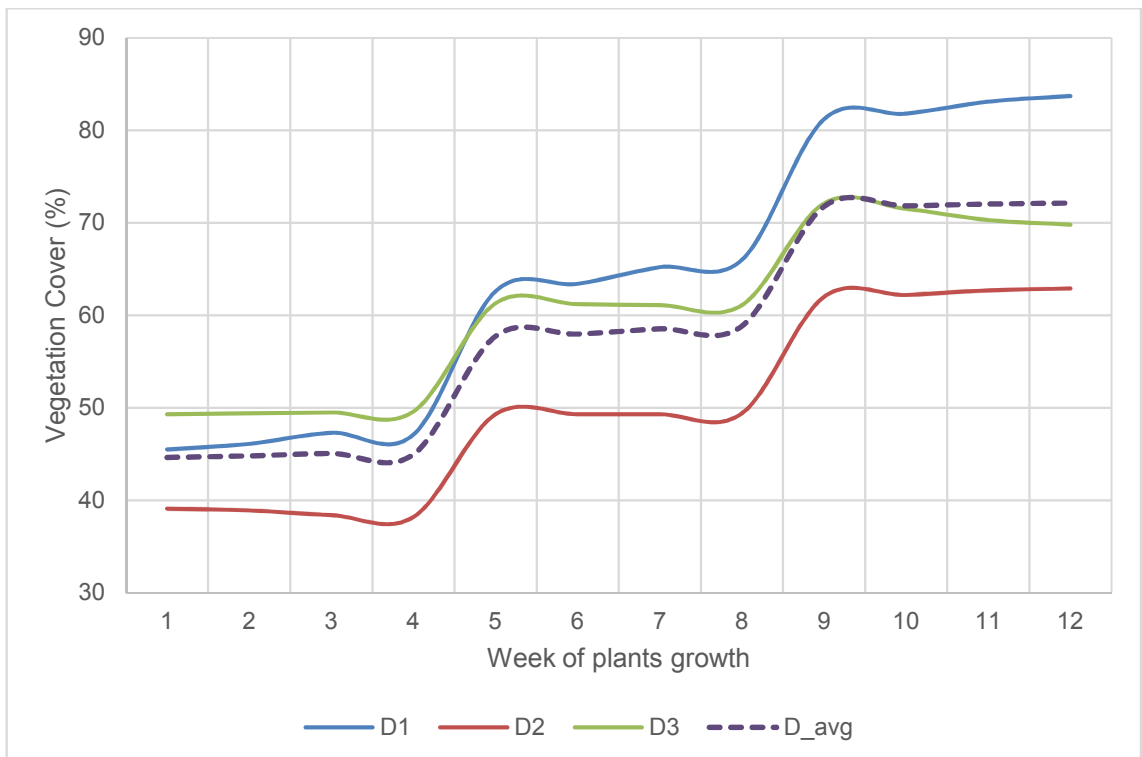


Figure 6.13 Vegetation cover over the 12-week testing programme for green roof design D. The vegetation cover for replicates D1, D2, and D3 is shown by solid lines, the average of replicates is shown by dashed line.

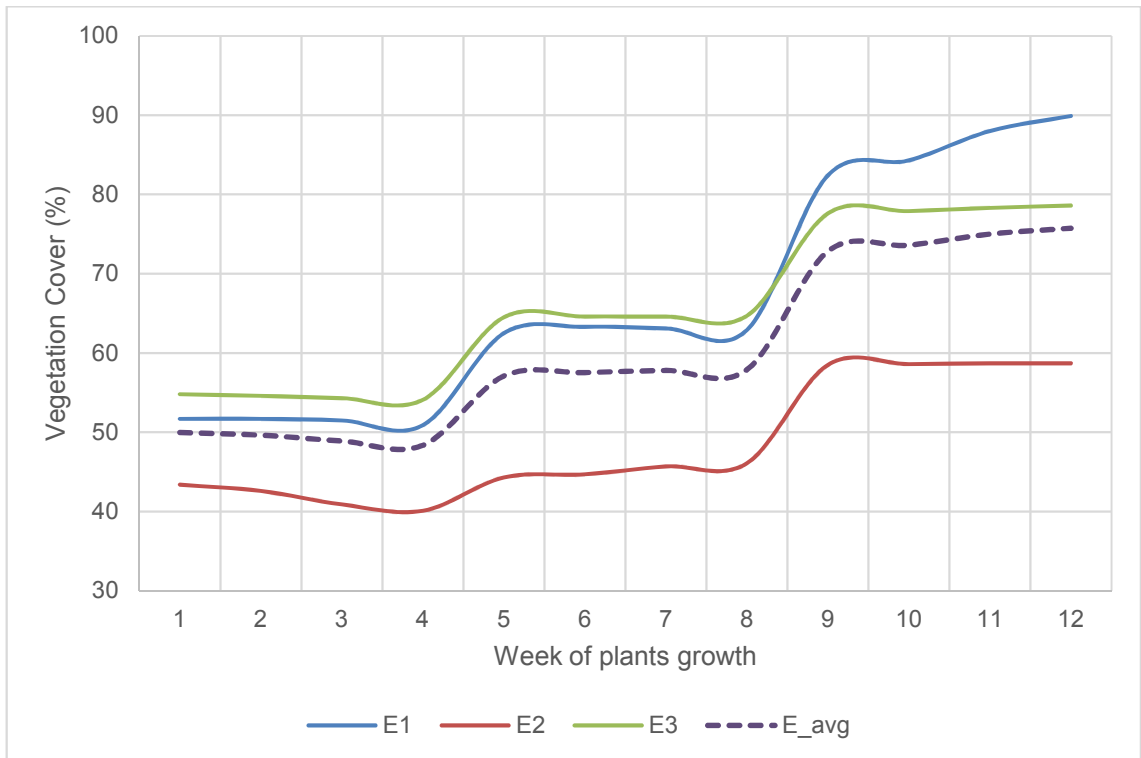


Figure 6.14 Vegetation cover over the 12-week testing programme for green roof design E. The vegetation cover for replicates E1, E2, and E3 is shown by solid lines, the average of replicates is shown by dashed line.

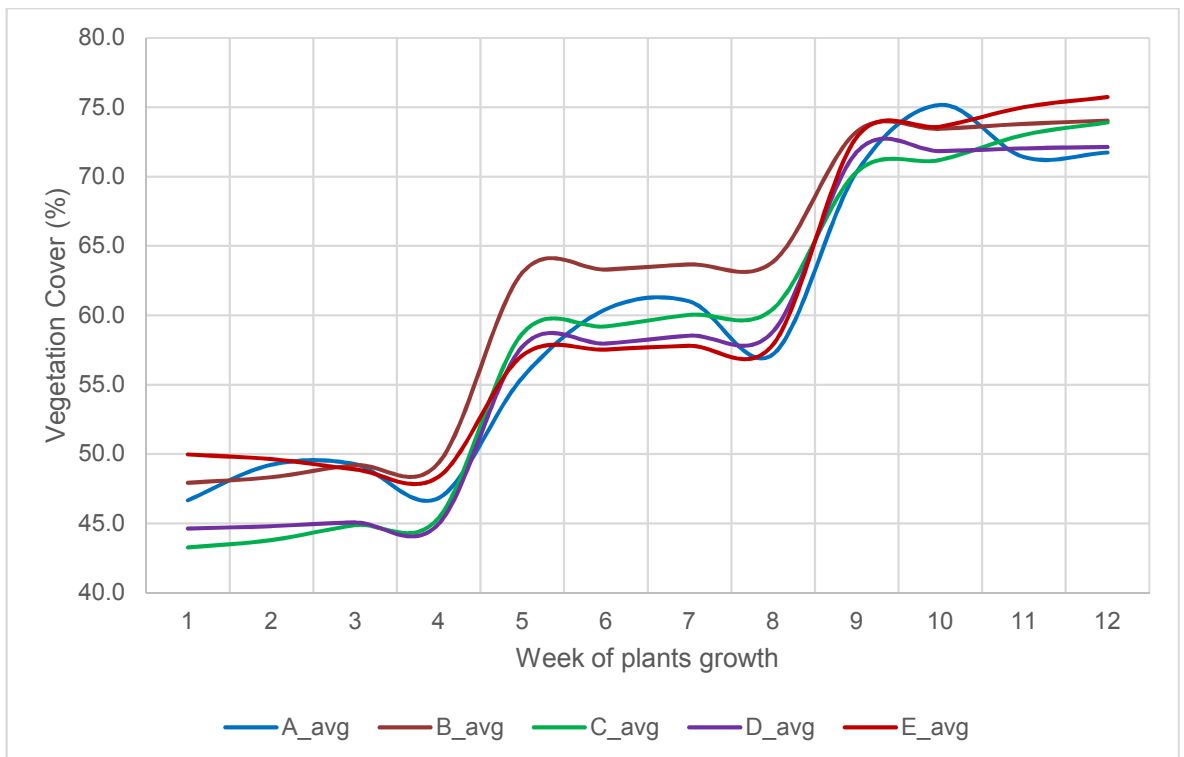


Figure 6.15 The comparison between average vegetation cover of each green roof design over the 12-week testing programme.

Table 6.10 Summary statistics of average vegetation cover data for all green roof designs: A, B, C, D, and E.

Summary Statistics, Average Vegetation Cover (%)						
Roof Type		A	B	C	D	E
Mean		59.56	61.93	58.68	58.35	60.36
Median		58.80	63.50	59.60	58.25	57.65
Percentiles	Min.	46.70	47.90	43.30	44.60	48.40
	25	49.28	49.35	45.28	45.08	49.90
	50	58.80	63.50	59.60	58.25	57.65
	75	70.58	73.25	70.52	71.80	73.00
	Max.	75.20	74.00	73.90	72.10	75.70
Shapiro-Wilk normality test	p-value	0.156	0.021	0.062	0.018	0.021
		- non-normal distribution ( $p < 0.05$ )				

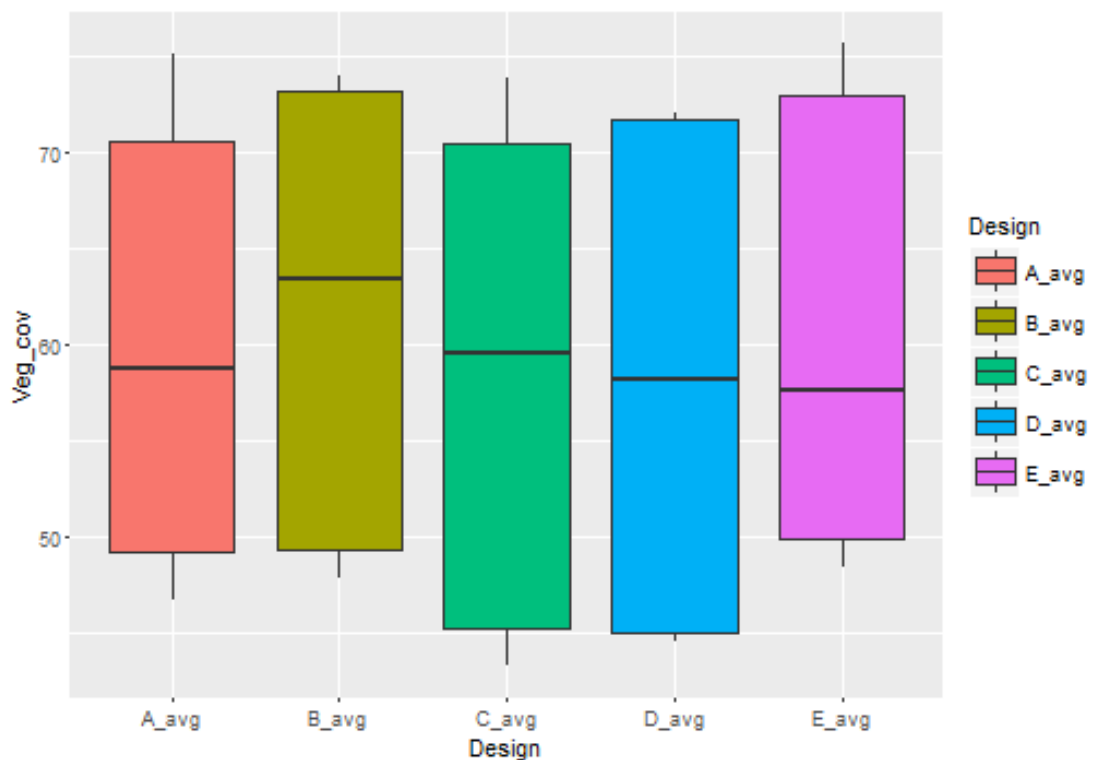


Figure 6.16 The average vegetation cover data distribution for all green roof designs: A, B, C, D, and E.

Table 6.11 P-values from Dunn's Kruskal-Wallis multiple comparison test results with Bonferroni correction applied for each combination of the green roof vegetation cover data sets. Highlighted numbers demonstrate a statistically significant difference between green roof designs.

Dunn's Kruskal-Wallis multiple comparison test – Vegetation Cover					
	A	B	C	D	E
A	-	1.000	1.000	1.000	1.000
B		-	1.000	1.000	1.000
C			-	1.000	1.000
D				-	1.000
E					-

 Null hypothesis of no statistically significant difference rejected ( $p < 0.05$ )

The vegetation cover increase followed a similar pattern across all green roofs during the period of laboratory tests. The only exception was green roof design A1, for which vegetation cover decreased significantly in week 4 and 8 of the tests. This appeared to be due to the death of certain plants, which were subsequently replaced. The laboratory conditions (high temperature, low air circulation) proved to be unfavourable for the survival of the cowslip, thus suggesting that this particular plant species may not be suitable for green roof laboratory testing (Figure 6.17). Additionally, slugs were discovered in some of the green roof trays feeding on plants (Figure 6.18).



rotten stems of cowslip growing in Crushed Red Brick



rotten stems of cowslip growing in Lytag

*Figure 6.17 Poorly performing cowslip. Its poor performance was observed across all green roof designs: (a) cowslip growing in Crushed Red Brick (b) cowslip growing in Lytag.*



*Figure 6.18 Slugs being found in green roof trays: (a) slug feeding on plant (b) slug trap – small container filled with beer sunk into the soil.*

Vegetation cover increased rapidly in week 5 and weeks 8 and 9, which followed the weeks of the rainfall simulation: 4 and 7 (Table 6.8), presumably due to plants use of water that was easily available. In that period plants increased their biomass. If there is no water available for longer time plants are likely to cease their growth (Graceson et al., 2014b). One could notice that the vegetation cover for replicate 2 for all green roof designs was lower than the vegetation cover for replicate 1 and 3. Replicate 2 of all green roofs was planted first, followed by replicates 3 and 1 (Table 6.8). The green roof replicates were planted a week apart, however, the plug plants were purchased and arrived at the same time and all of them were kept in the same laboratory conditions, resulting in their

simultaneous growth. Hence, the vegetation cover for the replicate 3 and 1 was higher than for the replicate 2 for all green roof designs.

Figure 6.16 and Table 6.22 show the distribution of the vegetation cover for the entire period of testing. Green roof design B demonstrates the highest median and the highest 3<sup>rd</sup> quartile (63.50% and 73.25%, respectively) of the average vegetation cover (Figure 6.16 and Table 6.22). However, the maximum vegetation cover for green roof design B is 74% and is lower than green roof design A, which is the conventional green roof (75.20%), and the green roof design E (75.50%). Green roof design D demonstrated slightly lower vegetation cover comparing to all green roof designs (median – 58.25%, maximum – 72.10%). Comparison of the average vegetation cover for different green roof designs did not show obvious differences (Figure 6.15). In the first weeks of the testing period green roof design C demonstrated the lowest average vegetation cover and green roof design E the highest. Following the first rainfall simulation the highest vegetation cover was observed for green roof design B, while the lowest average vegetation cover was recorded for green roof design E. At the end of the tests green roof design E demonstrated the highest average vegetation cover and green roof design A the lowest. No statistically significant differences in average vegetation cover between different green roof designs were confirmed by Dunn's Kruskal-Wallis multiple comparison test ( $p > 0.05$  for all green roof design combinations, Table 6.11).

The results show no clear indication of favourable green roof construction materials to encourage greater vegetation cover. The average vegetation cover across green roof designs follows closely the same pattern. This demonstrated the ability of each system to successfully support wildflowers development, at least in the short term. It should be noted that no biomass or height of plants were assessed in this study. Hence, only general comparison to the work of other researchers could be made. The results presented by Graceson et al. (2014b) were in opposition to the observations made in this part of the study. Their research demonstrated the influence of the green roof substrate type on the vegetation growth, with crushed brick being the least favourable as opposed to crushed tile or Lytag. Molineux et al. (2009) also investigated the effect of different type of the substrate on the growth of the green roof plants. The study showed that biomass of the plants grown on substrate made with sewage sludge pellets

is greater than for other types of substrate. Eksi and Rowe (2016) also recorded differences in vegetation growth in relation to the substrate type. Higher vegetation performance was noticed for expanded shale mix, as opposed to crushed porcelain or foamed glass. However, the authors highlighted that the material structure rather than the material type itself might have caused the difference. As presented in Chapter 3, the particle size distribution has an effect on material properties such as porosity or permeability. This, again, demonstrates that the careful analysis of the material properties is crucial to understanding of green roof performance. The same type of the material may result in a higher or lower performance, depending on its particle size distribution and grading.

#### **6.3.1.1 SUMMARY**

All green roof trays were plug-planted with the same number of wildflower species following the same time table. Digital image analysis of vegetation cover confirmed that all green roof designs supported vegetation growth similarly with all of the green roof designs demonstrating no statistically significant difference in average vegetation cover.

Laboratory conditions proved to be unfavourable for cowslip growth. It is not recommended to use this type of wildflower species in laboratory experiments where plants are exposed to high temperatures, heavy rainfall, and limited air circulation.

#### **6.3.2 GREEN ROOF RESPONSE TO THE SIMULATED RAINFALLS: THE EFFECT OF VEGETATION PRESENCE**

This section presents the analysis of the effect of vegetation presence on hydrological performance of the green roofs subjected to extreme rainfall events. The analysis was based on the retention as a main characteristic of the hydrological performance.

As opposed to in-situ experiments (Chapter 4), the observations for each replicate were independent, often with different laboratory microclimatic conditions. Hence, in order to increase the sample size, the observations of all replicates for each green roof design were combined. The hydrological performance data were considered in two groups: without vegetation and with vegetation. The group of observations for green roofs without vegetation was larger than the group of observations for green roofs with vegetation due to

repetition of the tests (211 and 180, respectively). Hence, to avoid bias due to the sample size the duplicated observations were removed resulting in 175 observations for the green roofs without vegetation.

To determine the nature of data distribution, the exploratory data analysis was carried out. The summary statistics for both green roof groups are presented in Table 6.12. The boxplots for are presented in Figure 6.19. The Q-Q plots and density histograms can be found in Appendix F.

Table 6.12 Summary statistics of retention data in relation to vegetation presence.

Summary Statistics - Retention (%)			
Green roof type	Without Vegetation	With Vegetation	
<b>N</b>	175	180	
<b>Mean</b>	21.62	19.61	
<b>Median</b>	13.00	9.00	
<b>Std. Deviation</b>	20.79	21.89	
<b>Percentiles</b>	<b>Min.</b>	0.00	0.00
	<b>25</b>	7.00	6.00
	<b>50</b>	13.00	9.00
	<b>75</b>	32.00	17.00
	<b>Max.</b>	91.00	78.00
<b>Shapiro-Wilk normality test</b>	<b>p-value</b>	5.56 x 10 <sup>-13</sup>	<2.20 x 10 <sup>-16</sup>
- non-normal distribution (p<0.05)			

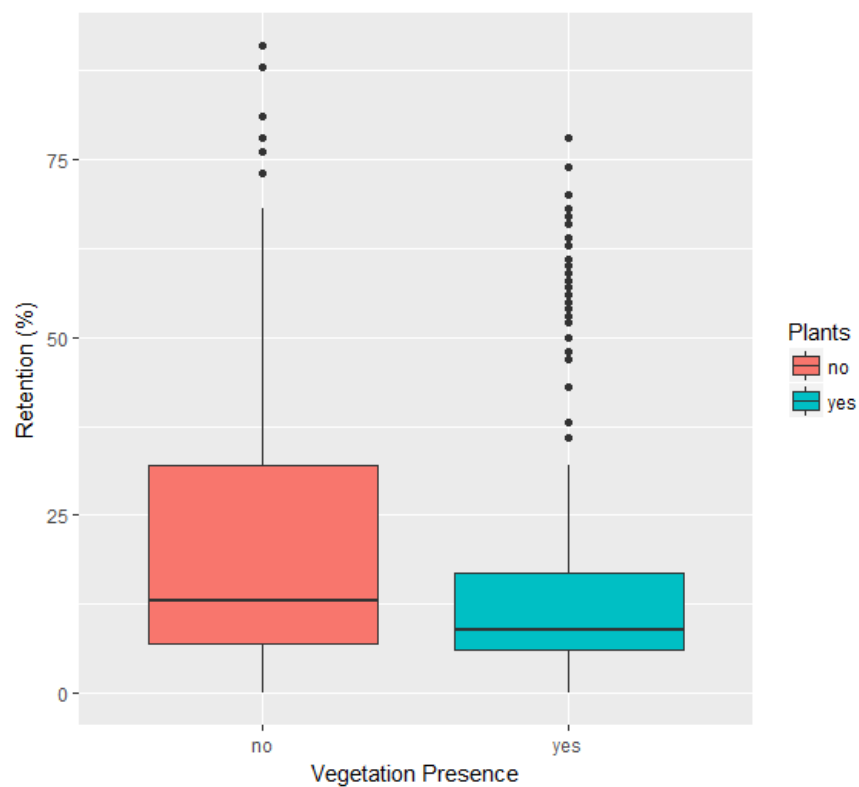


Figure 6.19 Stormwater retention data distribution for green roofs with and without vegetation.

Table 6.13 P-values from Mann-Whitney U test results with Bonferroni correction applied for each combination of the retention data sets. Highlighted numbers demonstrate a statistically significant difference between green roof with and without vegetation.

Mann-Whitney U test – Retention (%)		
Green roof type	Without Vegetation	With Vegetation
Without Vegetation	-	0.036
With Vegetation		-
<input type="checkbox"/> Null hypothesis of no statistically significant difference rejected ( $p < 0.05$ )		

Table 6.14 Median retention for each green roof design in relation to vegetation presence and p-values from Dunn’s Kruskal-Wallis multiple comparison test results with Bonferroni correction. Highlighted numbers demonstrate a statistically significant difference in retention between green roofs with and without vegetation.

Dunn’s Kruskal-Wallis multiple comparison test – Retention (%)						
		A	B	C	D	E
Without Vegetation		7.00	16.00	8.00	14.50	17.00
With Vegetation		6.00	10.50	8.00	9.50	11.50
p-value	Without – With Vegetation	0.66	0.27	0.57	0.31	0.04
<input type="checkbox"/> Null hypothesis of no statistically significant difference rejected ( $p < 0.05$ )						

Summary statistics and boxplot representation of retention data for each green roof designs demonstrated non-normal, positively skewed distribution (Table 6.12 and Figure 6.19).

The median retention for the green roofs without the vegetation was 13%. The median retention for the green roofs with vegetation was 9%. Mann-Whitney U test confirmed the significance of the difference in retention between vegetated and unvegetated green roofs (Table 6.13). The hydrological performance of green roofs with and without vegetation was also assessed in relation to the green roof design. The median retention for green roof C was the same for vegetated and unvegetated trays (8%). The median retention for all other vegetated green roof designs was lower than that of unvegetated. However, the difference was significant only for green roof design E (Table 6.14).

This result was surprising since many published studies presented opposite findings (VanWoert et al., 2005, Volder and Dvorak, 2014, Harper et al., 2015). Lower retention of green roofs with vegetation could have occurred due to the planting technique used in this study – plug planting. Implanting plug plants could have resulted in developing preferential flow paths for stormwater between the substrate material and that of plugs (Figure 6.20). This would be possible to happen at the early stage of a plants development when the root system is not well established, reducing green roof retention capacities. This is likely to change for mature green roofs with plants having well developed root system, which would influence the size distribution and connectivity of pores in the substrate, thus, leading to increased retention capacity of the green roof (Stovin et al., 2015).

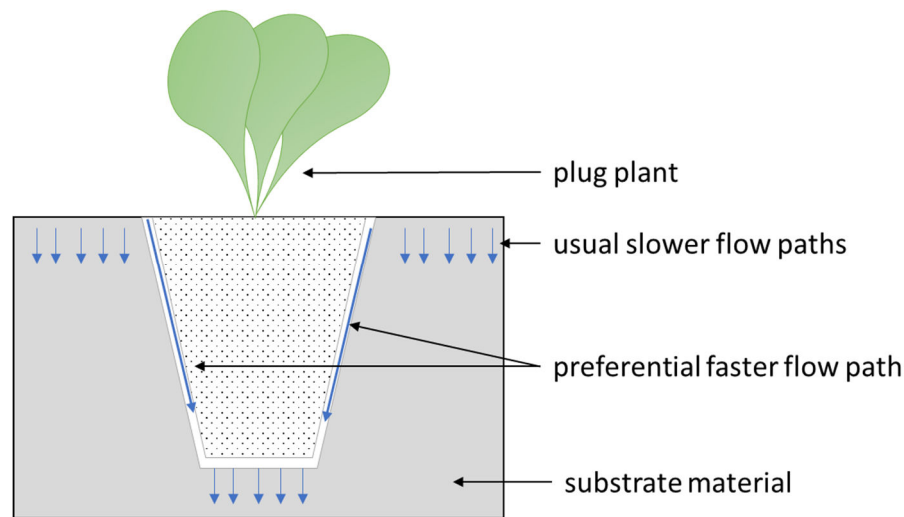


*Figure 6.20 The usual and preferential flow paths for stormwater through plug-planted green roof substrate.*

The assessment of the performance of unvegetated green roofs is crucial to determine their performance when the green roofs are not covered with vegetation such as at early stage, shortly after construction, at the period of plants germination and early development when seed-sowed. The results of this study demonstrated higher retention for the unvegetated roofs as opposed to vegetated green roofs in the early stage of plants development. Additional tests are recommended to investigate the differences between green roofs without and with vegetation for matured, fully developed green roofs.

### **6.3.3 GREEN ROOF RESPONSE TO THE SIMULATED RAINFALLS: EXPERIMENTAL REPLICATES**

This section presents the analysis of the green roof experimental replicates response to the simulated, extreme rainfall events. The overall hydrological performance of the experimental replicates of each green roof design was assessed based on the retention as a main characteristic of the hydrological performance. The exploratory data analysis was carried out to determine the nature of data distribution. The summary statistics for all green roof designs are presented in Table 6.15 to 6.19. The boxplots for all green roof designs are presented in Figure 6.21 to 6.25. The Q-Q plots and density histograms for all roofs can be found in Appendix G.

Due to the significantly higher retention of the unvegetated roofs of green roof design E (section 6.3.2), the green roofs without vegetation were not included in

this analysis. The analysis was performed on data set of 180 observations for green roof trays with vegetation.

The summary of factors that could have effect on green roof performance such as vegetation cover, air temperature and water content of the substrate prior to rainfall event are presented in Table 6.20.

It was assumed that the replicates of green roof designs would perform in a similar manner. Hence, the following null hypothesis was generated and tested: there is no significant difference in retention between green roofs of the same design. The null hypothesis was tested using the non-parametric Mann-Whitney U test. The results of the test for all green roof designs are presented in Table 6.21.

**Control: design A - Crushed Red Brick and Roofdrain40**

Table 6.15 Summary statistics of stormwater retention data for following green roofs: A-1, A-2, A-3. The retention data included observations for green roof trays with vegetation.

Summary Statistics, Retention (%)				
Roof type		A-1	A-2	A-3
<b>N</b>		12	12	12
<b>Mean</b>		19.83	16.42	19.75
<b>Median</b>		6.0	5.5	5.5
<b>Std. Deviation</b>		27.26	21.57	26.77
<b>Percentiles</b>	Min.	1.00	2.00	3.00
	25	3.00	3.75	4.00
	50	6.00	5.50	5.50
	75	23.00	17.25	19.50
	Max.	68.00	56.00	70.00
<b>Shapiro-Wilk normality test</b>	p-value	3.17 x 10 <sup>-4</sup>	2.13 x 10 <sup>-4</sup>	1.77 x 10 <sup>-4</sup>
<div style="display: flex; align-items: center;"> <div style="width: 20px; height: 10px; background-color: #cccccc; margin-right: 5px;"></div> <span>- non-normal distribution (p&lt;0.05)</span> </div>				

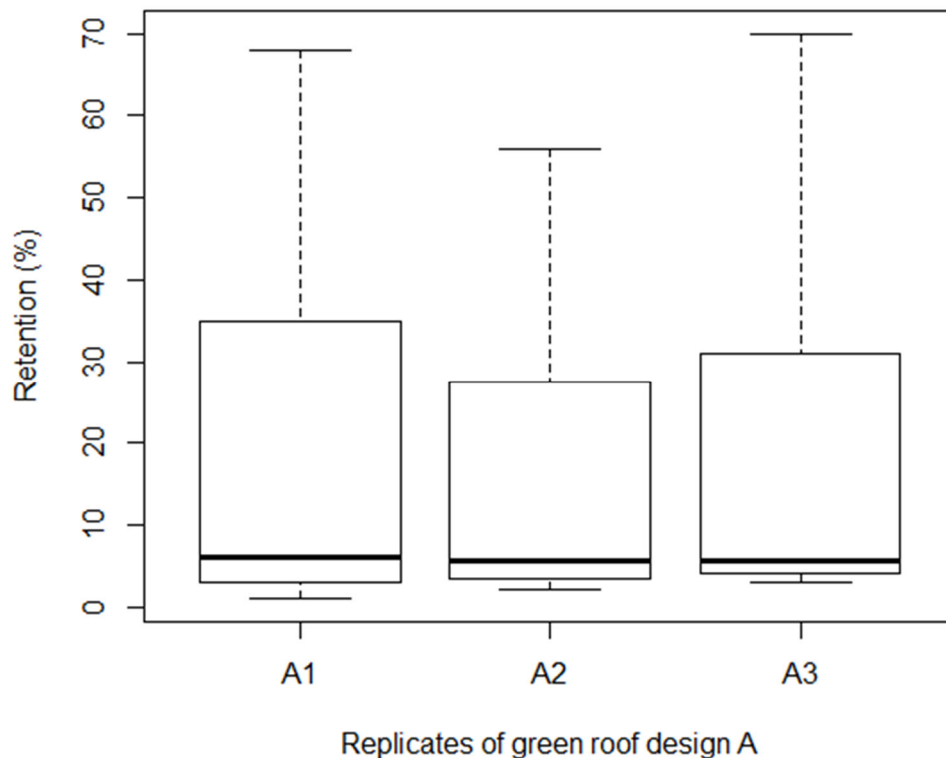


Figure 6.21 Retention data distribution for green roofs: A-1, A-2, A-3. The retention data included observations for green roof trays with vegetation.

## Treatment 1: design B – Sewage Sludge Pellets and Roofdrain40

Table 6.16 Summary statistics of stormwater retention data for following green roofs: B-1, B-2, B-3. The retention data included observations for green roof trays with vegetation.

Summary Statistics, Retention (%)				
Roof type		B-1	B-2	B-3
<b>N</b>		12	12	12
<b>Mean</b>		21.42	17.00	20.00
<b>Median</b>		11.00	9.00	11.00
<b>Std. Deviation</b>		23.53	20.11	19.56
<b>Percentiles</b>	Min.	0.00	0.00	8.00
	25	7.75	8.00	8.75
	50	11.00	9.00	11.00
	75	22.50	14.00	17.25
	Max.	66.00	67.00	61.00
<b>Shapiro-Wilk normality test</b>	p-value	1.42 x 10 <sup>-3</sup>	3.78 x 10 <sup>-3</sup>	2.42 x 10 <sup>-3</sup>
<div style="display: inline-block; width: 15px; height: 10px; background-color: #cccccc; border: 1px solid black;"></div> - non-normal distribution (p<0.05)				

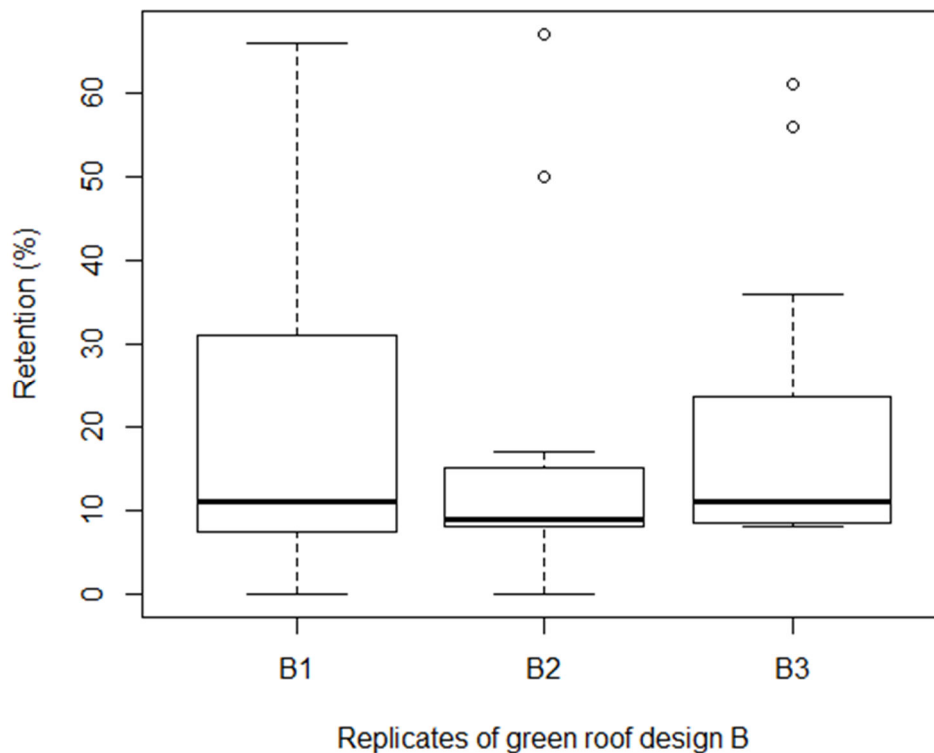


Figure 6.22 Retention data distribution for green roofs: B-1, B-2, B-3. The retention data included all observations for green roof trays with and without vegetation.

## Treatment 2: design C – Lytag and Roofdrain40

Table 6.17 Summary statistics of stormwater retention data for following green roofs: C-1, C-2, C-3. The retention data included observations for green roof trays with vegetation.

Summary Statistics, Retention (%)				
Roof type		C-1	C-2	C-3
<b>N</b>		12	12	12
<b>Mean</b>		22.58	17.75	21.17
<b>Median</b>		8.50	8.50	8.00
<b>Std. Deviation</b>		27.91	23.05	27.41
<b>Percentiles</b>	Min.	0.00	0.00	1.00
	25	5.75	3.25	5.50
	50	8.50	8.50	8.00
	75	27.00	28.50	22.75
	Max.	78.00	67.00	74.00
<b>Shapiro-Wilk normality test</b>	p-value	1.05 x 10 <sup>-3</sup>	1.99 x 10 <sup>-3</sup>	5.71 x 10 <sup>-4</sup>
<div style="display: flex; align-items: center;"> <div style="width: 20px; height: 10px; background-color: #cccccc; margin-right: 5px;"></div> <span>- non-normal distribution (p&lt;0.05)</span> </div>				

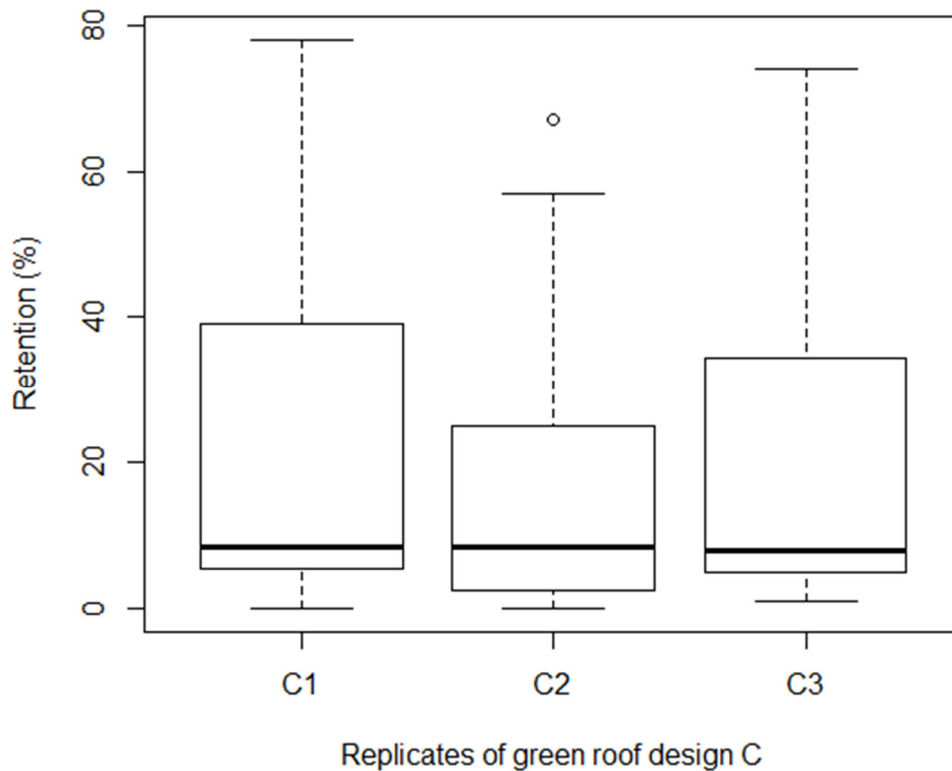


Figure 6.23 Retention data distribution for green roofs: C-1, C-2, C-3. The retention data included observations for green roof trays with vegetation.

### Treatment 3: design D – Crushed Red Brick and Granulated Rubber

Table 6.18 Summary statistics of stormwater retention data for following green roofs: D-1, D-2, D-3. The retention data included observations for green roof trays with vegetation.

Summary Statistics, Retention (%)				
Roof type		D-1	D-2	D-3
<b>N</b>		12	12	12
<b>Mean</b>		21.33	17.92	18.50
<b>Median</b>		12.50	9.00	9.50
<b>Std. Deviation</b>		20.72	18.61	19.97
<b>Percentiles</b>	Min.	4.00	4.00	3.00
	25	7.00	7.00	6.00
	50	12.50	9.00	9.50
	75	26.25	19.00	18.75
	Max.	57.00	55.00	61.00
<b>Shapiro-Wilk normality test</b>	p-value	1.54 x 10 <sup>-3</sup>	4.95 x 10 <sup>-4</sup>	1.42 x 10 <sup>-3</sup>
<div style="display: flex; align-items: center;"> <div style="width: 20px; height: 10px; background-color: #cccccc; margin-right: 5px;"></div> <span>- non-normal distribution (p&lt;0.05)</span> </div>				

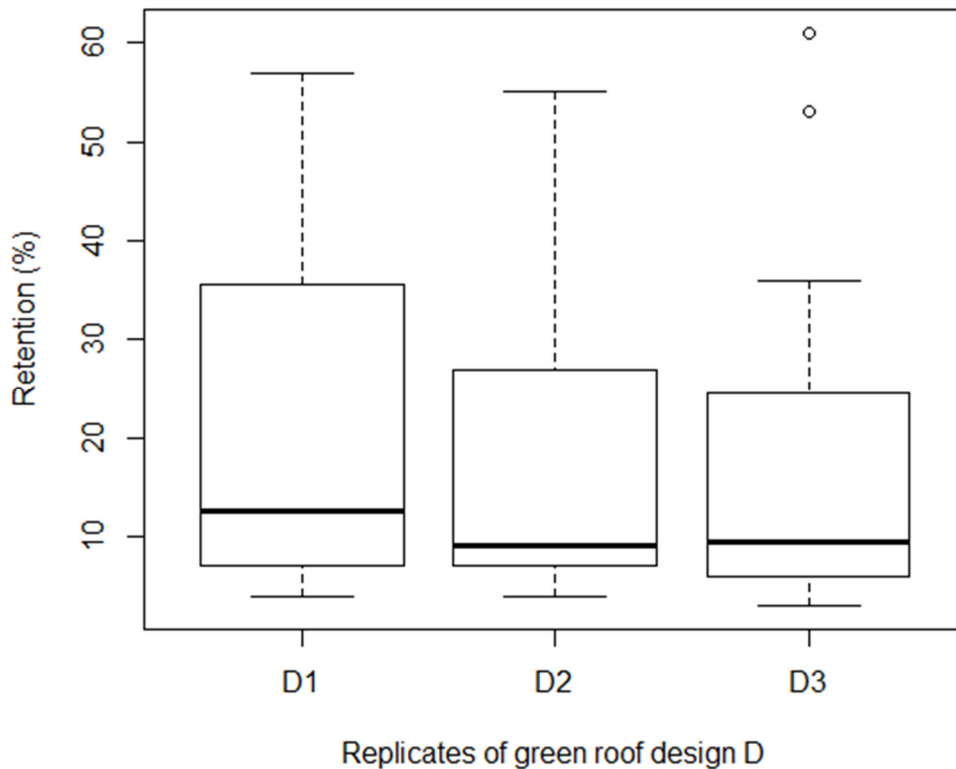


Figure 6.24 Retention data distribution for green roofs: D-1, D-2, D-3. The retention data included observations for green roof trays with vegetation.

## Treatment 4: design E – Crushed Red Brick and Wool-rich Carpet Shred

Table 6.19 Summary statistics of stormwater retention data for following green roofs: E-1, E-2, E-3. The retention data included observations for green roof trays with vegetation.

Summary Statistics, Retention (%)				
Roof type		E-1	E-2	E-3
<b>N</b>		12	12	12
<b>Mean</b>		24.08	15.17	21.25
<b>Median</b>		13.00	9.00	13.00
<b>Std. Deviation</b>		22.64	15.94	20.86
<b>Percentiles</b>	Min.	8.00	0.00	0.00
	25	10.00	6.75	10.00
	50	13.00	9.00	13.00
	75	26.25	15.50	21.75
	Max.	68.00	58.00	64.00
<b>Shapiro-Wilk normality test</b>	p-value	6.39 x 10 <sup>-4</sup>	2.36 x 10 <sup>-3</sup>	4.29 x 10 <sup>-3</sup>
<div style="background-color: #cccccc; width: 20px; height: 10px; display: inline-block; vertical-align: middle;"></div> - non-normal distribution (p<0.05)				

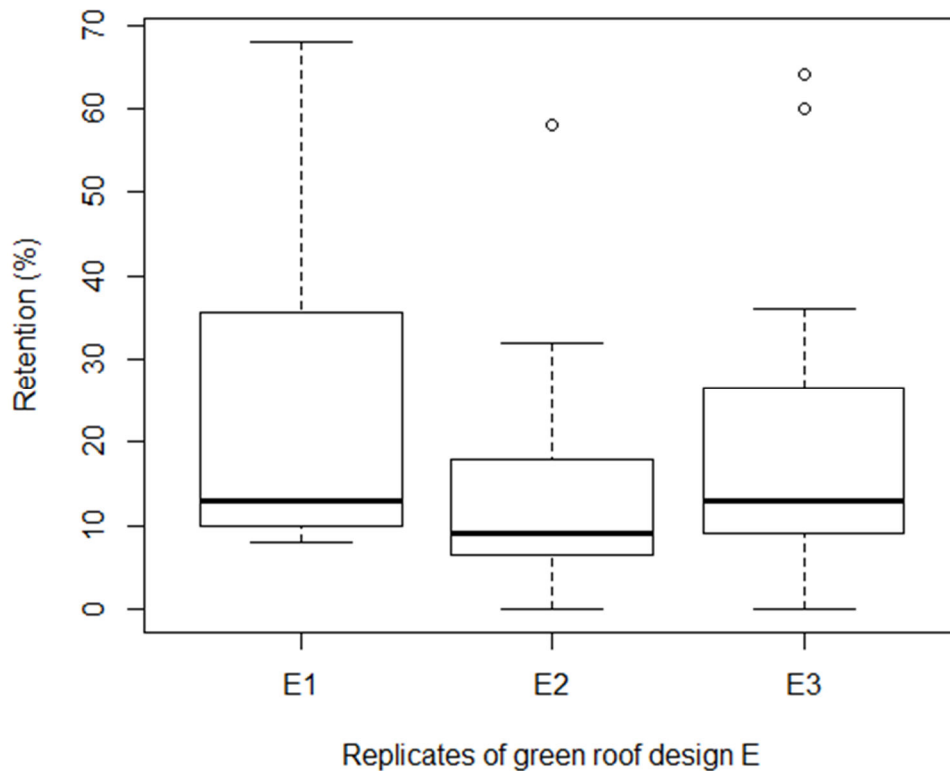


Figure 6.25 Retention data distribution for green roofs: E-1, E-2, E-3. The retention data included observations for green roof trays with vegetation.

Table 6.21 P-values from Mann-Whitney tests between replicates of the following green roof designs: A, B, C, D, and E. Highlighted numbers demonstrate no statistically significant difference in retention between green roof design replicates. The retention data included all observations for green roof trays with and without vegetation.

Green roof design	A			B			C			D			E		
	1	2	3	1	2	3	1	2	3	1	2	3	1	2	3
Replicate															
<b>1</b>	-	0.727	0.862	-	0.655	0.977	-	0.583	0.795	-	0.469	0.544	-	0.099	0.862
<b>2</b>	-	-	0.581	-	-	0.335	-	-	0.750	-	-	1.000	-	-	0.235
<b>3</b>	-	-	-	-	-	-	-	-	-	-	-	-	-	-	-
	- the null hypothesis of no difference should be accepted (p>0.05)														

Table 6.20 Median of vegetation cover, air temperature and substrate water content corresponding to each green roof design replicate. Italicised numbers show values that could have been possibly critical to green roof replicates performance such as low vegetation cover or high substrate water content.

Green roof design	A			B			C			D			E		
	1	2	3	1	2	3	1	2	3	1	2	3	1	2	3
Replicate															
<b>Vegetation Cover (%)</b>	62.20	51.65	62.35	69.15	57.60	62.58	63.45	56.20	59.20	64.30	49.30	61.15	63.00	45.20	64.60
<b>Temperature (°C)</b>	21.00	21.00	20.00	21.00	21.00	20.00	21.00	21.00	20.00	21.00	21.00	20.00	21.00	21.00	20.00
<b>Water Content Prior Tests (%)</b>	34.05	32.8	32.2	25.65	25.00	23.55	31.1	33.2	32.7	30.4	32.2	32.0	33.05	33.1	32.95

Summary statistics and boxplot representation of retention data for all green roof designs demonstrated non-normal, positively skewed distribution (Table 6.15 to 6.19. and Figure 6.21 to 6.25). Non-normal distribution of retention data for all green roof design was also confirmed by Shapiro-Wilk normality test results ( $p < 0.05$ ) (Table 6.15 to 6.19).

The exploratory data analysis of the retention of all green roof designs demonstrated absolute median retention differences of 0.5% to 4% between replicates. The lowest median retention was observed for the replicate 2 of all green roof designs, except green roof design C. These differences, however, were not significant as demonstrated by the Mann-Whitney U test results (Table 6.21). These results were as expected. There were no considerable differences in the median temperature and the median substrate water content between the replicates of all green roof designs (Table 6.20). There were, however, noticeable differences in the median vegetation cover, in particular for the replicates 2 of all green roof designs (Table 6.20). The lower median retention for the replicates 2 of green roof designs correlated with their lower median vegetation cover. However, these differences in the median vegetation cover did not cause significant differences in the median retention between replicates of all green roof design. Thus, the analysis of the retention of green roofs of the same design, concurred the hypothesis of no significant differences in retention between the replicates of the green roofs of the same design.

#### **6.3.4 GREEN ROOF RESPONSE TO THE SIMULATED RAINFALLS: GREEN ROOFS OF DIFFERENT DESIGN**

This section presents the analysis of the green roofs of different designs responses to the simulated, extreme rainfall events. The overall hydrological performance of each green roof design was assessed based on the runoff depth, retention, and peak flow reduction. The analysis was performed on a data set of 180 observations for the green roof trays with vegetation. In order to increase the sample size, the observations of all replicates for each green roof design were combined.

#### **6.3.4.1 OVERALL HYDROLOGICAL PERFORMANCE AND THE EFFECT OF GREEN ROOF DESIGN**

This section focuses on overall hydrological performance of the green roofs subjected to extreme rainfall events. It aims to explore general patterns as well as the influence of the design on hydrological performance of the green roofs. The exploratory data analysis was carried out to determine the nature of data distribution. Summary statistics of the green roof hydrological performance data are presented in Table 6.22 (runoff depth), Table 6.24 (retention) and Table 6.26 (peak flow reduction). Green roof hydrological performance data distribution is presented in Figure 6.26 (runoff depth), Figure 6.27 (retention) and Figure 6.28 (peak flow reduction).

The differences in hydrological performance between green roofs of different design was assessed using non-parametric Dunn's Kruskal-Wallis multiple comparison test with Bonferroni correction. The following hypothesis was tested: there is no significant difference in hydrological performance (runoff depth, retention, and peak flow reduction) between green roofs of different design. The results of the analysis are presented in Table 6.23 (runoff depth), Table 6.25 (retention), and Table 6.27 (peak flow reduction).

## Runoff depth

Table 6.22 Summary statistics of stormwater runoff depth data for the following green roofs: A, B, C, D, and E.

Summary Statistics						
Runoff depth (mm)	A	B	C	D	E	
<b>N</b>	36	36	36	36	36	
<b>Mean</b>	24.07	23.65	23.51	23.79	23.39	
<b>Median</b>	21.18	20.36	21.16	20.16	20.29	
<b>Std. Deviation</b>	12.83	11.84	12.55	11.97	11.56	
<b>Percentiles</b>	Min.	6.49	7.83	4.61	8.49	6.53
	25	17.40	17.62	16.72	16.48	16.80
	50	21.18	20.36	21.16	20.16	20.29
	75	28.75	27.60	28.97	28.54	27.72
	Max.	50.07	48.37	49.14	49.24	47.84
<b>Shapiro-Wilk normality test</b>	p-value	$3.61 \times 10^{-3}$	$2.04 \times 10^{-3}$	$2.63 \times 10^{-2}$	$7.88 \times 10^{-4}$	$2.52 \times 10^{-3}$
- non-normal distribution ( $p < 0.05$ )						

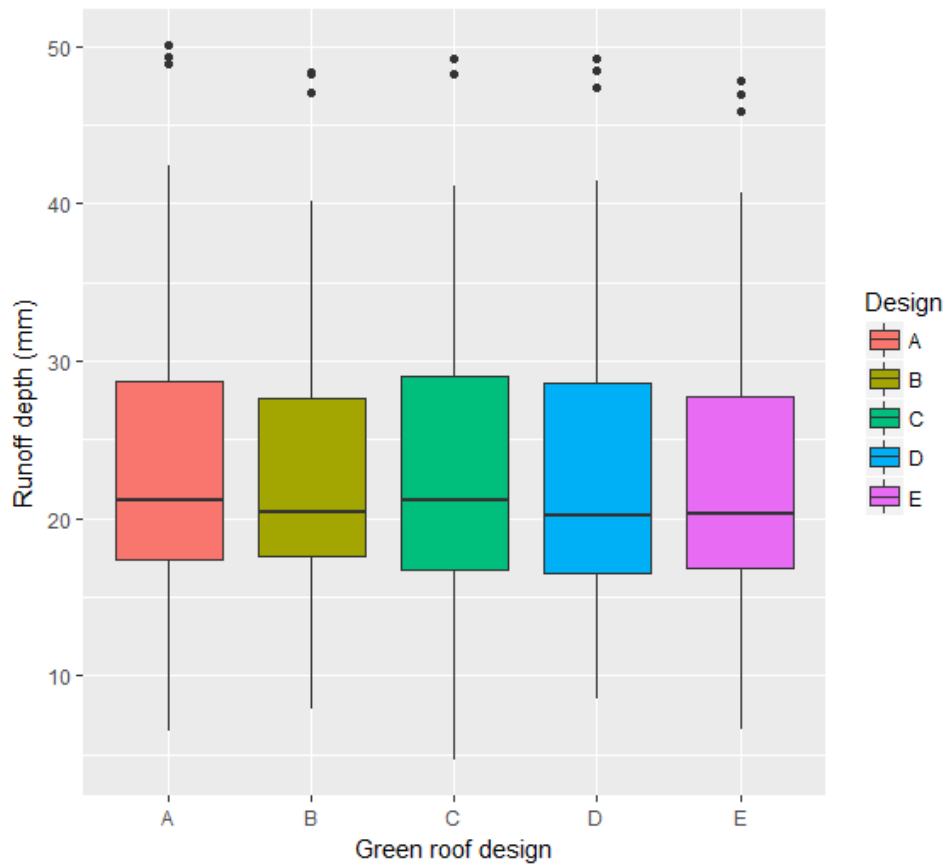


Figure 6.26 Stormwater runoff depth data distribution for green roofs designs A-E.

Table 6.23 P-values from Dunn's Kruskal-Wallis multiple comparison test results with Bonferroni correction applied for each combination of the runoff depth data sets. Highlighted numbers demonstrate a statistically significant difference between green roof designs.

Dunn's Kruskal-Wallis multiple comparison test – Runoff Depth					
	A	B	C	D	E
A	-	1.000	1.000	1.000	1.000
B		-	1.000	1.000	1.000
C			-	1.000	1.000
D				-	1.000
E					-

\* Uncorrected p-value  
 Null hypothesis of no statistically significant difference rejected

## Retention

Table 6.24 Summary statistics of stormwater retention data for selected green roofs.

Summary Statistics						
Retention (%)		A	B	C	D	E
<b>N</b>		36	36	36	36	36
<b>Mean</b>		18.67	19.47	20.50	19.25	20.17
<b>Median</b>		6	10.5	8	9.5	11.5
<b>Std. Deviation</b>		24.65	20.61	25.54	19.27	19.80
<b>Percentiles</b>	Min.	1.0	0.0	0.0	3.0	0.0
	25	4.0	8.0	4.75	7.0	8.75
	50	6.0	10.5	8.0	9.5	11.5
	75	20.25	14.75	20.75	21.75	18.50
	Max.	70.0	67.0	78.0	61.0	68.0
<b>Shapiro-Wilk normality test</b>	p-value	4.25 x 10 <sup>-8</sup>	1.49 x 10 <sup>-7</sup>	3.17 x 10 <sup>-7</sup>	4.69 x 10 <sup>-7</sup>	1.02 x 10 <sup>-6</sup>
<input type="checkbox"/>	- non-normal distribution (p<0.05)					

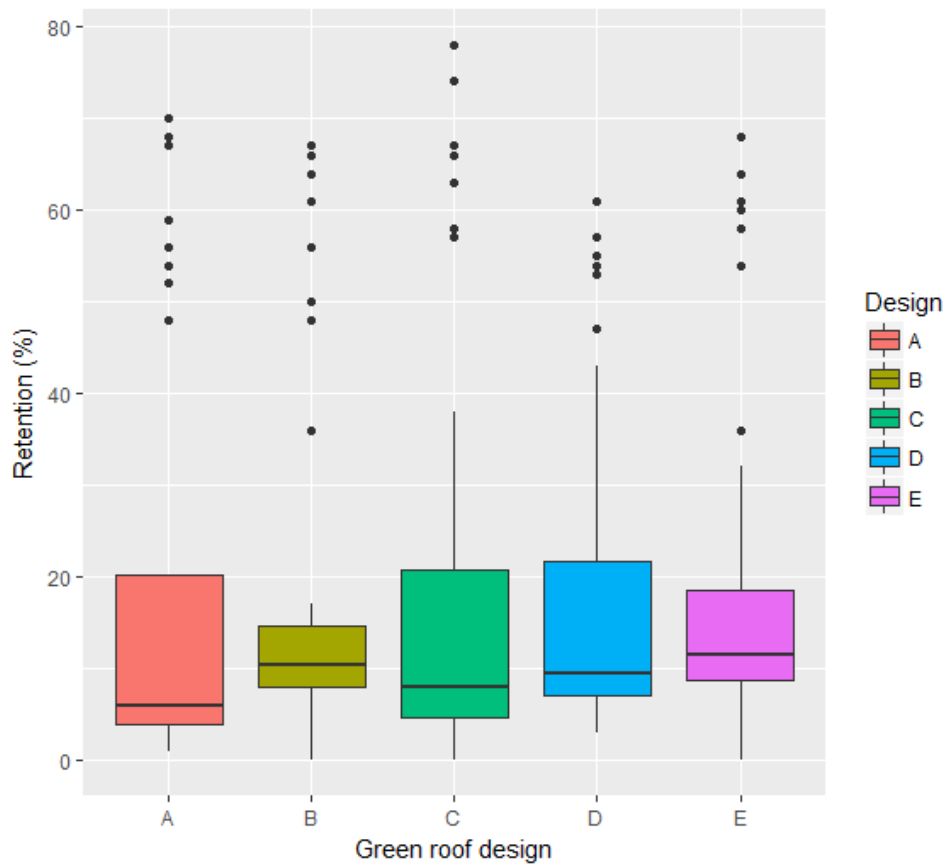


Figure 6.27 Stormwater retention data distribution for green roof designs A-E.

Table 6.25 P-values from Dunn’s Kruskal-Wallis multiple comparison test results with Bonferroni correction applied for each combination of the retention data sets. Highlighted numbers demonstrate a statistically significant difference between green roof designs. *Italicised numbers show a statistically significant difference between green roof designs based on uncorrected p-value.*

Dunn’s Kruskal-Wallis multiple comparison test – Retention					
	A	B	C	D	E
A	-	<i>0.065 / 0.006*</i>	1.000	<i>0.287 / 0.029*</i>	0.014
B		-	1.000	1.000	1.000
C			-	1.000	0.627
D				-	1.000
E					-

\* Uncorrected p-value  
 Null hypothesis of no statistically significant difference rejected

## Peak flow reduction

Table 6.26 Summary statistics of stormwater peak flow reduction data for selected green roofs.

Summary Statistics						
Peak Flow Reduction (%)	A	B	C	D	E	
<b>N</b>	36	36	36	36	36	
<b>Mean</b>	15.5	9.65	11.99	6.84	15.63	
<b>Median</b>	-2.3	0.6	-2.3	0.3	7.45	
<b>Std. Deviation</b>	33.08	23.58	33.64	18.50	20.95	
<b>Percentiles</b>	Min.	-9.1	-5.8	-11.0	-5.2	-2.3
	25	-5.2	-2.3	-6.4	-1.2	4.5
	50	-2.3	0.6	-2.3	0.3	7.45
	75	25.65	4.05	5.00	8.05	15.45
	Max.	100.00	100.00	100.00	100.00	100.00
<b>Shapiro-Wilk normality test</b>	p-value	1.92 x 10 <sup>-7</sup>	1.26 x 10 <sup>-8</sup>	1.50 x 10 <sup>-8</sup>	2.95 x 10 <sup>-9</sup>	5.09 x 10 <sup>-7</sup>
<div style="background-color: #cccccc; width: 20px; height: 10px; display: inline-block; margin-right: 5px;"></div> - non-normal distribution (p<0.05)						

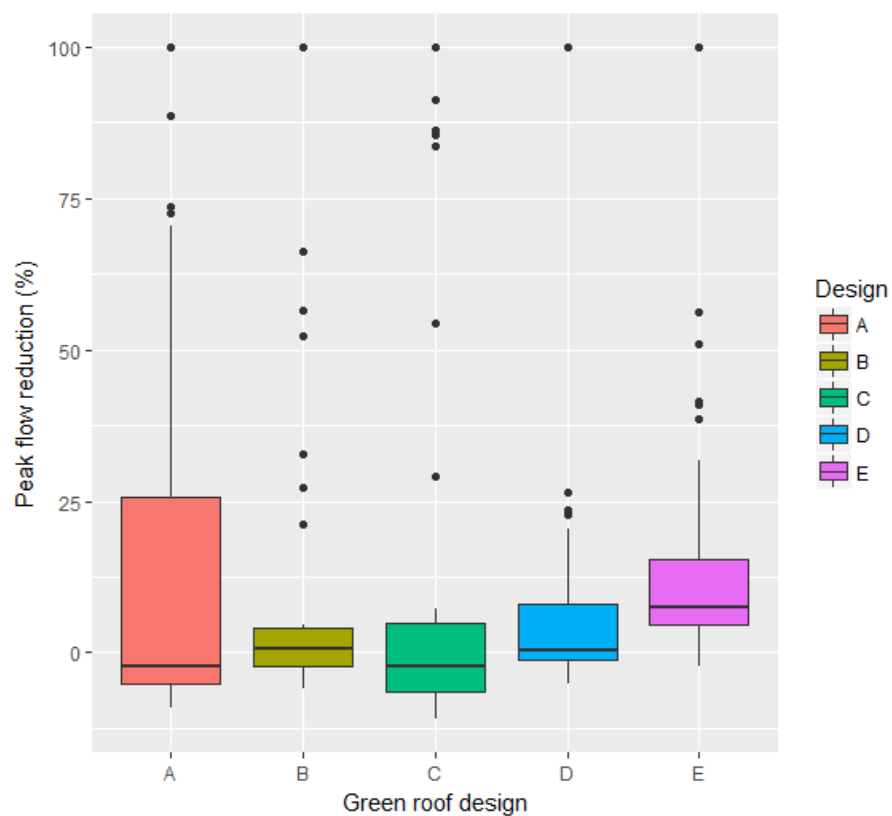


Figure 6.28 Stormwater peak flow reduction data distribution for green roof designs A-E.

Table 6.27 P-values from Dunn's Kruskal-Wallis multiple comparison test results with Bonferroni correction applied for each combination of the peak flow reduction data sets. Highlighted numbers demonstrate a statistically significant difference between green roof designs. Italicised numbers show a statistically significant difference between green roof designs based on uncorrected p-value.

Dunn's Kruskal-Wallis multiple comparison test – Peak Flow Reduction					
	A	B	C	D	E
A	-	1.000	1.000	1.000	0.001
B		-	0.839	1.000	0.047
C			-	0.715	5.244 x 10 <sup>-5</sup>
D				-	<i>0.059 / 0.006*</i>
E					-

\* Uncorrected p-value  
 Null hypothesis of no statistically significant difference rejected

Summary statistics and boxplot representation of runoff depth, retention, and peak flow reduction data for each green roof designs demonstrated non-normal, positively skewed distribution (Table 6.22, Table 6.24 and Table 6.26 and Figure 6.26, Figure 6.27 and Figure 6.28). Non-normal distribution of retention data for all green roof design was also confirmed by the Shapiro-Wilk normality test results ( $p < 0.05$ ). The general pattern of the retention and peak flow reduction distribution were in direct opposition to that observed in the in-situ experimental data analysis (Chapter 4). The in-situ retention and peak flow reduction data were negatively skewed with a high number of high-performance values. This was due to the high number of rainfall events of the return period below 2 years, which were mostly retained by the green roofs, resulting in a concentration of high retention and peak flow reduction observations. Contrary to that, laboratory data included only the observations of the green roof responses to the extreme rainfall events. Hence, a high concentration of low retention observations was present.

The median runoff depth ranged from 20.16mm for green roof design D, to 21.18mm for green roof design C (about 5% difference). The maximum runoff depths were in the range from 47.84mm (green roof design E) to 50.07mm (green roof design A) and occurred for merged rainfall events. The depth of the merged

rainfall events was twice of that of not merged. Hence, the amount of water discharged from green roofs for these rainfall events was also significantly higher. Clearly, the size of the rainfall event has an effect on green roof hydrologic responses. The influence of the magnitude of the rainfall event on green roof hydrological performance is discussed in detail in section 6.3.4.3.

Minimum runoff depths were ranging from 4.61mm for green roof design C, to 8.49mm for green roof design D. The minimum runoff depths were observed for rainfall events with long inter-event dry period and substrates with low water content prior to the event. These rainfall events characteristics were also correlated with the maximum retention values ranging from 61% for the green roof design D and 78% for the green roof design C. The highest retention for green roof designs A, C, D, and E corresponded to their lowest runoff depth. However, the characteristics of the rainfall with the maximum retention for green roof design B do not match the rainfall event with the lowest runoff depth. The highest retention for green roof design B was observed for a high rainfall event (1:100 year). This high retention could occur due to the higher vegetation cover.

The median retention varied from 6% for green roof design A to 11.5% for green roof design E. This means that the green roofs demonstrated low performance for half of the rainfall events. This could be related to inter-event dry period and substrate water content prior to the rainfall. The median IET was 35.5 hours (Table 6.28), which suggests that one and a half days could not have been enough to restore green roof retention capacity after an extreme rainfall event. The median substrate water content was 31.55% (Table 6.28) also suggesting that green roofs did not fully restore their retention capacity prior to the rainfall. No retention was observed for green roof designs B, C, and E, for rainfall events with short IET. Minimum retention for green roof design A and D were recorded for rainfall events with short IET and high substrate water content.

*Table 6.28 Summary statistics of inter-event dry period and substrate water content prior to the tests. This is based on observations green roof trays with vegetation, for all green roof designs.*

Summary Statistics		
Variable	IET (hours)	Water content (%)
<b>Mean</b>	98.13	30.02
<b>Percentiles</b>	Min.	17.00
	25	20.75
	50 (Median)	35.50
	75	59.50
	Max.	412.00

The results of the analysis of overall hydrological performance of the green roofs subjected to the extreme rainfall events agreed in general with the observations made for green roofs exposed to natural conditions. The green roof median retention of extreme rainfall events was low and median runoff depth high. This concurred with the findings of many previous studies stating that larger rainfall events produce a greater runoff depth (Getter et al., 2007) and result in lower retention (Fassman-Beck et al., 2013, Stovin et al., 2012, Carpenter and Kaluvakolanu, 2011, Simmons et al., 2008). However, given certain conditions such as long IET or low substrate water content prior to the rainfall event, the green roofs could retain a large proportion of the extreme rainfall as well. The relation between the inter-event dry period and the green roof retention capacity has been well documented (Villarreal and Bengtsson, 2005, Buccola and Spolek, 2011, Stovin, 2010). The longer the inter-event dry period, the longer the green roof has to restore its stormwater storage capacity (Stovin et al., 2013, Hathaway et al., 2008). The results presented in this study also showed higher retention capacity for the green roofs with higher vegetation cover. Higher vegetation cover results in higher evapotranspiration hence more rainfall can be retained within the green roof substrate (Morgan et al., 2013, Speak et al., 2013a, Czemieli Berndtsson, 2010).

The green roof response to the extreme rainfall events has not been yet, to the knowledge of the author, investigated and documented. Hence, there is little data available for meaningful comparison. There was only one extreme rainfall event

documented, amongst reviewed green roof studies in the UK (Chapter 2). The rainfall event of the return period of 1:61 year was recorded by Nawaz et al. (2015). The retention corresponding to this event was 10.7%. It is within the range of median retention (6% - 11.5%) observed in this study.

It was also anticipated that green roof design could have an effect on green roof responses to the extreme rainfall events. However, Dunn's Kruskal-Wallis multiple comparison test demonstrated no statistically significant differences in runoff depth between the green roofs of different design (Table 6.23). This result could have been obtained due to a large rainfall depths and a finite storage capacity of the green roofs. The quantity of water stored by the green roofs during the extreme rainfall events would not have been large enough, in comparison to the rainfall depth, to cause significant differences in the runoff depths. Influence of other factors such as rainfall event magnitude, vegetation presence or substrate water content, could also result in lack of significant differences in runoff depth between green roof designs.

In contrast to runoff depth analysis, Dunn's Kruskal-Wallis multiple comparison test results indicated statistically significant differences in retention between green roof designs A-B and A-D (for not corrected p-value), and A-E (Table 6.25). Inspection of the retention medians indicated that retention was significantly increased when the conventional drainage layer was replaced with an alternative one and when the conventional substrate material was replaced with Sewage Sludge Pellets. There was no significant difference in retention between control green roof design A and green roof design C, most likely due to similarities in grading, both Crushed Red Brick (green roof design A) and Lytag (green roof design C) are well-graded materials. Although the green roof design did not have an effect on runoff depth, test results clearly demonstrated its influence on stormwater retention ability of green roofs. More detailed analysis of the impact of the material properties on green roof retention capacities is discussed in section 6.3.4.2.

Results of the peak flow reduction analysis contrasted with all published peak flow reduction analysis outcomes. All published studies presented positive peak flow reduction values (Stovin et al., 2012, Fassman-Beck et al., 2013, Carpenter and Kaluvakolanu, 2011, Locatelli et al., 2014, Lee et al., 2015). This study results

demonstrated a high number of the negative peak flow reductions, especially for the green roof design A and design C (for more than a half of the observations). Such a result could have occurred due to the small scale of the green roof trays and very short runoff route resulting in very low concentration time. Numerous studies have reported a peak flow reduction results based on the large scale green roof monitoring. Fassman-Beck et al. (2013) obtained 62-90% of the peak flow reduction based on results from six tested roofs, Carpenter and Kaluvakolanu (2011) noted mean peak flow reduction of 88%. Few researchers documented peak flow reduction values for small scale green roof plots. Stovin et al. (2012) noted 58.67% of peak flow reduction for green roof plot 3m x 1m. Lee et al. (2015) tested small scale, 1m x 1m, green roof plots with peak flow reduction results being in the range between 9% to 29%. The peak flow reductions for small scale plots were smaller than these for the large scale green roofs. However, these results are not directly comparable due to different design of the green roofs, climatic conditions amongst others. The impact of the rainfall size, however, was observed by Locatelli et al. (2014) who reported 40%–78% peak flow reduction for return periods between 0.1 and 1, and 10%–36% for return periods between 5 and 10 years. This indicates that peak flow reduction decreases with increasing rainfall magnitude. Thus, the high number of the negative peak flow reduction values could have occurred due to the small scale of green roof plots and high magnitude of the rainfall events.

The Dunn's Kruskal-Wallis multiple comparison test identified statistically significant differences in peak flow reduction between green roof designs E-A, E-B, E-C, and E-D (for not corrected p-value) (Table 6.27). The peak flow reduction for green roof E was significantly higher than that for all other green roof designs. In the case of green roof design D, the corrected p-value suggests no significant difference in comparison to green roof design E. This could have been due to the fact that both of the green roof designs D and E had a drainage layer made of alternative materials, which could have influenced peak flow reduction.

However, this problem requires further investigation, perhaps additional laboratory tests including rainfall events of a lower return period, which would allow for deeper understanding of this problem.

#### **6.3.4.2 THE EFFECT OF MATERIAL PROPERTIES**

As detailed in the section 6.3.4.1 there were no significant differences in runoff depth between green roofs of different design. However, there were some significant variations in retention between green roof designs. The absence of the significant differences could have been accounted for by the small size samples used in the analysis. Thus, the relationship between the green roof design and its hydrologic responses was assessed in detail. Since green roof designs vary in substrate and drainage layer material type, the effect of green roof construction material properties on hydrological performance was assessed considering two groups of green roof designs. The first group included green roof designs A, B, and C, which differ in substrate material. The second group included green roof designs A, D, and E, which differ in drainage layer material. The relationship between median runoff depth and material properties (described and assessed in Chapter 3) for each green roof design is presented in Figure 6.29 to 6.32. The relationship between median retention and material properties for each green roof design is shown in Figure 6.33 to 6.36.

Figure 6.37 and Figure 6.38 presents time-series of per-event retention for each treatment green roof design B, C, D, and E in comparison to the control green roof design A.

## Runoff depth

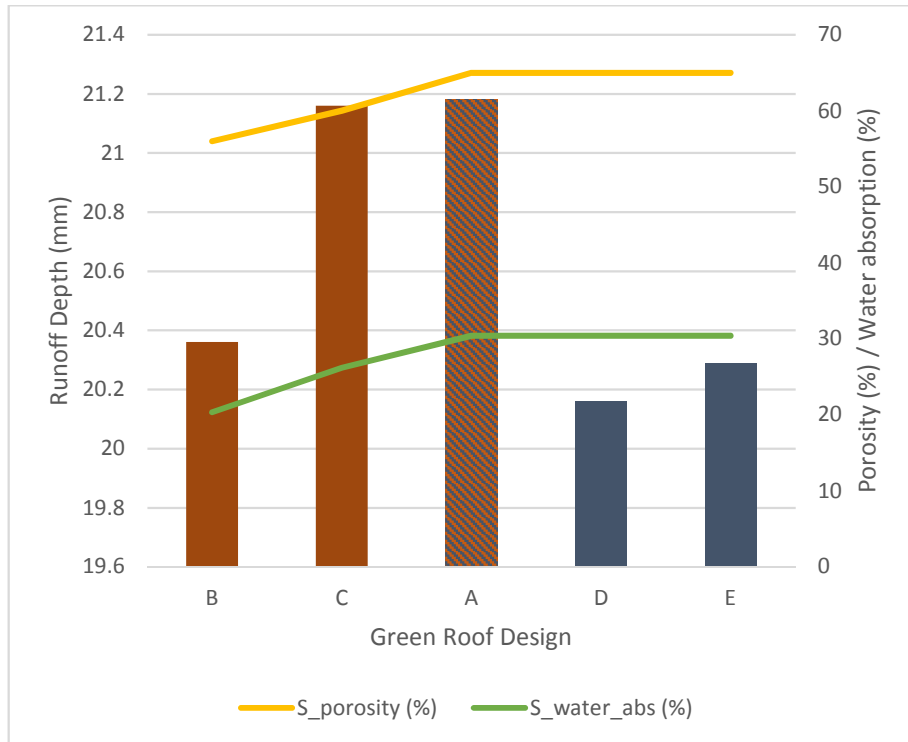


Figure 6.29 Relationship between runoff depth and substrate material porosity ( $S_{porosity}$ ) and water absorption ( $S_{water\_abs}$ ) for green roofs design A-E.

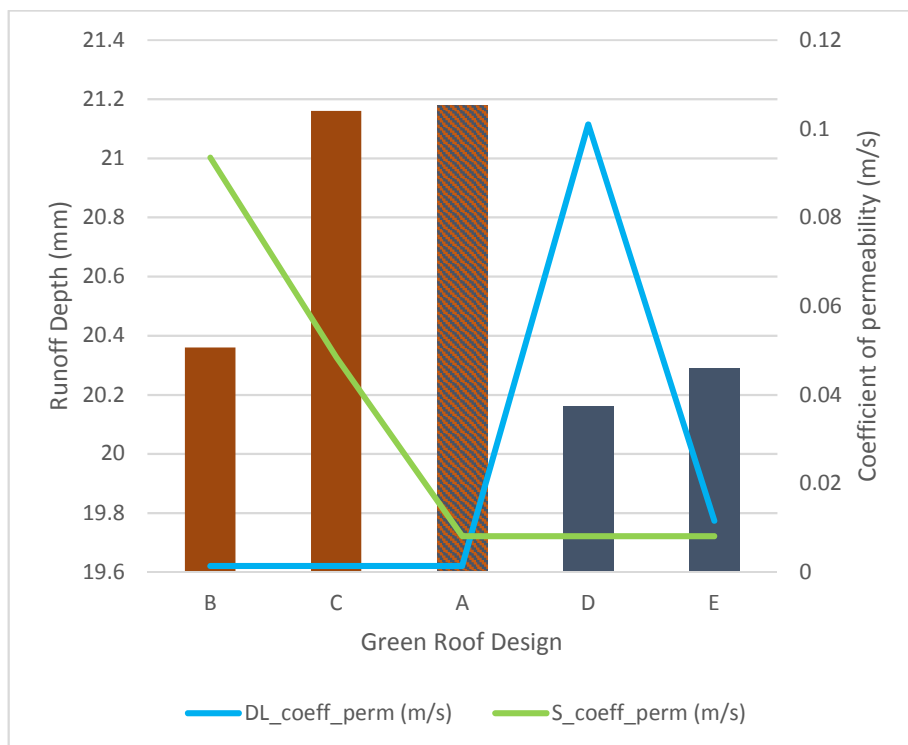


Figure 6.30 Relationship between runoff depth and coefficient of permeability of substrate material ( $S_{coeff\_perm}$ ) and drainage layer material ( $DL_{coeff\_perm}$ ) for green roofs design A-E.

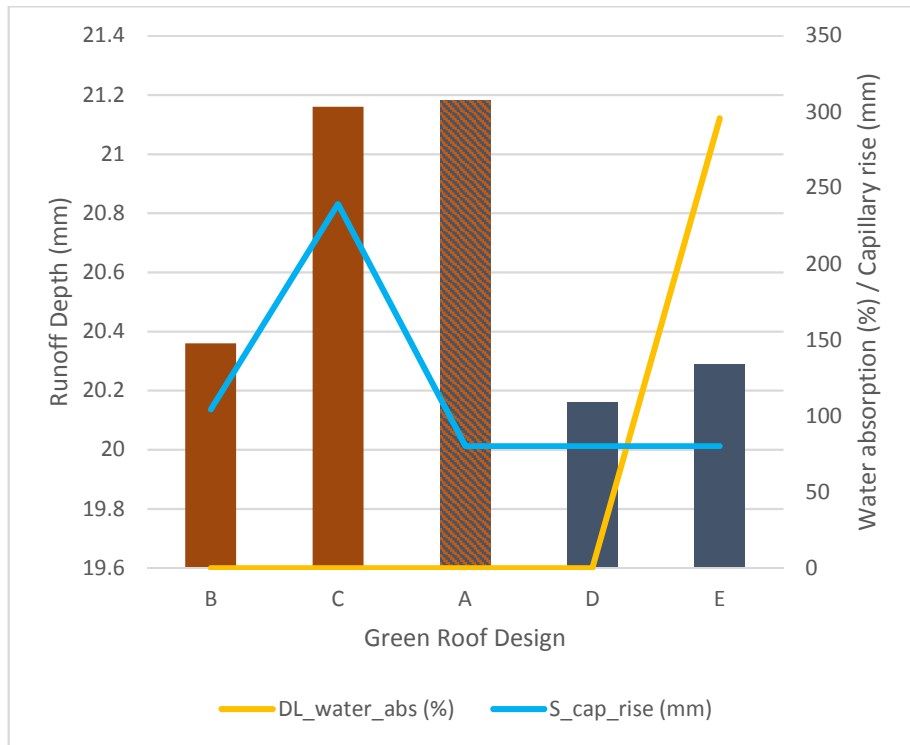


Figure 6.31 Relationship between runoff depth and water absorption of drainage layer material (DL\_water\_abs) and capillary rise of substrate material (S\_cap\_rise) for green roofs design A-E.

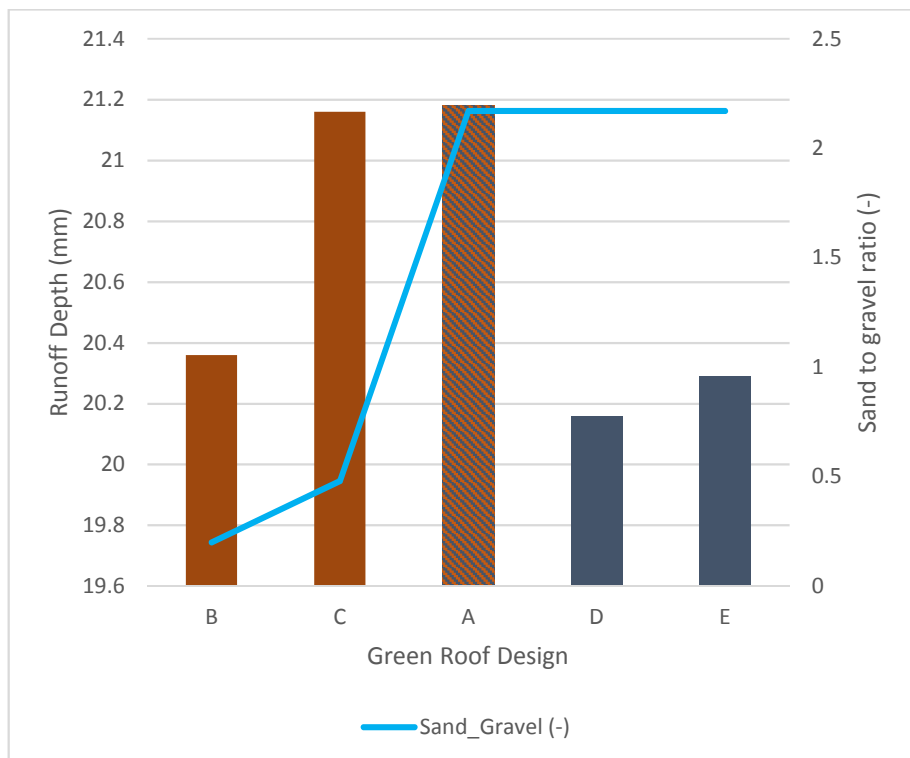


Figure 6.32 Relationship between runoff depth and sand to gravel ratio of substrate material for green roofs design A-E.

## Retention

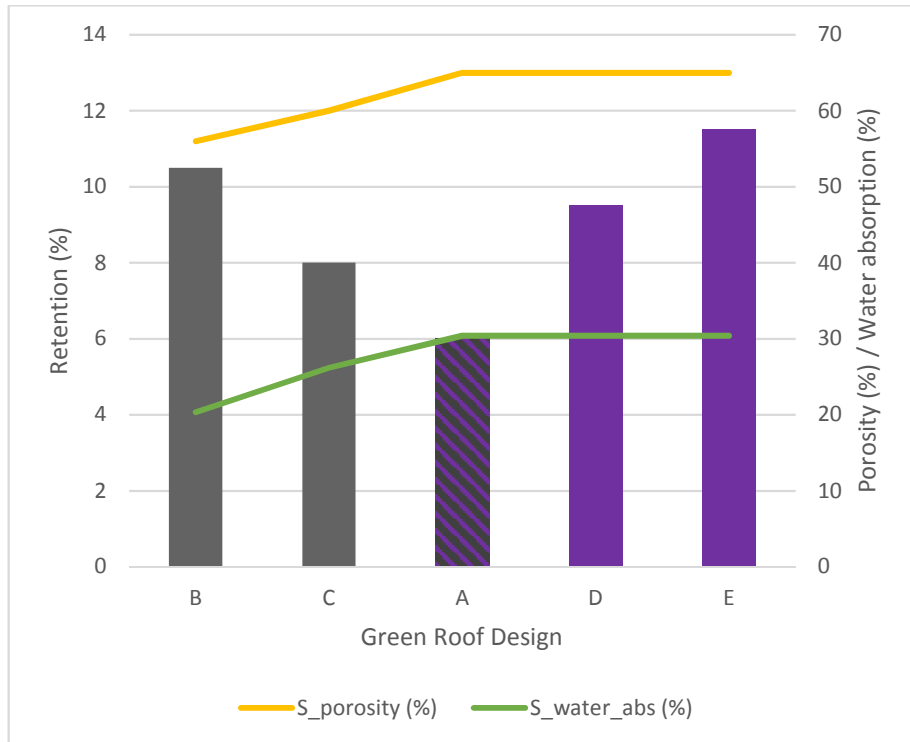


Figure 6.33 Relation between retention and substrate material porosity ( $S_{porosity}$ ) and water absorption ( $S_{water\_abs}$ ) for green roofs design A-E.

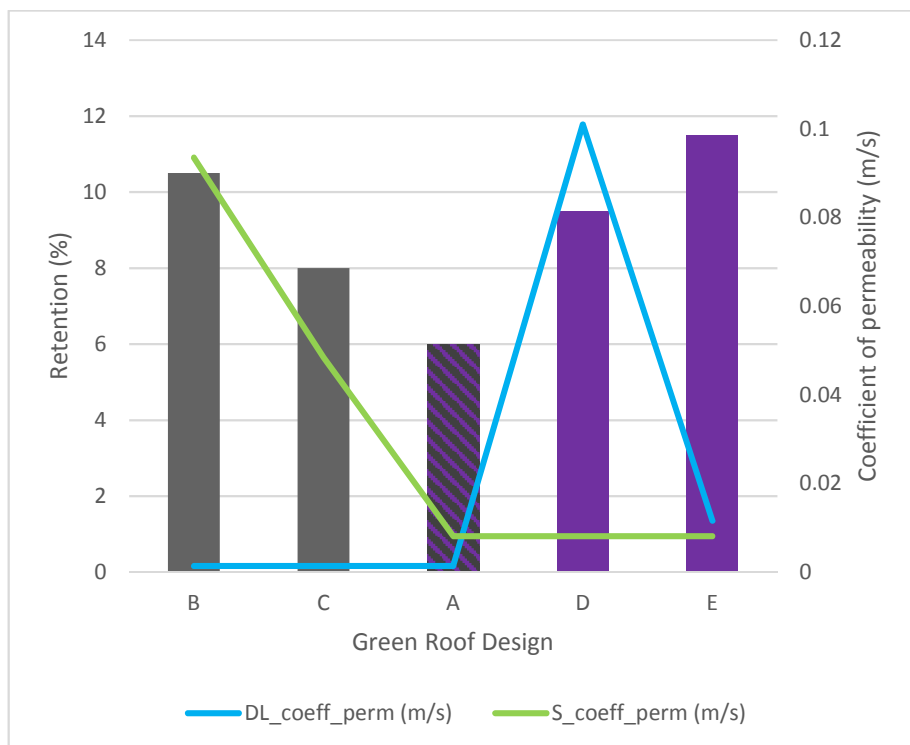


Figure 6.34 Relation between retention and coefficient of permeability of substrate material ( $S_{coeff\_perm}$ ) and drainage layer material ( $DL_{coeff\_perm}$ ) for green roofs design A-E.

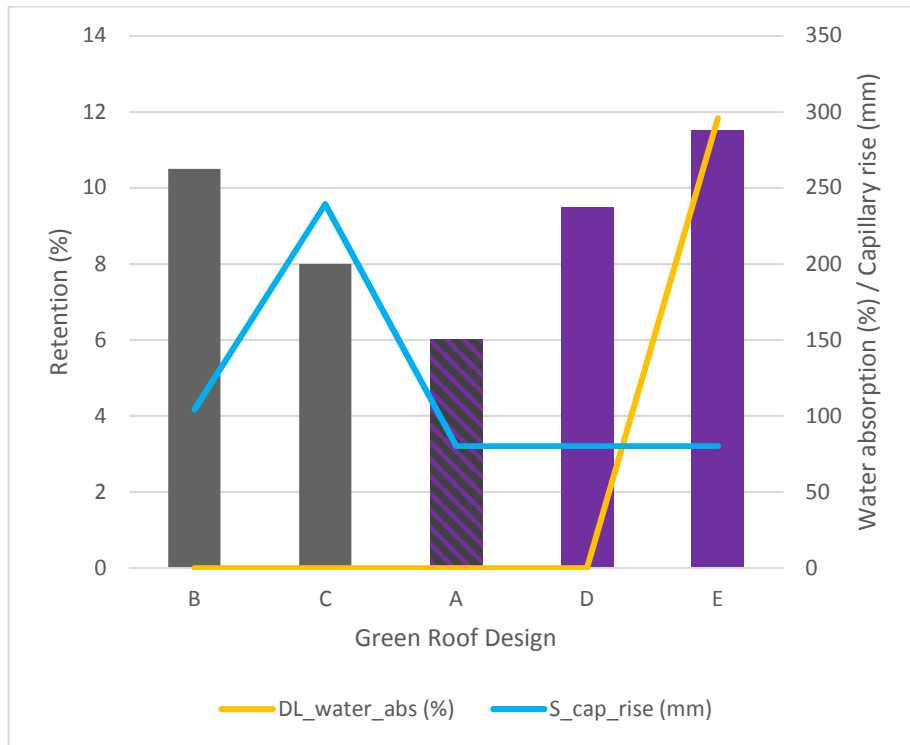


Figure 6.35 Relation between retention and water absorption of drainage layer material (DL\_water\_abs) and capillary rise of substrate material (S\_cap\_rise) for green roofs design A-E.

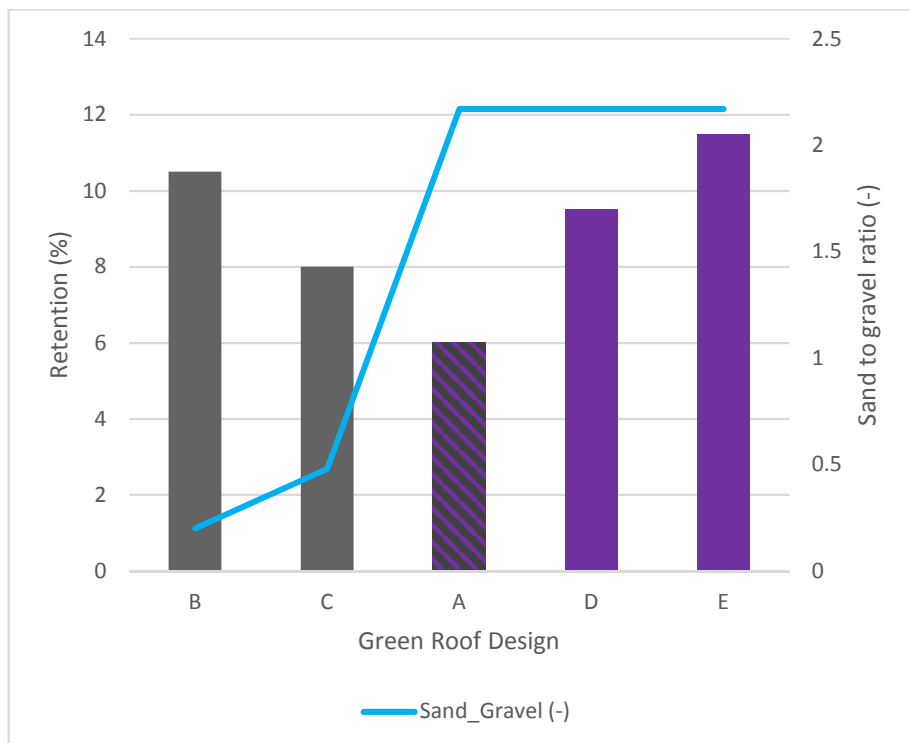


Figure 6.36 Relation between retention and sand to gravel ratio of substrate material for green roofs design A-E.

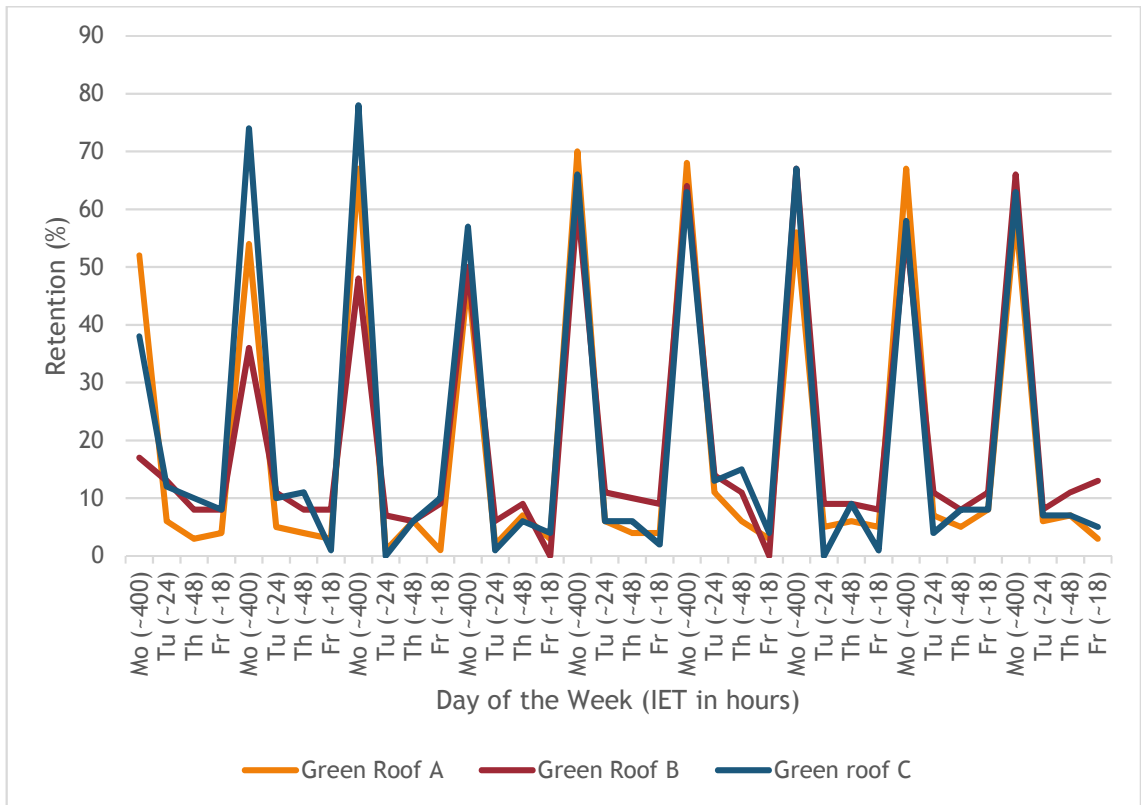


Figure 6.37 Time-series of per-event retention for the control green roof design A and treatment green roof designs B and C.

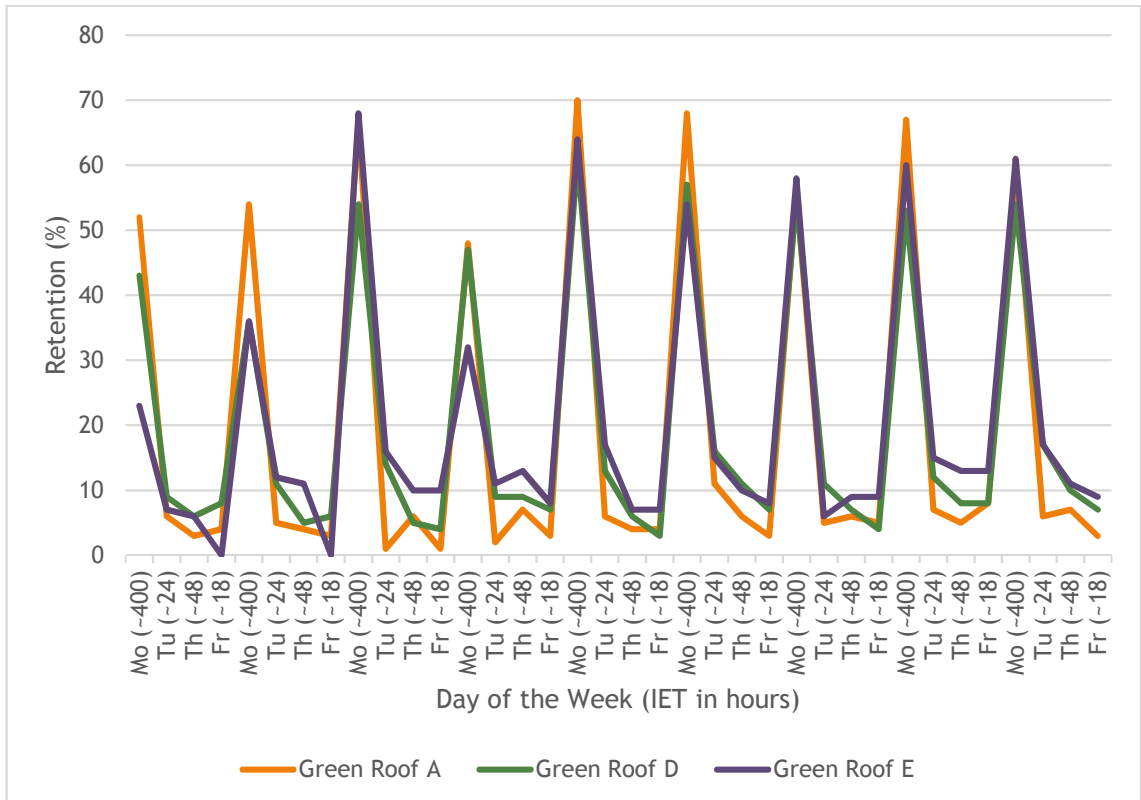
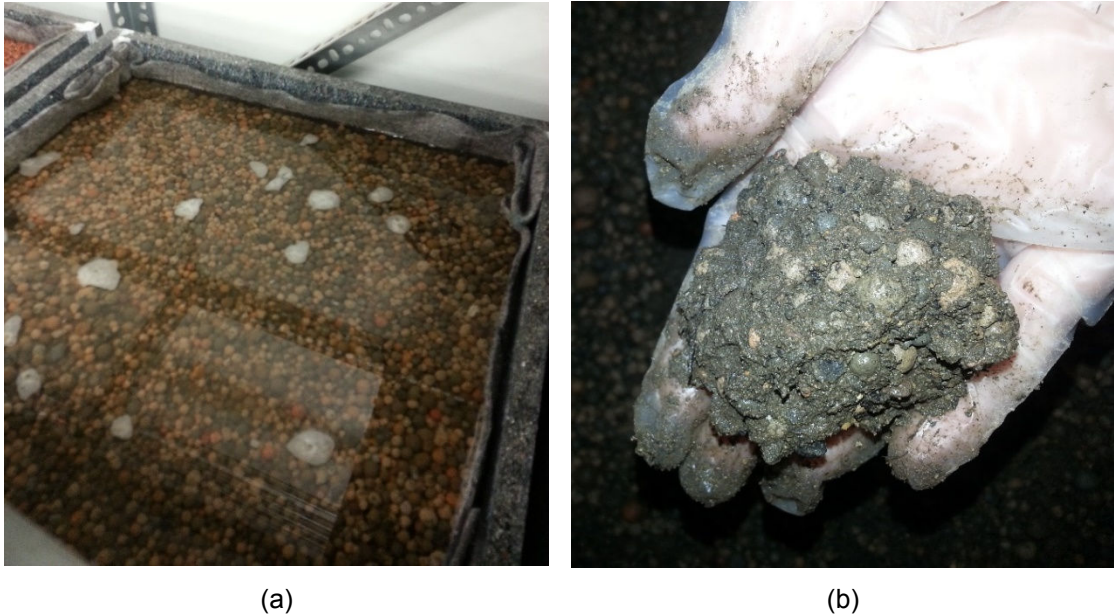


Figure 6.38 Time-series of per-event retention for the control green roof design A and treatment green roofs D and E.

### **Group 1 – substrate material: green roof designs A, B, and C**

Median runoff depths for the green roof designs A and C were similar. Median runoff depth for the green roof design B was about 4% lower than that for green roof design A. The highest median retention was observed for green roof design B (10.5%), followed by green roof design C (8%). The lowest median retention was recorded for green roof design A (6%). Figure 6.29 and Figure 6.33 show that the substrate material of green roof design B (Sewage Sludge Pellets) had the lowest porosity and water absorption in this group of green roof designs. It also had the highest permeability (Figure 6.30 and Figure 6.34), the lowest sand to gravel ratio (Figure 6.32 and Figure 6.36), and capillary rise at similar level to green roof design A (Figure 6.31 and Figure 6.35). Based on the material properties of Sewage Sludge Pellets the runoff depth should be expected to be higher and retention lower for green roof design B in comparison to control green roof design A. The outcome of the laboratory experiment was in direct contrast to the assumptions. Contradicting results were most likely obtained due to the structure of the substrate mix. Sewage Sledge Pellets material was poorly-graded, which resulted in particles segregation leading to deposition of fine particles on the top of the filter geotextile. The deposited fine particles could have created a layer of low permeability, preventing stormwater drainage and resulting in water logging (Figure 6.39). It is crucial that the green roof construction materials are well-graded to avoid material segregation, which can affect green roof performance. It needs to be stressed that material segregation and its consequences for the green roof performance could not be quantified during standard material properties tests. Hence, it is strongly recommended that, as part of the material properties tests, green roof systems are tested under laboratory conditions as well. This will provide a comprehensive understanding of their behaviour.



*Figure 6.39 Green roof design B water-logging problem: (a) green roof tray filled with undrained water (b) lump of deposited low permeability layer.*

Although median runoff depth for green roof design C was similar to the control green roof design A (21.16mm and 21.18mm respectively), the median retention for the green roof design C was higher (8% and 6%, respectively), but not significantly. The substrate material for green roof design C, Lytag, had a much higher capillary rise value (Figure 6.31 and Figure 6.35), which could have had some effect on the increase of green roof C retention capacity. Lower porosity and water absorption (Figure 6.29 and Figure 6.33) and higher coefficient of permeability (Figure 6.30 and Figure 6.34) would have had an opposite effect on stormwater retention of green roof design C.

The control green roof design A and green roof designs B and C, made with alternative substrate materials, demonstrated comparable retention capacity observed after a two-week dry period (retention peaks on Mondays, Figure 6.37). However, the retention ability significantly drops for subsequent extreme rainfall events (Tuesdays, Thursdays, and Fridays). For many subsequent rainfall events the retention of green roof A and C dropped to zero, especially on Tuesdays and Fridays. The rainfall events simulated on these days had short inter-event dry period of 24 and 18 hours, respectively. Clearly, these green roof designs did not restore their retention abilities fast enough to accommodate stormwater during the subsequent extreme rainfall event.

## **Group 2 – drainage layer material: green roof designs A, D, and E**

Looking at the green roofs with altered drainage layer, it was noticeable that both green roof designs D and E had lower median runoff depth (Figure 6.29) and higher retention than control green roof design A (Figure 6.33). However, only an increase in retention for green roof design E was statistically significant. This could be accounted by the extremely high water absorption of Wool-rich Carpet Shred. The drainage material properties do not seem to explain the differences in retention between green roof design D and A. The drainage layer of green roof design D (Granulated Rubber) had much higher coefficient of permeability, which would rather increase runoff than reduce. However, analysing time-series of per-event retention plot (Figure 6.38), the differences in retention patterns between green roof design A-D and A-E are noticeable.

All green roofs restored their retention ability after a two-week dry period. High retention was observed on Mondays, the first day of the test series after the break (peak values on graph, Figure 6.38). For the subsequent rainfall events (Tuesday, Thursday, and Friday) the retention for all green roofs dropped considerably. However, green roofs with drainage layers made of alternative materials had higher retention abilities for subsequent rainfall events than the control green roof design A. Green roof A was fitted with conventional “egg-box” shape drainage layer. This drainage layer accumulates water until is full. Once the water storage capacity is exhausted, any additional stormwater (eg. from next rainfall event) is discharged with none being retained. This type of drainage layer initially provides significant storage for stormwater but this falls to zero when filled. In contrast to the control drainage layer, tested alternative materials drain and restore their stormwater storage capacity prior the next rainfall event. Therefore, whilst initial storage ability is lower in comparison to control drainage layer, it provides more uniformly distributed stormwater storage capacity over multiple rainfall events. This response of granulated/fibre-like drainage layers to subsequent extreme rainfall events is more desirable in stormwater management. This type of drainage layer should be considered for use for drainage layer construction if a key objective of the green roof design is stormwater control.

The lowest median retention was observed for the control green roof design A. All other green roofs demonstrated higher median retention, which showed that green roofs made of alternative materials could perform as well as, or better than conventional green roofs.

Numerous researchers have investigated the effect of the material type on green hydrological performance (Stovin et al., 2015, Fassman-Beck et al., 2013, Simmons et al., 2008, Voyde et al., 2010, Graceson et al., 2013, Mickovski et al., 2013, Beck et al., 2011). However, only few assessed the influence of the properties of these materials on green roof hydrologic responses. Graceson et al. (2013) reported significant relationship between water holding capacity and retention of the green roofs but only when low water holding capacity materials were included in the model. In this study, the significance of the high retention of the green roof design E was possibly caused by extremely high water absorption of the Wool-rich Carpet Shred. The lower differences in water absorption of substrate materials did not affect significantly retention of green roof designs A, B, and C. It is, therefore, possible that only high differences in the water holding capacity or water absorption would result in a significant change in the green roof retention. Fassman-Beck et al. (2013) and Stovin et al. (2015) indicated the influence of material properties such as water holding capacity, permeability or porosity on hydrological performance of green roofs. However, they did not present detailed analysis of the relationship between these material properties and hydrologic responses of green roofs.

#### **6.3.4.3 THE EFFECT OF RAINFALL MAGNITUDE**

This section aims to explore the effect of the rainfall magnitude on overall hydrological performance of green roofs as well as on the hydrologic responses of each green roof design. The exploratory data analysis was carried out to determine the nature of data distribution. Summary statistics of the green roof hydrological performance data in relation to the rainfall magnitude are presented in Table 6.29 (runoff depth) and Table 6.31 (retention). Data distributions for green roof hydrological performance categorised by rainfall magnitude are presented in Figure 6.40 (runoff depth) and Figure 6.41 (retention).

The hydrological performance of the green roofs related to the rainfall magnitude was assessed considering two groups of rainfall events. The first group included

rainfall events of 1:30, 1:50 and 1:100 return period. The second group included merged rainfall events.

It was assumed that the rainfall magnitude would influence the green roof hydrological performance. Based on this assumption, the following null hypothesis was generated: there is no significant difference in green roof hydrological performance (runoff depth and retention) when subjected to rainfall events of different magnitude.

The hypothesis was tested using non-parametric Dunn's Kruskal-Wallis multiple comparison test with Bonferroni correction. The results for all green roof designs combined are presented in Table 6.29 and Table 6.30, and for each green roof design in Table 6.31 and Table 6.32.

## Runoff depth

Table 6.29 Summary statistics of runoff depth data in relation to rainfall event magnitude. Statistically significant differences are represented by *p*-values obtained from Dunn's Kruskal-Wallis multiple comparison test results with Bonferroni correction. Highlighted numbers demonstrate a statistically significant difference in runoff depth between rainfall events of different return period. Italicised numbers show a statistically significant difference between green roof designs based on uncorrected *p*-value.

Summary Statistics and Dunn's Kruskal-Wallis multiple comparison test results					
Return period		1 in 30	1 in 50	1 in 100	Merged
<b>N</b>		45	45	45	45
<b>Mean</b>		16.23	16.70	19.64	42.15
<b>Median</b>		18.36	19.45	23.49	40.12
<b>Std. Deviation</b>		4.61	5.5	6.61	4.56
<b>Percentiles</b>	<b>Min.</b>	4.61	6.49	8.6	36.28
	<b>25</b>	13.02	11.00	11.72	38.61
	<b>50</b>	18.36	19.45	23.49	40.12
	<b>75</b>	19.29	20.74	24.55	47.41
	<b>Max.</b>	21.08	22.60	26.53	50.70
<b>p-value</b>	<b>1 in 30</b>	-	1.000	5.64 x 10 <sup>-3</sup>	4.93 x 10 <sup>-21</sup>
	<b>1 in 50</b>		-	0.098 / 0.016*	2.12 x 10 <sup>-17</sup>
	<b>1 in 100</b>			-	1.91 x 10 <sup>-9</sup>
	<b>Merged</b>				-
* Uncorrected p-value <input type="checkbox"/> Null hypothesis of no statistically significant difference rejected (p<0.05)					

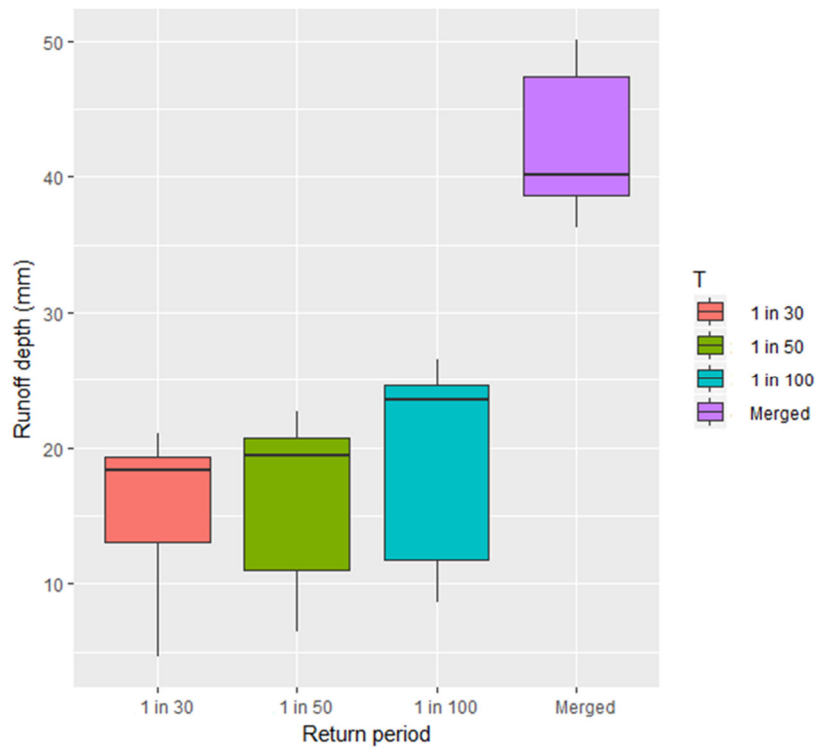


Figure 6.40 Stormwater runoff depth data distribution categorised by the rainfall magnitude.

Table 6.30 Median runoff depth for selected green roofs in relation to rainfall magnitude and p-values from Dunn’s Kruskal-Wallis multiple comparison test results with Bonferroni correction. Highlighted numbers demonstrate a statistically significant difference in runoff depth between rainfall events of different return period.

Dunn’s Kruskal-Wallis multiple comparison test – Runoff Depth (mm)						
Green roof design	A	B	C	D	E	
<b>1 in 30</b>	19.45	18.24	18.36	18.32	17.98	
<b>1 in 50</b>	20.72	19.45	20.74	19.17	18.62	
<b>1 in 100</b>	24.55	23.49	24.51	23.17	22.39	
<b>Merged</b>	41.31	39.51	41.07	39.92	39.43	
<b>p - value</b>	<b>1in30 – 1in50</b>	1.00	1.00	1.00	1.00	1.00
	<b>1in30 – 1in100</b>	0.56	0.99	0.51	0.67	1.00
	<b>1in30 – Merged</b>	6.95 x 10 <sup>-5</sup>	1.40 x 10 <sup>-4</sup>	5.65 x 10 <sup>-5</sup>	1.16 x 10 <sup>-4</sup>	3.08 x 10 <sup>-4</sup>
	<b>1in50 – 1in100</b>	1.00	1.00	1.00	1.00	1.00
	<b>1in50 – Merged</b>	9.37 x 10 <sup>-4</sup>	8.53 x 10 <sup>-4</sup>	1.12 x 10 <sup>-3</sup>	5.41 x 10 <sup>-4</sup>	3.72 x 10 <sup>-4</sup>
	<b>1in100 – Merged</b>	0.04	0.02	0.04	0.04	0.03
<span style="background-color: #cccccc; border: 1px solid black; display: inline-block; width: 15px; height: 10px; vertical-align: middle;"></span> Null hypothesis of no statistically significant difference rejected (p<0.05)						

## Retention

Table 6.31 Summary statistics of retention data in relation to rainfall event magnitude. Statistically significant differences are represented by *p*-values obtained from Dunn's Kruskal-Wallis multiple comparison test results with Bonferroni correction. Highlighted numbers demonstrate a statistically significant difference in retention between rainfall events of different return period. Italicised numbers show a statistically significant difference between green roof designs based on uncorrected *p*-value.

Summary Statistics and Dunn's Kruskal-Wallis multiple comparison test results					
Return Period		1 in 30	1 in 50	1 in 100	Merged
<b>N</b>		45	45	45	45
<b>Mean</b>		20.84	24.04	25.49	8.07
<b>Median</b>		10.00	11.00	11.00	8.00
<b>Std. Deviation</b>		22.40	24.87	25.07	2.64
<b>Percentiles</b>	<b>Min.</b>	0	0	0	3
	<b>25</b>	6	6	7	6
	<b>50</b>	10	11	11	8
	<b>75</b>	36	50	56	10
	<b>Max.</b>	78	70	67	15
<b>p - value</b>	<b>1 in 30</b>	-	1.000	1.000	<i>0.25 / 0.04*</i>
	<b>1 in 50</b>		-	1.000	<i>0.18 / 0.03*</i>
	<b>1 in 100</b>			-	0.03
	<b>Merged</b>				-
* Uncorrected p-value <input type="checkbox"/> Null hypothesis of no statistically significant difference rejected ( $p < 0.05$ )					

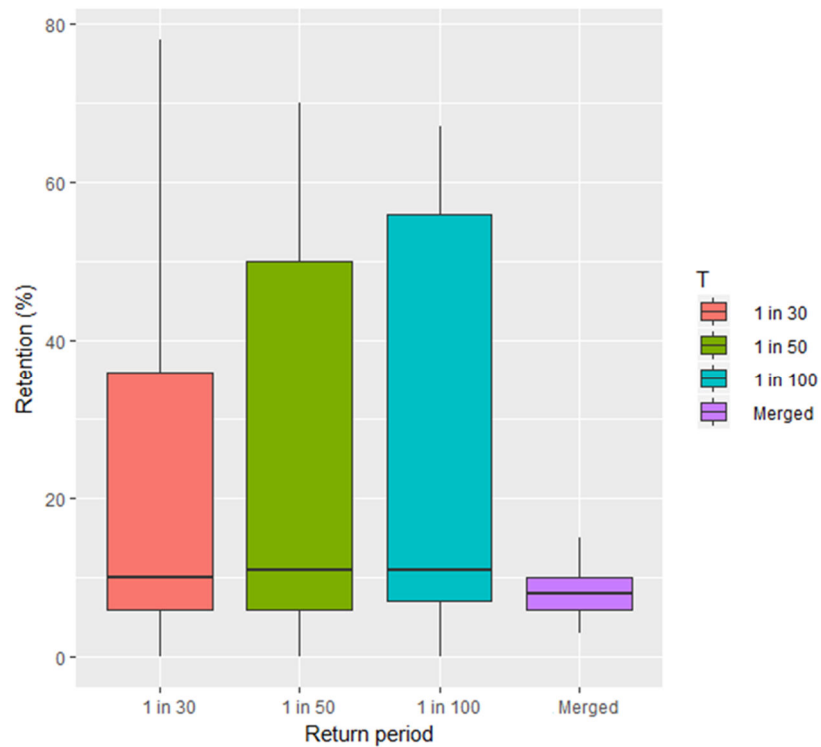


Figure 6.41 Stormwater retention data distribution categorised by the magnitude of rainfall event.

Table 6.32 Median retention for selected green roofs in relation to rainfall magnitude and p-values from Dunn's Kruskal-Wallis multiple comparison test results with Bonferroni correction. Highlighted numbers demonstrate a statistically significant difference in retention between rainfall events of different return period.

Dunn's Kruskal-Wallis multiple comparison test – Retention (%)						
Green roof design	A	B	C	D	E	
1 in 30	5	11	10	11	12	
1 in 50	6	11	6	13	15	
1 in 100	7	11	7	12	15	
Merged	6	9	8	7	10	
p - value	1in30 – 1in50	1.00	1.00	1.00	1.00	1.00
	1in30 – 1in100	1.00	1.00	1.00	1.00	1.00
	1in30 – Merged	1.00	1.00	1.00	0.65	1.00
	1in50 – 1in100	1.00	1.00	1.00	1.00	1.00
	1in50 – Merged	1.00	1.00	1.00	0.33	1.00
	1in100 – Merged	1.00	0.37	1.00	0.25 / 0.04*	0.67
* Uncorrected p-value						
Null hypothesis of no statistically significant difference rejected (p<0.05)						

### **Rainfall events of the return period of 1:30, 1:50 and 1:100 year**

Analysis of the categorised by rainfall magnitude data distribution presented high negative skewness for runoff depth (Figure 6.40) and high positive skewness for retention (Figure 6.41) for all rainfall events. This confirmed the high concentration of observation of high runoff depth and low retention.

As expected, the lowest median runoff depth was for 1:30 year rainfall events, the highest median runoff depth was observed for 1:100 year rainfall events (Table 6.29). The median retention, however, did not follow the expected pattern. A higher median retention was observed for the group of 1:100 and 1:50 year rainfall events (11%). A lower median retention was recorded for 1:30 year rainfall events (Table 6.31). It was unexpected because the highest median runoff depth was observed for 1:100 rainfall events, which should result in lower retention. One could also noticed an increase in the range of the 3<sup>rd</sup> quartile with an increase of the rainfall magnitude (Figure 6.41). This increase could have occurred due to a higher vegetation cover. The 1:100 year rainfall events were simulated during the three last weeks of the testing programme (Table 6.8) when all green roof trays had above 70% of an average vegetation cover (Figure 6.15). Higher vegetation cover results in greater evapotranspiration, thus more rainfall can be retained by green roof (Morgan et al., 2013, Speak et al., 2013a, Czemieli Berndtsson, 2010).

Dunn's Kruskal-Wallis multiple comparison test showed that the differences in retention were not significant for all magnitudes of rainfall events. In the case of runoff depth there was no significant difference between 1:30 and 1:50 year rainfall events. However, the median runoff depth for rainfall events of 1:100 year return period was significantly higher than these for 1:30 year and 1:50 year (for uncorrected p-value) rainfall events. The depth of a 1:100 rainfall event was much greater than these of 1:50 or 1:30 year rainfall events. Thus, the runoff depth corresponding to 1:100 year rainfall event was expected to be higher due to the limited storage capacity of the green roof. Larger rainfall event would generate a greater proportion of stormwater runoff (Getter et al., 2007).

Analysis of the effect of rainfall magnitude on the performance of the individual green roof designs demonstrated no significant differences in runoff depth and

retention. The absence of the significance could have been due to the small size of the samples.

The retention performance of each green roof design with regards to rainfall event magnitude reflected the overall retention data analysis (Table 6.24). The lowest retention was observed for green roof design A and the highest for green roof design E. There was no clear pattern in retention between green roof designs in regards to rainfall magnitude. The retention for green roof design A and E increased with increase of rainfall magnitude, as opposed to green roof design C. In the case of green roof design B, the median retention remained constant for all rainfall magnitudes. However, it need to be stressed that these differences were not significant.

The author found no published results showing the differences in green roof hydrological responses in relation to extreme rainfall events. In general, the results of this study agreed with observation that stated that the runoff increases with rainfall depth (Getter et al., 2007, Nawaz et al., 2015). A large number of observations, included in this study, were that of short IET and high substrate water content prior to the rainfall event. Thus, the substrates were of high saturation degree. As a result, high volumes of gravitational water entering the soil were subsequently discharged. The higher the magnitude of the rainfall the higher the runoff depth discharged.

However, the results of the retention analysis contrasted with these published stating that larger rainfall events result in lower retention (Fassman-Beck et al., 2013, Stovin et al., 2012, Carpenter and Kaluvakolanu, 2011, Simmons et al., 2008). The median retention did not increase significantly with the increase of the rainfall magnitude. Moreover, it was the same for rainfall events of return period of 1:50 and 1:100 year.

### **Merged rainfall events**

The group of merged rainfall events included rainfalls of the depth twice larger than these in the group of not merged (single) rainfall events. Subsequently, the runoff depth produced by these rainfalls were much greater comparing to single rainfall events (Figure 6.40). All of the observations in merged rainfall events group were of IET being about 48 hours. This time could not have been long

enough to allow green roofs to restore their stormwater retention capacity resulting in their low retention. Dunn's Kruskal-Wallis multiple comparison test showed significant differences between the group of merged rainfall events and other groups in runoff depth (Table 6.29) and retention (for uncorrected p-value) (Table 6.31). This was likely due to the merged rainfall event characteristics such as constant IET or high rainfall depth.

The case of merged rainfall events points at the problems emerging from combining rainfall events and its effect on retention values. Merging rainfalls results in increased duration and rainfall depth and consequently in changed retention (as a percentage of rainfall depth) and different return period. Hence, green roof responses to merged rainfall events cannot be directly compared with those to non-merged rainfalls. In author's view, analysis based on the merged rainfall events do not accurately reflect green roof performance. Clearly, there is a need for some general, universal assumptions to be set, in order to support the development of a universal model to predict green roof retention abilities or to quantify the runoff.

#### **6.3.4.4 SUMMARY**

The green roof hydrological behaviour (runoff depth, retention, peak flow reduction) was analysed for the green roofs of different design. The analysis was performed taking under consideration the effect of green roof design, green roof construction material properties, and magnitude of rainfall event. The following observations were made:

- Green roofs subjected to extreme rainfall events retained on average (median) from 6% to 11.5% depending on green roof design. The per-event retention ranged between 0% and 78% for all green roof designs. The result revealed that all green roofs, conventional and made of alternative materials could contribute to stormwater management during extreme rainfall events specific to the UK (London) climatic conditions.
- The runoff depth did not differ significantly between green roof designs, as opposed to the retention, which was significantly lower (for uncorrected p-value) for conventional green roof design A.
- Green roofs made of alternative materials perform as well as or better than the conventional green roof, with respect to retention.

- There was no clear relationship between green roof construction material properties and green roof hydrological performance in the case of substrate.
- Green roofs with altered drainage layer performed better than the conventional green roof. However, there was no clear relation between hydrological performance of these green roofs and the properties of the materials from which they were made. The only factor clearly differentiating control drainage layer from treatment drainage layers was material structure. Granulated/fibre-like materials showed higher retention abilities for subsequent extreme rainfall events. Hence, they should be investigated further for their use as a drainage layer, when the objective for green roof design is stormwater management.
- Granulate materials used as substrate layers should be well-graded to avoid material segregation and formation of reduced permeability layer, which could lead to water-logging on the roof. Water-logging would increase green roof weight, lead to damage of the green roof layers, increase the risk of leakage and as a result damage supporting structure.
- The maximum runoff depth and minimum retention was observed for green roofs with high water content, which provided evidence for a correlation between substrate water content prior to the rainfall event and hydrological performance of the green roofs. Substrate with lower water content has more capacity to accommodate additional water volumes since their voids are only partially filled with water.
- Contrary to expectation, peak flow reduction analysis demonstrated a high number of negative observations, which could not be fully explained in this research. Potential reasons include:
  - the small scale of the green roofs resulting in short distances of stormwater flow to outlet,
  - the nature of the runoff as a response to extreme rainfall events, have thus far not been investigated

The higher value of peak flow reduction is very undesirable for green roofs installed as stormwater management tool. Further investigation is needed to fully understand peak flow reduction abilities of green roofs subjected to extreme rainfall events.

- Runoff depth increased with rainfall magnitude for all green roof designs, but not significantly. There were also no significant differences in retention for all green roof designs in relation to rainfall event magnitude. Any differences observed may have been due to green roofs being more sensitive to other factors such as changes in vegetation cover, IET or substrate water content.

The analysis of the hydrological performance of green roofs demonstrated that green roofs do have an ability to mitigate stormwater, even when subjected to extreme rainfall events specific to UK (London) climatic conditions. Moreover, green roofs made of alternative materials performed comparably or better than the conventional green roofs. These are promising results showing that green roofs made with alternative materials could be possibly utilised as stormwater management tools and also contribute to recycling of waste materials. However, they should be further investigated as a full-scale green roof system to confirm their performance.

### **6.3.5 PRELIMINARY MULTIPLE LINEAR REGRESSION ANALYSIS**

This section presents the analysis of the relationship between hydrological performance characteristics such as runoff depth and retention and factors related to rainfall and laboratory microclimate conditions, green roof design, properties of the green roof construction materials, and vegetation cover. The initial predictor variables were as follows:

- rainfall characteristics: rainfall depth, IET
- soil and laboratory microclimate conditions: substrate water content prior to the rainfall, air temperature, air pressure
- substrate material properties: sand to gravel ratio, particle density, saturated density, bulk density, porosity, capillary rise, water absorption, coefficient of permeability
- drainage layer materials: saturated density, bulk density, water absorption, coefficient of permeability
- vegetation cover

The relationships between response and predictor variables were assessed using multiple linear regression analysis.

The analysis is based on a unique set of 180 observations of vegetated green roofs responses to extreme rainfall events specific to UK (London) climatic conditions. Hence, the models are limited to rainfall events of high magnitude and to the laboratory microclimate conditions with air temperatures ranging from 18°C to 22.5°C and median temperature 21°C. The selection of final predictor variables significant to the model was carried out using automatic stepwise process.

Table 6.33 summarises the results of multiple linear regression analysis for runoff depth, while Table 6.34 shows the results for retention. Figure 6.42 and Figure 6.43 present graphical verification of regression analysis assumptions for runoff depth and retention analysis, respectively.

### Runoff depth

*Table 6.33 Summary of multiple linear regression predicting runoff depth using rainfall depth [RD], inter-event time [IET], temperature [TEMP], substrate water content prior rainfall event [WC], substrate porosity [SPOR], drainage layer water absorption [DLWA] and substrate sand to gravel ratio [SSG] (N=180).*

Predictor	$\beta$	p-value
RD	<b>0.957</b>	<b>&lt;2.00 x10<sup>-16</sup> ***</b>
IET	-0.025	<2.00 x10 <sup>-16</sup> ***
TEMP	0.423	1.04 x10 <sup>-2</sup> *
WC	0.332	3.59 x10 <sup>-7</sup> ***
SSG	2.888	8.57 x10 <sup>-4</sup> ***
SPOR	-87.105	2.28 x10 <sup>-4</sup> ***
DLWA	-0.004	1.46 x10 <sup>-2</sup> *
<b>Linear Regression Model</b>	RUNOFF = 0.957*RD - 0.025*IET + 0.423*TEMP + 0.332*WC + 2.888*SSG - 87.105*SPOR -0.004*DLWA + 30.093  R <sup>2</sup> =0.969, Adjusted R <sup>2</sup> = 0.968, p< 2.2 x10 <sup>-16</sup>	
Significance codes: 0 '***' 0.001 '**' 0.01 '*' 0.05 '.' 0.1 ' ' 1.0		

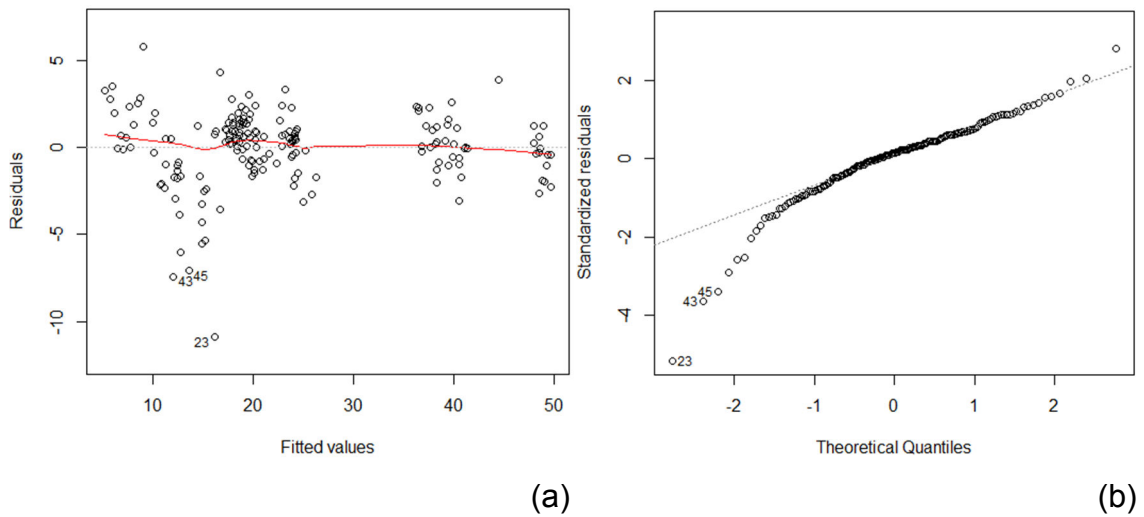


Figure 6.42 Linear regression model assumptions graphical tests (a) residuals vs. fitted values (b) residuals Q-Q plot.

## Retention

Table 6.34 Summary of multiple linear regression predicting retention using rainfall depth [RD], inter-event time [IET], temperature [TEMP], substrate water content prior rainfall event [WC], substrate porosity [SPOR], drainage layer water absorption [DLWA] and substrate sand to gravel ratio [SSG] (N=180).

Predictor	$\beta$	p-value
RD	-0.210	$3.17 \times 10^{-3}$ **
IET	0.100	$<2.00 \times 10^{-16}$ ***
TEMP	-1.428	$1.60 \times 10^{-5}$ ***
WC	-3.239	$9.60 \times 10^{-7}$ ***
SSG	-12.627	$1.11 \times 10^{-3}$ **
SPOR	386.696	$2.54 \times 10^{-4}$ ***
DLWA	0.012	$7.17 \times 10^{-2}$ •
<b>Linear Regression Model</b>	$\text{RET} = -0.210 \cdot \text{RD} + 0.100 \cdot \text{IET} - 1.428 \cdot \text{WC} - 3.239 \cdot \text{TEMP} - 12.627 \cdot \text{SSG} + 386.696 \cdot \text{SPOR} + 0.012 \cdot \text{DLWA} - 97.119$ $R^2=0.814, \text{ Adjusted } R^2 = 0.807, p < 2.2 \times 10^{-16}$	
Significance codes: 0 '***' 0.001 '**' 0.01 '*' 0.05 '.' 0.1 ' ' 1.0 ''		

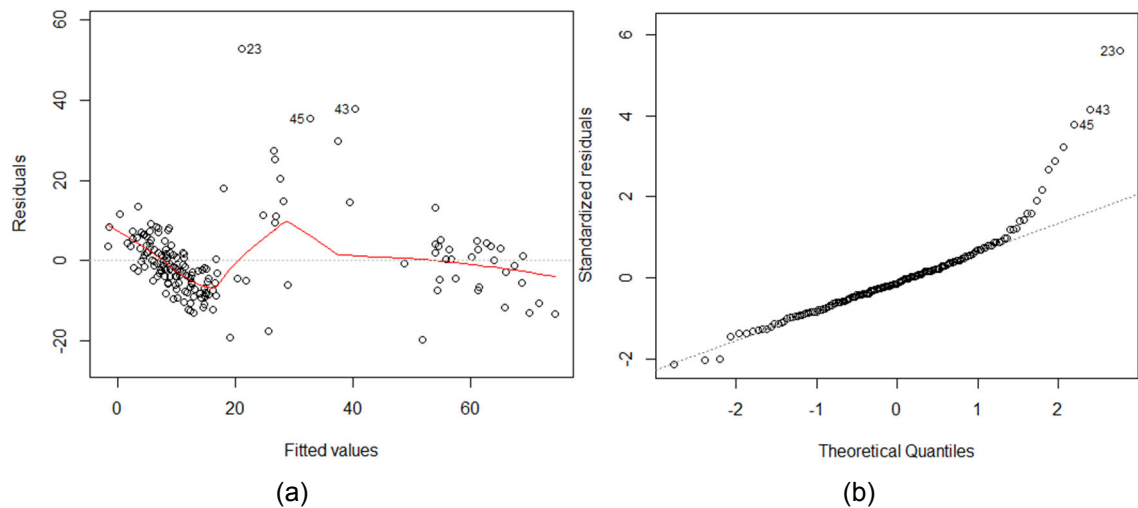


Figure 6.43 Retention linear regression model assumptions graphical tests (a) residuals vs. fitted values (b) residuals Q-Q plot.

The preliminary multiple linear regression model predicting runoff depth [RUNOFF] included following predictors: rainfall depth [RD], inter-event time [IET], temperature [TEMP], substrate water content prior rainfall event [WC], substrate porosity [SPOR], drainage layer water absorption [DLWA] and substrate sand to gravel ratio [SSG] (Table 6.33).

The preliminary runoff depth prediction model was characterised by high adjusted coefficient of determination  $R^2=0.865$ , indicating that 86.5% of the total variations in runoff depth was explained by the model. The significance of the model was also high ( $p < 2.2 \times 10^{-16}$ ). The model showed that the following predictor variables were highly significant for runoff depth prediction: rainfall depth (positive relationship), IET (negative relationship), water content (positive relationship), substrate sand to gravel ratio (positive relationship) and porosity (negative relationship) (all variables had a significance level of  $p \sim 0.00$ ). The model also included water absorption of the drainage layer (negative relationship) and temperature but their significance to the model was lower ( $p=0.015$  and  $p=0.010$ , respectively).

To validate the model the assumptions of independence of errors and normal distribution of errors were tested. The assumptions were validated by investigating two plots: residuals vs. fitted values and Q-Q plot of residuals (Figure 6.42). The residuals vs. fitted values plot demonstrates random distribution of residuals throughout the range of fitted values. The Q-Q plots

presented non-normal distribution of data although residuals partially fit the normal line.

The second model developed was a preliminary multiple linear regression model to predict retention. The model was developed using rainfall depth [RD], inter-event time [IET], temperature [TEMP], substrate water content prior rainfall event [WC], substrate porosity [SPOR], drainage layer water absorption [DLWA] and substrate sand to gravel ratio [SSG] (Table 6.34).

The adjusted coefficient of determination,  $R^2$  was 0.814, which suggests that 81.4% of the retention variations can be explained by regression model. The most significant predictor variables were: IET (positive relationship), temperature (negative relationship), substrate water content (negative relationship) and substrate porosity (negative relationship). The least significant factor to the model was water absorption of the drainage layer ( $p=0.072$ ).

The preliminary multiple linear regression model to predict regression failed the assumptions of independence of the errors and their normal distribution (Figure 6.43). The residuals were randomly situated for higher retentions, however they also highly concentrated for lower values. The random distribution of residuals around zero was expected. The Q-Q plots confirmed non-normal distribution of residuals.

Contrary to expectation, none of the models included vegetation cover, suggesting that other factors are more significant to runoff depth or retention changes. Both models, however, included water absorption of drainage layer confirming previous observation of significantly higher performance of green roof design E (Wool-rich Carpet Shred). Both models were strongly influenced by IET and substrate water content, which also concurred previous observations. Higher retention and lower runoff depth were observed for longer IET and lower substrate water content.

The runoff depth and retention models demonstrated the importance of material properties such as the sand to gravel ratio (as a representation of particle size distribution of substrate) and material porosity to green roof hydrological performance characteristics predictions. However, the relationship between runoff depth/retention and sand to gravel ratio was unexpected. The relationship

was positive for runoff depth and negative for retention, suggesting that more gravelly materials would produce less runoff. This result could have been biased by the performance of green roof design B (Sewage Sludge Pellets). Lower runoff depth observed for this green roof appeared to occur due to the material segregation and formation of a low permeability layer, not as a result of the low sand to gravel ratio. Also, the relationship between runoff depth/retention and temperature was unexpected as it is anticipated that higher temperature increases evapotranspiration restoring green roof stormwater storage capacity (Stovin et al., 2012, Fassman-Beck et al., 2013, Voyde et al., 2010). This assumption is, most likely, an effect of a simplification of the relationship between evapotranspiration and temperature. The evapotranspiration is, in fact, directly proportional to vapour pressure deficit. The vapour pressure deficit is the difference between the saturated vapour pressure at the temperature of the surface and the actual vapour pressure of the air above (Shaw, 2011). Although, there is a positive relationship between vapour pressure and the temperature, the increase of the air temperature does not necessarily result in higher evapotranspiration. It is a difference between the surface and the air vapour pressure (the difference in the surface and air temperature) that matters. Furthermore, there are other factors influencing evapotranspiration rates such as wind speed, solar radiation or water availability. The positive association between runoff depth and substrate porosity was expected since higher porosity means more space available for stormwater storage. However, the porosity does not reflect the size distribution and connectivity of pores, which are anticipated to have an influence on water movement in the soil (Gardner et al., 1999). These relationships require further investigation to fully understand their interrelatedness.

There was no study published, to the best knowledge of the author, on the effect of extreme rainfall events on a green roof hydrological performance. Thus, the results of the preliminary regression analysis were compared to the models developed based on monitoring of the green roofs exposed to natural conditions. The results of this study agreed with findings of other researchers demonstrating moderate negative relationship between retention and rainfall depth (Karteris et al., 2016, Stovin et al., 2012) and strong positive relationship between runoff depth and rainfall depth (Mentens et al., 2006, Schroll et al., 2011, Stovin et al.,

2012). Only few researchers attempted regression analysis to explain runoff depth/retention using other factors such as IET or vegetation performance. Nagase and Dunnett (2012) demonstrated moderate relationship between runoff depth and plant height, dry root weight and plant diameter. In this study the vegetation cover was included as a predictor variable, however, it was disregarded in the stepwise process due to low significance to both models. Wong and Jim (2015) reported moderate relationship between retention and IET as well as substrate water content prior to the rainfall. The common finding of all studies was a much higher coefficient of determination for runoff models than for retention models.

The preliminary multiple linear regression models had high coefficient of determination, however they did not fulfil the regression analysis assumptions. To further improve the model the influence of sand to gravel ratio and porosity on runoff depth should be investigated in more detail. Moreover, it should be stressed that the hydrological performance data include green roof responses to extreme rainfall events in laboratory microclimatic conditions similar to conditions that would be experienced during warm seasons. Thus, it may not be suitable to predict green roof retention or runoff depth for other than specified conditions. The regression models could be improved by variable transformation such as log transformation. Other models such as non-linear models should be also explored, especially models supported by machine learning techniques, which do not presume the nature of the response and predictor variables relationship.

The multiple linear regression analysis presented an excellent opportunity to contribute to general knowledge of the factors influencing green roof hydrological performance and the nature of its relationship. It is anticipated that the prediction of the runoff depth from green roofs of specific design would be highly beneficial to engineers, especially designing for urban water management. Current storm sewer design methods are based on required design storm selection and estimation of runoff flows resulting from the rainfall event. Hence, the prediction of runoff depth (or runoff flow) is more desirable than the retention. It does not mean that the retention shouldn't be assessed. Green roof retention capacity is a crucial characteristic in the early stage of green roof design, when the decision of the green roof system selection is made in order to fulfil design objectives.

## 6.4 CONCLUSIONS

The aim of this chapter was to assess the hydrological performance of the extensive green roofs under extreme UK, specifically London, climatic conditions. The data collected during small scale green roof laboratory experiment, using a custom designed (as a part of this research) rainfall simulator system were analysed. The analysis included Overall hydrological performance (stormwater runoff, retention, and peak flow reduction) hydrologic responses in relation to material properties rainfall magnitude and vegetation presence. The preliminary multiple linear regression analysis was carried out assessing the relationship between the extreme UK (London) rainfall conditions, properties of the green roof construction materials and hydrological performance of green roof (section 6.3.5).

This study was based on the UK (London) climatic conditions and specific materials available in the UK and thereby may not be relevant to other climatic or location contexts. The laboratory green roof experiment analysis led to the following conclusions:

1. Small scale extensive green roofs tested in this study subjected to extreme UK (London) climatic conditions retained from 5% to 24% (median retention), depending on green roof design. This result indicated that green roofs could support stormwater management in extreme rainfall conditions. This is crucial in the face of climate change which is leading to frequent extreme weather conditions including rainfalls. In highly dense urban areas, where on-ground stormwater management is limited, roof space has the greatest potential for dealing with excessive stormwater volumes.
2. The laboratory experiment results demonstrated that green roofs of the same design (substrate and drainage layer depth and material as well as vegetation type) behaved similarly.
3. Green roofs made using alternative construction materials performed as well as or better than the control green roofs, with respect to runoff depth and retention. Such design can ensure the multifunctionality of green roofs, not only as a stormwater management, but also as part of the waste management cycle, reducing the disposal of certain waste materials in landfill.

4. Drainage layer material structure may influence hydrological performance. Green roofs with granulated/fibre-like (alternative) materials as drainage layer showed higher retention abilities for subsequent extreme rainfall events than green roofs with conventional, “egg-box” shaped drainage layer. Hence, further investigation may be warranted to investigate the potential for using such alternative materials as a drainage layer, particularly when the key driver for green roof implementation is stormwater management.
5. Green roofs should be designed using carefully selected materials. The material properties influenced green roof hydrological performance, which was demonstrated through regression analysis. The most significant material properties included substrate porosity and drainage layer water absorption. Moreover, it is critical for the green roof construction material to be well-graded to avoid material segregation, which could potentially affect green roof performance. It must be stressed, however, that material segregation and its consequences for the green roof performance could not be assessed during standard material property tests within this study. It is recommended that further laboratory tests are carried out on the green roofs made of these materials to provide further insight on how this affects performance.
6. Maximum runoff depth and minimum retention was observed for green roofs with high water content. This indicated there was a strong relationship between substrate water content prior to the rainfall event and hydrological performance of the green roofs. Substrates with lower water content have more capacity to accommodate additional water volumes since their voids are only partially filled with water. This was confirmed by the regression analysis.
7. The runoff depth increased with increasing rainfall magnitude with no significant differences in data distribution between 1: 30 and 1: 50 rainfall events.
8. The peak flow reduction analysis demonstrated a high number of negative observations, which could not be fully explained in this study. Further investigation is needed to fully understand this unexpected behaviour.
9. The linear regression models for runoff depth and prediction for green roofs subjected to extreme rainfall events with the air temperature between

18°C and 22.5°C demonstrated high coefficients of determination and significance but failed regression assumptions. Further, comprehensive regression analysis is needed. Other models should be explored, especially models supported by machine learning techniques, which do not presume the nature of the response and predictor variables relationship. The prediction of runoff depth (or runoff flow) is significant to urban stormwater management engineering. Storm sewer system design is based on the estimation of runoff flows resulting from selected rainfalls. Hence, extra effort should be made to develop adequate prediction models to support engineering design. This research has gone part of the way to achieving that aim.

10. The execution of a green roof is crucial. The outlets should remain clear to allow unrestricted stormwater discharge. This is important, especially for green roof subjected to experimental tests, where the quality of data is paramount for the results.

The laboratory experiments, which included rainfall simulator design and construction, allowed for the collection of a substantial number of observations of green roof hydrological responses to extreme rainfall events specific to UK (London) climatic conditions. At the time of writing, the author was unable to find any similar studies for comparison. This research successfully fills that gap in knowledge. The results were encouraging, showing that green roofs have the ability to mitigate stormwater even when subjected to extreme rainfall events (1:30, 1:50 and 1:100 year rainfall events). Moreover, laboratory experiment data analysis complemented in-situ experimental data analysis. The similarities and differences between both experiments outcomes are discussed in Chapter 6. In addition, basic guidelines on sustainable green roof design in relation to hydrological performance are suggested, based on the outcomes of this research.

## **CHAPTER 7**

### **GREEN ROOF HYDROLOGICAL PERFORMANCE – AN OVERVIEW**

This chapter presents an overview of the hydrological performance of green roofs based on results of in-situ and laboratory experiments. It addresses the research objective relating to the assessment of the hydrological performance of the conventional extensive green roofs. This chapter collates and compares the results from the in-situ and laboratory experiments. Furthermore, the comparison between multiple linear regression models developed based on results from these two experiments (in-situ and laboratory) is made, presenting factors that influence the hydrological performance under common and extreme weather conditions. Finally, the research findings supporting sustainable green roof design in the UK are presented.

#### **7.1 HYDROLOGICAL BEHAVIOUR OF THE CONVENTIONAL GREEN ROOF (W/40/100 – ‘A’ DESIGN) BASED ON LABORATORY AND IN-SITU EXPERIMENTS**

The green roof made with 100mm Crushed Red Brick substrate, 40mm Roofdrain40 drainage layer and planted with wildflowers was tested in both in-situ and laboratory conditions. This green roof design was termed ‘W/40/100’ for in-situ test and ‘A’ for the laboratory test. Their hydrological behaviour was described in detail in Chapter 4 and 5, respectively.

The direct comparison was unattainable due to the lack of comparable rainfall events from both experiments. The in-situ experiment included rainfall events of return period below 2 years, with majority events having a return period below 1 year. The laboratory experiment included rainfalls of 30, 50 and 100 years return periods (Table 7.1 and Figure 7.1). The mean and median rainfall depths were

much higher for the laboratory experiment than those for the in-situ experiment, which resulted in different hydrological responses of these green roofs. Moreover, the number of observations for these two experiments varied significantly. For these reasons, the results from both experiments were not directly comparable. They could be, however, complementary.

*Table 7.1 Summary statistics of rainfall data sets recorded during the in-situ and laboratory experiments.*

Summary Statistics, Rainfall Depth (mm)			
Experiment		In-situ	Laboratory
<b>N</b>		181	36
<b>Mean</b>		8.69	28.77
<b>Percentiles</b>	Min.	2.00	20.57
	25	3.40	21.67
	50 (Median)	6.08	24.24
	75	10.89	30.12
	Max.	43.55	52.89

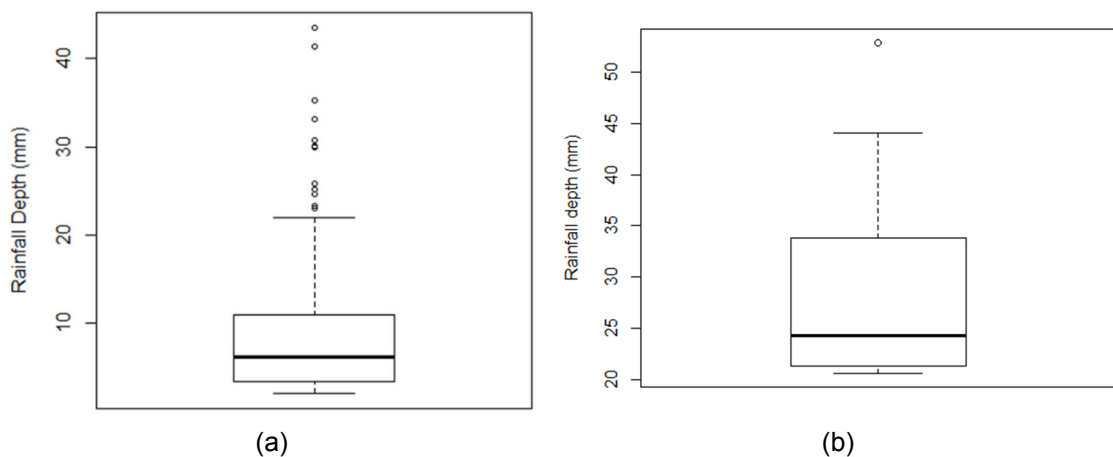


*Figure 7.1 Distribution of rainfall depth data (a) recorded during the in-situ experiment (b) recorded during the laboratory experiment.*

The comparison of the retention between the replicates of W/40/100 green roof design and A green roof design demonstrated high differences. In-situ test results showed full retention for about half of the rainfall events, while laboratory test results presented significantly lower median retentions, being between 5.5% and 6% (Table 7.2). The cumulative retention obtained during in-situ experiment was 61.9%, while during the laboratory experiment this was 16.3%. The high contrast

in retention responses is clearly shown in Figure 7.2. The in-situ experiment data were negatively skewed, whilst the data from laboratory experiment were positively skewed. In general, this confirmed the observations of other researchers of inverse relationship between rainfall depth and retention (Simmons et al., 2008, Carter and Rasmussen, 2006, VanWoert et al., 2005, Fassman-Beck et al., 2013, Stovin et al., 2012). A similar relationship was observed between median retention and rainfall depth for in-situ experiment, but not for laboratory experiment (Table 7.3). Interestingly, green roofs tested in laboratory conditions presented the ability to retain high quantities of stormwater with maximum retention values ranging between 77% to 81% (Table 7.3) in certain conditions. As explained in Chapter 6, in this case a higher retention was observed for rainfall events preceded by long inter-event dry period. Furthermore, the simulations of 100 year rainfall events were carried out on green roofs with higher vegetation coverage. This shows that the retention assessment is more complex, as factors such as inter-event dry period, rainfall duration, climatic conditions or vegetation coverage significantly influence the green roof hydrological behaviour. Moreover, these contrasting retention results show that the retention as a percentage of rainfall retained within the green roof, does not fully reflect green roof performance. Green roofs can retain limited amount of water regardless the magnitude of rainfall. Hence, it could be more useful to measure green roof retention capacity as a percentage of water retained in relation to maximum quantity of water that the green roof can hold, rather than in relation to rainfall.

*Table 7.2 Summary statistics of stormwater retention data for green roofs analysed for the in-situ experiment: W/40/100-1, W/40/100-2, W/40/100-3 and for the laboratory experiment: A-1, A-2, A-3.*

Summary Statistics, Retention (%)							
Roof type		W/40/100-1	W/40/100-2	W/40/100-3	A-1	A-2	A-3
	<b>Mean</b>	75.60	76.15	82.65	19.83	16.42	19.75
<b>Percentiles</b>	<b>Min.</b>	0.10	6.40	13.30	1.00	2.00	3.00
	<b>25</b>	44.80	47.42	66.22	3.00	3.75	4.00
	<b>50 (Median)</b>	99.30	99.85	100.00	6.00	5.50	5.50
	<b>75</b>	100.00	100.00	100.00	23.00	17.25	19.50
	<b>Max.</b>	100.00	100.00	100.00	68.00	56.00	70.00

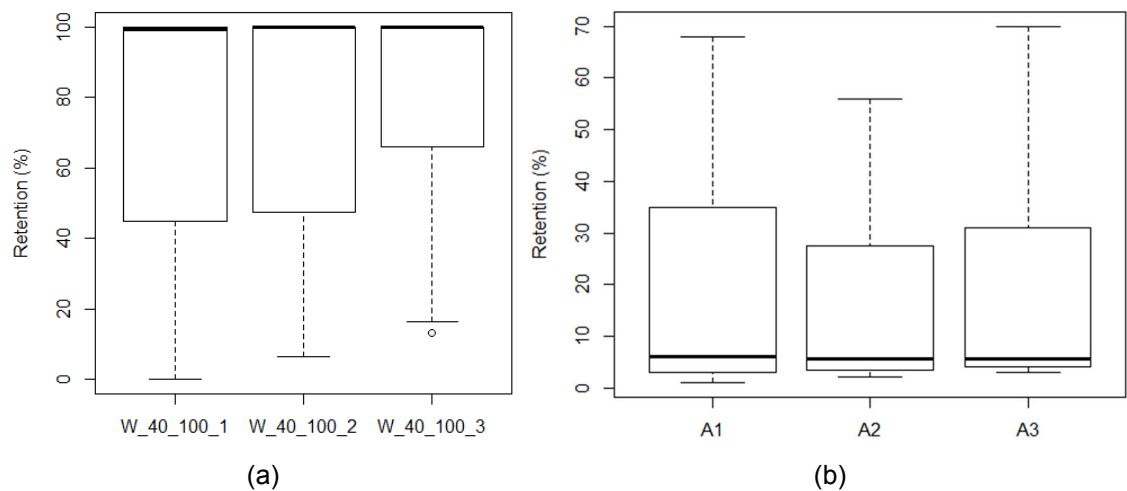


Figure 7.2 Retention data distribution (a) for green roofs investigated in-situ: W/40/100-1, W/40/100-2, W/40/100-3 (b) for green roofs investigated in laboratory: A-1, A-2, A-3.

Table 7.3 Median stormwater retention determined for different rainfall depth for the in-situ and laboratory experiment, where  $T$  is the return period of the rainfall event.

Experiment	Rainfall Depth (mm)	Retention (%)
In-situ	2 – 3.28	100.0
	3.29 – 5.81	100.0
	5.82 – 9.64	100.0
	>9.65	44.1
Laboratory	20.57 (T=30)	5.0
	22.04 (T=50)	6.0
	26.45 (T=100)	7.0

## 7.2 DISCUSSION OF PRELIMINARY MULTIPLE LINEAR REGRESSION MODELS DEVELOPED BASED ON RESULTS OF IN-SITU AND LABORATORY EXPERIMENTS

Preliminary multiple linear regression models to predict runoff depth and retention of green roofs were developed based on the data from in-situ and laboratory experiments and subsequently compared. It need to be noted that both types of models were based on a different set of initial predictor variables (Chapter 4 and 6). The laboratory data set included green roof material properties, but certain weather characteristics, such as dew point or wind speed, were not present. In

contrast, the in-situ data set included weather conditions variables but did not contain green roof material properties (Table 7.4). Hence, only partial comparison of models could be achieved. Table 7.5 presents models for runoff depth and Table 7.6 shows models for retention developed based on in-situ and laboratory data sets.

*Table 7.4 Summary of the predictor variables used to develop runoff depth and retention multiple linear regression models based on in-situ and laboratory data sets.*

Predictor variable	In-situ experiment	Laboratory experiment
Rainfall depth [RD]	+	+
Inter-event dry period [IET]	+	+
Rainfall duration [DUR]	+	
Rainfall intensity [INT]	+	
Air temperature [TEMP]	+	+
Air pressure [BAR]	+	+
Humidity [HUM]	+	
Dew point [DEW]	+	
Wind speed [WIND]	+	
THW index [THW]	+	
Soil water content [WC]		+
Substrate material properties		+
Drainage layer material properties		+

*Table 7.5 Multiple linear regression models to predict runoff depth based on in-situ and laboratory data sets.*

Experiment	Response Variable	Linear Regression Model	R <sup>2</sup> / Adjusted R <sup>2</sup>	p-value
In-situ	RUNOFF	$=0.514*RD + 0.025*DUR + 0.849*TEMP + 0.202*HUM - 0.958*DEW + 0.047*WIND - 1.275*BAR + 17.315$	0.750 / 0.749	< 2.2 x10 <sup>-16</sup>
Laboratory	RUNOFF	$=0.957*RD - 0.025*IET + 0.423*TEMP + 0.332*WC + 2.888*SSG - 87.105*SPOR - 0.004*DLWA + 30.093$	0.969 / 0.968	< 2.2 x10 <sup>-16</sup>

Table 7.6 Multiple linear regression models to predict retention based on in-situ and laboratory data sets.

Experiment	Response Variable	Linear Regression Model	R <sup>2</sup> / Adjusted R <sup>2</sup>	p-value
In-situ	RETENTION	$= - 1.173*RD - 0.172*DUR - 7.025*TEMP - 2.084*HUM + 8.740*DEW - 0.630*WIND + 11.500*BAR - 67.189$	0.419 / 0.416	< 2.2 x10 <sup>-16</sup>
Laboratory	RETENTION	$= - 0.210*RD + 0.100*IET - 1.428*WC - 3.239*TEMP - 12.627*SSG + 386.696*SPOR + 0.012*DLWA - 97.119$	0.814 / 0.807	< 2.2 x10 <sup>-16</sup>

The developed models for runoff depth and retention, based on data collected in laboratory and in-situ experiments (Chapter 4 and 6), demonstrated certain similarities. The common predictors, significant to runoff depth and retention models, were rainfall depth and temperature. The runoff depth models supported the assumption of positive relationship between the runoff and rainfall depth (Nawaz et al., 2015), which was also reflected by a negative relationship between the retention and rainfall depth in the retention models. Additionally, both runoff depth models also presented a positive relationship between the runoff depth and temperature, while both retention models showed a negative relationship between these two variables. This contradicts the assumption that green roofs perform better during warm seasons when higher temperatures result in higher evapotranspiration rates, thus restoring green roof retention abilities (Stovin et al., 2012, Fassman-Beck et al., 2013). As explained in Chapter 6, section 6.3.5, this assumption is, most likely, an effect of simplification of the relationship between evapotranspiration and temperature. The evapotranspiration depends on vapour pressure deficit as well as other factors, such as wind speed, solar radiation, or water availability. This adds to the complexity of the assessment of hydrological performance of green roofs.

The two other common predictor variables used to build the runoff depth and retention models were inter-event dry period and air pressure. The former was

significant for the models based on laboratory data, while the latter was significant for the models based on in-situ data. This may suggest that inter-event dry period is paramount for green roofs to restore their retention capacity when subjected to extreme rainfall events. This could, however, suggest that changes in weather conditions such as wind speed and dew point (constant in the laboratory environment) have greater influence on the green roofs retention abilities than the inter-event dry period. When the wind speed variable was not present, the inter-event dry period became significant for the green roof retention capacity restoration.

Both, in-situ and laboratory runoff depth models demonstrated high coefficient of determination, greater than 0.74. The retention model based on the laboratory data also had high coefficient of determination  $R^2=0.807$ . High coefficients of determination indicated that models explain a high proportion of the total variations in response variables. The retention model based on the in-situ data, however, demonstrated moderate coefficient of determination  $R^2=0.416$ , indicating that model did not fit the data well. All models did not meet the assumptions of independence of errors and normal distribution of errors and therefore they need further improvement.

Concluding, the preliminary multiple linear regression models developed in this study demonstrated limited ability to explain the runoff depth or retention as green roof responses to rainfall events. They do, however, confirm certain patterns such as influence of the rainfall depth on runoff depth or retention. These models should be improved by introducing missing variables and/or variable transformation. The use of a non-linear analysis could also result in more accurate runoff depth and retention models.

### **7.3 SUSTAINABLE GREEN ROOF DESIGN FOR HYDROLOGICAL PERFORMANCE IN THE UK - BEST PRACTICE**

This section outlines the research findings that could be of paramount importance to sustainable green roof design for hydrological performance in the UK. Currently, there is no British Standard regulating green roof design and installation. There is, however, a guidance developed by Green Roof Organisation (GRO) (The Green Roof Organisation, 2014). *The GRO Green Roof Code* is mainly based on the German FLL guidelines (FLL, 2008) with

adjustments to suit the UK market. The GRO code outlines the main considerations for green roof design, installation, and maintenance. However, the guidelines are very generic. For example, sections related to green roof materials and their properties are limited lacking technical details. These sections could be complemented by introducing findings of this research to support sustainable green roof design for hydrological performance.

### **Drainage layer and growing medium (substrate) materials**

The inclusion of a comprehensive list of materials suitable for green roof construction which are available in the UK, would support green roof design process. There is a variety of materials used as green roof substrate or drainage layer, but not listed in the GRO code (The Green Roof Organisation, 2014) or FLL guidelines (FLL, 2008). Such a list of green roof materials used and tested in the UK, based on published literature, is presented in Table 2.5. It is proposed that the list of substrate and drainage layer materials as well as substrate additives to be included in the GRO code in order to reflect a broad range of material selection.

The list should also be complemented by the alternative, sustainable materials tested in this study: Lytag and Sewage Sludge Pellets, as green roof substrate materials and Granulated Rubber and Wool-rich Carpet Shred as green roof drainage layer materials.

### **Properties of drainage layer and growing medium (substrate) materials**

It is proposed that drainage layer materials should be classified into the following groups based on their structure: i) mat/board type, such as 'egg-box' polymer mat ii) granulates, such as gravel or Granulated Rubber iii) fibres, such as Wool-rich Carpet Shred. Each group requires assessment of different properties, for example the particle size distribution is required for granulates but not for mats, the filling volume applies to mats/boards with water storage cells but not to granulates or fibres. Thus, a clear division and understanding of the properties of each group of the drainage layer materials would help green roof designers to select appropriate materials in order to achieve the project objectives.

In terms of properties of the substrate materials, special attention should be paid to the particle size distribution. The GRO code, following FLL guidelines, specifies

the maximum quantities for fine ( $d \leq 0.063\text{mm}$ ) and coarse ( $d > 4.0\text{mm}$ ) particles being 15% and 50%, respectively (FLL, 2008, The Green Roof Organisation, 2014). However, none of these guides advise on grading of the material. This study demonstrated that the use of poorly-graded material may result in material segregation. The consequences of the material segregation include the formation of impermeable layer leading to water logging or changes in water permeability of the substrate. Hence, it is proposed that substrate materials should be well-graded.

### **Assessment of green roof material properties**

The integrated approach to material properties analysis is of high importance to the green roof design. However, the GRO code does not list any British Standards related to material properties testing (The Green Roof Organisation, 2014). The recommendations of the German FLL guidelines refer to German national standards. This research demonstrated that appropriate British Standards can be successfully used for the assessment of the green roof material properties. The list of material properties and the corresponding British Standards used to assess them are presented in Table 3.2. In addition, void ratio, porosity, and saturated density should be derived from these properties.

*Table 7.7 British Standards describing the test methods for relevant material properties.*

<b>Material Property</b>	<b>Standard</b>
<b>Particle Size Distribution</b>	BS 1377-2:1990
<b>Loose Bulk Density</b>	BS 1377-2:1990
<b>Particle Density</b>	BS 1377-2:1990
<b>Water Permeability</b>	BS 1377-5:1990
<b>Water Absorption</b>	BS EN 1097-6:2013
<b>Organic Matter Content</b>	BS EN 13039:2011
<b>Void Ratio</b>	Equation 3.6, Chapter 3
<b>Porosity</b>	Equation 3.7, Chapter 3
<b>Saturated Density</b>	Equation 3.8, Chapter 3

It is also proposed to introduce laboratory tests of the green roof systems, in addition to tests of material properties, in order to assess the performance of the entire green roof system. The novel rainfall simulator setup and testing methods developed during the course of this study could become a base for such assessment.

### **General comments**

As the GRO code states, there are different types of green roofs, designed to fulfil different objectives from serving as a stormwater management tool to creating new wildlife habitats within urban environment (The Green Roof Organisation, 2014). There is a need for a multidisciplinary approach to green roof design (Nawaz et al., 2015, Fassman and Simcock, 2012). Hence, it is crucial for all professionals involved in the green roof design to have a common ground of understanding of green roof performance and appropriate guidelines to follow. This could be achieved by introducing well-defined terms related to green roof design. For example, the properties of the materials should be described in a clear, consistent manner to avoid confusion. This could eventually overcome the shortcomings of the FLL guidelines, such as the very different manner in which recommendations for particle size distribution for substrate and drainage layer are presented, which is confusing and could be misleading (Chapter 3). Another example of potential shortcoming can be found in the GRO code which includes 'weight ( $\text{kg/m}^2$ )' as a material property, when a density would be more appropriate and meaningful for green roof designers (especially for load calculations). Additionally, there is no indication of 'important performance characteristics' for substrate, which is provided in the drainage layer or filter layer sections. This supports the proposal of a comprehensive code, consistent in structure, content, and terminology, that would support a multidisciplinary approach to green roof design.

## **CHAPTER 8**

### **CONCLUSIONS AND RECOMMENDATIONS**

#### **8.1 OVERALL CONCLUSIONS**

Resilient cities have a capacity to survive, adapt and grow even when challenged by frequent and acute problems such as consequences of climate change or urban waste disposal. The negative effects of climate change include extreme weather, heat waves, flooding or rising sea levels. Poor urban waste management results in soil and ground water contamination and deterioration of living standards. In order to effectively deal with such problems, cities need novel sustainable solutions. Green roofs are one of the few stormwater management tools that offer close to source control that could support the development of resilient cities. They can retain and attenuate stormwater reducing flood risk in urban areas. They can also contribute to water cycle through evapotranspiration, thus improving urban microclimate. Additionally, if made of recycled or secondary materials (alternative materials), they can support urban waste management. However, the knowledge of hydrological performance of the green roofs made of alternative materials and green roofs subjected to extreme rainfall events is still limited.

This thesis has contributed to filling the void in knowledge on the hydrological performance of green roofs in the context of the United Kingdom. The key objective of this study was to assess the hydrological performance of extensive green roofs under UK climatic conditions. This included identification of alternative materials which could be used in the design of green roofs and assessment of their properties in relation to hydrological performance of green roofs, the evaluation of the hydrological performance of conventional extensive green roofs and finally investigation into the green roof hydrologic responses to

extreme rainfall events. These assessments were conducted using long-term in-situ experimental monitoring and detailed laboratory-based experiments. The key findings in this thesis are summarised in section 8.1.1 to 8.1.3.

### **8.1.1 GREEN ROOF MATERIALS AND THEIR PROPERTIES**

Alternative green roof materials were selected in this research after a critical review of the literature. The properties of the materials that were assessed in laboratory tests included: loose bulk density, particle density, saturated density, particle size distribution, porosity and void ratio, maximum capillary rise, coefficient of permeability and water absorption.

The analysis of the material properties confirmed that the type of the material used in the green roof design has an impact on the properties of the substrate and drainage layer, as green roof components. The composition of these materials affects its particle, bulk, and saturated densities. The material densities have great impact on the load imposed by the green roof to the supporting structure, but also affect the material transportation and green roof installation process. Amongst the tested materials, the lowest densities were obtained for Lytag ( $\rho_b = 0.78 \text{ Mg/m}^3$ ,  $\rho_s = 1.96 \text{ Mg/m}^3$ ,  $\rho_{\text{sat}} = 1.38 \text{ Mg/m}^3$ ) and Roofdrain40 ( $\rho_b = 0.064 \text{ Mg/m}^3$ ,  $\rho_{\text{sat}} = 0.415 \text{ Mg/m}^3$ ), hence these materials could be recommended as the best choice for lightweight green roof system.

The particle size distribution and grading of the granulate materials are of paramount importance to the performance of green roof systems. The type of the material determines its densities, but it is the particle size distribution that significantly impacts on other properties such as permeability or maximum capillary rise. Thus, the same type of material could demonstrate major differences in physical characteristics and performance, depending on the particle size distribution. Moreover, the laboratory-based experiments proved that poorly-graded materials, such as the Sewage Sludge Pellets used in this study, are not suitable materials for green roof construction. Hence, the granular materials selected for green roof construction should be well-graded.

Based on the above, this study concludes that properties-based, as opposed to type-based, selection of the materials for green roof layers should be used. It also highlights the importance of assessing properties of green roof construction materials collectively, as they are interconnected to each other. It is paramount

to use materials with appropriate characteristics to meet green roof design objectives specific to the individual project.

The highest water absorption amongst the substrate materials was observed for the Crushed Red Brick (30.41%), whilst the lowest one was for the Sewage Sludge Pellets (20.35%). Amongst the drainage layer materials, Wool-rich Carpet Shred had the highest water absorption (295.82%). Materials with the highest water absorption were expected to enhance the hydrological performance of green roofs. This was confirmed by the high median retention of green roofs with Wool-rich Carpet Shred drainage layer. The behaviour of green roofs with different substrates assessed was in complete opposition to that expected. The highest retention was observed for green roofs with Sewage Sludge Pellets substrate. This performance was, however, due to poor drainage as a result of material segregation and not to the effect of water absorption. This observation supports the recommendation of using well-graded materials for green roof construction, to avoid material segregation which could lead to water logging.

The preliminary multiple linear regression models demonstrated the significance of porosity of the substrate material and water absorption of drainage layer material in the prediction of runoff depth and retention. Additionally, particle size distribution (expressed as sand to gravel ratio) of the substrate material was significant to the retention model. These results suggest the importance of these material properties to the hydrological performance of green roofs. However, it needs to be noted that both developed models are preliminary models and they need subsequent improvement.

### **8.1.2 HYDROLOGICAL PERFORMANCE OF CONVENTIONAL EXTENSIVE GREEN ROOFS**

The hydrological performance of the conventional extensive green roofs was studied through in-situ and laboratory-based experiments. The in-situ experiment provided unique data based on long-term monitoring of twenty-four small scale green roofs, between July 2010 and August 2014 under UK (London) climatic conditions. The experimental setup included three replicates of eight green roof designs as a combination of the following: i) vegetation type: sedum and wildflower, ii) drainage layer depth: 25mm and 40mm, iii) substrate depth: 50mm and 100mm.

This study has demonstrated that extensive conventional green roofs are effective in retaining stormwater and reducing peak flow from rainfall events of return period less than 2 years. The median retention for all green roof designs was above 99%, the median runoff depth was less than 0.05mm and the median peak flow reduction was greater than 99%. This high hydrological performance of all green roof designs was obtained as a response to high number of small rainfall events with median rainfall depth of 6.08mm. The green roofs retention performance was reduced for larger rainfall events (rainfall depth > 9.65mm), due to finite retention capacity of green roofs. This was reflected by the cumulative retention for the entire monitoring period of 4 years that ranged from 61.5% (W/25/50) to 77.9% (S/40/100) across all green roof designs.

The laboratory tests of the conventional extensive green roof design (called 'A' in the laboratory experiment) subjected to extreme rainfall events of return period of 30, 50 and 100 years, resulted in median retention between 5.5% and 6%. The cumulative retention obtained during these tests was 16.3%. As expected, these results confirmed the finite retention capacity of the analysed conventional green roofs. The results also indicated much lower green roof performance under extreme rainfall events. However, it also demonstrated that green roofs have certain capacity to retain extreme rainfall events, given specific conditions such as long inter-event dry period prior to the extreme rainfall. This was concurred by the maximum retention which ranged between 77% and 81%. Concluding, the extensive conventional green roofs investigated in this study presented high ability to retain small rainfall events and limited ability to retain extreme rainfall events, thus presenting a potential as stormwater management tool in UK climate.

The variety of conventional green roof designs included in the in-situ experiment presented an opportunity to identify significant factors affecting their hydrological performance. The results of the in-situ experiment demonstrated that the green roof design did not have significant effect on runoff depth, retention, and peak flow reduction, except for the S/40/100 design. This particular design demonstrated high hydrological performance, suggesting that green roofs of deeper drainage and substrate layer would perform significantly better than those with shallower layers. In contrast, significant differences in retention were identified between replicates of the same green roof designs. These results

suggest that factors such as vegetation coverage, organic matter content, degree of compaction or roof construction imperfections may influence the green roof performance.

The preliminary multiple linear regression models confirmed the significance of the rainfall depth and temperature in predicting runoff depth and retention. Additionally, factors such as rainfall duration, air humidity, dew point, wind speed and air pressure were included in both models, which seem to have greater effect on the hydrological performance of green roofs than other factor such as inter-event dry period. The runoff depth model could explain 74.9% of the response variations ( $R^2=0.749$ ), while the retention model only 41.6% of the response variations ( $R^2=0.416$ ). However, both models did not meet the assumptions of independence of errors and normal distribution of errors, thus they need further improvement.

The effect of season on the green roof hydrological performance was also assessed. The results of analysis demonstrated that conventional extensive green roofs perform significantly better in warm seasons, such as spring and summer (with median retention being greater than 99% for all green roof designs), than in cold seasons, such as autumn (median retention ranging between 74.55% and 99.9%) and winter (median retention ranging between 41.5% and 93.9%). These differences could occur due to the rainfall event distribution, with larger events being present in autumn and winter, thus resulting in greater runoff depths. This could also be due to higher evapotranspiration in summer and spring, resulting in faster restoration of the retention capacity of green roofs.

Concluding, the assessment of the green roof hydrological performance is a complex problem, which involves a large number of factors affecting the green roof response to rainfalls. Although this study demonstrated significant influence of certain factors, such as rainfall depth and temperature, on hydrological performance, the impact of other factors like vegetation cover, organic matter content or degree of compaction was not assessed. All green roof designs assessed in the in-situ experiment presented a good hydrological performance under UK (London) climatic conditions. However, these results may not be relevant to other climatic or location context.

### **8.1.3 HYDROLOGICAL PERFORMANCE OF GREEN ROOFS MADE WITH ALTERNATIVE MATERIALS SUBJECTED TO EXTREME RAINFALL EVENTS**

The hydrological performance of the extensive green roofs made with alternative materials was studied through laboratory-based experiments. An experimental rainfall simulator laboratory setup and associated method of data collection have been developed by the author during the course of the research, in order to determine and compare the hydrological performance of green roofs of various designs subjected to extreme rainfall events, in a timely and efficient manner. The laboratory experiment provided a unique data set based on monitoring of fifteen small scale green roofs under UK (London) extreme climatic conditions. The experimental setup included three replicates of five green roof designs, including a conventional green roof made with Crushed Red Brick and Roofdrain40, and green roof designs made with alternative materials, such as Lytag and Sewage Sludge Pellets combined with Roofdrain40, and Granulated Rubber and Wool-rich Carpet Shred combined with Crushed Red Brick. The simulated rainfall events, specific to UK (London), included these of 1:30, 1:50 and 1:100 year return period.

This study assessed the capacity of extensive green roofs to retain stormwater from extreme rainfall events. The obtained median retention varied from 6% (Crushed Red Brick) to 11.5% (Wool-rich Carpet Shred), whilst the median runoff depth was between 20.16mm (Granulated Rubber) and 21.18mm (Crushed Red Brick). However, the median retention for individual green roofs ranged between 5.5% (Crushed Red Brick – replicate 2 and 3) and 13% (Wool-rich Carpet Shred – replicate 1 and 3). The results also demonstrated that green roofs have high ability to retain extreme rainfall events, given specific conditions such as long inter-event dry period or low substrate water content prior to the extreme rainfall. This was concurred by the maximum retention which ranged between 61% (Granulated Rubber) and 78% (Lytag). This concludes that the extensive green roofs investigated in this study presented limited ability to retain extreme rainfall events. However, the performance of green roofs varied from one design to another, and was influenced by factors, such as inter-event dry period and substrate water content, demonstrating potential of green roofs made of alternative materials as stormwater management tool in UK (London) climate.

The variety of green roof designs included in the laboratory experiment presented an opportunity to assess the impact of the selected materials and their properties on the hydrological performance of green roofs. The green roof design did not have significant effect on the runoff depth. This had, however, significant impact on retention. The Sewage Sludge Pellets, Granulated Rubber and Wool-rich Carpet Shred green roofs demonstrated significantly higher retention than the conventional green roof (Crushed Red Brick). These results suggested that replacement of the 'egg-box' drainage layer with granulated or fibre-like material could enhance the green roof retention. Moreover, the laboratory assessed green roofs with alternative drainage layer demonstrated higher retention abilities for subsequent extreme rainfall events than the green roofs with conventional, 'egg-box' shaped drainage layer. Hence, these alternative materials could be used as a drainage layer, when a green roof is designed as a stormwater management tool. The high retention of the Sewage Sludge Pellets based green roof design occurred as a result of reduced drainage due to material segregation. The green roof made with Lytag performed better than the conventional green roof (Crushed Red Brick) but this difference was not significant. This concludes that green roofs made of alternative materials performed as good as or better than the conventional green roofs in regards to runoff depth and retention. Hence, green roofs can not only be used as a stormwater management tool but also they can also improve waste management and reduce the disposal of certain waste materials to landfill.

The runoff depth was significantly influenced by the rainfall magnitude, with higher runoff depths being recorded for greater rainfall depths. However, it was not a significant factor affecting the retention of green roofs.

The preliminary multiple linear regression models demonstrated the significance of the rainfall depth and temperature for prediction of runoff depth and retention. Amongst other factors affecting these hydrologic responses of investigated green roofs were: inter-event dry period, water content of the substrate prior the event, vegetation and materials properties discussed in section 8.1.1. Substrates with lower water content have more capacity to accommodate additional water volumes since their voids are only partially filled with water. Long inter-event dry period allows green roofs to restore their retention capacity. The runoff depth model could explain 96.8% of the response variations ( $R^2=0.968$ ), while the

retention model 80.7% of the response variations ( $R^2=0.807$ ). However, it needs to be noted that both developed regression models were preliminary and they require further improvement.

The peak flow reduction analysis showed a high number of negative observations, which could not be fully explained in this study.

These results show that green roofs made of alternative materials can support the stormwater management in extreme rainfall conditions. This is crucial taking into consideration climate changes, resulting in frequent extreme weather conditions including extreme rainfalls. In highly dense urban areas, where on-ground stormwater management is limited, green roofs are potentially one of the best solutions to deal with excessive stormwater volumes.

## **8.2 CONTRIBUTION TO KNOWLEDGE**

This thesis has made original contributions to knowledge in relation to the assessment of the hydrological performance of extensive green roofs.

### **8.2.1 GREEN ROOF MATERIALS AND THEIR PROPERTIES**

This thesis has identified and selected alternative materials, suitable for the use in extensive green roof systems to enhance their hydrological performance, and available in the UK (section 7.3). Selected materials, such as Sewage Sludge Pellets and Granulated Rubber, have been investigated in previous green roof studies. However, their hydrological performance was not assessed. Wool-rich Carpet Shred was not, to the best knowledge of the author of this thesis, studied as a green roof construction material. This study filled these obvious gaps in the knowledge.

This study has also recommended the list of British Standards describing methods for testing of the material properties required to assess green roof hydrological performance (section 7.3).

### **8.2.2 EXPERIMENTAL SETUP TO ASSESS THE HYDROLOGICAL PERFORMANCE OF GREEN ROOFS IN LABORATORY CONDITIONS**

During the course of this study, an innovative rainfall simulator system to simulate a broad range of rainfall events for the assessment of the green roof hydrological performance was developed (Chapter 5). The experimental setup was designed

and built following critical evaluation of the strengths and weaknesses of in-situ and laboratory green roof monitoring systems identified in the literature.

The novel experimental setup required new testing procedures that has been developed and presented in this thesis. This laboratory testing method could be further improved through technical refinement and benchmarking.

### **8.2.3 HYDROLOGICAL PERFORMANCE OF GREEN ROOFS SUBJECTED TO EXTREME RAINFALL EVENTS**

To the author's knowledge, this thesis has assessed for the first time, at the large scale, through laboratory experiments, the hydrological performance of green roofs exposed to extreme rainfall events (Chapter 6). The results showed that green roofs have the ability to retain extreme rainfalls in specific conditions.

### **8.2.4 PREDICTION MODELS FOR THE HYDROLOGICAL PERFORMANCE OF THE GREEN ROOFS**

Based on green roofs hydrological performance data collected through long-term monitoring of in-situ green roofs and a unique data collected through laboratory experiments, preliminary multiple linear regression models to predict runoff depth and retention of green roof systems were developed (section 7.2). These models could be the basis for further development of tools for accurate prediction of green roof responses to rainfall events in order to assist green roof designers, standardisation bodies, specifiers, manufacturers, and contractors.

## **8.3 RECOMMENDATIONS FOR FURTHER WORK**

### **8.3.1 GREEN ROOF MATERIALS AND THEIR PROPERTIES**

This study demonstrated great potential of alternative materials to enhance the green roof hydrological performance. Their possible abilities to support other green roof functions, such as enhancement of biodiversity are, however, not fully known and this aspect should be explored.

Additional alternative materials could be identified and their properties investigated. A broad selection of these materials would assist green roof designers with the selection of appropriate materials in order to achieve the project's objectives.

### **8.3.2 IMPROVEMENT OF THE RAINFALL SIMULATOR SYSTEM**

An experimental method and setup have been developed to determine the hydrological performance of green roof systems in laboratory conditions. The current rainfall simulator system is manually-operated, hence only rainfall events of constant intensity can be simulated with high accuracy. Thus, the experimental method and setup can be further improved through technical refinement so that events of variable intensity could be also simulated.

### **8.3.3 IMPROVEMENT OF THE PREDICTION MODELS FOR THE HYDROLOGICAL PERFORMANCE OF THE GREEN ROOFS**

The multiple linear regression models of runoff depth and retention developed in this study are preliminary models. Therefore, they can be further improved in order to increase the accuracy of their predictions. The improvement of prediction models could be achieved through a more comprehensive regression analysis or the development of models supported by machine learning techniques, which do not presume the nature of the response and predictor variables relationship. Predictive modelling should concentrate on green roof runoff quantities in order to assess their impact on the drainage system, especially during extreme weather conditions.

## REFERENCES

- Aksoy, H., Unal, N. E., Cokgor, S., Gedikli, A., Yoon, J., Koca, K., Inci, S. B. and Eris, E. (2012) 'A rainfall simulator for laboratory-scale assessment of rainfall-runoff-sediment transport processes over a two-dimensional flume', *CATENA*, 98, pp. 63-72.
- Alexandri, E. and Jones, P. (2007) 'Developing a one-dimensional heat and mass transfer algorithm for describing the effect of green roofs on the built environment: Comparison with experimental results', *Building and Environment*, 42(8), pp. 2835-2849.
- Alfredo, K., Montalto, F. and Goldstein, A. (2010) 'Observed and Modeled Performance of Prototype Green Roof Test Plots Subjected to Simulated Low and High Intensity Precipitation in a Laboratory Experiment', *Journal of Hydrologic Engineering*, 15(6), pp. 444-457.
- Bates, A. J., Sadler, J. P., Greswell, R. B. and Mackay, R. (2015) 'Effects of recycled aggregate growth substrate on green roof vegetation development: A six year experiment', *Landscape and Urban Planning*, 135, pp. 22-31.
- Beck, D. A., Johnson, G. R. and Spolek, G. A. (2011) 'Amending greenroof soil with biochar to affect runoff water quantity and quality', *Environmental Pollution*, 159(8-9), pp. 2111-2118.
- Beecham, S. and Razzaghmanesh, M. (2015) 'Water quality and quantity investigation of green roofs in a dry climate', *Water Research*, 70, pp. 370-384.
- Bengtsson, L., Grahn, L. and Olsson, J. (2005) 'Hydrological function of a thin extensive green roof in southern Sweden', *Nordic Hydrology*, 36(3), pp. 259-268.
- Benvenuti, S. (2014) 'Wildflower green roofs for urban landscaping, ecological sustainability and biodiversity', *Landscape and Urban Planning*, 124, pp. 151-161.
- Berndtsson, J. C., Bengtsson, L. and Jinno, K. (2009) 'Runoff water quality from intensive and extensive vegetated roofs', *Ecological Engineering*, 35(3), pp. 369-380.

- Berretta, C., Poë, S. and Stovin, V. (2014) 'Moisture content behaviour in extensive green roofs during dry periods: The influence of vegetation and substrate characteristics', *Journal of Hydrology*, 511, pp. 374-386.
- Bianchini, F. and Hewage, K. (2012) 'How “green” are the green roofs? Lifecycle analysis of green roof materials', *Building and Environment*, 48(0), pp. 57-65.
- Biomass Energy Centre (2014) *Sewage sludge*. Available at: [http://www.biomassenergycentre.org.uk/portal/page?\\_pageid=75,18722&\\_dad=portal&\\_schema=PORTAL](http://www.biomassenergycentre.org.uk/portal/page?_pageid=75,18722&_dad=portal&_schema=PORTAL) (Accessed: 20 June 2014).
- Bliss, D. J., Neufeld, R. D. and Ries, R. J. (2009) 'Storm Water Runoff Mitigation Using a Green Roof', *Environmental Engineering Science*, 26(2), pp. 407-418.
- Bonham, C. D. (2013) *Measurements for Terrestrial Vegetation*. Wiley.
- Boningale Greensky (2016) *SkyPlug Specification*: Boningale Greensky. Available at: <http://www.boningale-greensky.co.uk/products/> (Accessed: 15 July 2016).
- Brenneisen, S. (2006) 'Space for urban wildlife: designing green roofs as habitats in Switzerland', *Urban Habitats*, 4(1), pp. 27-36.
- British Standards Institution (1990a) *BS 1377-2:1990: Methods of test for soils for civil engineering purposes. Classification tests*. London: British Standards Institution.
- British Standards Institution (1990b) *BS 1377-5:1990: Methods of test for soils for civil engineering purposes. Compressibility, permeability and durability tests*. London: British Standards Institution.
- British Standards Institution (1990c) *BS 1377-7:1990: Methods of test for soils for civil engineering purposes. Shear strength tests (total stress)*. London: British Standards Institution.
- British Standards Institution 2000. *BS EN 1097-6:2000: Tests for mechanical and physical properties of aggregates. Determination of particle density and water absorption*. London: British Standards Institution.
- British Standards Institution 2002. *NA to BS EN 1991-1-1:2002 UK National Annex to Eurocode 1: Actions on structures. Part 1-1: General actions — Densities, self-weight, imposed loads for buildings* London: British Standards Institution.

- British Standards Institution 2011. BS EN 13039:2011: Soil improvers and growing media. Determination of organic matter content and ash. London: British Standards Institution.
- British Standards Institution 2013. Drain and sewer systems outside buildings. British Standards Institution.
- Buccola, N. and Spolek, G. (2011) 'A Pilot-Scale Evaluation of Greenroof Runoff Retention, Detention, and Quality', *Water, Air, Soil Pollution*, 216(1), pp. 83-92.
- Butler, D. and Davies, J. (2010) *Urban Drainage, Third Edition*. CRC Press.
- Carbone, M., Garofalo, G., Nigro, G. and Piro, P. (2014) 'A Conceptual Model for Predicting Hydraulic Behaviour of a Green Roof', *Procedia Engineering*, 70(0), pp. 266-274.
- Carpenter, C. M., Todorov, D., Driscoll, C. T. and Montesdeoca, M. (2016) 'Water quantity and quality response of a green roof to storm events: Experimental and monitoring observations', *Environ Pollut.*
- Carpenter, D. D. and Kaluvakolanu, P. (2011) 'Effect of Roof Surface Type on Storm-Water Runoff from Full-Scale Roofs in a Temperate Climate', *Journal of Irrigation and Drainage Engineering*, 137(3), pp. 161-169.
- Carter, T. L. and Rasmussen, T. C. (2006) 'Hydrologic behavior of vegetated roofs', *JAWRA Journal of the American Water Resources Association*, 42(5), pp. 1261-1274.
- Castleton, H. F., Stovin, V., Beck, S. B. M. and Davison, J. B. (2010) 'Green roofs; building energy savings and the potential for retrofit', *Energy and Buildings*, 42(10), pp. 1582-1591.
- Coma, J., Pérez, G., Solé, C., Castell, A. and Cabeza, L. F. (2016) 'Thermal assessment of extensive green roofs as passive tool for energy savings in buildings', *Renewable Energy*, 85, pp. 1106-1115.
- Connop, S. April 2012. *RE: Barking Riverside tipping buckets calibration*. Type to Owczarek, K.
- Currie, B. A. and Bass, B. (2008) 'Estimates of air pollution mitigation with green plants and green roofs using the UFORE model', *Urban Ecosystems*, 11(4), pp. 409-422.
- Czemiel Berndtsson, J. (2010) 'Green roof performance towards management of runoff water quantity and quality: A review', *Ecological Engineering*, 36(4), pp. 351-360.

- Davis Instruments 2012. Rain Collector II Installation manual. Davis Instruments.
- Davis Instruments 2015. Vantage Pro2 Console Manual. Davis Instruments.
- DeJong-Hughes, J., Moncrief, J. F., Voorhees, W. B. and Swan, J. B. (2016) *Soil compaction: causes, effects and control*. University of Minnesota. Available at: <http://www.extension.umn.edu/agriculture/tillage/soil-compaction/> (Accessed: 20 July 2016).
- Department of the Environment, L., National Water Council, L. S. T. C. o. S. and Mains, W. (1981) *Design and Analysis of Urban Storm Drainage: the Wallingford Procedure: Volume 4: the Modified Rational Method*.
- DoE/NWC (1981) *Design and analysis of urban storm drainage : the Wallingford procedure*. National Water Council.
- Driscoll, E. D., Palhegyi, G. E., Strecker, E. W. and Shelley, P. E. (1989) *Analysis of Storm Event Characteristics for Selected Rainfall Gages Throughout the United States: Draft*. U.S. Environmental Protection Agency.
- Dunnett, N. and Kingsbury, N. I. (2008) *Planting green roofs and living walls*. Rev. and updated ed., [2nd ed.] edn. Portland, Or. ; London: Timber.
- EcoSchemes Ltd (2003) *Green Roofs: Their Existing Status and Potential for Conserving Biodiversity in Urban Areas*, Peterborough: English Nature. Available at: <https://books.google.co.uk/books?id=-RV9tgAACAAJ>.
- Ecosheet (2016) *Ecosheet Product Range*: Ecosheet. Available at: <http://www.ecosheet.com/products/> (Accessed: 15 July 2016).
- Eksi, M. and Rowe, D. B. (2016) 'Green roof substrates: Effect of recycled crushed porcelain and foamed glass on plant growth and water retention', *Urban Forestry & Urban Greening*, 20, pp. 81-88.
- Emorsgate Seeds (2016) *ER1F – Wild Flowers for Green Roofs*: Emorsgate Seeds. Available at: <http://wildseed.co.uk/mixtures/view/57/wild-flowers-for-green-roofs> (Accessed: 15 July 2016).
- European Tyre & Rubber Manufacturers' Association (2013) *Sustainable? ETRMA Annual Report 2012 - 2013*, Brussels: ETRMA - European Tyre & Rubber Manufacturers' Association. Available at: [http://www.etrma.org/uploads/Modules/Documentsmanager/etrma\\_annualreport-2012-2013.pdf](http://www.etrma.org/uploads/Modules/Documentsmanager/etrma_annualreport-2012-2013.pdf) (Accessed: 21 June 2014).
- Evans, E. J., Inglethorpe, S. J. D. and Wetton, P. D. (1999) *Evaluation Of Pumice And Scoria Samples From East Africa As Lightweight Aggregates* Keyworth: British Geological SurveyWG/99/15).

- Faraway, J. (2002) 'Practical Regression and Anova using R'.
- Farrell, C., Ang, X. Q. and Rayner, J. P. (2013) 'Water-retention additives increase plant available water in green roof substrates', *Ecological Engineering*, 52, pp. 112-118.
- Fassman-Beck, E., Voyde, E., Simcock, R. and Hong, Y. S. (2013) '4 Living roofs in 3 locations: Does configuration affect runoff mitigation?', *Journal of Hydrology*, 490(0), pp. 11-20.
- Fassman, E. and Simcock, R. (2012) 'Moisture Measurements as Performance Criteria for Extensive Living Roof Substrates', *Journal of Environmental Engineering*, 138(8).
- Fioretti, R., Palla, A., Lanza, L. G. and Principi, P. (2010) 'Green roof energy and water related performance in the Mediterranean climate', *Building and Environment*, 45(8), pp. 1890-1904.
- FLL 2008. Guidelines for the Planning, Construction and Maintenance of Green Roofing – Green Roofing Guideline. Bonn: Forschungsgesellschaft Landschaftsentwicklung Landschaftsbau e. V. (FLL).
- Forschungsgesellschaft Landschaftsentwicklung Landschaftsbau (2008) *Guidelines for the Planning, Construction and Maintenance of Green Roofing: Green Roofing Guideline*. Forschungsgesellschaft Landschaftsentwicklung Landschaftsbau.
- Gardner, C. M. K., Laryea, K. B. and Unger, P. W. (1999) *Soil Physical Constraints to Plant Growth and Crop Production*. Land and Water Development Division, Food and Agriculture Organization.
- Getter, K. L., Rowe, D. B. and Andresen, J. A. (2007) 'Quantifying the effect of slope on extensive green roof stormwater retention', *Ecological Engineering*, 31(4), pp. 225-231.
- Getter, K. L., Rowe, D. B., Robertson, G. P., Cregg, B. M. and Andresen, J. A. (2009) 'Carbon Sequestration Potential of Extensive Green Roofs', *Environmental Science & Technology*, 43(19), pp. 7564-7570.
- Graceson, A., Hare, M., Hall, N. and Monaghan, J. (2014a) 'Use of inorganic substrates and composted green waste in growing media for green roofs', *Biosystems Engineering*, 124, pp. 1-7.
- Graceson, A., Hare, M., Monaghan, J. and Hall, N. (2013) 'The water retention capabilities of growing media for green roofs', *Ecological Engineering*, 61, Part A(0), pp. 328-334.

- Graceson, A., Monaghan, J., Hall, N. and Hare, M. (2014b) 'Plant growth responses to different growing media for green roofs', *Ecological Engineering*, 69, pp. 196-200.
- Gregoire, B. G. and Clausen, J. C. (2011) 'Effect of a modular extensive green roof on stormwater runoff and water quality', *Ecological Engineering*, 37(6), pp. 963-969.
- Grismer, M. E. (2011) *Rainfall Simulation Studies – A Review of Designs, Performance and Erosion Measurement Variability*: Depts. of Hydrologic Sciences and Biological & Agricultural Engineering, UC Davis.
- Hakimdavar, R., Culligan, P. J., Finazzi, M., Barontini, S. and Ranzi, R. (2014) 'Scale dynamics of extensive green roofs: Quantifying the effect of drainage area and rainfall characteristics on observed and modeled green roof hydrologic performance', *Ecological Engineering*, 73(0), pp. 494-508.
- Harper, G. E., Limmer, M. A., Showalter, W. E. and Burken, J. G. (2015) 'Nine-month evaluation of runoff quality and quantity from an experiential green roof in Missouri, USA', *Ecological Engineering*, 78, pp. 127-133.
- Hathaway, A. M., Hunt, A. and Jennings, G. D. (2008) 'A field study of green roof hydrologic and water quality performance', *Transactions of the ASABE*, 51(1), pp. 37-44.
- Hawkins, E. (2016) *Climate spirals*. Available at: <http://www.climate-lab-book.ac.uk/spirals/> (Accessed: 20 July 2016).
- Hiltner, R. N., Lawrence, T. M. and Tollner, E. W. (2008) 'Modeling stormwater runoff from green roofs with HYDRUS-1D', *Journal of Hydrology*, 358(3-4), pp. 288-293.
- Introduction to Types of Green Roof* (2012): livingroofs.org. Available at: <http://livingroofs.org/2010022858/green-roof-types/greenrooftypes.html> (Accessed: 01 August 2012).
- Johkan, M., Shoji, K., Goto, F., Hashida, S.-n. and Yoshihara, T. (2010) 'Blue Light-emitting Diode Light Irradiation of Seedlings Improves Seedling Quality and Growth after Transplanting in Red Leaf Lettuce', *HortScience*, 45(12), pp. 1809-1814.
- Johnson, R. A. and Bhattacharyya, G. K. (2011) *Statistics : principles and methods*. 6th ed., International student edn. Hoboken, N.J.: Wiley.
- Karteris, M., Theodoridou, I., Mallinis, G., Tsiros, E. and Karteris, A. (2016) 'Towards a green sustainable strategy for Mediterranean cities: Assessing

- the benefits of large-scale green roofs implementation in Thessaloniki, Northern Greece, using environmental modelling, GIS and very high spatial resolution remote sensing data', *Renewable and Sustainable Energy Reviews*, 58, pp. 510-525.
- Kasmin, H. (2010) *Hydrological performance of green roofs*. University of Sheffield, Sheffield.
- Kosareo, L. and Ries, R. (2007) 'Comparative environmental life cycle assessment of green roofs', *Building and Environment*, 42(7), pp. 2606-2613.
- Kottek, M., Grieser, J., Beck, C., Rudolf, B. and Rubel, F. (2006) 'World Map of the Köppen-Geiger climate classification updated', *Meteorologische Zeitschrift*, 15(3), pp. 259-263(5).
- Krishnan, R. and Ahmad, H. 'Stormwater runoff mitigation on extensive green roof: a review on trends and factors'. *6th South East Asian Technical Universities Consortium (SEATUC) Symposium*, Malaysia.
- Ksiazek, K., Fant, J. and Skogen, K. (2012) 'An assessment of pollen limitation on Chicago green roofs', *Landscape and Urban Planning*, 107(4), pp. 401-408.
- Lee, J. S., Kim, J. T. and Lee, M. G. (2014) 'Mitigation of urban heat island effect and greenroofs', *Indoor and Built Environment*, 23(1), pp. 62-69.
- Lee, J. Y., Lee, M. J. and Han, M. (2015) 'A pilot study to evaluate runoff quantity from green roofs', *Journal of Environmental Management*, 152(0), pp. 171-176.
- Lewis-Beck, M. S. (1993) *Regression analysis*. London: Sage.
- Li, J.-f., Wai, O. W. H., Li, Y. S., Zhan, J.-m., Ho, Y. A., Li, J. and Lam, E. (2010) 'Effect of green roof on ambient CO<sub>2</sub> concentration', *Building and Environment*, 45(12), pp. 2644-2651.
- Liu, K. K. Y. (2003) 'Engineering performance of rooftop gardens through field evaluation', pp. 1-15.
- Locatelli, L., Mark, O., Mikkelsen, P. S., Arnbjerg-Nielsen, K., Bergen Jensen, M. and Binning, P. J. (2014) 'Modelling of green roof hydrological performance for urban drainage applications', *Journal of Hydrology*, 519, Part D(0), pp. 3237-3248.

- Lundholm, J., Macivor, J. S., Macdougall, Z. and Ranalli, M. (2010) 'Plant species and functional group combinations affect green roof ecosystem functions', *PLoS One*, 5(3), pp. e9677.
- Luo, H., Liu, X., Anderson, B. C., Zhang, K., Li, X., Huang, B., Li, M., Mo, Y., Fan, L., Shen, Q., Chen, F. and Jiang, M. (2015) 'Carbon sequestration potential of green roofs using mixed-sewage-sludge substrate in Chengdu World Modern Garden City', *Ecological Indicators*, 49, pp. 247-259.
- Lytag (2014) *Welcome to Lytag*. Available at: <http://www.lytag.net/> (Accessed: 20 June 2014).
- Macaulay, S. 'Diverting carpet waste from landfill', *Carpet Recycling UK Conference 2011*, Birmingham: Carpet Recycling UK.
- Macivor, J. S. and Lundholm, J. (2011) 'Performance evaluation of native plants suited to extensive green roof conditions in a maritime climate', *Ecological Engineering*, 37(3), pp. 407-417.
- Mansell, M. G. (2003) *Rural and urban hydrology*. London: Thomas Telford.
- Matlock, J. M. and Rowe, D. B. (2016) 'The suitability of crushed porcelain and foamed glass as alternatives to heat-expanded shale in green roof substrates: An assessment of plant growth, substrate moisture, and thermal regulation', *Ecological Engineering*, 94, pp. 244-254.
- McNeil, S. J., Sunderland, M. R. and Zaitseva, L. I. (2007) 'Closed-loop wool carpet recycling', *Resources, Conservation and Recycling*, 51(1), pp. 220-224.
- Mentens, J., Raes, D. and Hermy, M. (2006) 'Green roofs as a tool for solving the rainwater runoff problem in the urbanized 21st century?', *Landscape and Urban Planning*, 77(3), pp. 217-226.
- Met Office (2012) 'Met Office Integrated Data Archive System (MIDAS) Land and Marine Surface Stations Data (1853-current)'. Available at: <http://catalogue.ceda.ac.uk/uuid/220a65615218d5c9cc9e4785a3234bd0> (Accessed: 27 December 2016).
- Mickovski, S. B., Buss, K., McKenzie, B. M. and Sökmener, B. (2013) 'Laboratory study on the potential use of recycled inert construction waste material in the substrate mix for extensive green roofs', *Ecological Engineering*, 61, Part C(0), pp. 706-714.

- Molineux, C. J., Fentiman, C. H. and Gange, A. C. (2009) 'Characterising alternative recycled waste materials for use as green roof growing media in the UK', *Ecological Engineering*, 35(10), pp. 1507-1513.
- Molineux, C. J., Gange, A. C., Connop, S. P. and Newport, D. J. (2015) 'Using recycled aggregates in green roof substrates for plant diversity', *Ecological Engineering*, 82, pp. 596-604.
- Morgan, S., Celik, S. and Retzlaff, W. (2013) 'Green Roof Storm-Water Runoff Quantity and Quality', *Journal of Environmental Engineering*, 139(4), pp. 471-478.
- Murphy, J. M., Sexton, D. M. H., Jenkins, G. J., Boorman, P. M., Booth, B. B. B., Brown, C. C., Clark, R. T., Collins, M., Harris, G. R., Kendon, E. J., Betts, R. A., Brown, S. J., Howard, T. P., Humphrey, K. A., McCarthy, M. P., McDonald, R. E., Stephens, A., Wallace, C., Warren, R., Wilby, R. and Wood, R. A. (2009) *UK Climate Projections science report: Climate change projections*, Exeter.
- Nagase, A. and Dunnett, N. (2010) 'Drought tolerance in different vegetation types for extensive green roofs: Effects of watering and diversity', *Landscape and Urban Planning*, 97(4), pp. 318-327.
- Nagase, A. and Dunnett, N. (2011) 'The relationship between percentage of organic matter in substrate and plant growth in extensive green roofs', *Landscape and Urban Planning*, 103(2), pp. 230-236.
- Nagase, A. and Dunnett, N. (2012) 'Amount of water runoff from different vegetation types on extensive green roofs: Effects of plant species, diversity and plant structure', *Landscape and Urban Planning*, 104(3-4), pp. 356-363.
- Natural Environment Research, C. (1975) *Flood studies report*. London.
- Nawaz, R., McDonald, A. and Postoyko, S. (2015) 'Hydrological performance of a full-scale extensive green roof located in a temperate climate', *Ecological Engineering*, 82, pp. 66-80.
- Nektarios, P. A., Ntoulas, N., Nydrioti, E., Kokkinou, I., Bali, E.-M. and Amountzias, I. (2015) 'Drought stress response of Sedum sediforme grown in extensive green roof systems with different substrate types and depths', *Scientia Horticulturae*, 181, pp. 52-61.
- Nimmo, J. R. (2004) 'Porosity and Pore Size Distribution', *Encyclopedia of Soils in the Environment*, 3, pp. 295-303.

- NovaLynx Corporation 2007. Model 260-2595 Rain Gauge Calibrator Instruction Manual. Auburn: NovaLynx Corporation.
- Olszewski, M. W., Holmes, M. H. and Young, C. A. (2010) 'Assessment of physical properties and stonecrop growth in green roof substrates amended with compost and hydrogel', *HortTechnology*, 20(2), pp. 438-444.
- Ondoño, S., Bastida, F. and Moreno, J. L. (2014) 'Microbiological and biochemical properties of artificial substrates: A preliminary study of its application as Technosols or as a basis in Green Roof Systems', *Ecological Engineering*, 70, pp. 189-199.
- Ondono, S., Martinez-Sanchez, J. J. and Moreno, J. L. (2016) 'The composition and depth of green roof substrates affect the growth of *Silene vulgaris* and *Lagurus ovatus* species and the C and N sequestration under two irrigation conditions', *J Environ Manage*, 166, pp. 330-40.
- Owczarek, K., Ciupala, M. A., Connop, S. and Newport, D. 2016. Green roof runoff monitoring systems: Review - Draft. Unpublished article.
- Palla, A., Gnecco, I. and Lanza, L. G. (2010) 'Hydrologic Restoration in the Urban Environment Using Green Roofs', *Water*, 2(2), pp. 140-154.
- Palla, A., Sansalone, J. J., Gnecco, I. and Lanza, L. G. (2011) 'Storm water infiltration in a monitored green roof for hydrologic restoration', *Water Science & Technology*, 64(3), pp. 766.
- Pérez, G., Coma, J., Solé, C., Castell, A. and Cabeza, L. F. (2012) 'Green roofs as passive system for energy savings when using rubber crumbs as drainage layer', *Energy Procedia*, 30, pp. 452-460.
- Perez, G., Vila, A., Rincon, L., Sole, C. and Cabeza, L. F. (2012) 'Use of rubber crumbs as drainage layer in green roofs as potential energy improvement material', *Applied Energy*, 97, pp. 347-354.
- Planet Natural (2016) *Damping off*. Available at: <https://www.planetnatural.com/pest-problem-solver/plant-disease/damping-off/> (Accessed: 15 July 2016).
- Putwain, P., Haynes, G., Rawlinson, H., A.Walker and Cook, P. (2011) *Determination of the growing benefits of wool-rich carpet shred*, Warrington: Ecological Restoration Consultants.
- Qin, X., Wu, X., Chiew, Y.-M. and Li, Y. (2012) 'A Green Roof Test Bed for Stormwater Management and Reduction of Urban Heat Island Effect in

- Singapore', *British Journal of Environment & Climate Change*, 2(4), pp. 410-420.
- Razzaghmanesh, M. and Beecham, S. (2014) 'The hydrological behaviour of extensive and intensive green roofs in a dry climate', *Science of The Total Environment*, 499(0), pp. 284-296.
- Rincón, L., Coma, J., Pérez, G., Castell, A., Boer, D. and Cabeza, L. F. (2014) 'Environmental performance of recycled rubber as drainage layer in extensive green roofs. A comparative Life Cycle Assessment', *Building and Environment*, 74, pp. 22-30.
- Rowe, D. B. (2011) 'Green roofs as a means of pollution abatement', *Environmental Pollution*, 159(8–9), pp. 2100-2110.
- Sailor, D. J. and Hagos, M. (2011) 'An updated and expanded set of thermal property data for green roof growing media', *Energy and Buildings*, 43(9), pp. 2298-2303.
- Sanderson, M. (2010) *Changes in the frequency of extreme rainfall events for selected towns and cities*, Exeter: Met Office.
- Schroll, E., Lambrinos, J., Righetti, T. and Sandrock, D. (2011) 'The role of vegetation in regulating stormwater runoff from green roofs in a winter rainfall climate', *Ecological Engineering*, 37(4), pp. 595-600.
- Shaw, E. M. (2011) *Hydrology in practice*. 4th ed. edn. London: Spon Press.
- Simmons, M. T., Gardiner, B., Windhager, S. and Tinsley, J. (2008) 'Green roofs are not created equal: the hydrologic and thermal performance of six different extensive green roofs and reflective and non-reflective roofs in a sub-tropical climate', *Urban Ecosystems*, 11(4), pp. 339-348.
- Skinner, B. J. and Porter, S. C. (1995) *The blue planet : an introduction to earth system science*. New York ; Chichester: John Wiley.
- Smith, A. (2013) *Clay Bricks and Clay Blocks: a Resource Efficiency Action Plan*: WRAP and Brick Development Association.
- Snodgrass, E. C. and McIntyre, L. (2010) *The green roof manual : a professional guide to design, installation, and maintenance*. Portland, Or. ; London: Timber.
- Solano, L., Ristvey, A. G., Lea-Cox, J. D. and Cohan, S. M. (2012) 'Sequestering zinc from recycled crumb rubber in extensive green roof media', *Ecological Engineering*, 47, pp. 284-290.

- Spaans, M. and Waterhout, B. (2017) 'Building up resilience in cities worldwide – Rotterdam as participant in the 100 Resilient Cities Programme', *Cities*, 61, pp. 109-116.
- Speak, A. F., Rothwell, J. J., Lindley, S. J. and Smith, C. L. (2012) 'Urban particulate pollution reduction by four species of green roof vegetation in a UK city', *Atmospheric Environment*, 61(0), pp. 283-293.
- Speak, A. F., Rothwell, J. J., Lindley, S. J. and Smith, C. L. (2013a) 'Rainwater runoff retention on an aged intensive green roof', *Science of The Total Environment*, 461–462(0), pp. 28-38.
- Speak, A. F., Rothwell, J. J., Lindley, S. J. and Smith, C. L. (2013b) 'Reduction of the urban cooling effects of an intensive green roof due to vegetation damage', *Urban Climate*, 3, pp. 40-55.
- Stovin, V. (2010) 'The potential of green roofs to manage Urban Stormwater', *Water and Environment Journal*, 24(3), pp. 192-199.
- Stovin, V., Poe, S. and Berretta, C. (2013) 'A modelling study of long term green roof retention performance', *J Environ Manage*, 131, pp. 206-15.
- Stovin, V., Poë, S., De-Ville, S. and Berretta, C. (2015) 'The influence of substrate and vegetation configuration on green roof hydrological performance', *Ecological Engineering*, 85, pp. 159-172.
- Stovin, V., Vesuviano, G. and Kasmin, H. (2012) 'The hydrological performance of a green roof test bed under UK climatic conditions', *Journal of Hydrology*, 414–415(0), pp. 148-161.
- Susca, T., Gaffin, S. R. and Dell'Osso, G. R. (2011) 'Positive effects of vegetation: Urban heat island and green roofs', *Environmental Pollution*, 159(8–9), pp. 2119-2126.
- Takebayashi, H. and Moriyama, M. (2007) 'Surface heat budget on green roof and high reflection roof for mitigation of urban heat island', *Building and Environment*, 42(8), pp. 2971-2979.
- Teemusk, A. and Mander, U. (2006) 'The use of greenroofs for the mitigation of environmental problems in urban areas', in Mander, U., Brebbia, C.A. & Tiezzi, E. (eds.) *Sustainable City IV : Urban Regeneration and Sustainability Wit Transactions on Ecology and the Environment*, pp. 3-17.
- Teemusk, A. and Mander, U. (2007) 'Rainwater runoff quantity and quality performance from a greenroof: The effects of short-term events', *Ecological Engineering*, 30(3), pp. 271-277.

- The Green Roof Organisation (2014) *The GRO green roof code : green roof code of best practice for the UK 2014*. Sheffield: Groundwork Sheffield.
- Thomas, P. (2010) *FLOORING: A Resource Efficiency Action Plan*, London: Construction Products Association.
- Thuring, C. E., Berghage, R. D. and Beattie, D. J. (2010) 'Green Roof Plant Responses to Different Substrate Types and Depths under Various Drought Conditions', *HortTechnology*, 20(2), pp. 395-401.
- UK Meteorological Office (1948-current) 'UK climate - Historic station data'. Available at: [http://www.metoffice.gov.uk/pub/data/weather/uk/climate/stationdata/heat\\_hrowdata.txt](http://www.metoffice.gov.uk/pub/data/weather/uk/climate/stationdata/heat_hrowdata.txt) (Accessed: 2016).
- UK Meteorological Office (2016) *Southern England: climate*. Available at: <http://www.metoffice.gov.uk/climate/uk/regional-climates/so> (Accessed: 15 July 2016).
- University of East London (2010) *Barking Riverside green roof experiment: University of East London*. Available at: [http://www.uel.ac.uk/erg/documents/Greenroof\\_expt\\_leaflet.pdf](http://www.uel.ac.uk/erg/documents/Greenroof_expt_leaflet.pdf) (Accessed: 29 July 2012).
- Van Renterghem, T. and Botteldooren, D. (2011) 'In-situ measurements of sound propagating over extensive green roofs', *Building and Environment*, 46(3), pp. 729-738.
- Van Renterghem, T. and Botteldooren, D. (2014) 'Influence of rainfall on the noise shielding by a green roof', *Building and Environment*, 82(0), pp. 1-8.
- Van Seters, T., Rocha, L., Smith, D. and MacMillan, G. (2009) 'Evaluation of Green Roofs for Runoff Retention, Runoff Quality, and Leachability', *Water Quality Research Journal of Canada*, 44(1), pp. 33-47.
- VanWoert, N. D., Rowe, D. B., Andresen, J. A., Rugh, C. L., Fernandez, R. T. and Xiao, L. (2005) 'Green roof stormwater retention: effects of roof surface, slope, and media depth', *J Environ Qual*, 34(3), pp. 1036-44.
- Versini, P. A., Ramier, D., Berthier, E. and de Gouvello, B. (2015) 'Assessment of the hydrological impacts of green roof: from building scale to basin scale', *Journal of Hydrology*, (0).
- Vesuviano, G. and Stovin, V. (2013) 'A generic hydrological model for a green roof drainage layer', *Water Sci Technol*, 68(4), pp. 769-75.

- Vijayaraghavan, K. (2016) 'Green roofs: A critical review on the role of components, benefits, limitations and trends', *Renewable and Sustainable Energy Reviews*, 57, pp. 740-752.
- Vijayaraghavan, K. and Joshi, U. M. (2015) 'Application of seaweed as substrate additive in green roofs: Enhancement of water retention and sorption capacity', *Landscape and Urban Planning*, 143, pp. 25-32.
- Vijayaraghavan, K., Joshi, U. M. and Balasubramanian, R. (2012) 'A field study to evaluate runoff quality from green roofs', *Water Res*, 46(4), pp. 1337-45.
- Vijayaraghavan, K. and Raja, F. D. (2014) 'Design and development of green roof substrate to improve runoff water quality: Plant growth experiments and adsorption', *Water Research*, 63(0), pp. 94-101.
- Vijayaraghavan, K. and Raja, F. D. (2015) 'Pilot-scale evaluation of green roofs with Sargassum biomass as an additive to improve runoff quality', *Ecological Engineering*, 75(0), pp. 70-78.
- Vila, A., Pérez, G., Solé, C., Fernández, A. I. and Cabeza, L. F. (2012) 'Use of rubber crumbs as drainage layer in experimental green roofs', *Building and Environment*, 48, pp. 101-106.
- Villarreal, E. L. and Bengtsson, L. (2005) 'Response of a Sedum green-roof to individual rain events', *Ecological Engineering*, 25(1), pp. 1-7.
- Volder, A. and Dvorak, B. (2014) 'Event size, substrate water content and vegetation affect storm water retention efficiency of an un-irrigated extensive green roof system in Central Texas', *Sustainable Cities and Society*, 10(0), pp. 59-64.
- Voyde, E., Fassman, E. and Simcock, R. (2010) 'Hydrology of an extensive living roof under sub-tropical climate conditions in Auckland, New Zealand', *Journal of Hydrology*, 394(3-4), pp. 384-395.
- Water UK (2006) *Sewers for Adoption - A Design and Construction Guide for Developers*. 6 th edn. Wiltshire: WRc plc.
- Waterman 2012. Waterman extend their appointment on LYTAG.
- Whitlow, R. (1995) *Basic soil mechanics*. 3rd ed. edn. Harlow: Longman Scientific & Technical.
- Whittinghill, L. J., Rowe, D. B. and Cregg, B. M. (2013) 'Evaluation of Vegetable Production on Extensive Green Roofs', *Agroecology and Sustainable Food Systems*, 37(4), pp. 465-484.

- Wolf, D. and Lundholm, J. T. (2008) 'Water uptake in green roof microcosms: Effects of plant species and water availability', *Ecological Engineering*, 33(2), pp. 179-186.
- Wong, G. K. L. and Jim, C. Y. (2014) 'Quantitative hydrologic performance of extensive green roof under humid-tropical rainfall regime', *Ecological Engineering*, 70(0), pp. 366-378.
- Wong, G. K. L. and Jim, C. Y. (2015) 'Identifying keystone meteorological factors of green-roof stormwater retention to inform design and planning', *Landscape and Urban Planning*, 143, pp. 173-182.
- Yio, M. H., Stovin, V., Werdin, J. and Vesuviano, G. (2013) 'Experimental analysis of green roof substrate detention characteristics', *Water Sci Technol*, 68(7), pp. 1477-86.
- Young, T., Cameron, D. D., Sorrill, J., Edwards, T. and Phoenix, G. K. (2014) 'Importance of different components of green roof substrate on plant growth and physiological performance', *Urban Forestry & Urban Greening*, 13(3), pp. 507-516.

## APPENDIX A

### ABG Geosynthetic Meadow Mix and ABG Geosynthetic Finesse Roofdrain40 Manufacturer's specification



## ROOFDRAIN 40S1RXSSc3h

GEOCOMPOSITE DRAINAGE AND FLOW ATTENUATION LAYER

**ROOFDRAIN 40S1RXSSc3h** consists of a perforated cusped HDPE (High Density Polyethylene) core with selected geotextiles thermally bonded on each side. It is primarily intended for use under thin soil layers where the plant roots can reach down to the water in the core reservoirs. The core is perforated to allow the excess rainwater to flow into the underside and away through the **ROOFDRAIN** to the outlets. The upper textile is optimised for drainage performance and the lower textile protects the waterproofing system. Its major application is in extensive roof garden drainage where **ROOFDRAIN** provides a lightweight drainage layer and water reservoir to sustain plant growth.

For efficient storage and handling, the product is normally rolled "dimples inward", and will usually require to be turned over during installation.

**ROOFDRAIN 40S1RXSSc3h** makes extensive use of recycled polymers in its construction.

#### GEOTEXTILES

		Flat face	Dimple face	
Type		Heat treated non-woven	Non-woven felt	
Material		Polypropylene	Mixed pp & other recycled polymers	
Mass / unit area	(g/m <sup>2</sup> )	250	300 <sup>(3)</sup>	EN ISO 9864
Water flow at 50mm head	l/m <sup>2</sup> .sec	80	not determined <sup>(3,6)</sup>	EN ISO 11058
Breakthrough head	(mm)	0	not determined <sup>(3,6)</sup>	BS 6906 (3)
Pore size O <sub>90</sub>	(µm)	70	not determined <sup>(3,6)</sup>	EN ISO 12956
Static Puncture (CBR)	(N)	3 400	1 500 <sup>(3)</sup>	EN ISO 12236
Chemical resistance		Highly resistant to all common chemicals		

#### ROOFDRAIN

		Hydraulic gradient =			
		10%	3%	1%	
In-plane water flow at 20kPa	(l/m.s)	10.1	4.5	2.0	EN ISO 12958
based on structural boundary conditions as simulated by <b>HARD platen</b> testing					
Water flow normal to the plane	(l/m <sup>2</sup> .s)	1.4			
Thickness at 2kPa	(mm)	45		(nominal)	EN ISO 9863-1
Tensile strength (MD/CD)	(kN/m)	32 / 32			EN ISO 10319
Elongation at peak (MD/CD)	(%)	35 / 40			EN ISO 10319
Water reservoir volume <sup>(7)</sup>	(l/m <sup>2</sup> )	14			
Mass/unit area (dry)	(g/m <sup>2</sup> )	2 550			EN ISO 9864
Mass/unit area (saturated)	(g/m <sup>2</sup> )	16 600		(indicative)	EN ISO 9864
Life expectancy	(yrs)	120 years in pH 4 to 9 at 25°C			
Chemical resistance		Excellent resistance to common chemicals			EN 14030
Resistance to microbes		No significant effect			EN 12225
Waterproofing Compatibility		Fully compatible. All components compatible with potable water			
Health, safety, environment		INERT. No known health hazard. No precautions necessary			

#### NOTES

- (1) The geotextile is bonded to the core to prevent intrusion into and blockage of the drainage passage under the action of pressure of fill material. The textile is root-permeable; if a root barrier is required alternative textiles can be substituted or an additional layer of **ROOTEX** should be laid.
- (2) The values given are indicative and correspond to nominal results obtained in our laboratories and testing institutes. The above figures have been obtained from statistical interpretation of test results. In line with our policy of continuous improvement the right is reserved to make changes without notice at any time.
- (3) Unless otherwise stated allowable tolerances are ± 15% of the typical value except for recycled textile for which the values are indicative. The tolerance on roll length is 1.5% and on roll width is 1.0%.
- (4) The above figures have been obtained from statistical interpretation of test results.
- (5) Non-load bearing walls can be built off Roofdrain
- (6) The hydraulic performance of the dimple face textile does not influence overall product performance.
- (7) Water retention within the soil 20 – 40 litres (dependent on thickness of soil)
- (8) Final determination of the suitability of any information is the sole responsibility of the user. ABG will be pleased to discuss the use of this or any other product but responsibility for selection of a material and its application in any specific project remains with the user.
- (9) Refer to separate sheets for fixing instructions and packing dimensions.

## ABG Sedum, Meadow & Lawn Roof Media & Sedum Seed Medium

All mixes are based on specially matured and graded green compost to provide optimal stability, and minimal leaching of organic matter & nutrients, plus carefully selected and graded clay aggregate: recycled from virgin brick and tile.

- **Sedum Roof Medium** is based on 5 -14mm brick/tile & 10 – 25mm green compost
- **Meadow Roof Medium** is based on 2 - 5mm brick/tile & 0 - 10mm green compost
- **Lawn Roof Medium** is based on 2 - 5mm brick/tile & 0 - 10mm green compost & soil
- **Sedum Seed Medium** is based on 5 -14mm brick/tile & 0-8mm compost, fine bark & soil

All provide an air-filled porosity greater than 20% v/v – as advised by the Green Roof Centre, Sheffield (see below) – and thus good drainage, robust hardy growth and strong root action.

Properties		Typical Values	
		Sedum Roof	Meadow Roof
Laboratory bulk density	g/l	840	800
Organic matter	%DM	2	2
(from loss at 450°C)	g/litre	22	23
pH <sup>1</sup> (1:5 aqueous extract)		8.0	8.0
Electrical conductivity	µS/cm	380	400
(1:5 aqueous extract)	mS/m	38	40
Stability	mg CO <sub>2</sub> /g OM	1.3	1.3
<b>Nutrients</b>			
<u>Water-extractable</u>			
Ammoniacal nitrogen (NH <sub>4</sub> -N)	mg/l	10	10
as N			
Nitric nitrogen (NO <sub>3</sub> -N) as N	mg/l	20	20
NH <sub>4</sub> +NO <sub>3</sub> -N as N	mg/l	30	30
Calcium as Ca	mg/l	20	30
<u>CAT-extractable <sup>2</sup></u>			
Phosphorus as P	mg/l	6	12
Potassium as K	mg/l	216	300
Magnesium as Mg	mg/l	24	30
Sulphur as S	mg/l	6	16
Iron as Fe	mg/l	6	20
<u>Total Extractable</u>			
Nitrogen as N	mg/l	600	800
Phosphorus as P	mg/l	60	200

(values for elements such as K, Ca & Mg are not reported because inert forms of these elements in the aggregate would render the data meaningless)

### Particle size distribution (% air-dry sample passing)

	16.0mm	98	100
	8.0 mm	20	90
	4.0 mm	2	70
	1.0 mm	Nil	25
Air-filled porosity	% v/v	41.5	24.9
Water-holding capacity	% v/v	12.7	25.2
Solids	% v/v	45.8	49.9
Weeds and foreign matter		Nil	Nil

<sup>1</sup> This should not be compared with the pH of peat products (the optimal pH of peat products is much lower than for soils and composted materials).

<sup>2</sup> 'CAT' = aqueous solution of calcium chloride + DTPA (chelating agent) – an extractant originally developed for soils and now specified in UK and European standards for composted materials (eg PAS 100) because it is more appropriate for most nutrients than the water-extraction method originally developed for peat products only.

## APPENDIX B

Calibration curves for tipping bucket rain gauges measuring runoff from experimental green roof plots and control roof plots at Barking Riverside in-situ experiment

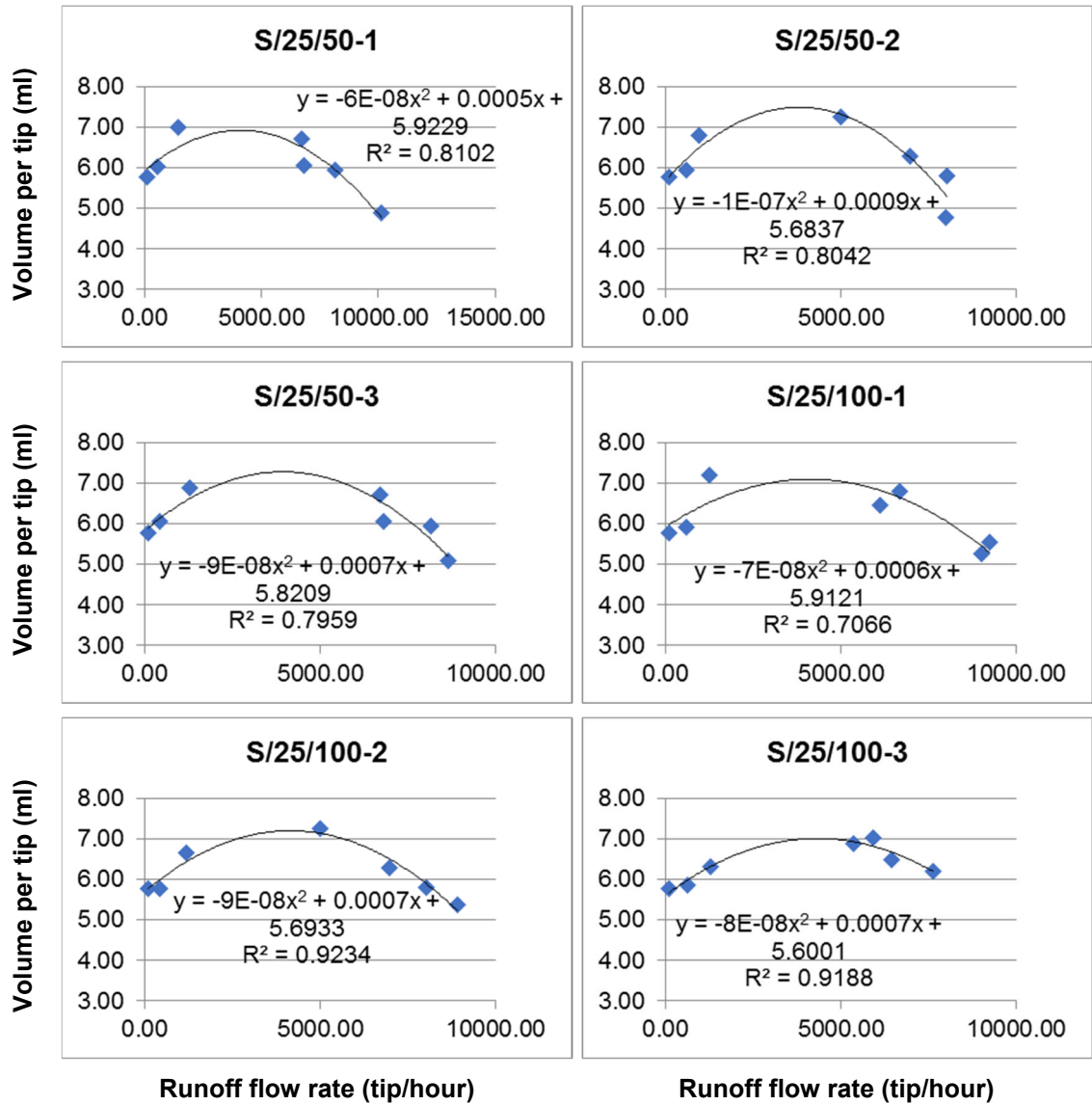


Figure B.1 Modelled calibration curves for the sedum green roof plots with drainage layer depth being 25mm.

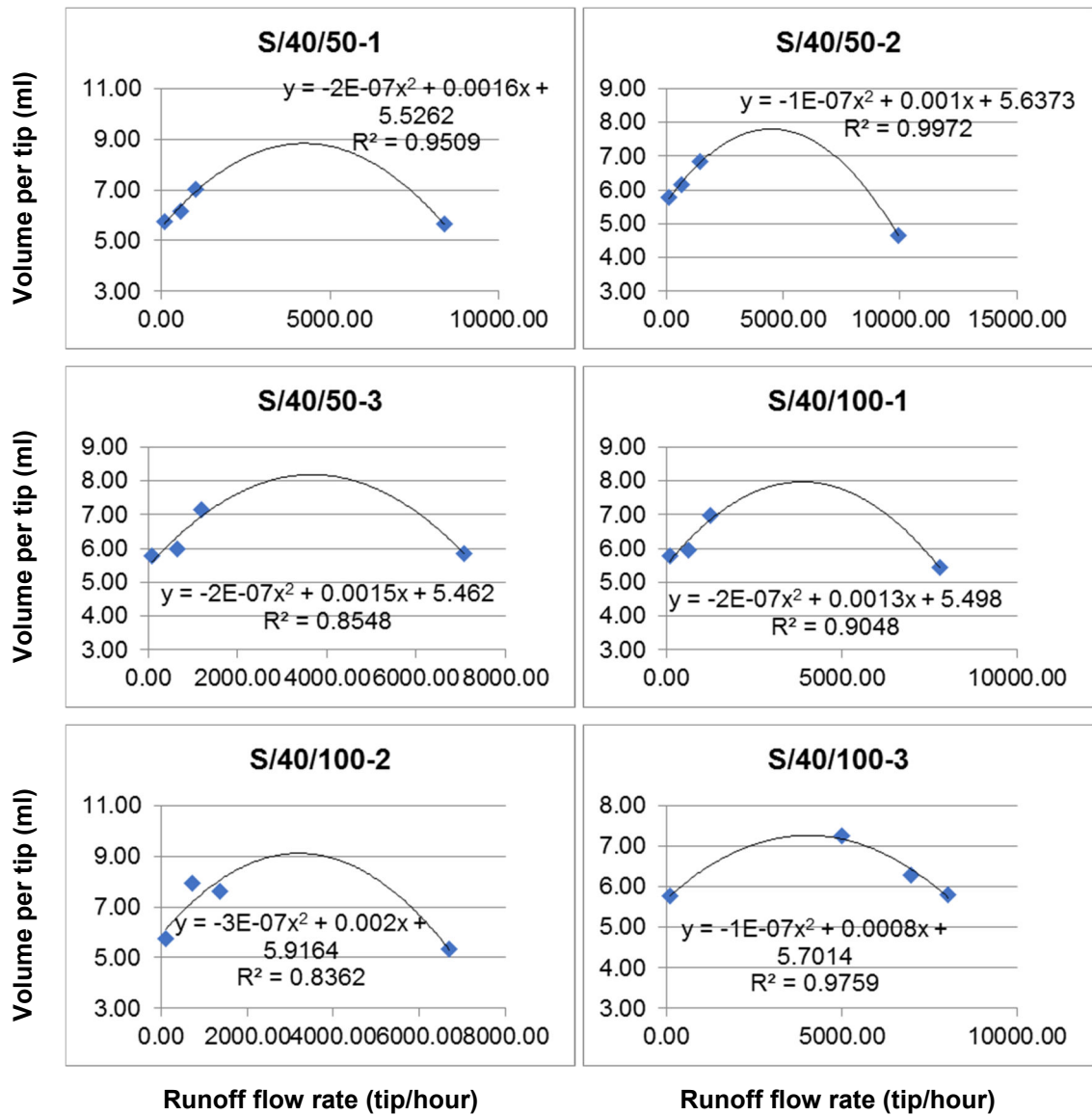


Figure B.2 Modelled calibration curves for the sedum green roof plots with drainage layer depth being 40mm.

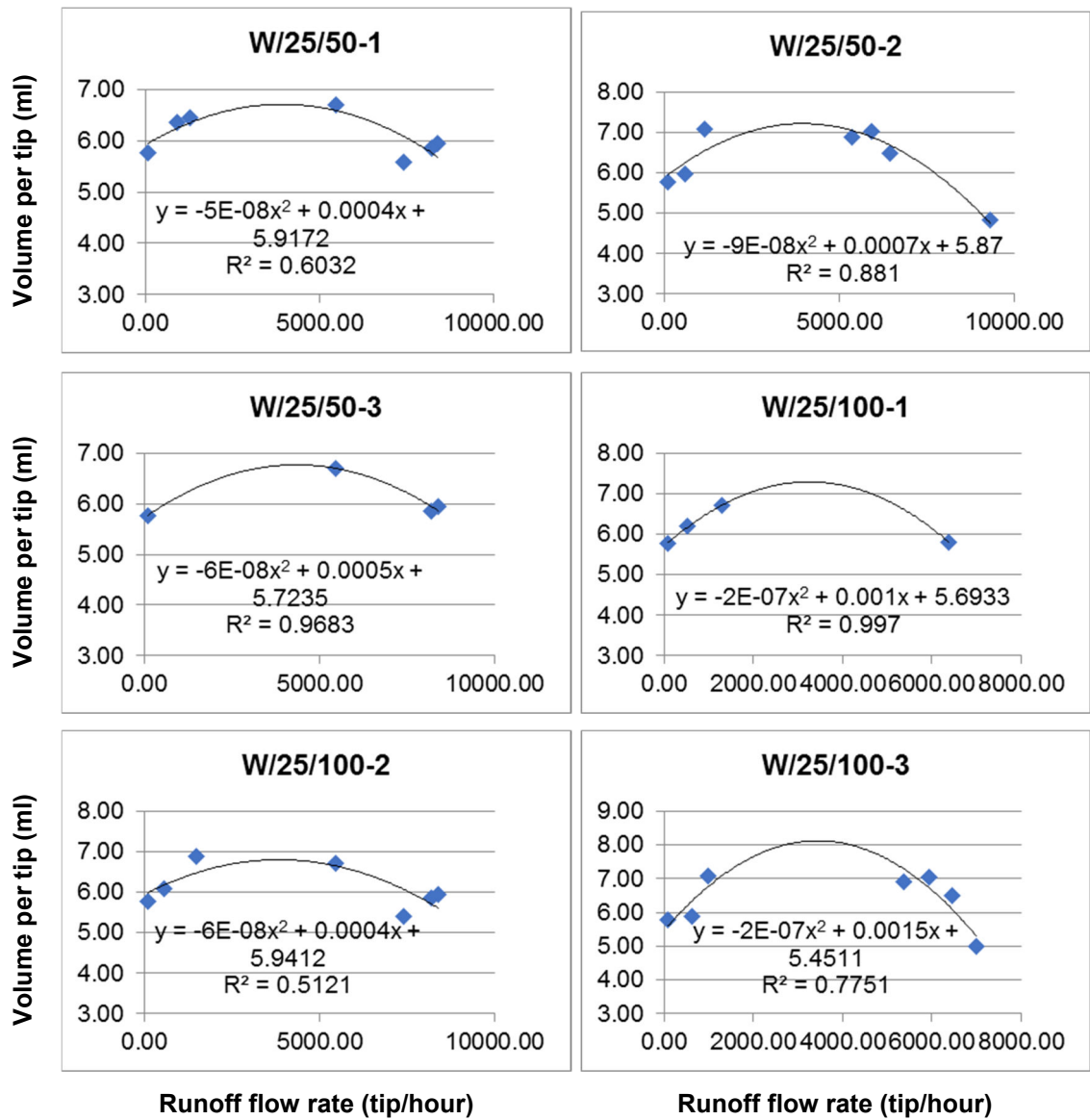


Figure B.3 Modelled calibration curves for the wildflower green roof plots with drainage layer depth being 25mm.

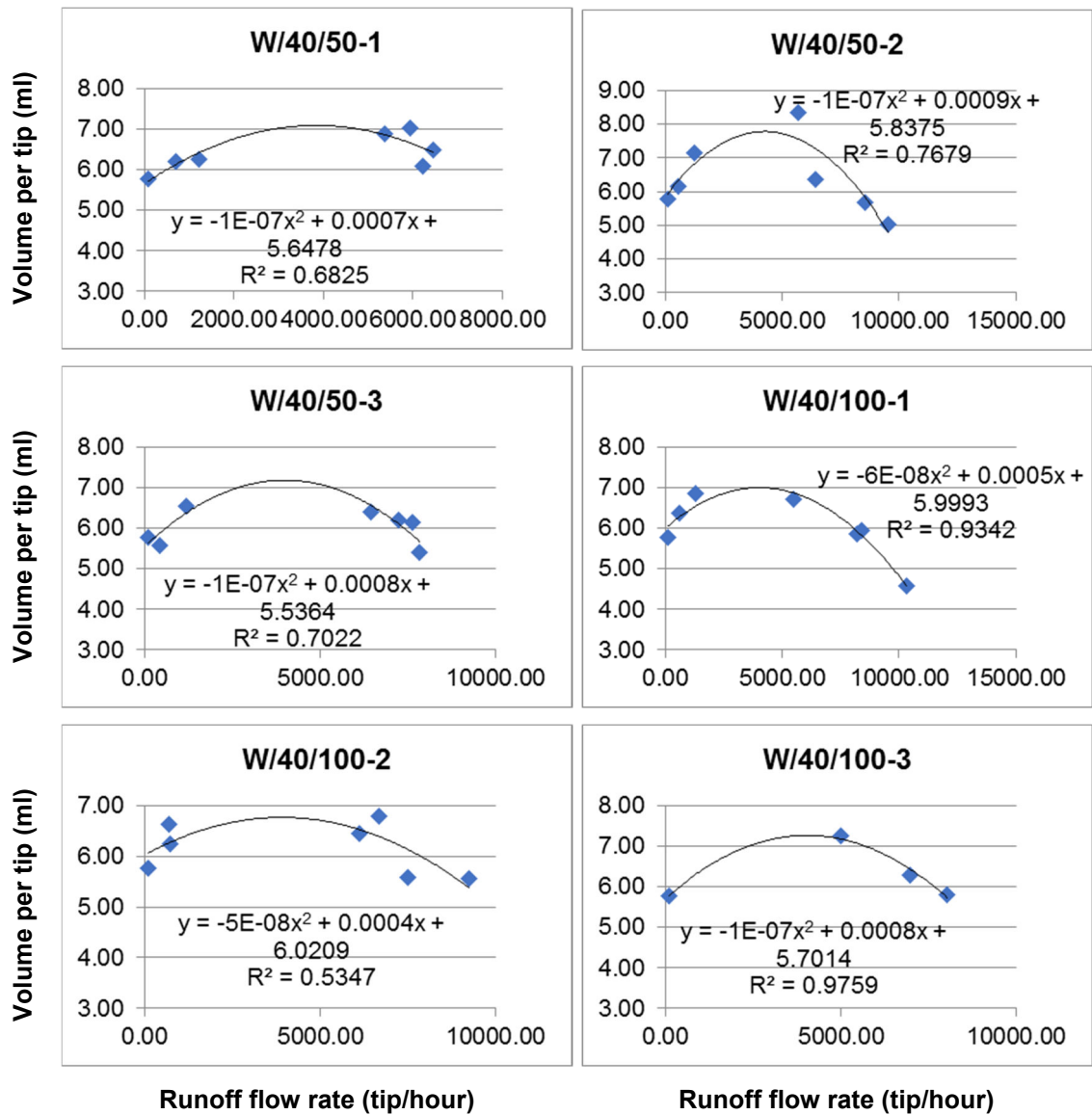


Figure B.4 Modelled calibration curves for the wildflower green roof plots with drainage layer depth being 40mm.

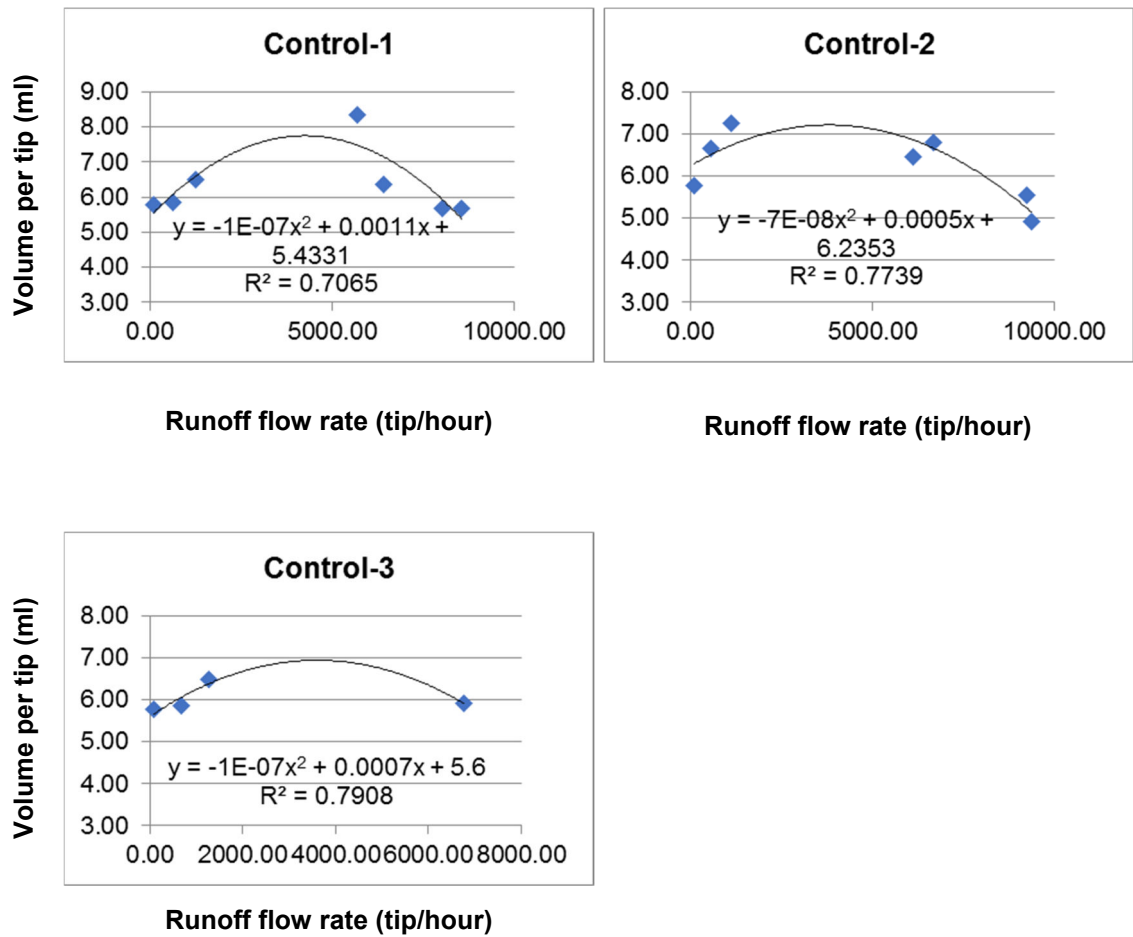


Figure B.5 Modelled calibration curves for the control roof plots.

## APPENDIX C

Barking Riverside in-situ experiment: Q-Q plots and density histograms for initial and final rainfall event data sets

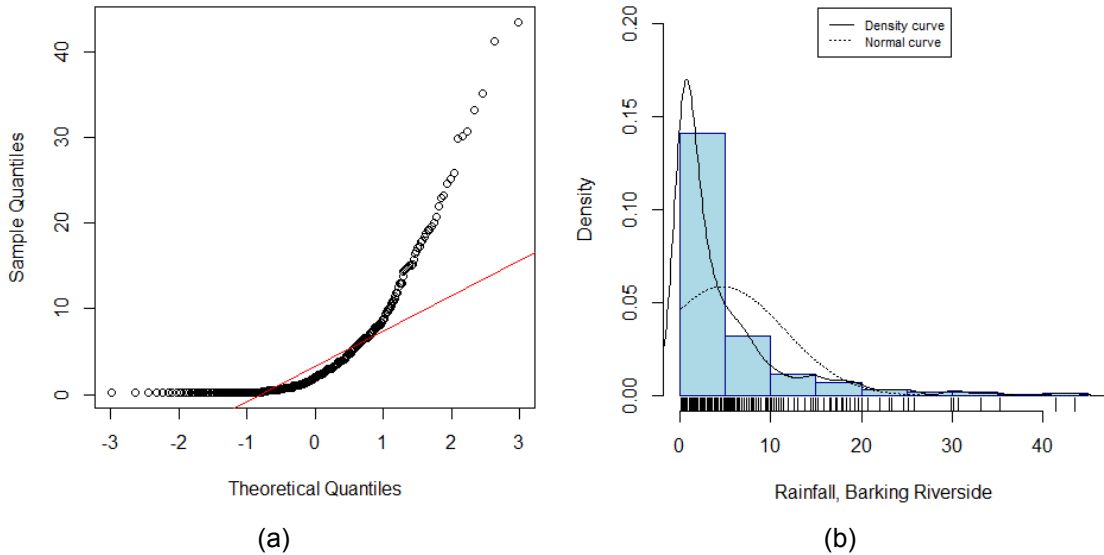


Figure C.1 Data exploratory analysis of rainfall at Barking Riverside – initial data set: (a) Q-Q plot showing relationship between sample and theoretical quantiles. It confirms non-normal distribution of rainfalls (b) histogram presenting the density of rainfall data. It shows exponential distribution of rainfalls.

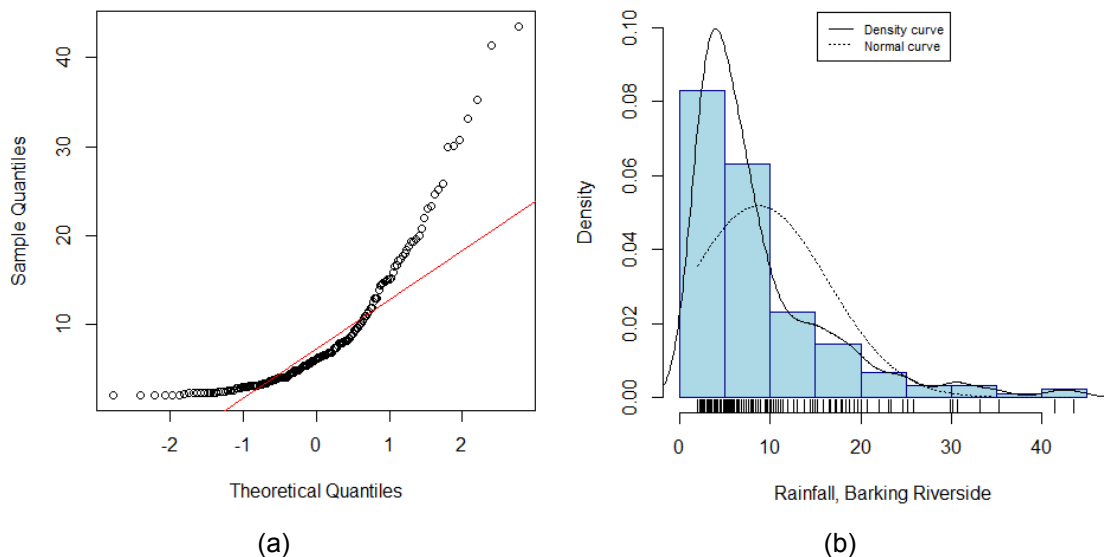


Figure C.2 Data exploratory analysis of rainfall at Barking Riverside – final data set: (a) Q-Q plot showing relationship between sample and theoretical quantiles. It confirms non-normal distribution of rainfalls (b) histogram presenting the density of rainfall data. It shows exponential distribution of rainfalls.

# APPENDIX D

Barking Riverside in-situ experiment: Q-Q plots and density histograms for retention data of each green roof experimental replicate

## Control roofs

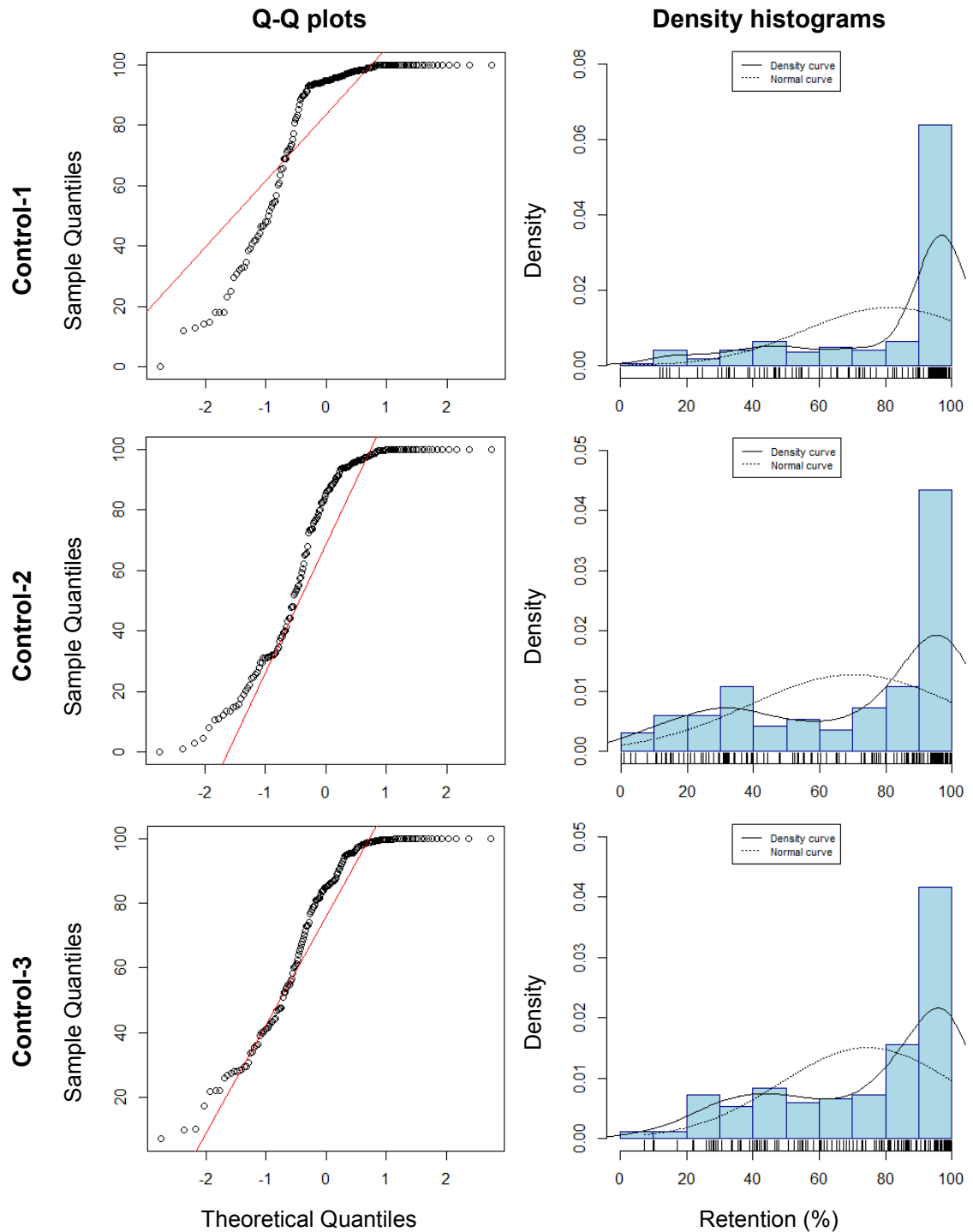
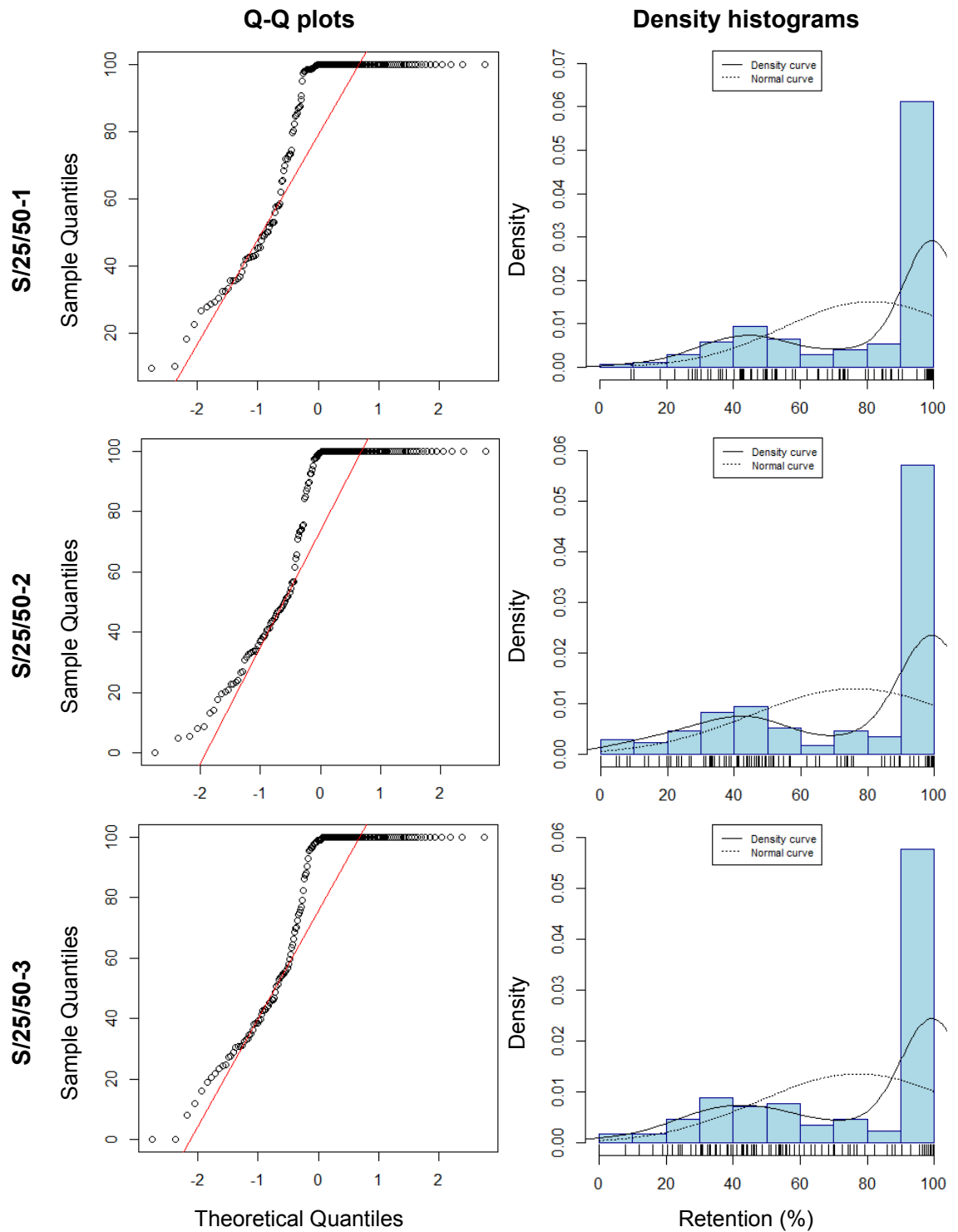


Figure D.1 Data exploratory analysis of retention data for replicates of control roof. Q-Q plots and density histograms confirm non-normal distribution of retention.

**Vegetation: Sedum, drainage layer: 25mm, substrate: 50mm (S/25/50)**



*Figure D.2 Data exploratory analysis of retention data for replicates of S/25/50 roof. Q-Q plots and density histograms confirm non-normal distribution of retention.*

Vegetation: Sedum, drainage layer: 25mm, substrate: 100mm (S/25/100)

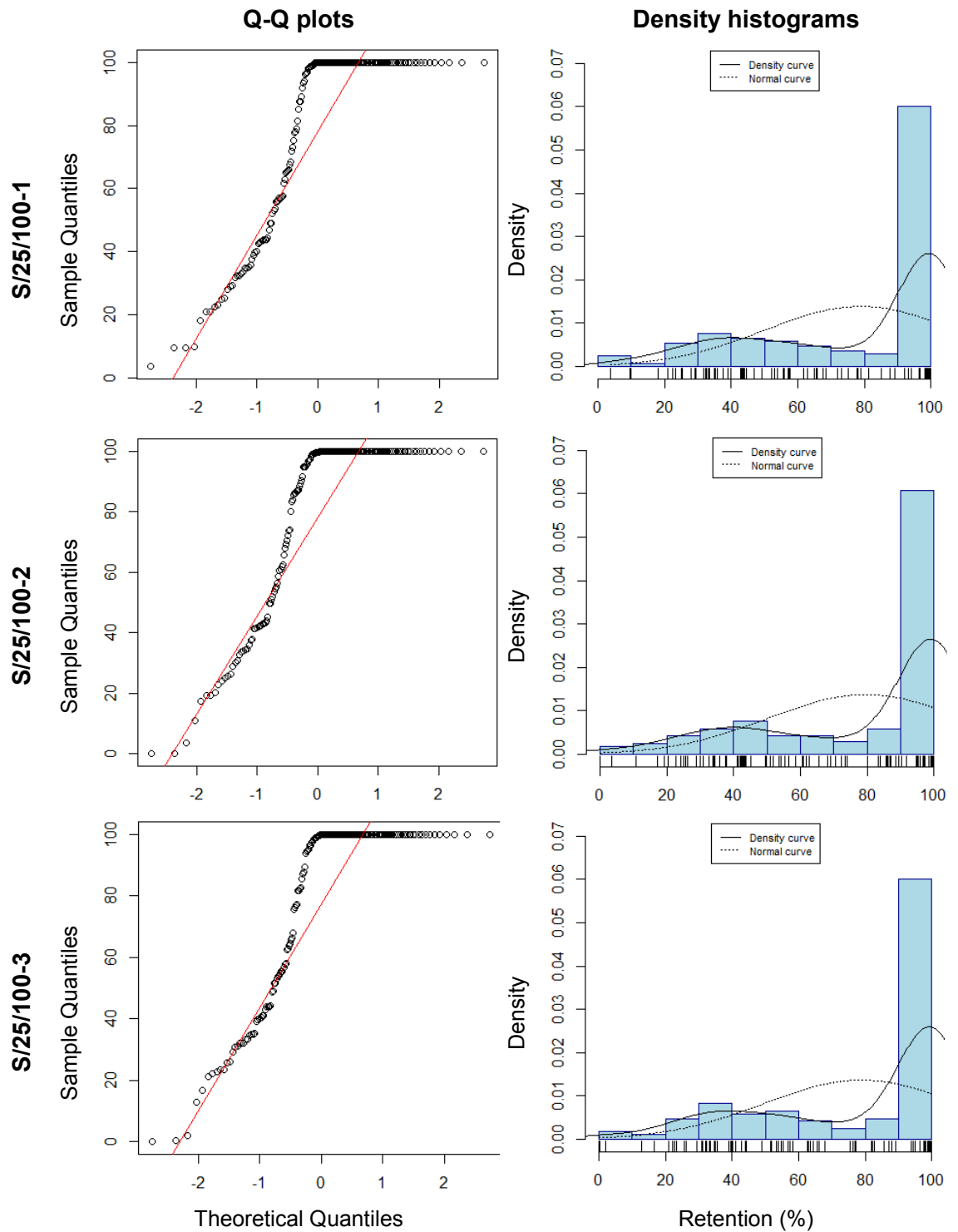


Figure D.3 Data exploratory analysis of retention data for replicates of S/25/100 roof. Q-Q plots and density histograms confirm non-normal distribution of retention.

Vegetation: Sedum, drainage layer: 40mm, substrate: 50mm (S/40/50)

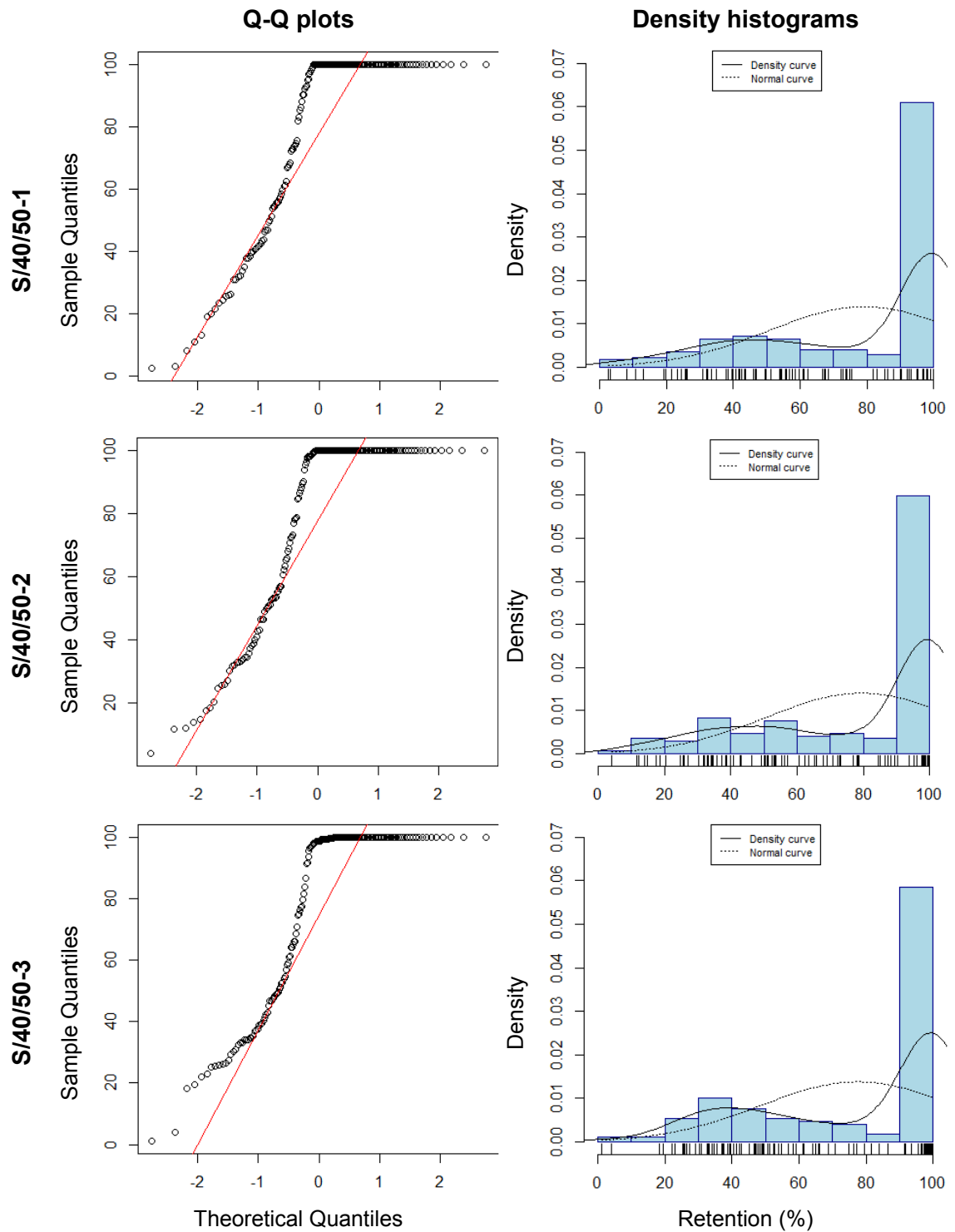


Figure D.4 Data exploratory analysis of retention data for replicates of S/40/50 roof. Q-Q plots and density histograms confirm non-normal distribution of retention.

Vegetation: Sedum, drainage layer: 40mm, substrate: 100mm (S/40/100)

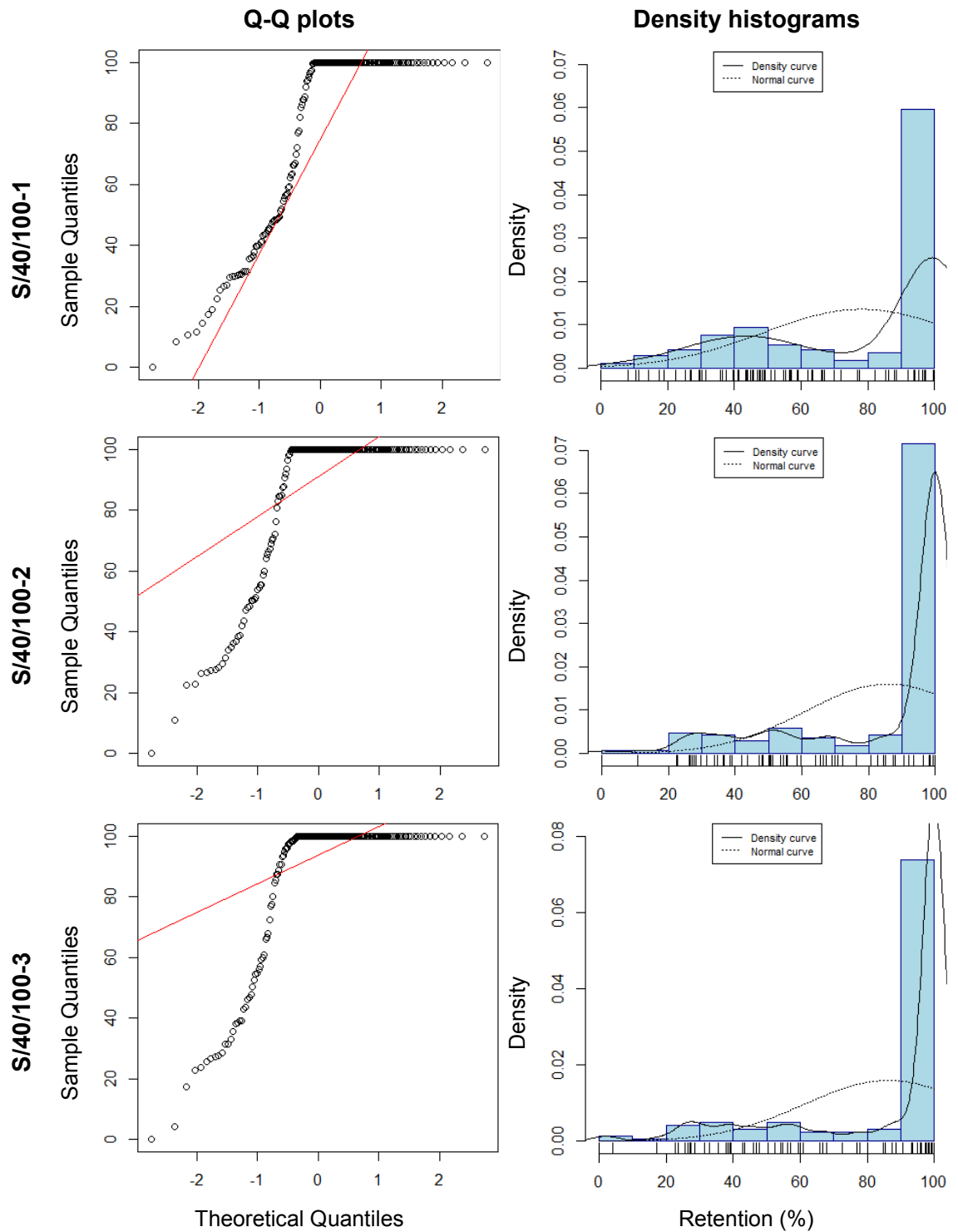


Figure D.5 Data exploratory analysis of retention data for replicates of S/40/100 roof. Q-Q plots and density histograms confirm non-normal distribution of retention.

Vegetation: Wildflower, drainage layer: 25mm, substrate: 50mm (W/25/50)

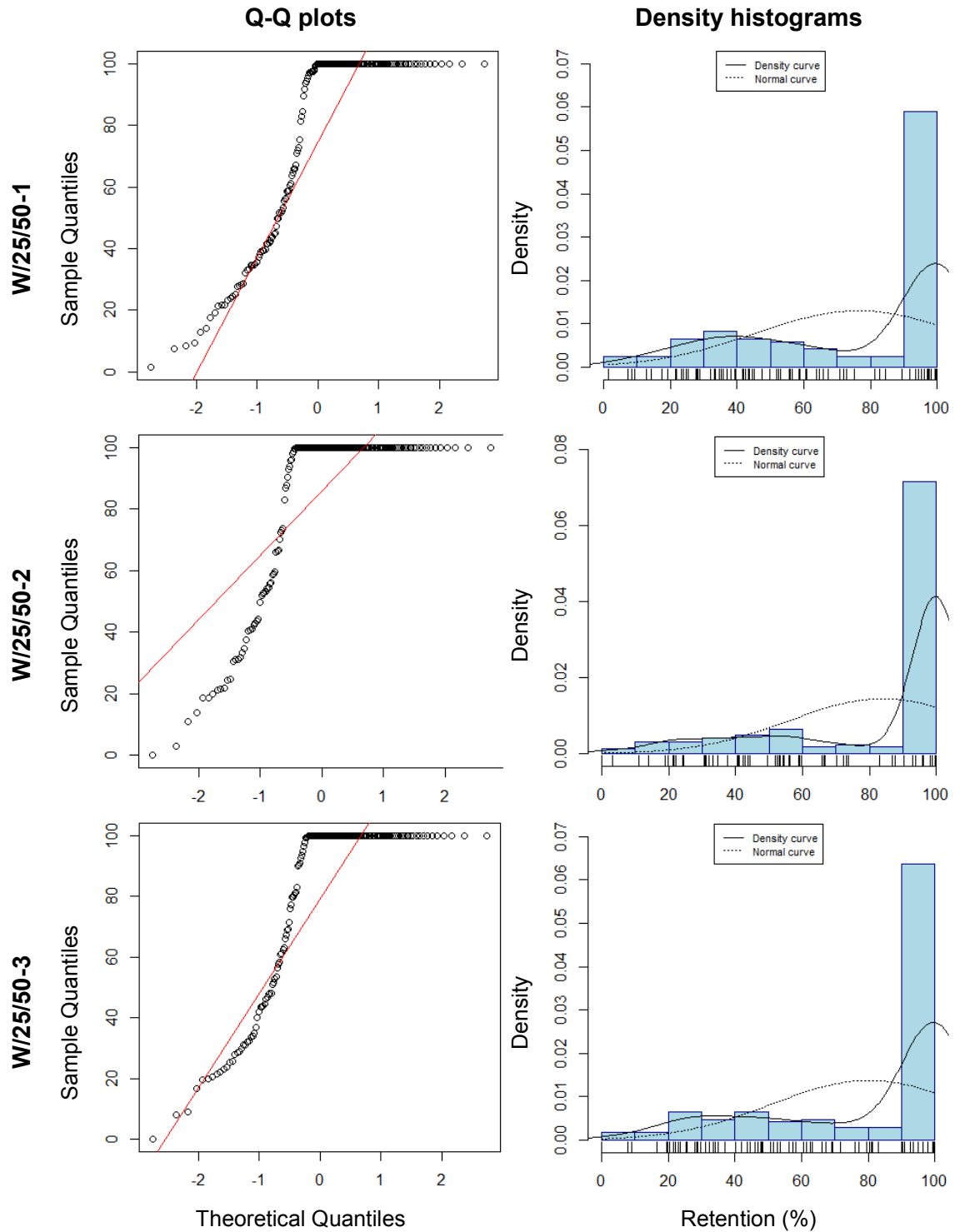


Figure D.6 Data exploratory analysis of retention data for replicates of W/25/50 roof. Q-Q plots and density histograms confirm non-normal distribution of retention.

Vegetation: Wildflower, drainage layer: 25mm, substrate: 100mm  
(W/25/100)

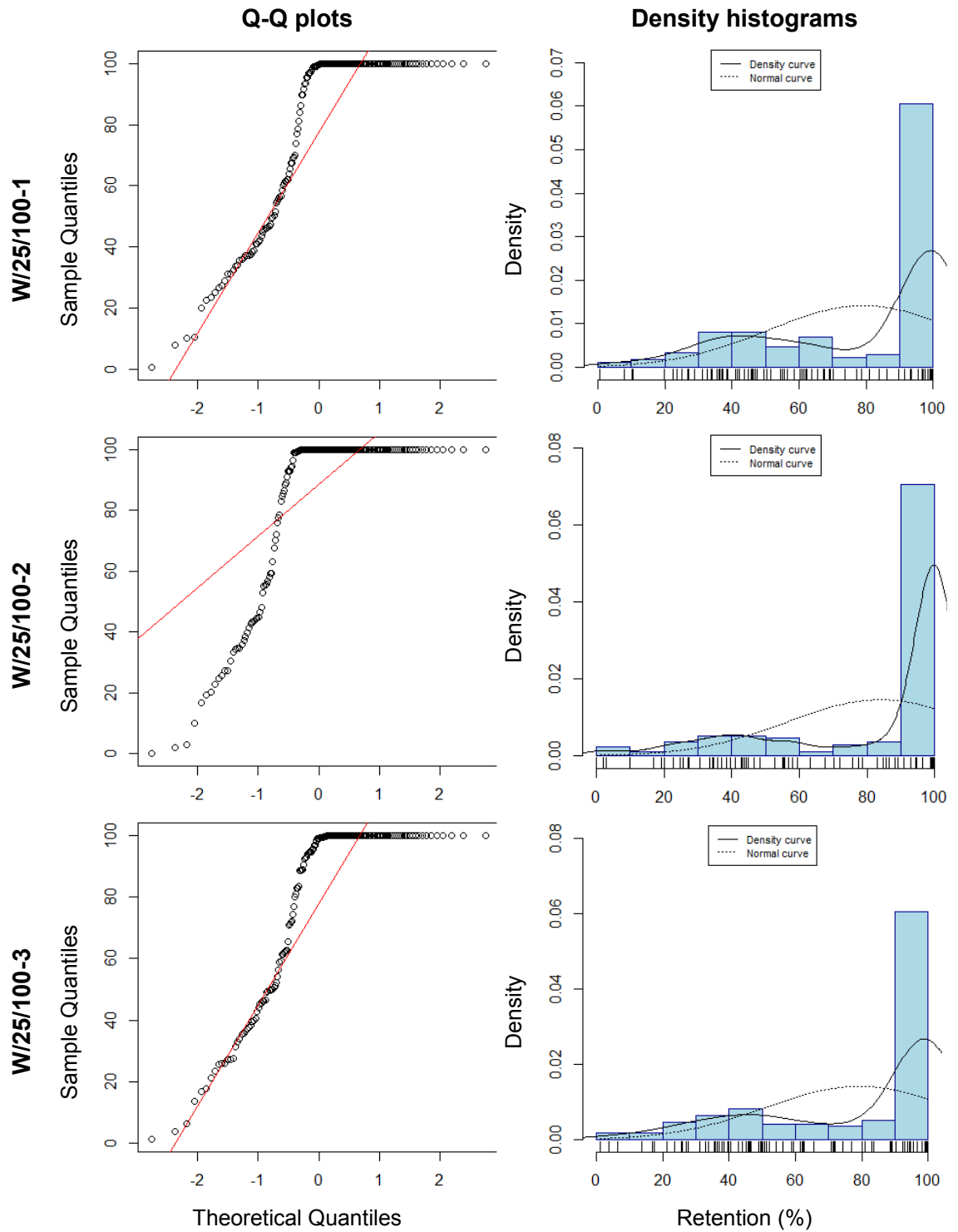


Figure D.7 Data exploratory analysis of retention data for replicates of W/25/100 roof. Q-Q plots and density histograms confirm non-normal distribution of retention.

Vegetation: Wildflower, drainage layer: 40mm, substrate: 50mm (W/40/50)

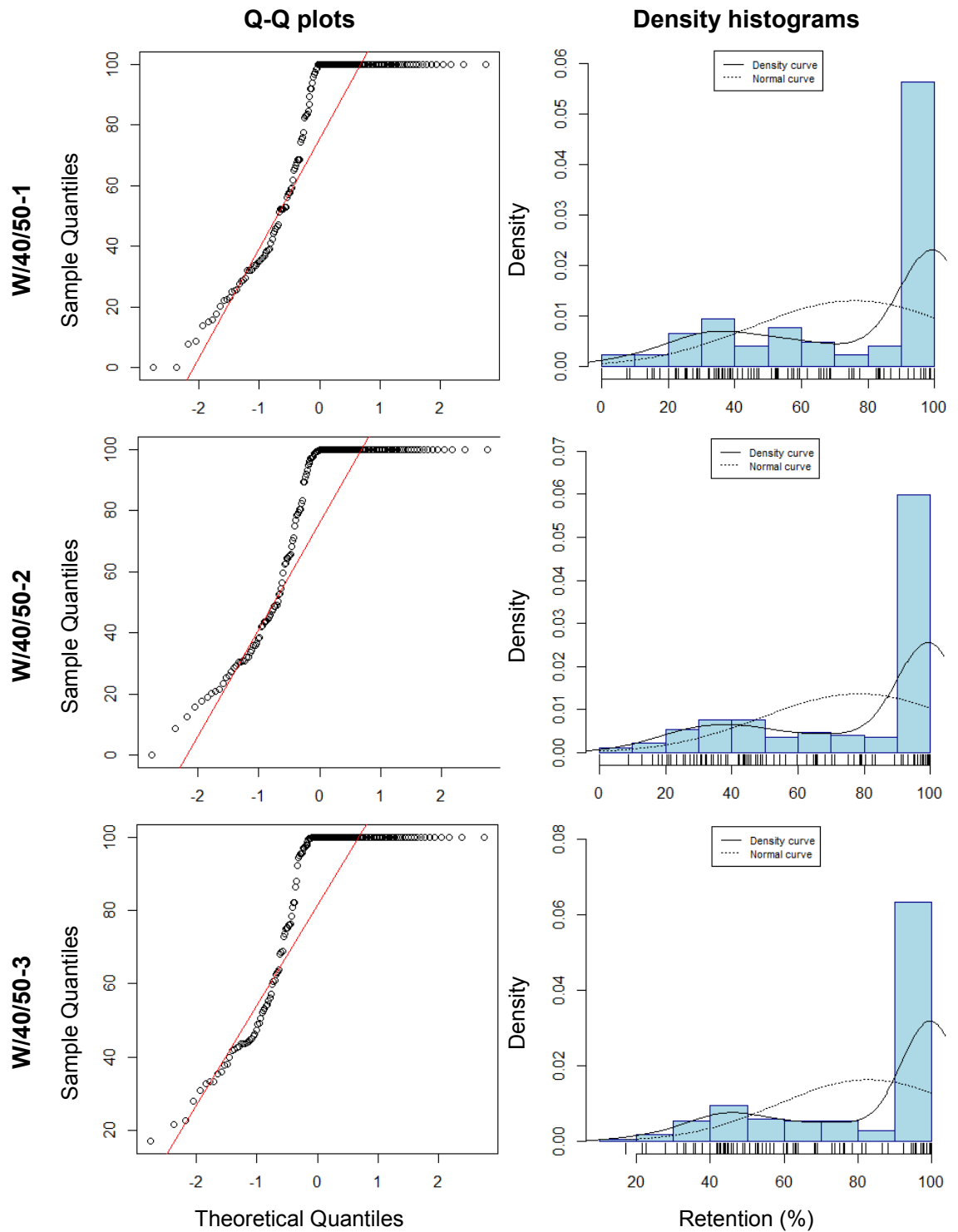


Figure D.8 Data exploratory analysis of retention data for replicates of W/40/50 roof. Q-Q plots and density histograms confirm non-normal distribution of retention.

Vegetation: Wildflower, drainage layer: 40mm, substrate: 100mm  
(W/40/100)

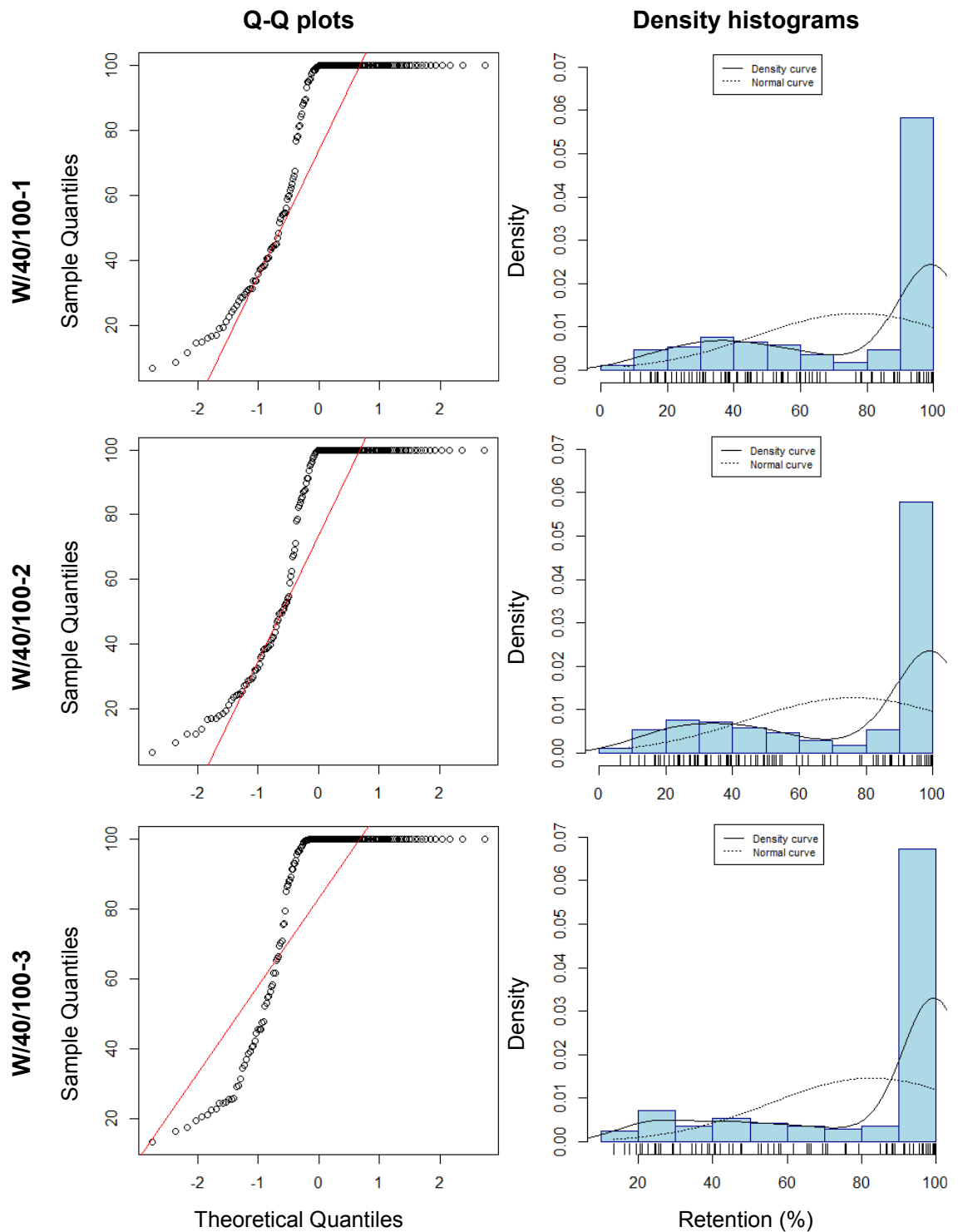
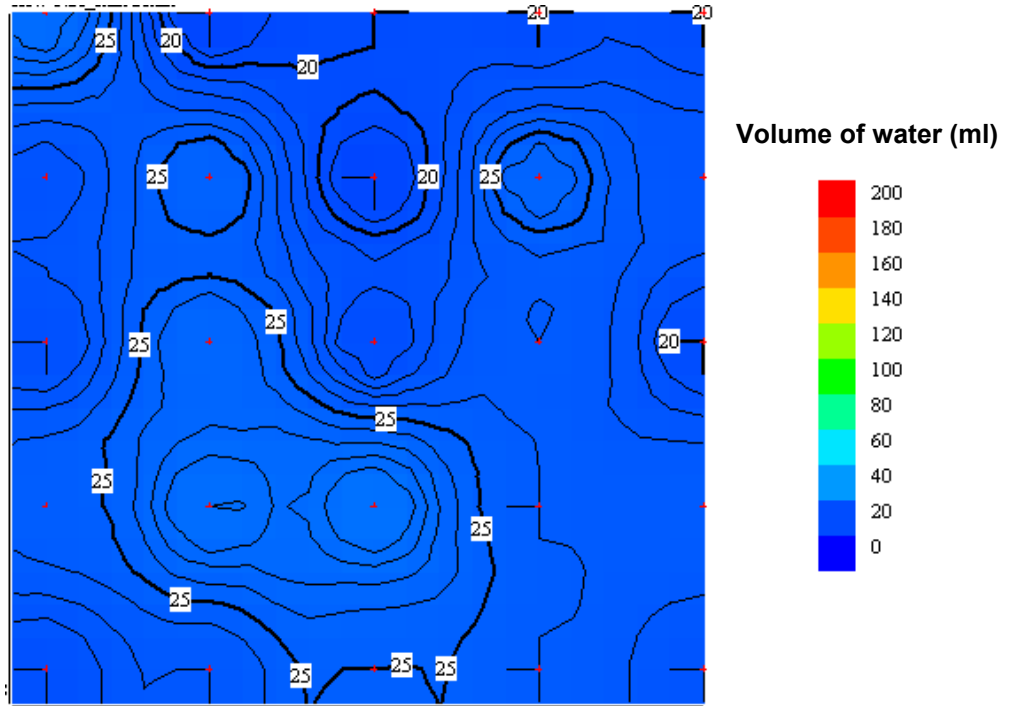


Figure D.9 Data exploratory analysis of retention data for replicates of W/40/100 roof. Q-Q plots and density histograms confirm non-normal distribution of retention.

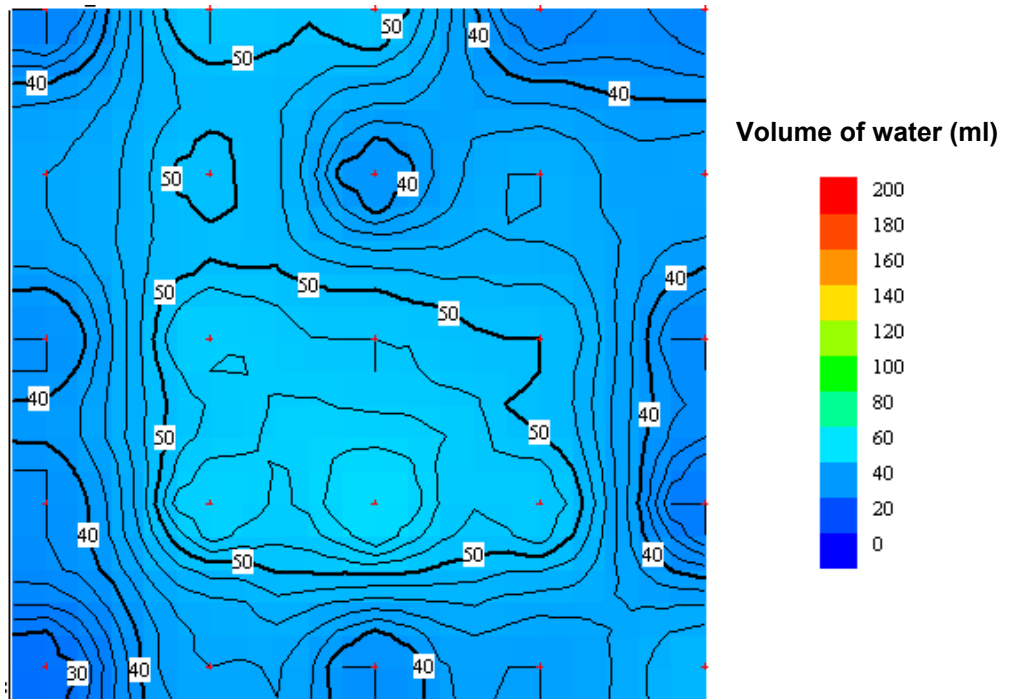
## APPENDIX E

Rainfall simulator calibration: the spatial distribution of simulated rainfall

**Actual flow rate: 0.145 l/min (displayed flow rate: 0.05 l/min)**



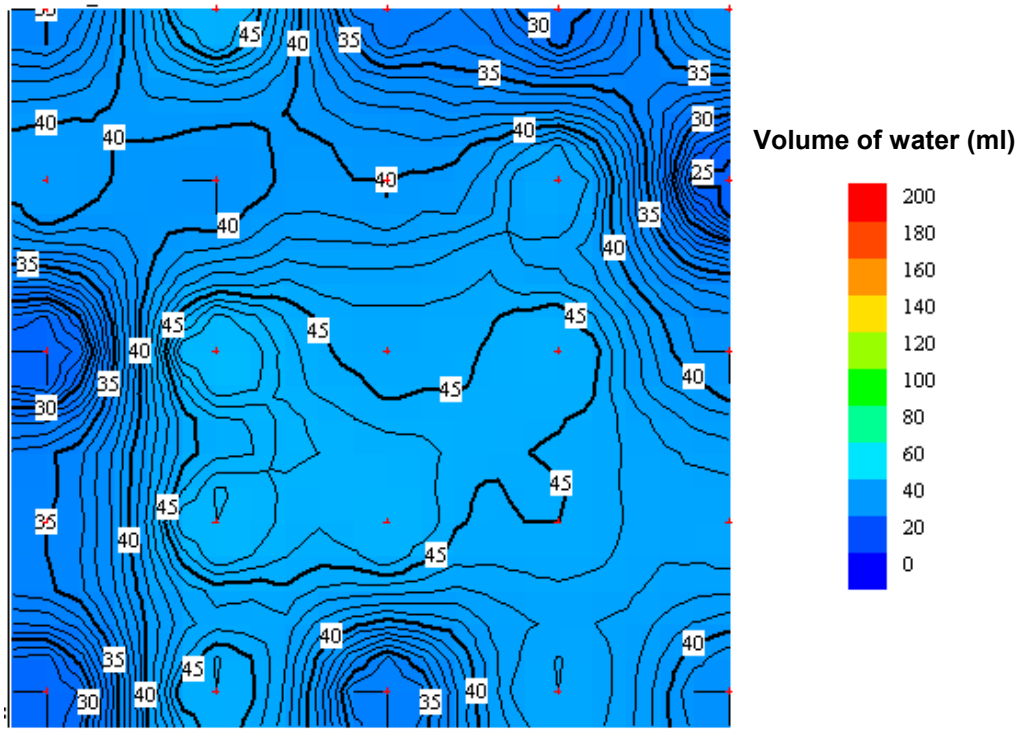
(a) duration: 5min



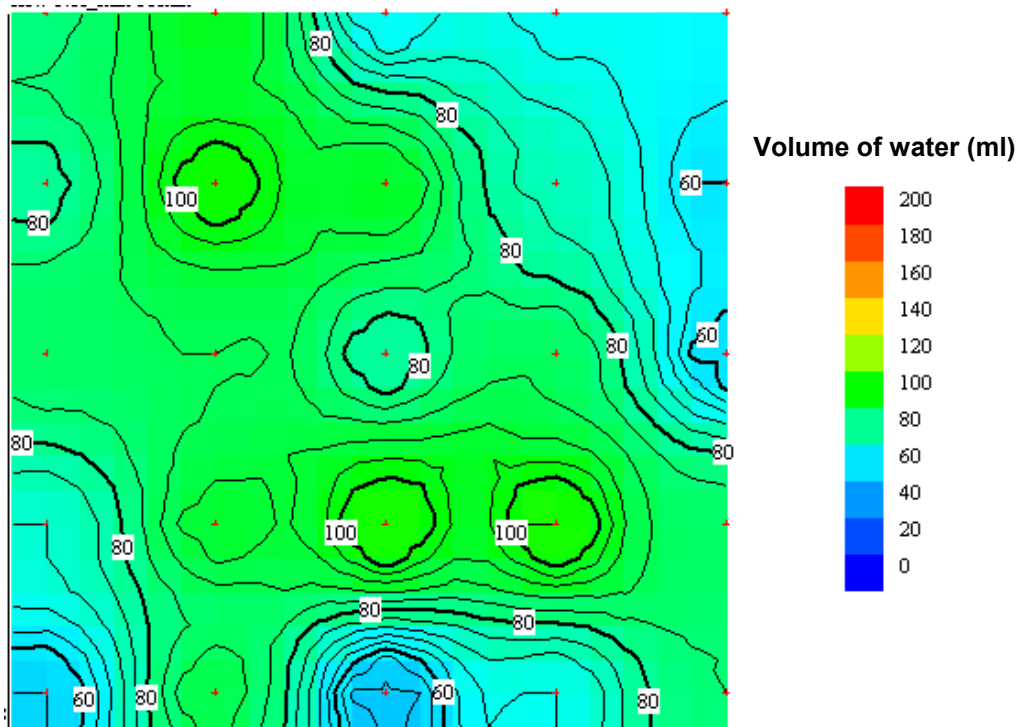
(b) duration: 10min

Figure E.1 Maps showing simulated rainfall distribution for the displayed flow rate of 0.05 l/min (a) test duration 5min (b) test duration 10min.

Actual flow rate: 0.255 l/min (displayed flow rate: 0.1 l/min)



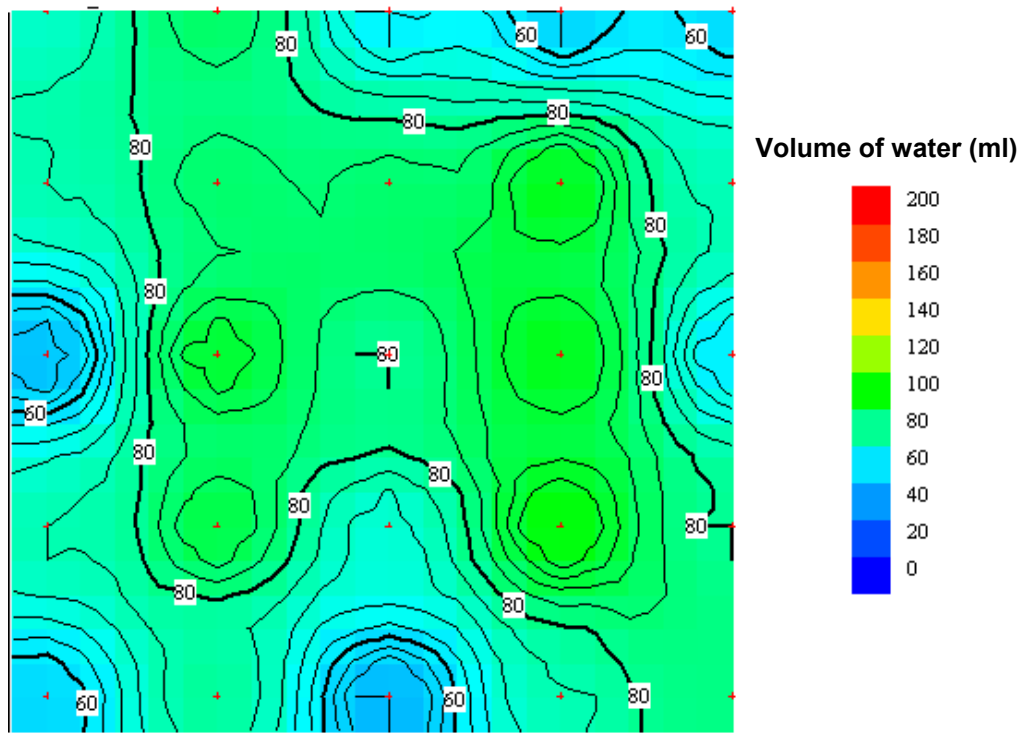
(a) duration: 5min



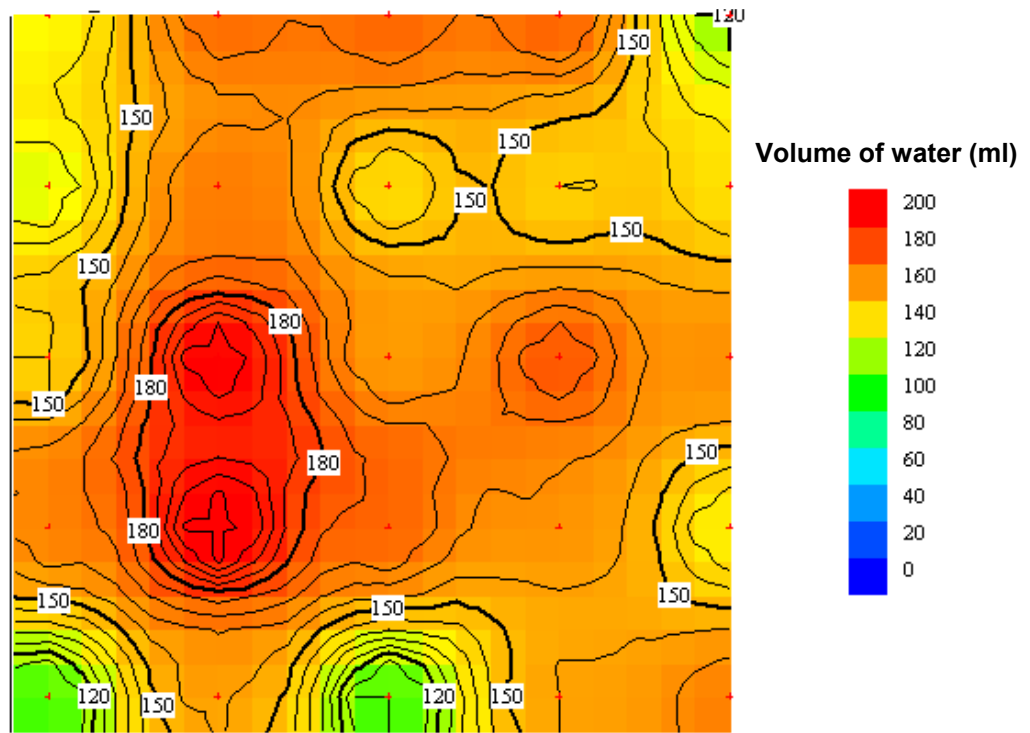
(b) duration: 10min

Figure E.2 Maps showing simulated rainfall distribution for the displayed flow rate of 0.1 l/min (a) test duration 5min (b) test duration 10min.

Actual flow rate: 0.489 l/min (displayed flow rate: 0.2 l/min)



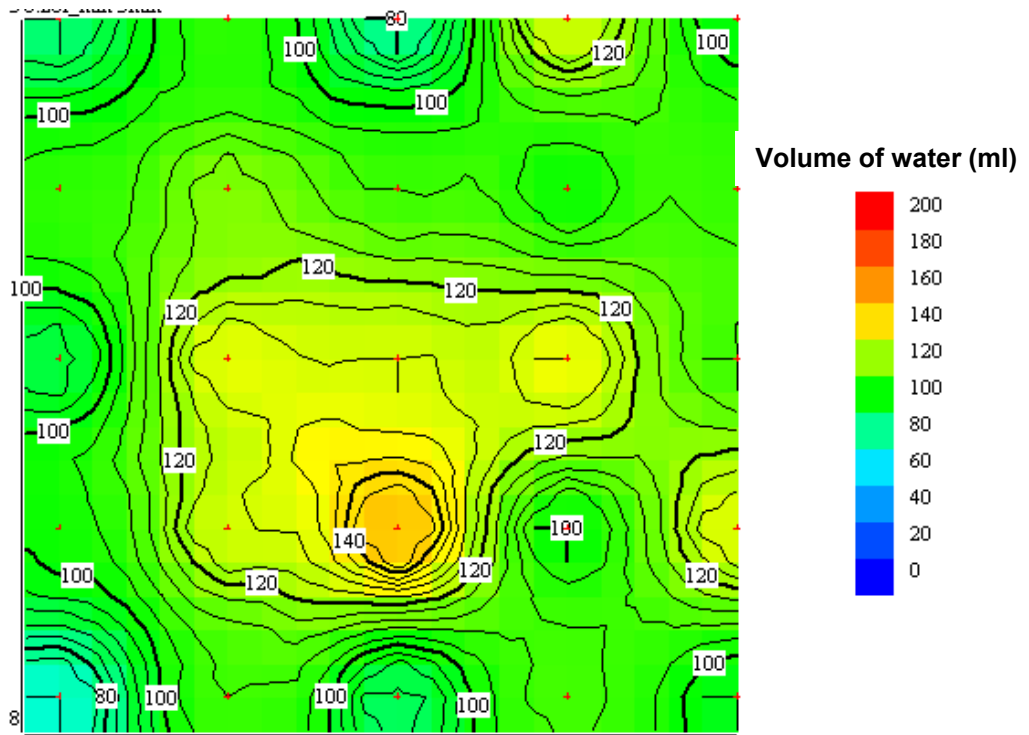
(a) duration: 5min



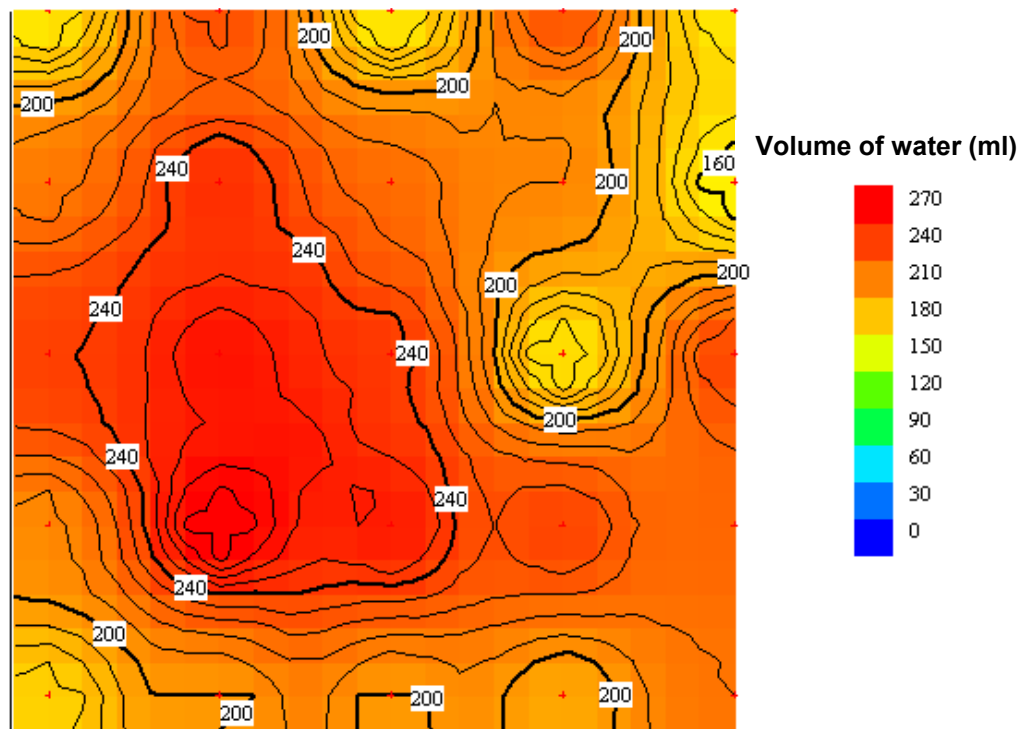
(b) duration: 10min

Figure E.3 Maps showing simulated rainfall distribution for the displayed flow rate of 0.2 l/min (a) test duration 5min (b) test duration 10min.

Actual flow rate: 0.685 l/min (displayed flow rate: 0.28 l/min)



(a) duration: 5min



(b) duration: 10min

Figure E.4 Maps showing simulated rainfall distribution for the displayed flow rate of 0.28 l/min (a) test duration 5min (b) test duration 10min.

## APPENDIX F

Laboratory experiment: Q-Q plots and density histograms for retention data of vegetated and unvegetated green roofs.

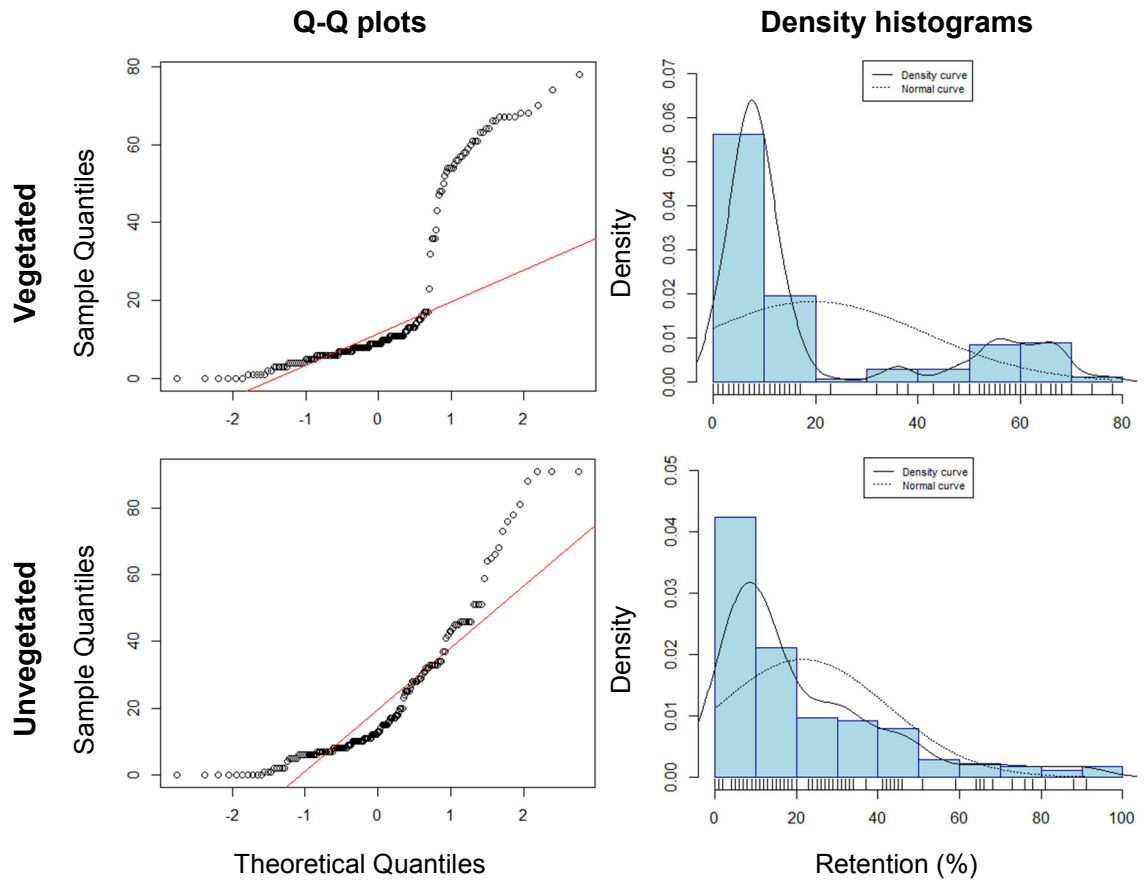


Figure F.1 Data exploratory analysis of retention data for vegetated and unvegetated green roofs. Each group includes all green roof designs. Q-Q plots and density histograms confirm non-normal distribution of retention.

# APPENDIX G

Laboratory experiment: Q-Q plots and density histograms for retention data of each green roof experimental replicate

**Control: design A - Crushed Red Brick and Roofdrain40**

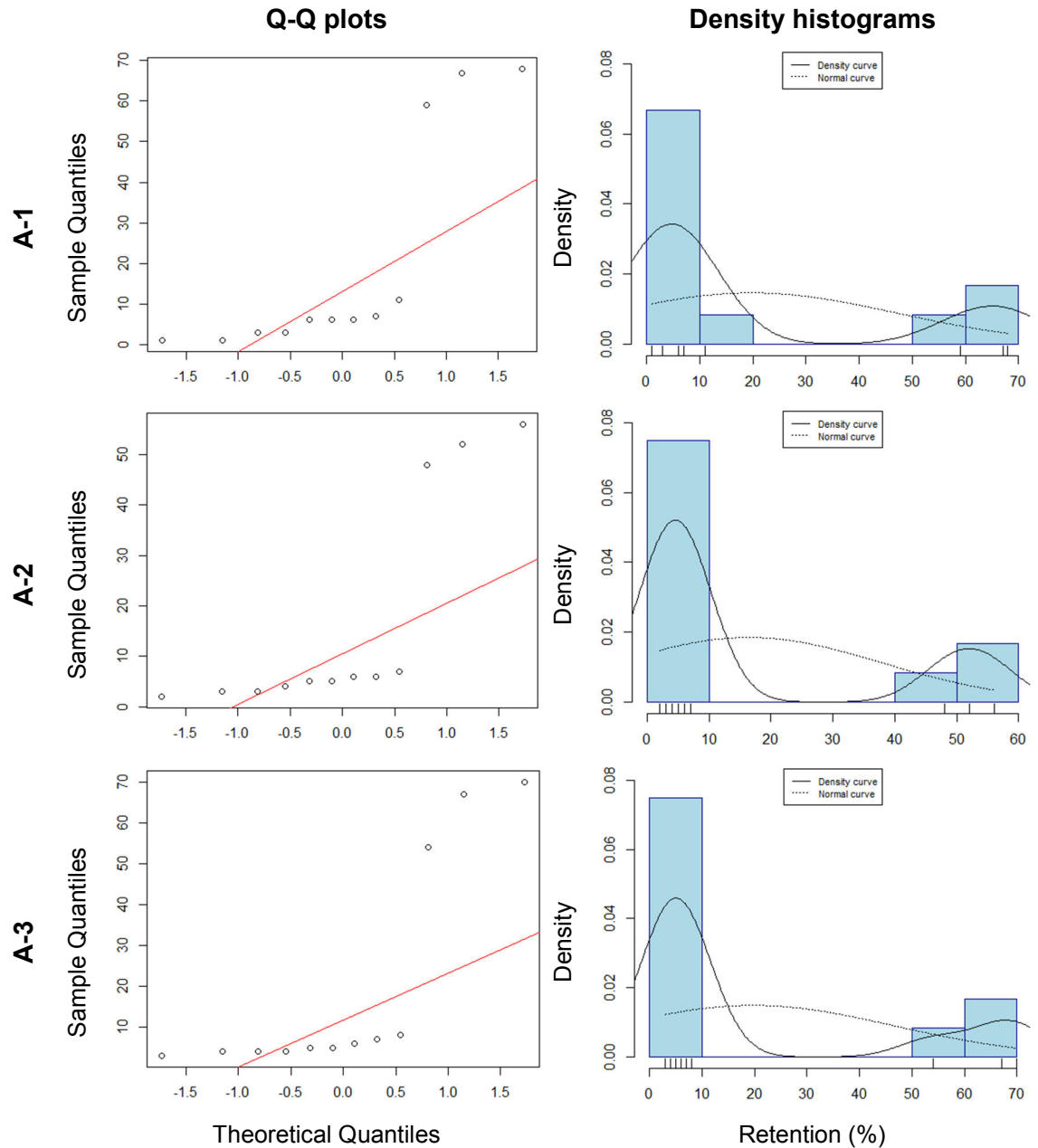


Figure G.1 Data exploratory analysis of retention data for replicates of green roof design A. Q-Q plots and density histograms confirm non-normal distribution of retention.

## Treatment 1: design B – Sewage Sludge Pellets and Roofdrain40

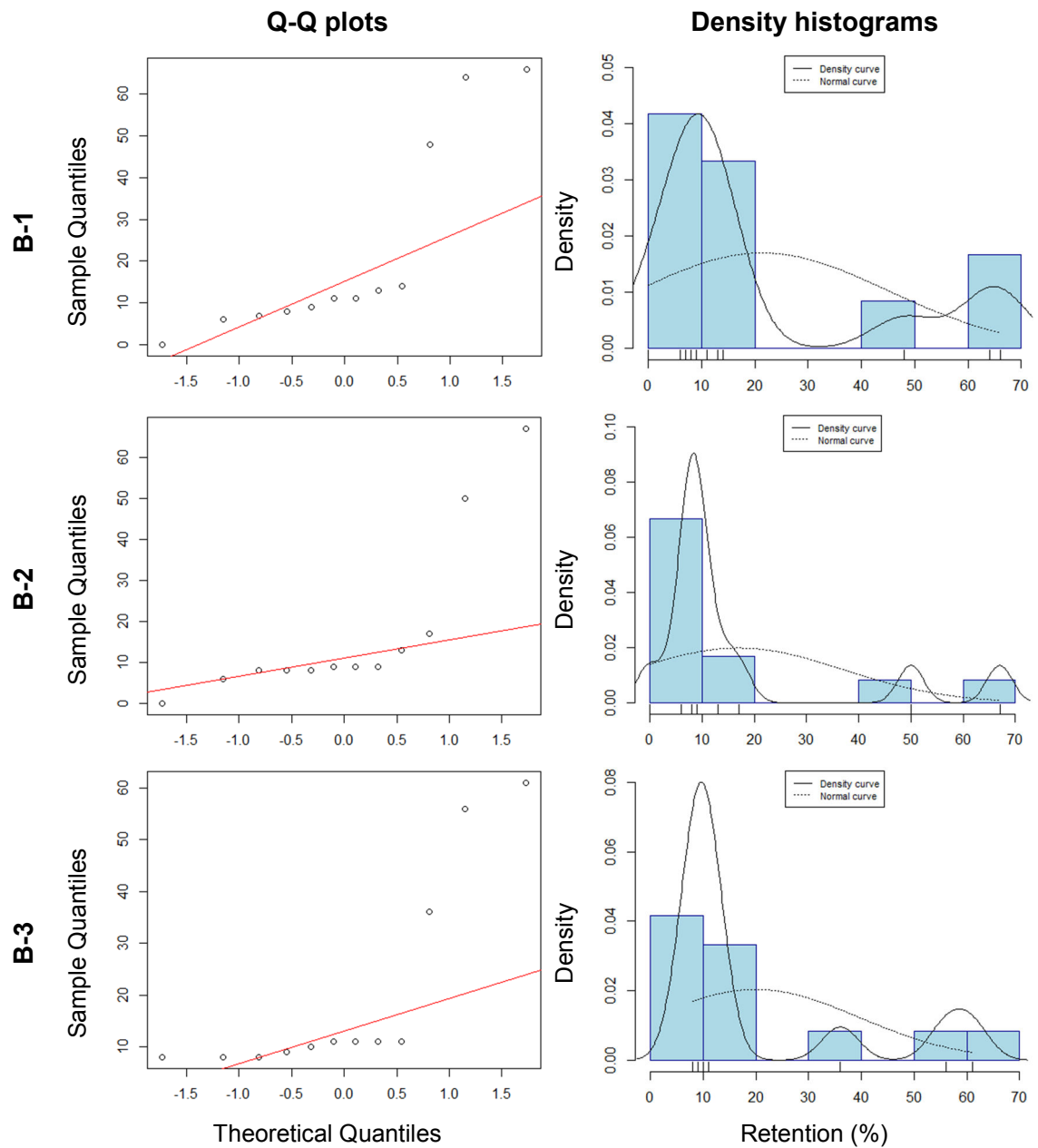


Figure G.2 Data exploratory analysis of retention data for replicates of green roof design B. Q-Q plots and density histograms confirm non-normal distribution of retention.

## Treatment 2: design C – Lytag and Roofdrain40

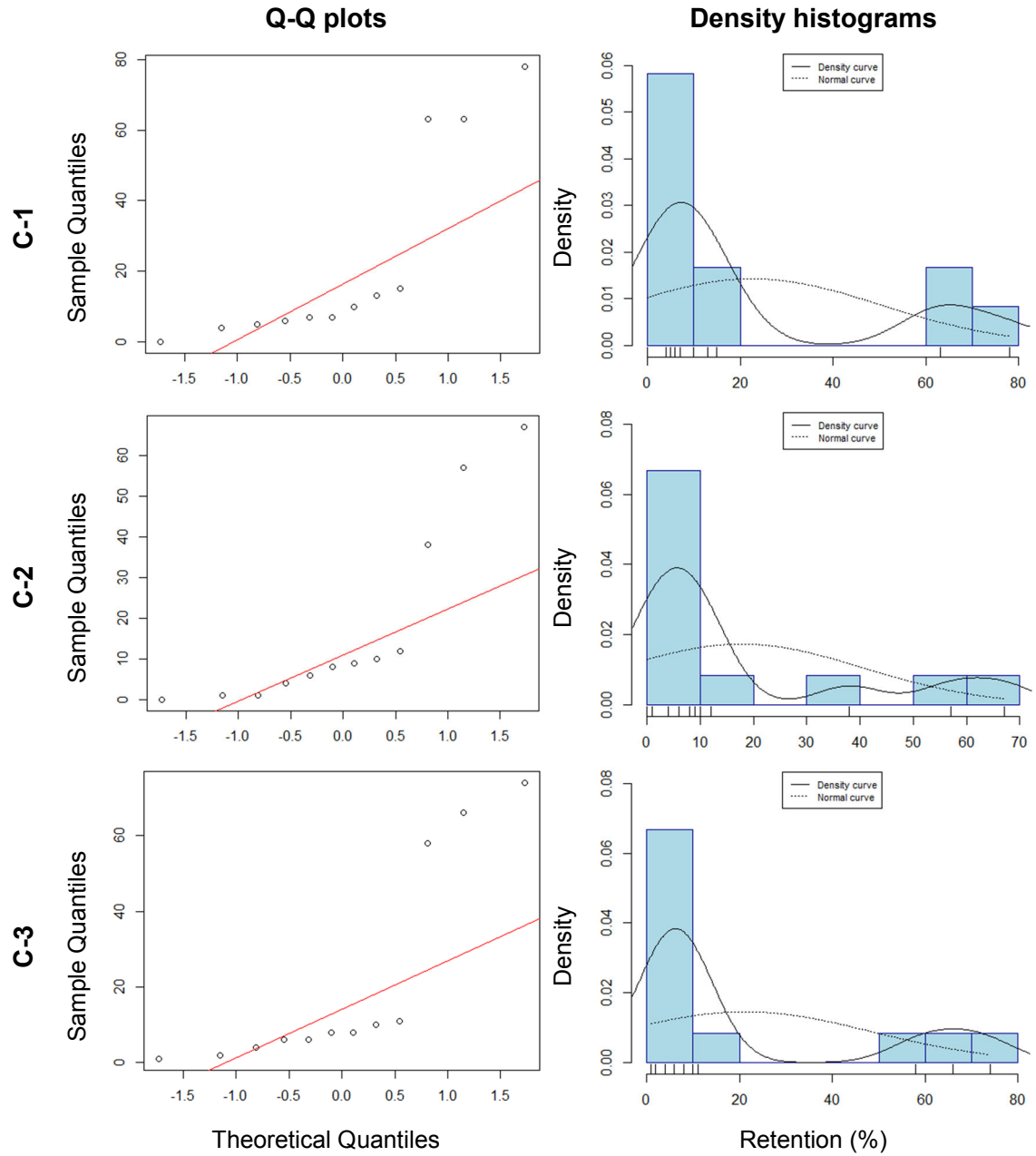


Figure G.3 Data exploratory analysis of retention data for replicates of green roof design C. Q-Q plots and density histograms confirm non-normal distribution of retention.

### Treatment 3: design D – Crushed Red Brick and Granulated Rubber

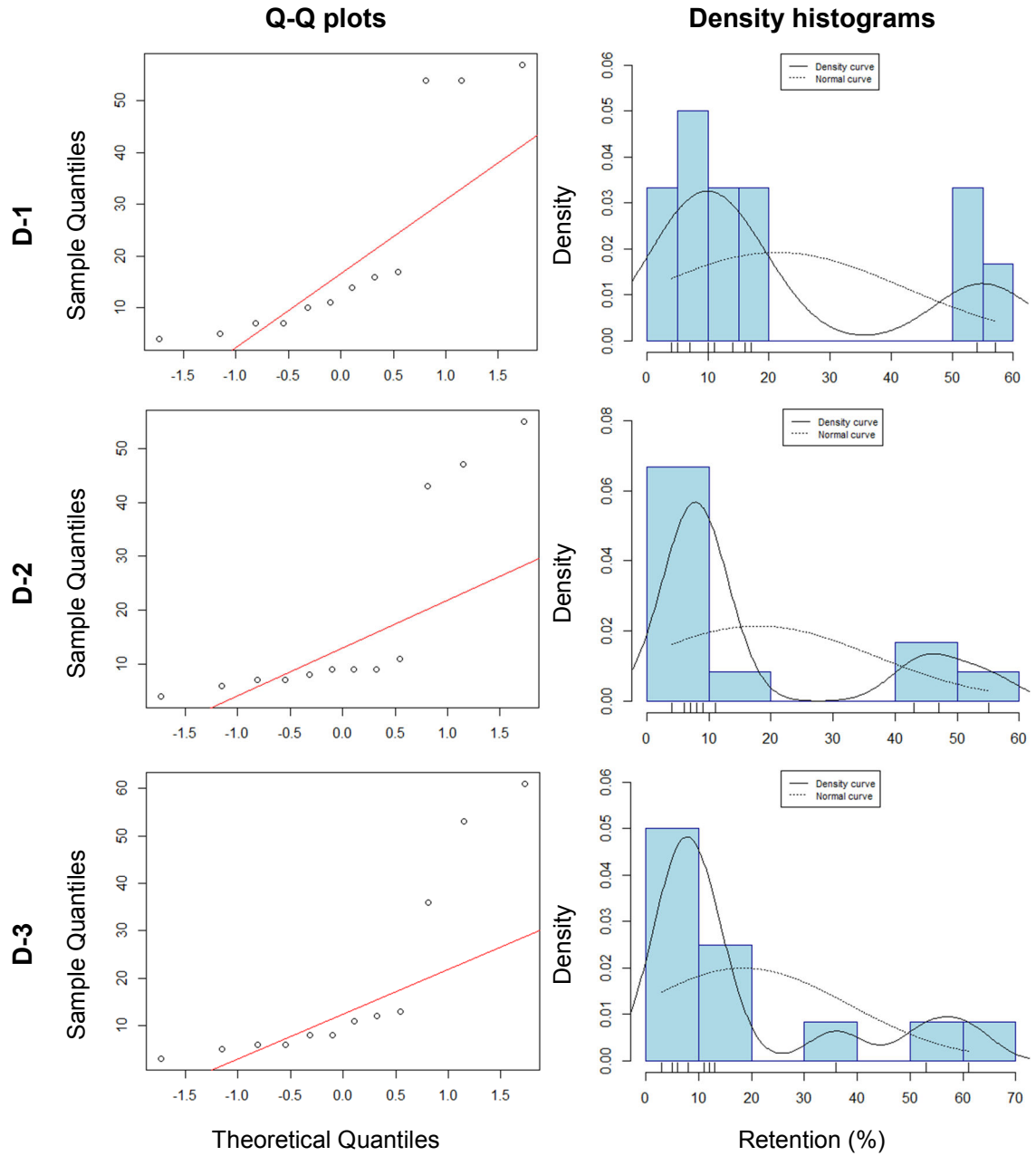
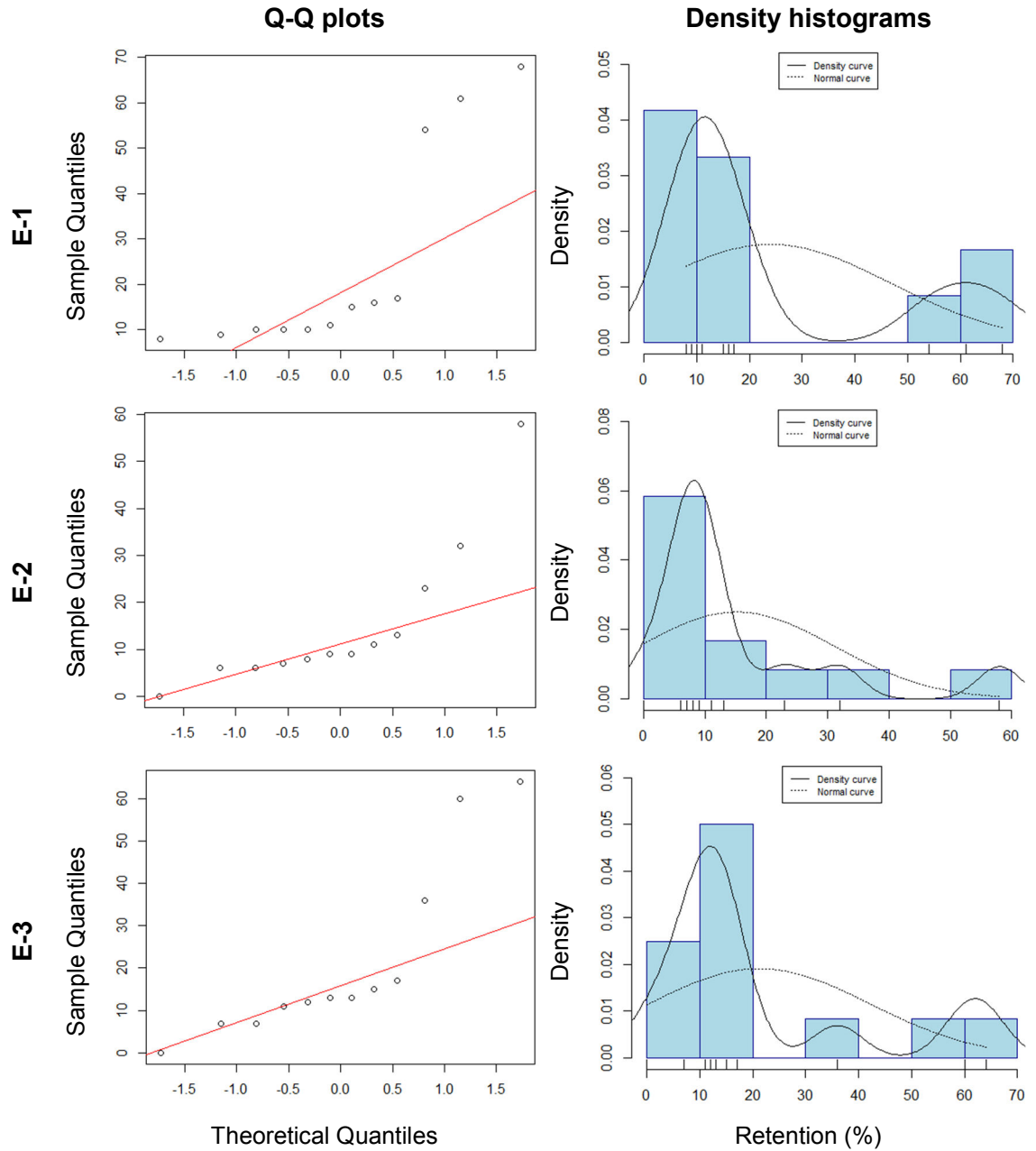


Figure G.4 Data exploratory analysis of retention data for replicates of green roof design D. Q-Q plots and density histograms confirm non-normal distribution of retention.

**Treatment 4: design E – Crushed Red Brick and Wool-rich Carpet Shred**



*Figure G.5 Data exploratory analysis of retention data for replicates of green roof design E. Q-Q plots and density histograms confirm non-normal distribution of retention.*